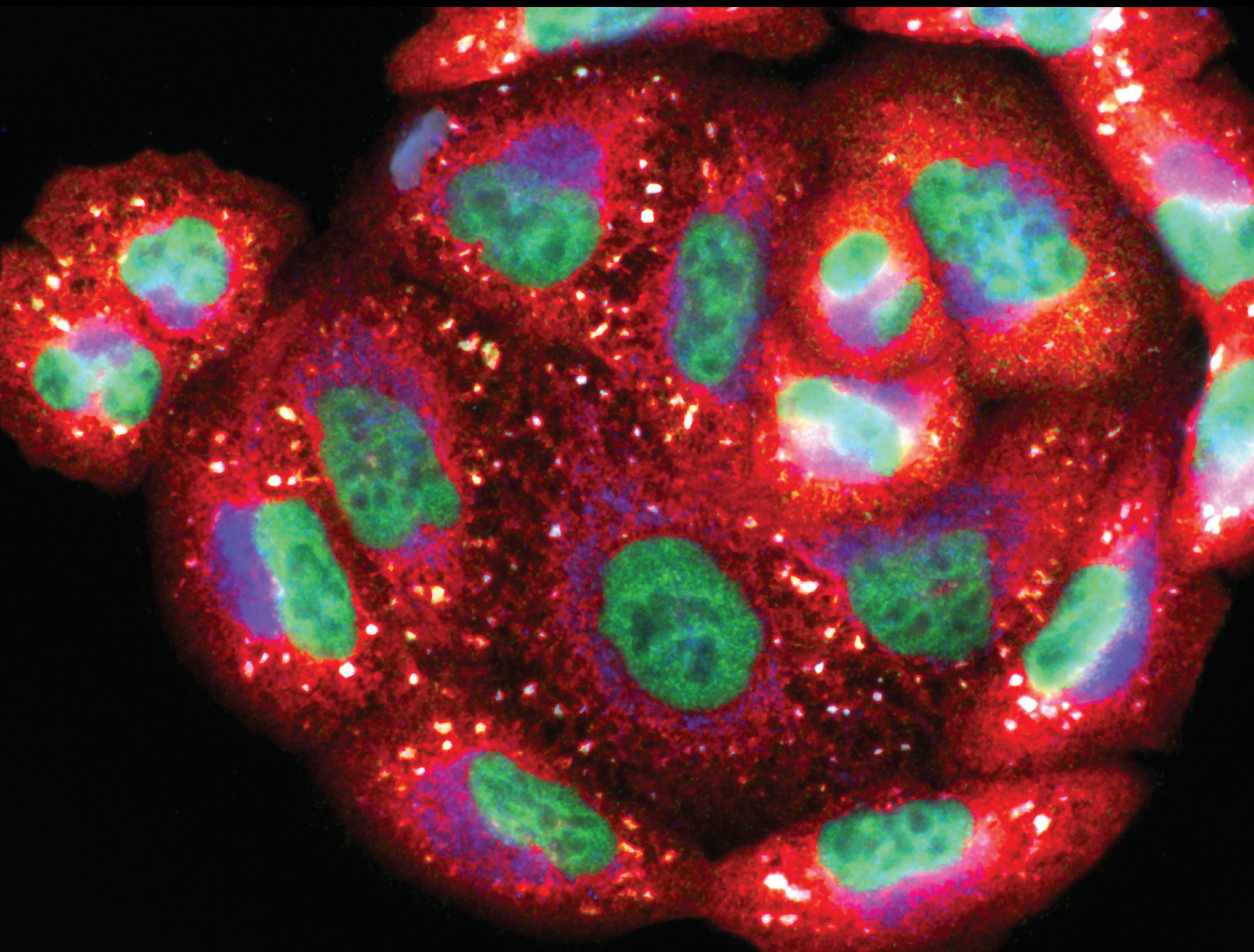


Bioactive Compounds of Food: Their Role in the Prevention and Treatment of Diseases 2022

Lead Guest Editor: Dr. Anderson Junger Teodoro

Guest Editors: Dr. Germán Gil, Dr. Felipe Leite Oliveira, and Dr. Cassiano
Felipe Gonçalves-de-Albuquerque

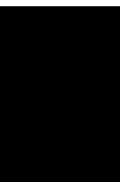




**Bioactive Compounds of Food: Their Role in
the Prevention and Treatment of Diseases 2022**

**Bioactive Compounds of Food: Their
Role in the Prevention and Treatment of
Diseases 2022**

Lead Guest Editor: Dr. Anderson Junger Teodoro
Guest Editors: Dr. Germán Gil, Dr. Felipe Leite
Oliveira, and Dr. Cassiano Felipe Gonçalves-de-
Albuquerque



Copyright © 2023 Hindawi Limited. All rights reserved.

This is a special issue published in "Oxidative Medicine and Cellular Longevity" All articles are open access articles distributed under the Creative Commons Attribution License, which permits unrestricted use, distribution, and reproduction in any medium, provided the original work is properly cited.

Chief Editor

Jeannette Vasquez-Vivar, USA

Associate Editors

Amjad Islam Aqib, Pakistan
Angel Catalá , Argentina
Cinzia Domenicotti , Italy
Janusz Gebicki , Australia
Aldrin V. Gomes , USA
Vladimir Jakovljevic , Serbia
Thomas Kietzmann , Finland
Juan C. Mayo , Spain
Ryuichi Morishita , Japan
Claudia Penna , Italy
Sachchida Nand Rai , India
Paola Rizzo , Italy
Mithun Sinha , USA
Daniele Vergara , Italy
Victor M. Victor , Spain

Academic Editors

Ammar AL-Farga , Saudi Arabia
Mohd Adnan , Saudi Arabia
Ivanov Alexander , Russia
Fabio Altieri , Italy
Daniel Dias Rufino Arcanjo , Brazil
Peter Backx, Canada
Amira Badr , Egypt
Damian Bailey, United Kingdom
Rengasamy Balakrishnan , Republic of Korea
Jiaolin Bao, China
Ji C. Bihl , USA
Hareram Birla, India
Abdelhakim Bouyahya, Morocco
Ralf Braun , Austria
Laura Bravo , Spain
Matt Brody , USA
Amadou Camara , USA
Marcio Carochio , Portugal
Peter Celec , Slovakia
Giselle Cerchiaro , Brazil
Arpita Chatterjee , USA
Shao-Yu Chen , USA
Yujie Chen, China
Deepak Chhangani , USA
Ferdinando Chiaradonna , Italy

Zhao Zhong Chong, USA
Fabio Ciccarone, Italy
Alin Ciobica , Romania
Ana Cipak Gasparovic , Croatia
Giuseppe Cirillo , Italy
Maria R. Ciriolo , Italy
Massimo Collino , Italy
Manuela Corte-Real , Portugal
Manuela Curcio, Italy
Domenico D'Arca , Italy
Francesca Danesi , Italy
Claudio De Lucia , USA
Damião De Sousa , Brazil
Enrico Desideri, Italy
Francesca Diomede , Italy
Raul Dominguez-Perles, Spain
Joël R. Drevet , France
Grégory Durand , France
Alessandra Durazzo , Italy
Javier Egea , Spain
Pablo A. Evelson , Argentina
Mohd Farhan, USA
Ioannis G. Fatouros , Greece
Gianna Ferretti , Italy
Swaran J. S. Flora , India
Maurizio Forte , Italy
Teresa I. Fortoul, Mexico
Anna Fracassi , USA
Rodrigo Franco , USA
Juan Gambini , Spain
Gerardo García-Rivas , Mexico
Husam Ghanim, USA
Jayeeta Ghose , USA
Rajeshwary Ghosh , USA
Lucia Gimeno-Mallench, Spain
Anna M. Giudetti , Italy
Daniela Giustarini , Italy
José Rodrigo Godoy, USA
Saeid Golbidi , Canada
Guohua Gong , China
Tilman Grune, Germany
Solomon Habtemariam , United Kingdom
Eva-Maria Hanschmann , Germany
Md Saquib Hasnain , India
Md Hassan , India










Tim Hofer , Norway
John D. Horowitz, Australia
Silvana Hrelia , Italy
Dragan Hrnčić, Serbia
Zebo Huang , China
Zhao Huang , China
Tarique Hussain , Pakistan
Stephan Immenschuh , Germany
Norsharina Ismail, Malaysia
Franco J. L. , Brazil
Sedat Kacar , USA
Andleeb Khan , Saudi Arabia
Kum Kum Khanna, Australia
Neelam Khaper , Canada
Ramoji Kosuru , USA
Demetrios Kouretas , Greece
Andrey V. Kozlov , Austria
Chan-Yen Kuo, Taiwan
Gaocai Li , China
Guoping Li , USA
Jin-Long Li , China
Qiangqiang Li , China
Xin-Feng Li , China
Jialiang Liang , China
Adam Lightfoot, United Kingdom
Christopher Horst Lillig , Germany
Paloma B. Liton , USA
Ana Lloret , Spain
Lorenzo Loffredo , Italy
Camilo López-Alarcón , Chile
Daniel Lopez-Malo , Spain
Massimo Lucarini , Italy
Hai-Chun Ma, China
Nageswara Madamanchi , USA
Kenneth Maiese , USA
Marco Malaguti , Italy
Steven McAnulty, USA
Antonio Desmond McCarthy , Argentina
Sonia Medina-Escudero , Spain
Pedro Mena , Italy
V́ctor M. Mendoza-Núñez , Mexico
Lidija Milkovic , Croatia
Alexandra Miller, USA
Sara Missaglia , Italy

Premysl Mladenka , Czech Republic
Sandra Moreno , Italy
Trevor A. Mori , Australia
Fabiana Morroni , Italy
Ange Mouithys-Mickalad, Belgium
Iordanis Mourouzis , Greece
Ryoji Nagai , Japan
Amit Kumar Nayak , India
Abderrahim Nemmar , United Arab Emirates
Xing Niu , China
Cristina Nocella, Italy
Susana Novella , Spain
Hassan Obied , Australia
Pál Pacher, USA
Pasquale Pagliaro , Italy
Dilipkumar Pal , India
Valentina Pallottini , Italy
Swapnil Pandey , USA
Mayur Parmar , USA
Vassilis Paschalis , Greece
Keshav Raj Paudel, Australia
Ilaria Peluso , Italy
Tiziana Persichini , Italy
Shazib Pervaiz , Singapore
Abdul Rehman Phull, Republic of Korea
Vincent Pialoux , France
Alessandro Poggi , Italy
Zsolt Radak , Hungary
Dario C. Ramirez , Argentina
Erika Ramos-Tovar , Mexico
Sid D. Ray , USA
Muneeb Rehman , Saudi Arabia
Hamid Reza Rezvani , France
Alessandra Ricelli, Italy
Francisco J. Romero , Spain
Joan Roselló-Catafau, Spain
Subhadeep Roy , India
Josep V. Rubert , The Netherlands
Sumbal Saba , Brazil
Kunihiro Sakuma, Japan
Gabriele Saretzki , United Kingdom
Luciano Saso , Italy
Nadja Schroder , Brazil

Anwen Shao , China
Iman Sherif, Egypt
Salah A Sheweita, Saudi Arabia
Xiaolei Shi, China
Manjari Singh, India
Giulia Sita , Italy
Ramachandran Srinivasan , India
Adrian Sturza , Romania
Kuo-hui Su , United Kingdom
Eisa Tahmasbpour Marzouni , Iran
Hailiang Tang, China
Carla Tatone , Italy
Shane Thomas , Australia
Carlo Gabriele Tocchetti , Italy
Angela Trovato Salinaro, Italy
Rosa Tundis , Italy
Kai Wang , China
Min-qi Wang , China
Natalie Ward , Australia
Grzegorz Wegrzyn, Poland
Philip Wenzel , Germany
Guangzhen Wu , China
Jianbo Xiao , Spain
Qiongming Xu , China
Liang-Jun Yan , USA
Guillermo Zalba , Spain
Jia Zhang , China
Junmin Zhang , China
Junli Zhao , USA
Chen-he Zhou , China
Yong Zhou , China
Mario Zoratti , Italy

Contents

Serum from Adolescents with High Polyphenol Intake Exhibits Improved Lipid Profile and Prevents Lipid Accumulation in HepG2 Human Liver Cells

Giuseppina Augimeri, Ennio Avolio , Giovanna Caparello, Angelo Galluccio, Daniela De Rose, Adele Vivacqua , Catia Morelli , Ines Barone , Stefania Catalano , Sebastiano Andò, Cinzia Giordano , Diego Sisci , Stefania D'Angelo , and Daniela Bonofiglio 

Research Article (12 pages), Article ID 1555942, Volume 2023 (2023)

Protective Effect of Dietary Polysaccharides from Yellow Passion Fruit Peel on DSS-Induced Colitis in Mice

Laryssa Regis Bueno , Bruna da Silva Soley , Kahlile Youssef Abboud , Isabella Wzorek França , Karien Sauruk da Silva , Natalia Mulinari Turin de Oliveira , Juliana Santos Barros, Marcelo Biondaro Gois , Lucimara Mach Côrtes Cordeiro , and Daniele Maria-Ferreira 


Research Article (15 pages), Article ID 6298662, Volume 2022 (2022)

Potential Functional Food Products and Molecular Mechanisms of *Portulaca Oleracea* L. on Anticancer Activity: A Review

Pâmela Gomes de Souza , Amauri Rosenthal , Ellen Mayra Menezes Ayres , and Anderson Junger Teodoro 



Review Article (9 pages), Article ID 7235412, Volume 2022 (2022)

Bioactivities and Mechanism of Actions of *Dendrobium officinale*: A Comprehensive Review

Xiaoyu Xu, Cheng Zhang, Ning Wang, Yu Xu, Guoyi Tang, Lin Xu, and Yibin Feng 








Review Article (21 pages), Article ID 6293355, Volume 2022 (2022)

The Ameliorative Role of Eugenol against Silver Nanoparticles-Induced Hepatotoxicity in Male Wistar Rats

Hany N. Yousef , Somaya S. Ibraheim, Ramadan A. Ramadan, and Hanaa R. Aboelwafa 



Research Article (18 pages), Article ID 3820848, Volume 2022 (2022)

Bovine Lactoferrin Induces Cell Death in Human Prostate Cancer Cells

Vanessa P. Rocha , Samir P. C. Campos , Caroline A. Barros , Pablo Trindade , Leticia R. Q. Souza, Triciana G. Silva, Etel R. P. Gimba , Anderson J. Teodoro , and Rafael B. Gonçalves 








Research Article (13 pages), Article ID 2187696, Volume 2022 (2022)

Hepatoprotective Mechanism of Ginsenoside Rg1 against Alcoholic Liver Damage Based on Gut Microbiota and Network Pharmacology

Ting Xia, Bin Fang, Chaoyan Kang, Yuxuan Zhao, Xiao Qiang, Xiaodong Zhang, Yiming Wang, Tian Zhong, Jianbo Xiao , and Min Wang 








Research Article (18 pages), Article ID 5025237, Volume 2022 (2022)

Luteolin-Rich Extract of *Thespesia garckeana* F. Hoffm. (Snot Apple) Contains Potential Drug-Like Candidates and Modulates Glycemic and Oxidoinflammatory Aberrations in Experimental Animals

Uchenna Blessing Alozieuwa, Bashir Lawal , Saidu Sani, Amos Sunday Onikanni, Obinna Osuji, Yunusa Olatunji Ibrahim, Shukurat Bisola Babalola, Gomaa Mostafa-Hedeab , Abdulrahman A. Alsayegh , Sarah Albogami, Gaber El-Saber Batiha , Alexander T. H. Wu , Hsu-Shan Huang , and Carlos Adam Conte-Junior 







Research Article (20 pages), Article ID 1215097, Volume 2022 (2022)

Quercetin Protects Ethanol-Induced Hepatocyte Pyroptosis via Scavenging Mitochondrial ROS and Promoting PGC-1 α -Regulated Mitochondrial Homeostasis in L02 Cells

Xingtao Zhao , Cheng Wang , Shu Dai , Yanfang Liu , Fang Zhang , Cheng Peng , and Yunxia Li 

Research Article (15 pages), Article ID 4591134, Volume 2022 (2022)

Role of Inflammation, Oxidative Stress, and Mitochondrial Changes in Premenstrual Psychosomatic Behavioral Symptoms with Anti-Inflammatory, Antioxidant Herbs, and Nutritional Supplements

Arshiya Sultana , Khaleequr Rahman , Md Belal Bin Heyat , Sumbul , Fajjan Akhtar , and Abdullah Y. Muaad 





Research Article (29 pages), Article ID 3599246, Volume 2022 (2022)

Theaflavin-3,3'-Digallate Protects Cartilage from Degradation by Modulating Inflammation and Antioxidant Pathways

Yun Teng, Zheyu Jin, Weizhi Ren, Minghao Lu, Mingzhuang Hou, Quan Zhou, Wenhao Wang, Huilin Yang , and Jun Zou 

Research Article (19 pages), Article ID 3047425, Volume 2022 (2022)

Mulberrin Confers Protection against Doxorubicin-Induced Cardiotoxicity via Regulating AKT Signaling Pathways in Mice

Peng Ye , Wen-Lan Li , Long-Tang Bao , and Wei Ke 



Research Article (18 pages), Article ID 2967142, Volume 2022 (2022)

Vitexin Mitigates *Staphylococcus aureus*-Induced Mastitis via Regulation of ROS/ER Stress/NF- κ B/MAPK Pathway

Yu Chen , Jing Yang , Zhi Huang , Baoyi Yin , Talha Umar , Cheng Yang , Xiangqian Zhang , Hongyuan Jing , Shuai Guo , Mengyao Guo , Ganzhen Deng , and Changwei Qiu 

Research Article (20 pages), Article ID 7977433, Volume 2022 (2022)








Delving the Role of *Caralluma fimbriata*: An Edible Wild Plant to Mitigate the Biomarkers of Metabolic Syndrome

Rimsha Anwar, Roshina Rabail, Allah Rakha , Marcin Bryla, Marek Roszko, Rana Muhammad Aadil , and Marek Kieliszek 

Review Article (17 pages), Article ID 5720372, Volume 2022 (2022)

Contents







Resveratrol as a Promising Polyphenol in Age-Associated Cardiac Alterations

Denise Börzsei , Judith Sebestyén, Renáta Szabó , Zelma Nadin Lesi, Andrea Pálszabó, Patrícia Pálszabó, András Szász, Dániel Priksz , Béla Juhász , Médea Veszelka , Zsolt Turcsán, Zoltán Deim, Csaba Varga , and Anikó Pósa 
Research Article (8 pages), Article ID 7911222, Volume 2022 (2022)



Novel Compound Polysaccharides from Chinese Herbal Medicines: Purification, Characterization, and Antioxidant Activities

Xu Yang , Haiyu Ji, Yingying Feng, Juan Yu, and Anjun Liu 
Research Article (10 pages), Article ID 9973419, Volume 2022 (2022)







***Carica papaya* L. Leaves: Deciphering Its Antioxidant Bioactives, Biological Activities, Innovative Products, and Safety Aspects**

Anshu Sharma, Ruchi Sharma, Munisha Sharma, Manoj Kumar , Mrunal Deepak Barbhai , José M. Lorenzo, Somesh Sharma, Mahesh Kumar Samota, Maria Atanassova, Gianluca Caruso , Mo. Naushad, Radha, Deepak Chandran , Pramod Prakash, Muzaffar Hasan, Nadeem Rais, Abhijit Dey , Dipendra Kumar Mahato, Sangram Dhumal, Surinder Singh, Marisennayya Senapathy, Sureshkumar Rajalingam, Marthandan Visvanathan, Lejaniya Abdul Kalam Saleena, and Mohamed Mekhemar 
Review Article (20 pages), Article ID 2451733, Volume 2022 (2022)

Epigallocatechin Gallate Relieved PM2.5-Induced Lung Fibrosis by Inhibiting Oxidative Damage and Epithelial-Mesenchymal Transition through AKT/mTOR Pathway

Zhou Zhongyin, Wang Wei, Xiong Juan , and Fan Guohua 
Research Article (11 pages), Article ID 7291774, Volume 2022 (2022)

Ginger for Healthy Ageing: A Systematic Review on Current Evidence of Its Antioxidant, Anti-Inflammatory, and Anticancer Properties

Mehtap Ozkur , Necla Benlier , Işıl Takan , Christina Vasileiou , Alexandros G. Georgakilas , Athanasia Pavlopoulou , Zafer Cetin , and Eyup Ilker Saygili 
Review Article (16 pages), Article ID 4748447, Volume 2022 (2022)

Research Article

Serum from Adolescents with High Polyphenol Intake Exhibits Improved Lipid Profile and Prevents Lipid Accumulation in HepG2 Human Liver Cells

Giuseppina Augimeri,¹ Ennio Avolio ,² Giovanna Caparello,² Angelo Galluccio,^{2,3} Daniela De Rose,¹ Adele Vivacqua ,¹ Catia Morelli ,¹ Ines Barone ,¹ Stefania Catalano ,^{1,4} Sebastiano Andò,^{1,4} Cinzia Giordano ,^{1,4} Diego Sisci ,^{1,4} Stefania D'Angelo ,⁵ and Daniela Bonofiglio ,^{1,4}

¹Department of Pharmacy, Health and Nutritional Sciences, University of Calabria, Rende, 87036 Cosenza, Italy

²Health Center Srl, 87100 Cosenza, Italy

³Department of Clinical and Experimental Medicine, University Magna Graecia, 88100 Catanzaro, Italy

⁴Centro Sanitario, University of Calabria, 87036 Arcavacata di Rende, Italy

⁵Department of Movement Sciences and Wellbeing, University of Naples "Parthenope", 80133 Naples, Italy

Correspondence should be addressed to Stefania D'Angelo; stefania.dangelo@uniparthenope.it

Received 11 April 2022; Revised 15 September 2022; Accepted 24 November 2022; Published 13 February 2023

Academic Editor: Felipe L. de Oliveira

Copyright © 2023 Giuseppina Augimeri et al. This is an open access article distributed under the Creative Commons Attribution License, which permits unrestricted use, distribution, and reproduction in any medium, provided the original work is properly cited.

The traditional Mediterranean diet (MD) is characterized by a high phenolic-rich food intake, including in particular vegetables and fruits, but also legumes, whole grain cereals, nuts, and extra virgin olive oil. Evidence for beneficial effects of polyphenols in humans depends on the amount consumed and on their bioavailability. Here, we evaluated the association between the estimated polyphenol intake by fruits and vegetables food source and serum biochemical parameters in healthy adolescents, recruited into the DIMENU research project. Categorizing adolescents into three groups according to their estimated total polyphenol intake, we found that adolescents who declared high consumption of polyphenols had a higher adherence to the MD and had a better serum lipid profile than adolescents consuming low amounts of polyphenols. Moreover, using human HepG2 liver cells treated with oleic acid as an in vitro model for studying lipid accumulation, we showed that intracellular lipid accumulation is alleviated by serum from adolescents consuming a polyphenol-rich diet following MD recommendations. Our data underline the importance of promoting adherence to the typical MD foods as a superior strategy to prevent metabolic and chronic diseases and to ensure a better quality of life among adolescents.

1. Introduction

It is well recognized that nutrition plays an important role in health status; particularly, a high plant-based diet rich in fruits and vegetables may provide protective effects against many noncommunicable diseases (NCDs), such as cardiovascular diseases, type 2 diabetes, and some types of cancer [1–3]. In the past 10 years, a rise in interest in fruit and vegetable consumption has been motivated by their content of polyphenols [4]. Fruits like apples, grapes, pears, and berries typically have

high amounts of polyphenols (200–300 mg per 100 g); also, vegetables, such as broccoli, carrots, and cabbages, contain a similar polyphenol content in fresh mass (100–300 mg per 100 g) [5, 6]. Apart from fruits and vegetables, other dietary sources of these phytochemicals include chocolate, tea, nuts, and olive oil as well as to a lesser extent dry legumes and whole grains [7]. Polyphenols are a very heterogeneous and widespread group of compounds, with more than 8000 different molecules characterized by the presence of one or more aromatic rings bearing hydroxyl groups [8]. Dietary polyphenols

are divided into four classes: flavonoids, phenolic acids, stilbenes, and lignans, which can exist in a glycosidic form (glycosides of flavonoids, lignans, and stilbenes) or as esters (phenolic acids esterified to polyols such as quinic acid) [9]. Flavonoids can be classified into six subclasses based on the specific heterocyclic ring involved: flavonols, flavones, isoflavones, flavanones, anthocyanins, and flavanols (catechins and proanthocyanidins). In addition, two classes of phenolic acids can be distinguished into benzoic acid derivatives and cinnamic acid derivatives [7, 10, 11]. The most common phenolic acids are caffeic acid and ferulic acid, which are the major phenolic compounds in coffee and cereals, respectively. The best-studied stilbene is resveratrol in grapes, grape products, and red wine [10, 12].

These bioactive compounds are responsible for some sensory and health properties of foods, such as bitterness, astringency, and antioxidant ability. However, the considerable diversity of their structures makes polyphenols different from other antioxidants. Furthermore, the conjugation reactions with methyl, sulfate, or glucuronide groups as well as the nature and amounts of metabolites formed by the gut microflora may influence their absorption and their bioavailability [6, 13, 14]. In addition, the intake of these compounds and their food sources are highly variable and are linked with dietary patterns, sex, socioeconomic factors, and the native foods of each region.

Many studies, including epidemiologic cohort and case-control studies, as well as preclinical studies, have shown that the regular consumption of polyphenol-rich foods may reduce the incidence of obesity, metabolic syndrome, and liver disorders [15]. For example, polyphenols like catechins, resveratrol, and curcumin have been found to inhibit lipogenesis and enhance energy expenditure, leading to weight loss and anti-obesogenic effects in different cell, animal, and human studies [16, 17]. Moreover, in human interventional trials, it has been widely demonstrated that polyphenols exert antioxidant and anti-inflammatory effects, preventing the progression of the metabolic syndrome [18].

Nonalcoholic fatty liver disease (NAFLD) is the most common chronic disease that may lead to severe pathologic conditions such as cirrhosis and hepatocellular carcinoma [19]. Adults as well as children with fatty liver display abnormal glucose and lipid metabolism [20]. The early events of NAFLD, studied in animals and in cell models of hepatic steatosis, including human hepatoblastoma HepG2 cell line [21], are triglyceride accumulation in the liver and insulin resistance, which is considerably affected by different causes such as hyperenergetic diets, sedentary lifestyle, and genetic factors. Fat accumulation in the liver is associated with lipotoxic hepatocellular injury due to elevated free fatty acids, free cholesterol, and other lipid metabolites. Thus, mitochondrial dysfunction with oxidative stress and endoplasmic reticulum stress-associated mechanisms are activated [22]. Currently, there is no agreement with respect to the pharmacological treatment of NAFLD, but lifestyle interventions based on exercise and a balanced diet for quality and quantity are considered the cornerstone of the NAFLD management [23].

The Mediterranean diet (MD), which is characterized by a high intake of vegetables, fruits, whole grain cereals,

legumes, low-fat dairy, and extra virgin olive oil, has been suggested to decrease the risk of many NCDs, including liver disorders [24–27]. It is worth noting that the optimal adherence to the MD has been associated with the reduced risk of development and progression of NAFLD, due to the nutraceutical effects of bioactive compounds such as fibers, omega-3 fatty acids, vitamins, and polyphenols [28, 29]. Despite the promising evidence about the possible role of polyphenols in NCDs [30, 31], data regarding their consumption at the population level is not strong enough to recommend dietary intake levels [32]. Identifying an optimal polyphenol consumption is particularly relevant in the young population. Indeed, a healthy dietary pattern based on the consumption of polyphenol-based foods in adolescence might prevent the development of several NCD in adulthood. In order to estimate the dietary intake of polyphenols, several web databases have been developed, among which the web-based Phenol-Explorer database is the most comprehensive electronic tool on polyphenol contents. Indeed, Phenol-Explorer database, using information on food composition, metabolism, and pharmacokinetics of polyphenols, retrieves a reliable estimation on the polyphenol content from dietary sources [11, 33, 34].

The aim of this study was to estimate polyphenol intake from fruits and vegetables food source documented in a 24-hour dietary recall, by using the Phenol-Explorer database, in healthy adolescents. According to their estimated total polyphenol intake, adolescents were categorized into three different groups in order to evaluate the impact of polyphenol intake on serum metabolic profile. Furthermore, the potential properties of serum from adolescents were also investigated using an *in vitro* cell culture model of lipid accumulation.

2. Materials and Methods

2.1. Study Population. The population sample was recruited into the DIMENU research project (Mediterranean Diet and Swimming-Calabria FESR-FSE 2014-2020, prot. 52243/2017), in which adolescents were enrolled by the Castrolibero Institute of Education (Cosenza, Italy) and by sports associations of the Calabria region, Italy [35–38]. As part of the DIMENU project, in the current study, we investigated the total population of 56 subjects (31 girls and 25 boys) aged between 14 and 17 years. The exclusion criteria from the study included health problems, drug use, supplement intake, any type of restrictive diet (i.e., low calorie, low carb, and low fat content) and cognitive, physical, or motor limitation. Ethical approval was obtained by the Ethics Committee of the University of Calabria, Italy (# 5727/2018) to conduct this study.

2.2. Anthropometric Parameters and Physical Activity Intensity Levels. In all participants, anthropometric data were collected using a validated protocol [39], in particular by measuring height and bodyweight; the body mass index (BMI) was calculated as previously reported [38]. Physical activity levels, based on the WHO recommendations [40], were classified according to the metabolic equivalents (METs), particularly physical inactivity (<3 metabolic

equivalents (METs), moderate PA (3 to 6 METs), and vigorous-intensity PA (>6 METs), using a questionnaire that we have described elsewhere [38].

2.3. Adherence to the Mediterranean Diet by KIDMED Test and Dietary Assessment by 24h Recall. The KIDMED test was used to assess the adherence to the MD, providing a score ranging from <0 to ≤12 according to the 16-point questions (12 positive and 4 negative items) [41]. Nutritionists collected daily meals from each subject through an in-depth interview of the 24-hour recall which investigated detailed data about food preparation methods, ingredients used, and amounts of each food consumed in reference to a common size container (e.g., bowls, cups, and glasses). The dietary survey was carried out the day before the interview and planned excluding the investigation of the food intake referring to the weekend. A photographic manual of portion sizes was used to visually estimate food amounts. Nutrient intakes were calculated by multiplying the portion weight by its nutrient content. Specific software MetaDieta software version 4.2.1. (Meteda s.r.l., Roma, Italy), which includes the Italian database, was used to analyze the energy and nutrient content of food intake.

2.4. Biochemical and Hormonal Measurements. After a 12-hour overnight fasting, venous blood samples were collected and centrifuged in order to obtain serum. The biochemical parameters were analyzed by a Konelab 20i chemistry analyzer (Thermo Electron Corporation, Vantaa, Finland) according to standard procedures. Serum C-reactive protein (CRP) levels were determined by immunonephelometry (GOLDSITE Diagnostics, Inc., Shenzhen, China). Serum insulin levels were detected with an enzyme-linked immunosorbent assay (ELISA) kit (NovaTec Immundiagnostica GmbH, Dietzenbach, Germany) following the manufacturer's instructions. The lowest detectable concentration of insulin was 0.25 μ IU/mL at a 95% confidence limit; the intra-assay variability was within ≤5%. Homeostasis model assessment for estimating insulin resistance (HOMA-IR) which was calculated as the product of fasting glucose concentration (mg/dL) and fasting insulin concentration was divided by 405. Erythrocyte sedimentation rate (ESR) was measured by the Wintrobe method.

2.5. Phenol-Explorer Database. Phenol-Explorer is an updated comprehensive database for natural polyphenols including food synthesis, processing, and humans' polyphenol metabolites (<http://phenol-explorer.eu-version3.6>). The last version of Phenol-Explorer database provides data on 502 polyphenol compounds in 452 plant-based foods collected from 638 scientific peer-reviewed articles and divided in the main polyphenol classes [42–44]. The Phenol-Explorer 3.6 database reports data that also consider the effects of cooking and food processing on polyphenol content. The data from total polyphenols in the database was expressed as total phenolics, which was determined by using the Folin-Ciocalteu assay; the value of the individual polyphenols was evaluated by chromatography [44, 45]. The only exception to the use of this method was for determination of total anthocyanins, using the pH differential

method [46]. Caution should be taken when comparing retention factors obtained by different methods, as polyphenols degraded during food cooking or processing may no longer be detectable by HPLC, but still keep an absorbance or ability to reduce the Folin reagent [44]. Total polyphenol content was calculated as the sum of the contents of individual compounds expressed in mg/100 g food fresh weight [45].

2.6. Estimation of Dietary Polyphenol Intake. The calculation of polyphenol intake was derived from matching the dietary assessment by 24h recall and food (fruits and vegetables) data in the Phenol-Explorer database. The fruit and vegetable intakes were calculated (in g) by following the portions sizes reported by each subject. An advanced search was carried out in the Phenol-Explorer database to retrieve mean content values for total polyphenols contained in the foods obtained. Total polyphenol intake was calculated as the sum of all individual polyphenol intakes from all food sources reported [13, 33, 34, 45].

2.7. Antioxidant Ability Assessed in Serum

2.7.1. FRAP Assay. The ferric reducing antioxidant power (FRAP) method measures the change in absorbance that occurs when the TPTZ (2,4,6-tris-pyridyl-S-triazine) (–Fe(III)) complex is reduced to the TPTZ-Fe²⁺ form in the presence of antioxidant compounds [47]. Briefly, the FRAP reagent was prepared by mixing 10 mM tris-pyridyl-S-triazine (TPTZ) solution in 40 mM HCl plus 20 mM FeCl₃ and 0.25 M sodium acetate buffer (pH 3.6) in a volume ratio of 1:1:10. The acetate buffer used in the FRAP assay was prepared by dissolving 1.90 g/L of sodium acetate in water and adjusted to pH 3.6 with 16.0 mL/L glacial acetic acid. An aliquot (6 μ L) of serum from adolescents stratified in three groups according to their polyphenol intake was mixed with 140 μ L of FRAP reagent and 0.06 μ L of H₂O. The absorbance of the reaction mixture was measured at 593 nm in Multiskan SkyHigh (Thermo Fisher Scientific, Waltham, MA, USA). A solution of FeSO₄ (1 mM) was used to obtain the calibration curve. 2,4,6-Tris-pyridyl-S-triazine (TPTZ), FeCl₃, FeSO₄, glacial acetic acid, and oleic acid were purchased from Sigma-Aldrich (Milan, Italy).

2.7.2. DPPH Assay. The 2,2-diphenyl-1-picrylhydrazyl (DPPH, Sigma-Aldrich) assay is based on the reduction of the purple DPPH• to 1,1-diphenyl-2-picryl hydrazine by antioxidant compounds [48]. Serum aliquots (100 μ L) were mixed with 100 μ L of methanol, incubated for 2 min, and then centrifuged (10 min, 48°C, 9500 = g). Supernatant samples were immediately tested for the DPPH radical scavenging activity. Briefly, 10 μ L of serum sample was mixed with 100 μ L of a 0.1 mM DPPH solution in absolute methanol and incubated in darkness at room temperature for 30 min. The absorbance was read at 520 nm in Multiskan SkyHigh (Thermo Fisher Scientific). The sample absorbance was compared with the absorbance of a control containing only methanol and DPPH solution. The percentage of DPPH inhibition

was calculated using the following equation:

$$\%IDPPH = \left[1 - \left(\frac{As}{A0} \right) \right] * 100, \quad (1)$$

where As is the absorbance of sample and A0 is the DPPH solution absorbance.

2.8. Cell Culture and Experimental Treatments. Human hepatocellular carcinoma HepG2 cells were obtained from American Type Culture Collection (ATCC, USA) and authenticated and stored according to the supplier's instruction. HepG2 cells were cultured in Eagle's Minimum Essential Medium (EMEM) (ATCC) and supplemented with 10% fetal bovine serum (FBS, Life Technologies) and 1% penicillin-streptomycin (Sigma-Aldrich) at 37°C in a humidified 5% CO₂ atmosphere. For staining of lipid droplets with Oil Red O, 140,000 HepG2 cells were seeded in 24-multiwell dishes for 24 hours. Subsequently, the cells were pretreated for 1 hour in serum-free medium with 10% of pooled serum of all adolescents as control and pooled serum from adolescents with low, medium, and high polyphenol intake before exposure of 0.1 mM oleic acid (OA) for 24 hours.

2.9. MTT Assay. HepG2 cells were seeded in a 24-well plate and exposed to different concentration (0.1-1 mM) of OA for 24 hours. Cell viability was determined with the 3-(4,5-dimethylthiazol-2-yl)-2,5-diphenyltetrazolium (MTT) assay, as previously described [49]. The results were expressed as a percentage of viable cells in comparison to the control (taken as 100%).

2.10. Staining of Lipid Droplets with Oil Red O. After incubation with oleic acid, HepG2 cells were washed with PBS and fixed with 4% paraformaldehyde for 30 minutes at room temperature. Then, the cells were stained with Oil Red O (Bio Optica, Milan, Italy) as described in the manufacturer's protocol and observed under a light microscope (Olympus). To quantify Oil Red O content, the cells were treated with 100% isopropanol and lipid accumulation was evaluated at 510 nm in Multiskan SkyHigh (Thermo Fisher Scientific).

2.11. Statistical Analysis. Data were reported as the mean and standard deviation (SD) or standard error of mean (SEM) as indicated. Table 1 shows the average values and SD of total cholesterol, low-density lipoprotein (LDL), and triglycerides (TG) along with the effect size, the corresponding 95% confidence intervals, and the *p* values, evaluated by equivalence test, between low and high polyphenol intake groups. Statistical differences between groups were evaluated by using parametric tests (one-way ANOVA and Student's *t*-test). The correlation between variables was evaluated by Spearman's correlation test. Statistical significance was set at *p* < 0.05.

3. Results

3.1. Characteristics of Participants and Total Polyphenol Intake. The general characteristics of the study population are presented in Table 2. A total of 56 adolescents with a mean age of 15.87 (±1.04) years old were included in the

final analysis, specifically 31 girls and 25 boys. Normal mean values of BMI were found in our population (22.96 ± 3.33). We also reported the data on the three intensity levels of the physical activity of participants, according to the guidelines established by the WHO [39]. In addition, the KIDMED test revealed a score < 4.52 (1st tertile), within 4.52-7.38 (2nd tertile) and > 9.52 (3rd tertile) and a mean score of 7.14 (±2.23), indicating an average adherence to the Mediterranean diet (MD) in our adolescents. The mean daily intake of total polyphenols was estimated at 434.46 (±514.27) mg/day, consisting of approximately 49% of flavonoids, 39% of phenolic acids, and 12% of other polyphenols. No differences were observed in the general characteristics according to sex (data not shown).

3.2. Total Polyphenol Intake Associates with Mediterranean Diet Adherence in Adolescents. Previous studies showed that the polyphenol intake is positively associated with the adherence to the Mediterranean diet in an adult Italian population [50], but there is no adequate data about this correlation in healthy adolescents. Testing the association between the total estimated polyphenol intake and the adherence to the MD in all adolescents, we found a significant linear increasing association (*r* = 0.411 and *p* = 0.001). We did not find any difference in the polyphenol intake according to sex, physical activity, or BMI (data not shown).

3.3. Mediterranean Diet Adherence and Dietary and Food Intakes of Adolescents Stratified according to Their Estimated Total Polyphenol Intake. Based on daily total polyphenol intake, we classified the study participants into the low, moderate, and high polyphenol intake groups (Table 3). We found that adolescents allocated in the highest tertile of total polyphenol consumption had significantly higher adherence to the MD than participants from the lowest tertile (8.21 ± 1.84 vs. 6.15 ± 2.22, *p* = 0.01).

Using a 24-hour dietary recall method, we evaluated the mean daily intakes of energy, macronutrients, and micronutrients in our adolescents grouped according to the estimated total polyphenol intake. As shown in Table 4, no statistically significant differences were found among the three groups in absolute intakes of energy and most macronutrients. However, we observed that adolescents with high polyphenols' consumption showed greater intakes of omega-3 fatty acids and soluble and insoluble dietary fibers than those with low polyphenols' consumption group. The same differences were revealed after energy adjustment (data not shown). As regarding the intakes of micronutrients, the mean levels of vitamin B5, B6, B8, B12, K, phosphorus, magnesium, selenium, potassium, and copper were increased in high compared to low consumers. Similarly, vitamins and minerals, except phosphorus and copper, displayed the significant differences after energy adjustment (data not shown). In addition, intake of water was greater in high than low and moderate polyphenol intake groups. Interestingly, the dietary total antioxidant capacity evaluated by the Oxygen Radical Absorbance Capacity (ORAC) showed increased total ORAC in adolescents with high compared with low intake group.

TABLE 1: The differences of total cholesterol, low-density lipoprotein cholesterol, and triglycerides values between low and high polyphenol intake (PI) groups.

Biomarkers	Average values and SD (mg/dL)	Effect size (mg/dL)	95% confidence interval (mg/dL)	p values
Total cholesterol	Low PI: 163.2 ± 37.1 High PI: 140.3 ± 20.6	22.9	3.0-42.9	0.025
LDL	Low PI: 93.3 ± 27.5 High PI: 74.9 ± 17.1	18.4	3.1-33.5	0.020
TG	Low PI: 112.1 ± 109.7 High PI: 55.6 ± 15.3	56.5	3.2-109.7	0.039

LDL: low-density lipoprotein; TG: triglycerides; PI: polyphenol intake; SD: standard deviation.

TABLE 2: General characteristics of all participants.

Total population (number of subjects)	56
Girls/boys (numbers)	31/25
Age (years)	15.87 ± 1.04
BMI (kg/m ²)	22.96 ± 3.33
BMI (kg/m ²) percentiles	73.51 ± 20.81
Physical activity intensity levels (number of subjects)	
Sedentary	14
Moderate	21
Vigorous	21
KIDMED score	7.14 ± 2.23
Total polyphenol intake (mean mg/day)	434.46 ± 514.27
Flavonoids (%)	49
Phenolic acids (%)	39
Other polyphenols (%)	12

BMI: body mass index. Data are expressed as mean ± SD.

TABLE 3: KIDMED score in adolescents grouped according to their total estimated total polyphenol consumption.

	Total polyphenol intake (mg/day)			p value
	Low (n = 19)	Moderate (n = 18)	High (n = 19)	
	<210	210-460	>460	*0.32 ¥ 0.0001 § 0.0002
KIDMED score	6.15 ± 2.22	7.05 ± 2.23	8.21 ± 1.84	*0.40 ¥ 0.01 § 0.23

*: low vs. moderate; ¥: low vs. high; §: moderate vs. high. Data are expressed as mean ± SD. Statistical differences were evaluated by a one-way ANOVA test. In bold are reported statistically significant values.

3.4. Antioxidant Activity of Serum Samples from Adolescents Classified according to their Estimated Total Polyphenol Consumption. Polyphenols have been largely studied for their effects on human health due to their potential antioxidant properties, which decrease the risk of several diseases, including metabolic disorders and cardiovascular and liver diseases [29, 51, 52]. Based on our results showing that the dietary total ORAC increased in high polyphenol consumers, we evaluated the potential antioxidant properties of serum samples from the adolescents enrolled in this study. We found that serum from high consumers displayed a significantly enhanced ferric reducing antioxidant activity than that from adolescents consuming moderate and low amounts of polyphenols (Figure 1(a)). Consistent with these results, we also observed that pooled serum from adolescents

consuming high amounts of polyphenols exhibited a higher percentage of inhibition against DPPH compared to the moderate and low polyphenol consumers (Figure 1(b)).

3.5. Biochemical, Metabolic, and Inflammatory Serum Profile from Adolescents Classified according to Their Estimated Total Polyphenol Intake. Serum levels of general, metabolic, and inflammatory biomarkers in subjects classified according to the tertiles of total polyphenols' consumption were evaluated, since no significant association between total polyphenol intake and serum biomarkers data was observed in all adolescents (Table 5). Although normal values of circulating biomarkers were found in our population sample, we observed significantly reduced serum levels of triglycerides (TG), total cholesterol, and low-density lipoprotein

TABLE 4: Energy and nutrient intakes from 24-hour recall in adolescents stratified with respect to the total polyphenol intake.

	Total polyphenol intake			<i>p</i> value
	Low	Moderate	High	
Primary energy sources				
Total energy (kcal)	1656.10 ± 426.74	1713.22 ± 517.21	1567.47 ± 408.86	* 0.92 ¥ 0.82 § 0.59
Total energy (kJ)	6929.144 ± 1785.48	7168.12 ± 2164.01	6558.31 ± 1710.67	* 0.92 ¥ 0.82 § 0.59
Total fat (g)	79.80 ± 20.78	77.49 ± 26.05	71.33 ± 33.74	* 0.96 ¥ 0.61 § 0.77
Total carbohydrate (g)	162.46 ± 81.63	180.12 ± 76.34	146.68 ± 49.93	* 0.73 ¥ 0.77 § 0.33
Total protein (g)	65.01 ± 20.66	71.36 ± 28.08	77.19 ± 21.75	* 1 ¥ 0.44 § 0.45
Animal protein (g)	37.63 ± 23.88	39.78 ± 23.52	49.60 ± 30.68	* 0.97 ¥ 0.35 § 0.50
Vegetable protein (g)	22.03 ± 10.04	23.66 ± 11.35	20.41 ± 8.10	* 0.87 ¥ 0.87 § 0.58
Fats				
SFA (g)	22.60 ± 11.33	20.03 ± 8.71	17.46 ± 10.90	* 0.73 ¥ 0.29 § 0.73
MUFA (g)	39.32 ± 14.09	40.48 ± 14.10	34.99 ± 20.80	* 0.95 ¥ 0.70 § 0.60
PUFA (g)	6.90 ± 2.56	8.20 ± 2.91	9.42 ± 6.27	* 0.62 ¥ 0.17 § 0.66
Vegetable fats (g)	46.95 ± 9.81	47.37 ± 18.85	41.24 ± 16.76	* 0.99 ¥ 0.51 § 0.47
Animal fats (g)	24.84 ± 22.19	21.91 ± 14.76	29.59 ± 30.18	* 0.92 ¥ 0.81 § 0.58
Omega-3 fatty acids (g)	0.84 ± 0.30	1.05 ± 0.55	1.57 ± 1.21	* 0.75 ¥ 0.02 § 0.12
Omega-6 fatty acids (g)	6.16 ± 2.10	6.45 ± 2.46	7.39 ± 5.42	* 0.97 ¥ 0.57 § 0.72
EPA (g)	0.05 ± 0.11	0.10 ± 0.20	0.16 ± 0.26	* 0.78 ¥ 0.23 § 0.58
DHA (g)	0.08 ± 0.18	0.13 ± 0.28	0.44 ± 0.94	* 0.96 ¥ 0.15 § 0.26
PUFA : SFA ratio	0.23 ± 0.21	0.22 ± 0.10	0.34 ± 0.24	* 0.99 ¥ 0.20 § 0.18
Cholesterol (mg)	182.10 ± 122.05	182.33 ± 119.99	249.63 ± 199.50	* 1 ¥ 0.36 § 0.38
Carbohydrates				
Starch (g)	96.80 ± 53.65	110.69 ± 62.37	79.80 ± 42.41	* 0.71 ¥ 0.59 § 0.19
Soluble sugars (g)	48.43 ± 36.01	51.71 ± 23.75	60.48 ± 20.79	* 0.93 ¥ 0.38 § 0.60
Glycemic index	60.50 ± 19.55	63.51 ± 18.10	53.70 ± 7.96	* 0.84 ¥ 0.40 § 0.16
Glycemic load	88.50 ± 66.71	93.57 ± 60.09	65.17 ± 27.00	* 0.96 ¥ 0.38 § 0.25
Fibers				
Total dietary fiber	12.95 ± 4.46	15.19 ± 6.51	15.21 ± 4.93	* 0.42 ¥ 0.40 § 1
Soluble dietary fiber	1.70 ± 1.14	2.47 ± 1.38	2.91 ± 1.50	* 0.20 ¥ 0.02 § 0.59
Insoluble dietary fiber	4.54 ± 2.46	7.75 ± 3.80	8.18 ± 4.15	* 0.02 ¥ 0.007 § 0.93
Vitamins				
Vitamin A eq. retinol (µg)	974.91 ± 717.13	1044.16 ± 624.45	1274.02 ± 686.88	* 0.95 ¥ 0.38 § 0.56
Vitamin B1 (mg)	1.15 ± 1.67	0.76 ± 0.29	0.87 ± 0.31	* 0.47 ¥ 0.66 § 0.95
Vitamin B2 (mg)	1.03 ± 0.47	1.17 ± 0.43	1.25 ± 0.55	* 0.67 ¥ 0.38 § 0.88
Vitamin B3 (mg)	15.79 ± 7.92	14.81 ± 7.73	17.65 ± 8.00	* 0.92 ¥ 0.75 § 0.52
Vitamin B5 (mg)	1.88 ± 1.49	2.43 ± 1.87	3.26 ± 1.70	* 0.59 ¥ 0.04 § 0.30
Vitamin B6 (mg)	1.45 ± 0.62	1.61 ± 0.60	2.06 ± 0.55	* 0.69 ¥ 0.008 § 0.06
Vitamin B8 (µg)	8.13 ± 5.93	12.34 ± 9.60	18.27 ± 13.97	* 0.43 ¥ 0.01 § 0.20
Folic acid (µg)	228.15 ± 100.30	250.29 ± 114.85	222.56 ± 91.12	* 0.79 ¥ 0.98 § 0.69
Vitamin B12 (µg)	1.98 ± 1.69	3.48 ± 3.13	4.41 ± 2.30	* 0.16 ¥ 0.01 § 0.48
Vitamin C (mg)	124.66 ± 176.75	98.81 ± 48.80	132.91 ± 83.16	* 0.78 ¥ 0.97 § 0.64
Vitamin K (µg)	1.33 ± 2.49	2.69 ± 4.26	6.11 ± 8.82	* 0.76 ¥ 0.04 § 0.19
Vitamin D (µg)	1.42 ± 1.80	1.66 ± 1.72	3.24 ± 4.91	* 0.97 ¥ 0.21 § 0.30
Vitamin E (mg)	12.67 ± 1.95	13.29 ± 4.34	13.16 ± 3.67	* 0.87 ¥ 0.87 § 0.58

TABLE 4: Continued.

Total ORAC ($\mu\text{mol TE}$)	3844.89 \pm 2347.86	4908.39 \pm 2772.36	7862.79 \pm 7217.15	* 0.77 ¥ 0.03 § 0.14
Minerals				
Calcium (mg)	412.11 \pm 196.85	560.11 \pm 257.10	630.17 \pm 296.5	* 0.87 ¥ 0.87 § 0.58
Phosphorus (mg)	738.68 \pm 341.02	948.54 \pm 397.10	1014.03 \pm 296.91	* 0.17 ¥ 0.04 § 0.83
Iodium (μg)	69.80 \pm 142.01	69.22 \pm 81.78	95.53 \pm 76.28	* 0.99 ¥ 0.73 § 0.73
Sodium (mg)	1356.37 \pm 1161.84	1000.35 \pm 859.83	1180.03 \pm 1087.92	* 0.56 ¥ 0.82 § 0.86
Iron (mg)	7.32 \pm 2.10	7.92 \pm 2.85	8.95 \pm 3.36	* 0.80 ¥ 0.19 § 0.51
Magnesium (mg)	134.95 \pm 81.02	226.42 \pm 155.94	223.36 \pm 71.31	* 0.04 ¥ 0.04 § 0.99
Selenium (μg)	16.09 \pm 12.34	37.98 \pm 44.53	67.91 \pm 60.71	* 0.31 ¥ 0.002 § 0.11
Potassium (mg)	2086.14 \pm 717.62	2609.25 \pm 939.23	2743.79 \pm 460.26	* 0.08 ¥ 0.02 § 0.84
Zinc (mg)	8.39 \pm 5.22	8.13 \pm 3.03	9.81 \pm 4.23	* 0.98 ¥ 0.56 § 0.46
Copper (mg)	0.61 \pm 0.39	0.86 \pm 0.57	1.19 \pm 0.90	* 0.49 ¥ 0.02 § 0.27
Water (g)	722.58 \pm 348.85	783.53 \pm 230.44	1096.57 \pm 522.33	* 0.88 ¥ 0.01 § 0.05

SFA: saturated fatty acid; MUFA: monounsaturated fatty acid; PUFA: polyunsaturated fatty acid; EPA: eicosapentaenoic acid; DHA: docosahexaenoic acid; ORAC: Oxygen Radical Absorbance Capacity; eq.: equivalent. *: low vs. moderate; ¥: low vs high; §: moderate vs. high. Statistical differences were evaluated by a one-way ANOVA test. In bold are reported statistically significant values.

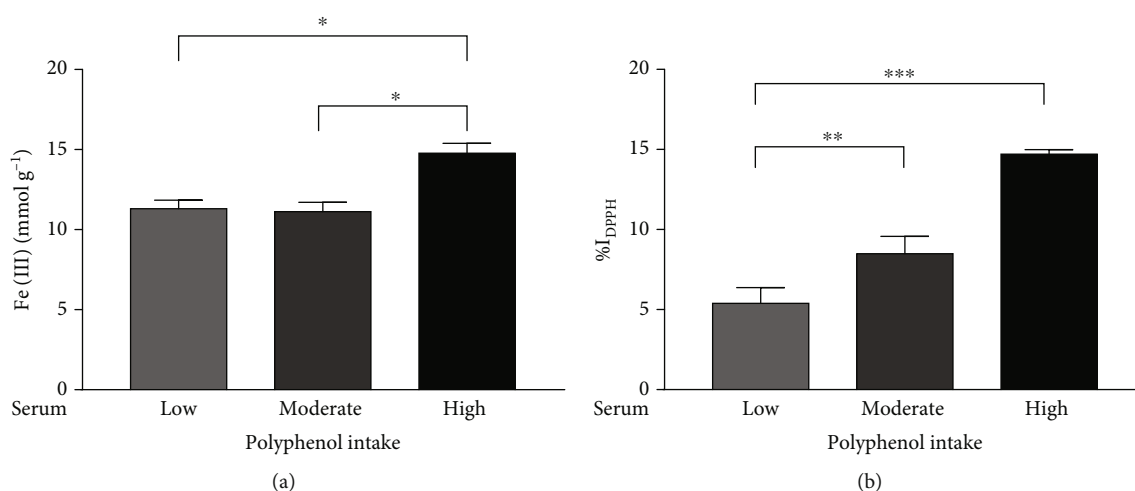


FIGURE 1: Antioxidant capacity assessed by ferric reducing ability (FRAP) assay (a) and percentage of inhibition against DPPH (b) in the pool of serum from adolescents with low, moderate, and high polyphenol intake (low, moderate, and high). The bar graphs showed the mean \pm SEM of 3 independent experiments. * $p < 0.05$, ** $p < 0.005$, and *** $p < 0.001$.

(LDL) along with ESR values in adolescents who declared high consumption of polyphenols.

3.6. Effects of Serum from Adolescents with Different Estimated Polyphenol Intake against Oleic Acid-Induced Lipid Accumulation in Human HepG2 Liver Cells. In order to investigate the properties of the serum from adolescents with different polyphenols' consumption in the prevention of the liver damage, we used human hepatocyte-derived cell line HepG2 exposed to oleic acid (OA), as the main alternative in vitro model for studying lipid accumulation. First, in order to evaluate the effects of OA on HepG2 cell viability, MTT assay was performed. We observed that OA at 0.1 mM did not display any cell toxicity (data not shown). Thus, we pretreated the cells with 10% of pooled serum from all adolescents as control and

pooled serum from adolescents with low, moderate, and high polyphenol intake, and we induced lipid accumulation with OA 0.1 mM for 24 hours (Figure 2(a)). Interestingly, serum from high polyphenol consumers reduced lipid accumulation compared to adolescents with low or moderate polyphenol intakes, as revealed by the quantification of intracellular lipid content, addressing the role of polyphenol-rich diet in the prevention of lipid accumulation (Figure 2(b)).

4. Discussion

In this study, we evidenced that serum from adolescents who declared a high intake of polyphenols displays antioxidant properties and protects against in vitro hepatic lipid accumulation, supporting the idea that a polyphenol-rich diet

TABLE 5: Serum biomarkers in adolescents stratified with respect to the estimated total polyphenol intake.

Serum biomarkers	Total polyphenol intake			<i>p</i> value
	Low	Moderate	High	
Glucose (mg/dL)	80.79 ± 8.30	78.22 ± 7.53	78.21 ± 5.53	* 0.53 ¥ 0.51 § 1
Insulin (mU/L)	10.38 ± 6.68	10.50 ± 6.85	8.73 ± 6.26	* 1 ¥ 0.69 § 0.67
HOMA-IR	2.09 ± 1.16	2.04 ± 1.36	1.69 ± 1.23	* 0.99 ¥ 0.60 § 0.68
TG (mg/dL)	112.05 ± 109.72	67.33 ± 31.91	55.63 ± 15.28	* 0.11 ¥ 0.03 § 0.86
Total cholesterol (mg/dL)	163.21 ± 37.06	154.11 ± 27.44	140.26 ± 20.56	* 0.61 ¥ 0.05 § 0.33
LDL (mg/dL)	93.26 ± 27.54	91.89 ± 22.76	74.95 ± 17.06	* 0.98 ¥ 0.04 § 0.07
HDL (mg/dL)	47.47 ± 10.13	48.89 ± 12.90	54.26 ± 10.66	* 0.92 ¥ 0.16 § 0.32
Creatinine (mg/dL)	0.92 ± 0.11	0.87 ± 0.12	0.87 ± 0.12	* 0.45 ¥ 0.42 § 1
Urea nitrogen (mg/dL)	28.74 ± 5.69	28.28 ± 6.05	31.53 ± 6.68	* 0.97 ¥ 0.35 § 0.25
Uric acid (mg/dL)	4.90 ± 1.16	4.88 ± 1.80	5.08 ± 1.56	* 1 ¥ 0.93 § 0.91
Total bilirubin (mg/dL)	0.99 ± 0.62	0.88 ± 0.37	1.21 ± 0.75	* 0.85 ¥ 0.49 § 0.22
Direct bilirubin (mg/dL)	0.27 ± 0.09	0.24 ± 0.07	0.29 ± 0.11	* 0.64 ¥ 0.75 § 0.25
ESR (mm/h)	18.74 ± 7.06	24.72 ± 16.22	13.58 ± 7.95	* 0.24 ¥ 0.33 § 0.01
CRP (mg/L)	1.27 ± 0.81	1.23 ± 0.64	1.12 ± 0.53	* 0.98 ¥ 0.77 § 0.87

HOMA-IR: Homeostasis model assessment for estimating insulin resistance; TG: triglyceride; LDL: low-density lipoprotein; HDL: high-density lipoprotein; ESR: erythrocyte sedimentation rate; CRP: serum C-reactive protein. *: low vs. moderate; ¥: low vs. high; §: moderate vs. high. Statistical differences were evaluated by a one-way ANOVA test. In bold are reported statistically significant values.

may have an important role in the prevention of metabolic and chronic diseases. Firstly, fruits and vegetables reported in 24-hour dietary recalls and the Phenol-Explorer database were matched, and the estimated total polyphenol intake in our population was calculated. Among adolescents enrolled in our study, the estimated intake of polyphenols was a mean of 434.46 mg/day, consisting of 49% of flavonoids, 39% of phenolic acids, and 13% of other polyphenols. These results are in agreement with the data described in the HELENA study investigating the dietary intake of polyphenols in European adolescents [53]. Analyzing the relationship between the estimated total polyphenol intake and the general characteristics of our population, we did not find any significant correlation between the consumption of polyphenols and sex, physical activity, or BMI. Interestingly, we evidenced a significant linear positive association between total polyphenol intake and the adherence to the MD. In particular, stratifying the adolescents into three groups based on their polyphenol intake (low, moderate, and high), KIDMED score revealed an optimal adherence to the MD (8.21 ± 1.84) in high polyphenols' consumers, suggesting that the health benefits of the MD could be related to the high intake of fruits and vegetables. Other authors have reported a linear correlation between MD and the intake of polyphenols [42, 50]. Nowadays, the MD is considered one of the healthiest eating patterns, due to high consumption of fruits and vegetables, which represent the main food sources of polyphenols, along with a high intake of legumes, nuts and whole grains, low-fat dairy, a moderate intake of fish, and reduced consumption of meat [54], thus providing a balanced intake of macro- and micronutrients. Analyzing the dietary intake assessment by 24-hour recall interview,

the primary energy sources in foods did not reflect the optimal proportions of daily intakes even though total energy intake is in the range of the suggested dietary intake allowances in our population according to the total polyphenol intake, suggesting a same quantitative dietary pattern among adolescents. However, in spite of the unchanged total energy intakes, we found qualitative differences in several nutrients among the three groups, which levels are in the average of the recommended allowances. In particular, the intakes of soluble and insoluble fibers and omega-3 fatty acids along with several vitamins and minerals significantly increased in high compared to low polyphenols' consumers, showing a good eating behavior and a better compliance with the MD pyramid recommendations. It is worth noting that in our adolescents, the primary energy sources in foods did not reflect the optimal proportions of daily intakes. The MD emphasizes eating foods like vegetables and fruits because of their elevated micronutrient content, in terms of vitamins, minerals, and phytochemicals, which are able to elicit different beneficial effects, including antioxidant properties. In our population, total antioxidant capacity from the diet evaluated by ORAC values resulted increased in adolescents who consume high amounts of polyphenols. These data correlated with the antioxidant power of the serum samples of our adolescents, measured by conventional total antioxidant assay methods. Those methods, based on the radical scavenging activity and redox potential of antioxidants, displayed in high polyphenol intake group an overall serum antioxidant capacity and predicted the body's antioxidant status. Another favorable effect of polyphenols is related to their ability in ameliorating lipid/lipoprotein metabolism and alleviating hyperlipidemia [55].

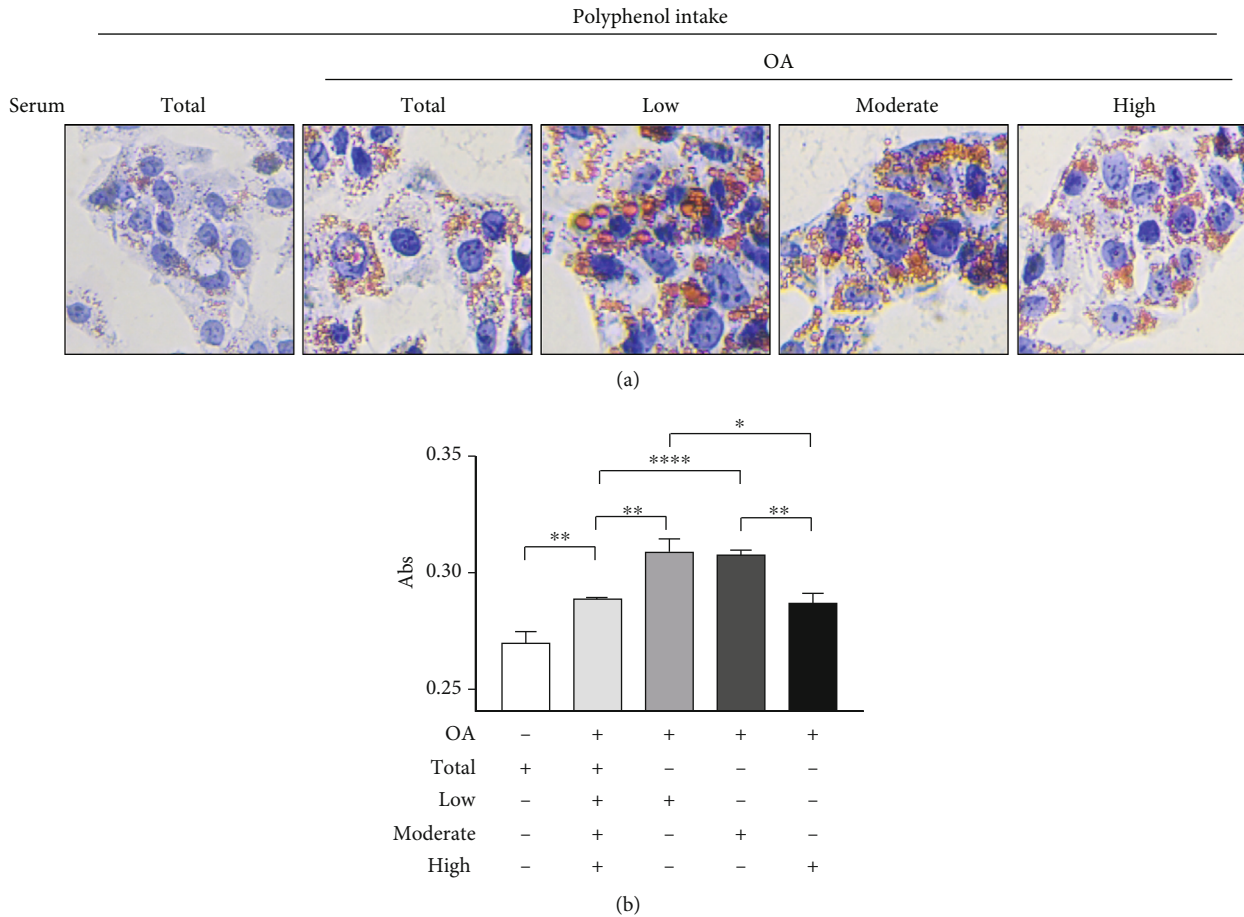


FIGURE 2: Lipid accumulation in human HepG2 liver cells treated with oleic acid in the presence of serum from adolescents. (a) HepG2 cells were pretreated with the pool of serum from all adolescents (total) or with the pool of serum from low, moderate, and high polyphenols' consumers (10% v/v), followed by the treatment with oleic acid (OA) 0.1 mM for 24 hours. Lipid accumulation was observed by Oil Red O staining. (b) HepG2 cells were treated with isopropanol, and the quantification of intracellular lipid accumulation was measured at 510 nm. The bar graphs showed the mean \pm SEM of 3 independent experiments, each performed in triplicate. * $p < 0.05$, ** $p < 0.005$, and **** $p < 0.0001$.

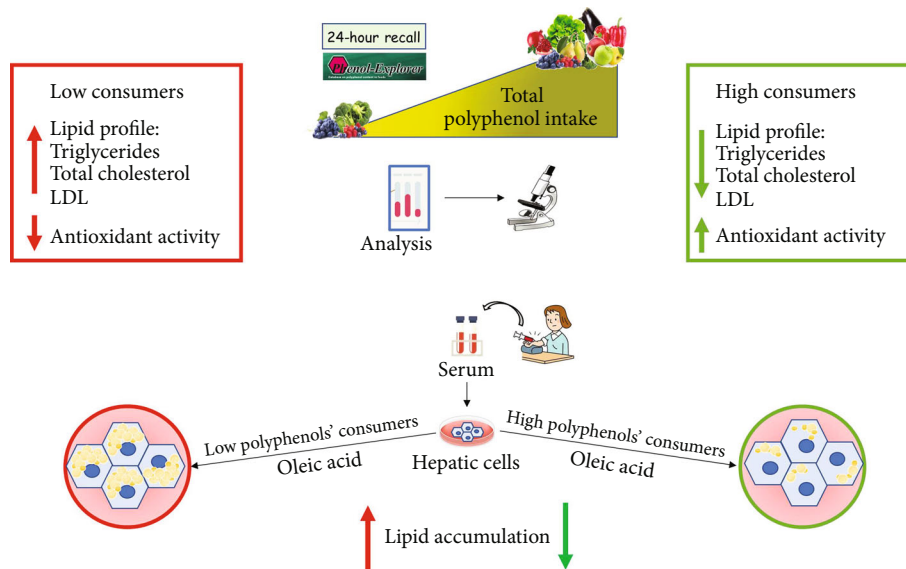


FIGURE 3: Graphical representation of the main results of our study.

However, although the common consumption of polyphenol-rich diet would maintain or improve the lipid profile of healthy participants [56–59], further studies are needed to clarify the preventive actions of these phytochemicals in healthy individuals. In addition, a crucial aspect that has to be investigated is to distinguish the specific effects of polyphenols versus those of many prohealth components (e.g., vitamins, fibers, and minerals) present in fruits and vegetables. Although we failed to observe a significant association between total polyphenol intake and serum biomarkers in all adolescents, maybe due to the small sample investigated, our data revealed a better lipid profile, in terms of reduced serum concentration of TG, total cholesterol, and LDL in healthy adolescents with high polyphenol intake. An imbalance between lipid acquisition and lipid disposal leads to a hepatic fat accumulation, which is of pivotal importance in the development of NAFLD, and it is also a risk factor for many other chronic metabolic diseases. Using an in vitro model of lipid accumulation represented by the OA-induced human HepG2 liver cells, we showed that intracellular lipid accumulation is alleviated by serum from adolescents consuming a polyphenol-rich diet and following MD recommendations. Although we cannot unravel whether polyphenol intake caused the lipid biomarkers or whether the lipid biomarkers led to changes in the diet in our study, we may speculate the benefits of healthy eating pattern in the complex pathology of NAFLD. Collectively, our findings are graphically reported in Figure 3.

This study includes some limitations, such as the relatively small sample size, particularly when the total sample was divided into the three groups, as well as the lack of direct methods to measure polyphenol serum levels. However, data from clinical setting together with experimental cell model strengthen the importance of improving healthy dietary habits in adolescents in an attempt to achieve clinical health outcomes.

5. Conclusions

Although further studies and deeper knowledge about polyphenol intakes and several prohealth components from the MD pattern might be helpful for planning targeted prevention strategies at an early age, we support and encourage the Mediterranean eating style for the prevalent fruit and vegetable consumption which should represent a protective choice against the development of NCDs, including NAFLD.

Data Availability

The data used to support the findings of this study are available from the corresponding author upon request.

Conflicts of Interest

The authors declare that there is no conflict of interest regarding the publication of this paper.

Acknowledgments

This work was supported by the EU Regional Operational Program Calabria, Italy (POR Calabria FESR-FSE 2014-

2020) DIMENU (prot. #52243/2017); by the Department of Excellence (Italian Law. 232/2016), the Department of Pharmacy, and the Health and Nutritional Sciences, University of Calabria, Italy; and by the Piano Triennale 2021-2023 University of Naples “Parthenope” - CUP 169I21000010006. We sincerely thank all participants enrolled from High School Istituto Istruzione Superiore-Valentini-Majorana, Castrolibero (CS, Italy). We are also thankful to all partners of the DIMENU project.

References










- [1] G. Grosso, F. Bella, J. Godos et al., “Possible role of diet in cancer: systematic review and multiple meta-analyses of dietary patterns, lifestyle factors, and cancer risk,” *Nutrition Reviews*, vol. 75, no. 6, pp. 405–419, 2017.
- [2] R. Meccariello and S. D’Angelo, “Impact of polyphenolic-food on longevity: an elixir of life. An overview,” *Antioxidants*, vol. 10, no. 4, p. 507, 2021.
- [3] C. Schwedhelm, H. Boeing, G. Hoffmann, K. Aleksandrova, and L. Schwingshackl, “Effect of diet on mortality and cancer recurrence among cancer survivors: a systematic review and meta-analysis of cohort studies,” *Nutrition Reviews*, vol. 74, no. 12, pp. 737–748, 2016.
- [4] C. G. Fraga, K. D. Croft, D. O. Kennedy, and F. A. Tomas-Barberan, “The effects of polyphenols and other bioactives on human health,” *Food & Function*, vol. 10, no. 2, pp. 514–528, 2019.
- [5] E. Cieřlik, A. Gręda, and W. Adamus, “Contents of polyphenols in fruit and vegetables,” *Food Chemistry*, vol. 94, no. 1, pp. 135–142, 2006.
- [6] A. Scalbert, C. Manach, C. Morand, C. Remesy, and L. Jimenez, “Dietary polyphenols and the prevention of diseases,” *Critical Reviews in Food Science and Nutrition*, vol. 45, no. 4, pp. 287–306, 2005.
- [7] K. B. Pandey and S. I. Rizvi, “Plant polyphenols as dietary antioxidants in human health and disease,” *Oxidative Medicine and Cellular Longevity*, vol. 2, no. 5, Article ID 897484, pp. 270–278, 2009.
- [8] D. Del Rio, A. Rodriguez-Mateos, J. P. Spencer, M. Tognolini, G. Borges, and A. Crozier, “Dietary (poly)phenolics in human health: structures, bioavailability, and evidence of protective effects against chronic diseases,” *Antioxidants & Redox Signaling*, vol. 18, no. 14, pp. 1818–1892, 2013.
- [9] R. Tsao, “Chemistry and biochemistry of dietary polyphenols,” *Nutrients*, vol. 2, no. 12, pp. 1231–1246, 2010.
- [10] C. Manach, A. Scalbert, C. Morand, C. Remesy, and L. Jimenez, “Polyphenols: food sources and bioavailability,” *The American Journal of Clinical Nutrition*, vol. 79, no. 5, pp. 727–747, 2004.
- [11] J. Perez-Jimenez, V. Neveu, F. Vos, and A. Scalbert, “Identification of the 100 richest dietary sources of polyphenols: an application of the phenol-explorer database,” *European Journal of Clinical Nutrition*, vol. 64, no. S3, pp. S112–S120, 2010.
- [12] M. Guasch-Ferre, J. Merino, Q. Sun, M. Fito, and J. Salas-Salvado, “Dietary polyphenols, Mediterranean diet, prediabetes, and type 2 diabetes: a narrative review of the evidence,” *Oxidative Medicine and Cellular Longevity*, vol. 2017, Article ID 6723931, 16 pages, 2017.

- [13] G. Grosso, U. Stepaniak, R. Topor-Madry, K. Szafraniec, and A. Pajak, "Estimated dietary intake and major food sources of polyphenols in the Polish arm of the HAPIEE study," *Nutrition*, vol. 30, no. 11-12, pp. 1398–1403, 2014.
- [14] C. Manach, G. Williamson, C. Morand, A. Scalbert, and C. Remesy, "Bioavailability and bioefficacy of polyphenols in humans. I. Review of 97 bioavailability studies," *The American Journal of Clinical Nutrition*, vol. 81, no. 1, pp. 230S–242S, 2005.
- [15] H. Cory, S. Passarelli, J. Szeto, M. Tamez, and J. Mattei, "The role of polyphenols in human health and food systems: a mini-review," *Frontiers in Nutrition*, vol. 5, p. 87, 2018.
- [16] S. Wang, N. Moustaid-Moussa, L. Chen et al., "Novel insights of dietary polyphenols and obesity," *The Journal of Nutritional Biochemistry*, vol. 25, no. 1, pp. 1–18, 2014.
- [17] M. Bose, J. D. Lambert, J. Ju, K. R. Reuhl, S. A. Shapses, and C. S. Yang, "The major green tea polyphenol, (-)-epigallocatechin-3-gallate, inhibits obesity, metabolic syndrome, and fatty liver disease in high-fat-fed mice," *The Journal of Nutrition*, vol. 138, no. 9, pp. 1677–1683, 2008.
- [18] G. Chiva-Blanch and L. Badimon, "Effects of polyphenol intake on metabolic syndrome: current evidences from human trials," *Oxidative Medicine and Cellular Longevity*, vol. 2017, Article ID 5812401, 18 pages, 2017.
- [19] P. Angulo, "Nonalcoholic fatty liver disease," *The New England Journal of Medicine*, vol. 346, no. 16, pp. 1221–1231, 2002.
- [20] A. Kotronen and H. Yki-Jarvinen, "Fatty liver," *Arteriosclerosis, Thrombosis, and Vascular Biology*, vol. 28, no. 1, pp. 27–38, 2008.
- [21] W. Cui, S. L. Chen, and K. Q. Hu, "Quantification and mechanisms of oleic acid-induced steatosis in HepG2 cells," *American Journal of Translational Research*, vol. 2, no. 1, pp. 95–104, 2010.
- [22] E. Buzzetti, M. Pinzani, and E. A. Tsochatzis, "The multiple-hit pathogenesis of non-alcoholic fatty liver disease (NAFLD)," *Metabolism*, vol. 65, no. 8, pp. 1038–1048, 2016.
- [23] "EASL-EASD-EASO clinical practice guidelines for the management of non-alcoholic fatty liver disease," *Journal of Hepatology*, vol. 64, no. 6, pp. 1388–1402, 2016.
- [24] G. Augimeri and D. Bonofiglio, "The Mediterranean diet as a source of natural compounds: does it represent a protective choice against cancer?," *Pharmaceuticals (Basel)*, vol. 14, no. 9, p. 920, 2021.
- [25] G. Augimeri, F. I. Montalto, C. Giordano et al., "Nutraceuticals in the Mediterranean diet: potential avenues for breast cancer treatment," *Nutrients*, vol. 13, no. 8, p. 2557, 2021.
- [26] M. Korre, M. A. Tsoukas, E. Frantzeskou, J. Yang, and S. N. Kales, "Mediterranean diet and workplace health promotion," *Current Cardiovascular Risk Reports*, vol. 8, no. 12, p. 416, 2014.
- [27] F. Sofi, F. Cesari, R. Abbate, G. F. Gensini, and A. Casini, "Adherence to Mediterranean diet and health status: meta-analysis," *BMJ*, vol. 337, no. sep11 2, article a1344, 2008.
- [28] C. Anania, F. M. Perla, F. Olivero, L. Pacifico, and C. Chiesa, "Mediterranean diet and nonalcoholic fatty liver disease," *World Journal of Gastroenterology*, vol. 24, no. 19, pp. 2083–2094, 2018.
- [29] I. Rodriguez-Ramiro, D. Vauzour, and A. M. Miniñane, "Polyphenols and non-alcoholic fatty liver disease: impact and mechanisms," *The Proceedings of the Nutrition Society*, vol. 75, no. 1, pp. 47–60, 2016.
- [30] M. Boccellino and S. D'Angelo, "Anti-obesity effects of polyphenol intake: current status and future possibilities," *International Journal of Molecular Sciences*, vol. 21, no. 16, p. 5642, 2020.
- [31] S. D'Angelo, "Current evidence on the effect of dietary polyphenols intake on brain health," *Current Nutrition & Food Science*, vol. 16, no. 8, pp. 1170–1182, 2020.
- [32] G. Williamson and B. Holst, "Dietary reference intake (DRI) value for dietary polyphenols: are we heading in the right direction?," *The British Journal of Nutrition*, vol. 99, Suppl 3, pp. S55–S58, 2008.
- [33] J. Perez-Jimenez, L. Fezeu, M. Touvier et al., "Dietary intake of 337 polyphenols in French adults," *The American Journal of Clinical Nutrition*, vol. 93, no. 6, pp. 1220–1228, 2011.
- [34] A. Tresserra-Rimbau, A. Medina-Remón, J. Pérez-Jiménez et al., "Dietary intake and major food sources of polyphenols in a Spanish population at high cardiovascular risk: the PRE-DIMED study," *Nutrition, Metabolism, and Cardiovascular Diseases*, vol. 23, no. 10, pp. 953–959, 2013.
- [35] G. Augimeri, A. Galluccio, G. Caparello et al., "Potential antioxidant and anti-inflammatory properties of serum from healthy adolescents with optimal Mediterranean diet adherence: findings from DIMENU cross-sectional study," *Antioxidants (Basel)*, vol. 10, no. 8, 2021.
- [36] A. Galluccio, G. Caparello, E. Avolio et al., "Self-perceived physical activity and adherence to the Mediterranean diet in healthy adolescents during COVID-19: findings from the DIMENU pilot study," *Healthcare*, vol. 9, no. 6, p. 622, 2021.
- [37] C. Morelli, E. Avolio, A. Galluccio et al., "Nutrition education program and physical activity improve the adherence to the Mediterranean diet: impact on inflammatory biomarker levels in healthy adolescents from the DIMENU longitudinal study," *Frontiers in Nutrition*, vol. 8, article 685247, 2021.
- [38] C. Morelli, E. Avolio, A. Galluccio et al., "Impact of vigorous-intensity physical activity on body composition parameters, lipid profile markers, and irisin levels in adolescents: a cross-sectional study," *Nutrients*, vol. 12, no. 3, p. 742, 2020.
- [39] WHO, "Physical status : the use of and interpretation of anthropometry , report of a WHO expert committee," World Health Organization, 1995.
- [40] WHO, "Global Recommendations on Physical Activity for Health," World Health Organization, Geneva, 2010.
- [41] S. García Cabrera, N. Herrera Fernandez, C. Rodríguez Hernandez, M. Nissensohn, B. Roman-Vinas, and L. Serra-Majem, "Kidmed test; prevalence of low adherence to the Mediterranean diet in children and young: a systematic review," *Nutrición Hospitalaria*, vol. 32, no. 6, pp. 2390–2399, 2015.
- [42] A. Kapolou, H. C. Karantonis, N. Rigopoulos, and A. E. Koutedidakis, "Association of mean daily polyphenols intake with Mediterranean diet adherence and anthropometric indices in healthy Greek adults: a retrospective study," *Applied Sciences*, vol. 11, no. 10, p. 4664, 2021.
- [43] V. Neveu, J. Perez-Jimenez, F. Vos et al., "Phenol-explorer: an online comprehensive database on polyphenol contents in foods," *Database*, vol. 2010, p. pap024, 2010.
- [44] J. A. Rothwell, J. Perez-Jimenez, V. Neveu et al., "Phenol-Explorer 3.0: a major update of the Phenol-Explorer database to incorporate data on the effects of food processing on polyphenol content," *Database*, vol. 2013, p. bat070, 2013.

- [45] S. Castro-Barquero, A. Tresserra-Rimbau, F. Vitelli-Storelli et al., "Dietary polyphenol intake is associated with HDL-cholesterol and a better profile of other components of the metabolic syndrome: a PREDIMED-plus sub-study," *Nutrients*, vol. 12, no. 3, p. 689, 2020.
- [46] P. Stratil, B. Klejdus, and V. Kuban, "Determination of total content of phenolic compounds and their antioxidant activity in vegetables—evaluation of spectrophotometric methods," *Journal of Agricultural and Food Chemistry*, vol. 54, no. 3, pp. 607–616, 2006.
- [47] I. F. Benzie and J. J. Strain, "The ferric reducing ability of plasma (FRAP) as a measure of "antioxidant power": the FRAP assay," *Analytical Biochemistry*, vol. 239, no. 1, pp. 70–76, 1996.
- [48] M. S. Blois, "Antioxidant determinations by the use of a stable free radical," *Nature*, vol. 181, no. 4617, pp. 1199–1200, 1958.
- [49] D. Rovito, G. Gionfriddo, I. Barone et al., "Ligand-activated PPAR γ downregulates CXCR4 gene expression through a novel identified PPAR response element and inhibits breast cancer progression," *Oncotarget*, vol. 7, no. 40, pp. 65109–65124, 2016.
- [50] J. Godos, G. Rapisarda, S. Marventano, F. Galvano, A. Mistretta, and G. Grosso, "Association between polyphenol intake and adherence to the Mediterranean diet in Sicily, southern Italy," *NFS Journal*, vol. 8, pp. 1–7, 2017.
- [51] L. Hooper, P. A. Kroon, E. B. Rimm et al., "Flavonoids, flavonoid-rich foods, and cardiovascular risk: a meta-analysis of randomized controlled trials," *The American Journal of Clinical Nutrition*, vol. 88, no. 1, pp. 38–50, 2008.
- [52] Y. J. Liu, J. Zhan, X. L. Liu, Y. Wang, J. Ji, and Q. Q. He, "Dietary flavonoids intake and risk of type 2 diabetes: a meta-analysis of prospective cohort studies," *Clinical Nutrition*, vol. 33, no. 1, pp. 59–63, 2014.
- [53] R. W. Wisnuwardani, S. De Henauw, O. Androustos et al., "Estimated dietary intake of polyphenols in European adolescents: the HELENA study," *European Journal of Nutrition*, vol. 58, no. 6, pp. 2345–2363, 2019.
- [54] C. Davis, J. Bryan, J. Hodgson, and K. Murphy, "Definition of the Mediterranean diet; a literature review," *Nutrients*, vol. 7, no. 11, pp. 9139–9153, 2015.
- [55] F. Feldman, M. Koudoufio, Y. Desjardins, S. Spahis, E. Delvin, and E. Levy, "Efficacy of polyphenols in the Management of dyslipidemia: a focus on clinical studies," *Nutrients*, vol. 13, no. 2, p. 672, 2021.
- [56] S. Bo, G. Ciccone, A. Castiglione et al., "Anti-inflammatory and antioxidant effects of resveratrol in healthy smokers a randomized, double-blind, placebo-controlled, cross-over trial," *Current Medicinal Chemistry*, vol. 20, no. 10, pp. 1323–1331, 2013.
- [57] P. Castilla, R. Echarri, A. Davalos et al., "Concentrated red grape juice exerts antioxidant, hypolipidemic, and antiinflammatory effects in both hemodialysis patients and healthy subjects," *The American Journal of Clinical Nutrition*, vol. 84, no. 1, pp. 252–262, 2006.
- [58] S. Martinez-Lopez, B. Sarria, J. L. Sierra-Cinos, L. Goya, R. Mateos, and L. Bravo, "Realistic intake of a flavanol-rich soluble cocoa product increases HDL-cholesterol without inducing anthropometric changes in healthy and moderately hypercholesterolemic subjects," *Food & Function*, vol. 5, no. 2, p. 364, 2014.
- [59] C. Tsang, N. F. Smail, S. Almoosawi, G. J. M. McDougall, and E. A. S. Al-Dujaili, "Antioxidant rich potato improves arterial stiffness in healthy adults," *Plant Foods for Human Nutrition*, vol. 73, no. 3, pp. 203–208, 2018.

Research Article

Protective Effect of Dietary Polysaccharides from Yellow Passion Fruit Peel on DSS-Induced Colitis in Mice

Laryssa Regis Bueno ^{1,2}, Bruna da Silva Soley ^{1,2}, Kahlile Youssef Abboud ³,
Isabella Wzorek França ^{1,2}, Karien Sauruk da Silva ^{1,2},
Natalia Mulinari Turin de Oliveira ^{1,2}, Juliana Santos Barros,⁴
Marcelo Biondaro Gois ^{4,5}, Lucimara Mach Côrtes Cordeiro ³,
and Daniele Maria-Ferreira ^{1,2}

¹Instituto de Pesquisa Pelé Pequeno Príncipe, Curitiba, 80250-060 PR, Brazil

²Faculdades Pequeno Príncipe, Programa de Pós-graduação em Biotecnologia Aplicada à Saúde da Criança e do Adolescente, Curitiba, 80230-020 PR, Brazil

³Department of Biochemistry and Molecular Biology, Federal University of Paraná, Curitiba, Paraná, Brazil

⁴Instituto de Ciências da Saúde, Universidade Federal da Bahia and Centro de Ciências da Saúde, Universidade Federal do Recôncavo da Bahia, Santo Antônio de Jesus, BA, Brazil

⁵Faculdade de Ciências da Saúde, Universidade Federal de Rondonópolis, Rondonópolis, MT, Brazil

Correspondence should be addressed to Daniele Maria-Ferreira; daniele.ferreira@pelepequenoprincipe.org.br

Received 11 April 2022; Revised 17 August 2022; Accepted 27 September 2022; Published 15 October 2022

Academic Editor: Anderson J. Teodoro

Copyright © 2022 Laryssa Regis Bueno et al. This is an open access article distributed under the Creative Commons Attribution License, which permits unrestricted use, distribution, and reproduction in any medium, provided the original work is properly cited.

Inflammatory bowel disease (IBD) is a complex inflammatory disorder characterized by chronic and spontaneously relapsing inflammation of the gastrointestinal tract. IBD includes two idiopathic disorders: Crohn's disease (CD) and ulcerative colitis (UC). In particular, UC causes inflammation and ulceration of the colon and rectum. There is no cure for UC. The pharmacological treatment is aimed at controlling and/or reducing the inflammatory process and promoting disease remission. The present study investigated the possible protective effects of soluble dietary fiber (SDF) isolated from yellow passion fruit peel in the dextran sulfate sodium- (DSS-) induced colitis model in mice, induced by 5% of DSS. The animals were treated with SDF (10, 30, or 100 mg/kg (po)), and the disease activity index was monitored. Colon tissues were collected, measured, and prepared for oxidative stress, inflammation, and histology analysis. SDF improved body weight loss, colon length, and disease activity index and prevented colonic oxidative stress by regulating GSH levels and SOD activity. Furthermore, SDF reduced colonic MPO activity, TNF- α , and IL-1 β levels and increased IL-10 and IL-6 levels. As observed by histological analysis, SDF treatment preserved the colonic tissue, the mucus barrier, and reduced inflammatory cell infiltration. Although this is a preliminary study, taken together, our data indicate that SDF may improve the course of DSS-UC. More studies are needed to explore and understand how SDF promotes this protection.

1. Introduction

Inflammatory bowel disease (IBD) is a general term used to describe chronic inflammatory conditions affecting the gastrointestinal tract, including Crohn's disease (CD) and ulcerative colitis (UC) [1]. IBD is a complex heterogeneous autoimmune

disease that presents as a remarkable characteristic of a defect in the protective epithelial intestinal barrier and deregulated immune activation [2]. Although the etiopathogenesis is not fully understood, it is known that IBD stems from an autoimmune background with a strong influence of genetic factors and dysregulated host immunological responses [3], the gut

microbiome [3, 4], and exposure to environmental triggers, such as ultraprocessed food intake [5] and psychological stress [6].

The incidence and prevalence of UC have increased worldwide [7], affecting patients of all age groups, particularly between the ages of 15–25 and 50–70 years [7–9]. The clinical presentation of UC includes anemia, weight loss, fever, watery and/or bloody diarrhea, and abdominal pain, which together contribute to an extreme decrease in the patient's quality of life, especially for those with active disease [7, 10]. UC is idiopathic, defined as a chronic, relapsing, and remitting inflammatory disease of the colon, and its diagnosis is based on endoscopic, histological, and laboratory evaluation [7]. The treatment must be adapted to the disease activity (mild, moderate, or severe) and the extent of the colon lesion [11]. Therapies use immunosuppressive and corticosteroid drugs [12], aminosalicylates [13], and monoclonal antibodies, such as anti-TNF- α [14] and integrin inhibitors [15]. The main purpose is to induce and maintain remission with the long-term goals of preventing disability, colectomy, and colorectal cancer [16]. However, in addition to the high cost, low efficacy, and side effects, the success of the treatment also depends on several other factors, such as patient adherence and dose optimization [17]. Therefore, various new therapeutic strategies with natural compounds have been studied for UC treatment [18].

Many studies have reported that dietary fibers (nondigestible polysaccharides) ameliorate intestinal barrier function through the improvement of gastrointestinal flora diversity [19–22] and reduction of intestinal barrier defects and inflammation [23]. Our research group has been dedicated to studying the polysaccharides obtained from biomass residues from the yellow passion fruit (*Passiflora edulis* f. *flavicarpa*), an unexplored coproduct of the juice industry. In addition to the already known nutritional value (vitamin B₃, iron, calcium, and phosphorus) [24], the consumption of passion fruit offers several beneficial therapeutic effects, including antioxidant, anti-inflammatory [25], hypoglycemic, and vasorelaxant [26]. It has also been observed that soluble dietary fibers from passion fruit peel flour presented an antigastric ulcer effect *in vivo* [27]. Therefore, our study is aimed at investigating whether soluble dietary fiber (SDF) from yellow passion fruit peel (*P. edulis* f. *flavicarpa*) could improve the course of ulcerative colitis induced by DSS in mice, by reducing the inflammatory process and promoting tissue healing.

2. Methods

2.1. Soluble Dietary Fiber Extraction. Soluble dietary fiber (SDF) was obtained from yellow passion fruit (*Passiflora edulis* f. *flavicarpa*) peel. Briefly, the fruits were washed, and the peel was separated from the pulp, cut into small pieces, and then dried at 50°C. The dried matter was made into flour and stored at room temperature until analysis as previously described [27]. SDF's relative molecular weight was 53 kDa; it is composed of 92% of GalA with high methyl esterified homogalacturonan [27].

2.2. Animals. All experimental protocols were approved by the Animal Use Ethics Committee of the *Instituto de Pesquisa*

Pelé Pequeno Príncipe (number 055-2020). All procedures followed the Guide for the Care and Use of Laboratory Animals (8th edition, National Research Council, 2011) and the Brazilian National Council for the Control of Animal Experimentation. Female Swiss mice (20–30 g), aged between 4 and 5 weeks, were provided by the Animal Facility of *Instituto Carlos Chagas, Fiocruz*, Curitiba, PR, and kept in plastic cages (maximum 12 animals per cage), covered by a layer of wood shavings. Animals were housed and fed in a controlled environment at a temperature of 25 ± 2°C and a 12 h light/dark cycle and acclimatized for at least 1 week before the experiments. Wood shavings and the environmental enrichment were changed every three days, and the animals were maintained with *ad libitum* access to standard laboratory chow and water. For the ulcerative colitis induction protocol, the animals were randomized, matched for weight, and identified according to their group.

2.3. Dextran Sodium Sulfate (DSS) Colitis Model. Acute ulcerative colitis was induced by 5% of DSS (dextran sodium sulfate, molecular weight: 40,000, Cayman Chemical Company), given to animals in drinking water for 5 consecutive days. On days 6 to 8, the DSS was replaced by normal drinking water. The disease's clinical course was monitored daily throughout the experimental protocol period, and weight loss, change in stool consistency, and rectal bleeding were scored (disease activity index (DAI)). On day 8, all animals were euthanized, and the colons were removed, measured, and stored for further analysis.

2.4. Pharmacological Treatments and Disease Activity Index (DAI). The experimental protocol and treatment are illustrated in Figure 1. Mice were divided into the following treatment groups: (i) control group that received only drinking water (control: water, 1 mL/kg (po)); (ii) DSS group, treated with vehicle and given DSS in drinking water (DSS: water, 1 mL/kg (po)); and (iii) SDF group, treated with SDF and given DSS in drinking water (SDF: 10, 30, or 100 mg/kg (po)).

The DAI was monitored daily and scored according to the animal's body weight changes as follows:

- (i) 0: increased or remained within 1% of the baseline
- (ii) 1: decreased by 1 to 5%
- (iii) 2: decreased by 5 to 10%
- (iv) 3: decreased by 10 to 15%
- (v) 4: decreased by more than 15%

The stool consistency was scored as follows:

- (i) 0: in the absence of diarrhea
- (ii) 2: if the stool did not stick to the animal's anus
- (iii) 4: if the animal presented liquid stool

The presence of blood in stool was scored as follows:

- (i) 0: if animals did not present blood in stool

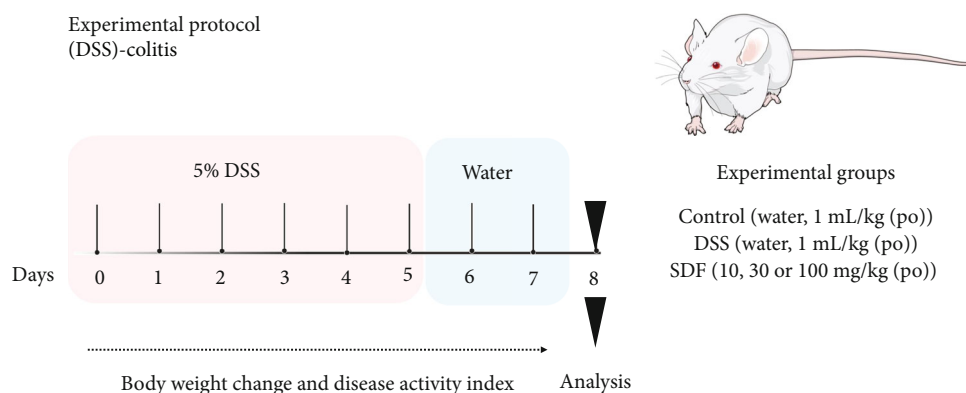


FIGURE 1: Experimental protocol for the induction of ulcerative colitis.

TABLE 1: Histopathological score.

Category	Inflammatory cell infiltrate			Intestinal histoarchitecture		
Criterion	Severity	Extent	Score 1	Epithelial changes	Mucosal histoarchitecture	Score 2
Definition	Mild	Mucosa	1	Focal erosions	—	1
	Moderate	Mucosa and submucosa	2	Erosions	Focal ulcerations, goblet cell depletion	2
	Marked	Transmural	3	Marked erosions	Extended ulcerations ± granulation tissue ± goblet cell depletion	3
Sum of scores 1 and 2						0–6

Score 0: normal.

(ii) 2: for moderate blood in stool

(iii) 4: for gross bleeding

At the end of the experimental protocol, the colon tissues were carefully removed and washed with 0.9% saline. The lengths were measured, and the tissues were stored at -80°C for further analysis.

2.5. Tissue Preparation. Animal tissues were homogenized in PBS (pH 7.4) containing protease inhibitor (Sigma FAST™). The homogenate was analyzed for glutathione (GSH) levels. The samples were centrifuged at 8,900 rpm at 4°C for 20 min. The supernatant was used to determine the superoxide dismutase (SOD) activity, cytokines, and protein levels. The pellet was resuspended in phosphate buffer with hexadecyltrimethylammonium (HTAB) and used to measure myeloperoxidase (MPO) activity.

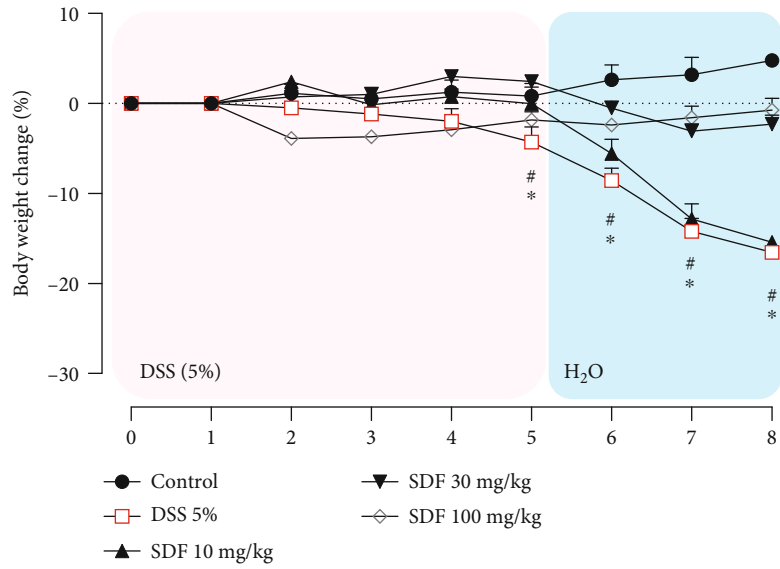
Cytokine levels (TNF- α , IL-1 β , IL-6, and IL-10) were evaluated using an enzyme-linked immunosorbent assay (ELISA) kit according to the manufacturer's recommendations (PeproTech Inc.). The protein concentration was determined by the method of Bradford (Bradford, 1976), using the bovine serum albumin standard curve. All results were read in a spectrophotometer as recommended and interpolated with their respective standard curves.

2.6. Determination of GSH Levels and SOD Activity. To determine the GSH levels, 50 μL of tissue homogenate was

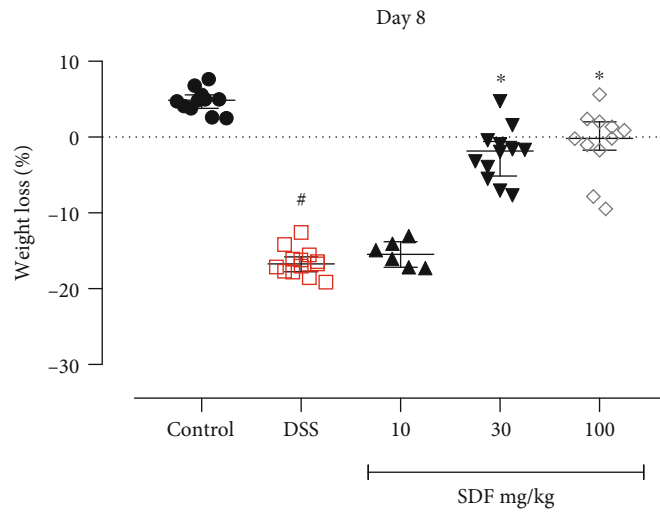
mixed with 40 μL trichloroacetic acid (12.5%) and vortexed for 10 min. The samples were then centrifuged for 15 min at 3,000 rpm at 4°C , and aliquots of 10 μL of the supernatant were mixed with Tris buffer (400 mM, pH 8.9) and 5,5'-dithiobis (2-nitrobenzoic acid) (DTNB, 10 mM). This solution reacts with GSH to generate a yellow compound (2-nitro-5-thiobenzoic acid). The reaction absorbance was measured using a spectrophotometer at 415 nm. All values were interpolated into a standard curve of GSH (0.375–3 μg), and the results were expressed as μg of GSH per mg of protein [28, 29].

Supernatant aliquots of 20 μL were added to a buffer solution containing 200 mM Tris HCl-EDTA (pH 8.5) and pyrogallol (1 mM) to measure the SOD activity. The samples were vortex for 1 min and incubated for 20 min at room temperature. The reaction was stopped with 1 N HCl. All samples were centrifuged for 4 min at 14,000 rpm. The absorbance was read by a spectrophotometer at 405 nm, and the amount of SOD that inhibited the pyrogallol oxidation by 50% was defined as one unit (U) of SOD activity (relative to the control of the test). The enzymatic activity was expressed as units per milligram of protein (U/mg of protein) [29].

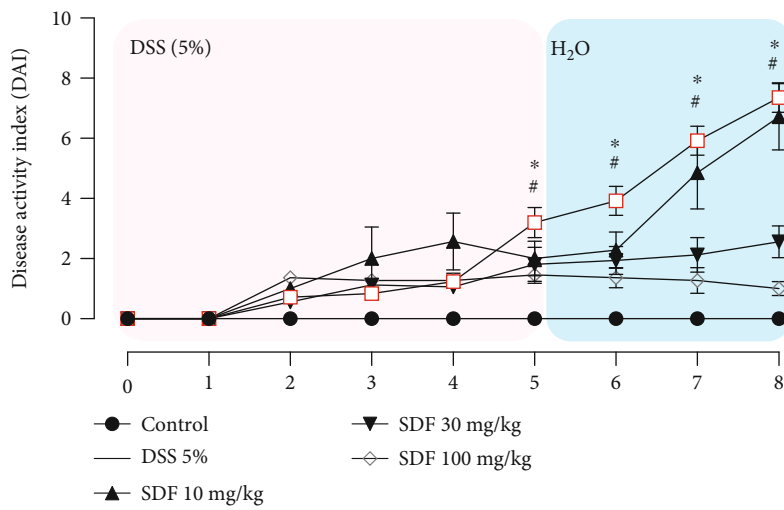
2.7. Quantification of MPO Activity. The MPO activity was determined by using the sample pellets. Briefly, the pellets were resuspended in 1 mL of potassium phosphate buffer (80 mM, pH 5.4) containing 0.5% hexadecyltrimethylammonium bromide (HTAB). After, the samples were centrifuged at 9,900 rpm for 20 min at 4°C . Then, 30 μL of the supernatant



(a)



(b)



(c)

FIGURE 2: Continued.

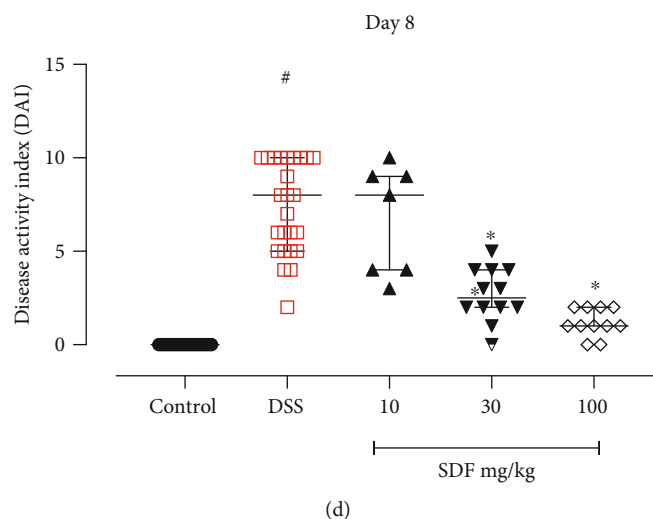


FIGURE 2: Effect of SDF on the (a) body weight change from day 1 to 8, (b) body weight change on day 8, (c) disease activity index from day 1 to 8, and (d) disease activity index on day 8. Animals received 5% of DSS in drinking water for 5 consecutive days followed by 2 days of water. Mice were orally treated, once a day, with vehicle (control or DSS groups: water, 1 mL/kg) or SDF (10, 30, or 100 mg/kg) for 7 days. Results are expressed as mean \pm S.E.M. or median with interquartile ranges and analyzed using two-way ANOVA followed by Bonferroni's multiple comparisons test, or Kruskal–Wallis followed by Dunn's, respectively. # $p < 0.05$, compared to control group; * $p < 0.05$, compared to the DSS group.

was mixed with 0.017% of H_2O_2 and 3,3',5,5'-tetramethylbenzidine (TMB, 18.4 mM). The reaction absorbance was measured at 620 nm, with the results expressed as optical density (OD)/mg of protein [30].

2.8. Determination of Cytokine Levels. Samples were centrifuged at 8,900 rpm at 4°C for 20 min, and the supernatant was used to measure cytokine levels; the levels of IL-1 β , TNF- α , IL-10, and IL-6 were evaluated using an enzyme-linked immunosorbent assay (ELISA) kit according to the manufacturer's recommendations (PeproTech). Each cytokine level was extrapolated from a standard curve (pg/mL), and the results were expressed as pg of each cytokine/mg of protein.

2.9. Histopathological and Immunohistochemical Assessment. Colon samples were collected from the same defined regions, fixed in 10% formalin (neon), and dehydrated sequentially in ethanol and ether for inclusion and construction of paraffin blocks. The paraffin blocks were sectioned in a microtome (7 μ m thickness cross-section). Slides containing the histological sections were deparaffinized and stained with hematoxylin and eosin (H&E) for histopathological evaluation. H&E-stained colonic tissue sections were blindly scored by assessing infiltration of the lamina propria with mononuclear cells, crypt hyperplasia, goblet cell depletion, and alteration of mucosal histoarchitecture (including epithelial erosion and mucosal ulceration), resulting in scores of 0 to 6 (Table 1) [31, 32]. Ten microscopic fields from each mouse, from at least 8 mice per group, were examined using a light microscope (Olympus® BX43F, Minato-Ku, Japan) and a 20x objective (and 40x or 100x if necessary to confirm structure). Slides were also stained for periodic acid Schiff (PAS) and Alcian Blue (AB), and stained mucin-like glyco-

protein positive pixels were captured and quantified with the ImageJ® software.

For immunohistochemical evaluation of mucin 1 (MUC-1), slides containing the histological sections were deparaffinized, incubated overnight with primary anti-MUC-1 antibodies (1:100, pH9) (rabbit polyclonal to MUC1 IgG, 1:100, Abcam), and revealed with 2, 3, diamino-benzidine complex + hydrogen peroxide substrate. Positive pixels were captured and quantified with the ImageJ® software.

2.10. Statistical Analysis. The Shapiro-Wilk test was used to assess the normality of the data. Statistical analysis was performed using Kruskal-Wallis, followed by Dunn's posttest for nonparametric data. The results were expressed as a median with interquartile ranges. One-way ANOVA or two-way ANOVA followed by Bonferroni's multiple comparisons posttest for multivariable analyses was applied to compare differences between multiple groups that presented parametric data. The results were expressed as means \pm SEM. Differences with $p < 0.05$ were considered statistically significant. All analysis was conducted using the GraphPad Prism software (GraphPad Software).

3. Results

3.1. SDF Treatment Alleviated DSS-Induced Colitis. The animals were treated orally once a day with SDF (10, 30, and 100 mg/kg) or vehicle (water, 1 mL/kg), from day 1 to day 7 (Figure 1) to assess the potential effect of SDF in the DSS-induced colitis model. The body weight change and DAI were evaluated according to the experimental protocol. At the end of the experiment (day 8), the animals were euthanized; the colons were collected, measured, and stored for further analysis.

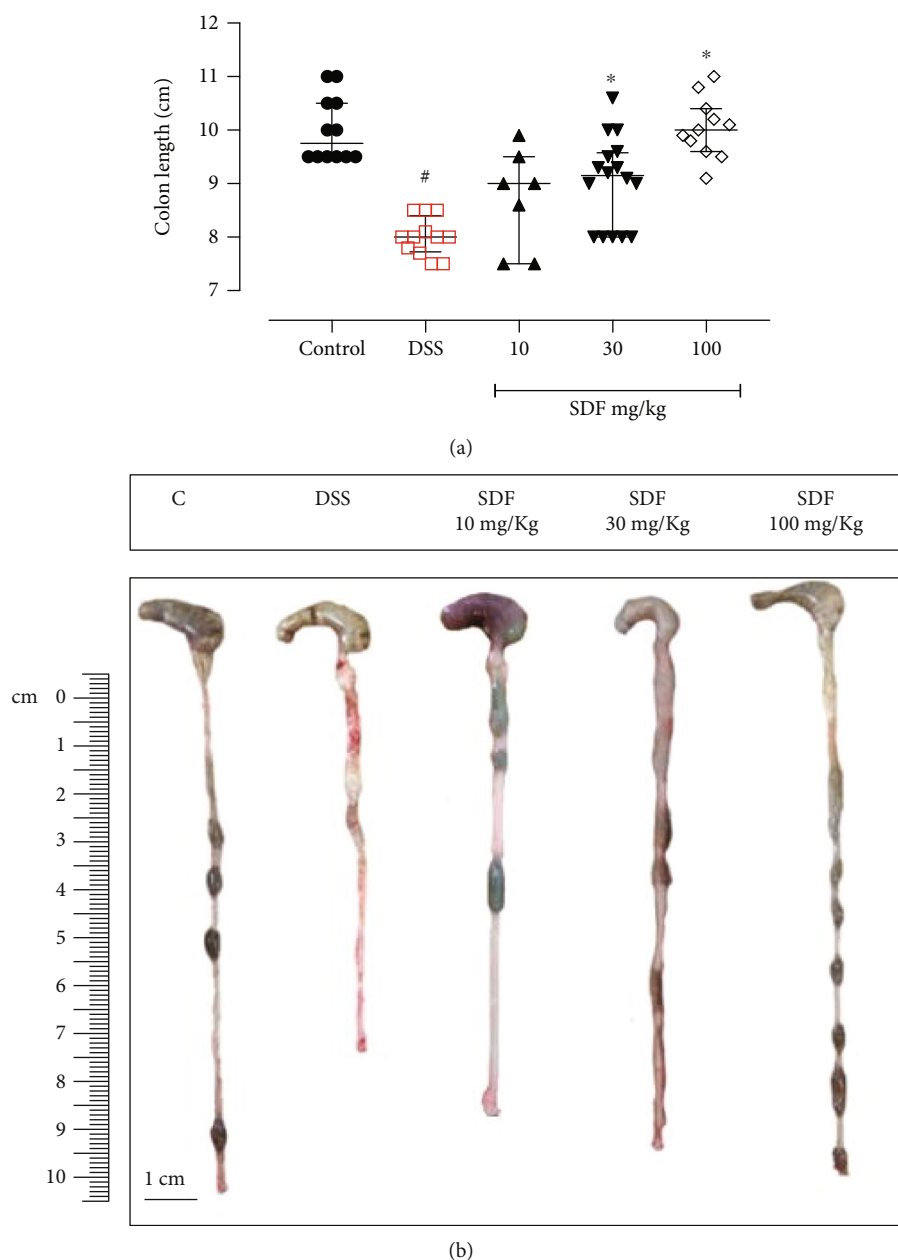


FIGURE 3: Effect of SDF on the mouse colon length. Animals received 5% of DSS in drinking water for 5 consecutive days followed by 2 days of water. Mice were orally treated, once a day, with vehicle (control or DSS groups: water, 1 mL/kg) or SDF (10, 30, or 100 mg/kg) for 7 days. Results are expressed as median with interquartile ranges and analyzed using Kruskal–Wallis followed by Dunn’s. # $p < 0.05$, compared to the control group; * $p < 0.05$, compared to the DSS group.

The animals that received DSS in drinking water and were treated with vehicle started to lose weight on day 5 (-4.29%, $p < 0.0017$), continuing up to day 8 (-16.53%, $p < 0.0001$) (Figures 2(a) and 2(b)) when compared to healthy mice (control group).

Furthermore, the DSS group presented an increased DAI (days 4, 5, 6, 7, and 8; $p = 0.0221$, $p < 0.0001$, $p < 0.000$, $p < 0.0001$, and $p < 0.0001$, respectively) (Figures 2(c) and 2(d)), as well as a reduced colon length (by 17%), when compared to the control group (median: 9.75 cm) (Figure 3).

The SDF treatment significantly prevented body weight loss (day 8, SDF 30 mg/kg: 86%; day 8, SDF 100 mg/kg:

95%, $p < 0.0001$ and $p < 0.0001$, respectively) (Figures 2(a) and 2(b)) and DAI development (day 8, median SDF 30 mg/kg: 2.5; and day 8, median SDF 100 mg/kg: 1.0, $p < 0.0001$ and $p < 0.0001$, respectively) when compared to the DSS group (median: 8.00) (Figures 2(c) and 2(d)). The treatment with SDF also prevented the reduction in colon length (SDF 30 mg/kg: 12%, $p < 0.05$; and SDF 100 mg/kg: 25%, $p < 0.001$) when compared to the DSS group (median: 8.0 cm) (Figure 3).

The SDF doses of 30 and 100 mg/kg prevented weight loss and the development of DAI when compared to the control group. Therefore, we decided to work only with the highest dose tested (100 mg/kg) in the subsequent experiments,

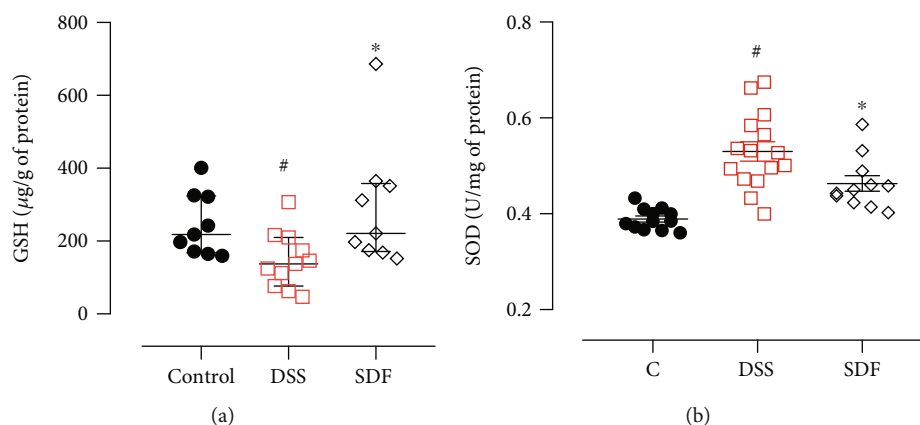


FIGURE 4: Effect of SDF on GSH (a) levels and SOD (b) activity. Animals received 5% of DSS in drinking water for 5 consecutive days followed by 2 days of water. Mice were orally treated, once a day, with vehicle (control or DSS groups: water, 1 mL/kg) or SDF (100 mg/kg) for 7 days. Results are expressed as mean \pm S.E.M. or median with interquartile ranges and analyzed using one- or two-way ANOVA followed by Bonferroni's multiple comparisons test, or Kruskal-Wallis followed by Dunn's, respectively. # $p < 0.05$, compared to the control group; * $p < 0.05$, compared to the DSS group.

considering that the DSS-induced ulcerative colitis model is a very aggressive inflammatory model.

3.2. SDF Decreased Colonic Oxidative Stress. The inflammatory damage induced by DSS brought about the infiltration of neutrophils and macrophages, generating excessive amounts of reactive oxygen species with a subsequent increase in oxidative stress [33]. Therefore, we measured the GSH levels and SOD activity to quantify these parameters.

The animals in the DSS group showed reduced GSH levels (median: 137.1 μ g/g of protein) and increased SOD activity (0.53 ± 0.02 U/mg of protein) compared to the control group (median GSH: 218.3 μ g/g of protein; median SOD: 0.38 ± 0.00 U/mg of protein) ($p = 0.0324$ and $p < 0.0001$, respectively). The SDF treatment restored the GSH (median: 221.5 μ g/g of protein) and SOD activity (0.45 ± 0.01 U/mg of protein) compared to the DSS group ($p = 0.0129$ and $p = 0.0135$, respectively) (Figures 4(a) and 4(b)).

3.3. SDF Regulated Colonic MPO Activity and Cytokine Secretion. Colon tissue damage in the DSS-induced ulcerative colitis model is directly linked to increased vascular permeability followed by tissue edema, increased cellular infiltration, such as neutrophils and macrophages, and a consequent increase in mucosal cytokine production [30]. Therefore, we measured colonic pro- and anti-inflammatory cytokines to explore whether SDF treatment could alleviate DSS colitis by regulating inflammation.

We did not observe significant differences in MPO activity between the DSS group (median: 0.20 mg of protein) and the control group (median: 0.15 mg of protein) ($p = 0.1076$). On the other hand, SDF treatment decreased the MPO activity (median: 0.09) ($p = 0.0101$) compared to the DSS group (Figure 5(a)).

An increase in tissue cytokines, including the proinflammatory cytokines IL-1 β and TNF- α , and a decrease in tissue IL-10 and IL-6 were observed in mice that received DSS and were treated with vehicle (IL-1 β : 5420 ± 583.9 pg/mg of

protein; TNF- α : 5841 ± 356.5 pg/mg of protein; IL-10: 4217 ± 525.6 pg/mg of protein; IL-6: 2264 ± 265.4 pg/mg of protein), compared to the control group (IL-1 β : 3598 ± 383.1 pg/mg of protein; TNF- α : 2746 ± 520.7 pg/mg of protein; IL-10: 9778 ± 1012 pg/mg of protein; IL-6: 6706 ± 499.2 pg/mg of protein) ($p < 0.05$, $p < 0.0001$, $p < 0.001$, and $p < 0.0001$, respectively). In the SDF group, these cytokines were significantly decreased (IL-1 β : 3843 ± 248.3 pg/mg of protein and TNF- α : 3492 ± 230.5 pg/mg of protein) ($p < 0.05$ and $p < 0.01$, respectively) and increased (IL-10: 7102 ± 877.1 pg/mg of protein and IL-6: 4746 ± 898.8 pg/mg protein) ($p < 0.05$ and $p < 0.05$, respectively) compared to the DSS group (Figures 5(b)–5(e)).

3.4. SDF Treatment Improved Microscopic Colon Damage in Mice. Colonic damage induced by oral administration of DSS includes the destruction of the intestinal mucosal barrier and is directly related to the disease progression [33]. Therefore, the colons were collected at the end of the experiment and processed for histological analysis. Then, we further evaluated the protective effect of SDF (100 mg/kg). H&E colon staining (Figure 6) showed that 5% of DSS destroyed the colon tissue, leading to the formation of extensive ulcerations, edema, and histopathological changes in the mucosa and submucosa. SDF (100 mg/kg) H&E-stained sections revealed a significant overall histological improvement, evidenced by a conserved mucosal architecture. Furthermore, the DSS group showed an increase in the histopathological score (median: 4) compared to the control group (median: 2) ($p < 0.0001$). SDF treatment reduced histopathological damage (median: 3) compared to the DSS group ($p < 0.0001$) (Figure 6(a)).

3.5. SDF Treatment Preserved the Mucus Layer. A handful of studies have already demonstrated that DSS-induced colonic damage is related to decreased gastric mucus content and secretion [33]. Therefore, we next evaluated if the protective effect of SDF could be associated with the maintenance of the colon's protective mucus barrier. The results show (Figures 7 and 8)

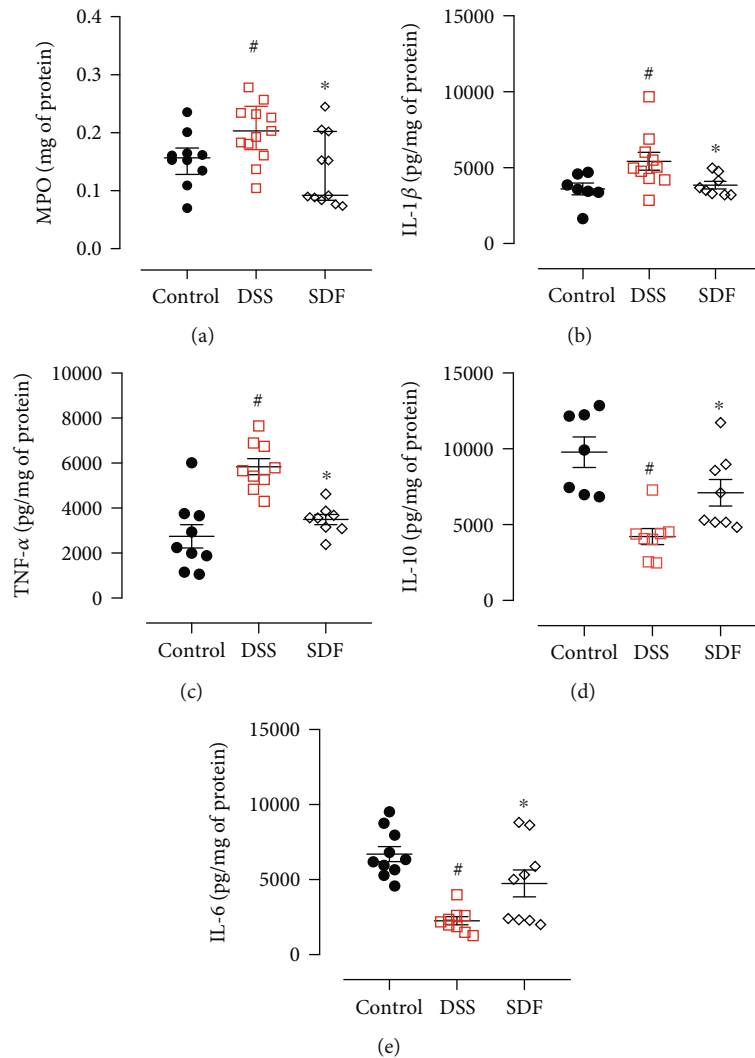


FIGURE 5: Effect of SDF on MPO activity (a) and IL-1 β (b), TNF- α (c), IL-10 (d), and IL-6 (e) levels. Animals received 5% of DSS in drinking water for 5 consecutive days followed by 2 days of water. Mice were orally treated, once a day, with vehicle (control or DSS groups: water, 1 mL/kg) or SDF (100 mg/kg) for 7 days. Results are expressed as mean \pm S.E.M. or median with interquartile ranges and analyzed using one- or two-way ANOVA followed by Bonferroni's multiple comparisons test, or Kruskal-Wallis followed by Dunn's, respectively. # p < 0.05, compared to the control group; * p < 0.05, compared to the DSS group.

that the administration of DSS induced a decrease in PAS and AB staining, indicative of neutral mucin and acid mucin-like glycoproteins (54% and 65%, respectively) ($p = 0.0016$ and $p < 0.0001$, respectively) compared to the control group. The treatment with SDF (100 mg/kg) increased the staining for PAS and AB by 80% and 155%, respectively ($p = 0.046$ and $p < 0.0005$, respectively), compared to the DSS group (34.71 ± 14.51 pixels/field and 2153 ± 613.7 pixels/field, respectively) (Figures 7 and 8).

To confirm the previous result, we performed an immunohistochemical analysis to determine the expression profile of the transmembrane mucin MUC-1. Animals with ulcerative colitis have reduced levels of MUC-1 (95%, $p < 0.0001$) when compared to the control group (Figure 9) (95804 ± 12615 pixels/field). The treatment with SDF (100 mg/kg) increased the labeling for MUC-1 by 300% ($p = 0.0297$) compared to the DSS group (14031 ± 2730 pixels/field) (Figure 9).

4. Discussion

Many natural products possess therapeutic and medicinal properties. Bioactive compounds, including polysaccharides formed by polymers of monosaccharides and characterized as macromolecules of high molecular weight, offer various biological activities, such as anti-inflammatory, that could be utilized to develop new IBD therapies [34]. For the first time, we show that the polysaccharides extracted from the yellow passion fruit peel protect mice from ulcerative colitis progression in the DSS model, ameliorate the mucosal barrier, and prevent DSS-induced inflammation.

Inflammatory bowel disease (IBD) consists of two major pathological subtypes: Crohn's disease (CD) and ulcerative colitis (UC) [1]. UC is described as a complex condition becoming increasingly critical globally [35]. The pathophysiology and underlying disease mechanisms remain unclear;

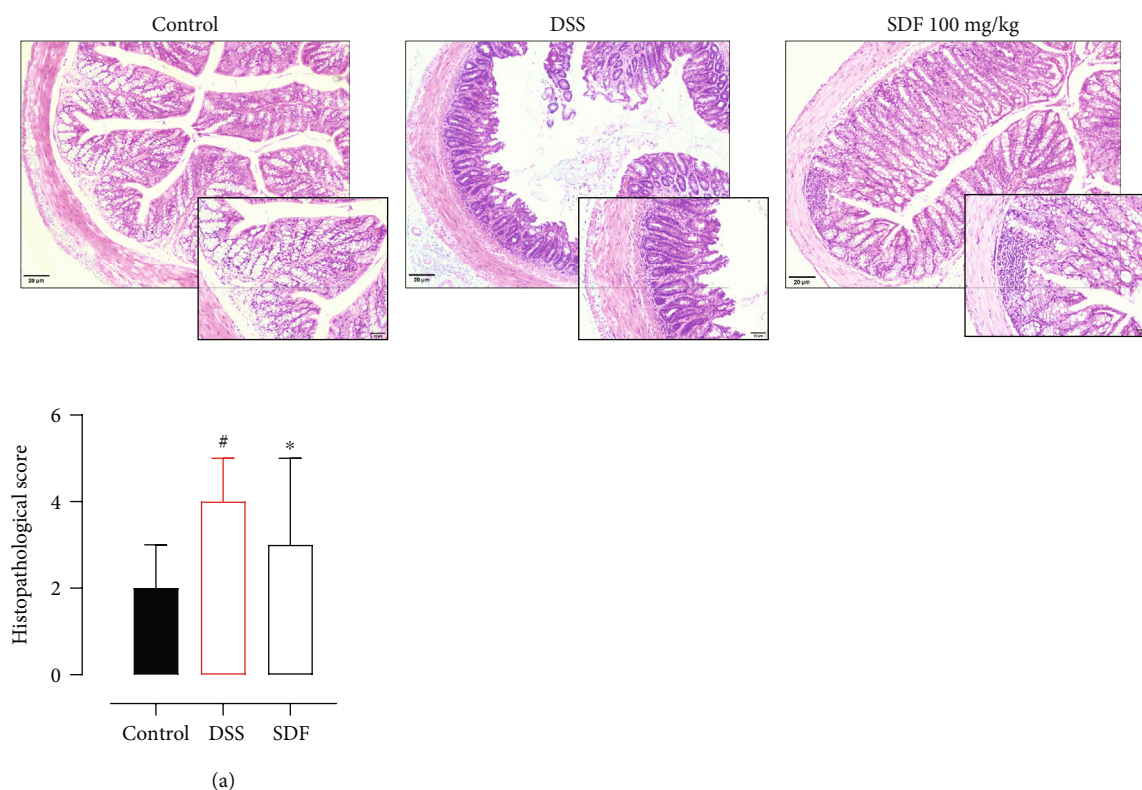


FIGURE 6: Effect of SDF on histological parameters and histopathological score (a). Hematoxylin and eosin-stained sections of colons, $\times 20$ (bars = $100 \mu\text{m}$). Animals received 5% of DSS in drinking water for 5 consecutive days followed by 2 days of water. Mice were orally treated, once a day, with vehicle (control or DSS groups: water, 1 mL/kg) or SDF (100 mg/kg) for 7 days. Results are expressed as median with interquartile ranges and analyzed using Kruskal–Wallis followed by Dunn's. # $p < 0.05$, compared to the control group; * $p < 0.05$, compared to the DSS group.

however, a handful of studies reported that the disease is directly related to genetic susceptibility, and its occurrence and development have been associated with immune disorders, environmental factors, and mucosal dysfunction [1]. Unfortunately, pharmacological and nonpharmacological strategies for the treatment of UC do not induce cure but aim to reduce symptoms and maintain effective clinical remission [36]. Therefore, the development of safe and effective treatments with a high capacity to maintain the remission of IBD patients is necessary.

There are several experimental models for studying inflammatory bowel disease. The DSS ulcerative colitis model is the most widely used due to its simplicity, high degree of uniformity, and reproducibility of the lesions [37, 38]. Administration of DSS in drinking water induces mucosal damage resulting from the disruption of the intestinal epithelial monolayer lining, luminal bacteria, and associated antigen translocation. Additionally, neutrophils and macrophage infiltration initially mediate oxidative stress and inflammation, contributing to the observed tissue damage [39, 40]. Animals exhibit marked body weight loss, altered stool consistency, and hematochezia [38].

Natural products are gaining ground as possible sources of new options for UC treatment. Several studies have shown that biomolecules have anti-inflammatory activity and can control IBD [18]. Polysaccharides isolated from natural products form one of the main classes of bioactive com-

pounds with therapeutic efficacy [41]. The consumption of nondigestible dietary fibers can provide health benefits and appears to reduce the risk of developing several conditions, including obesity, diabetes mellitus, heart disease, and metabolic syndrome [42, 43]. Interestingly, dietary fibers have also been associated with reducing the risk of developing inflammatory bowel disease, maintaining epithelial barrier integrity, and forming short-chain fatty acids that can inhibit the transcription of proinflammatory mediators [44].

As expected, DSS induced all the characteristics mentioned above in our experiments, including colon shortening. SDF treatment prevented weight loss and increased disease scores, including rectal bleeding, which is directly associated with the prevention of colon shortening [39]. Consequently, all the other aspects of the disease, including raised fur, hunched back, and reduced mobility, were improved. Several other studies have already demonstrated the protective effect of polysaccharides extracted from natural products in ulcerative colitis models [45–47]. Specifically, fruit polysaccharides also have such a protective effect. Zou et al. have demonstrated that *Ficus carica* polysaccharide attenuated DSS-induced ulcerative colitis in C57BL/6 mice by maintaining goblet cells and reducing inflammation [48]. Polysaccharides extracted from *Morinda citrifolia* Linn presented anti-inflammatory action in a mouse acetic acid-induced colitis model, reducing inflammatory cell infiltration and oxidative stress [49]. Related

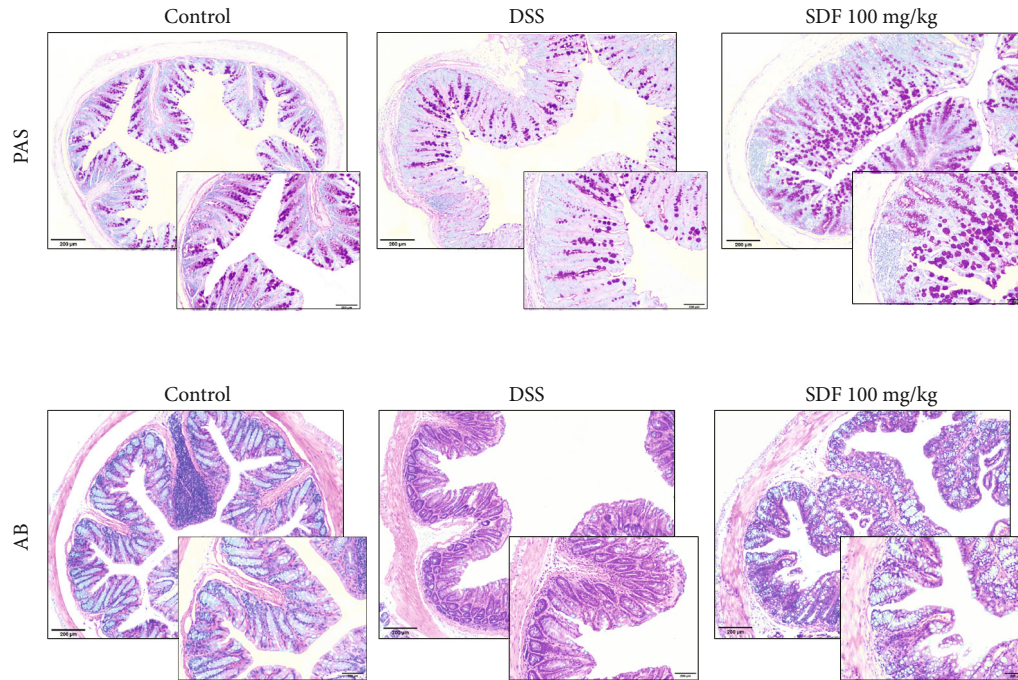


FIGURE 7: Effect of SDF on histochemical staining for neutral mucin-like glycoproteins (PAS) and acid mucin (Alcian Blue). Histochemical staining of colons for neutral mucin-like glycoproteins (PAS) and acid mucin (Alcian Blue), $\times 20$ (bars = $100 \mu\text{m}$). Animals received 5% of DSS in drinking water for 5 consecutive days followed by 2 days of water. Mice were orally treated, once a day, with vehicle (control or DSS groups: water, 1 mL/kg) or SDF (100 mg/kg) for 7 days.

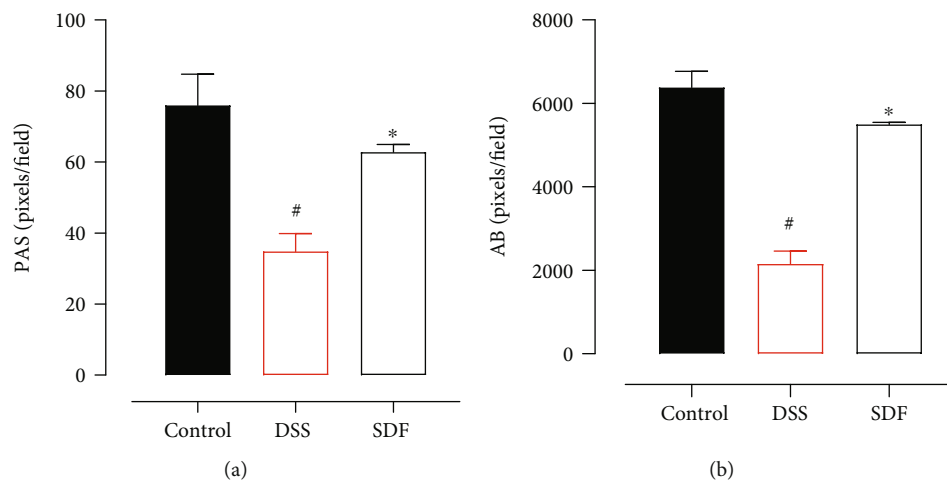


FIGURE 8: SDF preserves mucus secretion. Quantification of PAS (a) and Alcian Blue (b). Animals received 5% of DSS in drinking water for 5 consecutive days followed by 2 days of water. Mice were orally treated, once a day, with vehicle (control or DSS groups: water, 1 mL/kg) or SDF (100 mg/kg) for 7 days. Results are expressed as mean \pm S.E.M. followed by Bonferroni's multiple comparisons test. [#] $p < 0.05$, compared to the control group; ^{*} $p < 0.05$, compared to the DSS group.

oxidative stress and inflammation were quantified to understand the mechanisms of SDF protection further.

Inflammatory cell infiltration and oxidative stress play an important role in the pathological development, induction, and progression of ulcerative colitis [50]. As the disease progresses, the colonic tissue infiltration of leukocytes, neutrophils, and macrophages increases, resulting in a consequent uncontrolled generation of reactive nitrogen and oxygen metabolites that destroy tissue structures, including lipids, proteins,

and DNA [51]. Furthermore, the imbalance between pro- and anti-inflammatory cytokines contributes to compromised immune function and tissue damage [52]. For instance, TNF- α derived from dendritic cells, macrophages, and T cells can stimulate the production and release of other proinflammatory cytokines [2]. However, the intestine orchestrates a complex and organized system that contains multiple antioxidant methods of defense and protection mechanisms against inflammation to protect against damage, maintain intestinal

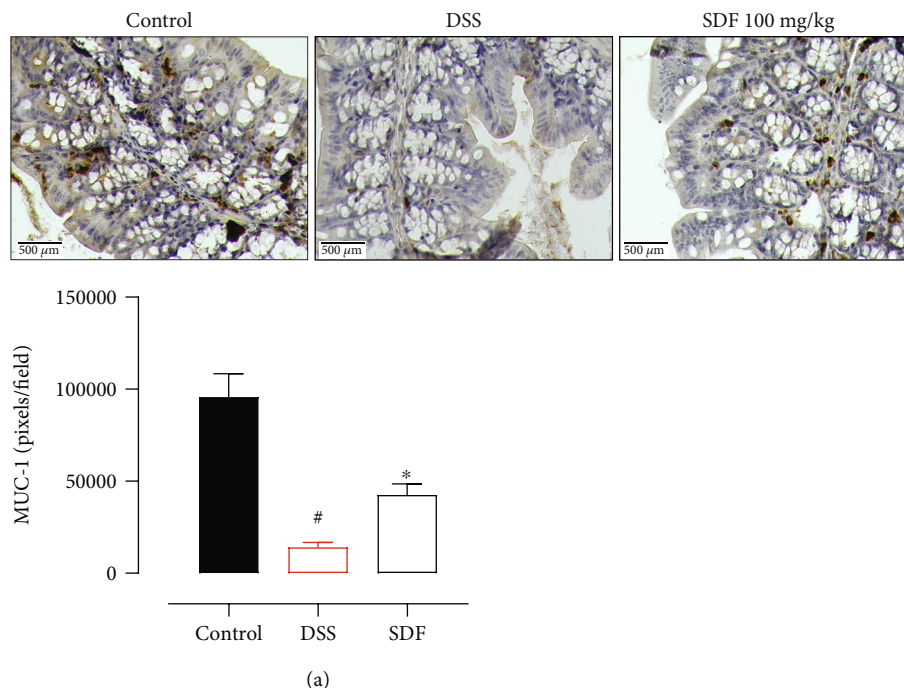


FIGURE 9: SDF preserves MUC-1 expression. Immunohistochemical staining of colons for MUC-1, $\times 40$ (bars = $500 \mu\text{m}$). Quantification of MUC-1 expression (a). Animals received 5% of DSS in drinking water for 5 consecutive days followed by 2 days of water. Mice were orally treated, once a day, with vehicle (control or DSS groups: water, 1 mL/kg) or SDF (100 mg/kg) for 7 days. Results are expressed as mean \pm S.E. M. followed by Bonferroni's multiple comparisons test. # $p < 0.05$, compared to the control group; * $p < 0.05$, compared to the DSS group.

integrity, and ensure general and immune homeostasis [53]. We observed in our experiments that SDF treatment prevented oxidative stress by maintaining GSH levels and SOD activity. We also observed that SDF treatment prevented the increase of MPO, TNF- α , and IL-1 β and the reduction of IL-10 and IL-6, suggesting a tissue-protective response and regulatory effect on inflammation. Along with preventing the general development of the disease, it is also possible to suggest that SDF ameliorated colonic inflammation in the DSS-induced ulcerative colitis model.

The inflammatory process observed in the DSS-induced ulcerative colitis model occurs probably due to the intestinal epithelium damage and dissemination of proinflammatory luminal microbial antigens to the underlying tissue [37, 39]. Therefore, reducing the inflammatory process represents an attractive alternative for the management of ulcerative colitis. Interestingly, it has been previously demonstrated that SDF had a protective effect on the stomach mucosa; administering SDF significantly reduced stomach gastric ulcer lesions in rats. The authors also showed that this protection might be related to maintaining GSH levels and gastric mucus secretion, corroborating our data [27]. In addition, it is well-known that the intestinal inflammatory process is directly related to motility dysfunction [54]. We observed through DAI that animals treated with SDF have a lower score of diarrhea when compared to DSS animals. In fact, fiber consumption may modulate gastrointestinal motility either by changes in the microbiota and fermentation end products or by modulating the bulk flow of material through the intestine [55–57]. Moreover, cumulative evidence has shown polysaccharides from different sources and with different structures regulate intestinal motility,

reduce diarrhea [58–61], and ameliorate constipation in animals [62–66], adults, and children [67].

Another important factor involved in the pathogenesis of ulcerative colitis is the permeation of the mucous barrier that occurs due to the reduction in the production and secretion of mucins and the stratification of the mucus layers [68]. Mucus barrier abnormalities, such as depleted upper crypt goblet cells, decreased core mucus components, and decreased mucin expression, allow bacterial penetration that could stimulate an abnormal immune system response leading to the development of local tissue inflammation [69]. Tissue inflammation and mucus layer depletion contribute to acute histological changes, which are directly associated with all the colitis aspects, including weight loss and diarrhea [37]. Histological damage, such as modification of normal mucosal histoarchitecture and erosions, and tissue cell infiltration are important changes observed [70, 71]. For this reason, in addition to microscopic analysis, we also assessed mucus preservation through PAS and AB staining and the expression profile of MUC-1. The PAS was employed to stain neutral mucins, and AB was used to stain acid mucin-like glycoproteins in the colon tissue; MUC-1 is transmembrane mucin, and the maintenance of its expression and secretion ensures tissue protection and corrects cell signaling and immune response and consequently intestinal homeostasis [69].

The microscopic examination of the colon sections showed a clear colonic epithelial destruction induced by DSS, with visible tissue damage. We observed a high histological score, which includes cellular infiltration, crypt hyperplasia, epithelial erosion, mucosal ulceration, and goblet cell depletion. The reduction of goblet cells corroborates the

results found for PAS and AB staining and MUC-1 expression. It is noteworthy that SDF treatment preserved the epithelial architecture. Histological analyses revealed a reduction in the histopathological score, composed of a reduction in the severity and extent of tissue damage, reduction of erosion, and maintenance of goblet cells. This evidence corroborates the maintenance of positive labeling indicative of mucin. Thus, it is possible to hypothesize that SDF treatment reinforces the protective barrier of the intestinal mucosa, maintaining normal mucus secretion, and thus, intestinal homeostasis.

Cumulative evidence has shown that natural polysaccharides may reinforce the intestinal protective barrier in several ways; furthermore, other studies have shown that these molecules can protect the mucus barrier [72, 73]. Interestingly, chronic or intermittent dietary fiber deficiency can cause erosion of the protective mucus layer, making it thinner and more susceptible to pathogens [74]. Strengthening of the epithelial and mucus barrier can occur, for example, by increased production of short-chain fatty acids (SCFAs) [75]. Increasing the abundance of intestinal *Bifidobacterium*, *Lactobacillus*, and *Escherichia coli* [75, 76] and inhibiting the growth of potentially pathogenic bacteria, such as *Clostridium*, also alleviate ulcerative colitis [77]. Some other authors suggest that polysaccharides reduce the expression of proinflammatory cytokines and MPO activity [76, 78–80].

Finally, we have presented here the protective role of SDF for the first time. However, the exact mechanism by which this polysaccharide extract provides colonic protection is still not entirely clear. Nondigestible polysaccharides have complex structures and may show beneficial properties through direct and indirect mechanisms [81]. The literature assumes that these molecules can, for example, serve as a substrate for bacterial fermentation in the large intestine. This produces SCFAs and other metabolites that interact with different receptors (G-protein-coupled receptors, including GPR41, GPR43, and GPR109A) to promote beneficial effects such as increased prostaglandin production and mucin expression (MUC-1, MUC-2, MUC-3, and MUC-4). Furthermore, it has been shown that polysaccharides extracted from natural products can directly inhibit COX overexpression [82] interact with different mucins through molecular mucoadhesive interactions [83] or interact with Toll-like receptors [84–87].

All these mechanisms could contribute to the observed intestinal protection promoted by SDF. Our results demonstrate that SDF might prevent the development of ulcerative colitis through several mechanisms, including colonic mucosal protection, decreased oxidative stress, and inflammation, ultimately resulting in the maintenance of mucus layer and tissue integrity. Although the exact protection mechanism has not yet been determined, the presented data indicate that SDF may represent an interesting option for managing acute ulcerative colitis. However, more studies are needed to explore and understand how SDF elicits its beneficial effects.

Data Availability

The data presented in the current study are available from the corresponding author on reasonable request.

Conflicts of Interest

The authors declare no competing interests.

Acknowledgments

This work was supported by the Instituto de Pesquisa Pelé Pequeno Príncipe (Brazil). L.R.B. is a master student and B.S. is a postdoctoral student, both receiving a grant from the Instituto de Pesquisa Pelé Pequeno Príncipe. I.F.W. is a master student receiving a grant from the Coordenação de Aperfeiçoamento de Pessoal de Nível Superior (CAPES; finance code 001; Brazil). N.M.T.d.O. and K.S.S. are PhD students, receiving a grant from the Coordenação de Aperfeiçoamento de Pessoal de Nível Superior (CAPES, Brazil), or Instituto de Pesquisa Pelé Pequeno Príncipe. L.M.C.C. received grant from CNPq (process numbers 404717/2016-0 and 307314/2018-9).

References

- [1] P. Hindryckx, F. Baert, A. Hart, F. Magro, A. Armuzzi, and L. Peyrinbiroulet, “Clinical trials in ulcerative colitis: a historical perspective,” *Journal of Crohn’s and Colitis*, vol. 9, no. 7, pp. 580–588, 2015.
- [2] B. Ahluwalia, L. Moraes, M. K. Magnusson, and L. Ohman, “Immunopathogenesis of inflammatory bowel disease and mechanisms of biological therapies,” *Scandinavian Journal of Gastroenterology*, vol. 53, no. 4, pp. 379–389, 2018.
- [3] J. L. Round and S. K. Mazmanian, “The gut microbiota shapes intestinal immune responses during health and disease,” *Nature Reviews Immunology*, vol. 9, no. 5, pp. 313–323, 2009.
- [4] A. Swidsinski, A. Ladhoff, A. Pernthaler et al., “Mucosal flora in inflammatory bowel disease,” *Gastroenterology*, vol. 122, no. 1, pp. 44–54, 2002.
- [5] N. Narula, E. C. L. Wong, M. Dehghan et al., “Association of ultra-processed food intake with risk of inflammatory bowel disease: prospective cohort study,” *Bmj*, vol. 374, 2021.
- [6] D. Sgambato, A. Miranda, R. Ranaldo, A. Federico, and M. Romano, “The role of stress in inflammatory bowel diseases,” *Current Pharmaceutical Design*, vol. 23, no. 27, pp. 3997–4002, 2017.
- [7] R. Ungaro, S. Mehandru, P. B. Allen, L. P. Biroulet, and J. Colombel, “Ulcerative colitis,” *The Lancet*, vol. 389, no. 10080, pp. 1756–1770, 2017.
- [8] G. P. Kotze, F. Steinwurz, C. Francisconi et al., “Review of the epidemiology and burden of ulcerative colitis in Latin America,” *Therapeutic Advances in Gastroenterology*, vol. 13, 2020.
- [9] D. T. Rubin, A. N. Ananthakrishnan, C. A. Siegel, B. G. Sauer, and M. D. Long, “ACG clinical guideline: ulcerative colitis in adults,” *Official Journal of the American College of Gastroenterology ACG*, vol. 114, no. 3, pp. 384–413, 2019.
- [10] M. D. Coates, M. Lahoti, D. G. Binion, E. M. Szigethy, M. D. Regueiro, and K. Bielefeldt, “Abdominal pain in ulcerative colitis,” *Inflammatory Bowel Diseases*, vol. 19, no. 10, pp. 2207–2214, 2013.
- [11] M. Kayal and S. Shah, “Ulcerative Colitis: Current and Emerging Treatment Strategies,” *Journal of Clinical Medicine*, vol. 9, no. 1, p. 94, 2019.
- [12] S. Danese, C. A. Siegel, and L. P. Biroulet, “Review article: integrating budesonide-MMX into treatment algorithms for mild-

- to-moderate ulcerative colitis,” *Alimentary Pharmacology & Therapeutics*, vol. 39, no. 10, pp. 1095–1103, 2014.
- [13] S. Singh, J. A. Proudfoot, P. S. Dulai et al., “No benefit of concomitant 5-aminosalicylates in patients with ulcerative colitis escalated to biologic therapy: pooled analysis of individual participant data from clinical trials,” *The American Journal of Gastroenterology*, vol. 113, no. 8, pp. 1197–1205, 2018.
- [14] R. W. Stidham, T. C. H. Lee, P. D. R. Higgins et al., “Systematic review with network meta-analysis: the efficacy of anti-tumour necrosis factor-alpha agents for the treatment of ulcerative colitis,” *Alimentary Pharmacology & Therapeutics*, vol. 39, no. 7, pp. 660–671, 2014.
- [15] S. J. Bickston, B. W. Behm, D. J. Tsoulis et al., “Vedolizumab for induction and maintenance of remission in ulcerative colitis,” *Cochrane Database of Systematic Reviews*, vol. 8, 2014.
- [16] K. Tripathi and J. D. Feuerstein, “New Developments in Ulcerative Colitis: Latest Evidence on Management, Treatment, and Maintenance,” *Drugs in Context*, vol. 8, 2019.
- [17] D. C. Baumgart and W. J. Sandborn, “Inflammatory bowel disease: clinical aspects and established and evolving therapies,” *The Lancet*, vol. 369, no. 9573, pp. 1641–1657, 2007.
- [18] Y. E. Joo, “Natural product-derived drugs for the treatment of inflammatory bowel diseases,” *Intestinal Research*, vol. 12, no. 2, pp. 103–109, 2014.
- [19] W. Cheng, J. Lu, B. Li et al., “Effect of functional oligosaccharides and ordinary dietary fiber on intestinal microbiota diversity,” *Frontiers in Microbiology*, vol. 8, p. 1750, 2017.
- [20] M. S. Elshahed, M. Anca, A. C. Aprotosoae, and M. A. Farag, “Pectin in Diet: Interactions with the Human Microbiome, Role in Gut Homeostasis, and Nutrient-Drug Interactions,” *Carbohydrate Polymers*, vol. 255, article 117388, 2021.
- [21] K. E. B. Knudsen, H. N. Laerke, M. S. Hedemann et al., “Impact of diet-modulated butyrate production on intestinal barrier function and inflammation,” *Nutrients*, vol. 10, no. 10, p. 1499, 2018.
- [22] Q. Song, Y. Wang, L. Huang et al., “Review of the Relation Ships among Polysaccharides, Gut Microbiota, and Human Health,” *Food Research International*, vol. 140, article 109858, 2021.
- [23] T. V. Hung and T. Zuzuki, “Dietary fermentable fiber reduces intestinal barrier defects and inflammation in colitic mice,” *The Journal of Nutrition*, vol. 146, no. 10, pp. 1970–1979, 2016.
- [24] K. R. V. Cordova, T. M. M. T. B. Gama, C. M. G. Winter, G. K. Neto, and R. J. S. Freitas, “Características físico-químicas da casca do maracujá amarelo (*Passiflora edulis flavicarpa* Degener) obtida por secagem,” *Boletim do Centro de Pesquisa de Processamento de Alimentos*, vol. 23, no. 2, 2005.
- [25] A. Y. Coqueiro, J. R. R. Pereira, and F. Galante, “Peel flour of the *Passiflora edulis* f. *flavicarpa*, (yellow passion fruit): from therapeutic potentials to side effects,” *Revista Brasileira de Plantas Mediciniais*, vol. 18, no. 2, pp. 563–569, 2016.
- [26] B. Cabral, R. H. Bortolin, T. A. F. Goncalves et al., “Hypoglycemic and vasorelaxant effect of *Passiflora edulis* fruit peel by-product,” *Plant Foods for Human Nutrition*, vol. 76, no. 4, pp. 466–471, 2021.
- [27] K. Y. Abboud, B. B. Luz, J. L. Dallazen et al., “Gastroprotective effect of soluble dietary fibres from yellow passion fruit (*Passiflora edulis* f. *flavicarpa*) peel against ethanol-induced ulcer in rats,” *Journal of Functional Foods*, vol. 54, pp. 552–558, 2019.
- [28] J. Sedlak and R. H. Lindsay, “Estimation of total, protein-bound, and nonprotein sulphhydryl groups in tissue with Ellman’s reagent,” *Analytical Biochemistry*, vol. 25, no. 1, pp. 192–205, 1968.
- [29] S. Marklund and G. Marklund, “Involvement of the superoxide anion radical in the autoxidation of pyrogallol and a convenient assay for superoxide dismutase,” *European Journal of Biochemistry*, vol. 47, no. 3, pp. 469–474, 1974.
- [30] L. M. De Young, J. B. Kheifets, S. J. Ballaron, and J. M. Young, “Edema and cell infiltration in the phorbol ester-treated mouse ear are temporally separate and can be differentially modulated by pharmacologic agents,” *Agents and Actions*, vol. 26, no. 3, pp. 335–341, 1989.
- [31] D. J. Berg, N. Davidson, R. Kühn et al., “Enterocolitis and colon cancer in interleukin-10-deficient mice are associated with aberrant cytokine production and CD4(+) TH1-like responses,” *The Journal of Clinical Investigation*, vol. 98, no. 4, pp. 1010–1020, 1996.
- [32] U. Erben, C. Loddenkemper, K. Doerfel et al., “A guide to histomorphological evaluation of intestinal inflammation in mouse models,” *International Journal of Clinical and Experimental Pathology*, vol. 7, no. 8, pp. 4557–4576, 2014.
- [33] S. Hwang, S. Hwang, M. Jo, C. G. Lee, and K. J. Rhee, “Oral administration of Korean propolis extract ameliorates DSS-induced colitis in BALB/c mice,” *International Journal of Medical Sciences*, vol. 17, no. 13, pp. 1984–1991, 2020.
- [34] L. Duan, S. Cheng, L. Li, Y. Liu, D. Wang, and G. Liu, “Natural anti-inflammatory compounds as drug candidates for inflammatory bowel disease,” *Frontiers in Pharmacology*, vol. 12, 2021.
- [35] D. P. Venegas, M. K. Fuente, G. Landskron et al., “Short Chain Fatty Acids (SCFAs)-Mediated Gut Epithelial and Immune Regulation and Its Relevance for Inflammatory Bowel Diseases,” *Frontiers in Immunology*, vol. 277, 2019.
- [36] J. Meier and A. Sturm, “Current treatment of ulcerative colitis,” *World Journal of Gastroenterology: WJG*, vol. 17, no. 27, pp. 3204–3212, 2011.
- [37] D. D. Eichele and K. K. Kharbanda, “Dextran sodium sulfate colitis murine model: an indispensable tool for advancing our understanding of inflammatory bowel diseases pathogenesis,” *World Journal of Gastroenterology*, vol. 23, no. 33, pp. 6016–6029, 2017.
- [38] M. Perse and A. Cerar, “Dextran sodium sulphate colitis mouse model: traps and tricks,” *Journal of Biomedicine and Biotechnology*, vol. 2012, Article ID 718617, 13 pages, 2012.
- [39] B. Chassaing, J. D. Aitken, M. Malleshappa, and M. V. Kumar, “Dextran sulfate sodium (DSS)-induced colitis in mice,” *Current Protocols in Immunology*, vol. 104, pp. 15–25, 2014.
- [40] G. K. Meers, H. Bohnenberger, H. M. Reichardt, F. Luhder, and S. D. Reichardt, “Impaired resolution of DSS-induced colitis in mice lacking the glucocorticoid receptor in myeloid cells,” *PloS One*, vol. 13, no. 1, article e0190846, 2018.
- [41] X. Ji, M. Yin, H. Nie, and Y. Liu, “A review of isolation, chemical properties, and bioactivities of polysaccharides from *Blettia striata*,” *BioMed Research International*, vol. 2020, Article ID 5391379, 11 pages, 2020.
- [42] A. M. P. Lottenberg, P. L. T. Fan, and V. Buonacorso, “Effects of dietary fiber intake on inflammation in chronic diseases,” *Einstein (São Paulo)*, vol. 8, pp. 254–258, 2010.
- [43] F. Saura-Calixto, “Dietary fiber as a carrier of dietary antioxidants: an essential physiological function,” *Journal of Agricultural and Food Chemistry*, vol. 59, no. 1, pp. 43–49, 2011.

- [44] M. Gajendran, P. Loganathan, A. P. Catinella, and J. G. Hashash, "A comprehensive review and update on Crohn's disease," *Disease-a-Month*, vol. 64, no. 2, pp. 20–57, 2018.
- [45] Y. Sun, J. Huo, S. Zhong, J. Zhu, Y. Li, and X. Li, "Chemical structure and anti-inflammatory activity of a branched polysaccharide isolated from *Phellinus baumii*," *Carbohydrate Polymers*, vol. 268, article 118214, 2021.
- [46] X. Zhao, H. Liu, Y. Wu et al., "Intervention with the crude polysaccharides of *Physalis pubescens* L. mitigates colitis by preventing oxidative damage, aberrant immune responses, and dysbacteriosis," *Journal of Food Science*, vol. 85, no. 8, pp. 2596–2607, 2020.
- [47] W. Yang, P. Zhao, X. Li, L. Guo, and W. Gao, "The Potential Roles of Natural Plant Polysaccharides in Inflammatory Bowel Disease: A Review," *Carbohydrate Polymers*, vol. 277, article 118821, 2022.
- [48] Q. Zou, X. Zhang, X. Liu et al., "Ficus carica polysaccharide attenuates DSS-induced ulcerative colitis in C57BL/6 mice," *Food & Function*, vol. 11, no. 7, pp. 6666–6679, 2020.
- [49] J. A. Batista, D. A. Magalhaes, S. G. Sousa et al., "Polysaccharides derived from *Morinda citrifolia* Linn reduce inflammatory markers during experimental colitis," *Journal of Ethnopharmacology*, vol. 248, article 112303, 2020.
- [50] M. A. Alzoughaibi, "Concepts of oxidative stress and antioxidant defense in Crohn's disease," *World Journal of Gastroenterology: WJG*, vol. 19, no. 39, pp. 6540–6547, 2013.
- [51] G. Jena, P. P. Trivedi, and B. Sandala, "Oxidative stress in ulcerative colitis: an old concept but a new concern," *Free Radical Research*, vol. 46, no. 11, pp. 1339–1345, 2012.
- [52] M. F. Neurath, "Cytokines in inflammatory bowel disease," *Nature Reviews Immunology*, vol. 14, no. 5, pp. 329–342, 2014.
- [53] F. Biasi, F. Leonarduzzi, P. I. Oteiza, and G. Poli, "Inflammatory bowel disease: mechanisms, redox considerations, and therapeutic targets," *Antioxidants & Redox Signaling*, vol. 19, no. 14, pp. 1711–1747, 2013.
- [54] G. Bassotti, E. Antonelli, V. Villanacci, M. P. Dore, and G. M. Pes, "Abnormal gut motility in inflammatory bowel disease: an update," *Techniques in Coloproctology*, vol. 24, no. 4, pp. 275–282, 2020.
- [55] R. Havenaar, "Intestinal health functions of colonic microbial metabolites: a review," *Beneficial Microbes*, vol. 2, no. 2, pp. 103–114, 2011.
- [56] F. Backhed, R. E. Ley, J. L. Sonnenburg, D. A. Peterson, and J. I. Gordon, "Host-bacterial mutualism in the human intestine," *Science*, vol. 307, no. 5717, pp. 1915–1920, 2005.
- [57] D. S. Gray, "The clinical uses of dietary fiber," *American Family Physician*, vol. 51, pp. 419–419, 1995.
- [58] N. M. T. Oliveira, B. B. Luz, V. S. Schneider et al., "Dietary polysaccharides from guavira pomace, a co-product from the fruit pulp industry, display therapeutic application in gut disorders," *Food Research International*, vol. 156, article 111291, 2022.
- [59] H. Y. Pan, C. Q. Zhang, X. Q. Zhang et al., "A galacturonan from *Dioscorea opposita* Thunb. regulates fecal and impairs IL-1 and IL-6 expression in diarrhea mice," *Glycoconjugate Journal*, vol. 39, no. 1, pp. 131–141, 2022.
- [60] D. D. Ren, S. S. Li, H. M. Lin et al., "Panax quinquefolius polysaccharides ameliorate antibiotic-associated diarrhoea induced by lincomycin hydrochloride in rats via the MAPK signaling pathways," *Journal of Immunology Research*, vol. 2022, Article ID 4126273, 19 pages, 2022.
- [61] D. Sacks, B. Baxter, B. C. V. Campbell et al., "Multisociety consensus quality improvement revised consensus statement for endovascular therapy of acute ischemic stroke," *International Journal of Stroke*, vol. 13, no. 6, pp. 612–632, 2018.
- [62] X. Ren, Y. Gamallat, B. Zhang, and Y. Xin, "Enteromorpha and polysaccharides from enteromorpha ameliorate loperamide-induced constipation in mice," *Biomedicine & Pharmacotherapy*, vol. 96, pp. 1075–1081, 2017.
- [63] Y. Lu, J. Zhang, Z. Zhang et al., "Konjac glucomannan with probiotics acts as a combination laxative to relieve constipation in mice by increasing short-chain fatty acid metabolism and 5-hydroxytryptamine hormone release," *Nutrition*, vol. 84, article 111112, 2021.
- [64] K. Li, L. Zhu, H. Li et al., "Structural characterization and rheological properties of a pectin with anti-constipation activity from the roots of *Arctium lappa* L.," *Carbohydrate Polymers*, vol. 215, pp. 119–129, 2019.
- [65] M. R. P. Rao, D. U. Warriar, S. R. Gaikwad, and P. M. Shevate, "Phosphorylation of psyllium seed polysaccharide and its characterization," *International Journal of Biological Macromolecules*, vol. 85, pp. 317–326, 2016.
- [66] T. Li, X. Lu, and X. Yang, "Stachyose-enriched α -galacto-oligosaccharides regulate gut microbiota and relieve constipation in mice," *Journal of Agricultural and Food Chemistry*, vol. 61, no. 48, pp. 11825–11831, 2013.
- [67] E. R. Ceresola, R. Ferrarese, A. Preti, and F. Canducci, "Targeting patients' microbiota with probiotics and natural fibers in adults and children with constipation," *European Review for Medical and Pharmacological Sciences*, vol. 22, no. 20, pp. 7045–7057, 2018.
- [68] J. A. Grondin, Y. H. Kwon, P. M. Far, S. Haq, and W. I. Khan, "Mucins in intestinal mucosal defense and inflammation: learning from clinical and experimental studies," *Frontiers in Immunology*, vol. 11, 2020.
- [69] M. E. V. Johansson, "Mucus layers in inflammatory bowel disease," *Inflammatory Bowel Diseases*, vol. 20, no. 11, pp. 2124–2131, 2014.
- [70] M. K. Jeengar, D. Thummuri, M. Magnusson, V. G. M. Naidu, and S. Uppugunduri, "Uridine ameliorates dextran sulfate sodium (DSS)-induced colitis in mice," *Scientific Reports*, vol. 7, no. 1, 2017.
- [71] X. Xu, S. Lin, Y. Yang et al., "Histological and ultrastructural changes of the colon in dextran sodium sulfate-induced mouse colitis," *Experimental and Therapeutic Medicine*, vol. 20, no. 3, pp. 1987–1994, 2020.
- [72] D. T. Wu, H. Guo, S. Lin, S. C. Lam, L. Z. R. Lin, and W. Qin, "Review of the structural characterization, quality evaluation, and industrial application of Lycium barbarum polysaccharides," *Trends in Food Science & Technology*, vol. 79, pp. 171–183, 2018.
- [73] Y. Nie, Q. Lin, and F. Luo, "Effects of Non-Starch Polysaccharides on Inflammatory Bowel Disease," *International Journal of Molecular Sciences*, vol. 18, no. 7, 2017.
- [74] M. S. Desai, A. M. Seekatz, K. Koropatkin et al., "A dietary fiber-deprived gut microbiota degrades the colonic mucus barrier and enhances pathogen susceptibility," *Cell*, vol. 167, no. 5, pp. 1339–1353.e21, 2016.
- [75] M. H. Chen, K. S. Swanson, G. C. Fahey Jr. et al., "In vitro fermentation of xylooligosaccharides produced from *Miscanthus × giganteus* by human fecal microbiota," *Journal of Agricultural and Food Chemistry*, vol. 64, no. 1, pp. 262–267, 2016.

- [76] P. D. Cani, A. Jacques, M. A. Iglesias et al., "Metabolic endotoxemia initiates obesity and insulin resistance," *Diabetes*, vol. 56, no. 7, pp. 1761–1772, 2007.
- [77] M. Vrese and P. R. Marteau, "Probiotics and prebiotics: effects on diarrhea," in *Bioactive Foods in Promoting Health*, pp. 205–227, Elsevier, 2007.
- [78] S. G. Krylova, L. A. Efimova, E. P. Zueva et al., "Gastroprotective effect of nonstarch polysaccharide calcium pectate under experimental conditions," *Bulletin of Experimental Biology and Medicine*, vol. 145, no. 6, pp. 731–734, 2008.
- [79] Y. Yue, S. Wu, Z. Li et al., "Wild jujube polysaccharides protect against experimental inflammatory bowel disease by enabling enhanced intestinal barrier function," *Food & Function*, vol. 6, no. 8, pp. 2568–2577, 2015.
- [80] L. Shi, Q. Lin, T. Yang et al., "Oral administration of *Lentinus edodes* β -glucans ameliorates DSS-induced ulcerative colitis in mice via MAPK-Elk-1 and MAPK-PPAR γ pathways," *Food & Function*, vol. 7, no. 11, pp. 4614–4627, 2016.
- [81] Y. Zhao, B. Yan, Z. Wang, M. Li, and W. Zhao, "Natural Polysaccharides with Immunomodulatory Activities," *Mini Reviews in Medicinal Chemistry*, vol. 20, no. 2, pp. 96–106, 2020.
- [82] C. Deng, H. Fu, J. Shang, J. Chen, and X. Xu, "Dectin-1 mediates the immunoenhancement effect of the polysaccharide from *Dictyophora indusiata*," *International Journal of Biological Macromolecules*, vol. 109, pp. 369–374, 2018.
- [83] O. W. Meldrum, G. E. Yakubov, G. Gartaula, M. A. McGuckin, and M. J. Gidley, "Mucoadhesive functionality of cell wall structures from fruits and grains: electrostatic and polymer network interactions mediated by soluble dietary polysaccharides," *Scientific Reports*, vol. 7, no. 1, pp. 1–15, 2017.
- [84] M. Yin, Y. Zhang, and H. Li, "Advances in research on immunoregulation of macrophages by plant polysaccharides," *Frontiers in Immunology*, vol. 10, 2019.
- [85] X. Chen, G. Yu, S. Fan et al., "Sargassum fusiforme polysaccharide activates nuclear factor kappa-B (NF- κ B) and induces cytokine production via Toll-like receptors," *Carbohydrate Polymers*, vol. 105, pp. 113–120, 2014.
- [86] H. S. Kim, B. R. Shin, H. K. Lee et al., "Dendritic cell activation by polysaccharide isolated from *Angelica dahurica*," *Food and Chemical Toxicology*, vol. 55, pp. 241–247, 2013.
- [87] X. Zhang, J. Wang, Z. Xu, Z. Li, S. Feng, and H. Lu, "The impact of rhubarb polysaccharides on Toll-like receptor 4-mediated activation of macrophages," *International Immunopharmacology*, vol. 17, no. 4, pp. 1116–1119, 2013.

Review Article

Potential Functional Food Products and Molecular Mechanisms of *Portulaca Oleracea* L. on Anticancer Activity: A Review

Pâmela Gomes de Souza ^{1,2}, Amauri Rosenthal ³, Ellen Mayra Menezes Ayres ^{1,2}, and Anderson Junger Teodoro ^{1,4}

¹Graduate Program in Food and Nutrition, Federal University of the State of Rio de Janeiro (UNIRIO), Av. Pasteur, 296, Urca, Rio de Janeiro, RJ, Brazil

²Laboratory of Sensory and Consumer Science, Graduate Program in Food and Nutrition, Federal University of the State of Rio de Janeiro (UNIRIO), Av. Pasteur, 296, Urca, Rio de Janeiro, RJ, Brazil

³Embrapa Food Technology, Av. das Américas, 29501, Guaratiba, Rio de Janeiro, RJ, Brazil

⁴Department of Nutrition and Dietetics, Universidade Federal Fluminense Rua Mário Santos Braga, 30 Niterói RJ, Brazil

Correspondence should be addressed to Anderson Junger Teodoro; atteodoro@gmail.com

Received 14 June 2022; Revised 1 September 2022; Accepted 10 September 2022; Published 20 September 2022

Academic Editor: Alexandros Georgakilas

Copyright © 2022 Pâmela Gomes de Souza et al. This is an open access article distributed under the Creative Commons Attribution License, which permits unrestricted use, distribution, and reproduction in any medium, provided the original work is properly cited.

Portulaca oleracea Linn. (*P. oleracea* L.) has recently gained attention as a functional food due to the chemical composition of this plant regarding bioactive compounds. The special attention to the use of *P. oleracea* as an ingredient in functional food products is also due to the promotion of sustainable food. It is an unconventional food plant, and its consumption may contribute to preserving biodiversity due to its cultivation in a polyculture system. Food sovereignty may be achieved, among other strategies, with the consumption of unconventional food plants that are more resistant in nature and easily cultivated in small places. *P. oleracea* grows spontaneously and may be found in streets and sidewalks, or it may be cultivated with seeds and cuttings propagation. The culinary versatility of *P. oleracea* opens up opportunities to explore the development of sustainable, functional food products. This mini-review shows that functional food products developed from *P. oleracea* are already available at the research level, but it is expected that more scientific literature focusing on the development of *P. oleracea* functional products with proven anticancer activities may be released in the near future. Polysaccharides, some phenolic compounds, alkaloids, and cerebrosides are associated with the inhibition and prevention of carcinogenesis through *in vitro* and *in vivo* investigations. The anticancer activities of *P. oleracea*, its bioactive compounds, and the involved molecular mechanisms have been reported in the literature. The importance of further elucidating the cancer inhibition mechanisms is in the interest of forthcoming applications in the development of food products with anticancer properties for implementation in the human diet.

1. Introduction

The common purslane (*P. oleracea* L.) is a herbaceous succulent annual plant from the Portulacaceae family, native to the Middle East and India [1, 2]. It may be found on roadsides, gardens, and cultivated areas in the tropical and subtropical regions [3, 4]. There are various cultivars of *P. oleracea* distributed worldwide, mainly with morphological

differences, with the common purslane having green-red stems, obovate leaves, yellow flowers, and single-layered petals, while the ornamental purslane produces flowers of different colors [1]. The stems and leaves have a slightly acid and salty taste and are usually consumed in salads, soups, and stews [5, 6]. It is an edible plant in regions of European, Mediterranean, African, and Asia countries and Australia [6]. In Brazil, *P. oleracea* is known as an “unconventional

food plant”, a term referring to plants that are not part of the usual consumption of most of the population in a particular region, country, or even the planet because basic food is very homogeneous, with the use of few food species [7].

P. oleracea has a high nutritional value and many antioxidant properties due to its phenolic compound and omega-3 fatty acid abundance, particularly α -linolenic acid. It is well-known in traditional Chinese medicine [2]. for its use in diuretic, febrifuge, antiseptic, antispasmodic, and vermifuge treatments [8]. Among its various pharmacological properties are its anti-inflammatory [9], antioxidative [10], renoprotective [11], neuroprotective [12], hepatoprotective [13], and muscle-relaxing effects [14].

Anticarcinogenic activities have been reported for *P. oleracea*. Investigations were carried out to screen the activities for antihepatocellular carcinoma [15, 16], colon cancer [17], glioblastoma multiforme [18], ovarian cancer [19] sarcoma [20], lung cancer [16], anti-cervical [21], gastric cancer [22], and pancreatic cancer [23]. *P. oleracea* contains bioactive compounds with antioxidant properties, act on metastasis and invasion, modulate the immune system, and inhibit tumor formation [19, 24, 25, 4].

Thus, this mini-review aimed to assemble the anticancer effects of bioactive compounds of *P. oleracea*, demonstrating the molecular mechanisms and the potential for the development of functional food products with anticancer properties.

2. The Nutritional Value and Bioactive Compounds of *P. Oleracea*

Proximate analyses of *P. oleracea* components including leaves, seeds, stems, buds, and flowers, have been performed. Ash, fiber, protein, and fat approximate contents of *P. oleracea* leaves as 20.56%, 36.27%, 12.82%, and 3.75%, respectively, are found on a dry matter basis [26]. *P. oleracea* also contains minerals in its leaves with concentration values approximate such as potassium (3710 mg/100 g of dry matter), calcium (2390 mg/100 g), nitrogen (2170 mg/100 g), magnesium (580 mg/100 g), phosphorus (350 mg/100 g), sulfur (200 mg/100 g), iron (32.4 mg/100 g), manganese (5.8 mg/100 g), boron (2.8 mg/100 g), zinc (2 mg/100 g), and copper (1.1 mg/100 g) [26]. This study showed higher levels of potassium, calcium, magnesium, phosphorus, and iron when compared to those of spinach (336 mg/100 g of dry matter, 98 mg/100 g, 82 mg/100 g, 25 mg/100 g, and 0.4 mg/100 g, respectively) [27].

P. oleracea contains high amounts of Omega-3 fatty acids, as discussed by Siriamornpun and Suttajit [28] that found higher levels of Omega-3 fatty acids in fresh leaves, with 523.146 ± 2.29 mg/100 g, while, for stems and flowers, the authors reported 148.87 ± 3.30 mg/100 g and 216.17 ± 1.16 mg/100 g, respectively. Other plants (analysis of leaves in dry matter) contain lower levels of Omega-3 fatty acids than *P. oleracea*, such as mint (194.9 mg/100 g), watercress (179.6 mg/100 g), spinach (129.2 mg/100 g), parsley (124.8 mg/100 g), and broccoli (110.3 mg/100 g) (analysis of leaves in dry matter) [29]. Omega-3 fatty acids may have pharmacological effects such as anti-hyperlipidemic, antimicrobial, anti-inflammatory, neuroprotective and nephropro-

TECTIVE activities [3, 30, 31, 32, 11]. *P. oleracea* also contains high levels of tocopherols, vitamin A, β -carotene and ascorbic acid [3, 32–34]. Antimicrobial and antioxidant activities were related to these compounds [3, 33].

High concentrations of oxalic acid have also been detected in *P. oleracea*. The intake of oxalic acid provided by the diet with *P. oleracea* may form complexes with minerals such as calcium and iron (insoluble salts) or sodium, magnesium, and potassium (soluble salts), reducing their bioavailability and possibly leading to the development of kidney stones through the formation of calcium oxalate crystals [35]. Thus, consumption of *P. oleracea* should be moderated by individuals with a propensity to develop kidney stones. Amounts of 23.45 ± 0.45 g, 5.58 ± 0.18 g, and 9.09 ± 0.12 g of total oxalates per kilogram of fresh weight oxalates were obtained in fresh leaves, stems, and buds, respectively, with 75.0% being soluble oxalates in the stems and buds, and only 27.5% in the leaves [36]. The authors reported a 66.7% reduction ($p < 0.001$) of soluble oxalates after cooking the leaves for a short time, discarding the water, and pickling them with white vinegar [36]. Some other bioactive compounds from secondary metabolism of *P. oleracea* such as flavonoids, alkaloids, terpenoids and their pharmacological activity can be seen in Table 1.

Flavonoids (a class of phenolic compounds) in *P. oleracea* were associated with anti-fertility, antimicrobial, antioxidant and antidiabetic effects [37–40]. Combined effects of polyunsaturated fatty acids, flavonoids and polysaccharides on hypoglycaemic, hypolipidaemic and insulin resistance reducer effects through ingestion of *P. oleracea* seeds in clinical test with humans were observed [40]. Other phenolic compounds (Polyphenols and phenolic acids) in *P. oleracea* have antioxidant and antimutagenic effects [41–43].

Other bioactive compounds with pharmacological importance in *P. oleracea* are alkaloids and terpenes. Anticancer, anti-inflammatory and antioxidant effects were described for alkaloids found in this plant while hepatoprotective, antibacterial, antifungal and anti-hypoxia effects were described for terpenes of *P. oleracea* [44–48].

3. Potential Antioxidant of the *P. Oleracea*

This plant is rich in antioxidants such as vitamin A, tocopherols, ascorbic acid, beta-carotene, and phenolic compounds [33, 49]. Beta-carotene was found in *P. oleracea* with content ranging from 21 μ g/g to 30 μ g/g of fresh mass in leaves and 3.6 μ g/g to 6.5 μ g/g of fresh mass in stems [50]. The antioxidant potential was measured at different growth stages (15, 30, 45, and 60 days) of aerial parts of *P. oleracea* [49]. The total phenolic content (TPC) for the young shoots at 15 days was significantly lower than at 30, 45, and 60 days, while the ascorbic acid content (AAC) did not show a significant decrease from the developing to the mature stage. According to the study, the IC50 value of 1,1-diphenyl-2-picrylhydrazyl (DPPH) free radical scavenging activity ranged from 1.30 ± 0.04 mg/ml (60 days) to 1.71 ± 0.04 mg/ml (15 days), while the ascorbic acid equivalent antioxidant content (AEAC) values ranged from 229.5 ± 7.9 mg AA/100 g (15 days) to 319.3 ± 8.7 mg AA/100 g (60 days), the TPC varied

TABLE 1: Some classes of bioactive compounds from secondary metabolism of *P. oleracea* and their pharmacological activity.

Compounds	Plant structure	Form (fresh or dry)	Pharmacological activity	References
Flavonoids	Aerial part	Dry	Antifertility	[37]
	Aerial part	Dry	Antimicrobial	[38]
	Leaves	Fresh	Antioxidant	[39]
	Seeds	Dry	Antidiabetic	[40]
Polyphenols	Leaf, stem and flower	Dry	Antioxidant	[41]
	Whole plant	Fresh	Antimutagenic	[42]
Phenolic acids	Aerial parts	Dry	Antioxidant	[43]
	Aerial part	Dry	Anticancer	[44]
Alkaloids	Whole plant	Fresh	Anti-inflammatory	[45]
	Whole plant	Dry	Antioxidant	[46]
Terpenes	Whole plant	Dry	Hepatoprotective, antibacterial and antifungal	[47]
	Aerial part	Dry	Anti-hypoxia	[48]

from 174.5 ± 8.5 mg GAE/100 g (15 days) to 348.5 ± 7.9 mg GAE/100 g (60 days), the AAC varied from 60.5 ± 2.1 mg/100 g (60 days) to 86.5 ± 3.9 mg/100 g (15 days), and the ferric reducing antioxidant power (FRAP) ranged from 1.8 ± 0.1 mg GAE/g (15 days) to 4.3 ± 0.1 mg GAE/g (60 days). Thus, mature plants (60 days) of *P. oleracea* had higher TPC and antioxidant activities than immature plants.

The dry weights of the samples (leaves, flowers, and stems) from two different locations were investigated for potential antioxidant activity by Silva and Carvalho [41], who found that stems had a higher total phenolic content and total antioxidant activity than the flowers and leaves. The oil from seeds, leaves, and stems of *P. oleracea* were analyzed and found that the peroxide value was significantly higher for seed oil and the lowest for stem oil [51]. Furthermore, the highest ascorbic acid content was found for *P. oleracea* seed oil (41.67%), followed by leaf oil (32.29%), and the highest DPPH was obtained for leaf oil (12.55%), followed by seed oil (2.05%). Values for lettuce (IC₅₀ = 17.07 mg/ml), artichoke (IC₅₀ = 18.14 mg/ml), turmeric (IC₅₀ = 21.14 mg/ml), spinach (IC₅₀ = 22.87 mg/ml), and escarole (IC₅₀ = 32.2 mg/ml) were reported by Tiveron et al. [52], showing that *P. oleracea* presents the lowest IC₅₀ necessary to reduce 50% of DPPH free radicals.

4. Functional Food Products and *P. Oleracea*

The *P. oleracea* plant may be used as an ingredient in functional food products due to its nutritional value and bioactive compounds that will be incorporated into the formulations.

The use of the *P. oleracea* plant as food may not only enhance the nutrients and bioactive composition of functional products but also influence their sensory and technological characteristics. Although it is well-known that sensory acceptance by consumers is essential for a product's commercial success on the market, few studies in the literature have reported the application of *P. oleracea* in products and its performance or the sensory profile of such products.

Regarding the technological aspect, the incorporation of the durum wheat flour with 5% of *P. oleracea* to bread resulted in the improvement of the rheological characteristics, an increase in antioxidant properties, and a decrease in the Omega-6-to-Omega-3 ratio, which is beneficial for human health, in addition to improving the sensorial quality [53].

The durum wheat spaghetti fortified with 10% of *P. oleracea*, a potential functional food, was appreciated by consumers. It showed a high concentration of α -linolenic acids (Omega-3), total phenolic compounds, and antioxidant properties, so that, considering 100 g of pasta per day, it is possible to obtain 75 mg of essential linoleic acid and 9 mg of linolenic acid, along with a four-fold increase in total phenolic compounds [54]. The Omega-3 fatty acids can also inhibit carcinogenesis and slow tumor growth, as demonstrated by *in vitro*, *in vivo*, and clinical investigations [55].

The analysis of bread incorporated with four different concentrations of *P. oleracea* powder (0%, 5%, 10%, and 15%) showed increasing water absorption capacity, stability under the mixer, and softening levels as the *P. oleracea* powder concentration in the samples increased. The protein, fat, total ash, moisture, and fiber contents also increased along with the *P. oleracea* concentrations [56]. However, the bread with 15% of *P. oleracea* powder showed a decreased farinograph quality number and presented the lowest scores for sensory properties and color, taste, texture, and overall liking. The optimized formulation containing 10% of *P. oleracea* powder had the highest acceptance.

P. oleracea has also been used to produce powder mixtures with two other plant species, *Amaranthus hybridus* L. and *Chenopodium berlandieri* L. The powder mixtures containing *P. oleracea* showed more significant contents of phenolic compounds, with an increase in the antioxidant activity [57].

Another innovative functional product assessed was a fermented *P. oleracea* juice added with a selected lactic acid bacteria. Results demonstrated an increase in total antioxidants, preserved vitamin C, A, and E levels, and increased contents of vitamin B2 and phenolic compounds. In addition, decreased levels of pro-inflammatory mediators and

TABLE 2: Bioactive compounds of *P. oleracea*, types of extracts, and molecular mechanisms for cancer inhibition.

<i>In vitro</i>	Experimental model	<i>In vivo</i>	Compounds	Types of extract	Types of cancer inhibited	Mechanisms and results	References
		Rats	Polysaccharides	Aqueous extract	Ovarian	Scavenge superoxide anion, (DPPH-), nitric oxide, and hydroxyl radicals Inhibit RBC hemolysis	[19]
	Human cancer cell lines SF-268, NCI-H460, K-562, SGC-7901, and SMMC-7721		Homoisoflavonoids	Hydroalcoholic extract		Spleen, thymocyte, T and B lymphocyte proliferation	[61]
		Mice	Polysaccharides	Aqueous extract	Cervical	Sub-G1 phase cell cycle arrest, triggering DNA damage Inducing apoptosis	[21]
	Treatment of HeLa cell	Mice	Polysaccharides	Aqueous extract		Inhibit the growth of transplantable sarcoma 180 Increase in the number of white blood cells (WBC) and CD4+ T-lymphocytes	[20]
		Rats	Polysaccharides	Aqueous extract	Gastric	Increase in the CD4 ⁺ /CD8 ⁺ ratio Interleukin-2 (IL-2), interleukin-4 (IL-4), and tumor necrosis factor-alpha (TNF- α) was enhanced Provide dose-dependent protection against MNGG-induced oxidative injury by enhancing SOD, CAT, GSH-Px	[22]
	Human lung (K562 and A549) and breast (MCF-7 and MDA-MB-435) cancer cell lines		Alkaloids	Hydroalcoholic extract	Lung Breast	Moderate cytotoxic activities against A549 and weak cytotoxic activities against K562. The compounds showed low cytotoxic activity against MCF-7 and MDA-MB-435 cells.	[54]
	Human hepatocellular carcinoma cells			Seed alcoholic extract	Hepatocellular	Significantly reduced the cell viability of HepG2.	[15]
	The uterine cervical carcinoma (U14) cell line		Polysaccharides	Aqueous extract	Cervical	Upregulated the expression of CD80, CD86, CD83 Increase in IL-12, TLR-4, Decrease in IL-10	[29]
	Human HL60 cell line		Portulacerebroside A	Aqueous extract	Leukemia	Mitochondrial membrane potential ROS accumulated Increase in RNA expressions and protein levels of Bax/Bcl-2, caspase-3, and caspase-9	[49]
	HepG2 and A-549 cell lines			Seed oil	Liver Lung	ERK1/2, JNK1/2 and p38 MAPK pathway were blocked Significant cytotoxicity and inhibition of growth of the liver cancer (HepG2) and lung cancer (A-549) cell lines	[20]
	Human liver cancer HCCLM3 cells		Portulacerebroside A	Aqueous extract	Liver	Increase in RNA and protein expression levels of TIMP-2 and nm23-H1 Inhibition of the mRNA expression of MTA1, MMP-2, and MMP-9	[23]

TABLE 2: Continued.

<i>In vitro</i>	Experimental model	<i>In vivo</i>	Compounds	Types of extract	Types of cancer inhibited	Mechanisms and results	References
	Cervical cancer HeLa cells, esophageal cancer Eca-109 cells and breast cancer MCF-7 cells			Seed oil	Cervical Esophageal Breast	Suppression of the protein expression of MTA1, RhoA, Rac1/Cdc42, MMP-2, but not RhoC and MMP-9 Stronger inhibitory effect on the proliferation of MCF-7 cells and significantly inhibited the proliferation of HeLa cells and Eca-109 cells	[51]
	PANC-1 cancer cell line			Aqueous extract	Pancreatic	Significant effect on apoptosis in pancreatic cell line and high expression of P53 and reduction of CDK gene expression	[23]
	Human colon adenocarcinoma (HCT-15) and normal (Vero) cell line			Chloroform extract	Colon adenocarcinoma	Chloroform extract does not have cytotoxic activity and was not safe to normal Vero cell line.	[67]
	Colon cancer cells (HT-29) and HT-29 cancer stem cells			Ethyl alcohol extract	Colon Stem cells	Inhibited the proliferation of both HT-29 cancer cells and HT-29 cancer stem cells Significantly decreased the expression of the Notch1 and β -catenin genes in both cell types Decrease HeLa cell proliferation	[52]
	The human cervical cancer HeLa cells.			Aqueous extract	Cervical	Upregulate Bax level and downregulate Bcl-2 level in a concentration-dependent manner Inhibit the protein expression levels of TLR4, MyD88, TRAF6, AP-1 and NF- κ B subunit P65 Reduce the production of cytokine/chemokine	[50]
	The mouse cervical carcinoma U14 cells			Aqueous extract	Intestinal	Dendritic cell (DC) apoptosis in U14-bearing mice Increase intestinal DC survival Stimulate the TLR4-PI3K/AKT-NF- κ B signaling pathway	[48]
	Human glioblastoma cancer cell line (U-87)			Hydroethanolic extract		Cytotoxicity and apoptogenic effects Anti-NF- κ B activity along with two upstream ROS and NO mechanisms	[17]

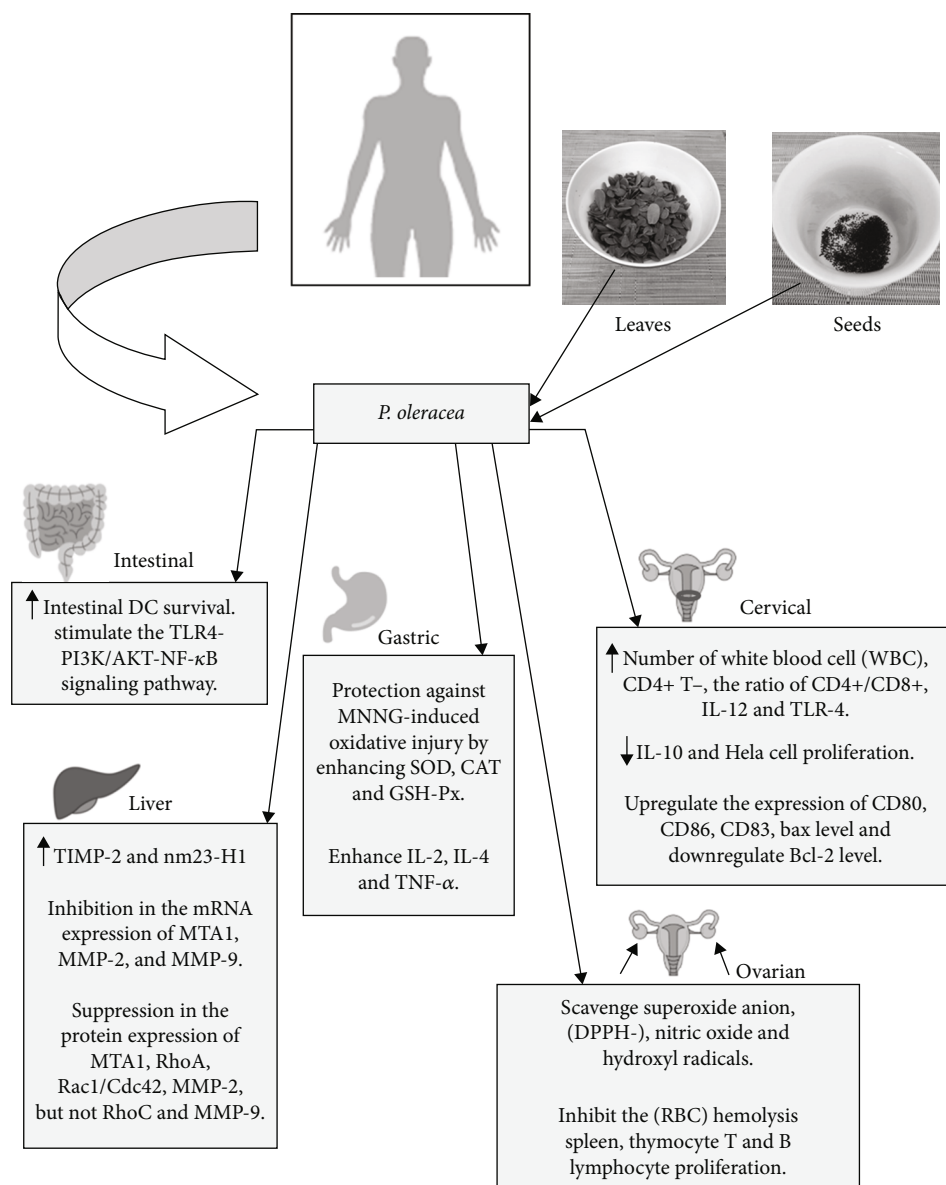


FIGURE 1: Some possible mechanisms of *P. oleracea* for anticancer activity.

reactive oxygen species were observed, with a consequent increase in the restorative characteristics of the use of *P. oleracea* juice for intestinal inflammation and epithelial injury [58].

The combination of yogurt or coconut plant extract or coconut cream with fresh leaves of *P. oleracea* reduced the overall oxalate content by simple dilution. The soluble oxalate content decreased from 53.0% to 10.7% when *P. oleracea* leaves were added to yogurt. However, the coconut plant extract and coconut cream had no effect on the percentage of soluble oxalate content but provided the mixture with an acceptable flavor [59].

The addition of fresh purslane leaves (ranging from 1% to 10%, w/w) to tomato sauces resulted in a decrease of total soluble solids from 9.57°Bx to 9.20°Bx, beneficially impacting sugar reduction. On the other hand, the amount of protein significantly increased from 0.12% to 1.83% from the lowest to the highest concentrations, respectively [60].

5. Bioactive Compounds of *P. Oleracea* on Anticancer Activity

P. oleracea presents phytochemicals and nutrients associated with anticarcinogenic properties. The 12% reduction in the activity of the mutagenic nitrosation mixture may be attributed to the ascorbic acid (vitamin C), α and β -carotene, chlorophyll, and polyphenols of the *P. oleracea* extract obtained through a standard juice extractor [42].

Phenolic compounds such as kaempferol and apigenin from a hydroethanolic extract of *P. oleracea* have effects *in vitro* against human glioma cells, and homoisoflavonoids showed *in vitro* selective cytotoxic activity for SF-268, NCI-H460, and SGC-7901 cell lines, as shown Table 2 [18, 61].

Polysaccharides from *P. oleracea* act on free radicals through the antioxidant mechanism, modulating the immune system, which may be preventive and therapeutic

in rat ovarian and gastric cancer and mouse cervical cancer and sarcomas, as shown Table 2 [19–22, 62].

Another bioactivity from *P. oleracea* is portulacacerebroside A, a cerebroside compound that suppresses the invasion and metastasis of liver cancer HCCLM3 cells and acts in leucocythemia treatment are shown in Table 2 [24, 63].

Polysaccharides showed activity against ovarian cancer by inhibiting the red blood cell (RBC) hemolysis in the spleen, thymocyte, and T and B lymphocyte proliferation [19]. These compounds also act against cervical cancer through Sub-G1 phase cell cycle arrest triggering DNA damage, inhibit the growth of transplantable sarcoma 180, increase the number of white blood cells (WBC), CD4+ T-, the CD4+/CD8+ ratio, IL-12, and TLR-4, decrease IL-10 and HeLa cell proliferation, reduce the production of cytokine/chemokine and the expression levels of CD80, CD86, CD83, Bax, and downregulate the Bcl-2 level in a concentration-dependent manner. In addition, polysaccharides inhibit the protein expression levels of TLR4, myeloid differentiation primary response 88 (MyD88), TNF receptor associated Factor 6 (TRAF6), activator protein-1 (AP-1), and factor nuclear kappa B (NF- κ B) subunit P65 [20, 21, 63, 64].

In gastric cancer, interleukins (IL-2 and IL-4) and TNF- α were enhanced by polysaccharides that also provide dose-dependent protection against N-methyl-N'-nitro-N-nitrosoguanidine (MNNG) induced oxidative injury by enhancing Superoxide dismutase (SOD), catalase (CAT), and glutathione (GSH-Px) [22]. In addition to acting against ovarian, gastric, and cervical cancer, polysaccharides also work against intestinal cancer by stimulating the TLR4-PI3K/AKT-NF- κ B signaling pathway and Anti-NF- κ B activity along with two upstream ROS and NO mechanisms [18, 62], showing the importance of studying these molecules in *P. oleracea* matrices.

The cerebroside compound, Portulacacerebroside A, affects leukemia and cervical, liver, esophageal, breast, and colon cancer and cancer stem cells [16, 24, 63, 65, 66]. Some mechanisms involved with Portulacacerebroside A have increased RNA expressions and protein levels of Bax/Bcl-2, caspase-3, and caspase-9, protein expression levels of TIMP-2 and nm23-H1, inhibition of the mRNA expression of MTA1, MMP-2, and MMP-9, RhoA, Rac1/Cdc42, MMP-2, and downregulation of the expression of the Notch1 and β -catenin genes.

Alkaloids inhibited lung and breast cancer through moderate cytotoxic activities against A549, weak cytotoxic activities against K562, and low cytotoxic activity against MCF-7 and MDA-MB-435 cells.

Some possible mechanisms of *P. oleracea* for anticancer activity are represented in Figure 1. The bioactivity of *P. oleracea* and the potential to develop new products from this underused plant in some regions deserve attention regarding its valorization as a functional food and its pharmacological properties. Different anticancer mechanisms of *P. oleracea* were explored and reported in this review. Aqueous extracts, seed oil, and hydroethanolic extracts present cytotoxicity to cancer cell lines while chloroform extract does not have cytotoxic activity [67]. Further studies will be needed to determine anticancer activity in particular food matrices and beverages.

6. Conclusion

The *P. oleracea* plant may be promising for developing and innovating potential functional food products. The high levels of antioxidants such as phenolic compounds, carotenoids, and other nutrients such as minerals and Omega-3 fatty acids are supported by functional food studies. Research has indicated the anticancer activity of *P. oleracea* extracts. Polysaccharides, some phenolic compounds, alkaloids, and cerebroside detected in *P. oleracea* and contained in aqueous extracts, seed oil, and hydroethanolic extracts are associated with inhibition and prevention of carcinogenesis. However, more studies are needed to prove the anticancer activity of food products containing *P. oleracea* as an ingredient to promote health benefits to the consumers.

Data Availability

The data used to support the findings of this study are included within the article.

Conflicts of Interest

The authors declare that there is no conflict of interest.

Acknowledgments

This project was funded by the Brazilian National Council for Scientific and Technological Development (142514/2020-9) and the Coordination for the Improvement of Higher Education Personnel.

References

- [1] M. Alam, A. S. Juraimi, M. Y. Rafii et al., "Genetic improvement of purslane (*Portulaca oleracea* L.) and its future prospects," *Molecular Biology Reports*, vol. 41, no. 11, pp. 7395–7411, 2014.
- [2] M. Iranshahy, M. Javadi, M. Iranshahi et al., "A review of traditional uses, phytochemistry and pharmacology of *Portulaca oleracea* L.," *Journal of Ethnopharmacology*, vol. 205, pp. 158–172, 2017.
- [3] M. K. Uddin, A. S. Juraimi, M. S. Hossain, M. A. U. Nahar, M. E. Ali, and M. M. Rahman, "Purslane weed (*Portulaca oleracea*): A prospective plant source of nutrition, omega-3 fatty acid, and antioxidant attributes," *The Scientific World Journal*, vol. 2014, Article ID 951019, 6 pages, 2014.
- [4] V. B. Rahimi, F. Ajam, H. Rakhshandeh, and V. R. Askari, "A pharmacological review on *Portulaca oleracea* L.: focusing on anti-inflammatory, anti-oxidant, immuno-modulatory and antitumor activities," *Korean Pharmacopuncture Institute*, vol. 22, no. 1, pp. 7–15, 2019.
- [5] Y. Y. Lim and E. P. L. Quah, "Antioxidant properties of different cultivars of *Portulaca oleracea*," *Food Chemistry*, vol. 103, no. 3, pp. 734–740, 2007.
- [6] B. Nemzer, F. Al-TaHER, and N. Abshiru, "Phytochemical composition and nutritional value of different plant parts in two cultivated and wild purslane (*Portulaca oleracea* L.) genotypes," *Food Chemistry*, vol. 320, article 126621, 2020.

- [7] V. F. Kinnup and H. Lorenzi, *Plantas Alimentícias Não-Convencionais (PANC) no Brasil*, Instituto Plantarum de Estudos da Flora, São Paulo, 2014.
- [8] L. Xiang, X. Dongming, W. Wang, R. Wang, Y. Ding, and L. Du, "Alkaloids from *Portulaca oleracea* L.," *Phytochemistry*, vol. 66, no. 21, pp. 2595–2601, 2005.
- [9] K. Chan, M. W. Islam, M. Kamil et al., "The analgesic and anti-inflammatory effects of *Portulaca oleracea* L. subsp. *sativa* (Haw.) Celak," *Journal of Ethnopharmacology*, vol. 73, no. 3, pp. 445–451, 2000.
- [10] M. A. Dkhil, A. E. A. Moniem, S. Al-Quraishy, and R. A. Saleh, "Antioxidant effect of purslane (*Portulaca oleracea*) and its mechanism of action," *Journal of Medicinal Plants Research*, vol. 5, no. 9, pp. 1589–1593, 2011.
- [11] W. Hozayen, M. Bastawy, and H. Elshafeey, "Effects of aqueous purslane (*Portulaca Oleracea*) extract and fish oil on gentamicin nephrotoxicity in albino rats," *Nature and Science*, vol. 9, no. 2, pp. 47–62, 2011.
- [12] C. Q. Wang and G. Q. Yang, "Betacyanins from *Portulaca oleracea* L. ameliorate cognition deficits and attenuate oxidative damage induced by D-galactose in the brains of senescent mice," *Phytomedicine*, vol. 17, no. 7, pp. 527–532, 2010.
- [13] A. Eidi, P. Mortazavi, J. Z. Moghadam, and M. Mardani, "Hepatoprotective effects of *Portulaca oleracea* extract against CCl₄-induced damage in rats," *Pharmaceutical Biology*, vol. 53, no. 7, pp. 1042–1051, 2015.
- [14] M. Gonnella, M. Charfeddine, G. Conversa, and P. Santamaria, "Purslane: a review of its potential for health and agricultural aspects," *European Journal of Plant Science and Biotechnology*, vol. 4, no. 1, pp. 131–136, 2010.
- [15] N. N. Farshori, E. S. S. Al-Sheddi, M. M. Al-Oqail, J. Musarrat, A. A. Al-Khedhairi, and M. A. Siddiqui, "Cytotoxicity assessments of *Portulaca oleracea* and *Petroselinum sativum* seed extracts on human hepatocellular carcinoma cells (HepG2)," *Asian Pacific Journal of Cancer Prevention*, vol. 15, no. 16, pp. 6633–6638, 2014.
- [16] E. S. Al-Sheddi, N. N. Farshori, M. M. Al-Oqail, J. Musarrat, A. A. Al-Khedhairi, and M. A. Siddiqui, "*Portulaca oleracea* seed oil exerts cytotoxic effects on human liver cancer (HepG2) and human lung cancer (A-549) cell lines," *Asian Pacific Journal of Cancer Prevention*, vol. 16, no. 8, pp. 3383–3387, 2015.
- [17] G. P. Asnani and C. R. Kokare, "In vitro and in vivo evaluation of colon cancer targeted epichlorohydrin crosslinked *Portulaca*-alginate beads," *Biomolecular Concepts*, vol. 9, no. 1, pp. 190–199, 2018.
- [18] V. B. Rahimi, S. H. Mousavi, S. Haghghi, S. Soheili-Far, and V. R. Askari, "Cytotoxicity and apoptogenic properties of the standardized extract of *Portulaca oleracea* on glioblastoma multiforme cancer cell line (U-87): a mechanistic study," *EXCLI Journal*, vol. 18, pp. 165–186, 2019.
- [19] C. Youguo, S. Zongji, and C. XiaoPing, "Evaluation of free radicals scavenging and immunity-modulatory activities of Purslane polysaccharides," *International Journal of Biological Macromolecules*, vol. 45, no. 5, pp. 448–452, 2009.
- [20] H. Shen, G. Tangg, G. Zeng et al., "Purification and characterization of an antitumor polysaccharide from *Portulaca oleracea* L.," *Carbohydrate Polymers*, vol. 93, no. 2, pp. 395–400, 2013.
- [21] R. Zhao, X. Gao, Y. Cai et al., "Antitumor activity of *Portulaca oleracea* L. polysaccharides against cervical carcinoma in vitro and in vivo," *Carbohydrate Polymers*, vol. 96, no. 2, pp. 376–383, 2013.
- [22] Y. Li, Y. Hu, S. Shi, and L. Jiang, "Evaluation of antioxidant and immuno-enhancing activities of Purslane polysaccharides in gastric cancer rats," *International Journal of Biological Macromolecules*, vol. 68, pp. 113–116, 2014.
- [23] S. Alipour, L. Pishkar, and V. Chaleshi, "Cytotoxic effect of *Portulaca Oleracea* extract on the regulation of CDK1 and P53 gene expression in pancreatic cancer cell line," *Nutrition and Cancer*, vol. 74, no. 5, pp. 1792–1801, 2022.
- [24] Q. Ji, G. Y. Zheng, W. Xia et al., "Inhibition of invasion and metastasis of human liver cancer HCCLM3 cells by portulacerebroside a," *Pharmaceutical Biology*, vol. 53, no. 5, pp. 773–780, 2015.
- [25] V. R. Askari, S. A. R. Rezaee, K. Abnous, M. Iranshahi, and M. H. Boskabady, "The influence of hydro-ethanolic extract of *Portulaca oleracea* L. on Th₁/Th₂ balance in isolated human lymphocytes," *Journal of Ethnopharmacology*, vol. 194, pp. 1112–1121, 2016.
- [26] D. C. S. Oliveira, C. Wobeto, M. R. Zanuzo, and C. Severgnini, "Composição mineral e teor de ácido ascórbico nas folhas de quatro espécies olerícolas não-convencionais," *Horticultura Brasileira*, vol. 31, no. 3, pp. 472–475, 2013.
- [27] NEPA/UNICAMP, *Tabela Brasileira de Composição de Alimentos*, NEPA/UNICAMP, Campinas, 2011.
- [28] S. Siriamornpun and M. Suttajit, "Microchemical components and antioxidant activity of different morphological parts of Thai wild purslane (*Portulaca oleracea*)," *Weed Science*, vol. 58, no. 3, pp. 182–188, 2010.
- [29] C. Pereira, D. Li, and A. J. Sinclair, "The alpha-linolenic acid content of green vegetables commonly available in Australia," *International Journal for Vitamin and Nutrition Research*, vol. 71, no. 4, pp. 223–228, 2001.
- [30] A. P. Simpopoulos, "Omega-3 fatty acids and antioxidants in edible wild plants," *Biological Research*, vol. 37, no. 2, pp. 263–277, 2004.
- [31] F. Naem and S. H. Khan, "Purslane (*Portulaca oleracea* L.) as phytochemical substance—a review," *Journal of Herbs, Spices and Medicinal Plants*, vol. 19, no. 3, pp. 216–232, 2013.
- [32] R. Zhao, T. Zhang, H. Zhao, and Y. Cai, "Effects of *Portulaca oleracea* L. Polysaccharides on phenotypic and functional maturation of murine bone marrow derived dendritic cells," *Nutrition and Cancer*, vol. 67, no. 6, pp. 987–993, 2015.
- [33] S. Petropoulos, A. Karkanis, N. Martins, and I. C. F. R. Ferreira, "Phytochemical composition and bioactive compounds of common purslane (*Portulaca oleracea* L.) as affected by crop management practices," *Trends in Food Science & Technology*, vol. 55, pp. 1–10, 2016.
- [34] M. M. S. Viana, L. A. Carlos, E. C. Silva, S. M. F. Pereira, D. B. Oliveira, and M. L. V. Assis, "Composição fitoquímica e potencial antioxidante de hortaliças não convencionais," *Horticultura Brasileira*, vol. 33, no. 4, pp. 504–509, 2015.
- [35] U. R. Palaniswamy, B. Bible, and R. J. McAvoy, "OXALIC acid concentrations in purslane (*Portulaca oleracea* L.) is altered by the stage of harvest and the nitrate to ammonium ratios in hydroponics," *Acta Horticulturae*, vol. 629, no. 629, pp. 299–305, 2004.
- [36] G. Y. Poeydomenge and G. P. Savage, "Oxalate content of raw and cooked purslane," *Journal of Food, Agriculture and Environment*, vol. 5, no. 1, pp. 124–128, 2007.
- [37] H. B. Nayaka, R. L. Londonkar, M. K. Umesh, and A. Tukappa, "Antibacterial attributes of apigenin, isolated from *Portulaca oleracea* L.," *International Journal of Bacteriology*, vol. 2014, Article ID 175851, 8 pages, 2014.

- [38] Y.-K. Du, L. Jing, X.-M. Li et al., "Flavonoids extract from *Portulaca oleracea* L. induce Staphylococcus aureus death by apoptosislike pathway," *International Journal of Food Properties*, vol. 20, no. 1, pp. 534–542, 2017.
- [39] V. Scari, M. R. Loizzo, R. Tundis, A. Mincione, and T. M. Pellicano, "Portulaca oleracea L. (purslane) extracts display antioxidant and hypoglycaemic effects," *Journal of Applied Botany and Food Quality*, vol. 91, pp. 39–46, 2018.
- [40] M.-I. K. El-Sayed, "Effects of *Portulaca oleracea* L. seeds in treatment of type-2 diabetes mellitus patients as adjunctive and alternative therapy," *Journal of Ethnopharmacology*, vol. 137, no. 1, pp. 643–651, 2011.
- [41] R. Silva and I. S. Carvalho, "In vitro antioxidant activity, phenolic compounds and protective effect against DNA damage provided by leaves, stems and flowers of *Portulaca oleracea* (purslane)," *Natural Product Communications*, vol. 9, no. 1, pp. 45–50, 2014.
- [42] S. Caballero-Salazar, R. Riverón-Negrete, M. G. Ordáz-Tellez, F. Abdullaev, and J. J. Espinosa-Aguirre, "Evaluation of the antimutagenic activity of different vegetable extracts using an *In Vitro* screening test," *Proceedings of the Western Pharmacology Society*, vol. 45, pp. 101–103, 2022.
- [43] N. Erkan, "Antioxidant activity and phenolic compounds of fractions from *Portulaca oleracea* L.," *Food Chemistry*, vol. 133, no. 3, pp. 775–781, 2012.
- [44] J. L. Tian, X. Liang, P. Y. Gao et al., "Two new alkaloids from *Portulaca oleracea* and their cytotoxic activities," *Journal of Asian Natural Products Research*, vol. 16, no. 3, pp. 259–264, 2014.
- [45] Y. Meng, Z. Ying, Z. Xiang et al., "The anti-inflammation and pharmacokinetics of a novel alkaloid from *Portulaca oleracea* L.," *Journal of Pharmacy and Pharmacology*, vol. 68, no. 3, pp. 397–405, 2016.
- [46] Z. Yang, C. Liu, L. Xiang, and Y. Zheng, "Phenolic alkaloids as a new class of antioxidants in *Portulaca oleracea*," *Phytotherapy Research*, vol. 23, no. 7, pp. 1032–1035, 2009.
- [47] E. S. Elkhayat, S. R. M. Ibrahim, and M. A. Aziz, "Portulene, a new diterpene from *Portulaca oleracea* L.," *Journal of Asian Natural Products Research*, vol. 10, no. 11, pp. 1039–1043, 2008.
- [48] C.-J. Chen, W.-Y. Wang, X.-L. Wang et al., "Anti-hypoxic activity of the ethanol extract from *Portulaca oleracea* in mice," *Journal of Ethnopharmacology*, vol. 124, pp. 246–250, 2009.
- [49] M. K. Uddin, A. S. Juraimi, M. E. Ali, and M. R. Ismail, "Evaluation of antioxidant properties and mineral composition of purslane (*Portulaca oleracea* L.) at different growth stages," *International Journal of Molecular Sciences*, vol. 13, no. 8, pp. 10257–10267, 2012.
- [50] L. Liu, P. Howe, Y. F. Zhou, Z. Q. Xu, C. Hocart, and R. Zhang, "Fatty acids and β -carotene in Australian purslane (*Portulaca oleracea*) varieties," *Journal of Chromatography A*, vol. 893, no. 1, pp. 207–213, 2000.
- [51] M. Desta, A. Molla, and Z. Yusuf, "Characterization of physico-chemical properties and antioxidant activity of oil from seed, leaf and stem of purslane (*Portulaca oleracea* L.)," *Biotechnology Reports*, vol. 27, pp. 1–5, 2020.
- [52] A. P. Tiveron, P. S. Melo, K. B. Bergamaschi, T. M. F. S. Vieira, M. A. B. Regitano-d'Arce, and S. M. Alencar, "Antioxidant activity of Brazilian vegetables and its relation with phenolic composition," *International Journal of Molecular Sciences*, vol. 13, no. 7, pp. 8943–8957, 2012.
- [53] M. G. Melilli, V. D. Stefano, F. Sciacca et al., "Improvement of fatty acid profile in durum wheat breads supplemented with *Portulaca oleracea* L. quality traits of purslane-fortified bread," *Food*, vol. 9, no. 6, 2020.
- [54] M. G. Melilli, A. Pagliaro, S. Scandurra, C. Gentile, and V. di Stefano, "Omega-3 rich foods: durum wheat spaghetti fortified with *Portulaca oleracea*," *Food Bioscience*, vol. 37, article 100730, 2020.
- [55] J. Y. Lee, T. B. Sim, J. E. Lee, and H. K. Na, "Chemopreventive and chemotherapeutic effects of fish oil derived omega-3 polyunsaturated fatty acids on colon carcinogenesis," *Clinical Nutrition Research*, vol. 6, no. 3, pp. 147–160, 2017.
- [56] L. N. Delvarianzadeh, M. Nafchi, and H. Ebrahimi, "Physicochemical, rheological, and sensory evaluation of voluminous breads enriched by purslane (*Portulaca oleracea* L.)," *Italian Journal of Food Science*, vol. 32, pp. 815–830, 2020.
- [57] Y. O. Santiago-Saenz, C. U. López-Palestina, J. Gutiérrez-Tlahque, R. Monroy-Torres, J. M. Pinedo-Espinoza, and A. D. Hernández-Fuentes, "Nutritional and functional evaluation of three powder mixtures based on mexican quelites: alternative ingredients to formulate food supplements," *Food Science and Technology*, vol. 40, no. 4, pp. 1029–1037, 2020.
- [58] R. Di Cagno, P. Filannino, O. Vincentini, V. Cantatore, I. Cavoski, and M. Gobbetti, "Fermented *portulaca oleracea* L. juice: a novel functional beverage with potential ameliorating effects on the intestinal inflammation and epithelial injury," *Nutrients*, vol. 11, no. 2, p. 248, 2019.
- [59] A. G. Moreau and G. P. Savage, "Oxalate content of purslane leaves and the effect of combining them with yoghurt or coconut products," *Journal of Food Composition and Analysis*, vol. 22, no. 4, pp. 303–306, 2009.
- [60] L. C. Apostol, S. Ropciuc, A. E. Prisacaru, and E. Albu, "Characterization of tomato sauce enriched with purslane (*Portulaca oleracea*) leaves," *Journal of Hygienic Engineering and Design*, vol. 31, pp. 127–132, 2020.
- [61] J. Yan, L. R. Sun, Z. Y. Zhou et al., "Homoisoflavonoids from the medicinal plant *Portulaca oleracea*," *Phytochemistry*, vol. 80, pp. 37–41, 2012.
- [62] R. Zhao, X. Shao, G. Jia et al., "Anti-cervical carcinoma effect of *Portulaca oleracea* L. polysaccharides by oral administration on intestinal dendritic cells," *BMC Complementary and Alternative Medicine*, vol. 19, no. 1, pp. 1–10, 2019.
- [63] Q. Ye, N. Zhang, K. Chen, J. Zhu, and H. Jiang, "Effects of portulacerebroside a on apoptosis of human leukemia HL60 cells and p38/JNK signaling pathway," *International Journal of Clinical and Experimental Pathology*, vol. 8, no. 11, pp. 13968–13977, 2015.
- [64] R. Zhao, T. Zhang, B. Ma, and X. Li, "Antitumor activity of *Portulaca Oleracea* L. polysaccharide on HeLa cells through inducing TLR4/NF- κ B signaling," *Nutrition and Cancer*, vol. 69, no. 1, pp. 131–139, 2017.
- [65] G. Guo, L. Yue, S. Fan, S. Jing, and L. H. Yan, "Antioxidant and antiproliferative activities of purslane seed oil," *Journal of Hypertension*, vol. 5, no. 2, pp. 01–19, 2016.
- [66] H. Jin, L. Chen, S. Wang, and D. Chao, "*Portulaca oleracea* extract can inhibit nodule formation of colon cancer stem cells by regulating gene expression of the notch signal transduction pathway," *Tumor Biology*, vol. 39, no. 7, pp. 101042831770869–101042831770869, 2017.
- [67] P. Y. Mali, "Assessment of cytotoxicity of *Portulaca oleracea* Linn. Against human colon adenocarcinoma and vero cell line," *Ayu*, vol. 36, no. 4, pp. 432–436, 2015.

Review Article

Bioactivities and Mechanism of Actions of *Dendrobium officinale*: A Comprehensive Review

Xiaoyu Xu,¹ Cheng Zhang,¹ Ning Wang,¹ Yu Xu,^{2,3} Guoyi Tang,¹ Lin Xu,¹ and Yibin Feng¹ 

¹School of Chinese Medicine, Li Ka Shing Faculty of Medicine, The University of Hong Kong, Hong Kong 999077, China

²School of Pharmacy, Shanghai University of Traditional Chinese Medicine, Shanghai 201203, China

³Engineering Research Center of Shanghai Colleges for TCM New Drug Discovery, Shanghai 201203, China

Correspondence should be addressed to Yibin Feng; yfeng@hku.hk

Received 1 June 2022; Revised 27 July 2022; Accepted 18 August 2022; Published 16 September 2022

Academic Editor: Felipe L. de Oliveira

Copyright © 2022 Xiaoyu Xu et al. This is an open access article distributed under the Creative Commons Attribution License, which permits unrestricted use, distribution, and reproduction in any medium, provided the original work is properly cited.

Dendrobium officinale has a long history of being consumed as a functional food and medicinal herb for preventing and managing diseases. The phytochemical studies revealed that *Dendrobium officinale* contained abundant bioactive compounds, such as bibenzyls, polysaccharides, flavonoids, and alkaloids. The experimental studies showed that *Dendrobium officinale* and its bioactive compounds exerted multiple biological properties like antioxidant, anti-inflammatory, and immune-regulatory activities and showed various health benefits like anticancer, antidiabetes, cardiovascular protective, gastrointestinal modulatory, hepatoprotective, lung protective, and neuroprotective effects. In this review, we summarize the phytochemical studies, bioactivities, and the mechanism of actions of *Dendrobium officinale*, and the safety and current challenges are also discussed, which might provide new perspectives for its development of drug and functional food as well as clinical applications.

1. Introduction

Dendrobium officinale Kimura et Migo, belonging to the *Dendrobium* of *Orchidaceae* genus, is widely used as a medicinal and functional food product [1]. It originated from Nanling Mountains and Yungui Plateau in China, and its cultivation migrated northward or eastward subsequently [2]. *Dendrobium officinale* was originally used as a tonic herbal medicine to treat stomach disorders and promote the secretion of body fluid in Chinese medicine [1]. It also has a long history as a food ingredient in Yunnan and Zhejiang Province in China, and the main ways of consumption are making instant food, soup, dishes, juices, tea, and wine. In particular, the dried stem of *Dendrobium officinale* (*Dendrobii officinalis*) has been documented in Chinese Pharmacopoeia for medicinal usage and is officially listed in “Medicine and Drug Homology,” which indicates that *Dendrobium officinale* might be feasible for long-term consumption with high safety [3].

Increasing pharmacological studies have found that *Dendrobium officinale* has a high nutritional and medicinal

value, such as antioxidant, immune-regulatory, anti-inflammatory, anticancer, antidiabetic, and hepatoprotective activities [4, 5]. These health benefits are mainly attributed to its abundant bioactive compounds, such as flavonoids, bibenzyls, polysaccharides, and alkaloids [6]. As a natural plant product, *Dendrobium officinale* poses little toxicity and side effects to human health, and it could combine with other herbal medicines in Chinese medicine decoction for the treatment of diseases. Since the present chemical drugs and therapy could cause some side effects in patients, it is essential to develop natural-derived drugs and adjuvant supplements with fewer side effects for patients. Hence, phytochemicals and herbal therapeutics have gained lots of attention for investigation in various disease treatments. *Dendrobium officinale* might be a promising dietary supplement and functional food in the prevention and management of diseases, and its bioactivities and mechanisms of action are worthy of exploration [7]. This review summarized the updated knowledge of the phytochemical studies, bioactivities, health benefits, related mechanism of action, and safety of *Dendrobium officinale*. The current challenge

and outlooks of *Dendrobium officinale*-related research are also discussed, providing new and critical viewpoints for developing medicinal and functional food in the future.

2. Phytochemical Studies

2.1. Bioactive Compounds. A large body of studies shows that *Dendrobium officinale* contains various bioactive compounds, such as polysaccharides, flavonoids, bibenzyls, and alkaloids [4, 7–9] (Figure 1). The tissue analysis found that the stems, leaves, and protocorm-like bodies of *Dendrobium officinale* had the highest content of polysaccharides, flavonoids, and alkaloids, respectively [10]. Among the bioactive compounds, polysaccharides are the major medicinal compound that is often utilized to investigate the therapeutic effects of *Dendrobium officinale*. It is mainly isolated from the stems of *Dendrobium officinale* with a yield rate of over 30% [11]. The chemical analysis showed that the polysaccharides mainly contained mannose and glucose with a structure of (1 → 4)-linked- β -D-mannopyranosyl and β -D-glucopyranosyl residues [12, 13]. Dendronan® is a new polysaccharide O-acetyl-glucomannan isolated from *Dendrobium officinale* with a relatively detailed chemical structure, and it was identified as the ratio of mannose to glucose (6.9:1) [14]. However, some polysaccharides with large molecular weight or absence of certain chemical groups might have low biological activities, and thus, some modifications could be considered for improving the bioavailability of polysaccharides from *Dendrobium officinale*, such as fermentation, degradation, or grafting [15, 16]. Furthermore, the relationship between structural characteristics and biological properties of *Dendrobium officinale* polysaccharides needs more in-depth investigation.

Additionally, the metabolic profile of *Dendrobium officinale* found that leaves contained more flavonoids than other parts, and flavonoids were considered the important antioxidant source [17–19]. A total of 14 major phenolic compounds including 1 quercetin-type flavonol, rutin, and 13 apigenin-type flavones like apigenin 6-C- β -D-glucoside-8-C- α -L-rhamnoside were identified from the leaves of *Dendrobium officinale*. And the major flavonoid compound was rutin with a content of 1.33 to 2.89 mg/g from leaves [19]. Moreover, naringenin was the flavonoid compound only found produced in the stems of *Dendrobium officinale* [10].

Bibenzyl is one of the most active ingredients in *Dendrobium officinale*, and the gigantol and dendrocandin are the most common bibenzyl compounds from *Dendrobium officinale* [4]. The phytochemical study found that the root tissues of *Dendrobium officinale* contained the highest amount of bibenzyl, such as erianin and gigantol. And the transcriptomic analysis revealed that cytochrome P450 genes and other enzymatic genes were functionally associated with the biosynthesis and accumulation of bibenzyl, which might help increase the content of bibenzyl for drug production and industrialization of *Dendrobium officinale* [20]. Several bibenzyl compounds have also been found in the leaves of *Dendrobium officinale*, such as the new derivate denofficin,

dendrocandin B, 4,4'-dihydroxy-3,5-dimethoxy bibenzyl, gigantol, and densiflorol [21].

Alkaloids were found abundant in protocorm-like bodies of *Dendrobium officinale*, which might be more available for producing alkaloids than other organs. The study also found that the enzymes involved in the alkaloid biosynthesis were strictosidine β -D-glucosidase, geissoschizine synthase, and vinorine synthase in *Dendrobium officinale* [10]. Additionally, the key enzyme-encoding genes associated with the alkaloid biosynthesis had higher activities in the leaves than that in the stems of *Dendrobium officinale* [22].

Due to the increasing demand and rare resources of wild type, there are more and more adulterations of *Dendrobium officinale*, and it negatively affects the sustainable utilization of this medicinal plant and food resource and increases the potential health risk of using cheaper and poorer products. The composition of ingredients contributes to the quantitative chemotypic variation and characteristics within difference [23]. Hence, some methods targeting the specific compounds of *Dendrobium officinale* have been developed for distinguishment. For example, the quantifications of naringenin, bibenzyls, and the ratios of mannose to glucose of polysaccharides could be used as key elements to distinguish from other similar spices [24]. Additionally, the combined analysis of HPLC fingerprints, HPLC-ESI-MS, and HPTLC found that violanthin and isoviolanthin were specific components for *Dendrobium officinale*, which could distinguish it from *Dendrobium devonianum* [25].

Overall, the phytochemical studies found abundant bioactive components in *Dendrobium officinale*, and they are closely associated with various bioactivities and health benefits. The identification of chemical structures of some major compounds as well as biosynthesis-related gene encoding enzymes is important for the exploration and protection of *Dendrobium officinale*. On the other hand, the chemical composition of *Dendrobium officinale* could be used to distinguish the plant from different sources. These findings facilitate a better understanding of the phytochemical variation of *Dendrobium officinale*, contributing to better quality control.

2.2. Influential Factors. The varied growth environment and origins with different natural resources lead to significant differences in the yield, quality, and even medicinal values of *Dendrobium officinale*. Samples from Zhejiang, Fujian, Yunnan, and Jiangxi Provinces resulted in different compositions of the active compounds, of which only the sample from Yunnan Province had three unique medicinal components, and only the sample from Jiangxi Province had no toxic component [26]. Hence, *Dendrobium officinale* from different regions need more investigations for better collection, protection, and utilization.

The quality and biological activities of *Dendrobium officinale* could be influenced by the processing methods and storage conditions [27–29]. The reduction in the grinding particle size could result in better physical properties and higher solubility of protein and polysaccharides, which led to better bioavailability and stronger antioxidant activity than crude ground products [27]. In addition, heat might

ROS. The treatment of polysaccharides at a high dose of 9.6 g/kg could protect against the precancerous lesions of gastric cancer (PLGC) in rats by activating the Nrf2 pathway and its downstream antioxidant enzymes like heme oxygenase 1 (HO-1) and NAD(P)H: quinone oxidoreductase-1 (NQO-1). The treatment also reduced the levels of 8-hydroxy-deoxyguanosine (8-OHdG) which was one of the predominant biomarkers of free radical-induced oxidative stress [34, 35]. In addition, polysaccharides could reduce oxidative stress-induced injuries by elevating the activity of the antioxidant enzyme superoxide dismutase (SOD) and decreasing the level of malonaldehyde (MDA), a product of polyunsaturated fatty acid peroxidation, in rats with type 2 diabetes treated at the dose of 20, 40, 80 and 160 mg/kg b.w. [36]. Like other natural products, *Dendrobium officinale* could also work as a dietary antioxidant supplement. However, its induction of antioxidant defenses may fail to reach effective concentration and the significant effects on human study. More importantly, some progression of diseases might be attributed to oxidative stress as the secondary contributor instead of the primary cause, and thus, the antioxidant properties of *Dendrobium officinale* may not pose a significant influence on the diseases [37].

3.2. Anti-inflammatory Activity. Chronic inflammation is a vital risk factor for various diseases such as diabetes, cancer, and cardiovascular diseases, and thus, the effective inhibition of inflammation facilitates the control and prevention of many chronic diseases. The *in vivo* and *in vitro* studies revealed that *Dendrobium officinale* and its bioactive compounds could inhibit inflammation by modulating inflammatory cytokines and related mediators. Sjogren's syndrome is a chronic autoimmune disorder of the affected glands with lymphocytic infiltration and dysfunction of aquaporin 5 (AQP5). A clinical study was conducted with 16 female patients with the deficient secretion of saliva, and they randomly received the extracts at the dose of 0.5 g/5 mL three times daily for one week. The results revealed that the treatment improved the function of glands by regulating the expression of AQP5 in labial glands and increasing saliva secretion [38]. The mouse model with Sjogren's syndrome further demonstrated the underlying mechanism that *Dendrobium officinale* polysaccharides (20 mg/mL) could reduce the expression of proinflammatory cytokines like tumor necrosis factor- α (TNF- α), interleukin-1 beta (IL-1 β), and IL-6, which attenuated the immune-mediated inflammation and maintained the balance of inflammatory cytokines [39]. Additionally, the pretreatment of polysaccharides at the dose of 1 μ g/mL could inhibit the TNF- α -induced apoptosis of human salivary gland cell line A-253 cells, indicating its potential of protecting the salivary glands and ameliorating Sjogren's syndrome [40]. Polysaccharides (1.5 g/kg) reduced brain inflammation and seizures, which were mainly involved in inhibiting the expressions of IL-1 β and TNF- α as well as mitogen-activated protein kinase (MAPK) signaling pathways in pentetrazol-induced epileptic rats [41]. Moreover, the polysaccharides isolated from the leaves could also mitigate the inflammation in LPS-stimulated THP-1 cells, and it could

protect the cells against cytotoxicity and reduce the formation of ROS, which may be associated with the inhibition of TLR-4, myeloid differentiation factor (MyD88), and tumor necrosis factor receptor-associated factor-6 (TRAF-6) [42].

3.3. Immune-regulatory Activity. *Dendrobium officinale* and its bioactive compounds have been reported to have the capability of regulating the immune system via cytokines and immune cells. For instance, 25 μ g/mL of the purified polysaccharides stimulated the immune activities by activating the extracellular signal-regulated kinases 1/2 (ERK1/2) and NF- κ B signaling pathways in human leukemia monocytic cell line THP-1 cells [43]. In addition, the treatment of 2,3-*O*-acetylated-1,4- β -*D*-glucomannan (100 μ g/mL) could target chemotactic cytokines like chemokine (C-C motif) ligands 4 (CCL4) and interferon gamma-induced protein 10 (IP-10) to stimulate the immune response in THP-1 cells, and these effects were mainly associated with the activation of NF- κ B which was regulated through the Toll-like receptor 4 (TLR4) signaling pathway [44].

The immune cells are also affected by the treatment of *Dendrobium officinale*. The purified polysaccharide with the main structure of *O*-acetyl-glucomannan at the dose of 40, 80, and 160 mg/kg b.w. promoted the proliferation of splenocytes; regulated the spleen lymphocyte subsets; increased the levels of serum immunoglobulin M (IgM), IgG, and haemolysin; and improved the phagocytotic function in cyclophosphamide-induced immunosuppressed mice [45]. Moreover, some subfractions of polysaccharides exhibited immunomodulating activity and enhanced the immune response by increasing the proliferation of splenocytes and macrophages, the secretion of cytokines like TNF- α , and the production of NO as well as phagocytosis [46–48]. In addition, the treatment of *Dendrobium officinale* polysaccharides at the dose of 1 μ g/mL in Sjogren's syndrome model could reduce the abnormal infiltration and apoptosis of lymphocytes, attenuate the dysfunction of AQP5, and induce the translocation of AQP5 by activating M3 muscarinic receptors, which indicated its ability to improve the immunity [39, 49].

Moreover, the immune-regulatory activity of *Dendrobium officinale* is closely associated with gut microbiota. The feeding of 0.25% polysaccharides increased the abundance of the gut microbiota *Parabacteroides*, in which *Parabacteroides*_sp_HGS0025 was positively associated with the butyrate, IgM, IL-10, and interferon-alpha (IFN- α) in the intestine and blood of mice. It indicated that polysaccharides could improve immunity by regulating the intestinal microbiota and its metabolites like butyrate [50].

4. Health Benefits

4.1. Anticancer Effects. *Dendrobium officinale* has therapeutic potential in cancer prevention and treatment. Its potential mechanism of action is mainly involved in reducing cancer cell growth and proliferation, triggering apoptosis, and increasing autophagy. And therefore, the adjuvant use

of *Dendrobium officinale* might be utilized as a simple, safe, but feasible therapy for cancer treatment.

Cancer cells have little apoptosis, and they could shift to malignant cells for lasting existence, induce tumor metastasis, and increase resistance to anticancer drugs [51]. The polysaccharides from *Dendrobium officinale* had the capability of triggering apoptosis to limit cancer progression. The apoptosis of cancer cells is mainly mediated by the antiapoptotic and proapoptotic cytokines and pathways. The well-known antiapoptotic factors include proteins like Bcl-2, Bcl-extra large (Bcl-xL), and Mcl-1, while the proapoptotic factors involve proteins like Bax, Bcl-2 homologous antagonist killer (Bak), Bcl-2 interacting killer (Bik), p53, and caspase-3 [52]. A study found that the polysaccharide extracted by hot water was effective in dose-dependently inhibiting the growth of liver hepatocellular carcinoma cell line HepG2 cells by increasing the ROS level, decreasing mitochondrial membrane potential, and inducing apoptosis with the downregulation of antiapoptotic protein Bcl-2 and upregulation of proapoptotic protein Bax expressions [53]. In addition, the polysaccharides effectively inhibited the proliferation of osteosarcoma U2OS and Saos-2 cells. It had a synergistic effect with cisplatin, which increased the cisplatin-induced apoptosis by upregulating the expression of proapoptotic factors p53, Bax, and Bak, downregulating the expression of antiapoptotic factors Bcl-2 and Mcl-1, and increasing the ratios of cleaved caspase-9 to caspase-9, cleaved caspase-3 to caspase-3, and cleaved poly (ADP-ribose) polymerase (PARP) to PARP [54]. Moreover, after being degraded into smaller molecules, the fractions of polysaccharides exerted inhibitory effects on the proliferation of human cervical carcinoma HeLa cells and induced apoptosis by upregulating the expression of ERK, Jun N-terminal kinase (JNK), and p38 [12].

The regulation of the Wnt signaling pathway is also closely associated with tumorigenesis. PLGC is a major phase in the progression of gastric cancer, which might be a potential target for the treatment of gastric cancer. The polysaccharides prepared from *Dendrobium officinale* were found to ameliorate the MNNG-PLGC in rats via the Wnt/ β -catenin pathway, downregulating the expressions of Wnt2 β and glycogen synthase kinase 3 beta (Gsk3 β), proliferating cell nuclear antigen (PCNA), and cyclinD1. In addition, the results of serum endogenous metabolites revealed that the change in betaine was the most significant, indicating that betaine may be a key contributor to the anticancer effects of *Dendrobium officinale* polysaccharides [55].

Furthermore, mitochondria are considered important in apoptosis, and a high level of ROS generated from mitochondria could induce apoptosis in cancer cells, suggesting that targeting the mitochondrial function or ROS stimulation might be feasible in cancer cell treatment [56]. An in vitro study with colon cancer cell line CT26 cells showed that the polysaccharides isolated from *Dendrobium officinale* reduced the proliferation of cells and induced cytotoxic autophagy as well as mitochondrial dysfunction via the ROS-AMP-activated protein kinase- (AMPK-) autophagy pathway [57].

On the other hand, *Dendrobium officinale* could prevent the growth of tumors by improving the host function and responses. For instance, the polysaccharide of *Dendrobium officinale* reduced colon tumorigenesis by preserving the intestinal barrier function and improving immune response to the tumor microenvironments in mice with colorectal cancer. The intestinal barrier function was restored by increasing the expression of zonula occludens-1 (ZO-1) and occludin, and the immune response was increased to exert anticancer effects via the tumor infiltrated CD8(+) cytotoxic T lymphocytes (CTLs) and the expression of programmed death-1 (PD-1) on CTLs [58].

The potential anticancer activity of *Dendrobium officinale* could potentiate the efficacy of anticancer agents or chemotherapy. Its polysaccharides inhibited the growth of human colorectal cancer HT-29 cells and reduced the metastasis of tumors in the zebrafish model, and the treatment increased the anticancer efficacy of 5-fluorouracil, which induced apoptosis via the mitochondrial-dependent intrinsic apoptotic pathway. These results indicated that *Dendrobium officinale* is a potential candidate for colorectal cancer therapy alone or in the combination with chemotherapy medication [59].

Notably, the molecular weight and structure of compounds in *Dendrobium officinale* might influence its anticancer activities. A study compared the anticancer properties of carbohydrates in *Dendrobium officinale* with different molecular weights, including monosaccharides, oligosaccharides, and polysaccharides. It was reported that polysaccharides had better anticancer properties than monosaccharides and oligosaccharides, suggesting that the efficacy of carbohydrate drugs largely depends on the molecular weight of the cancer treatment [54]. Moreover, the modification and use of vehicles could promote bioavailability and increase the bioactive function of *Dendrobium officinale*. The gold nanoparticle synthesized from the extracts of *Dendrobium officinale* showed better anticancer effects without increasing toxicity to the host [60]. In addition to the polysaccharides, there are also new derivatives from *Dendrobium officinale* with significant anticancer activities. A study found that several new phenanthrene and 9,10-dihydrophenanthrene derivative compounds showed cytotoxicity against cancer cell lines, HI-60 and THP-1 cells, and one of the compounds had a most significant effect with IC50 values of 11.96 and 8.92 μ M, respectively [61].

4.2. Antidiabetic Effects. Diabetes mellitus is a metabolic disorder and global health concern with complicated factors. The rapid development of modern society leads to unhealthy eating behavior, less physical activities, and overloaded stress management, which increases the risk of diabetes in adolescents and young adults [62]. In addition, the occurrence of diabetes increases the risk of complications that are still costly to be controlled by current drugs, such as diabetic retinopathy and nephropathy [63]. Numerous studies reveal that many herbal medicines and their bioactive compounds show significant hypoglycemic effects mainly by regulating glucose metabolism, improving insulin sensitivity and insulin resistance, and restoring the damaged pancreas [64].

Dendrobium officinale as a medicinal herbal plant has a long history of being used to attenuate the symptoms of diabetes which is also called “Xiaoke” disease in China. The hypoglycemic efficacy of *Dendrobium officinale* makes it a common ingredient in Xiaoke decoction for type 2 diabetes treatment [65].

Some enzymes are involved in glycemic control, such as α -glucosidase and α -amylase, and they have been developed as therapeutic targets for type 2 diabetes prevention and treatment [66]. Several main antidiabetic compounds were identified based on the inhibition of α -glucosidase and α -amylase activities in *Dendrobium officinale*. The crude extract of its stems was reported to have IC50 values of 78.1 μ g/mL on α -glucosidase activity and 116.7 μ g/mL α -amylase activity. Moreover, there were six compounds associated with α -glucosidase inhibition, such as N-p-coumaroyltyramine and 3,4,4'-trihydroxy-5-methoxybibenzyl. And 3,4-dihydroxy-4',5-dimethoxybibenzyl was the only identified compound with α -amylase inhibitory activities [67]. Type 2 diabetes is tightly related to abnormal metabolisms, such as hepatic glucose metabolism, insulin resistance, and low-grade inflammation. *Dendrobium officinale* polysaccharides could decrease the levels of fasting blood glucose, insulin, glycated serum protein, and serum lipid profile and alleviate pancreatic injury as well as the dysregulated metabolism of bile acids and amino acids in type 2 diabetic rats [36]. In addition, it could regulate the hepatic glucose metabolism via the glucagon-mediated signaling pathways as well as the liver-glycogen structure in HFD/STZ-induced diabetic mice [68]. Furthermore, the polysaccharides reduced the fasting blood sugar levels in mice by increasing insulin in serum and stimulating the glucagon-like peptide-1 (GLP-1) secretion which is an important hormone regulator in the progression of diabetes. And the in vitro study showed that the stimulated GLP-1 secretion may be related to the Ca^{2+} /calmodulin-dependent protein kinase (CaMK) and p38-MAPK pathways in the murine enteroendocrine cell line STC-1 cells [69]. *Dendrobium officinale* extracts could prevent STZ-induced type 1 diabetes in mice, which increased the level of liver glycogen and taurine and upregulated energy and amino acid metabolism [70].

Apart from type 1 and type 2 diabetes, diabetic complications are also recognized as a severe health concern. *Dendrobium officinale* polysaccharides were demonstrated to ameliorate diabetic cataracts in rats, and it could reduce the severity of the opacity of the lens by downregulating the microRNA-125b and MAPK signaling pathways, in which the level of microRNA-125b was positively correlated with the levels of ERK1, ERK2, Raf, and Ras [71].

4.3. Gastrointestinal Modulation. In the past two decades, numerous findings have revealed that the gut microbiota and its derived microbial products are key influential factors in the host metabolism, and dysbiosis is tightly linked to a high risk of many metabolic diseases [72]. The polysaccharides of *Dendrobium officinale* could regulate the composition and abundance of gut microbiota and its metabolites in mice, which increased the beneficial bacterium like *Ruminococcus*, *Eubacterium*, *Clostridium*, *Bifidobacterium*, *Para-*

bacteroides, and *Akkermansia muciniphila* and decreased the harmful bacteria like *Proteobacteria* and further modulated the production of butyrate [50]. In addition, *Dendrobium officinale* increased the diversity of intestinal mucosal flora in mice fed with HFD, which enhanced the abundance of *Ochrobactrum* and reduced the abundance of *Bifidobacterium* and *Ruminococcus*, and it further influenced the metabolism of carbohydrate, energy, and amino acid as well as gut microbiota to reduce HFD-induced negative effects [73].

As the most abundant and common microbial metabolites, short-chain fatty acids (SCFAs) play an important role in the gut and metabolic health. Studies found that SCFAs mediated the G-protein coupled receptors (GPCRs), such as GPCR41 and GPCR43, and the regulation of the SCFA-GPCR pathway by *Dendrobium officinale* could alleviate metabolic disorders [74, 75]. Moreover, the enzymatic fragments of polysaccharides could protect against dextran sulfate sodium- (DSS-) induced colitis by ameliorating the gut microbiota dysbiosis. The treatment inhibited the proinflammatory cytokines, restored SCFA levels, increased GPCR levels, and regulated the gut microbiota, which increased the abundance of *Bacteroides*, *Lactobacillus*, and *Ruminococcaceae* and reduced the abundance of *Proteobacteria* [74]. On the other hand, the polysaccharides were found little absorbed and would be degraded into SCFAs in the large intestine after the oral administration, and thus, its modulatory effects on gut microbiota were considered the main contributor to its bioactivities [76].

Dendrobium officinale could not only alleviate metabolic disorders via the modulation of intestinal microbiota and microbial products but also improve gut health to maintain host homeostasis (Figure 2). An in vitro fermentation study showed that polysaccharides from *Dendrobium officinale* increased the levels of SCFAs which mainly contained the acetic, propionic, and butyric acids, and it changed the gut microbiota community and accelerated the metabolic pathways of amino acid and fatty acids. The results suggested that the polysaccharides had probiotic effects improving gastrointestinal health [77]. On the other hand, the polysaccharides could ameliorate inflammatory bowel disease by increasing miR-433-3p in the intestinal small extracellular vesicle. The increased delivery of miR-433-3p reduced the inflammation from excessive macrophage activity in the intestine by inhibiting the MAPK signaling pathway, which was beneficial for maintaining the intestinal microenvironment [78]. Besides, the O-acetyl-glucomannan extracted from *Dendrobium officinale* was found to improve the colonic microenvironment and benefit colon health in mice, which increased the content of SCFAs, colonic length, and fecal moisture and reduced the colonic pH and defecation time [79]. Furthermore, the ethanol-induced gastric mucosal injury could be protected by the polysaccharides from *Dendrobium officinale* leaves consisting of mannose, galacturonic acid, glucose, galactose, and arabinose, and it could improve antioxidant capacity and reduce the apoptosis in human gastric epithelial cell line GES-1 cells via the AMPK/mTOR signaling pathway [80].

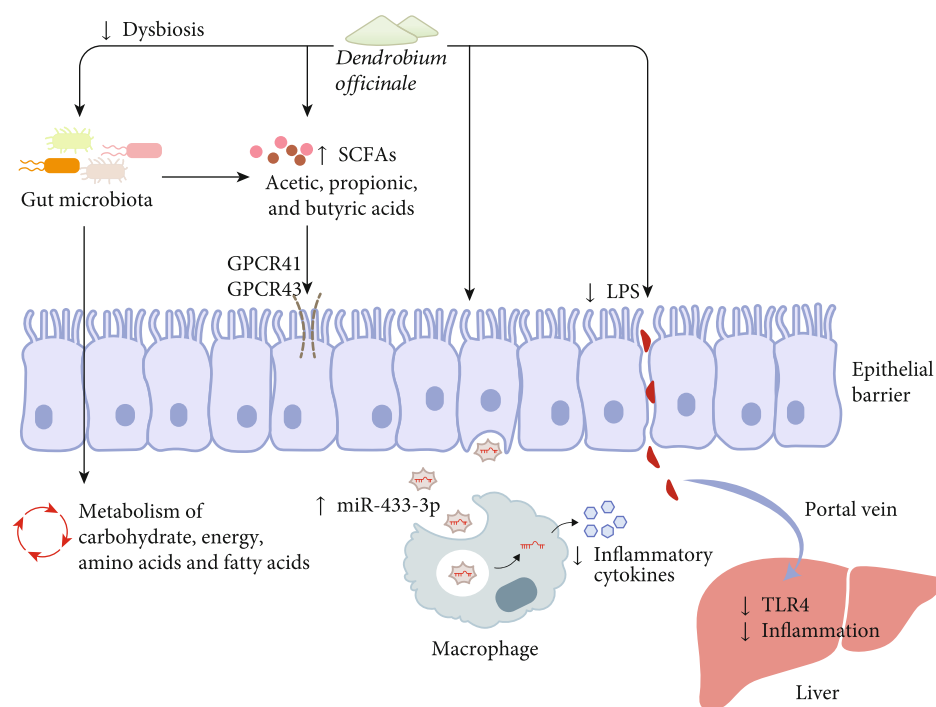


FIGURE 2: The gastrointestinal modulatory activities of *Dendrobium officinale* via several pathways.

The gut-liver axis has attracted great attention in the field of liver diseases since the gut-derived products could be transported directly to the liver via the portal vein, and the liver could give feedback via the bile and antibody secretion to the intestine [81]. After the mice were withdrawn from the high sugar and high-fat diet, *Dendrobium officinale* accelerated the liver recovery and inhibited the lipid deposition as well as inflammatory lesions in the liver, which was involved in modulating the gut microbiota and suppressing the activation of LPS-TLR4-associated inflammatory mediators in mice with NAFLD [79]. However, little is known about the underlying mechanism of action, and it is necessary to shift from the descriptive interaction analysis between the treatment of *Dendrobium officinale* and gut microbiota composition to cause-and-effect studies. And more microbiota-targeted interventions could be conducted to improve metabolic health in humans.

4.4. Cardiovascular Protection. Cardiovascular diseases remain a major threat to public health and human life, and it is caused by various pathological factors such as oxidative stress and inflammation [82]. It has been reported that *Dendrobium officinale* exerted cardiovascular-protective effects mainly by defending against oxidative stress, reducing the apoptosis of cardiomyocytes, and suppressing inflammation. The polysaccharides of *Dendrobium officinale* protected cardiomyocytes against oxidative stress-induced apoptosis by reducing ROS production, restoring mitochondrial membrane potential, regulating apoptosis-related protein, and increasing the activity of antioxidant enzymes, and these effects were possibly associated with the regulation of phosphoinositide 3-kinases (PI3K)/Akt and MAPK pathways [82, 83]. Moreover, *Dendrobium officinale* extracts had pro-

TECTIVE potential against diabetic cardiomyopathy in STZ-induced diabetic mice, which inhibited oxidative stress, decreased cardiac lipid accumulation as well as deposition of collagen, downregulated the expression of several proinflammatory cytokines, and reduced cardiac fibrosis [84]. Furthermore, *Dendrobium officinale* could ameliorate the aberrant cardio condition through the regulation of metabolism. In the rat model of unhealthy diet-induced metabolic hypertension, *Dendrobium officinale* could alleviate hypertension by reducing lipid abnormalities and improving the function of gastrointestinal as well as vascular endothelial relaxation, which may be mediated by activating the SCFA-GPCR 43/41 pathway [75, 85]. Besides, the water-soluble extracts of *Dendrobium officinale* alleviated cardiac injury and fibrosis in HFD/STZ-induced diabetic mice with a 12-week daily administration, which was potentially implicated in increasing lipid transport, reducing insulin resistance, and inhibiting the EMT signaling pathway [86].

4.5. Liver Protection. *Dendrobium officinale* could also confer protection against liver injuries and improve liver functions against different forms of liver injuries, such as drug-, chemical-, and acute alcohol-induced injuries and nonalcoholic fatty liver diseases (NAFLD). The polysaccharides from *Dendrobium officinale* could attenuate the acetaminophen-induced hepatotoxicity in mice by reducing the oxidative stress and activating the Nrf2-Keap1 signaling pathway, in which the levels of alanine aminotransferase (ALT), aspartate aminotransferase (AST), ROS, MDA, and myeloperoxidase (MPO) were decreased; the levels of GSH, CAT, and T-AOC were increased, and the Nrf2 nuclear translocation was activated [87]. Additionally, alcoholic liver diseases are characterized by disrupted ethanol metabolism and stimulated

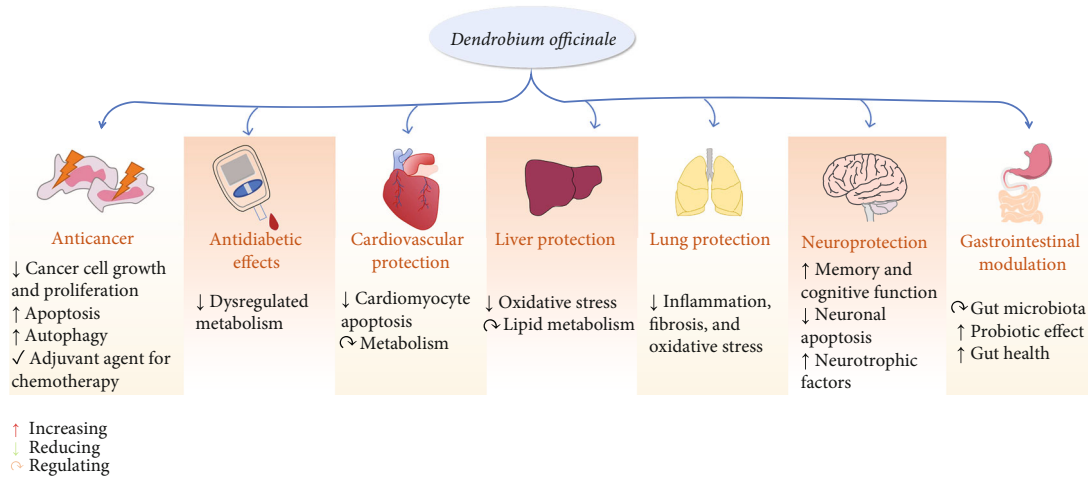


FIGURE 3: A summary of the health benefits of *Dendrobium officinale*.

oxidative stress. The NIR fluorescence imaging showed that the polysaccharides from *Dendrobium officinale* could protect against acute alcoholic liver injury in vivo by increasing the antioxidant levels, in which the level of GSH was balanced in the liver [88]. In addition, the alcohol-induced liver injury could be mitigated by the extracts of the *Dendrobium officinale* flower, which was associated with its antioxidant and anti-inflammatory activities. The flower extracts treatment reduced the serum levels of ALT, AST, TC, and TG and increased the activities of the antioxidant enzymes. It was associated with the downregulation of hepatic cytochrome P450 2E1 (CYP2E1) and upregulation of Nrf2, HO-1, and NQO1. Moreover, it inhibited inflammation by downregulating TLR-4 and NF- κ B p65 [89].

NAFLD is often caused by excessive lipid accumulation or steatosis due to an unhealthy diet pattern with little or no alcohol consumption. After the high-sucrose and high-fat diet was stopped, the 3-week administration of *Dendrobium officinale* could reduce the hepatic lipid accumulation, regulate the metabolism of fatty acid, and improve the histopathology of the liver in NAFLD mice. It may increase the β -oxidation and reduce the synthesis, desaturation, and uptake of fatty acids and alleviate the abnormality of major phospholipids in the liver of mice [90]. Furthermore, the polysaccharides could also reduce the disturbed hepatic lipid metabolism involved with the fatty acid, glycerolipid, and glycerophospholipid, and it restored the metabolism of ceramide and bile acids in type 2 diabetic rats [85].

4.6. Lung Protection. Due to climate changes and personal unhealthy lifestyles, the risk of chronic respiratory disease and acute lung injury goes high in these decades. Chronic obstructive pulmonary disease increases airway inflammation and leads to respiratory dysfunction. Cigarette smoke is a vital risk factor for the incidence of chronic obstructive pulmonary disease, and it could induce mucus hypersecretion and viscosity. Both in vitro and in vivo studies found that *Dendrobium officinale* polysaccharides attenuated the cigarette smoke-induced mucus hypersecretion and viscosity by inhibiting mucus secretory granules and downregulating the expression of mucin-5AC (MUC5AC) [91]. Moreover,

a randomized, double-blind, and placebo-controlled clinical trial was conducted on 40 patients with smoking habits and mild airflow obstruction, and patients randomly received 1.2 g *Dendrobium officinale* polysaccharides thrice daily. The treatment of polysaccharides could significantly ameliorate lung functions and reduce the serum levels of proinflammatory mediators (IL-6, IL-8, CRP, and TNF- α), and the expression of MUC5AC was decreased, and AQP5 was increased [92]. Additionally, it could decline cigarette smoke-induced oxidative stress in the lung and decrease the number of lymphocytes as well as monocytes in serum, which reduced the infiltration of inflammatory cells in lung tissue and inflammation indicators in serum. These effects might be mediated by inhibiting MAPK and NF- κ B signaling pathways [93].

The polysaccharides of *Dendrobium officinale* attenuated the bleomycin-induced pulmonary inflammation and fibrosis in rats by inhibiting the transforming growth factor-beta 1- (TGF- β 1-) Smad2/3 signaling pathway, and it effectively suppressed the transformation of alveolar epithelial type II cells into myofibroblasts and reduced the expression of Smad2/3 and fibronectin in rats [94]. Besides, colitis-induced secondary lung injury could be attenuated by the polysaccharides, which reduced inflammation and oxidative stress. The treatment inhibited the protein expression of TLR4 and increased the protein expressions of Nrf2, HO-1, and NQO-1 both in mice and in LPS-stimulated BEAS2B cells, indicating that TLR4 and Nrf2 signaling pathways played an important role in it [95].

4.7. Neuroprotection. *Dendrobium officinale* plays a crucial role in protecting the nervous system potentially by reducing neurological damage and improving memory as well as cognitive function. The extracts of *Dendrobium officinale* reduced the impaired neurobehaviors and enhanced the antioxidant capacity in neonatal rats with hypoxic-ischemic brain damage (HIBD), and it protected against HIBD by inhibiting neuronal apoptosis and increasing the expression of neurotrophic factors [96]. Additionally, its polysaccharides could attenuate learning and memory disabilities in mice, and these effects may be mediated by

TABLE 1: The health benefits and related molecular mechanisms of *Dendrobium officinale* extracts.

Type of study	Object	Dosage	Effects	Potential mechanisms	References
<i>Antidiabetes</i>					
In vivo	Male STZ-induced diabetic C57BL/6 mice	300 and 700 mg/kg b.w.	Decreased the levels of blood glucose Increased the levels of glycogen in liver Upregulated the energy and amino acid metabolism	↑ Citrate, pyruvate, alanine, isoleucine, histidine, and glutamine in serum ↑ Alanine and taurine in liver	[70]
In vivo	Male STZ-induced type 1 diabetic Sprague-Dawley rats	1 g/kg b.w.	Decreased the levels of serum TC, TG, BUN, and CREA Attenuated the hypoalgesia and histopathological changes of vital organs induced by hyperglycemia Prevented early complications in type 1 diabetes	↑ GSH-Px	[117]
<i>Gastrointestinal modulation</i>					
In vivo	Male and female Kunming mice	2.37 g/kg b.w.	Increased the diversity of intestinal mucosal flora Changed the carbohydrate, energy, and amino acid metabolism of intestinal mucosal flora Reduced the negative effects induced by HFD Regulated the gut microbiota Prevented lipid deposition and inflammatory lesions in the liver Inhibiting LPS-TLR4-associated inflammatory mediator activation Accelerated liver recovery	↑ <i>Ochrobactrum</i> ↓ <i>Bifidobacterium</i> and <i>Ruminococcus</i>	[73]
In vivo	Male ICR mice	0.2 and 0.6 g/kg b.w.		NA	[79]
<i>Cardiovascular protection</i>					
In vivo	Male Kunming mice	75, 150, and 300 mg/kg b.w.	Protected against myocardial ischemia Reduced the infarct size and the number of apoptotic cardiomyocytes	↑ SOD ↑ Meis1 ↓ CK-MB and LDH ↓ MDA	[118]
In vivo	Male STZ-induced diabetic Kunming mice	75, 150, and 300 mg/kg b.w.	Decreased the ratio of heart to body weight Ameliorated the cardia injury Reduced cardiac lipid accumulation, deposition of collagen, oxidative stress, and cardiac fibrosis Downregulated the proinflammatory cytokines	↑ T-SOD ↓ MDA ↓ TGF- β , collagen-1, fibronectin, NF- κ B, TNF- α , and IL-1 β	[84]
In vivo	Male STZ-induced diabetic Kunming male mice	75, 150, and 300 mg/kg b.w.	Decreased the ratio of heart to body weight Ameliorated the cardia injury Reduced cardiac lipid accumulation, deposition of collagen, oxidative stress, and cardiac fibrosis Downregulated the proinflammatory cytokines	↑ T-SOD ↓ MDA ↓ TGF- β , collagen-1, fibronectin, NF- κ B, TNF- α , and IL-1 β	[84]
In vivo	Male Sprague-Dawley rats with ACHSFD-induced metabolic hypertension	400 and 600 mg/kg b.w.	Lowered blood pressure Improved lipid abnormalities, intestinal flora, and the vascular endothelial relaxation function	↑ SCFA-GPCR43/41 pathway	[75]
In vivo	HFD/STZ-induced diabetic mice	75, 150, and 300 mg/kg b.w.	Reduced cardiac injury and fibrosis Suppressed insulin resistance Accelerated lipid transport	↑ PPAR- α , p-IRS1, and E-cadherin ↑ HDL-C ↓ TC, TG, and LDL-C	[86]

TABLE 1: Continued.

<i>Liver protection</i>					↓ TGF- β 1, p-JNK, Twist, Snail1, and Vimentin	
In vivo	Male Kunming mice	50, 100, and 200 mg/kg b.w.	Mitigated the alcohol-induced liver injury Reduced the degeneration, inflammatory infiltration, and lipid droplet accumulation in liver		↑ GSH, SOD, GSH-Px, and CAT ↑ Nrf2, HO-1, and NQO1 ↓ ALT, AST, TC, and TG ↓ MDA ↓ CYP2E1 ↓ TLR-4 and NF- κ B p65	[89]
<i>Neuroprotection</i>						
In vivo	Male and female neonatal Sprague-Dawley rats	75, 150, and 300 mg/kg b.w.	Protected against hypoxic-ischemic brain damage Alleviated the impaired neurobehaviors and antioxidant capacity Enhanced the neuronal apoptosis Enhanced the expression of neurotrophic factors		↑ SOD ↑ Bcl-2 ↑ KCC2 ↓ NOS, NO, and MDA ↓ Cleaved caspase-3 and Bax ↓ HIF-1 α and HDAC1	[96]
In vivo	Male ICR mice	1 and 3 g/kg b.w.	Reduced the depression-like behavior (decreased sucrose consumption and increased immobile time)		↑ NGF and BDNF	[98]
In vitro	PC12 cells	1, 3, and 10 μ g/mL	Potentiated the neurite outgrowth treatment		↑ Neurofilaments	
<i>Antifatigue</i>						
In vivo	Male BALB/c mice		Improved the fatigue resistance Increased the antioxidant activity Inhibited the decrease in glycogen storage		↑ PGC-1 α	[103]

NA: not applicable.

TABLE 2: The health benefits and related molecular mechanisms of *Dendrobium officinale* polysaccharides.

Type of study	Object	Dosage	Effects	Potential mechanisms	References
<i>Anticancer</i>					
In vitro	Colon cancer cell line CT26 cells	0, 400, and 800 $\mu\text{g}/\text{mL}$	Induced mitochondrial dysfunction and autophagy Reduced the cell proliferation	\uparrow ROS-AMPK-autophagy pathway	[57]
In vitro	Colon cancer cell line HT-29 cells	25, 50, 100, 200, and 400 $\mu\text{g}/\text{mL}$	Inhibited the proliferation of cells Induced cell apoptosis	\uparrow Mitochondria-dependent intrinsic apoptotic pathway	[59]
In vivo	Zebrafish	27.8, 83.3, and 250 $\mu\text{g}/\text{mL}$	Inhibited tumor metastasis	NA	
In vivo	Male BALB/c mice with AOM/DSS-induced colorectal cancer	50, 100, and 200 mg/kg b.w.	Alleviated chronic colitis and colon damage Reduced the formation and growth of colon tumor Restored the intestinal barrier function Improved antitumor immune response in the tumor microenvironments	\uparrow ZO-1 and occludin \uparrow Metabolic ability of tumor infiltrated CD8(+) CTLs \uparrow PD-1	[58]
In vivo	Male Wistar rats	2.4 and 4.8 g/kg b.w.	Inhibited the gastric carcinogenesis Exerted the antioxidative effect Induced cell apoptosis	\uparrow GSH-Px and IL-2 \uparrow IL-10 \uparrow Bax and caspase-3 \downarrow 8-OHdG and MDA \downarrow Activin A, Agrin, IL-1 α , ICAM-1, and TIMP-1 \downarrow Bcl-2	[119]
In vitro	Liver hepatocellular carcinoma cell line HepG2 cells	50, 100, 200, and 400 $\mu\text{g}/\text{mL}$	Inhibited cell growth Induced apoptosis Altered mitochondrial function	\uparrow ROS \uparrow Bax \downarrow Bcl-2	[53]
In vitro	Human osteosarcoma cell line U2OS and Saos-2 cells	12.5, 25, 50, 100, and 200 $\mu\text{g}/\text{mL}$	Inhibited the proliferation of cells Increased cisplatin-induced cell apoptosis	\uparrow p53, Bax, and Bak \uparrow The ratios of cleaved caspase-9 to caspase-9, cleaved caspase-3 to caspase-3, and cleaved PARP to PARP \downarrow Bcl-2 and Mcl-1	[54]
In vitro	Human cervical carcinoma HeLa cells	25, 50, 100, 200, and 400 $\mu\text{g}/\text{mL}$	Inhibited the proliferation of cells Induced the apoptosis	\uparrow ERK, JNK, and p38	[12]
In vivo	Male Wistar rats	2.4, 4.8, and 9.6 g/kg b.w.	Prevented MNNG-induced PLGC Reduced liver and kidney damage	\uparrow Nrf2 signaling pathway \uparrow HO-1 and NQO-1 \downarrow 8-OHdG	[34]
In vivo	Male Sprague-Dawley rats	2.4, 4.8, and 9.6 g/kg b.w.	Inhibited MNNG-induced PLGC Modulated serum endogenous metabolites	\downarrow Wnt2 β , Gsk3 β , PCNA, and CyclinD1	[55]
<i>Antidiabetes</i>					
In vivo	Streptozotocin-induced diabetic male Sprague-Dawley rats	25 and 100 mg/kg b.w.	Lowered the fasting blood sugar levels	$\text{Ca}^{2+}/\text{CaM}/\text{CaMKII}$ and MAPK signaling pathways	[69]
In vitro	Murine enteroendocrine cell line STC-1 cells	0, 0.2, 2, 20, 200, and 2000 $\mu\text{g}/\text{mL}$	Increased serum insulin and GLP-1 secretion		

TABLE 2: Continued.

In vivo	Streptozotocin-induced diabetic male Wistar rats	20, 40, 80, and 160 mg/kg b.w.	Decreased the levels of fasting blood glucose, insulin, glycosylated serum protein, and serum lipid profile Alleviated the pancreatic injury Reduced the oxidative stress injury Promoted hepatic glycogen synthesis	↑ SOD ↓ MDA	[36]
In vivo	Male HFD/STZ-induced diabetic C57BL/6J mice	100, 200, and 400 mg/kg b.w.	Reduced the degradation of hepatic glycogen and hepatic gluconeogenesis Reversed the instability of the liver glycogen structure Ameliorated hepatic glucose metabolism	NA	[68]
<i>Gastrointestinal protection</i>					
In vitro	Human gastric mucosal epithelial HFE145 cells	31.25, 62.5, 125, 250, and 500 µg/mL	Ameliorated H ₂ O ₂ -induced apoptosis Decreased the number of apoptotic cells in both early and late apoptosis stages Improved the nuclei morphology changes	↑ Bcl-2 ↓ ROS, caspase-3, PARP cleavage, and Bax ↓ NF-κB activation	[33]
In vivo	Male Sprague-Dawley rats	124 and 248 mg/kg b.w.	Reduced the ethanol-induced gastric mucosal injury, mucin loss, and apoptosis Regulated the small intestinal immune function	↓ The ratio of Bax to Bcl2	
In vivo	Female ICR mice	0.5 and 2 mg/kg b.w.	Modulated intestinal mucosal structures Influenced the production of immune cytokine production	NA	[16]
In vivo	Male BALB/c mice	200 mg/kg b.w.	Improved the diversity of gut microbiota Alleviated dextran sulfate sodium-induced colitis	↑ SCFAs ↑ GPRs ↑ <i>Bacteroides</i> , <i>Lactobacillus</i> , and <i>Ruminococcaceae</i> ↓ cTNF-α, IL-6, IL-1β ↓ <i>Proteobacteria</i>	[74]
In vivo	Male Sprague-Dawley rats	100 and 400 mg/kg b.w.	Reduced gastric mucosal injury score and pathological injury Increased the antioxidant activity	↑ p-AMPK, LC3β, HO-1, and Beclin-1 ↑ Bcl-2	[80]
In vitro	Human gastric epithelial cell line GES-1 cells	62.5, 125, and 250 µg/mL	Alleviated cell apoptosis	↓ p-mTOR and p62 ↓ Caspase-3 and Bax	
<i>Cardiovascular protection</i>					
In vitro	H9c2 cardiomyocytes	6.25, 12.5, and 25 µg/mL	Increased the survival rate of cells and antioxidant enzyme activity Reduced the LDH leakage, lipid peroxidation damage, ROS production, and the mitochondrial membrane potential Ameliorated H ₂ O ₂ -induced apoptosis	↑ The ratios of p-Akt to Akt and p-ERK to ERK ↑ The ratios of Bcl-2 to Bax ↓ The ratios of p-p38 to p38, p-JNK to JNK, and p-PI3K to PI3K	[82]

TABLE 2: Continued.

<i>Liver protection</i>					
In vivo	Male Wistar rats	20, 40, 80, and 160 mg/kg b.w.	Ameliorated the liver metabolism Balanced the metabolism of ceramide and bile acids Reduced oxidative stress, inflammation, and hepatic lipid accumulation	NA	[85]
In vivo	Male ICR mice	50, 100, and 200 mg/kg b.w.	Attenuated acetaminophen-induced liver injury Triggered the dissociation of Nrf2 from Nrf2-Keap1 complex Promoted the nuclear translocation of Nrf2	↑ GSH and CAT ↑ GCLC, GCLM, HO-1, and NQO1 ↑ Nrf2-Keap1 signaling pathway ↓ ALT, AST, ROS, MDA, and MPO	[87]
In vivo	Male C57BL/6J	100, 200, and 400 mg/kg b.w.	Maintained the balance of GSH content in liver Protected against acute alcoholic liver injury	NA	[88]
In vivo	Male ICR mice	0.6 g/kg b.w.	Decreased TG and FA content in the liver Reduced C16:0/C14:0 and C18:1/C18:0 in FAs Increased C20:4/C20:3 and C22:4/C22:3 in FAs Inhibited the saturated FAs Improved the dysregulated levels of major phospholipids in the liver	↑ CPT1- α and ACOX1 ↓ FAS, SCD-1, and FATP2	[90]
<i>Lung protection</i>					
In vivo	Male Sprague-Dawley rats	200 mg/kg b.w.	Alleviated bleomycin-induced pulmonary inflammation and fibrosis Reduced the transformation of rat alveolar epithelial type II cells into myofibroblasts	↓ TGF- β 1-Smad2/3 signaling pathway ↓ Smad2/3, p-Smad2/3, collagen I, and fibronectin	[94]
In vitro	Human bronchial epithelial cells	0.01, 0.1, and 1 μ g/mL	Ameliorated the cigarette smoke-induced mucus hypersecretion and viscosity	↓ MUC5AC ↓ Mucus secretory granules	[91]
In vivo	Male Sprague-Dawley rats	50 and 200 mg/kg b.w.			
In vitro	Mouse lung epithelial cells	0.01, 0.1, and 1 μ g/mL	Ameliorated the lung functions and inflammation in chronic obstructive pulmonary disease	↑ AQP5 ↓ MUC5AC	[92]
In vivo	Sprague-Dawley rats	5, 10, and 20 mg/mL			
A randomized, double-blind, and placebo-controlled clinical trial					
	Active cigarette smokers over 40 years old with mild airflow obstruction	1.2 g thrice daily			
<i>Neuroprotection</i>					
In vivo	Pentetrazol-induced epileptic male Sprague-Dawley rats	1.5 g/kg b.w.	Reduced brain inflammation and seizures	↓ IL-1 and TNF- α ↓ MAPK signaling pathways	[41]
In vivo	Female Kunming mice	140 mg/kg b.w.	Ameliorated the learning and memory disability Reduced the oxidative stress and neuroinflammation	↑ Nrf2/HO-1 pathway	[97]

TABLE 2: Continued.

<i>Antiosteoporosis</i>					
In vitro	Bone marrow mesenchymal stem cells	100, 200, and 400 $\mu\text{g}/\text{mL}$	Enhanced osteogenic differentiation of BMSCs Inhibited adipogenic differentiation		
In vivo	Fifteen-month-old mice	150 mg/kg b.w.	Increased the bone mass Reduced the accumulation of marrow adipose tissue and oxidative stress Prevented the age-related osteoporosis	\uparrow Nrf2 signaling pathway	[100]
In vitro	RAW264.7 cells	40 and 80 $\mu\text{g}/\text{mL}$	Alleviated estradiol deficiency Maintained calcium and phosphorus homeostasis		
In vivo	Female Wistar rats	150, 300, and 600 mg/kg b.w.	Improved uterine and femoral physical parameters and bone microarchitecture Inhibited osteoclastogenesis and the expression of some osteoclast-specific genes	NA	[101]
<i>Antiobesity</i>					
In vitro	Hepatocytes, C2C12 myoblasts, and 3T3-L1 preadipocytes	200 $\mu\text{g}/\text{mL}$	Ameliorated the insulin resistance		
In vivo	Male C57BL/6 mice and ob/ob mice	150 mg/kg b.w.	Reduced insulin resistance and visceral adipose tissue inflammation Decreased the HFD-induced liver lipid accumulation	\uparrow PPAR- γ \uparrow HDL-C \downarrow TG, FFA, TC, and LDL-C	[104]
<i>Laxation</i>					
In vivo	Male and female ICR mice	29, 57, and 114 mg/kg b.w.	Attenuated constipation Increased the gastrointestinal transit ratio Improved the fecal output characteristics	\uparrow Motilin, gastrin, acetylcholinesterase, and substance P \downarrow Somatostatin	[105]

NA: not applicable.

regulating the Nrf2/HO-1 pathway and inhibiting the activation of astrocytes and microglia in cognitive decline [97]. Moreover, the flower of *Dendrobium officinale* was found to attenuate the depression-like behavior in mice with the increase in sucrose consumption and decrease in immobile time, which may be mediated by the increased expression of nerve growth factor (NGF) and brain-derived neurotrophic factor (BDNF) in hippocampus. And the regulation of neurotrophic factor expression was also verified in astrocytes through a cAMP-dependent mechanism, plasminogen, and MMP-9 [98]. However, the capacity to cross the blood-brain barrier determines the direct action of natural products in the central nervous system. The extracts of *Dendrobium officinale* may contain complex biomacromolecules that fail to cross the blood-brain barrier, and thus, they may influence brain functions via some indirect pathways like the gut-microbiota-brain axis after oral intake [99].

4.8. Other Health Benefits. There are also other bioactivities and health benefits of *Dendrobium officinale*. Its polysaccharide has confirmed its antiosteoporosis activity through

increasing osteogenic differentiation of bone marrow mesenchymal stem cells (BMSCs) and reducing adipogenic differentiation. The in vitro study revealed that the polysaccharides restored the H_2O_2 -induced abnormal cell differentiation, while the in vivo study showed that it increased the bone mass and reduced the marrow adipose tissue as well as the oxidative stress in the aged mice, in which the activation of the Nrf2 antioxidant signaling pathway was considered the main contributor to these effects against age-related osteoporosis [100]. It also ameliorated the ovariectomy- and receptor activator expression of the NF- κB ligand- (RANKL-) induced osteoporosis by improving the bone microarchitecture, preventing bone loss, inhibiting osteoclastogenesis, and reducing the expression of osteoclast-specific markers [101].

Moreover, *Dendrobium officinale* and its bioactive compounds exert potent antifatigue effects. The 4-week treatment of polysaccharides with glucomannan in size of 730 kDa could ameliorate the fatigue in mice and reduce the indicators of fatigue, such as the increased levels of lactic dehydrogenase (LDH), blood urea nitrogen (BUN), MDA, creatine

phosphokinase (CK), and lactic acid (LD) and the decreased levels of serum SOD/glutathione peroxidase (GSH-Px) and gastrocnemius glycogen [102]. Also, the extracts attenuated fatigue and improved fatigue resistance of mice by maintaining the glycogen storage, reducing oxidative stress, and promoting the expression of peroxisome proliferator-activated receptor-gamma coactivator 1-alpha (PGC-1 α) [103].

In addition, *Dendrobium officinale* showed potential antiobesity activity. The polysaccharides could reduce palmitic acid-induced insulin resistance in vitro by activating the expression of peroxisome proliferator-activated receptor-gamma (PPAR- γ). It also declined the abnormal lipid metabolism and reduced the inflammation of visceral adipose tissue in both diets and genetically induced obese mouse models [104]. Furthermore, both the ultrafine powder and polysaccharides with glucose and mannose (14:1) exerted laxative activity and alleviated constipation by improving the colonic motility function, increasing gastrointestinal transit ratio, and regulating the gut hormones like motilin, gastrin, acetyl cholinesterase, substance P, and somatostatin [1, 105].

As mentioned above, a growing body of evidence indicates that as a traditional medicine and food homologous plant, *Dendrobium officinale* has diverse biological properties and health benefits (Figure 3). The bioactivities and related mechanism of actions of *Dendrobium officinale* extracts are shown in Table 1, while that of its polysaccharides is summarized in Table 2.

5. Safety

With the widespread usage and consumption of *Dendrobium officinale*, it is essential to assure its safety and quality from aspects of cultivation, preparations, and storage. Although there is a risk for herbal plants to be contaminated by heavy metals and pesticide residue, it is often safe to consume within a certain dose range [106]. A total of 43 different pesticides were found in *Dendrobium officinale* samples from three different growing regions, of which dimethomorph was the highest one. But the risk assessment demonstrated that there was no potential exposure risk of pesticides in *Dendrobium officinale* to human health in both the long and short terms [3]. In addition, the analysis of liquid chromatography-tandem mass spectrometry with 12 pesticides showed that the half-lives of pesticides were 0.9-14.4 days, and trifloxystrobin and fluopyram required the longest interval to harvest (42 days). The chronic and acute risk assessment data illustrated that the residues of these 12 pesticides in *Dendrobium officinale* posed no harmful effect on human health. The chronic and acute risk quotients of common pesticides were quite low, indicating that *Dendrobium officinale* showed little toxicity as dietary consumption in the general population [107]. There was little report about the significant toxicity induced by the consumption of *Dendrobium officinale*. On the other hand, the daily intake should not exceed 12 g according to *Chinese Pharmacopoeia* (2020 Edition), and it is not recommended for pregnant and lactating women and infants. More clinical studies are in

demand for the risk assessment of humans under exposure to *Dendrobium officinale*.

In short, *Dendrobium officinale* is a relatively safe herbal product with high edibility and various bioactivities. Apart from controlling the safety and quality during plantation, processing, and storage, it is still essential to manage the consumption within an effective but safe dosage and proper duration for patients as a therapeutical agent or dietary supplement.

6. Challenges and Outlooks

Although *Dendrobium officinale* might be a potential candidate for dietary supplements in disease treatment, some challenges are needed to be considered in future work. As a traditional Chinese herbal medicine, *Dendrobium officinale* is often used in combination with other herbal medicines as complicated formulations. Thus, the relationship between major active compounds and diseases remains vague, and the synergistic therapeutic effects of formulations might complicate the investigation of the mechanism of individual ingredients [108]. In the last decade, increasing studies have utilized computational methods to explore this complex interaction, such as network pharmacology and bioinformatics, which could establish the model of “compound-protein/gene-disease” via databases to identify the role of certain compounds in disease treatment and predict the therapeutic targets [109]. Many studies on traditional Chinese medicine have used high-throughput transcriptomic screening for investigating the molecular effects of herbs or ingredients, which might help explore novel molecular mechanisms and support the modernization of herbal medicines and herb-derived drug discovery [110].

Most studies have concentrated on the crude polysaccharides of *Dendrobium officinale*, but their bioactivities are closely associated with the structure features, molecular weight, and ratio of components like galactose, glucose, and mannose [111]. The alkali-soluble polysaccharide from *Dendrobium officinale* showed better effects on the proliferation of lactic acid bacteria and Bifidobacteria during the fermentation than the water-soluble polysaccharide, which is mainly attributed to its higher level of total sugar, uronic acid, glucose, and mannose as well as the lower level of sugar [112]. Hence, more attention should be paid to investigations of structure-activity relationships of *Dendrobium officinale* polysaccharides [113]. On the other hand, more efforts are now being made on the identification and characterization of the structural features and compositions of *Dendrobium officinale* polysaccharide fractions, but few of them have been standardized and developed as individual ingredients or drugs for extensive pharmacological research, which might hinder the definition of mechanism and clinical application. Additionally, the quality of *Dendrobium officinale* is susceptible to multiple factors like the cultivation origin, processing, and storage procedures. In particular, the processing methods are used to extract and purify *Dendrobium officinale*, and it might result in the modification of the chemical structure or degradation of active compounds, negatively affecting their bioavailability.

Moreover, like most herbal medicines, the pharmacokinetic, absorption, distribution, metabolism, and excretion studies of *Dendrobium officinale* are rarely documented, and the present pharmacokinetic studies mainly concentrated on several herbal medicines, like curcumin, ginseng, and ginger [114, 115]. However, these studies are essential for modern drug development and clinical application. The effective dose levels, tissue distribution, and metabolites of *Dendrobium officinale* are important elements for its bioactivities and action targets, which should be further analyzed by pharmacokinetic, absorption, distribution, metabolism, and excretion studies [116].

Although *Dendrobium officinale* has a long history of being used as formulations in folk, clinical study about its individual effects on human health is still scarce and limited. More detailed and large-scale clinical trials are warranted to assess its bioactivities and therapeutical effects on different diseases.

7. Conclusion

Dendrobium officinale has been widely used as a functional food and herbal medicine for preventing and managing many disorders. The phytochemical studies showed that *Dendrobium officinale* contains abundant bioactive compounds, such as bibenzyls, polysaccharides, flavonoids, and alkaloids. The experimental investigations revealed that *Dendrobium officinale* exerted antioxidant, anti-inflammatory, and immune-regulatory properties. It had a diversity of pharmaceutical effects like anticancer, antidiabetes, gastrointestinal modulatory, cardiovascular protective, hepatoprotective, lung protective, and neuroprotective activities. Hence, *Dendrobium officinale* could be considered the potential agent of adjuvant supplements for disease treatment. However, most studies focused on crude polysaccharides as the major medicinal compound, and few new components were purified for investigations. Although *Dendrobium officinale* has been used for a long time in folk, detailed and large-scale clinical studies are still warranted to demonstrate the pharmacological effects and mechanisms in humans. In addition, more investigations combining different modern technologies are needed for better control of the quality and safety of *Dendrobium officinale*.

Abbreviations

8-OHdG:	8-Hydroxy-deoxyguanosine
ACHSFD:	Overconsumption of alcohol and high sugar and fat diets
ACOX1:	Aryl-coenzyme A oxidase
ALT:	Alanine aminotransferase
AMPK:	AMP-activated protein kinase
AQP5:	Aquaporin 5
AST:	Aspartate aminotransferase
Bak:	Bcl-2 homologous antagonist killer
Bax:	Bcl-2-associated X protein
Bcl-2:	B-cell lymphoma-2
Bcl-xL:	Bcl-extra large
BDNF:	Brain-derived neurotrophic factor

Bik:	Bcl-2 interacting killer
BMSCs:	Bone marrow mesenchymal stem cells
BUN:	Blood urea nitrogen
CaM:	Calmodulin
CaMK:	Calmodulin-dependent protein kinase
CAT:	Catalase
CCL4:	Chemokine (C-C motif) ligands 4
CK:	Creatine kinase
CPT1- α :	Carnitine palmitoyltransferase 1-alpha
CTLs:	Cytotoxic T lymphocytes
DSS:	Dextran sulfate sodium
ERK:	Extracellular signal-regulated kinases
FAS:	Fatty acid synthase
FATP2:	Fatty acid transport protein 2
FFA:	Free fatty acid
GCLC:	Glutamate-cysteine ligase catalytic subunit
GCLM:	Glutamate-cysteine ligase regulatory subunit
GLP-1:	Glucagon-like peptide-1
GPCR:	G-protein-coupled receptor
GSH:	Glutathione
GSH-Px:	Glutathione peroxidase
Gsk3 β :	Glycogen synthase kinase 3 beta
HDAC1:	Histone deacetylase 1
HDL-C:	High-density lipoprotein cholesterol
HFD:	High-fat diet
HIBD:	Hypoxic-ischemic brain damage
HO-1:	Heme oxygenase 1
ICAM-1:	Intercellular adhesion molecule 1
IFN- α :	Interferon alpha
IgM:	Immunoglobulin M
IL-1 β :	Interleukin-1 beta
IP-10:	Interferon gamma-induced protein 10
JNK:	Jun N-terminal kinase
KCC2:	K ⁺ -Cl ⁻ cotransporter 2
LD:	Lactic acid
LDH:	Lactate dehydrogenase
LDL-C:	Low-density lipoprotein cholesterol
MAPK:	Mitogen-activated protein kinases
MDA:	Malonaldehyde
MNNG:	1-Methyl-3-nitro-1-nitrosoguanidine
MPO:	Myeloperoxidase
MUC5AC:	Mucin-5AC
MyD88:	Myeloid differentiation factor
NAFLD:	Nonalcoholic fatty liver diseases
NF- κ B:	Nuclear factor kappa-B
NGF:	Nerve growth factor
NO:	Nitric oxide
NOS:	Nitric oxide synthase
NQO-1:	NAD(P)H: quinone oxidoreductase-1
Nrf2:	Nuclear factor erythroid 2-related factor 2
PARP:	Poly (ADP-ribose) polymerase
PCNA:	Proliferating cell nuclear antigen
PD-1:	Programmed death-1
PGC-1 α :	Peroxisome proliferator-activated receptor gamma coactivator 1-alpha
PI3K:	Phosphoinositide 3-kinases
PLGC:	Precancerous lesions of gastric cancer
p-IRS1:	Phosphorylation of insulin receptor substrate 1
ROS:	Reactive oxygen species

SCD-1:	Stearoyl-coenzyme A desaturase-1
SCFA:	Short-chain fatty acid
TC:	Total cholesterol
TG:	Triglyceride
TGF- β 1:	Transforming growth factor beta 1
TIMP-1:	Tissue inhibitor of matrix metalloproteinase-1
TLR4:	Toll-like receptor 4
TNF- α :	Tumor necrosis factor- α
TRAF-6:	Tumor necrosis factor receptor-associated factor-6
ZO-1:	Zonula occludens-1.

Conflicts of Interest

The authors declare no conflicts of interest.

Authors' Contributions

Xiaoyu Xu worked on conceptualization, writing, original draft preparation, and writing review and editing; Cheng Zhang worked on writing, original draft preparation, and writing review and editing; Ning Wang worked on conceptualization, writing review and editing, resources, and supervision; Yu Xu worked on resources and writing review and editing; Guoyi Tang worked on methodology and writing review and editing; Lin Xu worked on writing, original draft preparation, and data curation; Yibin Feng worked on conceptualization, funding acquisition, project administration, supervision, resources, and writing review and editing.

Acknowledgments

This work was supported by the Gala Family Trust (200007008), Contract Research (260007830 and 260007482), Health and Medical Research Fund (15162961, 16172751, and 18192141), and Hong Kong Chinese Medicine Development Fund (Project Code: 19SB2/002A).

References

- [1] D. D. Luo, C. Qu, Z. B. Zhang et al., "Granularity and laxative effect of ultrafine powder of *Dendrobium officinale*," *Journal of Medicinal Food*, vol. 20, no. 2, pp. 180–188, 2017.
- [2] B. Hou, J. Luo, Y. Zhang, Z. Niu, Q. Xue, and X. Ding, "Iteration expansion and regional evolution: phylogeography of *Dendrobium officinale* and four related taxa in southern China," *Scientific Reports*, vol. 7, no. 1, 2017.
- [3] Z. Xu, L. Li, Y. Xu et al., "Pesticide multi-residues in *Dendrobium officinale* Kimura et Migo: Method validation, residue levels and dietary exposure risk assessment," *Food Chemistry*, vol. 343, article 128490, 2021.
- [4] H. Tang, T. Zhao, Y. Sheng, T. Zheng, L. Fu, and Y. Zhang, "Dendrobium officinale Kimura et Migo: A Review on Its Ethnopharmacology, Phytochemistry, Pharmacology, and Industrialization," *Evidence-Based Complementary and Alternative Medicine*, vol. 2017, Article ID 7436259, 19 pages, 2017.
- [5] L. Yan, X. Wang, H. Liu et al., "The genome of *Dendrobium officinale* illuminates the biology of the important traditional Chinese orchid herb," *Molecular Plant*, vol. 8, no. 6, pp. 922–934, 2015.
- [6] F. Wu, Y. Zhang, W. Liu, N. Zhu, J. Chen, and Z. Sun, "Comparison of torrefied and lyophilized *Dendrobium officinale* Caulis (Tiepishihu) by Fourier transform infrared spectroscopy and two-dimensional correlation spectroscopy," *Journal of Molecular Structure*, vol. 1204, article 127554, 2020.
- [7] W. Chen, J. Lu, J. Zhang et al., "Traditional Uses, phytochemistry, pharmacology, and quality control of *dendrobium officinale* kimura et migo," *Frontiers in Pharmacology*, vol. 2026, 2021.
- [8] Y. Yuan, J. Zhang, X. Liu, M. Meng, J. Wang, and J. Lin, "Tissue-specific transcriptome for *Dendrobium officinale* reveals genes involved in flavonoid biosynthesis," *Genomics*, vol. 112, no. 2, pp. 1781–1794, 2020.
- [9] Z. Ren, F. Qiu, Y. Wang et al., "Network Analysis of Transcriptome and LC-MS Reveals a Possible Biosynthesis Pathway of Anthocyanins in *Dendrobium officinale*," *Biomed Research International*, vol. 2020, Article ID 6512895, 10 pages, 2020.
- [10] Z. Wang, W. Jiang, Y. Liu et al., "Putative genes in alkaloid biosynthesis identified in *Dendrobium officinale* by correlating the contents of major bioactive metabolites with genes expression between Protocorm-like bodies and leaves," *BMC Genomics*, vol. 22, 2021.
- [11] C. Shen, H. Guo, H. Chen et al., "Identification and analysis of genes associated with the synthesis of bioactive constituents in *Dendrobium officinale* using RNA-Seq," *Scientific Reports*, vol. 7, 2017.
- [12] W. Yu, Z. Ren, X. Zhang et al., "Structural Characterization of Polysaccharides from *Dendrobium officinale* and Their Effects on Apoptosis of HeLa Cell Line," *Molecules*, vol. 23, article 248410, 2018.
- [13] Q. L. Luo, Z. H. Tang, X. F. Zhang et al., "Chemical properties and antioxidant activity of a water-soluble polysaccharide from *Dendrobium officinale*," *International Journal of Biological Macromolecules*, vol. 89, pp. 219–227, 2016.
- [14] X. Xing, S. W. Cui, S. Nie, G. O. Phillips, H. D. Goff, and Q. Wang, "Study on *Dendrobium officinale* O-acetylglucosaminan (*Dendronan*[®]): part II. Fine structures of O-acetylated residues," *Carbohydrate Polymers*, vol. 117, pp. 422–433, 2015.
- [15] S. Huang, F. Chen, H. Cheng, and G. Huang, "Modification and application of polysaccharide from traditional Chinese medicine such as *Dendrobium officinale*," *International Journal of Biological Macromolecules*, vol. 157, pp. 385–393, 2020.
- [16] S. Z. Xie, B. Liu, D. D. Zhang, X. Q. Zha, L. H. Pan, and J. P. Luo, "Intestinal immunomodulating activity and structural characterization of a new polysaccharide from stems of *Dendrobium officinale*," *Food & Function*, vol. 7, no. 6, pp. 2789–2799, 2016.
- [17] H. Cao, Y. Ji, S. Li et al., "Extensive Metabolic Profiles of Leaves and Stems from the Medicinal Plant *Dendrobium officinale* Kimura et Migo," *Metabolites*, vol. 9, article 21510, 2019.
- [18] S. Zheng, Y. Zhu, C. Jiao et al., "Extraction and Analysis of Gigantol from *Dendrobium officinale* with Response Surface Methodology," *Molecules*, vol. 23, 2018.
- [19] Y. Zhang, L. Zhang, J. Liu, J. Liang, J. Si, and S. Wu, "Dendrobium officinale leaves as a new antioxidant source," *Journal of Functional Foods*, vol. 37, pp. 400–415, 2017.
- [20] O. I. Adejobi, J. Guan, L. Yang et al., "Transcriptomic Analyses Shed Light on Critical Genes Associated with Bibenzyl

- Biosynthesis in *Dendrobium officinale*,” *Plant-Basel*, vol. 10, p. 633, 2021.
- [21] G. Ren, W. Z. Deng, Y. F. Xie et al., “Bibenzyl Derivatives From Leaves of *Dendrobium officinale*,” *Natural Product Communications*, vol. 15, no. 2, 2020.
- [22] X. Guo, Y. Li, C. Li et al., “Analysis of the *Dendrobium officinale* transcriptome reveals putative alkaloid biosynthetic genes and genetic markers,” *Gene*, vol. 527, no. 1, pp. 131–138, 2013.
- [23] J. Yang, X. Han, H. Y. Wang et al., “Comparison of metabolomics of *Dendrobium officinale* in different habitats by UPLC-Q-TOF-MS,” *Biochemical Systematic and Ecology*, vol. 89, article 104007, 2020.
- [24] X. Chen, F. Wang, Y. Wang et al., “Discrimination of the rare medicinal plant *Dendrobium officinale* based on naringenin, bibenzyl, and polysaccharides,” *Science China-Life Sciences*, vol. 55, no. 12, pp. 1092–1099, 2012.
- [25] Z. Ye, J. R. Dai, C. G. Zhang et al., “Chemical Differentiation of *Dendrobium officinale* and *Dendrobium devonianum* by Using HPLC Fingerprints, HPLC-ESI-MS, and HPTLC Analyses,” *Evidence-Based Complementary and Alternative Medicine*, vol. 2017, Article ID 8647212, 9 pages, 2017.
- [26] J. Hu, W. Huang, F. Zhang, X. Luo, Y. Chen, and J. Xie, “Variability of Volatile Compounds in the Medicinal Plant *Dendrobium officinale* from Different Regions,” *Molecules*, vol. 25, article 504621, 2020.
- [27] Q. Meng, H. Fan, D. Xu et al., “Superfine grinding improves the bioaccessibility and antioxidant properties of *Dendrobium officinale* powders,” *International Journal of Food Science and Technology*, vol. 52, no. 6, pp. 1440–1451, 2017.
- [28] Q. Meng, H. Fan, Y. Li, and L. Zhang, “Effect of drying methods on physico-chemical properties and antioxidant activity of *Dendrobium officinale*,” *Journal of Food Measurement and Characterization*, vol. 12, no. 1, pp. 1–10, 2018.
- [29] B. Wang, W. Zhang, X. Bai, C. Li, and D. Xiang, “Rheological and physicochemical properties of polysaccharides extracted from stems of *Dendrobium officinale*,” *Food Hydrocolloids*, vol. 103, article 105706, 2020.
- [30] S. Xing, X. Zhang, H. Ke, J. Lin, Y. Huang, and G. Wei, “Physicochemical properties of polysaccharides from *Dendrobium officinale* by fractional precipitation and their preliminary antioxidant and anti-HepG2 cells activities in vitro,” *Chemistry Central Journal*, vol. 12, 2018.
- [31] L. A. He, X. T. Yan, J. Liang et al., “Comparison of different extraction methods for polysaccharides from *Dendrobium officinale* stem,” *Carbohydrate Polymers*, vol. 198, pp. 101–108, 2018.
- [32] Z. Yu, Z. Yang, J. A. T. Da Silva, J. Luo, and J. Duan, “Influence of low temperature on physiology and bioactivity of postharvest *Dendrobium officinale* stems,” *Postharvest Biology and Technology*, vol. 148, pp. 97–106, 2019.
- [33] Q. Zeng, C. H. Ko, W. S. Siu et al., “Polysaccharides of *Dendrobium officinale* Kimura & Migo protect gastric mucosal cell against oxidative damage-induced apoptosis in vitro and in vivo,” *Journal of Ethnopharmacology*, vol. 208, pp. 214–224, 2017.
- [34] Y. Zhao, Y. Sun, G. Wang, S. Ge, and H. Liu, “*Dendrobium officinale* polysaccharides protect against MNNG-induced PLGC in rats via activating the NRF2 and antioxidant enzymes HO-1 and NQO-1,” *Oxidative Medicine and Cellular Longevity*, vol. 2019, Article ID 9310245, 11 pages, 2019.
- [35] A. Valavanidis, T. Vlachogianni, and C. Fiotakis, “8-Hydroxy-2'-deoxyguanosine (8-OHdG): a critical biomarker of oxidative stress and carcinogenesis,” *Journal of Environmental Science and Health Part C-Environmental Carcinogenesis & Ecotoxicology Reviews*, vol. 27, no. 2, pp. 120–139, 2009.
- [36] H. Chen, Q. Nie, J. Hu, X. Huang, W. Huang, and S. Nie, “Metabolism amelioration of *Dendrobium officinale* polysaccharide on type II diabetic rats,” *Food Hydrocolloids*, vol. 102, article 105582, 2020.
- [37] H. J. Forman and H. Q. Zhang, “Targeting oxidative stress in disease: promise and limitations of antioxidant therapy,” *Nature Reviews Drug Discovery*, vol. 20, no. 9, pp. 689–709, 2021.
- [38] L. Xiao, T. B. Ng, Y. B. Feng et al., “*Dendrobium candidum* extract increases the expression of aquaporin-5 in labial glands from patients with Sjögren’s syndrome,” *Phytomedicine*, vol. 18, no. 2-3, pp. 194–198, 2011.
- [39] X. Lin, P. C. Shaw, S. C. Sze, Y. Tong, and Y. Zhang, “*Dendrobium officinale* polysaccharides ameliorate the abnormality of aquaporin 5, pro-inflammatory cytokines and inhibit apoptosis in the experimental Sjögren’s syndrome mice,” *International Immunopharmacology*, vol. 11, no. 12, pp. 2025–2032, 2011.
- [40] L. Xiang, C. W. S. Sze, T. B. Ng et al., “Polysaccharides of *Dendrobium officinale* inhibit TNF- α -induced apoptosis in A-253 cell line,” *Inflammation Research*, vol. 62, no. 3, pp. 313–324, 2013.
- [41] L. Zhang, H. Peng, J. Xu et al., “Effects of *dendrobium officinale* polysaccharides on brain inflammation of epileptic rats,” *International Journal of Polymer Science*, vol. 2019, Article ID 9058161, 6 pages, 2019.
- [42] M. Zhang, J. Wu, J. Han, H. Shu, and K. Liu, “Isolation of polysaccharides from *Dendrobium officinale* leaves and anti-inflammatory activity in LPS-stimulated THP-1 cells,” *Chemistry Central Journal*, vol. 12, pp. 1–9, 2018.
- [43] T. B. He, Y. P. Huang, L. Yang et al., “Structural characterization and immunomodulating activity of polysaccharide from *Dendrobium officinale*,” *International Journal of Biological Macromolecules*, vol. 83, pp. 34–41, 2016.
- [44] Y. P. Huang, T. B. He, X. D. Cuan, X. J. Wang, J. M. Hu, and J. Sheng, “1,4-beta-D-Glucomannan from *Dendrobium officinale* Activates NF-kappa B via TLR4 to Regulate the Immune Response,” *Molecules*, vol. 23, article 265810, Article ID 2018, p. 2658.
- [45] X. Huang, S. Nie, H. Cai et al., “Study on *Dendrobium officinale* O-acetyl-glucomannan (*Dendronan*): part IV. Immunomodulatory activity in vivo,” *Journal of Functional Foods*, vol. 15, pp. 525–532, 2015.
- [46] S. Tao, Z. Lei, K. Huang et al., “Structural characterization and immunomodulatory activity of two novel polysaccharides derived from the stem of *Dendrobium officinale* Kimura et Migo,” *Journal of Functional Foods*, vol. 57, pp. 121–134, 2019.
- [47] Y. J. Zeng, H. R. Yang, H. F. Wang, M. H. Zong, and W. Y. Lou, “Immune enhancement activity of a novel polysaccharide produced by *Dendrobium officinale* endophytic fungus *Fusarium solani* DO7,” *Journal of Functional Foods*, vol. 53, pp. 266–275, 2019.
- [48] K. Huang, Y. Li, S. Tao et al., “Purification, Characterization and Biological Activity of Polysaccharides from *Dendrobium officinale*,” *Molecules*, vol. 21, no. 6, 2016.

- [49] X. Lin, J. Liu, W. Chung et al., "Polysaccharides of *Dendrobium officinale* induce aquaporin 5 translocation by activating M3 muscarinic receptors," *Planta Medica*, vol. 81, no. 2, pp. 130–137, 2015.
- [50] M. Li, H. Yue, Y. Wang et al., "Intestinal microbes derived butyrate is related to the immunomodulatory activities of *Dendrobium officinale* polysaccharide," *International Journal of Biological Macromolecules*, vol. 149, pp. 717–723, 2020.
- [51] R. S. Wong, "Apoptosis in cancer: from pathogenesis to treatment," *Journal of Experimental and Clinical Cancer Research*, vol. 30, pp. 1–4, 2011.
- [52] M. A. O'Brien and R. Kirby, "Apoptosis: a review of proapoptotic and anti-apoptotic pathways and dysregulation in disease," *Journal of Veterinary Emergency and Critical Care*, vol. 18, no. 6, pp. 572–585, 2008.
- [53] Y. Wei, L. Wang, D. Wang et al., "Characterization and anti-tumor activity of a polysaccharide isolated from *Dendrobium officinale* grown in the Huoshan County," *Chinese Medicine*, vol. 13, p. 1, 2018.
- [54] X. Zhang, S. Duan, S. Tao et al., "Polysaccharides from *Dendrobium officinale* inhibit proliferation of osteosarcoma cells and enhance cisplatin-induced apoptosis," *Journal of Functional Foods*, vol. 73, article 104143, 2020.
- [55] Y. Zhao, B. Li, G. Wang et al., "Dendrobium officinale Polysaccharides Inhibit 1-Methyl-2-Nitro-1-Nitrosoguanidine Induced Precancerous Lesions of Gastric Cancer in Rats through Regulating Wnt/beta-Catenin Pathway and Altering Serum Endogenous Metabolites," *Molecules*, vol. 24, article 266014, 2019.
- [56] T. Zaidieh, J. R. Smith, K. E. Ball, and Q. An, "ROS as a novel indicator to predict anticancer drug efficacy," *BMC Cancer*, vol. 19, no. 1, pp. 1–4, 2019.
- [57] K. Zhang, X. Zhou, J. Wang et al., "Dendrobium officinale polysaccharide triggers mitochondrial disorder to induce colon cancer cell death via ROS-AMPK-autophagy pathway," *Carbohydrate Polymers*, vol. 264, p. 118018, 2021.
- [58] J. Liang, H. Li, J. Chen et al., "Dendrobium officinale polysaccharides alleviate colon tumorigenesis via restoring intestinal barrier function and enhancing anti-tumor immune response," *Pharmacological Research*, vol. 148, article 104417, 2019.
- [59] S. Tao, C. Huang, Z. Tan et al., "Effect of the polysaccharides derived from *Dendrobium officinale* stems on human HT-29 colorectal cancer cells and a zebrafish model," *Food Bioscience*, vol. 41, article 100995, 2021.
- [60] W. Zhao, J. Li, C. Zhong, X. Zhang, and Y. Bao, "Green synthesis of gold nanoparticles from *Dendrobium officinale* and its anticancer effect on liver cancer," *Drug Delivery*, vol. 28, no. 1, pp. 985–994, 2021.
- [61] G. Y. Zhao, B. W. Deng, C. Y. Zhang, Y. D. Cui, J. Y. Bi, and G. G. Zhang, "New phenanthrene and 9, 10-dihydrophenanthrene derivatives from the stems of *Dendrobium officinale* with their cytotoxic activities," *Journal of Natural Medicines*, vol. 72, no. 1, pp. 246–251, 2018.
- [62] N. Lascar, J. Brown, H. Pattison, A. H. Barnett, C. J. Bailey, and S. Bellary, "Type 2 diabetes in adolescents and young adults," *Lancet Diabetes & Endocrinology*, vol. 6, no. 1, pp. 69–80, 2018.
- [63] A. K. Jugran, S. Rawat, H. P. Devkota, I. D. Bhatt, and R. S. Rawal, "Diabetes and plant-derived natural products: from ethnopharmacological approaches to their potential for modern drug discovery and development," *Phytotherapy Research*, vol. 35, no. 1, pp. 223–245, 2021.
- [64] X. Gong, M. Y. Ji, J. P. Xu, C. H. Zhang, and M. H. Li, "Hypoglycemic effects of bioactive ingredients from medicine food homology and medicinal health food species used in China," *Critical Reviews in Food Science and Nutrition*, vol. 60, no. 14, pp. 2303–2326, 2020.
- [65] B. Pang, Q. Zhou, T. Y. Zhao et al., "Innovative Thoughts on Treating Diabetes from the Perspective of Traditional Chinese Medicine," *Evidence-Based Complementary and Alternative Medicine*, vol. 2015, Article ID 905432, 12 pages, 2015.
- [66] C. Figueroa-Benavides, M. J. Matos, M. Peñaloza-Amion et al., "Targeting α -(1,4)-Glucosidase in diabetes mellitus type 2: the role of new synthetic Coumarins as potent inhibitors," *Current Topics in Medicinal Chemistry*, vol. 18, no. 27, pp. 2327–2337, 2018.
- [67] C. Chu, T. Li, H. A. Pedersen, K. T. Kongstad, J. Yan, and D. Staerk, "Antidiabetic constituents of *Dendrobium officinale* as determined by high-resolution profiling of radical scavenging and α -glucosidase and α -amylase inhibition combined with HPLC-PDA-HRMS-SPE-NMR analysis," *Phytochemistry Letters*, vol. 31, pp. 47–52, 2019.
- [68] Y. Liu, L. Yang, Y. Zhang et al., "Dendrobium officinale polysaccharide ameliorates diabetic hepatic glucose metabolism via glucagon-mediated signaling pathways and modifying liver-glycogen structure," *Journal of Ethnopharmacology*, vol. 248, article 112308, 2020.
- [69] M. T. Kuang, J. Y. Li, X. B. Yang et al., "Structural characterization and hypoglycemic effect via stimulating glucagon-like peptide-1 secretion of two polysaccharides from *Dendrobium officinale*," *Carbohydrate Polymers*, vol. 241, 2020.
- [70] H. Zheng, L. Pan, P. Xu et al., "An NMR-Based Metabolomic Approach to Unravel the Preventive Effect of Water-Soluble Extract from *Dendrobium officinale* Kimura & Migo on Streptozotocin-Induced Diabetes in Mice," *Molecules*, vol. 22, p. 15439, 2017.
- [71] Z. Y. Chen, Q. Lan, S. Chen et al., "Effects of *Dendrobium candidum* polysaccharides on microRNA-125b and mitogen-activated protein kinase signaling pathways in diabetic cataract rats," *Traditional Medicine Research*, vol. 6, no. 5, p. 45, 2021.
- [72] Y. Fan and O. Pedersen, "Gut microbiota in human metabolic health and disease," *Nature Reviews Microbiology*, vol. 19, no. 1, pp. 55–71, 2021.
- [73] X. Li, X. Peng, K. Guo, and Z. Tan, "Bacterial diversity in intestinal mucosa of mice fed with *Dendrobium officinale* and high-fat diet," *3 Biotech*, vol. 11, 2021.
- [74] Y. Zhang, Z. Wu, J. Liu et al., "Identification of the core active structure of a *Dendrobium officinale* polysaccharide and its protective effect against dextran sulfate sodium-induced colitis via alleviating gut microbiota dysbiosis," *Food Research International*, vol. 137, article 109641, 2020.
- [75] B. Li, X. He, H. Jin et al., "Beneficial effects of *Dendrobium officinale* on metabolic hypertensive rats by triggering the enteric-origin SCFA-GPCR43/41 pathway," *Food & Function*, vol. 12, no. 12, pp. 5524–5538, 2021.
- [76] L. Li, H. Yao, X. Li et al., "Destiny of *Dendrobium officinale* polysaccharide after oral administration: indigestible and nonabsorbing, ends in modulating gut microbiota," *Journal of Agricultural and Food Chemistry*, vol. 67, no. 21, pp. 5968–5977, 2019.

- [77] Y. Fu, J. Zhang, K. Chen et al., "An in vitro fermentation study on the effects of *Dendrobium officinale* polysaccharides on human intestinal microbiota from fecal microbiota transplantation donors," *Journal of Functional Foods*, vol. 53, pp. 44–53, 2019.
- [78] H. F. Liu, J. X. Liang, Y. M. Zhong et al., "Dendrobium officinale polysaccharide alleviates intestinal inflammation by promoting small extracellular vesicle packaging of miR-433-3p," *Journal of Agricultural and Food Chemistry*, vol. 69, no. 45, pp. 13510–13523, 2021.
- [79] S. S. Lei, B. Li, Y. H. Chen et al., "Dendrobium officinale, a traditional Chinese edible and officinal plant, accelerates liver recovery by regulating the gut-liver axis in NAFLD mice," *Journal of Functional Foods*, vol. 61, 2019.
- [80] Y. Ke, L. Zhan, T. Lu et al., "Polysaccharides of *Dendrobium officinale* Kimura & Migo leaves protect against ethanol-induced gastric mucosal injury via the AMPK/mTOR signaling pathway in vitro and in vivo," *Frontiers in Pharmacology*, vol. 11, article 526349, 2020.
- [81] A. Albillos, A. de Gottardi, and M. Rescigno, "The gut-liver axis in liver disease: pathophysiological basis for therapy," *Journal of Hepatology*, vol. 72, no. 3, pp. 558–577, 2020.
- [82] J. Y. Zhang, Y. Guo, J. P. Si, X. B. Sun, G. B. Sun, and J. J. Liu, "A polysaccharide of *Dendrobium officinale* ameliorates H₂O₂-induced apoptosis in H9c2 cardiomyocytes via PI3K/AKT and MAPK pathways," *International Journal of Biological Macromolecules*, vol. 104, pp. 1–10, 2017.
- [83] X. Zhao, M. Dou, Z. Zhang, D. Zhang, and C. Huang, "Protective effect of *Dendrobium officinale* polysaccharides on H₂O₂-induced injury in H9c2 cardiomyocytes," *Biomedicine and Pharmacotherapy*, vol. 94, pp. 72–78, 2017.
- [84] Z. Zhang, D. Zhang, M. Dou, Z. Li, J. Zhang, and X. Zhao, "Dendrobium officinale Kimura et Migo attenuates diabetic cardiomyopathy through inhibiting oxidative stress, inflammation and fibrosis in streptozotocin-induced mice," *Biomedicine and Pharmacotherapy*, vol. 84, pp. 1350–1358, 2016.
- [85] J. Yang, H. Chen, Q. Nie, X. Huang, and S. Nie, "Dendrobium officinale polysaccharide ameliorates the liver metabolism disorders of type II diabetic rats," *International Journal of Biological Macromolecules*, vol. 164, pp. 1939–1948, 2020.
- [86] J. Zeng, D. Li, Z. Li, J. Zhang, and X. Zhao, "Dendrobium officinale attenuates myocardial fibrosis via inhibiting EMT signaling pathway in HFD/STZ-induced diabetic mice," *Biological & Pharmaceutical Bulletin*, vol. 43, no. 5, pp. 864–872, 2020.
- [87] G. Lin, D. Luo, J. Liu et al., "Hepatoprotective effect of polysaccharides isolated from *Dendrobium officinale* against acetaminophen-induced liver injury in mice via regulation of the Nrf2-Keap1 signaling pathway," *Oxidative Medicine and Cellular Longevity*, vol. 2018, Article ID 6962439, 10 pages, 2018.
- [88] G. Nie, Y. Zhang, Z. H. Zhou et al., "Dynamic evaluation of the protective effect of *Dendrobium officinale* polysaccharide on acute alcoholic liver injury mice in vitro and in vivo by NIR fluorescence imaging," *Analytical and Bioanalytical Chemistry*, vol. 413, no. 23, pp. 5715–5724, 2021.
- [89] Y. L. Wu, S. H. Huang, C. M. He et al., "Dendrobium officinale flower extraction mitigates alcohol-induced liver injury in mice: role of antisteatosis, antioxidative, and anti-inflammatory," *Evidence-Based Complementary and Alternative Medicine*, vol. 2020, Article ID 1421853, 12 pages, 2020.
- [90] S. S. Lei, N. Y. Zhang, F. C. Zhou et al., "Dendrobium officinale regulates fatty acid metabolism to ameliorate liver lipid accumulation in NAFLD mice," *Evidence-Based Complementary and Alternative Medicine*, vol. 2021, Article ID 6689727, 12 pages, 2021.
- [91] R. Chen, Y. Liang, M. S. M. Ip, K. Y. Zhang, and J. C. W. Mak, "Amelioration of cigarette smoke-induced mucus hypersecretion and viscosity by *Dendrobium officinale* polysaccharides in vitro and in vivo," *Oxidative Medicine and Cellular Longevity*, vol. 2020, Article ID 8217642, 10 pages, 2020.
- [92] T. H. Song, X. X. Chen, S. C. W. Tang et al., "Dendrobium officinale polysaccharides ameliorated pulmonary function while inhibiting mucin-5AC and stimulating aquaporin-5 expression," *Journal of Functional Foods*, vol. 21, pp. 359–371, 2016.
- [93] Y. Liang, R. Du, R. Chen et al., "Therapeutic potential and mechanism of *Dendrobium officinale* polysaccharides on cigarette smoke-induced airway inflammation in rat," *Biomedicine and Pharmacotherapy*, vol. 143, article 112101, 2021.
- [94] J. Chen, J. Lu, B. Wang et al., "Polysaccharides from *Dendrobium officinale* inhibit bleomycin-induced pulmonary fibrosis via the TGFβ1-Smad2/3 axis," *International Journal of Biological Macromolecules*, vol. 118, pp. 2163–2175, 2018.
- [95] Y. Wen, H. Xiao, Y. Liu et al., "Polysaccharides from *Dendrobium officinale* ameliorate colitis-induced lung injury via inhibiting inflammation and oxidative stress," *Chemico-Biological Interactions*, vol. 347, p. 109615, 2021.
- [96] X. L. Li and M. Hong, "Aqueous extract of *Dendrobium officinale* confers neuroprotection against hypoxic-ischemic brain damage in neonatal rats," *Kaohsiung Journal of Medical Sciences*, vol. 36, no. 1, pp. 43–53, 2020.
- [97] J. Liang, Y. Wu, H. Yuan et al., "Dendrobium officinale polysaccharides attenuate learning and memory disabilities via anti-oxidant and anti-inflammatory actions," *International Journal of Biological Macromolecules*, vol. 126, pp. 414–426, 2019.
- [98] Y. Zhu, M. Liu, C. Cao et al., "Dendrobium officinale flos increases neurotrophic factor expression in the hippocampus of chronic unpredictable mild stress-exposed mice and in astrocyte primary culture and potentiates NGF-induced neuronal differentiation in PC12 cells," *Phytotherapy Research*, vol. 35, no. 5, pp. 2665–2677, 2021.
- [99] Q. P. Zhang, J. Cheng, Q. Liu, G. H. Xu, C. F. Li, and L. T. Yi, "Dendrobium officinale polysaccharides alleviate depression-like symptoms via regulating gut microbiota-neuroinflammation in perimenopausal mice," *Journal of Functional Foods*, vol. 88, 2022.
- [100] H. Peng, M. Yang, Q. Guo, T. Su, Y. Xiao, and Z. Y. Xia, "Dendrobium officinale polysaccharides regulate age-related lineage commitment between osteogenic and adipogenic differentiation," *Cell Proliferation*, vol. 52, 2019.
- [101] Q. Wang, C. T. Zi, J. Wang et al., "Dendrobium officinale orchid extract prevents ovariectomy-induced osteoporosis in vivo and inhibits RANKL-induced osteoclast differentiation in vitro," *Frontiers in Pharmacology*, vol. 8, 2017.
- [102] W. Wei, Z. P. Li, T. Zhu et al., "Anti-fatigue effects of the unique polysaccharide marker of *Dendrobium officinale* on BALB/c mice," *Molecules*, vol. 22, no. 1, p. 155, 2017.
- [103] S. Kim, K. Jo, B. S. Byun et al., "Chemical and biological properties of puffed *Dendrobium officinale* extracts: evaluation of

- antioxidant and anti-fatigue activities,” *Journal of Functional Foods*, vol. 73, 2020.
- [104] J. Qu, S. Tan, X. Xie et al., “Dendrobium officinale polysaccharide attenuates insulin resistance and abnormal lipid metabolism in obese mice,” *Frontiers in Pharmacology*, vol. 12, 2021.
- [105] D. D. Luo, C. Qu, G. S. Lin et al., “Character and laxative activity of polysaccharides isolated from *Dendrobium officinale*,” *Journal of Functional Foods*, vol. 34, pp. 106–117, 2017.
- [106] J. Yang, X. Dong, X. Zhen et al., “Metal organic framework assisted in situ complexation for miniaturized solid phase extraction of organic mercury in fish and *Dendrobium officinale*,” *Talanta*, vol. 209, 2020.
- [107] Y. Fu, Q. S. Wang, L. Zhang, S. P. Ling, H. Y. Jia, and Y. L. Wu, “Dissipation, occurrence, and risk assessment of 12 pesticides in *Dendrobium officinale* Kimura et Migo,” *Ecotoxicology and Environmental Safety*, vol. 222, 2021.
- [108] X. Zhou, S. W. Seto, D. Chang et al., “Synergistic effects of Chinese herbal medicine: a comprehensive review of methodology and current research,” *Frontiers in Pharmacology*, vol. 7, p. 201, 2016.
- [109] R. Z. Zhang, X. Zhu, H. Bai, and K. Ning, “Network pharmacology databases for traditional Chinese medicine: review and assessment,” *Frontiers in Pharmacology*, vol. 10, p. 123, 2019.
- [110] S. Fang, L. Dong, L. Liu et al., “HERB: a high-throughput experiment- and reference-guided database of traditional Chinese medicine,” *Nucleic Acids Research*, vol. 49, no. D1, pp. D1197–D1206, 2020.
- [111] M. L. Jin, K. Zhao, Q. S. Huang, C. L. Xu, and P. Shang, “Isolation, structure and bioactivities of the polysaccharides from *Angelica sinensis* (Oliv.) Diels: a review,” *Carbohydrate Polymers*, vol. 89, no. 3, pp. 713–722, 2012.
- [112] L. Xing, Y. L. Miao, N. Li, L. Jiang, and J. Y. Chen, “Molecular structure features and lactic acid fermentation behaviors of water- and alkali-soluble polysaccharides from *Dendrobium officinale*,” *Journal of Food Science and Technology-Mysore*, vol. 58, no. 2, pp. 532–540, 2021.
- [113] D. D. Wang, S. Shao, Y. Q. Zhang, D. Q. Zhao, and M. X. Wang, “Insight into polysaccharides from *Panax ginseng* C. A. Meyer in improving intestinal inflammation: modulating intestinal microbiota and autophagy,” *Frontiers in Immunology*, vol. 12, article 683911, 2021.
- [114] X. Y. Xu, X. Meng, S. Li, R. Y. Gan, Y. Li, and H. B. Li, “Bioactivity, health benefits, and related molecular mechanisms of curcumin: current progress, challenges, and perspectives,” *Nutrients*, vol. 10, no. 10, p. 1553, 2018.
- [115] S. M. He, E. Chan, and S. F. Zhou, “ADME properties of herbal medicines in humans: evidence, challenges and strategies,” *Current Pharmaceutical Design*, vol. 17, no. 4, pp. 357–407, 2011.
- [116] X. W. Chen, K. B. Sneed, and S. F. Zhou, “Pharmacokinetic profiles of anticancer herbal medicines in humans and the clinical implications,” *Current Medicinal Chemistry*, vol. 18, no. 21, pp. 3190–3210, 2011.
- [117] S. Z. Hou, C. Y. Liang, H. Z. Liu et al., “*Dendrobium officinale* prevents early complications in streptozotocin-induced diabetic rats,” *Evidence-Based Complementary and Alternative Medicine*, vol. 2016, Article ID 6385850, 10 pages, 2016.
- [118] M. M. Dou, Z. H. Zhang, Z. B. Li, J. Zhang, and X. Y. Zhao, “Cardioprotective potential of *Dendrobium officinale* Kimura et Migo against myocardial ischemia in mice,” *Molecular Medicine Reports*, vol. 14, no. 5, pp. 4407–4414, 2016.
- [119] Y. Zhao, Y. Liu, X. M. Lan et al., “Effect of *Dendrobium officinale* extraction on gastric carcinogenesis in rats,” *Evidence-Based Complementary and Alternative Medicine*, vol. 2016, Article ID 1213090, 8 pages, 2016.

Research Article

The Ameliorative Role of Eugenol against Silver Nanoparticles-Induced Hepatotoxicity in Male Wistar Rats

Hany N. Yousef , Somaya S. Ibraheim, Ramadan A. Ramadan, and Hanaa R. Aboelwafa 

Department of Biological and Geological Sciences, Faculty of Education, Ain Shams University, Cairo 11566, Egypt

Correspondence should be addressed to Hany N. Yousef; hany_barsoum@edu.asu.edu.eg

Received 30 April 2022; Revised 4 July 2022; Accepted 3 August 2022; Published 10 September 2022

Academic Editor: Cassiano Felipe Gonçalves-de-Albuquerque

Copyright © 2022 Hany N. Yousef et al. This is an open access article distributed under the Creative Commons Attribution License, which permits unrestricted use, distribution, and reproduction in any medium, provided the original work is properly cited.

Background. Silver nanoparticles (AgNPs) utilization is becoming increasingly popular. The existing investigation evaluates the ameliorative impact of eugenol (Eug) against the toxic influences of AgNPs on rats' liver. **Methods.** Sixty adult male rats were enrolled equally into control, Eug (100 mg kg⁻¹ orally), AgNPs-low dose (1 mg kg⁻¹ i.p), AgNPs-high dose (2 mg kg⁻¹ i.p), Eug + AgNPs-low dose (100 mg kg⁻¹ orally + 1 mg kg⁻¹ i.p), and Eug + AgNPs high dose (100 mg kg⁻¹ orally + 2 mg kg⁻¹ i.p). All the groups were treated daily for 30 days, subsequently serum aspartate transaminase (AST), alanine transaminase (ALT), alkaline phosphatase (ALP), total protein, total albumin, lactate dehydrogenase (LDH), total oxidative capacity (TOC), malondialdehyde (MDA), tumor necrosis factor-alpha (TNF- α), total antioxidant capacity (TAC), and interleukin 6 (IL-6) levels were measured; hepatic tissues superoxide dismutase (SOD), catalase (CAT), reduced glutathione (GSH), and glutathione peroxidase (GPx) levels were evaluated; histopathology and histomorphometry were documented in the liver of all groups; and Bcl-2, P53, Caspase-3, and TNF- α reactive proteins were also immunohistochemically detected. **Results.** AgNPs significantly triggered oxidative stress in hepatic tissues, characterized by elevated levels of AST, ALT, ALP, LDH, TOC, MDA, TNF- α , and IL-6 correlating with considerable decline in total protein, total albumin, TAC, SOD, CAT, GSH, and GPx. These changes were paralleled with histopathological alterations remarkable by devastation of the ordinary hepatic structure, with decrease in the numbers of normal hepatocytes, elevation in the numbers of necrotic hepatocytes, periportal and centrilobular inflammatory cells, deteriorated Kupffer cells, and dilated/congested central and portal veins. Alongside, a marked diminution in Bcl-2 immunoreactivity and a significant elevation in P53, Caspase-3, and TNF- α immunoreactivities were recorded. Supplementation of AgNPs-treated animals with Eug reversed most of the biochemical, histopathological, and immunohistochemical changes. **Conclusion.** This study proposed that Eug has an ameliorative effect against AgNPs-induced hepatotoxicity.

1. Introduction

Nanoparticles (NPs) are materials with a particle magnitude ranging from 1 to 100 nm that may be of natural inception or can be created by human industrial activities. Owing to their size, surface charge, and surface area, NPs possess unique physicochemical characteristics [1]. There is an expanding demand for using NPs in drug and medical services, materials science, industrial and household applications, electronics, energy harvesting, and mechanical industries [2].

Silver nanoparticles (AgNPs) attracted immense research attention worldwide consequent to their eminent

physical, chemical, and biological advantages. AgNPs are utilized as antimicrobial substances in many industries like biomedicine [3], cosmetics [4], food packaging [5], textile coating [6], and water disinfection [7]. AgNPs are also employed in many other fields, such as molecular imaging [8], drug delivery, and anticancer therapeutics [9].

The expanding utilization of nanomaterials in our daily life increases environmental worries. AgNPs can either purposely or unpurposely enter the human body via inhalation, drinking, ingestion, skin uptake, or intravenous injection [2]. Inside the body, AgNPs can translocate and accumulate in different tissues, including the liver, heart, lungs, kidneys,

and nervous tissues, where they interfere with the metabolic pathways inside the cells and exert adverse effects and toxicity [10]. The liver is a prime accumulation site of circulatory AgNPs, which cause cellular injury and toxic effects on it [11].

The mechanisms underlying AgNPs-induced cytotoxicity and genotoxicity are unclear. The liberation of silver ions and formation of reactive oxygen species (ROS) are proposed to be the possible reasons for the toxic impacts of AgNPs [12]. The increased intracellular ROS levels induce oxidative stress and subsequent lipid peroxidation and cellular macromolecular damage, which eventually leads to cell death [13].

Numerous investigations have emphasized the antioxidant potential of phytochemicals [14]. Eugenol (Eug; 1-allyl-4-hydroxy-3-methoxybenzene [$C_{10}H_{12}O_2$]) is a phenolic phytochemical abundantly present in clove, cinnamon, and basil and is used as a flavoring substance in foods and cosmetics and as a preservative in foods [15]. Eug has several pharmacological activities, including antimicrobial [16], antioxidant [17], anti-inflammatory [18], and anticancer [19] efficiencies.

According to the current literature, very rare and non-specific studies on the protective impact of Eug in reducing AgNPs-induced hepatotoxicity in male rats have been done. Thus, the present study's objective was to elucidate Eug's potential ameliorative effect against AgNPs-induced hepatotoxicity in male rats employing biochemical, histological, histomorphometrical, and immunohistochemical approaches.

2. Materials and Methods

2.1. Chemicals Used. Silver nitrate ($AgNO_3$, 99%), gelatin, and eugenol (Eug, 99%) were obtained from Sigma-Aldrich (St. Louis, MO, USA). Additional reagents and chemicals used were of high analytical grade and pureness.

2.2. Synthesis of AgNPs. AgNPs were synthesized using $AgNO_3$ and gelatin via the microwave method according to [20]. 16.987 g of $AgNO_3$ was dissolved in 100 mL of deionized distilled water for 20 min. Next, 1 g of gelatin soluble in deionized distilled water was added to AgNPs. The solution was stirred at 60°C for 24 h on a direct hot plate and then subjected to microwave irradiation at 700 watts for 5 min. All samples were naturally chilled at room temperature, and carefully covered and capped.

2.3. Physicochemical Characterization of AgNPs. Ultraviolet-visible (UV-VIS) spectroscopy (JASCO V-550 UV/VIS double-beam spectrophotometer, Tokyo, Japan) was used for the primary characterization of the synthesized AgNPs and to monitor their synthesis and stability. The crystallinity of AgNPs was characterized using an X-ray diffractometer (XRD) employing $CuK\alpha$ radiation. The sample was scanned over a 2θ range of 10°-80°. The chemical state and elemental composition were measured via X-ray photoelectron spectroscopy (XPS). The morphology of NPs was investigated by scanning electron microscopy (SEM) operating at

20 kV. Transmission electron microscopy (TEM) was performed to monitor the size and morphological stability of AgNPs [21]. AgNPs samples from the stock suspensions were sonicated in nanopure water for 30 min at room temperature. Then, a drop from the dilute specimen solution was dropped onto an amorphous carbon-coated copper grid and air dried, generating a monolayer. The particle diameters of the synthesized AgNPs were assessed using the software image analysis program over various shots of TEM photomicrographs for the intended specimen [22] at the Central Laboratory, Faculty of Agriculture, Cairo University, Egypt.

2.4. Experimental Animals. Sixty males of albino rats (*Rattus norvegicus*) of nearly equal age and weighing 180-200 g were obtained from the Schistosoma Biological Supply Program, Theodor Bilharz Research Institute, El-Giza, Egypt. The rats were kept in clean plastic crates supplied with wood shavings and fed a regular rodent pellet diet, besides water *ad libitum* at room temperature ($25 \pm 2^\circ C$), with a 12/12-h light-dark period and $55 \pm 5\%$ relative humidity. Before experimentation, all rats were allowed to adapt for a week. This study was in compliance with the international standards for animal laboratory treatment set by the local Institutional Animal Ethics Committee of Ain Shams University for the use and treatment of animals.

2.5. Experimental Design. The rats were put into six groups, each with 10 animals. They were treated daily at 9 a.m. for 30 days as follows:

Control group: healthy rats intraperitoneally (i.p.) injected with 1 mL deionized distilled water (vehicle for AgNPs) and orally received 1 mL corn oil (vehicle for Eug) by oral gavage.

Eug-treated group: rats were orally given Eug (100 mg kg^{-1} body weight) suspended in 1 mL of corn oil by oral gavage. This dose was calculated according to the dose used in previous rat studies [23].

AgNPs-low-dose-treated group: rats were i.p. treated with AgNPs (1 mg kg^{-1} body weight) dissolved in 1 mL of deionized distilled water.

AgNPs-high-dose-treated group: rats were i.p. treated with AgNPs (2 mg kg^{-1} body weight) dissolved in 1 mL of deionized distilled water.

The low and high doses of AgNPs were selected based on those used in previous investigations [2].

Eug + AgNPs-low-dose-treated group: rats were orally given Eug (100 mg kg^{-1} body weight) paralleled with i.p. injection of AgNPs-low dose (1 mg kg^{-1} body weight).

Eug + AgNPs-high-dose-treated group: rats were orally given Eug (100 mg kg^{-1} body weight) paralleled with i.p. injection of AgNPs-high dose (2 mg kg^{-1} body weight).

2.6. Collection of Sera and Tissue Samples. At the end of all treatments, the rats were fasted nightly, and in the following morning, they were anesthetized with light ether anesthesia. Using cardiac puncture, samples of blood were obtained and centrifuged for 10 minutes at $1500 \times g$ and $4^\circ C$ to get sera that were promptly preserved at $-80^\circ C$ until usage. The

TABLE 1: The utilized antibodies in the immunohistochemical investigation.

Antibody	Code	Clone	Antigen retrieval	Dilution	Sources	Company
Bcl-2	MA5-11757	100/D5	PBS, pH 7.4 with 0.2% BSA	1 : 50	Mouse/IgG1, kappa	Thermo Fisher Scientific (USA)
P53	MA5-12557	DO-7	PBS, pH 7.4	1 : 100-1 : 200	Mouse/IgG2b, kappa	Thermo Fisher Scientific
Caspase-3	MA5-11516	3CSP01 (7.1.44)	PBS, pH 7.4, with 0.2% BSA	1 : 50-1 : 100	Mouse/IgG2a	Thermo Fisher Scientific
TNF- α	MA5-23720	28401	PBS with 5% trehalose	8-25 μ g/mL	Mouse/IgG1	Thermo Fisher Scientific

livers of dissected rats were segregated out and instantly rinsed with ice-cold 0.9% NaCl physiological saline, and then they were kept frozen at -80°C for additional biochemical investigations, while the other liver specimens were excised and prepared for the histological, histomorphometrical, and immunohistochemical studies.

2.7. Preparation of Liver Homogenates. Using Ultra Turrax tissue homogenizer, specimens from the liver were homogenized in pH 7.4 ice-cold phosphate-buffered saline (PBS) to obtain a 10% solution (w/v). 0.16 mg/mL heparin was added to PBS to eliminate any erythrocytes and clots. The obtained homogenate was centrifuged for 15 min at $9000 \times g$ and 4°C , and then the clear supernatant was separated and preserved frozen at -80°C for subsequent biochemical assays. Hepatic protein content in every sample was determined using the previously reported procedures [24] which used bovine serum albumin as a standard.

2.8. Biochemical Assessment

2.8.1. Liver Function Biomarkers. Colorimetric assay kits specific for liver function biomarkers (aspartate aminotransferase (AST), alanine aminotransferase (ALT), alkaline phosphatase (ALP), lactate dehydrogenase (LDH), total protein, and total albumin) were purchased from EGY-CHEM for lab technology (BioMed, Germany) and used in conjunction with UV-VIS spectrophotometer (Shimadzu, Kyoto, Japan). Measuring the activities of AST, ALT, and ALP were based on protocols previously described by [25], while activity of LDH was depended on the protocol of [26]. Serum total protein and albumin levels were determined using the methods outlined by [27, 28], respectively.

2.8.2. Oxidative Stress Biomarkers in Sera. Total antioxidant capacity (TAC) and total oxidant capacity (TOC) were estimated in sera utilizing colorimetric assay kits manufactured by Biomedica Medizinprodukte GmbH, Germany, following the procedures formerly described by [29, 30], respectively.

2.8.3. Oxidative Stress Biomarkers in Liver Tissues. Levels of lipid peroxidation (LPO) were assessed depending on the production of thiobarbituric acid reactive substances (TBARS) and expressed as the extent of malondialdehyde (MDA) formation using a colorimetric assay kit (Biodiagnostic, Egypt) according to [31].

The effectiveness of antioxidants in the liver tissues including superoxide dismutase (SOD), catalase (CAT), reduced glutathione (GSH), and glutathione peroxidase (GPx) were assayed using commercially accessible colorimet-

ric kits (Biodiagnostic, Egypt) utilizing a UV-VIS spectrophotometer (Shimadzu, Kyoto, Japan). The protocol previously published by [32] was applied to estimate the effectiveness of SOD, whereas CAT activity was assayed by H_2O_2 consumption according to the method proposed by [33], while the techniques previously depicted by [34, 35] were used for measuring the activities of GSH and GPx, respectively.

2.8.4. Proinflammatory Markers in Liver Tissues. Two proinflammatory cytokines, tumor necrosis factor- α (TNF- α) and interleukin 6 (IL-6), had been assessed in the liver tissues. TNF- α levels were measured using a commercially accessible enzyme-linked immunosorbent assay (ELISA) kits (catalog number: CSB-E11987r, Cusabio Biotech Co., Ltd.) following the manufacturer's protocol. Meanwhile, the concentration of IL-6 had been assessed using the Rat IL-6 Quantikine ELISA Kit subsequent to the instructions described by the manufacturer (R&D Systems, Inc., Minneapolis, USA).

2.9. Histological Preparation. Samples of the liver of both control and treated animals were cut into tiny portions that instantly fixed for 24 h in 10% buffered formalin solution; after that they were proceeded for the routine protocol of paraffin sectioning previously described by [36]. 4-6- μm -thick paraffin sections were stained with Ehrlich's hematoxylin and eosin (H&E), dehydrated in a set of graded ethyl alcohol concentrations, cleared in xylene, mounted in DPX, and examined and photographed using compound light microscope (Olympus CX 31) provided with a Panasonic CD-220 camera.

2.10. Histomorphometrical Estimation. Six random fields from H&E-stained liver sections of all animal groups were selected and histomorphometrically analyzed using a computed image analysis system (Leica QWin, 500 Software, Germany) in the Department of Oral and Dental Pathology, Faculty of Dental Medicine, Al-Azhar University. The numbers of normal hepatocytes, necrotic hepatocytes, deteriorated Kupffer cells, and infiltrating inflammatory cells in the periportal areas (portal inflammation) and in the centrilobular zones (centrilobular inflammation) were estimated. In addition, the numbers of dilated/congested central and portal veins were recorded.

2.11. Immunohistochemical Preparation. Immunohistochemical localization of Bcl-2, P53, Caspase-3, and TNF- α reactive proteins was performed according to the standard Avidin-Biotin Complex (ABC) protocol [37]. 5- μm -thick

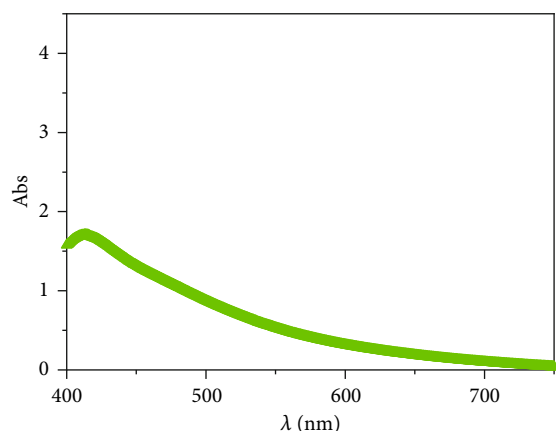


FIGURE 1: UV-VIS spectrum of AgNPs showing a maximum absorption peak at 413 nm wavelength using 1 g of gelatin via the microwave protocol.

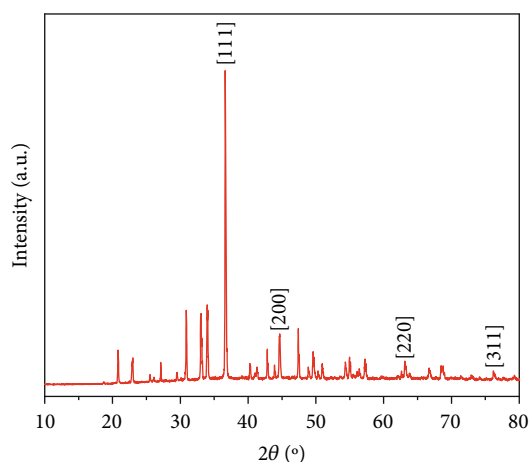


FIGURE 2: XRD pattern of biosynthesized AgNPs.

buffered formalin-fixed and paraffin-embedded hepatic tissue sectors were deparaffinized, rehydrated, and washed for 10 min in PBS. Endogenous peroxidase efficacy was obstructed with 3% hydrogen peroxide. After that, slides were incubated for 1–2 h at room temperature with the convenient dilution of the primary antibodies as represented in Table 1, followed in a refrigerator nightly at 4°C. Subsequently, they were rinsed in PBS, incubated for 10 min with biotinylated goat antipolyvalent, and then incubated for 1 h with ABC. Next, the sections were rinsed in PBS and incubated in diaminobenzidine tetrahydrochloride (pH 7.2) with 10 mL H₂O₂ for 7–9 min forward by PBS. Finally, sections were counterstained with Mayer's hematoxylin, dehydrated, cleared, and covered by cover slips. Negative control slides in the absence of primary antibodies were included for each parameter. The antibodies and all reagents were utilized in concurrence with the manufacturer's directives and recommendations.

2.12. Image Analysis. The quantification of immunoreactivity of active Bcl-2, P53, Caspase-3, and TNF- α proteins was assessed using the image analysis to estimate the per-

centage of positive immunostained cells related to the number of all cells assessed for each parameter [38]. The cells were regarded as positive if there was cytoplasmic and/or membranous brown coloration. A computational image analysis system (Leica QWin 500, Germany) at the Department of Oral and Dental Pathology, Faculty of Girls' Dental Medicine, Al-Azhar University, was used to process the images. For each parameter, six randomly selected high-power fields ($\times 200$) were captured in each slide with a standard measuring frame of an area 11434.9 mm². The image analyzer was initially adjusted automatically to transform the image analyzer program's measurement units (pixels) into real micrometer units. For statistical analysis, mean percentages of immunoreactive regions were calculated for all samples in each group.

2.13. Statistical Analysis. The biochemical, histomorphometrical, and immunohistochemical data recorded in the current investigation were tabulated and statistically analyzed. The values of six samples/group for all experimental animal sets were expressed as mean \pm standard error of mean (SEM). Statistical differences among rats' groups were estimated using one-way analysis of variance (ANOVA) subsequent by Tukey post hoc test utilizing the IBM SPSS Statistics for Windows, version 22 (IBM Corp., Armonk, N.Y., USA). Statistical significance was considered when a *P* value was less than 0.05.

3. Results

3.1. Physicochemical Characterization of Prepared AgNPs

3.1.1. UV-VIS Spectroscopy. The formation of AgNPs was confirmed by using UV-VIS spectrophotometer. At room temperature, the UV-VIS spectrum of AgNPs showed peak single-band absorption (surface plasmon resonance (SPR)) 1.8 at a wavelength of 413 nm using 1 g of gelatin via the microwave method marked in Figure 1.

3.1.2. X-Ray Diffraction (XRD) Analysis. The crystal structure of AgNPs was characterized by XRD (Figure 2). The results showed prominent peaks at $2\theta = 37.0$, 44.6 , 63.1 , and 76.2 , which were assigned to Ag (111), (200), (220), and (311) planes, respectively. These observed planes indicate that AgNPs had a face-centered cube structure and good crystallinity [39, 40]. The observed values agree with the reference of face-centered cubic structure from the Joint Committee of Powder Diffraction Standard (JCPDS No 03-065-2871). The additional peaks detected in the sample were attributed to the presence of AgNO₃ and AgO.

3.1.3. X-Ray Photoelectron Spectroscopy (XPS) Analysis. The XPS results revealed the presence of Ag, C, N, and O atoms according to their binding energies, as shown in Figure 3. There are four peaks in the survey spectra at around 286 eV (C 1s), 370 eV (Ag 3d), 401 eV (N 1s), and 534 eV (O 1s). The elemental compositions determined from XPS analysis were 5.08, 80.87, 1.53, and 12.53 atomic % for Ag, C, N, and O, respectively.

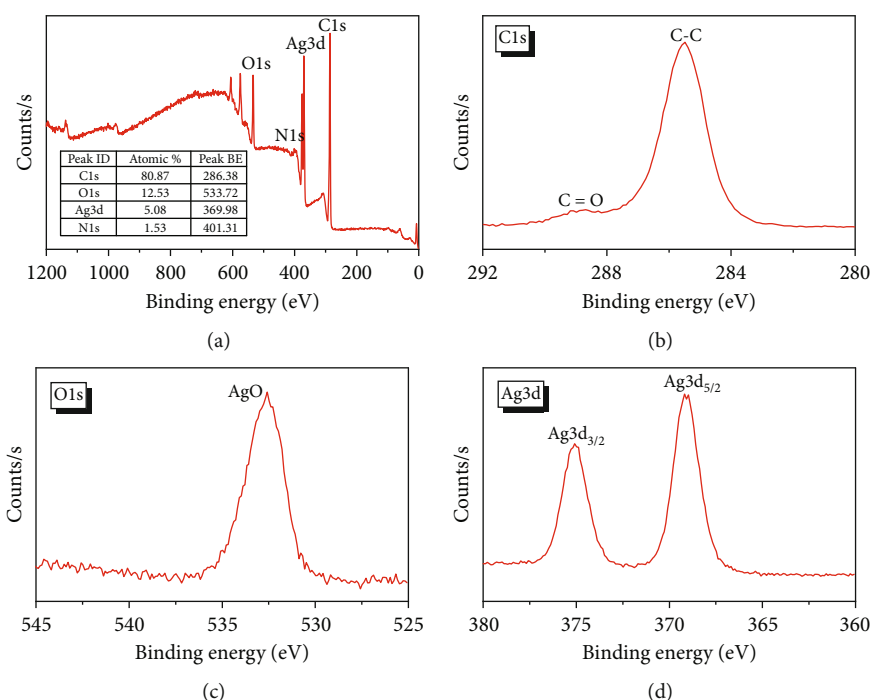


FIGURE 3: XPS spectra of AgNPs; (a) survey scan and high-resolution spectra of (b) C1s, (c) O1s, and (d) Ag3d.

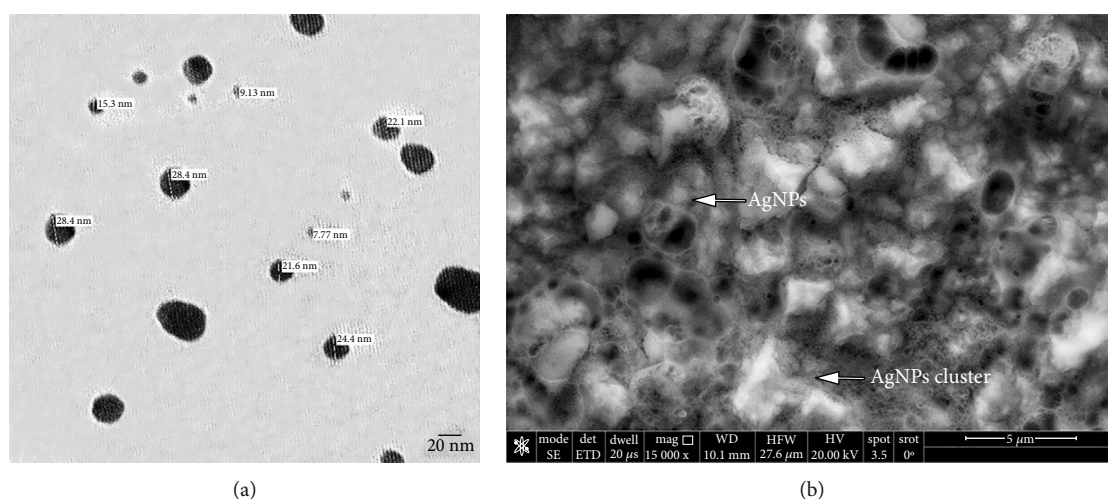


FIGURE 4: (a) TEM photomicrograph of AgNPs showing spherical forms and excellent particle dispersion with sizes ranging from 7.7 nm to 28.4 nm using 1 g of gelatin by the microwave technique ($\times 250,000$). (b) SEM image showing spherical AgNPs embedded with gelatin obtained at 20 kV electron high tension (EHT).

The high-resolution XPS C1s spectrum of the AgNPs showed two peaks at 285.7 and 288.9 eV corresponding to sp^3 C-C and C=O/C-O-Ag on the AgNPs surface (Figure 3(b)). Moreover, the high binding energy of O 1s at 532.3 eV was related to metal-OH bonds [41] (Figure 3(c)). The most noticeable signal in the XPS spectrum was that for Ag 3d, which comprises two spin-orbit peaks at 368.7 (Ag $3d_{5/2}$) and 375.1 (Ag $3d_{3/2}$) eV separated by around 6.0 eV (Figure 3(d)), which agree with the previously reported results [39, 41]. Together, these results illustrated the successful preparation of AgNPs.

3.1.4. Surface Morphology. The morphology of the bio-synthesized AgNPs was observed at 20 nm using TEM (Figure 4(a)). TEM analysis showed that the synthesized AgNPs were monodispersed, transparent, spherical, and highly crystalline with a normal small size (7.77–28.4 nm), smooth surface, well-distribution, and no agglomeration and were deemed suitable for utilization in this study. The SEM analysis (Figure 4(b)) of AgNPs showed that the NPs synthesized were spherical in shape [42], which correlated with the observed morphology of TEM image. Some aggregated particles of AgNPs were observed in the prepared

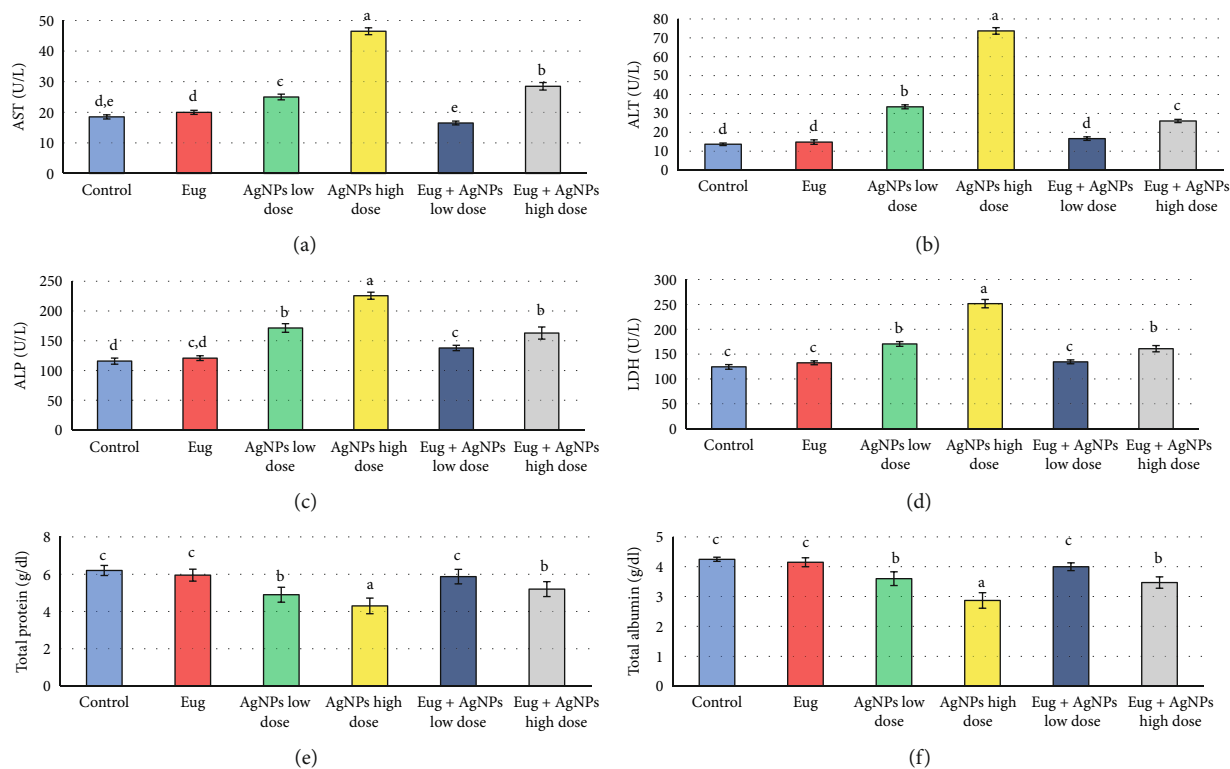


FIGURE 5: Liver function biomarkers: (a) aspartate aminotransferase (AST), (b) alanine aminotransferase (ALT), (c) alkaline phosphatase (ALP), (d) lactate dehydrogenase (LDH), (e) total protein, and (e) total albumin in the control and treated animal groups. Data are expressed as Mean \pm SEM ($n = 6$). Columns with different superscript letters are significantly different at the 0.05 level (one-way ANOVA).

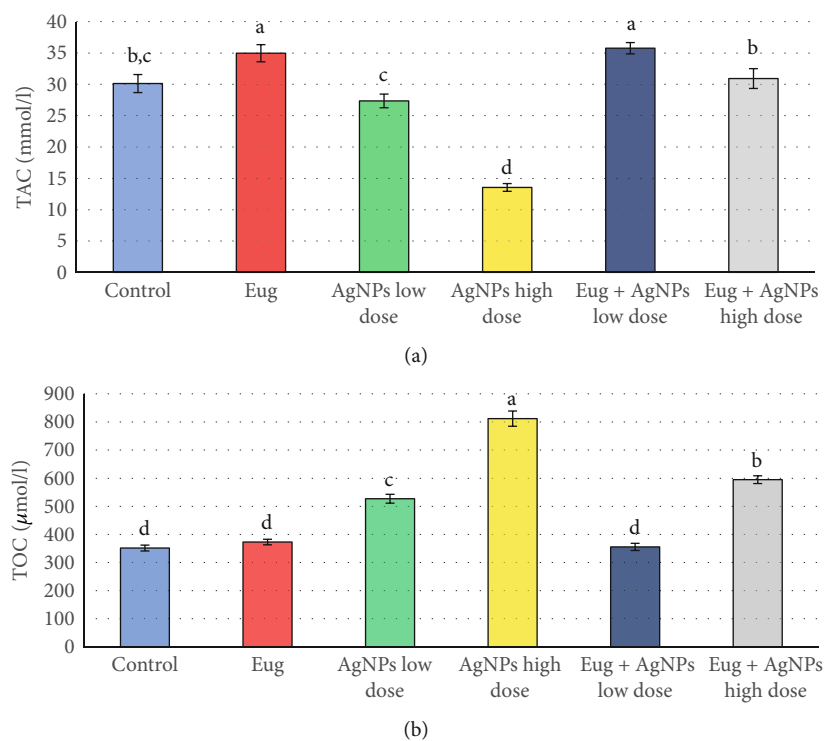


FIGURE 6: (a) Total antioxidant capacity (TAC) and (b) total oxidant capacity (TOC) in sera of the control and treated animal groups. Data are expressed as mean \pm SEM ($n = 6$). Columns with different superscript letters are significantly different at the 0.05 level (one-way ANOVA).

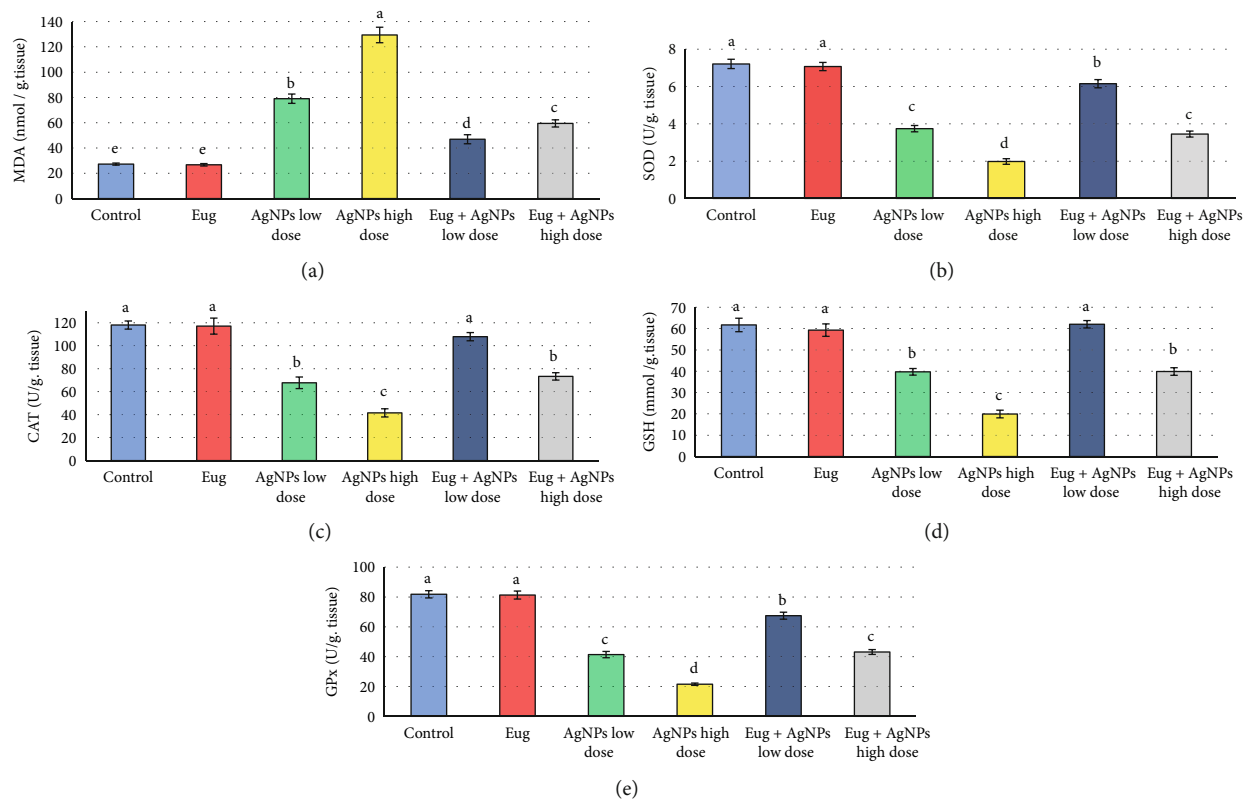


FIGURE 7: Oxidative stress biomarkers: (a) malondialdehyde (MDA), (b) superoxide dismutase (SOD), (c) catalase (CAT), (d) reduced glutathione (GSH), and (e) glutathione peroxidase (GPx) in the liver tissues of the control and treated animal groups. Data are expressed as mean \pm SEM ($n = 6$). Columns with different superscript letters are significantly different at the 0.05 level (one-way ANOVA).

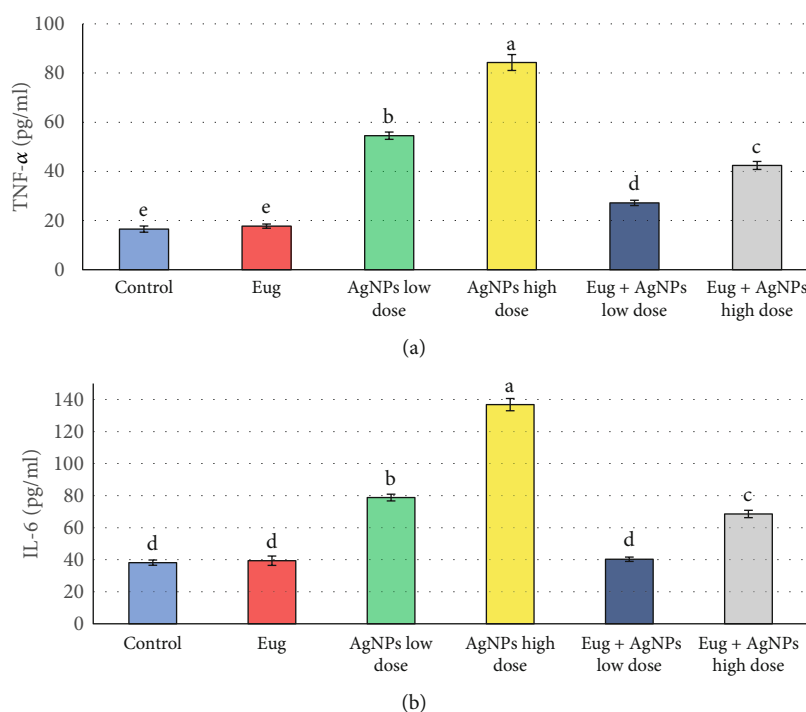


FIGURE 8: Inflammatory biomarkers: (a) tumor necrosis factor-alpha (TNF- α) and (b) interleukin 6 (IL-6) in the liver tissues of the control and treated animal groups. Data are expressed as mean \pm SEM ($n = 6$). Columns with different superscript letters are significantly different at the 0.05 level (one-way ANOVA).

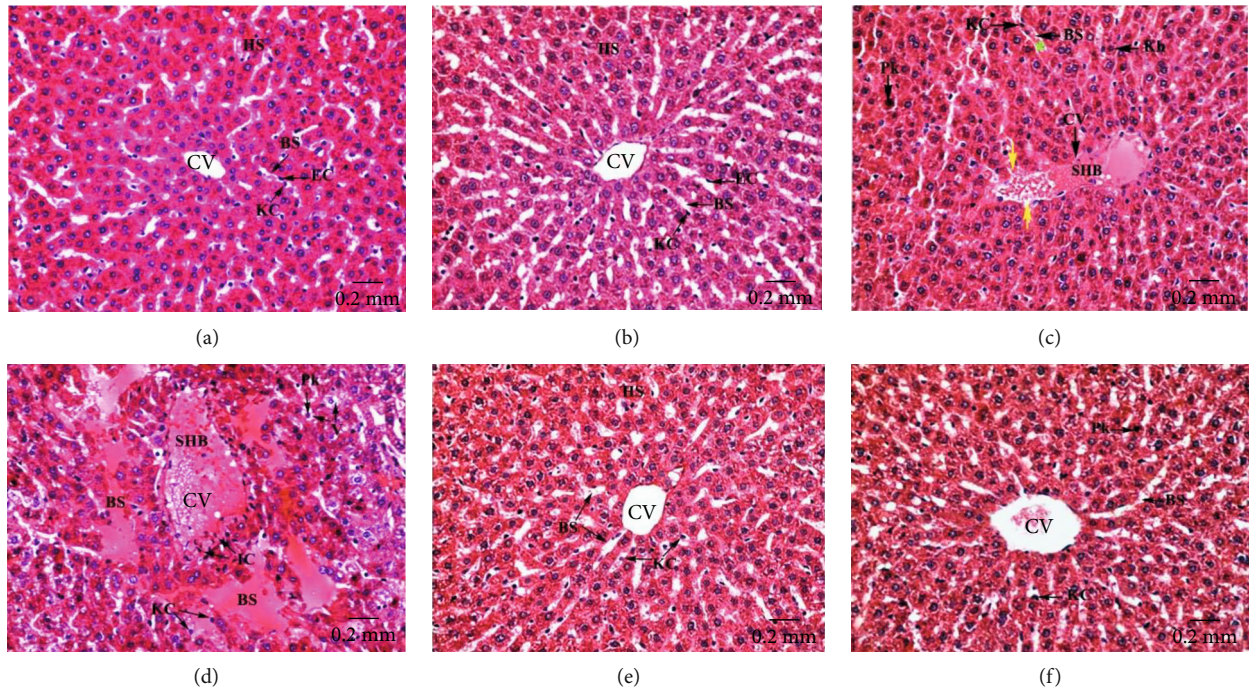


FIGURE 9: Centrilobular zones of hepatic tissues stained with H&E revealing (a) well-organized hepatic strands (HS) which expanded around a narrowed central vein (CV) and segregated by normal blood sinusoids (BS) appeared enveloped by attached endothelial (EC) and Kupffer (KC) cells in control rats; (b) intact hepatic architecture in Eug-treated rats; (c) dilated and congested central vein (CV) possesses severe stagnant hemorrhagic blood (SHB) in its lumen, and its surrounding endothelium seemed destructed (yellow arrow), and the hepatic blood sinusoids (BS) are dilated and congested with stagnant blood (green asterisk), and their Kupffer cells (KC) appeared more rounded and often pushed into the sinusoidal lumen, as well as hepatocytes showed pyknotic nuclei (Pk), and the others revealed nuclear karyorrhexis (Kh) in AgNPs-low-dose-treated rats; (d) severely dilated and congested central vein (CV) having stagnant blood masses (SHB) and infiltrating inflammatory cells (IC) in its lumen and also aggregated in the surrounding connective tissues, besides enlarged blood sinusoids (BS) with swollen and detached Kupffer cells (KC), disorderly hepatic strands with necrotic hepatocytes having pyknotic nuclei (Pk) and rather vacuolated cytoplasm (V) in AgNPs-high-dose-treated rats; (e) conspicuous amelioration in the structure of hepatic strands (HS), blood sinusoids (BS), and central veins (CV) in Eug + AgNPs-low-dose-treated rats; (f) almost intact architecture of the central vein (CV), blood sinusoids (BS), and hepatocytes with some of them still showing rather nuclear pyknosis (Pk) in Eug + AgNPs-high-dose-treated rats.

sample. The size of the silver particles got larger due to agglomeration of the smaller ones as the bio-organic molecules could stabilize and cap the individual particles [43, 44].

3.2. Biochemical Analysis. To evaluate liver injury, liver function enzymes (AST, ALT, ALP, and LDH), total protein, and total albumin levels and oxidant/antioxidant parameters (TAC and TOC) in sera, as well as antioxidant parameters (MDA, SOD, CAT, GSH, and GPX) and inflammation markers (IL-6 and TNF- α) in liver tissues, were evaluated.

The influences of AgNPs toxicity and the protective effects of Eug on liver function biomarkers of rats are shown in Figure 5. Eug administration alone did not have significant ($P > 0.05$) effects on the measured liver function indices in comparison with the control. Meanwhile, treatment of rats with AgNPs, either the low or high dose, caused marked increase ($P \leq 0.05$) in AST (35.21% and 151.49%), ALT (145.12% and 439.02%), ALP (48.10% and 94.91%), and LDH (37.14% and 102.31%) paralleled with a significant decline ($P \leq 0.05$) in total protein (-20.85% and -30.65%) and albumin (-15.66% and -32.47%) compared with the values of control animals. Levels of AST, ALT, LDH, total proteins, and total albumin were restored approximately to

the normal levels in rats treated with AgNPs-low dose in combination with Eug. While supplementation of Eug to the rats received the high dose of AgNPs caused modulation of the liver function parameters compared with the animals exposed to the high dose of AgNPs, but they were still considerably different ($P \leq 0.05$) comparable to the control values.

Figure 6 represents the serum TAC and TOC levels in the rats of all groups. The recorded data exhibited a significant rise ($P \leq 0.05$) in TAC level (16.07%) in Eug-treated group when contrasted with control group. On contrarily, nonsignificant decline ($P > 0.05$) and significant diminution ($P \leq 0.05$) were recorded in TAC levels of the AgNPs-low-dose-treated rats (-9.19%) and the AgNPs-high-dose-treated rats (-55.01%), respectively, when contrasted with control group. Addition of Eug to the rats injected with AgNPs, both low and high doses, caused modulation of the levels of TAC relative to that recorded in the animals administered AgNPs alone; nevertheless, it was significantly different ($P \leq 0.05$) compared with the control values in case of the high dose AgNPs-treated rats. Regarding TOC, administration of Eug solely did not produce significant ($P > 0.05$) effects on the levels of this parameter when compared with the control

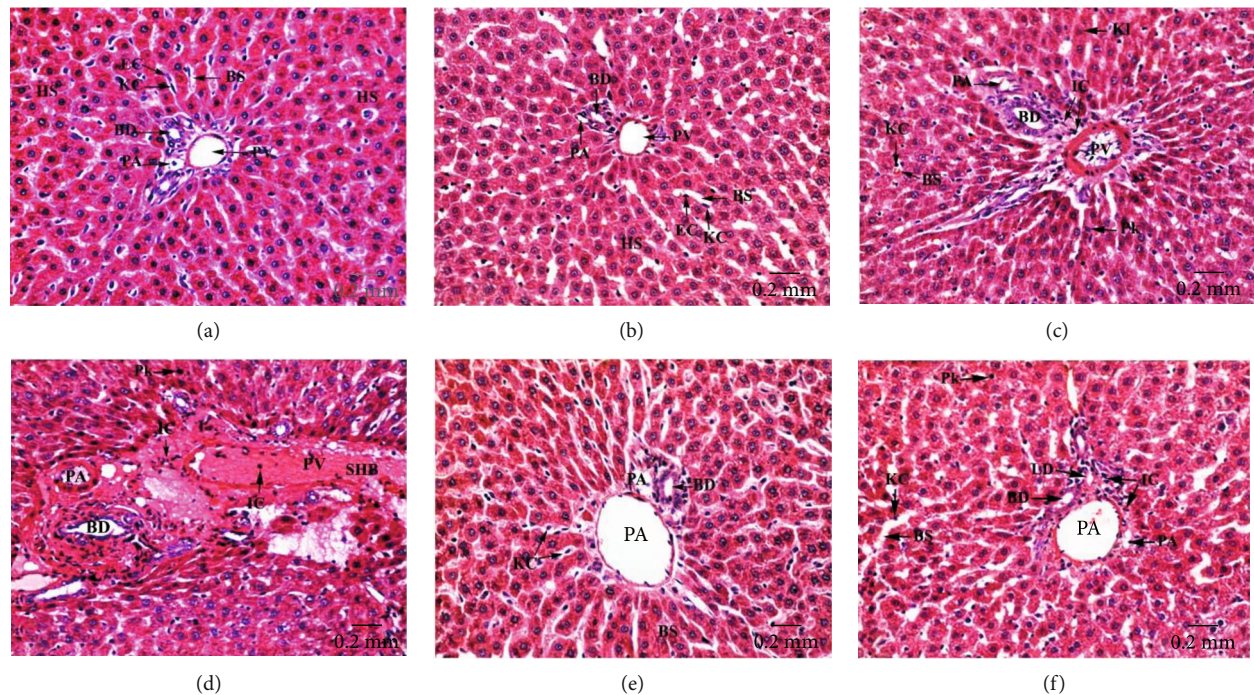


FIGURE 10: Periportal zones of hepatic tissues stained with H&E revealing (a) regular hepatic architecture with well-organized radiating hepatic strands (HS) surrounding the portal tract that formed of regular hepatic portal artery (PA), hepatic portal vein (PV), and bile ductule (BD) in control rats; (b) regular hepatic structure in Eug-treated rats; (c) devastated hepatic portal artery (PA), hepatic portal vein (PV), and bile ductule (BD) with thickened boundaries, infiltrating inflammatory cells (IC) in the surrounding connective tissues and inside their lumina, besides necrotic hepatocytes with pyknotic (Pk) or karyolysed (KI) nuclei and blood sinusoids (BS) having swollen Kupffer cells (KC) pushed in their lumens are obviously noticed in AgNPs-low-dose-treated rats; (d) severely dilated and congested hepatic portal vein (PV) and portal artery (PA) having stagnant blood masses (SHB) and infiltrating inflammatory cells (IC) in their lumens and also aggregated outside them, besides deteriorated bile ductules (BD) with thickened and deformed epithelia. Also, disorderly hepatic strands with necrotic hepatocytes having pyknotic (PK) nuclei are observed in AgNPs-high-dose-treated rats; (e) conspicuous improvement in the histological structure of the hepatic tissues with intact portal triad and hepatic strands in Eug + AgNPs-low-dose-treated rats; (f) restoration of the hepatic architecture with few infiltrating inflammatory cells (IC) and hepatocytes with pyknotic (Pk) nuclei are noticed in Eug + AgNPs-high-dose-treated rats.

group, while the incredible rise ($P \leq 0.05$) in levels of TOC of AgNPs-low-dose-treated rats (49.90%) and AgNPs-high-dose-treated rats (130.98%) was recorded when contrasted with the control group, whereas treatment of rats with AgNPs-low dose in combination with Eug returned the values of TOC to be very close to those of the control animals (355.5 ± 12.76 vs. 351.5 ± 10.44 , $P \geq 0.05$), while administration of Eug to the rats treated with the high dose of AgNPs caused amelioration of this parameter when contrasted with the animals treated to AgNPs alone, and this value was yet significantly different ($P \leq 0.05$) proportional to the control values.

Levels of MDA, SOD, CAT, GSH, and GPx in hepatic tissues of the control and treated animal groups were assessed to monitor the oxidative stress state. Figure 7 demonstrated that administration of Eug alone did not produce significant ($P > 0.05$) effects on these oxidative stress indices compared with the control. Meanwhile, low- and high-dose AgNPs-treated rats were subjected to oxidative stress which was confirmed by significant elevation ($P \leq 0.05$) in MDA levels (189.72% and 374.63%) accompanied by marked

decline ($P \leq 0.05$) in levels of SOD (-48.07% and -72.54%), CAT (-42.61% and -64.80%), GSH (-35.63% and -67.69%), and GPx (-49.39% and -73.67%) in comparison with the control group. Eug + AgNPs-low-dose and Eug + AgNPs-high-dose-treated groups showed marked modulation ($P \leq 0.05$) of the evaluated oxidative stress biomarkers compared with the animals subjected to AgNPs-low dose and AgNPs-high dose; but most of these parameters were significantly different ($P \leq 0.05$) relative to the recorded control values.

Levels of inflammatory biomarkers (TNF- α and IL-6) in liver tissues were investigated in all groups, and the within-group values of these parameters were compared (Figure 8). Rats received Eug solely displayed nonsignificant ($P > 0.05$) changes in the levels of TNF- α and IL-6 when compared with the control. Meanwhile, treatment of rats with AgNPs resulted in marked elevation ($P \leq 0.05$) in levels of TNF- α (230.07% and 410.31%) and IL-6 (106.40% and 258.36%) for the low dose and high dose of AgNPs, respectively, compared with those of control animals. Administration of Eug along with AgNPs (both low or high doses)

TABLE 2: Histomorphometrical analysis of the hepatic tissue components in control and treated animal groups.

Parameters	Animal groups					
	Control	Eug	AgNPs-low dose	AgNPs-high dose	Eug + AgNPs-low dose	Eug + AgNPs-high dose
Number of normal hepatocytes	316 ± 15.3 ^a	300 ± 0 ^a	260 ± 0 ^b	176 ± 0.775 ^c	290 ± 0 ^a	240 ± 0 ^b
% change	0	-5.06%	-17.72%	-44.30%	-8.23%	-24.05%
Number of necrotic hepatocytes	5.2 ± 0 ^f	7.2 ± 0 ^e	20.2 ± 0 ^c	63.8 ± 0 ^a	12.6 ± 0 ^d	21.6 ± 0 ^b
% change	0	38.46%	288.46%	1126.92%	142.31%	315.38%
Number of deteriorated Kupffer cells	12 ± 0.316 ^d	14 ± 0 ^d	23.4 ± 0 ^c	58 ± 2.47 ^a	16.2 ± 0 ^d	28.6 ± 0 ^b
% change	0	16.67%	95.00%	383.33%	35.00%	138.33%
Number of periportal inflammatory cells	10.2 ± 0 ^f	12.6 ± 0 ^e	35 ± 0 ^c	80.6 ± 0 ^a	18.2 ± 0 ^d	40.4 ± 0 ^b
% change	0	23.53%	243.14%	690.20%	78.43%	296.08%
Number of centrilobular inflammatory cells	6.8 ± 0 ^d	8.4 ± 0.6 ^d	20.4 ± 0 ^c	41.6 ± 3.89 ^a	12.8 ± 0 ^d	28.6 ± 0 ^b
% change	0	23.53%	200.00%	511.76%	88.24%	320.59%
Number of dilated/congested central veins	0.4 ± 0.245 ^c	0.6 ± 0.245 ^c	2 ± 0 ^b	4.8 ± 0 ^a	1 ± 0 ^c	1.8 ± 0 ^b
% change	0	50.00%	400.00%	1100.00%	150.00%	200.00%
Number of dilated/congested portal veins	0.6 ± 0.245 ^c	0.8 ± 0.2 ^c	2 ± 0 ^b	4.6 ± 0.245 ^a	1.2 ± 0 ^c	2.4 ± 0 ^b
% change	0	33.33%	233.33%	666.67%	100.00%	200.00%

Data are presented as Mean ± SEM and % change ($n = 6$ in each group). Within the same row, values preceded by different superscript letters differ significantly at the 0.05 level (one-way ANOVA and the Tukey test). Eug: eugenol; AgNPs: silver nanoparticles.

significantly ameliorated these changes and recovered to the control levels.

3.3. Histological Results. Liver sections of the control and Eug-treated rats revealed ordinary parenchymal architecture of the hepatic tissues in both centrilobular (Figures 9(a) and 9(b)) and the periportal (Figures 10(a) and 10(b)) zones, where well-organized radiating hepatic strands seemed expanded, surrounding the narrowed central veins and also around the portal tracts that formed of the regular hepatic portal veins, hepatic portal arteries, and bile ductules. Besides, normal blood sinusoids lined with attached endothelial and Kupffer cells were observed, while examination of the centrilobular (Figure 9(c)) and the periportal (Figure 10(c)) areas of liver sections of AgNPs-low-dose-treated rats revealed dilated and congested central veins, hepatic portal veins, and hepatic portal arteries which showed thickened and eroded lining membranes surrounded by infiltrating inflammatory cells. Necrotic hepatocytes appeared with nuclear pyknosis, karyorrhexis, and karyolysis. Besides, congested hepatic blood sinusoids with detached endothelial cells and rounded Kupffer cells appeared pushed into the sinusoidal lumen were seen. Moreover, the hepatic tissues of AgNPs-high-dose-treated rats showed massive pathological changes in the centrilobular (Figure 9(d)) and the periportal (Figure 10(d)) zones, where the hepatic cords missed their typical arrangement and the majority of hepatocytes degenerated, having vacuolated cytoplasm and pyknotic, karyorrhectic, or karyolysed nuclei. The central veins, hepatic portal veins, and hepatic portal arteries were disfigured, dilated, and severely congested with intense masses of hemolyzed blood in their lumina, besides infiltration of inflammatory lymphocytes around their con-

finer. In certain areas, the endothelial lining of most of these blood vessels looked corroded and damaged. Furthermore, the blood sinusoids showed destruction and congestion and lined with swollen activated Kupffer cells which appeared separated from their boundaries. Otherwise, Eug + AgNPs-low-dose-treated rats illustrated remarkable refinement in the hepatic architecture of both centrilobular (Figure 9(e)) and the periportal (Figure 10(e)) zones, with most of the hepatocytes and blood sinusoids appeared well-organized. Also, the central and hepatic portal veins, as well as the hepatic portal arteries appeared intact. Similarly, Eug + AgNPs-high-dose-treated rats manifested a nearly well-organized hepatic architecture in the centrilobular (Figure 9(f)) and periportal (Figure 10(f)) zones.

3.4. Histomorphometrical Results. As illustrated in Table 2, the hepatic tissues of both AgNPs-low-dose and AgNPs-high-dose-treated rats manifested a significant decline ($P \leq 0.05$) in the numbers of normal hepatocytes and a considerable rise ($P \leq 0.05$) in the numbers of necrotic hepatocytes, infiltrating inflammatory cells in the periportal and centrilobular zones, and deteriorated Kupffer cells. In addition, the numbers of dilated/congested central and portal veins were significantly elevated ($P \leq 0.05$) compared with control and Eug-treated rats. Otherwise, Eug + AgNPs-low-dose- and Eug + AgNPs-high-dose-treated rats showed amelioration of these impaired parameters observed after AgNPs treatment. Necrotic hepatocytes and infiltrating inflammatory cells significantly ($P \leq 0.05$) decreased in the centrilobular and periportal zones of the hepatic tissues of Eug + AgNPs-low-dose- and Eug + AgNPs-high-dose-treated rats. Meanwhile, a significant ($P \leq 0.05$) elevation in the numbers of deteriorated Kupffer cells, and dilated/congested

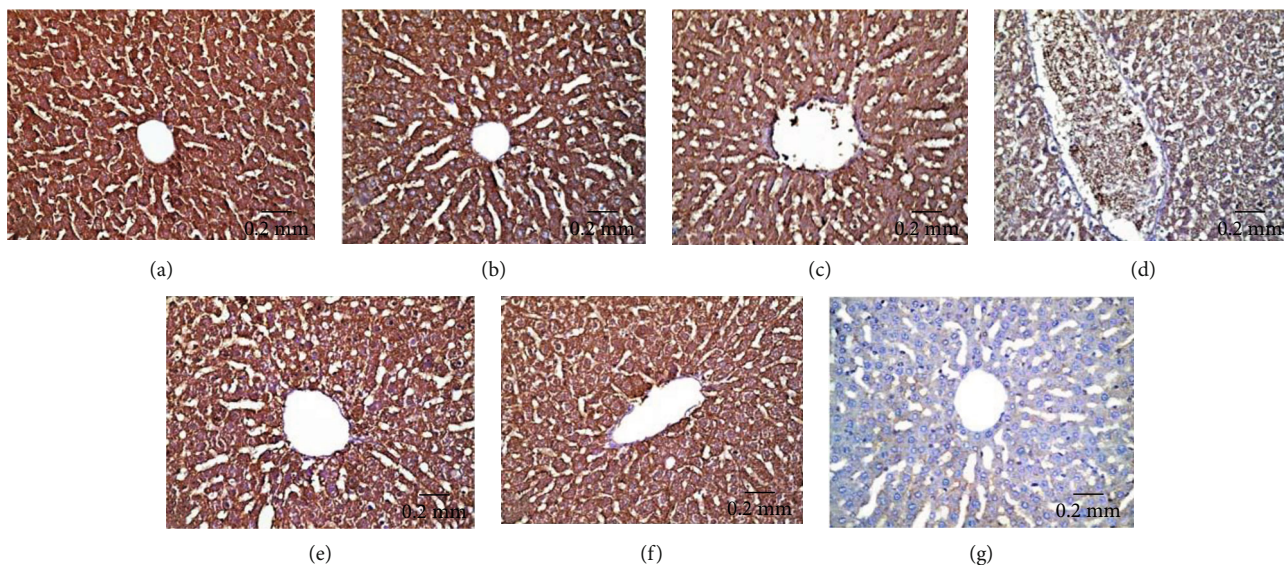


FIGURE 11: Immunohistochemical expression of Bcl-2 in hepatic tissues illustrating (a and b) strong reaction in control and Eug-treated group, respectively; (c) moderate reactivity in the AgNPs-low-dose-treated group; (d) weak immunostainability in the AgNPs-high-dose-treated group; (e) strong immunostaining in cotreatment of Eug with AgNPs-low-dose-treated group; (f) moderate immunostainability in Eug + AgNPs-high-dose-treated group; (g) no staining in negative control.

TABLE 3: Immunohistochemical image analysis of the area percentage of Bcl-2, P53, Caspase-3, and TNF- α immunoexpression in hepatic tissues of control and treated animal groups.

Parameters	Animal groups					
	Control	Eug	AgNPs-low dose	AgNPs-high dose	Eug + AgNPs-low dose	Eug + AgNPs-high dose
Bcl-2	67.8 \pm 1.78 ^a	65.1 \pm 3.76 ^a	55.6 \pm 0 ^{bc}	42.1 \pm 0.51 ^d	62.4 \pm 0 ^{ab}	53.6 \pm 0 ^c
% change	0	-3.98%	-17.99%	-37.91%	-7.96%	-20.94%
P53	20.8 \pm 2.27 ^c	25.8 \pm 0.58 ^c	42.8 \pm 4.12 ^b	63 \pm 3.66 ^a	28.2 \pm 0 ^c	45.5 \pm 0 ^b
% change	0	24.04%	105.77%	202.88%	35.58%	118.75%
Caspase-3	20.74 \pm 2.06 ^c	26 \pm 0 ^c	40.4 \pm 0 ^b	67.57 \pm 2.19 ^a	29 \pm 0 ^c	43 \pm 0 ^b
% change	0	25.31%	94.71%	225.64%	39.77%	107.24%
TNF- α	22 \pm 2.97 ^c	26.6 \pm 0.75 ^c	39.8 \pm 2.44 ^b	68.6 \pm 4.23 ^a	28.6 \pm 0 ^c	40.1 \pm 0 ^b
% change	0	20.91%	80.91%	211.82%	30.00%	82.27%

Data are presented as Mean \pm SEM and % change ($n=6$ in each group). Within the same row, values preceded by different superscript letters differ significantly at the 0.05 level (one-way ANOVA and the Tukey test). Eug: eugenol; AgNPs: silver nanoparticles.

central and portal veins, with a marked ($P \leq 0.05$) depletion in the number of normal hepatocytes were recorded in Eug + AgNPs-low-dose- and Eug + AgNPs-high-dose-treated rats relative to the control rats but showed modulation of these parameters compared with rats treated with AgNPs alone. Eug-treated rats did not show any significant different in these parameters, except for the number of necrotic hepatocytes and infiltrating inflammatory cells, indicating a significant change ($P \leq 0.05$) from all other groups.

3.5. Immunohistochemical Results

3.5.1. Bcl-2 Immunoreactivity. Bcl-2 immunoexpression in hepatic tissues of experimental animal groups is illustrated

in Figures 11(a)–11(g). AgNPs-low-dose-treated rats showed moderate Bcl-2 immunoreactivity (Figure 11(c)), whereas AgNPs-high-dose-treated rats revealed weak Bcl-2 immunoreactivity (Figure 11(d)) compared with the control (Figure 11(a)) and Eug-treated rat (Figure 11(b)) groups which showed strong Bcl-2 immunoreactivity. However, treatment of rats with Eug paralleled with AgNPs upregulated the immunoexpression of Bcl-2 in both the AgNPs-low-dose (Figure 11(e)) and AgNPs-high-dose (Figure 11(f)) groups. Negative control sample revealed negative immunoreactivity (Figure 11(g)). As shown in Table 3, Eug-treated rats did not exhibit significant change ($P > 0.05$) in the value of the area percentage of Bcl-2 immunoexpression in comparable with that of control rats. Meanwhile, a significant

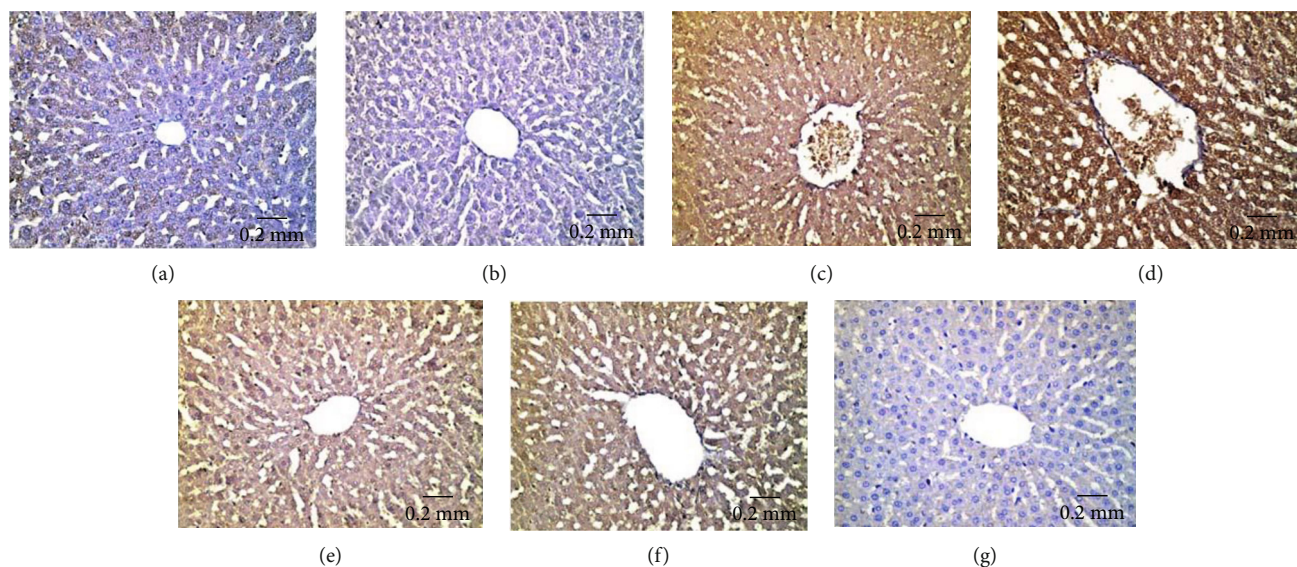


FIGURE 12: Immunohistochemical expression of P53 in hepatic tissues revealing (a and b) weak immunostainability in the control and Eug-treated groups, respectively; (c) moderate positive immunostainability in the AgNPs-low-dose-treated group; (d) relatively strong positive immunoreaction in the AgNPs-high-dose-treated group; (e) weak positive affinity for P53 in the Eug + ANPs-low-dose-treated group, (f) moderate immunoreactivity in the Eug + ANPs-high-dose-treated group; (g) negative immunostaining in negative control.

decline ($P \leq 0.05$) in the area percentage of Bcl-2 immunoreaction was recorded in the AgNPs-low-dose- and AgNPs-high-dose-treated groups, which was significantly ($P \leq 0.05$) modulated in the rats cotreated with Eug.

3.5.2. P53 Immunoreactivity. Hepatic tissues of control (Figure 12(a)) and Eug-treated (Figure 12(b)) rats revealed weak P53 immunoreactivity, whereas the rats treated with AgNPs-low dose manifested a moderate P53 immunoreactivity (Figure 12(c)). Furthermore, AgNPs-high-dose-treated rats exhibited intense positive stainability for P53 (Figure 12(d)). Meanwhile, Eug + AgNPs-low-dose-treated rats showed mild P53 immunoreactivity (Figure 12(e)), whereas Eug + AgNPs-high-dose-treated rats illustrated moderate reaction for P53 immunostaining (Figure 12(f)). There was no staining in negative control samples (Figure 12(g)). As revealed in Table 3, Eug-treated rats did not reveal any significant difference ($P > 0.05$) in the area percentage of P53 immunoreaction compared with the value of control group, whereas a significant elevation ($P \leq 0.05$) in the area percentage of P53 immunoreaction was recorded in both AgNPs-low-dose and AgNPs-high-dose-treated groups. However, a significant rise ($P \leq 0.05$) in the area percentage of P53 immunoreaction was recorded for both Eug + AgNPs-low-dose- and Eug + AgNPs-high-dose-treated rats relative to the control group.

3.5.3. Caspase-3 Immunoreactivity. Immunohistochemical examination of hepatic tissues of the control (Figure 13(a)) and Eug-treated (Figure 13(b)) groups exhibited weak Caspase-3 immunostainability, while liver sections of AgNPs-low-dose-treated rats showed strong positive Caspase-3 immunoreactivity (Figure 13(c)). Hepatic tissues

of AgNPs-high-dose-treated rats manifested an intense immunostainability for Caspase-3 (Figure 13(d)). Eug coadministered with both AgNPs-low-dose- and AgNPs-high-dose-treated groups illustrated moderate Caspase-3 immunoreactivity (Figures 13(e) and 13(f)), respectively. No staining was observed in negative control section (Figure 13(g)). According to Table 3, Eug-treated rats did not show a significant increase ($P > 0.05$) in the area percentage of Caspase-3 immunoreaction relative to control rats, while low-dose and high-dose AgNPs-treated rats evoked a significant increase ($P \leq 0.05$) in the area percentage of Caspase-3 immunoreaction in comparable with control animals. Concomitant administration of Eug to the rats treated with low and high doses of AgNPs caused modulation of the area percentage of Caspase-3 immunoreaction in contrast with the AgNPs-low- or high-dose-treated groups but still showed a significant elevation ($P \leq 0.05$) compared with the control group.

3.5.4. TNF- α Immunoreactivity. The liver sections of the control (Figure 14(a)) and Eug-treated (Figure 14(b)) groups showed negative TNF- α immunohistochemical reactivity, whereas the liver sections of AgNPs-low-dose-treated rats (Figure 14(c)) and AgNPs-high-dose-treated rats (Figure 14(d)) showed strong positive TNF- α immunostainability. Meanwhile, the hepatic tissues of Eug coadministered with the AgNPs-low-dose- (Figure 14(e)) or AgNPs-high-dose-treated (Figure 14(f)) groups illustrated mild TNF- α immunoreactivity compared with rats treated with low or high dose of AgNPs alone. Figure 14(g) shows no immunoreaction in negative control sample. As revealed in Table 3, Eug-treated rats did not exhibit significant ($P > 0.05$) difference in the area percentage of TNF- α immunoreaction compared to control rats, while low- and high-

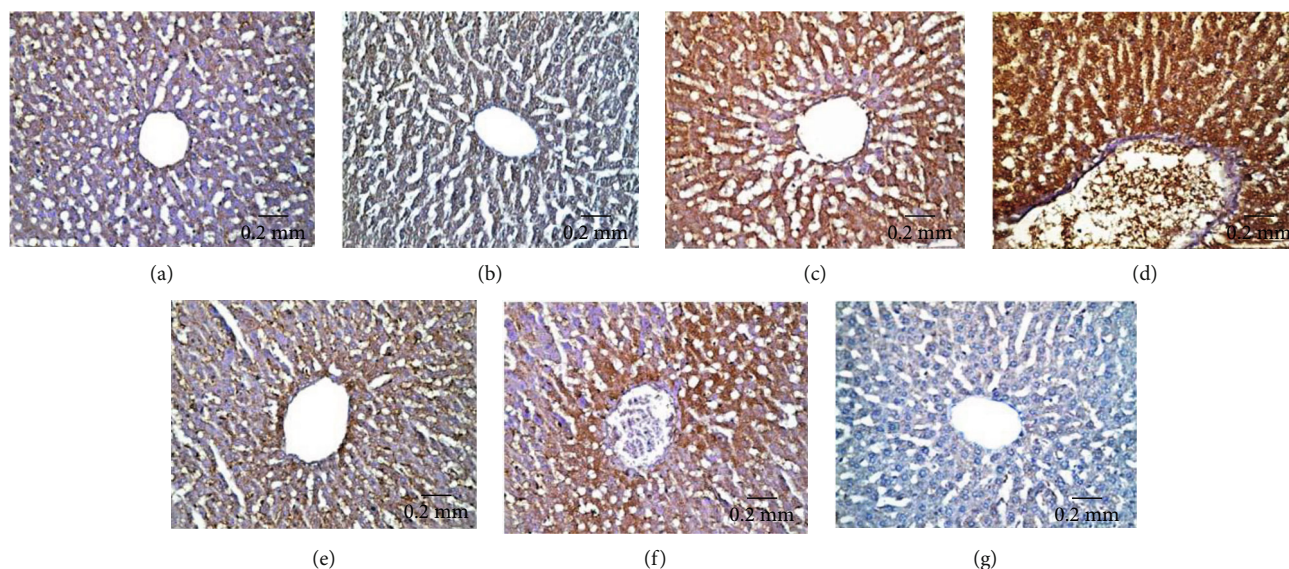


FIGURE 13: Immunohistochemical expression of Caspase-3 in hepatic tissues showing (a and b) a weak immunostainability in the control and Eug-treated groups, respectively, (c) moderate immunoreaction in the AgNPs-low-dose-treated group, (d) strong positive immunostainability in AgNPs-high-dose-treated group, (e and f) moderate immunoreaction in both Eug + AgNPs-low- and high-dose-treated groups, (g) no stainability in negative control.

dose AgNPs-treated rats evoked a significant rise ($P \leq 0.05$) in the area percentage of TNF- α immunoexpression compared with those of control group. However, accompanying administration of Eug to low- or high-dose AgNPs-treated rats showed amendment of TNF- α immunoexpression compared with the rats subjected to AgNPs low or high doses alone.

4. Discussion

The usage of NPs is becoming increasingly popular in various disciplines. Due to their minuscule size and unique chemical and physical characteristics, AgNPs have become one of the most commercialized NPs worldwide. While the use of AgNPs for biological applications is increasing, our knowledge and understanding of how they affect living cells and biochemical structures is still lacking [45]. Therefore, the potential toxicity of AgNPs in different body organs is an important research area. Regarding AgNPs toxicity, there are no published studies on the ameliorating role of Eug against the toxic influences of AgNPs.

Among varied organs, the liver is the principal objective organ of AgNPs' effects via all exposure pathways [2, 46, 47]. Thus, the current investigation was aimed to prepare and characterize AgNPs and to evaluate their toxicity on the biochemical, histological, histomorphometrical, and immunohistochemical characteristics of the hepatic tissues of adult rats. Furthermore, the ameliorative role of Eug in the hepatic structure and function against AgNPs-induced hepatotoxicity was investigated.

The present results revealed that the microwave technique reduces AgNPs with variable-rate microwave radiation. The microwave technique speeds up chemical reactions from days or hours to minutes. With an absorbance peak at 413 nm, microwave irradiation allows homo-

geneous heating for NPs formation and aids in the ripening of these nanomaterials without agglomeration [48]. The sample synthesized at 413 nm was used to trigger hepatotoxicity [2], and it facilitated AgNPs passage into the hepatocytes.

The current study revealed that the applied doses of AgNPs significantly increased serum AST, ALT, ALP, and LDH levels, which are the most indicative markers of structural deterioration of hepatocytes because these enzymes are located in the cytoplasm and released into the blood due to the loss of functional membrane integrity and cellular leakage [49]. Additionally, AgNPs induced a significant drop in serum total protein and albumin levels, indicating a decrease in protein synthesis and/or an increase in protein catabolism [50]. Our findings were consistent with previous studies [51], which showed that an AgNPs overdose might cause liver deterioration. Administration of Eug alleviated AgNPs-induced hepatotoxicity, as indicated by significant decline in AST, ALT, ALP, and LDH levels and marked elevation of total protein and total albumin levels, revealing the preservation of the functional integrity of hepatocytes. These findings were consistent with those previously published by [52], who found that cotreatment of Eug with cadmium considerably improves AST, ALT, ALP, and LDH levels in rats. Eug has antihepatotoxic activity, making it a suitable dietary supplement for treating hepatic damage [53].

Free radicals are extremely reactive molecules that originate as ordinary byproducts of metabolic activities in living cells. These chemicals include reactive nitrogen (RNS) and oxygen (ROS) species which can speedily interact with different macromolecules (proteins, carbohydrates, lipids, and nucleic acids) inside the cells, significantly damaging cellular structures [54]. Living cells produce endogenous antioxidative factors to buffer such synthesized free radicals, protecting cells from oxidative harm. CAT, SOD, GPx, and GSH

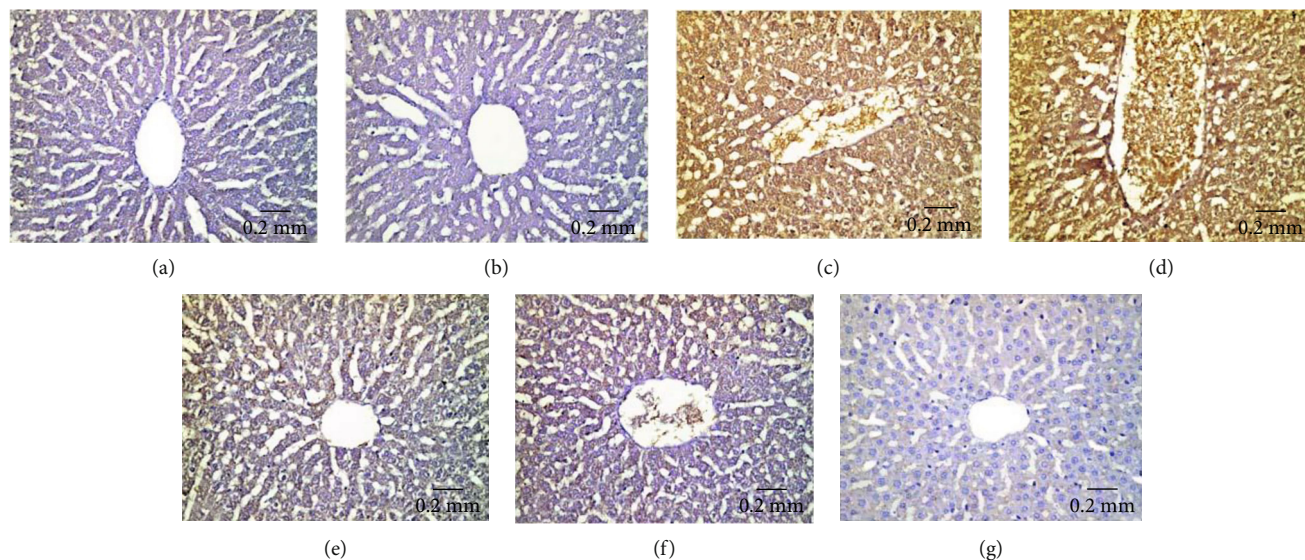


FIGURE 14: Immunohistochemical expression of TNF- α in hepatic tissues showing (a and b) negative immunohistochemical reactivity in control and Eug-treated rats, respectively; (c) moderate immunostainability in the AgNPs-low-dose-treated group; (d) strong immunostainability in the AgNPs-high-dose-treated group; (e) mild immunostainability in the Eug + AgNPs-low-dose-treated group; (f) weak immunoreactivity in the Eug + AgNPs-high-dose-treated group; (g) no immunostainability in negative control.

are the most prevalent endogenous antioxidant molecules [55]. When the produced free radicals exceed the cell's ability to counteract them with antioxidant molecules, oxidative stress occurs [56]. MDA is also a key indicator of oxidative stress in biological systems, and it is formed by ROS-induced peroxidation of membrane lipids, resulting in membrane damage and degradation [57].

The increased serum TOC level and the decreased TAC level, along with significantly increased LPO levels, reduced GSH levels, and decreased efficacy of CAT, SOD, and GPx in hepatic tissues of rats administered AgNPs, suggest that LPO is enhanced, causing excess free radical production, which triggers a chain interaction of direct and indirect bond formation with cellular molecules, impairing pivotal cellular activities and potentially leading to significant cell destruction and death [58]. The mitochondria are essential cellular targets of AgNPs-induced toxicity because AgNPs affect mitochondrial membrane permeability and interfere with their respiratory chain, resulting in ROS generation, necrosis, and apoptosis [59]. Previous studies have also revealed oxidative stress following AgNPs administration, which is consistent with our findings [2, 46, 60]. However, cotreatment of Eug with AgNPs induces the protective influence of Eug against the AgNPs-induced adverse alterations in oxidative stress biomarkers. Eug prevents LPO by disrupting the chain reaction by trapping active oxygen and being metabolized to a dimer (dieugenol), which prevents LPO at the level of free radical chain reaction propagation [61].

TNF- α and IL-6 are proinflammatory cytokines that are involved in immunological retrogradation by mediating tissue inflammation and organ injury [62]. Rats intoxicated with AgNPs showed significantly elevated hepatic TNF- α and IL-6 levels, indicating that AgNPs primarily influence macrophage activities and promote liver injury development. Our findings are consistent with earlier researches that

found inflammation in the rat's liver after AgNPs treatment [52, 63]. Nuclear factor-kappa B (NF- κ B) is a protein complex required for activating the inflammatory cascade that causes IL-6 and TNF- α transcription [64]. Inflammasomes are multiprotein complexes that initiate inflammatory reactivity [65]. AgNPs activate both NF- κ B transcriptional and inflammasome paths, indicating the participation of these paths in the molecular mechanism underlying AgNPs' inflammatory effects [66]. The current results revealed marked suppression of the overproduction of the tested cytokines in the liver tissues of rats treated with Eug concomitant with AgNPs-low or AgNPs-high doses. Eug has long been recognized for its anti-inflammatory properties, since it inhibits varied inflammation-related signaling routes containing the NF- κ B pathway [52].

The present biochemical outcomes were proved by our histological, histomorphometrical, and immunohistochemical observations. Histopathologically, varied alterations reflecting the hepatotoxic effects of AgNPs, included hepatocellular degeneration, lymphocytic infiltration, hepatocytic necrosis/apoptosis, dilatation/congestion of blood vessels, and dilation of sinusoidal spaces were the most identified hepatic abnormalities. In addition, the two applied doses of AgNPs significantly increased the numbers of necrotic hepatocytes, infiltrating inflammatory cells, deteriorated Kupffer cells, dilated/congested central and portal veins, besides significantly decreasing the numbers of normal hepatic cells, which are the most indicative signs of hepatic structural damage. Furthermore, the pathological responses of hepatic tissues to AgNPs were dose dependent, since the high AgNPs dose was more efficient compared with the low dose.

The majority of hepatocytes of AgNPs-treated rats manifested severe degeneration distinguished by clear signs of necrosis. Such degradation could be associated with leakage of lysosomal hydrolytic enzymes, as well as disruption of

hepatocyte membrane function, which causes a huge influx of water and Na⁺, leading to cytoplasmic degeneration [67]. Furthermore, necrosis is triggered by an attack on the cell organelles, particularly the endoplasmic reticulum, mitochondria, and nucleus, which disrupts their functions [68]. In this study, necrosis was evidenced by GSH depletion and diminishing in CAT and SOD activities [2].

The current study's findings manifested that vascular congestion was virtually a constant hallmark in hepatic tissues of AgNPs-treated rats, where some of these blood vessels had distorted contours owing to the surrounding fibrosis. Blood extravasation was also seen. Sinusoidal dilatation has also been elucidated as a result of hepatocyte necrosis or injury of the lining sinusoidal endothelial tissue [69]. Furthermore, the prominence and swelling of Kupffer cells were among the most noticeable AgNPs toxicity. These lesions are ascribed to the vital role of Kupffer cells in bodily protective mechanism versus detoxification of AgNPs-induced hepatic oxidative stress, because Kupffer cells are the first cells exposed to the hazardous compounds entering the liver via the portal vein [47, 70].

The hepatic tissues of AgNPs-treated rats showed dispersed inflammatory cell infiltration in the centrilobular and periportal zones, indicating that AgNPs interact with the interstitial hepatic tissues, causing a variety of immunological responses [71]. Comparable results were reported by [2], who confirmed that leukocytosis is found in AgNPs-treated animals.

The present immunohistochemical findings showed that AgNPs-mediated cell death is connected with apoptosis, which was confirmed by significant decline in Bcl-2 immunoreactivity and elevation in P53 and Caspase-3 immunoreactivities after low- and high-dose AgNPs treatment. Bcl-2, an antiapoptotic protein that is overexpressed in many cancers, inhibits the intrinsic mitochondria-mediated cell death process by preventing mitochondrial membrane permeabilization, which causes proapoptotic chemical leakage [72]. Moreover, Bcl-2 gene family controls caspase activation in the intrinsic apoptosis pathway, which is induced by intracellular harm, such as DNA damage [73]. The activation of P53 is linked to apoptosis induction and also regulates the expression of other apoptosis-related proteins [74]. [75] believed that the stimulation of apoptosis and alteration of gene expression of the apoptosis-associated genes Bcl-2 and P53 is responsible for cancer cell death induced by biogenic metal NPs. Caspase-3 is an apoptotic marker that can be triggered by both intrinsic and extrinsic apoptotic pathways, resulting in DNA breakage [76]. These changes can be attributed to AgNPs aggregation in tissues [77] or to the AgNPs' effect on mitochondrial activity, reducing cell viability [46].

Intracellular AgNPs toxicity can be brought on by different processes, especially excessive ROS generation. AgNPs possess unique characteristics that enable them to penetrate cell membranes and other biological barriers, causing cellular malfunction or destruction [47]. Oxidative stress increases intracellular ROS, as confirmed by our biochemical results. Metal oxide NPs trigger DNA damage and cell death through ROS generation and oxidative damage [78]. ROS

can trigger cell death via two separate cell death mechanisms, apoptosis and necrosis. ROS also activate caspases, which are believed to execute apoptosis. These modifications can eventually lead to organ malfunction or even cancer [79]. Since biochemical decrease in GPx, CAT, and SOD essentially results in oxidative stress-induced cell death, such apoptotic effects could potentially be a consequence of the AgNPs-induced intercellular oxidative stress [2]. [80] illustrated that nanochelating-based AgNPs cause mild apoptosis/necrosis in mice, as well as changes in numerous clinical variables, such as blood parameters and liver enzymes.

Although TNF- α is released from primary hepatocytes, it is implicated in the proinflammatory response and cell-to-cell communication, and its signaling is linked to many autoimmune and inflammatory diseases. TNF- α is primarily formed by macrophages in inflammatory tissues, and it is involved in angiogenesis, wound healing, and tumor formation [81]. In this study, TNF- α expression was not detected in normal liver specimens but was overexpressed in liver tissues of AgNPs-treated rats. Our findings are in line with those of other researchers who found higher TNF- α production in chronic liver disease [82].

On the other side, coadministration of Eug alongside AgNPs attenuated the intensity of the histopathological and histomorphometrical changes in the hepatic tissues of rats treated with low and high doses of AgNPs. Also, concomitant treatment with Eug into rats exposed to AgNPs modulated the immunohistochemical expression of Bcl-2, P53, Caspase-3, and TNF- α reactive proteins. These results are consistent with those reported by [52, 53, 61]. The hepatoprotective efficiency of Eug can be attributed to its ability to stabilize hepatocyte membranes by preventing LPO and improving antioxidant enzyme activity, besides its free radical scavenging and anti-inflammatory properties.

5. Conclusions

The current investigation established that exposing rats to AgNPs caused oxidative stress and inflammation, which resulted in hepatotoxicity. Our results also provide a new insight into the ameliorative role of Eug supplementation against AgNPs-induced hepatotoxicity due to its antioxidant, antiapoptotic, and anti-inflammatory properties. Finally, we suggest using Eug as a preventive agent along with AgNPs to minimize its hepatotoxicity.

Data Availability

The data presented in this study are available on request from the corresponding author.

Conflicts of Interest

The authors declare no competing interests.

Acknowledgments

The authors express their gratitude to Prof. Dr. Yahia I.S. and Dr. Hussien M.S.A., Nanoscience Laboratory for Environmental and Bio-medical Applications (NLEBA), Department of Physics, Faculty of Education, Ain Shams University, Roxy, 11757 Cairo, Egypt, for their cooperation and beneficial help in synthesis of AgNPs in their laboratory.

References




- [1] R. Singh and H. S. Nalwa, "Medical applications of nanoparticles in biological imaging, cell labeling, antimicrobial agents, and anticancer nanodrugs," *Journal of Biomedical Nanotechnology*, vol. 7, no. 4, pp. 489–503, 2011.
- [2] M. M. El Mahdy, T. A. S. Eldin, H. S. Aly, F. F. Mohammed, and M. I. Shaalan, "Evaluation of hepatotoxic and genotoxic potential of silver nanoparticles in albino rats," *Experimental and Toxicologic Pathology*, vol. 67, no. 1, pp. 21–29, 2015.
- [3] I. A. Nedelcu, A. Ficaï, M. Sonmez, D. Ficaï, O. Oprea, and E. Andronescu, "Silver based materials for biomedical applications," *Current Organic Chemistry*, vol. 18, no. 2, pp. 173–184, 2014.
- [4] M. E. K. Kraeling, V. D. Topping, Z. M. Keltner et al., "In vitro_ percutaneous penetration of silver nanoparticles in pig and human skin," *Regulatory Toxicology and Pharmacology*, vol. 95, pp. 314–322, 2018.
- [5] S. Kumar, A. Shukla, P. P. Baul, A. Mitra, and D. Halder, "Biodegradable hybrid nanocomposites of chitosan/gelatin and silver nanoparticles for active food packaging applications," *Food Packaging and Shelf Life*, vol. 16, pp. 178–184, 2018.
- [6] Y. Zhou and R.-C. Tang, "Facile and eco-friendly fabrication of AgNPs coated silk for antibacterial and antioxidant textiles using honeysuckle extract," *Journal of Photochemistry and Photobiology B: Biology*, vol. 178, pp. 463–471, 2018.
- [7] T. A. Dankovich and D. G. Gray, "Bactericidal paper impregnated with silver nanoparticles for point-of-use water treatment," *Environmental Science & Technology*, vol. 45, no. 5, pp. 1992–1998, 2011.
- [8] S. J. Lee, A. R. Morrill, and M. Moskovits, "Hot spots in silver nanowire bundles for surface-enhanced Raman spectroscopy," *Journal of the American Chemical Society*, vol. 128, no. 7, pp. 2200–2201, 2006.
- [9] W. Park and K. Na, "Advances in the synthesis and application of nanoparticles for drug delivery," *WIREs Nanomedicine and Nanobiotechnology*, vol. 7, no. 4, pp. 494–508, 2015.
- [10] Z. Ferdous and A. Nemmar, "Health impact of silver nanoparticles: a review of the biodistribution and toxicity following various routes of exposure," *International Journal of Molecular Sciences*, vol. 21, no. 7, p. 2375, 2020.
- [11] B. K. Gaiser, S. Hirn, A. Kermanizadeh et al., "Effects of silver nanoparticles on the liver and hepatocytes in vitro," *Toxicological Sciences*, vol. 131, no. 2, pp. 537–547, 2013.
- [12] A. K. Patlolla, D. Hackett, and P. B. Tchounwou, "Silver nanoparticle-induced oxidative stress-dependent toxicity in Sprague-Dawley rats," *Molecular and Cellular Biochemistry*, vol. 399, no. 1–2, pp. 257–268, 2015.
- [13] D. McShan, P. C. Ray, and H. Yu, "Molecular toxicity mechanism of nanosilver," *Journal of Food and Drug Analysis*, vol. 22, no. 1, pp. 116–127, 2014.
- [14] C. Forni, F. Facchiano, M. Bartoli et al., "Beneficial role of phytochemicals on oxidative stress and age-related diseases," *BioMed Research International*, vol. 2019, Article ID 8748253, 16 pages, 2019.
- [15] A. A. Khalil, U. . Rahman, M. R. Khan, A. Sahar, T. Mehmood, and M. Khan, "Essential oil eugenol: sources, extraction techniques and nutraceutical perspectives," *RSC Advances*, vol. 7, no. 52, pp. 32669–32681, 2017.
- [16] A. K. Mishra, A. Mishra, H. K. Kehri, B. Sharma, and A. K. Pandey, "Inhibitory activity of Indian spice plant *Cinnamomum zeylanicum* extracts against *Alternaria solani* and *Curvularia lunata*, the pathogenic dematiaceous moulds," *Annals of Clinical Microbiology and Antimicrobials*, vol. 8, pp. 1–7, 2009.
- [17] M. A. Murcia, I. Egea, F. Romojaro, P. Parras, A. M. Jiménez, and M. Martínez-Tomé, "Antioxidant evaluation in dessert spices compared with common food additives. Influence of irradiation procedure," *Journal of Agricultural and Food Chemistry*, vol. 52, no. 7, pp. 1872–1881, 2004.
- [18] Y. T. Tung, M. T. Chua, S. Y. Wang, and S. T. Chang, "Anti-inflammation activities of essential oil and its constituents from indigenous cinnamon (*Cinnamomum osmophloeum*) twigs," *Bioresource Technology*, vol. 99, no. 9, pp. 3908–3913, 2008.
- [19] E. Dervis, A. Yurt Kilcar, E. I. Medine et al., "In vitro incorporation of radioiodinated eugenol on adenocarcinoma cell lines (Caco2, MCF7, and PC3)," *Cancer Biotherapy & Radiopharmaceuticals*, vol. 32, no. 3, pp. 75–81, 2017.
- [20] H. Y. Zahran, M. Kilany, I. S. Yahia, O. Albulym, M. S. A. Hussien, and M. M. Abutalib, "Facile microwave synthesis of silver nanoplates: optical plasmonic and antimicrobial activity," *Materials Research Express*, vol. 6, no. 9, p. 095073, 2019.
- [21] X. F. Zhang, Z. G. Liu, W. Shen, and S. Gurunathan, "Silver nanoparticles: synthesis, characterization, properties, applications, and therapeutic approaches," *International Journal of Molecular Sciences*, vol. 17, no. 9, p. 1534, 2016.
- [22] M. J. Dykstra and L. E. Reuss, *Biological Electron Microscopy: Theory, Techniques, and Troubleshooting*, Springer, US, 2003.
- [23] A. C. Reddy and B. R. Lokesh, "Effect of curcumin and eugenol on iron-induced hepatic toxicity in rats," *Toxicology*, vol. 107, no. 1, pp. 39–45, 1996.
- [24] O. H. Lowry, N. J. Rosebrough, A. L. Farr, and R. J. Randall, "Protein measurement with the Folin phenol reagent," *Journal of Biological Chemistry*, vol. 193, no. 1, pp. 265–275, 1951.
- [25] N. W. Tietz, *Fundamentals of Clinical Chemistry*, Saunders (W.B.) Co Ltd, 1976.
- [26] A. Vassault, M. C. Azzedine, and M. Bailly, "Protocole de validation de techniques. Commission Validation de techniques," *Annales de Biologie Clinique*, vol. 44, pp. 686–718, 1986.
- [27] W. Armstrong and C. Carr, "Estimation of serum total protein," in *Physiological Chemistry Laboratory Directions*, Burges Publishing Co, USA, 3rd ed. edition, 1964.
- [28] B. T. Dumas, W. Ard Watson, and H. G. Biggs, "Albumin standards and the measurement of serum albumin with bromocresol green," *Clinica Chimica Acta*, vol. 31, no. 1, pp. 87–96, 1971.
- [29] D. Koracevic, G. Koracevic, V. Djordjevic, S. Andrejevic, and V. Cosic, "Method for the measurement of antioxidant activity in human fluids," *Journal of Clinical Pathology*, vol. 54, no. 5, pp. 356–361, 2001.

- [30] F. Tatzber, S. Griebenow, W. Wonisch, and R. Winkler, "Dual method for the determination of peroxidase activity and total peroxides- iodide leads to a significant increase of peroxidase activity in human sera," *Analytical Biochemistry*, vol. 316, no. 2, pp. 147–153, 2003.
- [31] J. A. Buege and S. D. Aust, "Microsomal lipid peroxidation," *Methods in Enzymology*, vol. 52, pp. 302–310, 1978.
- [32] M. Nishikimi, N. Appaji Rao, and K. Yagi, "The occurrence of superoxide anion in the reaction of reduced phenazine methosulfate and molecular oxygen," *Biochemical and Biophysical Research Communications*, vol. 46, no. 2, pp. 849–854, 1972.
- [33] H. Aebi, "Catalase in vitro," in *Methods in Enzymology*, pp. 121–126, Academic Press, 1984.
- [34] E. Beutler, O. Duron, and B. M. Kelly, "Improved method for the determination of blood glutathione," *The Journal of Laboratory and Clinical Medicine*, vol. 61, pp. 882–888, 1963.
- [35] D. E. Paglia and W. N. Valentine, "Studies on the quantitative and qualitative characterization of erythrocyte glutathione peroxidase," *The Journal of Laboratory and Clinical Medicine*, vol. 70, no. 1, pp. 158–169, 1967.
- [36] J. D. Bancroft and M. Gamble, Eds., "Theory and Practice of Histological Techniques," Edinburgh: Churchill Livingstone, Sixth edition, 2008.
- [37] K. Petrosyan, R. Tamayo, and D. Joseph, "Sensitivity of a novel biotin-free detection reagent (Powervision+TM/SUP) for immunohistochemistry," *Journal of Histotechnology*, vol. 25, no. 4, pp. 247–250, 2002.
- [38] Y. R. Van Eycke, J. Allard, I. Salmon, O. Debeir, and C. Decaestecker, "Image processing in digital pathology: an opportunity to solve inter-batch variability of immunohistochemical staining," *Scientific Reports*, vol. 7, no. 1, p. 42964, 2017.
- [39] M. J. Mofolo, P. Kadhila, K. C. Chinsebu, S. Mashele, and M. Sekhoacha, "Green synthesis of silver nanoparticles from extracts of *Pechuel-oeschea leubnitziae*: their anti-proliferative activity against the U87 cell line," *Inorganic and Nano-Metal Chemistry*, vol. 50, no. 10, pp. 949–955, 2020.
- [40] Z. Liu, L. Wang, X. Zhao, Y. Luo, K. Zheng, and M. Wu, "Highly effective antibacterial grafted chitosan for construction of durable antibacterial fabrics," *International Journal of Biological Macromolecules*, vol. 209, pp. 963–971, 2022.
- [41] G. Ghodake, S. Shinde, R. G. Saratale et al., "Whey peptide-encapsulated silver nanoparticles as a colorimetric and spectrophotometric probe for palladium(II)," *Microchimica Acta*, vol. 186, no. 12, p. 763, 2019.
- [42] P. Bhuyar, M. H. A. Rahim, S. Sundararaju, R. Ramaraj, G. P. Maniam, and N. Govindan, "Synthesis of silver nanoparticles using marine macroalgae *Padina* sp. and its antibacterial activity towards pathogenic bacteria," *Beni-Suef University Journal of Basic and Applied Sciences*, vol. 9, no. 1, p. 3, 2020.
- [43] Z. Shah, T. Gul, S. Ali Khan et al., "Synthesis of high surface area AgNPs from *Dodonaea viscosa* plant for the removal of pathogenic microbes and persistent organic pollutants," *Materials Science and Engineering: B*, vol. 263, p. 114770, 2021.
- [44] K. Jyoti, M. Baunthiyal, and A. Singh, "Characterization of silver nanoparticles synthesized using *Urtica dioica* Linn. leaves and their synergistic effects with antibiotics," *Journal of Radiation Research and Applied Sciences*, vol. 9, no. 3, pp. 217–227, 2016.
- [45] M. A. Islam, M. V. Jacob, and E. Antunes, "A critical review on silver nanoparticles: from synthesis and applications to its mitigation through low-cost adsorption by biochar," *Journal of Environmental Management*, vol. 281, p. 111918, 2021.
- [46] S. M. Hussain, K. L. Hess, J. M. Gearhart, K. T. Geiss, and J. J. Schlager, "In vitro toxicity of nanoparticles in BRL 3A rat liver cells," *Toxicology In Vitro*, vol. 19, no. 7, pp. 975–983, 2005.
- [47] M. Pourhamzeh, Z. Gholami Mahmoudian, M. Saidijam, M. J. Asari, and Z. Alizadeh, "The effect of silver nanoparticles on the biochemical parameters of liver function in serum, and the expression of Caspase-3 in the liver tissues of male rats," *Avicenna Journal of Medical Biochemistry*, vol. 4, no. 2, pp. 7–35557, 2016.
- [48] J. Pal, M. K. Deb, and D. K. Deshmukh, "Microwave-assisted synthesis of silver nanoparticles using benzo-18-crown-6 as reducing and stabilizing agent," *Applied Nanoscience*, vol. 4, no. 4, pp. 507–510, 2014.
- [49] S. S. Chaung, C. C. Lin, J. Lin, K. H. Yu, Y. F. Hsu, and M. H. Yen, "The hepatoprotective effects of Limonium sinense against carbon tetrachloride and β -D-galactosamine intoxication in rats," *Phytotherapy Research*, vol. 17, no. 7, pp. 784–791, 2003.
- [50] M. A. Abdel-Wahhab and S. E. Aly, "Antioxidant property of *Nigella sativa* (black cumin) and *Syzygium aromaticum* (clove) in rats during aflatoxicosis," *Journal of Applied Toxicology*, vol. 25, no. 3, pp. 218–223, 2005.
- [51] I. F. Mosa, M. Youssef, T. Shalaby, and O. F. Mosa, "The protective role of tannic acid against possible hepatonephrotoxicity induced by silver nanoparticles on male rats," *Sanamed*, vol. 14, no. 2, pp. 131–145, 2019.
- [52] A. Kumar, N. J. Siddiqi, S. T. Alrashood, H. A. Khan, A. Dubey, and B. Sharma, "Protective effect of eugenol on hepatic inflammation and oxidative stress induced by cadmium in male rats," *Biomedicine & Pharmacotherapy*, vol. 139, p. 111588, 2021.
- [53] A. Marchese, R. Barbieri, E. Coppo et al., "Antimicrobial activity of eugenol and essential oils containing eugenol: a mechanistic viewpoint," *Critical Reviews in Microbiology*, vol. 43, no. 6, pp. 668–689, 2017.
- [54] K. Brieger, S. Schiavone, F. J. Miller, and K. H. Krause, "Reactive oxygen species: from health to disease," *Swiss Medical Weekly*, vol. 142, no. w13659, pp. 1–14, 2012.
- [55] T. A. F. Aguilar, B. C. H. Navarro, and J. A. M. Pérez, *Endogenous Antioxidants: A Review of their Role in Oxidative Stress*, IntechOpen, London, UK, 2016.
- [56] A. Ozcan and M. Ogun, *Biochemistry of Reactive Oxygen and Nitrogen Species, in Basic Principles and Clinical Significance of Oxidative Stress*, S. J. T. Gowder, Ed., IntechOpen, London, UK, 2015.
- [57] C. J. Busch and C. J. Binder, "Malondialdehyde epitopes as mediators of sterile inflammation," *Biochimica et Biophysica Acta (BBA) - Molecular and Cell Biology of Lipids*, vol. 1862, no. 4, pp. 398–406, 2017.
- [58] B. Halliwell, "Free radicals, antioxidants, and human disease: curiosity, cause, or consequence?," *Lancet*, vol. 344, no. 8924, pp. 721–724, 1994.

- [59] A. Loghman, "Histopathologic and apoptotic effect of nanosilver in liver of broiler chickens," *African Journal of Biotechnology*, vol. 11, no. 22, pp. 6207–6211, 2012.
- [60] E. M. Abd Elmaksoud, N. M. Taha, M. A. Lebda, and M. A. Kamel, "The possible protective role of alpha-lipoic acid on nanosilver particle-induced hepatotoxicity in male rats," *Biochemistry Letters*, vol. 14, no. 1, pp. 85–97, 2019.
- [61] M. Ogata, M. Hoshi, S. Urano, and T. Endo, "Antioxidant activity of eugenol and related monomeric and dimeric compounds," *Chemical and Pharmaceutical Bulletin*, vol. 48, no. 10, pp. 1467–1469, 2000.
- [62] B. R. Lauwerys and F. A. Houssiau, *Involvement of Cytokines in the Pathogenesis of Systemic Lupus Erythematosus, in Cytokines and Chemokines in Autoimmune Disease*, P. Santamaria and P. H. Hackett, Eds., Springer, New York, 2003.
- [63] R. Ebabe Elle, S. Gaillot, J. Vidé et al., "Dietary exposure to silver nanoparticles in Sprague-Dawley rats: effects on oxidative stress and inflammation," *Food and Chemical Toxicology*, vol. 60, pp. 297–301, 2013.
- [64] T. Shabab, R. Khanabdali, S. Z. Moghadamtousi, H. A. Kadir, and G. Mohan, "Neuroinflammation pathways: a general review," *International Journal of Neuroscience*, vol. 127, no. 7, pp. 624–633, 2017.
- [65] H. Guo, J. B. Callaway, and J. P. Ting, "Inflammasomes: mechanism of action, role in disease, and therapeutics," *Nature Medicine*, vol. 21, no. 7, pp. 677–687, 2015.
- [66] A. Fehaid, R. Fujii, T. Sato, and A. Taniguchi, "Silver nanoparticles affect the inflammatory response in a lung epithelial cell line," *The Open Biotechnology Journal*, vol. 14, no. 1, pp. 113–123, 2020.
- [67] U. Del Monte, "Swelling of hepatocytes injured by oxidative stress suggests pathological changes related to macromolecular crowding," *Medical Hypotheses*, vol. 64, no. 4, pp. 818–825, 2005.
- [68] A. Singh, T. K. Bhat, and O. P. Sharma, "Clinical biochemistry of hepatotoxicity," *Journal of Clinical Toxicology*, vol. 4, no. 1, 2011.
- [69] L. L. Oligny and J. Lough, "Hepatic sinusoidal ectasia," *Human Pathology*, vol. 23, no. 8, pp. 953–956, 1992.
- [70] A. Neyrinck, "Modulation of Kupffer cell activity: physiopathological consequences on hepatic metabolism," *Bulletin et Mémoires de l'Académie Royale de Médecine de Belgique*, vol. 159, no. 5-6, pp. 358–366, 2004.
- [71] D. Johar, J. C. Roth, G. H. Bay, J. N. Walker, T. J. Krocak, and M. Los, "Inflammatory response, reactive oxygen species, programmed (necrotic-like and apoptotic) cell death and cancer," *Roczniki Akademii Medycznej w Białymstoku*, vol. 49, pp. 31–39, 2004.
- [72] S. L. Chan and V. C. Yu, "Proteins of the bcl-2 family in apoptosis signalling: from mechanistic insights to therapeutic opportunities," *Clinical and Experimental Pharmacology & Physiology*, vol. 31, no. 3, pp. 119–128, 2004.
- [73] S. Cory and J. M. Adams, "The Bcl2 family: regulators of the cellular life-or-death switch," *Nature Reviews Cancer*, vol. 2, no. 9, pp. 647–656, 2002.
- [74] P. May and E. May, "Twenty years of p53 research: structural and functional aspects of the p53 protein," *Oncogene*, vol. 18, no. 53, pp. 7621–7636, 1999.
- [75] H. Banu, N. Renuka, S. M. Faheem et al., "Gold and silver nanoparticles biomimetically synthesized using date palm pollen extract induce apoptosis and regulate p53 and Bcl-2 expression in human breast adenocarcinoma cells," *Biological Trace Element Research*, vol. 186, no. 1, pp. 122–134, 2018.
- [76] W. Ma, L. Jing, A. Valladares et al., "Silver nanoparticle exposure induced mitochondrial stress, Caspase-3 activation and cell death: amelioration by sodium selenite," *International Journal of Biological Sciences*, vol. 11, no. 8, pp. 860–867, 2015.
- [77] F. A. Sulaiman, O. S. Adeyemi, M. A. Akanji et al., "Biochemical and morphological alterations caused by silver nanoparticles in Wistar rats," *Journal of Acute Medicine*, vol. 5, no. 4, pp. 96–102, 2015.
- [78] M. J. Piao, K. A. Kang, I. K. Lee et al., "Silver nanoparticles induce oxidative cell damage in human liver cells through inhibition of reduced glutathione and induction of mitochondria-involved apoptosis," *Toxicology Letters*, vol. 201, no. 1, pp. 92–100, 2011.
- [79] K. Rahman, "Studies on free radicals, antioxidants, and co-factors," *Clinical Interventions in Aging*, vol. 2, no. 2, pp. 219–236, 2007.
- [80] S. M. Hoseini-Alfatemi, F. Fallah, S. Armin, M. Hafizi, A. Karimi, and S. Kalanaky, "Evaluation of blood and liver cytotoxicity and apoptosis-necrosis induced by nanochelating based silver nanoparticles in mouse model," *Iranian Journal of Pharmaceutical Research: IJPR*, vol. 19, no. 2, pp. 207–218, 2020.
- [81] Y. M. Yang and E. Seki, "TNF α in liver fibrosis," *Current Pathobiology Reports*, vol. 3, no. 4, pp. 253–261, 2015.
- [82] G. W. McCaughan, M. D. Gorrell, G. A. Bishop et al., "Molecular pathogenesis of liver disease: an approach to hepatic inflammation, cirrhosis and liver transplant tolerance," *Immunological Reviews*, vol. 174, no. 1, pp. 172–191, 2000.

Research Article

Bovine Lactoferrin Induces Cell Death in Human Prostate Cancer Cells

Vanessa P. Rocha ^{1,2} **Samir P. C. Campos** ³ **Caroline A. Barros** ^{1,4} **Pablo Trindade** ^{2,5}
Leticia R. Q. Souza⁵ **Triciana G. Silva**⁶ **Etel R. P. Gimba** ^{7,8} **Anderson J. Teodoro** ⁹
and Rafael B. Gonçalves ^{1,2}

¹Department of Biochemistry, Biomedical Institute, UNIRIO, 20211-040, Brazil

²Cell and Molecular Biology Graduate Program, UNIRIO, 20211-040, Brazil

³Medical Biochemistry Institute, UFRJ, 21941-590, Brazil

⁴Multicentre Graduate Program in Biochemistry and Molecular Biology, IFRJ, 20270-021, Brazil

⁵D'Or Institute for Research and Education-IDOR, 22281-100, Brazil

⁶National Center for Structural Biology and Bioimaging, CENABIO, UFRJ, 21941-902, Brazil

⁷Natural Science Department, UFF, 28895-532, Brazil

⁸Cellular and Molecular Oncology Program, National Institute of Cancer (INCA), 20231-050, Brazil

⁹Department of Nutrition and Dietetics, UFF, 22290-250, Brazil

Correspondence should be addressed to Rafael B. Gonçalves; rafael.braga@unirio.br

Received 7 March 2022; Accepted 22 August 2022; Published 2 September 2022

Academic Editor: Alessandra Durazzo

Copyright © 2022 Vanessa P. Rocha et al. This is an open access article distributed under the Creative Commons Attribution License, which permits unrestricted use, distribution, and reproduction in any medium, provided the original work is properly cited.

Bovine lactoferrin (bLf) is a multifunctional protein widely associated with anticancer activity. Prostate cancer is the second most frequent type of cancer worldwide. This study was aimed at evaluating the influence of bLf on cell viability, cell cycle progression, reactive oxygen species (ROS) production, and rate of apoptosis in the human prostate cancer cell line (DU-145). MTT assay and trypan blue exclusion were used to analyze cell viability. Morphological changes were analyzed through optical microscopy after 24 h and 48 h of bLf treatment. FITC-bLf internalization and cellular damage were observed within 24 h by confocal fluorescence microscopy. Cell cycle analyses were performed by flow cytometry and propidium iodide. For caspases 3/7 activation and reactive oxygen species production evaluation, cells were live-imaged using the high-throughput system Operetta. The cell viability assays demonstrated that bLf induces cell death and morphological changes after 24 h and 48 h of treatment compared to control on DU-145 cells. The bLf internalization was detected in DU-145 cells, G₁-phase arrest of the cell cycle, caspase 3/7 activation, and increased oxidative stress on bLf-treated cells. Our data support that bLf has an important anticancer activity, thus offering new perspectives in preventing and treating prostate cancer.

1. Introduction

Bovine Lactoferrin (bLf) is found in cattle and is an iron-binding protein. bLf is present in several exocrine secretions, such as tears, saliva, milk, and cervical mucus. It has a molecular mass of approximately 80 kDa [1, 2]. This protein can be found in two conformational states. The conformational state “apo-” (apo-bLf) represents the protein not bound to ferric ions, while the conformational state “holo-”

(holo-bLf) represents the protein bound to two ferric ions. Lf binds to the ferric ion in a very high affinity, approximately 10⁻²⁰ M of affinity constant (K_D), and some of its physiological functions rely on that iron-binding property. Holo-bLf has a more compact, stable structure and is less sensitive to thermal denaturation and proteolysis due to the iron bond in its structure, compared to apo-bLf [3–5]. bLf has proven to be a great model for studying biological activities, including iron transport, immunomodulatory,

anti-inflammatory, antiviral, antioxidant, and antitumor properties. Due to its multiple biological functions, bLf structural changes have been widely associated with immune enhancement and anticarcinogenic properties [1, 4–6].

Currently, great attention has been given initiatives aimed at preventing cancer. This disease alone is the second leading cause of death in the United States and a major public health problem worldwide. Counting about 19.3 million new cases of cancer per year worldwide accounting for nearly 10 million deaths in 2020. The coronavirus disease 2019 (COVID-19) pandemic drastically affected the diagnosis and treatment of cancer, which has led to an increase in mortality rates [7–9].

Robust evidence points out bLf as a promising biomolecule in cancer research. For instance, a previous study reported that treatment with bLf could suppress colon carcinogenesis by inducing elevated Fas expression, activation of caspases 3 and 8, and inductance ion of DNA fragmentation, which led to apoptosis of cancer cells in rat colon mucosa [10, 11]. Similarly, other studies demonstrated that bLf decreased the growth of colon, lung, bladder, and breast cancer cells. Induction of apoptosis in colon, lung, stomach, and breast cancer cells has also been reported [11–19].

Prostate cancer is the leading cancer diagnosis among men and the third most common diagnosis overall, with 1,414,259 expected cases in 2020, the fifth leading cause of cancer death in the United States [7, 20].

Recent evidence reported that bLf inhibits proliferation, induces apoptosis and intracellular acidification, and disturbs lysosomal acidification in the PC-3 prostate cancer cell line. This work suggests that the bLf mechanism of action is mediated by the V-ATPase pump in the plasma membrane, hindering its activity and decreasing acidity, thus limiting prostate cancer progression and metastasis formation [21].

New treatment options for prostate cancer are being used, and several recent studies for its treatment are being conducted. However, despite all the advances, the morbidity and mortality of prostate cancer have increased worldwide [22]. Bioactive compounds have been associated with modifying specific carcinogenic processes [23]. Therefore, this study is aimed at evaluating the cytotoxic effects of bLf on its apo- and holo- forms in the DU-145 cell line of prostate cancer.

2. Materials and Methods

2.1. Standards and Chemicals. All chemicals used in this work were of analytical grade. The water was distilled and deionized using a Millipore water purification system. Bovine lactoferrin was purchased from Life Extension (Florida, USA). The nitrilotriacetic acid, ferric nitrate, and Dulbecco's cell culture medium was obtained from Sigma-Aldrich Chemical Company (St. Louis, MO). Fetal bovine serum was purchased from Gibco™, Thermo Fisher Scientific (Waltham, Massachusetts, EUA). Tissue culture flasks were purchased from Greiner Bio-One International GmbH (Kremsmünster, Austria).

2.2. Preparation of bLf Forms: Apo-Lactoferrin. Bovine apo-lactoferrin was prepared from capsules containing 300 mg

of protein (Life Extension, USA). Phosphate saline buffer (PBS) (140 mM NaCl, 2.7 mM KCl, 10 mM Na₂HPO₄, and 1.8 mM KH₂PO₄ at pH 7.4) was used for protein solubilization. The capsule contained cellulose, and to separate it from the protein, four cycles of centrifugation of 10 minutes each was performed at an angular speed of 7000 rpm (12,052 × g) at 4°C. Then, apo-bLf was filtered using a sterile nitrocellulose membrane of a 0.22 μm pore (Millipore, USA) in an ESCO biosafety cabin, aliquoted, and frozen at -20°C. Finally, apo-bLf concentration was measured by an absorbance spectrophotometer at a 280 nm wavelength, using a molar extinction coefficient of 1.27 [24, 25].

2.3. Preparation of bLf Forms: Holo-Lactoferrin. Holo-lactoferrin was prepared from apo-bLf [3]. Apo-bLf stock was diluted in 10 mM Tris buffer, 75 mM NaCl, and pH 7.2. After dilution, a FeNTA solution (9.9 mM ferric nitrate and 8.5 mM nitrilotriacetic acid, deionized water) was added in a 2:1 ratio (FeNTA:bLf solution). The pH of the solution was adjusted to 7.0 and incubated for one hour at 4°C. Subsequently, the sample was dialyzed against a buffer with 25 mM Tris, 150 mM NaCl pH 7.5 at 4°C for 48 h. A dialysis membrane with a cut-off of 10 kDa was used, and the buffer was changed every 5 h. Then, the holo-bLf was filtered on a sterile nitrocellulose membrane of a 0.22 μm pore (Millipore, USA) in an ESCO biosafety cabin, aliquoted, and frozen at -20°C. Finally, the protein concentration was then measured in a spectrophotometer at a 280 nm wavelength, using the molar extinction coefficient of 1.51 holo-bLf. The presence of iron ions was verified using a spectrophotometric absorbance reading at 465 nm [3, 26, 27].

2.4. Cell Culture. The cell line was obtained from the Neoplastic Biomarkers Group (Nacional Institute of Cancer-INCA), which certified its identity and quality. The human prostate carcinoma cell line DU-145 (ATCC-HTB-81) was maintained routinely in high-glucose Dulbecco's Modified Eagle Medium (DMEM) (Sigma, New York, NY, USA), supplemented with a 10% fetal bovine serum (FBS) and 1% penicillin-streptomycin (PS) (Sigma, New York, NY, USA), pH 7.4, under 5% CO₂ atmosphere and 37°C. Once the cells reached 80% of confluence, they were dissociated with a 0.05% trypsin-ethylenediamine tetraacetic acid (EDTA) and subcultured in 25 or 75 cm² plastic flasks at a 25 × 10⁴ cells/cm² density, every two days, following ATCC instructions.

2.5. Cell Viability Assays: MTT Assay. Cell viability was determined by a 3-(4,5-dimethylthiazol-2-yl)-2,5-diphenyltetrazolium bromide (MTT) colorimetric test (Amresco, USA) [28]. By this test, the quantification of MTT reduction in formazan characterizes a detection of metabolic activity that is linked to cell viability. 96-well plates were prepared using 1.0 × 10⁴ cells/well for this analysis. After 24 h, the cells were washed, and 100 μL of apo- and holo-bLf solution was added to the wells at concentrations of 2, 4, 8, and 16 mg/mL (diluted in the culture medium described above). As a negative control, DMEM was used. After 24 h and 48 h of incubation, the bLf was removed, the wells were washed, and a solution of 200 μL MTT (Sigma) was added in PBS.

The plate was incubated for 3 hours at 37°C. After this period, the plate was analyzed on a spectrophotometer using absorbance at 570 nm and 650 nm. Wells with negative control were considered 100% in cell viability. Triton X-100 0.1% was used as a 100% death control to normalize calculations. This experiment was repeated in triplicate with independent preparations.

2.6. Cell Viability Assays: Cell Counting with Neubauer Chamber. The experiment is based on viable cells' selective permeability and was not stained by trypan blue since dead cells undergo changes in the membrane that affect their selective permeability, thus allowing the blue dye to enter [29]. The tests were performed by cultivating the cells in 24-well plates and kept with a 500 μ L of culture medium at 37°C until reaching a 90% confluence. Then, the medium was removed, and the cells were washed with PBS. The culture medium was placed in the control, and concentrations of apo-bLf and holo-bLf 2, 4, 8, and 16 mg/mL prepared with the culture medium were placed in their respective wells. After treatment for 24 h and 48 h, the cells were trypsinized and resuspended in a 200 μ L of the medium. 10 μ L of that suspension was collected and mixed with a 10 μ L of 0.4% trypan blue (Gibco) solution in PBS. 10 μ L was collected and placed in the Neubauer chamber for cell counting from the last suspension. Cells in the four outer quadrants were counted. Live and dead cells were distinguished by staining. Finally, cell concentration was calculated, and a percentage graph was made.

2.7. Cell Morphology Analysis. The analysis of cell morphology was carried out using images of cells in culture after 24 h and 48 h of treatment using both forms of bLf. The cells were placed in a 24-well plate. After reaching a 90% confluence, the culture medium was removed, and the cells were washed with warm PBS and incubated with concentrations of 0, 2, 4, 8, and 16 mg/mL apo- and holo-bLf for 24 h and 48 h. Images were obtained using an EVOS™ optical microscope (Thermo Fisher) and EVOSTM 20X Objective lens (Plan-Fluor INF/1.2). Three images per well were obtained, as to know: center, upper right quadrant, and lower left quadrant (close to the board's limit). Experiments were carried out in triplicate. Images were acquired at an image resolution of 1280 \times 960 pixels, 24-bit RGB. By using Image J software (1.53c), images were first converted to an 8-bit monochrome image. Then, levels were adjusted to visualize the cell structures better, regulating the brightness and contrast curve. Images were calibrated to adapt to the actual pixel size using the Evos reference bar. Next, the bars were included, and the images were analyzed.

2.8. Bovine Lactoferrin Cell Internalization Assays. We performed the bLf labeling with fluorescein isothiocyanate (FITC) for cell internalization assays at a 1:10 molar ratio for one hour at 4°C. For the labeling process, lactoferrin was incubated in primary phosphate buffer (2.5% Na₂HPO₄·x7H₂O and 0.082% NaH₂PO₄) at pH 8. To remove all free FITC, successive centrifugations using PBS at pH 7.4 (5 times) were performed using a Vivaspin filter unit (GE

Health Care, USA) with a cut-off molecular weight of 30 kDa [30]. We proceeded with a sterile filtration of the labeled apo- and holo-bLf using a 0.22 μ m syringe-driven filter unit. The proteins were used on the same day for the experiments. The cells were plated on a commercial "CELL-view™ Slide" plate (Greiner Bio-One) to proceed with the investigations. After an 80% confluence, the cells were washed with 100 μ L of PBS and incubated with apo- and holo-bLf-FITC conjugates (8 and 16 mg/mL) diluted in DMEM 4°C for 15 min. Subsequently, to remove unbound bLf, cells were washed with ice-cold PBS and immediately incubated with DMEM. After interaction with bLf, cells were kept under a 5% CO₂ atmosphere and 37°C for 24 h. After treatment, the cells were washed with warm PBS and fixed with 3.7% paraformaldehyde in PBS for 15 minutes at room temperature. The study of lactoferrin cellular localization occurred through Laser Scanning Confocal Fluorescence Microscopy (LSCFM) using the LSM 510 Meta Confocal Microscope (Zeiss Inc., Oberkochen) and EC Plan-Neofluar 40x/1.30 Oil DIC M27 (Zeiss Inc.) objective lens.

2.9. Cell Cycle Analysis. Cell cycle analysis was performed using propidium iodide staining. The cells were plated on a 6-well plate, and after reaching a 90% confluence, cells were treated with 1.5 mL of apo-bLf and holo-bLf at concentrations of 2, 4, 8, and 16 mg/mL. Control cells were kept with a culture medium only. After 24 h and 48 h of bLf treatment, cells were washed with PBS and dissociated using trypsin. 1 \times 10⁵ cells were collected from each treatment and mixed with cold Vindelov's solution [31]. After incubation for 15 minutes, protected from light, cell suspensions were analyzed using a BD FACSAria II cytometer (BD Biosciences). Twenty thousand events were then analyzed by flow cytometer on the fluorochrome PI channel (488 nm excitation laser and long pass filter 556 and band pass filter 616/23 for emission). Data were analyzed using the FlowJo™ v10.7.2 Software (BD Biosciences).

2.10. Analysis of Oxidative Stress and Activation of Apoptosis. The probe test for the assessment of oxidative stress and activation of apoptosis was carried out using the Operetta High-Content Imaging System and two different probe solutions, one containing the dihydroethidium (DHE) reagent (Thermo Fisher #D1168) and Hoechst 33342 (Thermo Fisher #H1399), with a final concentration of 5 μ M and 1 μ M, respectively. The other solution contained the reagent CellEvent™ Caspase-3/7 Green Detection Reagent (Thermo Fisher #C10423) and Hoechst 33342 (Thermo Fisher #H1399), with a final concentration of 2 μ M and 1 μ M. The cells were placed in a 96-well plate (Greiner Bio-One #655090). Each well had 2000 to 2500 cells. After 24 h of cell growth, the plates were treated with 100 μ L of apo-bLf and holo-bLf in 2, 4, 8, and 16 mg/mL for 24 h and 48 h. Then, the medium containing the compounds was removed. 50 μ L of the probe solutions was added with each solution in each specific plate, diluted with DMEM culture medium without phenol red. The plates were incubated at 37°C, 5% CO₂ for 30 min, and placed in the Operetta High Content Imaging System (Perkin Elmer) at 37°C and a 5% CO₂.

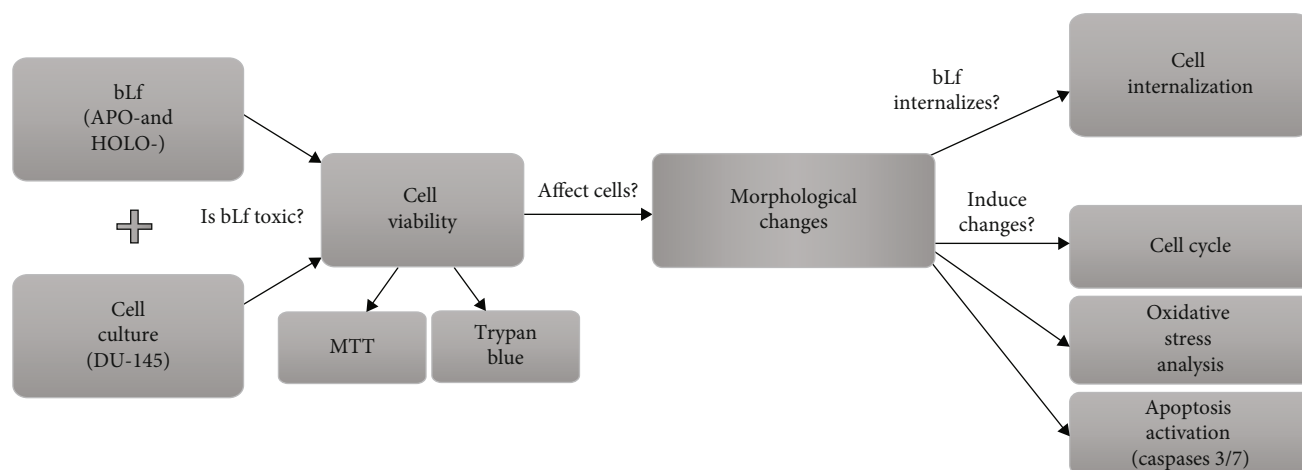


FIGURE 1: Graphical scheme of the study approach.

The images were obtained with the 20x objective and high numerical openings (NA) (PerkinElmer, USA). Data were analyzed using the Harmony 5.1 high-content image analysis software (PerkinElmer, USA). Nine independent fields were evaluated from wells in triplicate by experimental conditions. The results were demonstrated with a bar graph showing the positive cells for caspase 3/7 and DHE.

2.11. Statistical Analysis. The results are presented as mean with the corresponding standard deviation. Data were analyzed using the statistical software GraphPad Prism (version 6.01, GraphPad Software, San Diego, CA). One-way variance (ANOVA) using the Bonferroni post hoc test at a confidence level of 95% was used to test cell viability, cell cycle, and apoptosis.

2.12. Graphical Scheme. Figure 1 shows the graphical scheme of the study approach. It contains all the methodologies used.

3. Results

3.1. bLf Induces Cell Death in the DU-145 Cell Line. The effect of both forms of bLf (apo-bLf and holo-bLf) on cell viability was evaluated by two different approaches, MTT assay and trypan blue exclusion test (Figure 2). The screening of cytotoxic activity demonstrated that apo-bLf and holo-bLf reduced DU-145 cell viability using MTT assay. No differences were detected between the control group and cells exposed to 2, 4, and 8 mg/mL apo-bLf following a 24 h treatment. However, we observed a decrease of 80% in average viability after a 48 h of apo-bLf exposure with 2 and 4 mg/mL and a reduction of 70% following an 8 mg/mL treatment. In addition, the highest concentration of apo-bLf (16 mg/mL) induced the most significant reduction in cell viability, up to 60% ($p < 0.0001$) and 40% ($p < 0.01$) after 24 h and 48 h, respectively (Figure 2(a)).

After 24 h, treatment with 2 and 4 mg/mL holo-bLf (Figure 2(b)) induced a reduction of 25% in cell viability compared to control ($p < 0.05$). After 48 h, no cytotoxic

effects were observed following holo-bLf exposure (2 and 4 mg/mL). In contrast, the concentration of 8 mg/mL holo-bLf resulted in a drop in cell viability of 65% ($p < 0.01$) in 24 h and a decline of around 40% in 48 h ($p < 0.05$). Reductions of 50% and 90% of cell viability were observed using 16 mg/mL holo-bLf after 24 h and 48 h, respectively ($p < 0.01$).

To validate MTT findings, we also performed a trypan blue exclusion analysis to determine the number of viable cells in response to bLf treatment (Figures 2(c) and 2(d)). No significant difference in 24 h treatment with apo-bLf on all tested concentrations was observed (Figure 2(c)). However, after a 48 h treatment, we observed a reduction in cell viability of 30% ($p < 0.01$), 40% ($p < 0.001$), and more than 80% ($p < 0.0001$) following 4, 8, and 16 mg/mL apo-bLf, respectively. No significant differences were observed in lower concentrations of holo-bLf (2, 4, and 8 mg/mL) after 24 h treatment (Figure 2(d)). In turn, 16 mg/mL holo-bLf resulted in a 50% reduction in cell viability ($p < 0.0001$). Following 48 h treatment, a reduction in cell viability by approximately 40% ($p < 0.001$), 20% ($p < 0.01$), 60% ($p < 0.0001$), and 80% ($p < 0.0001$) was observed when using of 2, 4, 8, and 16 mg/mL holo-bLf, respectively.

3.2. bLf Causes Morphological Changes in the DU-145 Cell Line. In addition to the robust reduction in cell viability upon bLf treatment in the DU-145 cell line, evident changes in the morphology of the remaining cells (Figure 3) were observed. Treatment with both apo- and holo-bLf affected the cell shape so that most cells exhibited a stretched morphology and a reduced cell area (Figure 3(a)).

In addition, an increase in the number of intracellular granules could be primarily seen in the concentration of 16 mg/mL 24 h posttreatment and of 8 mg/mL 48 h post-treatment (Figure 3(b)). It is important to note that these morphological changes were more pronounced at 8 mg/mL with holo-bLf when compared to apo-bLf treatment.

3.3. bLf Internalizes and Causes DU-145 Cell Damage. Once we found that bLf induced DU-145 cell morphological

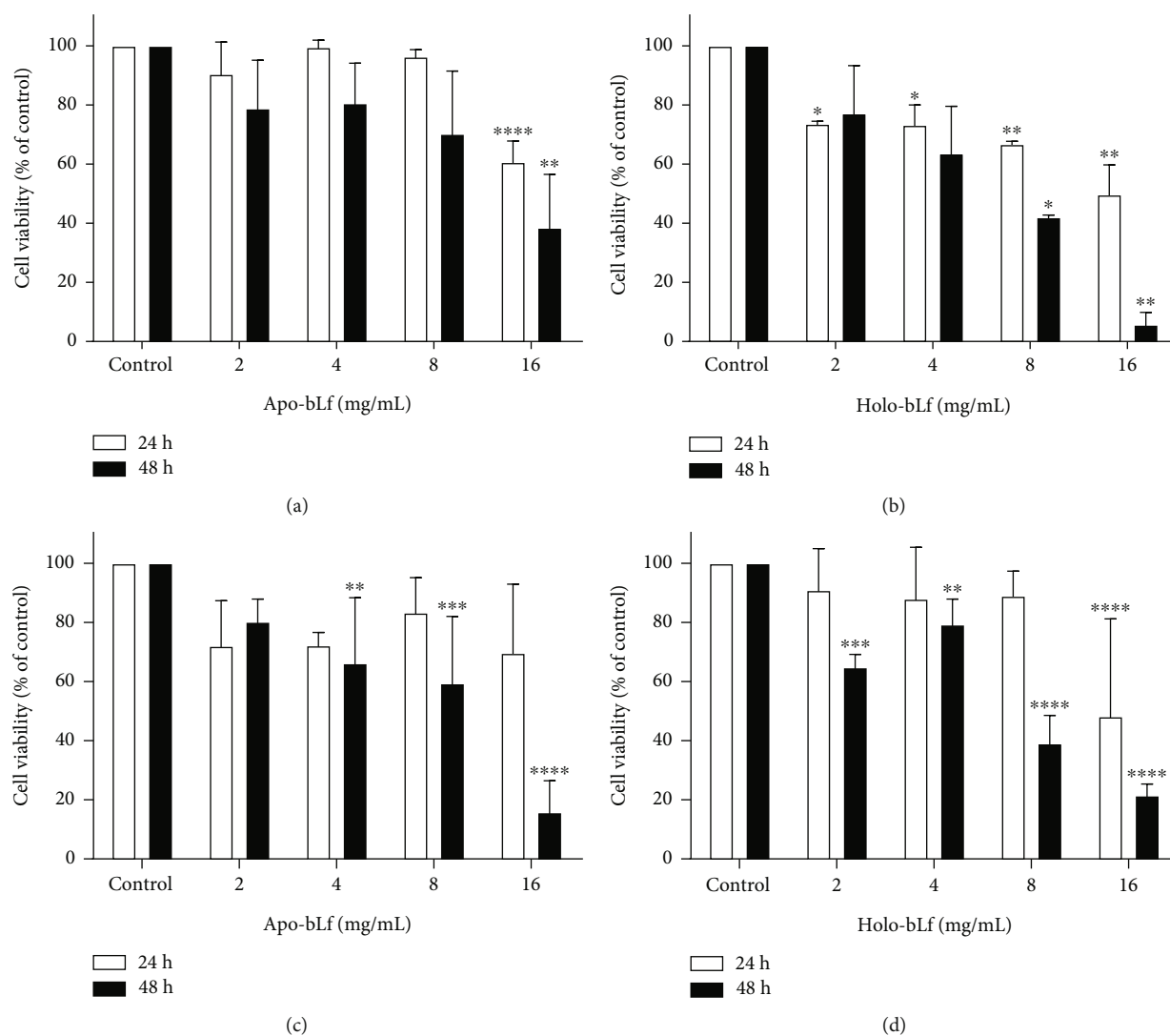


FIGURE 2: bLf induces cell death in the DU-145 cell line. DU-145 cells were treated for 24 h and 48 h with 2, 4, 8, and 16 mg/mL of apo-bLf and holo-bLf. In the negative control, the culture medium was used. Values were plotted as percentages concerning the negative control, which represents 100% of viability. (a) MTT assay and apo-bLf treatment; (b) MTT assay and holo-bLf treatment; (c) trypan blue exclusion and apo-bLf treatment; (d) trypan blue exclusion and holo-bLf treatment. Graphs (a) and (b) represent two separate experiments with replicates. Graphs (c) and (d) represent three separate experiments. The experiment is expressed as mean \pm SD. Significant differences between untreated and treated cells were compared using the one-way ANOVA test, with Bonferroni post hoc test (* $p < 0.05$; ** $p < 0.01$; *** $p < 0.001$; **** $p < 0.0001$).

changes and cell death, we then tested whether apo- and holo-bLf forms were internalized in DU-145 cells. For that, bLf forms were stained with FITC, and the images were obtained after 24 h of bLf treatment (Figure 4).

Using a fluorescence confocal microscope, we observed that FITC-stained apo- and holo-bLf were internalized at both tested concentrations. Moreover, lactoferrin internalization was more efficient in the highest concentration (16 mg/mL) of apo- and holo-bLf.

3.4. bLf Induces Cell Cycle Arrest in DU-145 Cells. We then aimed to evaluate whether the internalized apo- and holo-bLf were able to alter the cell cycle of DU-145 cells. Table 1 demonstrates that treatment with 16 mg/mL of holo-bLf increased 22.9% and 29.4% the percentage of cells

in the G_0/G_1 phase compared to control cells in 24 h and 48 h, respectively. The increase of cells in the G_0/G_1 phase was higher following a 48 h exposure than a 24 h. Apo-bLf treatment did not show any statistical difference in cell cycle distribution compared to control.

3.5. bLf Treatment Induces an Increase in Oxidative Stress and Activates Caspases 3/7 in the DU-145 Cell Line. We further investigated how bLf inhibited cell cycle progression and decreased cell viability. Figure 5 is aimed at verifying possible oxidative stress changes and apoptosis activation induced by bLf in DU-145 cells. Live probes for reactive oxidative species (ROS) and apoptosis, DHE, and caspase 3/7 were used in a High-Content Imaging System to quantify these physiological changes.

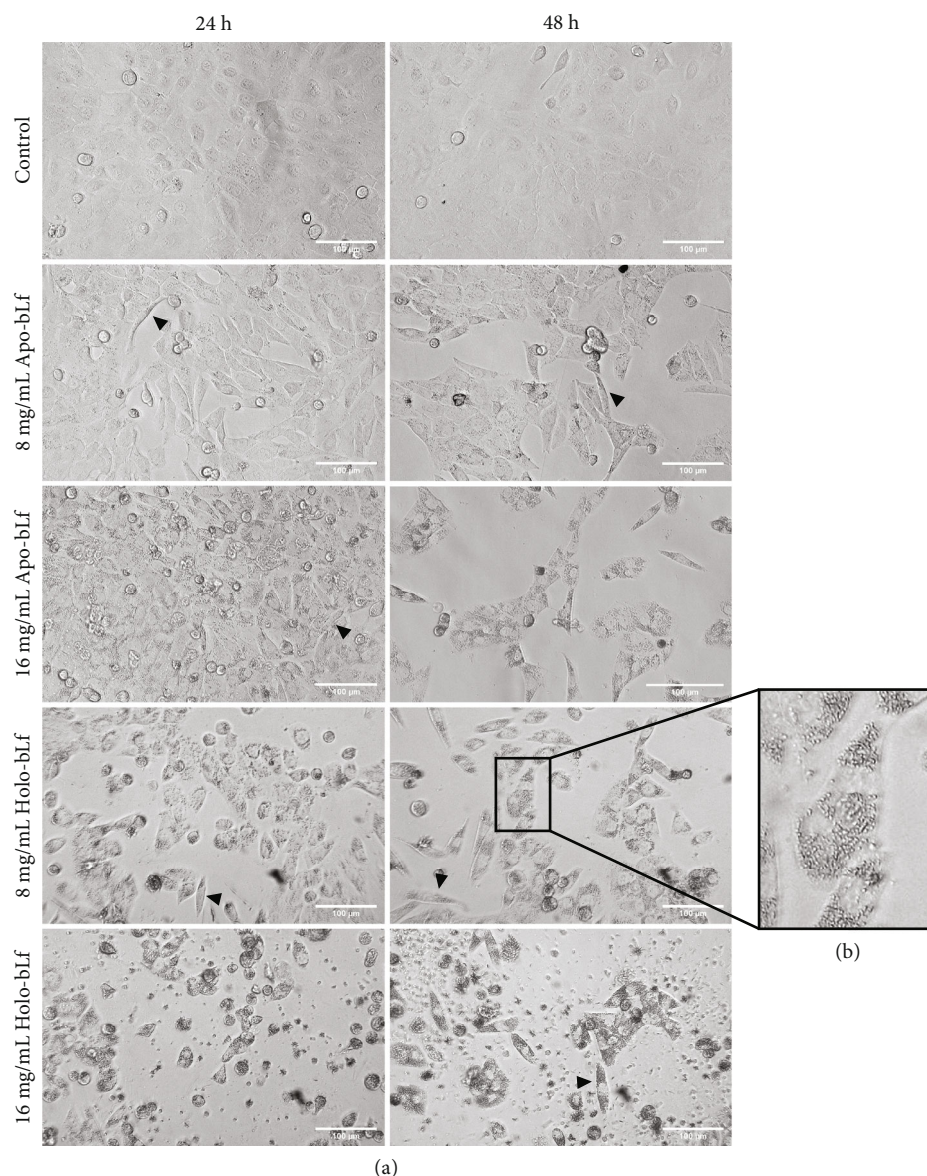


FIGURE 3: bLf causes morphological changes in the DU-145 cell line. To verify the effects of bLf, selected images were taken using an EVOS microscope. (a) DU-145 cells were treated for 24 and 48 h with apo-bLf and holo-bLf at 8 and 16 mg/mL. (b) Zoom in of 8 mg/mL after 48 h treatment showing intracellular granules. The control cell received only a culture medium. The white bars represent a distance of 100 μm . Arrowheads indicate stretched morphology.

Figures 5(a) and (b) show that both apo- and holo-bLf exposure increased DHE labelling when compared to the control. In 24 h, treatment with apo-bLf showed an increase of DHE-positive cells, being 7% with 2 mg/mL ($p < 0.01$), 12% with 4 mg/mL ($p < 0.0001$), 17% with 8 mg/mL ($p < 0.0001$), and 21% with 16 mg/mL ($p < 0.0001$) treatments. Holo-bLf also showed an increase of DHE-positive cells, being 8.5% with 2 mg/mL ($p < 0.01$), 11% with 4 mg/mL ($p < 0.0001$), 16% with 8 mg/mL ($p < 0.0001$), and 23% with 16 mg/mL ($p < 0.0001$) concentrations. After 48 h treatment, only holo-bLf with 16 mg/mL showed statistical difference in relation to control, increasing up to 12% the DHE-positive cells population.

In 24 h and 48 h treatments, we observed a concentration-dependent effect of both bLf forms on increasing DHE

labeling. However, both apo- and holo-bLf structures exhibited higher increases in DHE labeling after 24 h in comparison to 48 h treatment.

On the other hand, the detection of activated caspases 3/7 was higher following a 48 h exposure with bLf than the 24 h experimental group (Figures 5(c) and 5(d)). After 24 h, apo-bLf showed an increase in activated caspases 3/7 labelling on concentrations of 8 mg/mL with 7.3% of positive cells ($p < 0.001$) and 16 mg/mL 10% ($p < 0.0001$) compared to the control group. At the same time of treatment, 24 h, holo-bLf induced caspase 3/7 activation only on the treatment using 16 mg/mL, thus presenting a 16.5% of activated caspase-positive cells.

After a 48 h of bLf treatment, apo-bLf demonstrated a dose-dependent caspase activation, showing the percentage

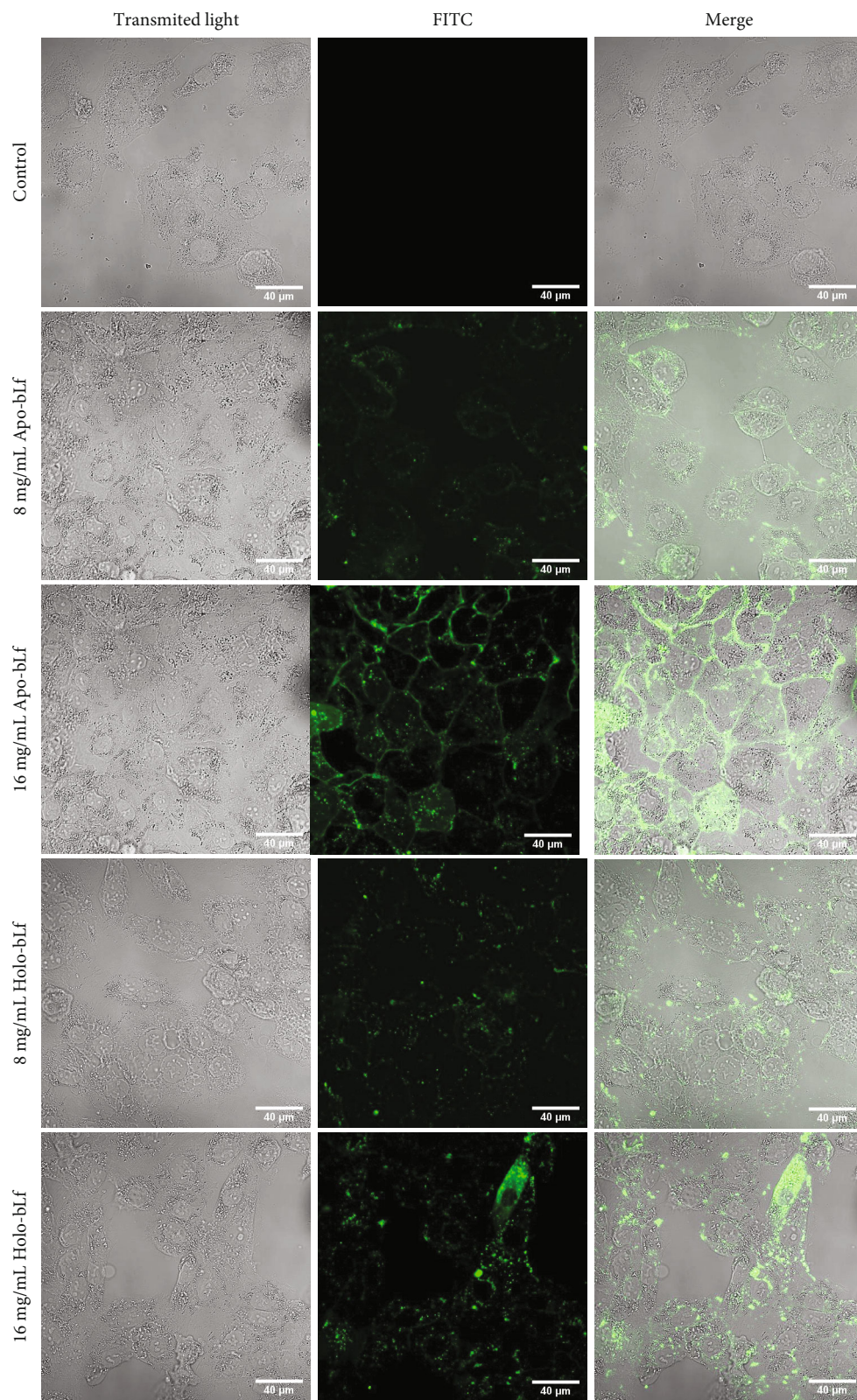


FIGURE 4: bLf internalizes and causes DU-145 cell damage. DU-145 cells were incubated with apo- and holo-bLf labeled with FITC for 24 h at 8 and 16 mg/mL concentrations. The images were obtained using fluorescence confocal microscopy (LSM 510 META Confocal Laser Scanning Microscope) and EC Plan-Neofluar 40x/1.30 Oil DIC M27 (Zeiss Inc.) objective lens. The white bars represent a distance of 40 μm.

TABLE 1: bLf modulates cell cycle of DU-145 cell line. The table below shows the percentage of cells in each cell cycle phase determined by flow cytometry. This table represents three different experiments expressed as mean \pm SD. The one-way ANOVA test compared significant differences between untreated and treated cells with the Bonferroni post hoc test.

	24 h treatment			48 h treatment		
	G ₀ /G ₁ (%)	S (%)	G ₂ /M (%)	G ₀ /G ₁ (%)	S (%)	G ₂ /M (%)
Control	44.1 \pm 3.6	27.5 \pm 5.4	13.9 \pm 0.9	46 \pm 6.9	22.7 \pm 8.8	14.4 \pm 3.6
Apo-bLf 2 mg/mL	45.4 \pm 2.8	22.9 \pm 6.8	13.3 \pm 2.5	54.2 \pm 7.4	17 \pm 7.1	12.4 \pm 3.7
Apo-bLf 4 mg/mL	41.1 \pm 2.2	26.3 \pm 4.5	13.8 \pm 1.1	51.6 \pm 5.4	18.9 \pm 5.2	13.5 \pm 3.6
Apo-bLf 8 mg/mL	42.4 \pm 5.4	23.3 \pm 3.9	14.4 \pm 1.3	53.4 \pm 3.4	18 \pm 7.7	14.3 \pm 4.9
Apo-bLf 16 mg/mL	53.7 \pm 1.4	20.5 \pm 1.2	13.3 \pm 2.4	50.5 \pm 3.7	18.8 \pm 4.9	12.8 \pm 6.1
Holo-bLf 2 mg/mL	46.9 \pm 9.5	24.4 \pm 7.3	15.3 \pm 2.5	56.2 \pm 4.7	18.6 \pm 9.8	15.1 \pm 2.3
Holo-bLf 4 mg/mL	47.1 \pm 6.6	22.3 \pm 5.3	16.4 \pm 3.5	57.2 \pm 3.8	19.3 \pm 9.1	15.4 \pm 2.1
Holo-bLf 8 mg/mL	51.4 \pm 4.3	21.3 \pm 1.4	13.9 \pm 1.9	63.5 \pm 4.5	18 \pm 6.7	12.4 \pm 1.6
Holo-bLf 16 mg/mL	67.0 ^a \pm 11.3	14 \pm 4.7	11.3 \pm 4.1	75.4 ^b \pm 9.9	11.3 \pm 3.8	10.8 \pm 4.2

*Different letters indicate statistical difference compared to control (^a $p < 0.05$; ^b $p < 0.01$).

of activated caspase 3/7 positive cells of 6.3% with 4 mg/mL ($p < 0.01$), 20.5% with 8 mg/mL ($p < 0.0001$), and 34% with 16 mg/mL ($p < 0.0001$). In addition, holo-bLf-treated cells also presented a dose dependent on caspase activation, with 10% with 4 mg/mL ($p < 0.05$), 28% with 8 mg/mL ($p < 0.0001$), and 49% with 16 mg/mL ($p < 0.0001$). At this stage, holo-bLf presented a higher effect on DU-145 caspases 3/7 activation than apo-bLf.

4. Discussion

Prostate cancer significantly challenges the health systems in many parts of the world. Even with a high survival rate when it is circumscribed, metastatic prostate cancer is primarily incurable even after discovering so many types of therapies. Despite all the efforts, prostate cancer is still one of the most frequent and lethal types of cancer. One of the most significant difficulties in reducing mortality is the lack of a broad spectrum of effective therapies against the considerable tumor heterogeneity at genetic and cellular levels, a considerable disease feature. Therefore, studies for the prevention and treatment of cancer are critical and have expanded over the years. There is still a demand for the development of compound effective for the induction of specific cell death [32, 33].

The structure of apo- and holo-bLf and differences in structural stability were investigated by our research group previously. This work showed that the presence of the iron ion in the holo-bLf structure promotes changes in its tertiary structure, when evaluating the tryptophan microenvironments and the interaction with the extrinsic fluorescent probe bis-ANS. In addition, holo-bLf has shown to have greater structural stability against chemical and physical disruptors [34].

Previous studies reported substantial antitumor effects of bLf, explicitly targeting tumor cells with no side effects on nontumorigenic cell lines (normal human intestinal epithelial cells and fibroblast). It has been shown that a semisaturated iron bLf (with 21% iron ions) is an important antitumor compound, as it selectively inhibits PC-3 cell

growth at a concentration of 14 mg/mL. Based on this study, the concentrations used in this work were chosen better to achieve the desired antitumor bLf effect [21, 35].

Even though some studies demonstrated the antitumor bLf activity [17, 21, 35–37], little is known about the possible effects and differences of the two conformational states, holo- and apo-bLf. Therefore, we sought to compare them to better understand these differences in antitumor activity.

To investigate the cytotoxic effects of bLf, we performed an MTT assay and trypan blue exclusion. It was possible to observe that cell viability decreased in a dose- and time-dependent manner when compared to control, and these effects were more intense following holo-bLf exposure (Figure 2).

A previous study on antitumor activity was developed with conjugation of bLf and doxorubicin in prostate cancer cell lines. The conjugation of both molecules proved to be more effective against cancer development by increasing cytotoxicity to cancer cells but presenting lower toxicity to normal cells compared to doxorubicin-treated cells alone [32].

Morphological changes induced by bLf treatment were characterized by an increase in the number of intracellular granules and induction of stretched morphology (Figure 3). Few cells were left in bLf-treated wells to confirm the viability results. Together, these results demonstrate that bLf affects the cell morphology of DU-145 cells compared to the control. Although both apo- and holo-bLf cause similar morphological changes in dose- and time-dependent effects, treatment with holo-bLf showed to be more robust when compared to apo-bLf treatment.

The internalization of apo- and holo-bLf in the DU-145 cell line allowed us to infer that both bLf forms possibly interact with intracellular targets (Figure 4). This type of interaction between DU-145 cells and bLf can be explained because this protein has a positive charge in the N-terminal region that can interact with the negative charge of heparin and glycosaminoglycans present on cell surfaces [30, 38]. In addition, it is already known that lactoferrin can bind to low-density lipoprotein receptors and proteins

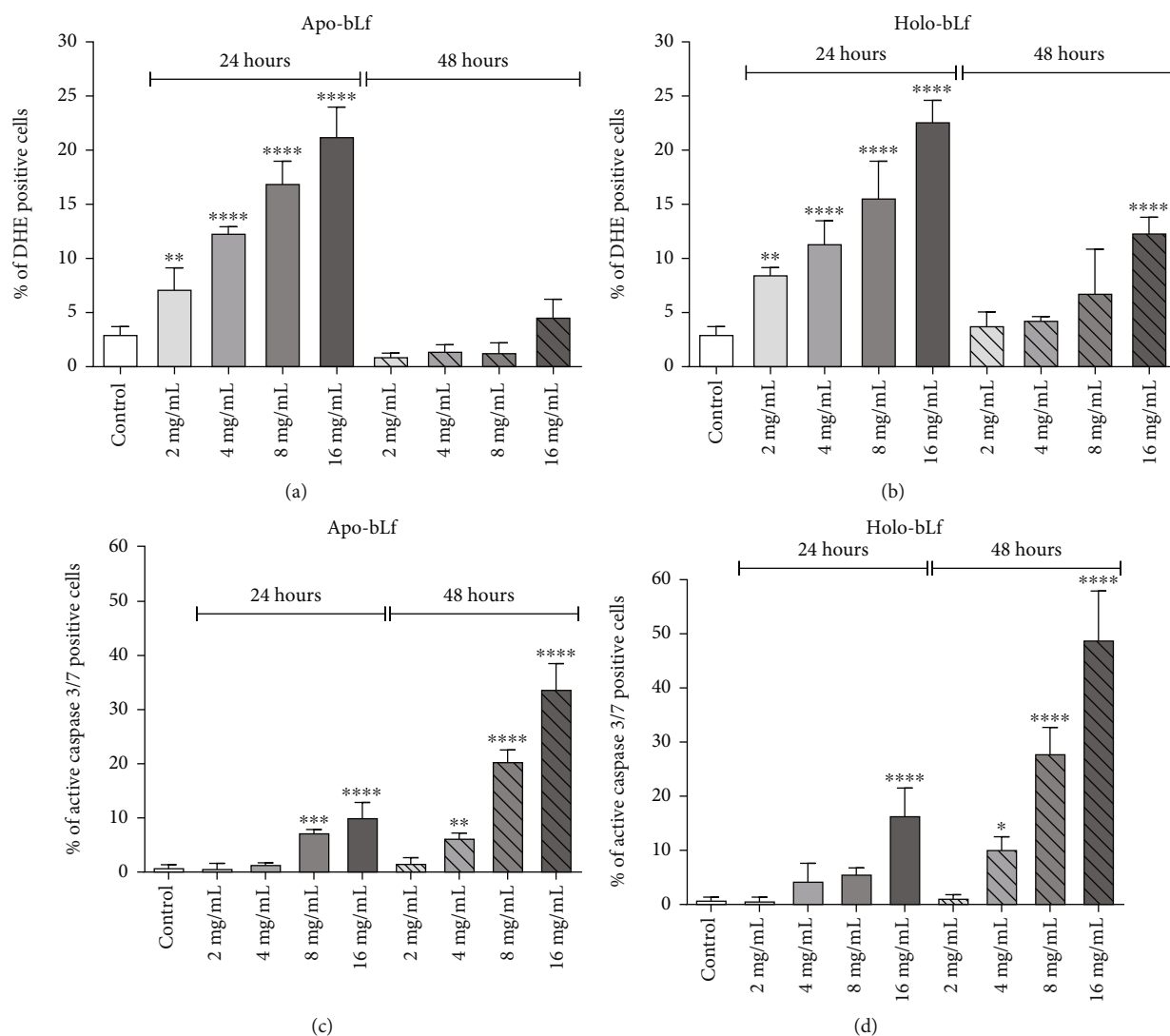


FIGURE 5: DU-145 cell treatment with apo- and holo-bLf induces oxidative stress and activates caspases 3/7. Cells were treated with 2, 4, 8, and 16 mg/mL of apo- and holo-bLf for 24 and 48 h and analyzed in high-throughput system Operetta. (a) Oxidative stress with apo-bLf treatment through dihydroethidium- (DHE-) labeled cell. (b) Oxidative stress with holo-bLf treatment through dihydroethidium- (DHE-) labeled cell. (c) Caspases 3/7 activation with apo-bLf treatment through CellEvent Caspase 3/7 Green Detection Reagent. (d) Caspases 3/7 activation with holo-bLf treatment through CellEvent Caspase 3/7 Green Detection Reagent. These graphics represent one distinct experiment with replicates. The experiment is expressed as mean \pm SD. Significant differences between untreated and treated cells were compared by the one-way ANOVA test, with Bonferroni post hoc test (* $p < 0.05$; ** $p < 0.01$; *** $p < 0.001$; **** $p < 0.0001$).

related to the low-density lipoprotein receptor [38]. Another way of cellular bLf internalization that has been highly characterized is facilitated by receptor-mediated endocytosis, and then, bLf enters the endo-lysosome [32, 39, 40].

Cancer diseases characteristically induce alterations of normal growth signaling pathways. Tumor cells present a growth advantage since the regulators that govern the progression of the G_1 phase of the cell cycle are natural oncogenesis targets. Therefore, analysis of the cell cycle progression has been pointed out as an essential tool for identifying new antitumor treatments. A decrease in cell division can inhibit tumor growth, thus inducing a delay in cancer development. Many studies that aim to propose antitumor remedies observed cell arrest in the G_0/G_1 phase and other results [41–43].

During the present work, we also quantified the percentage of cells at different cell cycle stages upon bLf administration (Table 1). In our culture conditions, most DU-145 cell lines showed to be at the G_0/G_1 phase, which accounts for $\sim 45\%$ of cells. The administration of apo-bLf does not modulate the DU-145 cell cycle on all concentrations and treatment times analyzed, although increasing G_0/G_1 population was observed upon a 16 mg/mL treatment. In turn, holo-bLf showed a dependent concentration increase in cells at G_0/G_1 , which was even higher than the observed with apo-bLf exposure, which accounts for a $\sim 75\%$ of cells in a 16 mg/mL, thus showing that holo-bLf induces cell cycle arrest at the G_0/G_1 phase.

Previous studies showed that bLf induces cell cycle arrest at the G_0/G_1 phase in highly metastatic oral mucosa and

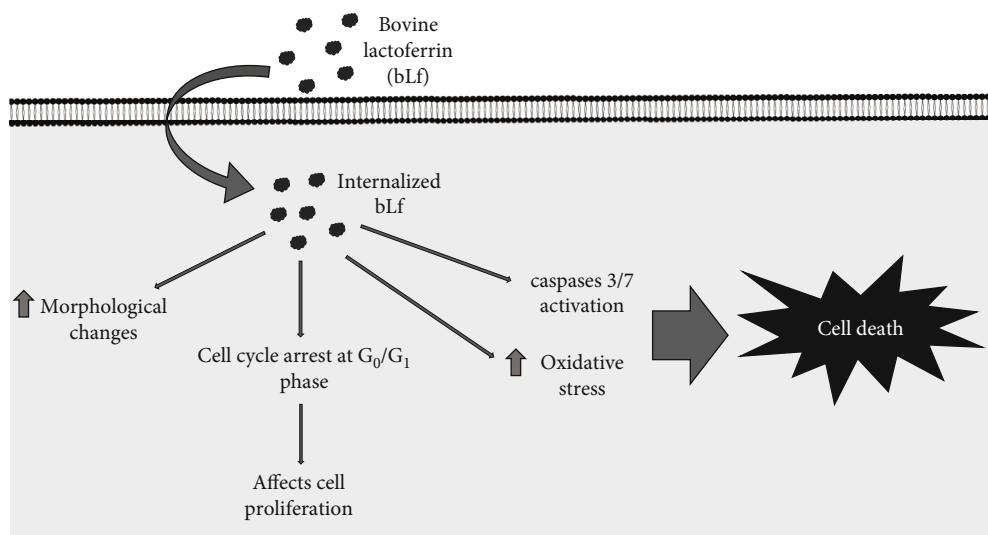


FIGURE 6: General scheme of the bLf effects on DU-145 cells. Diagram indicates internalization of bLf (apo- and holo-), increased oxidative stress, induction of morphological changes, apoptosis, and cell cycle arrest in the G₀/G₁ phase.

breast cancer cells [44, 45]. Our preliminary results corroborate previous findings described in the literature concerning the action of bLf and suggest that this protein may affect the cell cycle of cancer cells.

Detection of oxidative stress was carried out using DHE, a fluorescent probe used to detect ROS, as it undergoes a nonspecific oxidation process [46]. Our results (Figure 5) showed that bLf treatment increased oxidative stress levels in DU-145 cells in 24 h. This could be related to oxidative stress-induced cancer cell death. These data are in accordance with other published data that also showed increased ROS levels in less than 24 h upon Lf treatment in cancer cell lines [47, 48]. However, unlike most published data, we decided to perform ROS production analysis up to 48 h post bLf treatment. Although there is a dose-dependent increase in ROS production after a 24 h of bLf treatment, ROS levels at 48 h are smaller than at 24 h. Those data suggest that the ROS production induced by bLf could be transitory and time-dependent.

This difference could be explained, at least partially, because of bLf availability. In this context, cells could consume bLf or degrade in medium at the initial, thus supporting ROS production at 24 h but not at 48 h. Moreover, due to the chronology of the events, ROS detected in 24 h may be the inducer of cell death observed in 48 h. Therefore, those affected by bLf died. In holo-bLf-treated cells, lower levels of ROS in 48 h than 24 h were detected but higher than apo-bLf at the same time. Unpublished results from our group showed that holo-bLf presented more excellent structural stability than apo-bLf, which could be why we can still see the effect of this protein even after 48 h of treatment.

ROS plays an important role in cancer and is usually associated with promoting protumorigenic signaling, thus facilitating cancer cell proliferation, survival, and adaptation to hypoxia. Nevertheless, ROS can also promote antitumorigenic signaling and trigger oxidative stress-induced cancer cell death. Compared with normal cells, cancer cells elevated

ROS levels, thus altering the environment, making them more vulnerable to ROS-manipulation therapies. Disturbance in ROS levels changes cellular redox balance leading to oxidative stress, damage to mitochondria, and consequent apoptosis induction [49]. This may destroy cancer cells while sparing normal cells [46]. For instance, lanperisone, an identified compound, was able to act as a selective killer of Kras-mutant cancer cells that increased the steady-state levels of ROS [50]. As in our work, an article shows that apo-bLf treatment induces ROS production and depletion of cellular GSH on HeLa cells [48].

Caspases are aspartate-specific cysteine proteases that play essential roles in two main pathways that mediate apoptosis, the extrinsic/death and intrinsic-/mitochondria-dependent pathways [51–53]. Apoptosis or programmed cell death is a fundamental process for both health and disease that plays a vital role in carcinogenesis, immune system, embryonic development, maturation, and cytotoxic effector function [54]. Apoptosis promotion is one of the proposed mechanisms against cancer [35, 55].

We have shown evidence that bLf exhibited proapoptotic activities. Caspase 3/7 labeling was induced by apo-bLf and holo-bLf administration (Figure 5). CellEvent™ Caspase-3/7 assay used in this study is a substrate for activated caspases 3/7, so it is only fluorescent when caspases 3/7 are activated [56]. These results suggest that one of the mechanisms by which bLf engages their antitumor effects in prostate cancer is promoting apoptosis, thus corroborating with previous discoveries and cell viability experiments [35, 57].

Most of our results indicate that holo-bLf presented more antitumor effects when compared to apo-bLf. This was expected due to the conformation differences between apo- and holo-bLf [58]. The iron bond induces the structure to a more closed form; apo- has a more open and, consequently, more dynamic system than holo-. Thus, iron increases the stability of the protein since its structure is more closed and less susceptible to denaturation and proteolysis [4].

Thus, we can highlight the importance of using the holo-form of bLf in this work, since most papers use only the apo-form. Our results show that iron binding leads to an increase in the antitumor potential of this protein. New findings can expand the mechanism of action and protein expression involved in bLf effect. The results are relevant, as they will not only help research but will also contribute to a possible treatment for prostate cancer in the future. bLf has been shown to be very efficient against tumor cells *in vitro* studies, being an emerging biopharmaceutical [17, 21, 35–37]. Hence, some factors must be considered for its future use, as it may be a noninvasive and possibly preventive alternative for tumors. In addition, its low cost, mainly for public health systems, combined with its probable absence of side effects comparing to classic chemotherapy, makes bLf a promising candidate for antitumor.

Our results indicate that bLf may present antitumor activities by activating signaling pathways including, cell cycle arrest in the G₀/G₁ phase, apoptosis, and increase of ROS (Figure 6), thus corroborating with previous findings in the literature [35]. More studies on the apo- and holo-bLf mechanisms in cancer inhibition are needed.

5. Conclusions

In conclusion, the data presented in this work showed that treatments using bovine lactoferrin (apo- and holo-bLf forms) gave an antitumor effect in the prostate cancer cell line (DU-145). The holo-bLf form seems to be the substance with the highest potential for *in vivo* studies, thus offering a series of views on the use of these compounds in the prevention and treatment of prostate cancer, probably due to the iron binding. However, a more detailed investigation is needed to address better this issue and other cellular mechanisms activated by lactoferrin.

Data Availability

The data used to support the findings in this paper are available from the corresponding author upon request.

Conflicts of Interest

The authors declare that there is no conflict of interest regarding the publication of this paper.

Acknowledgments

This study is dedicated to the memory of Antônio Flavio da Rocha, beloved grandfather; few understand the importance of academic education as he did. Special thanks are due to Dra. Tais H. Kasai-Brunswick from the National Center of Structural Biology and Bioimaging-CENABIO/UFRJ, Dra. Andréa Cheble de Oliveira from UFRJ, and Dr. Stevens Rehen from IDOR (D'Or Institute for Research and Education) for all their support. We are grateful to the Multi-User Research Lab 01 (Laboratório de Pesquisa Multiusuário 01 (LPM-01)) of the Federal University of the State of Rio de Janeiro (UNIRIO) for using its facilities and the 15th Inter-

national Conference on Lactoferrin Structure, Function and Applications for the scientific dissemination. This work was supported in part by grants from Fundação Carlos Chagas Filho de Amparo à Pesquisa do Estado do Rio de Janeiro (FAPERJ) to RBG and AJT (grant numbers 211.039/2019 and 210.145/2016) and Coordenação de Aperfeiçoamento de Pessoal de Nível Superior (CAPES) to VPR.

References

- [1] H. Wakabayashi, K. Yamauchi, and M. Takase, "Lactoferrin research, technology and applications," *International Dairy Journal*, vol. 16, no. 11, pp. 1241–1251, 2006.
- [2] A. M. Di Biase, A. Pietrantonio, A. Tinari et al., "Heparin-interacting sites of bovine lactoferrin are involved in anti-adenovirus activity," *Journal of Medical Virology*, vol. 69, no. 4, pp. 495–502, 2003.
- [3] H. Bokkhim, N. Bansal, L. Grndahl, and B. Bhandari, "Physico-chemical properties of different forms of bovine lactoferrin," *Food Chemistry*, vol. 141, no. 3, pp. 3007–3013, 2013.
- [4] E. N. Baker and H. M. Baker, "A structural framework for understanding the multifunctional character of lactoferrin," *Biochimie*, vol. 91, no. 1, pp. 3–10, 2009.
- [5] S. A. Moore, B. F. Anderson, C. R. Groom, M. Haridas, and E. N. Baker, "Three-dimensional structure of diferric bovine lactoferrin at 2.8 Å resolution," *Journal of Molecular Biology*, vol. 274, no. 2, pp. 222–236, 1997.
- [6] J. L. Gifford, H. N. Hunter, and H. J. Vogel, "Lactoferricin," *Cellular and Molecular Life Sciences*, vol. 62, no. 22, pp. 2588–2598, 2005.
- [7] H. Sung, J. Ferlay, R. L. Siegel et al., "Global cancer statistics 2020: GLOBOCAN estimates of incidence and mortality worldwide for 36 cancers in 185 countries," *CA: a Cancer Journal for Clinicians*, vol. 71, no. 3, pp. 209–249, 2021.
- [8] J. Ferlay, M. Ervik, F. Lam et al., *Global cancer observatory: cancer today*. International Agency for Research on Cancer, WHO (World Health Organization), Lyon, France, 2020.
- [9] R. L. Siegel, K. D. Miller, H. E. Fuchs, and A. Jemal, "Cancer statistics, 2022," *CA: a Cancer Journal for Clinicians*, vol. 72, no. 1, pp. 7–33, 2022.
- [10] J. A. Gibbons, J. R. Kanwar, and R. K. Kanwar, "Iron-free and iron-saturated bovine lactoferrin inhibit survivin expression and differentially modulate apoptosis in breast cancer," *BMC Cancer*, vol. 15, no. 1, pp. 1–16, 2015.
- [11] H. Tsuda, K. Sekine, N. Takasuka, H. Toriyama-Baba, and M. Iigo, "Prevention of colon carcinogenesis and carcinoma metastasis by orally administered bovine lactoferrin in animals," *BioFactors*, vol. 12, no. 1-4, pp. 83–88, 2000.
- [12] C. Masuda, H. Wanibuchi, K. Sekine et al., "Chemopreventive effects of bovine lactoferrin on N-butyl-N-(4-hydroxybutyl)-nitrosamine-induced rat bladder carcinogenesis," *Japanese Journal of Cancer Research*, vol. 91, no. 6, pp. 582–588, 2000.
- [13] Y. Yamada, R. Sato, S. Kobayashi et al., "The antiproliferative effect of bovine lactoferrin on canine mammary gland tumor cells," *The Journal of Veterinary Medical Science*, vol. 70, no. 5, pp. 443–448, 2008.
- [14] Y. Ushida, K. Sekine, T. Kuhara et al., "Possible chemopreventive effects of bovine lactoferrin on esophagus and lung carcinogenesis in the rat," *Japanese Journal of Cancer Research*, vol. 90, no. 3, pp. 262–267, 1999.

- [15] M. Iigo, T. Kuhara, Y. Ushida, K. Sekine, M. A. Moore, and H. Tsuda, "Inhibitory effects of bovine lactoferrin on colon carcinoma 26 lung metastasis in mice," *Clinical & Experimental Metastasis*, vol. 17, no. 1, pp. 43–49, 1999.
- [16] J. A. Gibbons, R. K. Kanwar, and J. R. Kanwar, "Lactoferrin and cancer in different cancer models," *Frontiers in Bioscience - Scholar*, vol. S3, no. 3, pp. 1080–1088, 2011.
- [17] X. X. Xu, H. R. Jiang, H. B. Li, T. N. Zhang, Q. Zhou, and N. Liu, "Apoptosis of stomach cancer cell SGC-7901 and regulation of Akt signaling way induced by bovine lactoferrin," *Journal of Dairy Science*, vol. 93, no. 6, pp. 2344–2350, 2010.
- [18] L. Rodrigues, J. Teixeira, F. Schmitt, M. Paulsson, and H. L. Månsson, "Lactoferrin and cancer disease prevention," *Critical Reviews in Food Science and Nutrition*, vol. 49, no. 3, pp. 203–217, 2009.
- [19] C. Freiburghaus, B. Janicke, H. Lindmark-Månsson, S. M. Oredsson, and M. A. Paulsson, "Lactoferricin treatment decreases the rate of cell proliferation of a human colon cancer cell line," *Journal of Dairy Science*, vol. 92, no. 6, pp. 2477–2484, 2009.
- [20] NIH National Cancer Institute Cancer Facts & Figures 2020, "American cancer society," *Cancer Journal for Clinicians*, 2020.
- [21] J. P. Guedes, C. S. Pereira, L. R. Rodrigues, and M. Côrte-Real, "Bovine milk lactoferrin selectively kills highly metastatic prostate cancer PC-3 and osteosarcoma MG-63 cells *In Vitro*," *Frontiers in Oncology*, vol. 8, pp. 1–12, 2018.
- [22] T. V. Zadovnyi, N. Y. Lukianova, T. V. Borikun, and V. F. Chekhun, "Effects of exogenous lactoferrin on phenotypic profile and invasiveness of human prostate cancer cells (DU-145 and LNCaP) *in vitro*," *Experimental Oncology*, vol. 40, no. 3, pp. 184–189, 2018.
- [23] S. A. Ross and C. D. Davis, "MicroRNA, nutrition, and cancer prevention," *Advances in Nutrition*, vol. 2, no. 6, pp. 472–485, 2011.
- [24] H. Shimazaki, "On the occurrence of silician magnetites," *Resource Geology*, vol. 48, no. 1, pp. 23–29, 1998.
- [25] C. B. Denani, A. Real-Hohn, C. A. M. de Carvalho, A. M. O. Gomes, and R. B. Gonçalves, "Lactoferrin affects rhinovirus B-14 entry into H1-HeLa cells," *Archives of Virology*, vol. 166, no. 4, pp. 1203–1211, 2021.
- [26] M. L. Groves, "The isolation of a red protein from Milk2," *Journal of the American Chemical Society*, vol. 82, no. 13, pp. 3345–3350, 1960.
- [27] P. H. C. Van Berkel, M. E. J. Geerts, H. A. Van Veen et al., "Glycosylated and unglycosylated human lactoferrins both bind iron and show identical affinities towards human lysozyme and bacterial lipopolysaccharide, but differ in their susceptibilities towards tryptic proteolysis," *The Biochemical Journal*, vol. 312, no. 1, pp. 107–114, 1995.
- [28] T. Mosmann, "Rapid colorimetric assay for cellular growth and survival: application to proliferation and cytotoxicity assays," *Journal of Immunological Methods*, vol. 65, no. 1-2, pp. 55–63, 1983.
- [29] R. Khosravi-Far, R. A. Lockshin, and Z. Zakeri, "Programmed cell death: general principles for studying cell," in *Methods*, Academic Press/Elsevier, San Diego, California, 2008.
- [30] C. A. M. Carvalho, I. P. Sousa, J. L. Silva, A. C. Oliveira, R. B. Gonçalves, and A. M. O. Gomes, "Inhibition of Mayaro virus infection by bovine lactoferrin," *Virology*, vol. 452-453, pp. 297–302, 2014.
- [31] L. L. Vindelov, "Flow microfluorometric analysis of nuclear DNA in cells from solid tumors and cell suspensions. A new method for rapid isolation and straining of nuclei," *Virchows Archiv B Cell Pathology*, vol. 24, no. 1, pp. 227–242, 1977.
- [32] J. S. Shankaranarayanan, J. R. Kanwar, A. J. A. Al-Juhaishi, and R. K. Kanwar, "Doxorubicin conjugated to immunomodulatory anticancer Lactoferrin displays improved cytotoxicity overcoming prostate cancer chemo resistance and inhibits tumour development in TRAMP mice," *Scientific Reports*, vol. 6, pp. 1–16, 2016.
- [33] G. Wang, D. Zhao, D. J. Spring, and R. A. Depinho, "Genetics and biology of prostate cancer," *Genes & Development*, vol. 32, no. 17-18, pp. 1105–1140, 2018.
- [34] C. A. Barros, D. Sanches, C. A. M. Carvalho et al., "Influence of iron binding in the structural stability and cellular internalization of bovine lactoferrin," *Heliyon*, vol. 7, no. 9, 2021.
- [35] R. Jiang and B. Lönnnerdal, "Bovine lactoferrin and lactoferricin exert antitumor activities on human colorectal cancer cells (HT-29) by activating various signaling pathways," *Biochemistry and Cell Biology*, vol. 95, no. 1, pp. 99–109, 2017.
- [36] D. A. Ramírez-Sánchez, I. G. Arredondo-Beltrán, A. Canizalez-Roman et al., "Bovine lactoferrin and lactoferrin peptides affect endometrial and cervical cancer cell lines," *Biochemistry and Cell Biology*, vol. 99, no. 1, pp. 149–158, 2021.
- [37] A. Najmafshar, M. Rostami, J. Varshosaz, D. Norouzian, and S. Z. A. Samsam Shariat, "Enhanced antitumor activity of bovine lactoferrin through immobilization onto functionalized nano graphene oxide: an *in vitro/in vivo* study," *Drug Delivery*, vol. 27, no. 1, pp. 1236–1247, 2020.
- [38] J. H. Andersen, H. Jenssen, K. Sandvik, and T. J. Gutteberg, "Anti-HSV activity of lactoferrin and lactoferricin is dependent on the presence of heparan sulphate at the cell surface," *Journal of Medical Virology*, vol. 74, no. 2, pp. 262–271, 2004.
- [39] R. M. Samarasinghe, R. K. Kanwar, and J. R. Kanwar, "The effect of oral administration of iron saturated-bovine lactoferrin encapsulated chitosan-nanocarriers on osteoarthritis," *Biomaterials*, vol. 35, no. 26, pp. 7522–7534, 2014.
- [40] R. K. Kanwar and J. R. Kanwar, "Immunomodulatory lactoferrin in the regulation of apoptosis modulatory proteins in cancer," *Protein and Peptide Letters*, vol. 20, no. 4, pp. 450–458, 2013.
- [41] J. A. Diehl, "Cycling to cancer with cyclin D1," *Cancer Biology & Therapy*, vol. 1, no. 3, pp. 226–231, 2002.
- [42] C. Yu, H. Cao, X. He et al., "Cyclin-dependent kinase inhibitor 3 (CDKN3) plays a critical role in prostate cancer via regulating cell cycle and DNA replication signaling," *Biomedicine & Pharmacotherapy*, vol. 96, pp. 1109–1118, 2017.
- [43] G. Albayrak, E. Konac, A. U. Dikmen, and C. Y. Bilen, "Memantine induces apoptosis and inhibits cell cycle progression in LNCaP prostate cancer cells," *Human & Experimental Toxicology*, vol. 37, no. 9, pp. 953–958, 2018.
- [44] C. Chea, M. Miyauchi, T. Inubushi et al., "Molecular mechanism of inhibitory effects of bovine lactoferrin on the growth of oral squamous cell carcinoma," *PLoS One*, vol. 13, no. 1, article e0191683, 2018.
- [45] Y. Zhang, A. Nicolau, C. F. Lima, and L. R. Rodrigues, "Bovine lactoferrin induces cell cycle arrest and inhibits mTOR signaling in breast cancer cells," *Nutrition and Cancer*, vol. 66, no. 8, pp. 1371–1385, 2014.
- [46] C. R. Reczek and N. S. Chandel, "The two faces of reactive oxygen species in cancer," *Annual Review of Cancer Biology*, vol. 1, no. 1, pp. 79–98, 2017.

- [47] I. V. Zalutskii, N. Y. Lukianova, D. M. Storchai et al., "Influence of exogenous lactoferrin on the oxidant/antioxidant balance and molecular profile of hormone receptor-positive and -negative human breast cancer cells in vitro," *Experimental Oncology*, vol. 39, no. 2, pp. 106–111, 2017.
- [48] C. Luzi, F. Brisdelli, R. Iorio et al., "Apoptotic effects of bovine apo-lactoferrin on HeLa tumor cells," *Cell Biochemistry and Function*, vol. 35, no. 1, pp. 33–41, 2017.
- [49] B. P. George and H. Abrahamse, "Increased oxidative stress induced by Rubus bioactive compounds induce apoptotic cell death in human breast cancer cells," *Oxidative Medicine and Cellular Longevity*, vol. 2019, Article ID 6797921, 18 pages, 2019.
- [50] A. T. Shaw, M. M. Winslow, M. Magendantz et al., "Selective killing of K-ras mutant cancer cells by small molecule inducers of oxidative stress," *Proceedings of the National Academy of Sciences of the United States of America*, vol. 108, no. 21, pp. 8773–8778, 2011.
- [51] A. Ashkenazi and V. M. Dixit, "Death receptors: signaling and modulation," *Science*, vol. 281, no. 5381, pp. 1305–1308, 1998.
- [52] D. R. Green and J. C. Reed, "Mitochondria and apoptosis," *Science*, vol. 281, no. 5381, pp. 1309–1312, 1998.
- [53] W. C. Earnshaw, L. M. Martins, and S. H. Kaufmann, "Mammalian caspases: structure, activation, substrates, and functions during apoptosis," *Annual Review of Biochemistry*, vol. 68, no. 1, pp. 383–424, 1999.
- [54] T. A. Fleisher, "Apoptosis," *Immunology*, vol. 78, no. 3, pp. 245–250, 1997.
- [55] D. Hanahan and R. A. Weinberg, "Hallmarks of cancer: the next generation," *Cell*, vol. 144, no. 5, pp. 646–674, 2011.
- [56] B. S. Mandavilli, M. Yan, and S. Clarke, "Cell-based high content analysis of cell proliferation and apoptosis," *Methods in Molecular Biology*, vol. 1683, pp. 47–57, 2018.
- [57] W. R. Pan, P. W. Chen, Y. L. S. Chen, H. C. Hsu, C. C. Lin, and W. J. Chen, "Bovine lactoferricin B induces apoptosis of human gastric cancer cell line AGS by inhibition of autophagy at a late stage," *Journal of Dairy Science*, vol. 96, no. 12, pp. 7511–7520, 2013.
- [58] T. B. Baker, M. E. Piper, D. E. McCarthy, M. R. Majeskie, and M. C. Fiore, "Addiction motivation reformulated: an affective processing model of negative reinforcement," *Psychological Review*, vol. 111, no. 1, pp. 33–51, 2004.

Research Article

Hepatoprotective Mechanism of Ginsenoside Rg1 against Alcoholic Liver Damage Based on Gut Microbiota and Network Pharmacology

Ting Xia,¹ Bin Fang,¹ Chaoyan Kang,¹ Yuxuan Zhao,¹ Xiao Qiang,¹ Xiaodong Zhang,¹ Yiming Wang,¹ Tian Zhong,² Jianbo Xiao ^{3,4} and Min Wang ¹

¹State Key Laboratory of Food Nutrition and Safety, Key Laboratory of Industrial Fermentation Microbiology, College of Biotechnology, Tianjin University of Science and Technology, Tianjin 300457, China

²Faculty of Medicine, Macau University of Science and Technology, Taipa, Macau 999078, China

³Universidad de Vigo, Department of Analytical and Food Chemistry, Faculty of Sciences, 32004 Ourense, Spain

⁴International Research Center for Food Nutrition and Safety, Jiangsu University, Zhenjiang 212013, China

Correspondence should be addressed to Jianbo Xiao; jianboxiao@yahoo.com and Min Wang; minw@tust.edu.cn

Received 21 May 2022; Revised 30 June 2022; Accepted 18 July 2022; Published 23 August 2022

Academic Editor: Felipe L. de Oliveira

Copyright © 2022 Ting Xia et al. This is an open access article distributed under the Creative Commons Attribution License, which permits unrestricted use, distribution, and reproduction in any medium, provided the original work is properly cited.

Alcoholic liver disease (ALD) is a major public health problem worldwide, which needs to be effective prevention. Ginsenoside Rg1 (GRg1), a bioactive ingredient extracted from ginseng, has benefit effects on health. In this study, 11 potential targets of GRg1 against ALD were firstly obtained by network pharmacology. KEGG pathway enrichment showed that GRg1-target-ALD was closely related to Toll-like receptor (TLR) and nuclear factor-kappa B (NF- κ B) signaling pathways. In addition, GRg1 decreased antioxidant levels and increased oxidative levels in alcohol-treated mice, which alleviated oxidative stress-induced hepatic damage. GRg1 enhanced intestinal barrier function *via* upregulating the levels of tight junction protein and immunoglobulin A. GRg1 also reduced alcohol-induced inflammation by suppressing TLR4/NF- κ B pathway, which was consistent with the prediction of network targets. Moreover, GRg1 altered GM population, and *Verrucomicrobia*, *Bacteroidetes*, *Akkermansia*, *Bacteroides*, *Lachnospiraceae_NK4A136_group*, and *Alloprevotella* played positive association with intestinal barrier indicators and negative correlation with hepatic inflammation biomarkers. The results suggest that GRg1 administration might be a promising strategy for protection of alcohol-induced liver damage.

1. Introduction

Alcoholic liver disease (ALD) is an ubiquitous health burden around the world, which causes progression of liver damage [1, 2]. It has been demonstrated that oxidative stress is a major pathogenesis of alcohol-induced liver damage, which is closely related to the development of ALD [3]. Alcohol administration induces reactive oxygen species (ROS) generation and oxidative products, which leads to the destruction of antioxidative system [4]. Previous study has reported that excess ROS induced by alcohol can activate Kupffer cells and produce proinflammatory factors [5].

Emerging studies have proved that the alteration of gut microbiota (GM) is a causative factor in ALD [6, 7]. Mean-

while, excessive alcohol intake destroys the integrity of intestinal barrier and promotes lipopolysaccharides (LPS) releasing from intestine to liver through blood circulation [8]. Toll-like receptor 4 (TLR4) is activated by LPS in Kupffer cells and induces the expression of p-nuclear factor-kappa B (p-NF- κ B). TLR4/nuclear factor-kappa B (NF- κ B) pathway results in the release of inflammatory factors, which subsequently contributes to liver damage [9]. Therefore, alteration of GM and inhibition of inflammatory could be an effective strategy to prevent alcohol-induced liver injury.

Ginsenosides are bioactive compounds extracted from *Panax ginseng* C.A. Meyer, which have many pharmacological properties including anti-inflammation, antioxidant activity, and anticancer [10, 11]. Among these ginsenosides,

ginsenoside Rg1 (GRg1) accounts for about 0.22% in sun-dried ginseng and *Radix ginseng rubra*, which is a major bioactive component [12]. Recent studies reported that GRg1 displayed remarkable antioxidant activity and exhibited protection of liver injury [13, 14]. However, the effect and mechanism of GRg1 on GM in mice with alcoholic liver damage remain unclear.

Recently, network pharmacology is used to estimate the molecular mechanism of drugs from multiple dimensions. It reveals the potentially complex relationship between drugs and their targets according to “disease-target-ingredient-drug” network model [15]. This method has been successfully used in the research of Chinese herbal medicine, especially in seeking of bioactive ingredients and their therapeutic targets [16]. Therefore, network pharmacology can provide a valid strategy to further explore the potential targets of GRg1 to prevent ALD.

In this study, the potential ALD targets of GRg1 were predicted through network pharmacology firstly. The effects of GRg1 on ethanol-induced liver injury were investigated *in vivo*. The potential targeted pathway was explored to verify the analysis of network pharmacology. Moreover, GM composition and gut barrier were explored in the intestine. GM interplayed with host indexes was estimated in ethanol-treated mice. The findings would provide an alternative agent from ginseng for ALD prevention.

2. Materials and Methods

2.1. Materials. GRg1 (purity $\geq 98\%$) was obtained from Beijing Beina Chuanglian Biotechnology Technology Research Institute (Beijing, China), which was dissolved with distilled water. The structure of GRg1 is shown in Figure 1. Silymarin was purchased from Madaus AG. (Cologne, Germany), which was dissolved with olive oil. The primary antibodies against TLR4 (Santa Cruz Biotechnology, Santa Cruz, CA, USA) and p-NF- κ B p65 (Abcam, Cambridge, UK), and the second antibody (Cell Signaling Technology, Danvers, MA, USA) was purchased.

2.2. Network Pharmacology Analysis. The information of bioactive ingredients of ginseng was obtained from Traditional Chinese Medicine Systems Pharmacology Database (TCMSP). The corresponding targets of these ingredients were screened through HERB (<http://herb.ac.cn/>), TCMSP, and literature retrieval. In addition, ALD as the key word was screened in the GeneCards databases (<https://www.genecards.org/>). The targets related to ALD were analyzed according to relevance score ≥ 40 . All targets were converted into their gene names by Uniport database.

The targets of bioactive components in ginseng associated with ALD were determined by R x64 3.6.3 and represented in Venn diagrams. The network analysis of herb-ingredient-target-disease was visualized by Cytoscape 3.6.1. The shared targets were upload to STRING for analysis of protein-protein interaction (PPI), and then, protein type was set as Homo Sapiens. The data were saved and enriched by R x64 3.6.3. Meanwhile, the clusterProfiler package in R

x64 3.6.3 was used to label and visualize KEGG pathway, to predict the pathway expression of these targets.

2.3. Design of Animal Experiments. Forty male ICR mice (6 weeks old, 18–22 g) were provided by Beijing Vital River Laboratory Animal Technology Co., Ltd. (Beijing, China). The pathogen-free environment for raising experimental mice was provided by the Animal Committee of Nankai University (SYXK2019-0001, permission date: Jan 11, 2019). We conducted animal experiments following animal ethics. The schematic diagram of animal experimental protocol was shown in Figure S1. The dose of GRg1 administered by gavage was 10 mg/kg body weight (b.w.) and 40 mg/kg b.w. [17, 18]. ICR mice were randomized into the groups of control, alcohol, alcohol + silymarin (100 mg/kg b.w.), alcohol + low-dose GRg1 (10 mg/kg b.w.), and alcohol + high-dose GRg1 (40 mg/kg b.w.). The control group was orally administrated with distilled water, and the alcohol group was given by gavage with alcohol (Sigma-Aldrich, St. Louis, MO, USA) for 30 days with an increased dose (2–6 g/kg b.w.). Silymarin (100 mg/kg b.w.) and GRg1 (10 and 40 mg/kg b.w., respectively) were given to alcohol + silymarin and alcohol + GRg1 groups and then to alcohol by daily gavage 2 h later. After 12 h, the mice were anesthetized with sodium pentobarbital (50 mg/kg, i.p.) and euthanized by cervical dislocation. The serum in each mouse was obtained by blood centrifugation, and then, the liver and intestinal tissues of the mice were immediately placed in refrigerator (-80°C).

2.4. Histopathological Observation. The liver and colon tissues were removed by laparotomy and immersed in formaldehyde solution. Tissues were embedded in paraffin wax. Then, the tissue samples were cut into 5–8 μm thickness and stained by hematoxylin-eosin (H&E) and Alcian blue-periodic acid Schiff (AB-PAS), respectively. The degree of inflammation and lipid accumulation of in these tissues was observed.

2.5. Analysis of Biochemical Indexes. The circulating levels of alanine aminotransferase (ALT), aspartate aminotransferase (AST), lactate dehydrogenase (LDH), and alkaline phosphatase (AKP) were measured by detection kits (Nanjing Jiancheng Bioengineering Institute, Nanjing, China). Hepatic levels of malondialdehyde (MDA), glutathione peroxidase (GSH-Px), glutathione (GSH), catalase (CAT), and superoxide dismutase (SOD) were detected by detection kits of Nanjing Jiancheng Bioengineering Institute.

2.6. Enzyme-Linked Immunosorbent Assay (ELISA). The liver and colon tissue samples were grinded into homogenate. The sample supernatant of serum, liver, and colon was obtained after centrifugation. The total protein contents were measured by a BCA protein kit. The levels of LPS, tumor necrosis factor α (TNF- α), interleukin-1 beta (IL-1 β), interleukin-6 (IL-6), transforming growth factor- β 1 (TGF- β 1), ROS, 8-hydroxy-2'-deoxyguanosine (8-OHdG), 4-hydroxynonenal (4-HNE), and immunoglobulin A (IgA) in each sample were measured by ELISA reader (Tecan, Salzburg, Austria).

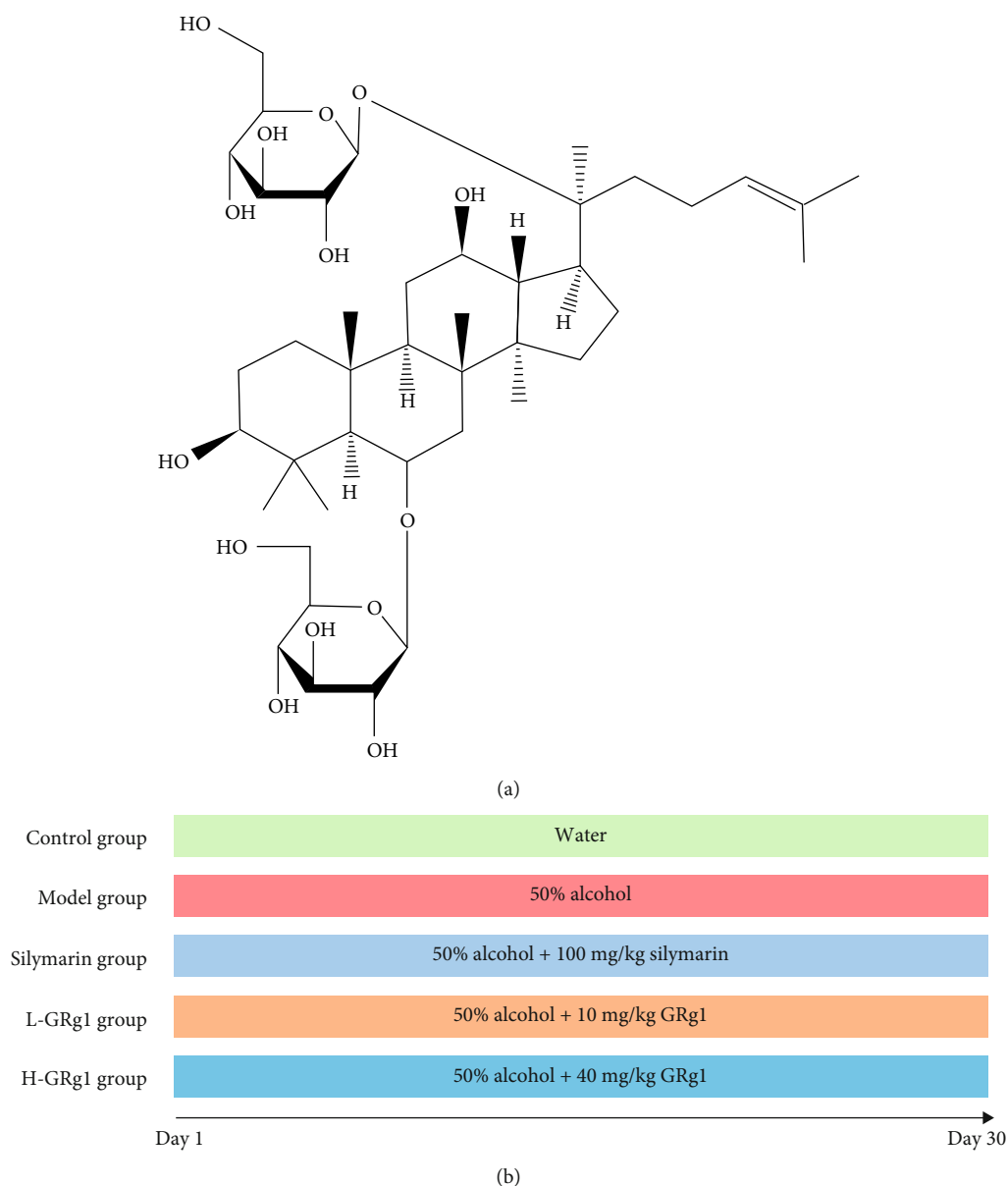


FIGURE 1: Chemical structure of GRg1.

2.7. Analysis of Reverse Transcription-Quantitative Polymerase Chain Reaction (RT-qPCR). The extraction kit (Promega Corporation, Madison, WI, USA) was used to extract the total RNA of colonic tissue, which were transcribed into cDNA. The concentrations of RNA were measured by NanoPhotometer™ P300 spectrophotometer (Implen, Munchen, Germany). GAPDH gene primers were selected as internal reference genes to determine the mRNA levels of zonula occludens-1 (ZO-1), occludin, and claudin. Sequences of primers were placed in Table 1. SYBR Green PCR Master Mix kit (Vazyme Biotech Co., Ltd Nanjing, China) was applied to carry out PCR reaction. The conditions of reaction were 5 min 95°C, 10 s 95°C, 30 s 60°C, and 40 cycles. $2^{-\Delta\Delta Ct}$ method was used to measure the relative mRNA expression.

2.8. Western Blotting Analysis. The total protein content in each sample of liver and colon was determined. Separation of proteins from different samples was separated by sodium dodecyl sulfate-polyacrylamide gel electrophoresis (10-15%) and then transferred to polyvinylidene fluoride (PVDF) membrane. The membranes were sealed and incubated with the primary antibodies and then washed and incubated with secondary antibodies at 25°C. Finally, protein expression of membranes was presented by an odyssey infrared imaging system.

2.9. DNA Sequencing of GM and Bioinformatic Analysis. The cecal contents of each sample were obtained in a super-clean worktable. The total microbial DNA of cecum contents was extracted by a DNA kit (Omega Biotek, Norcross, GA,

TABLE 1: Primer sequences used for RT-qPCR assay.

Genes	Forward (5'-3')	Reverse (5'-3')
GAPDH	ATTCAACGGCACAGTCAAGG	GCAGAAGGGGCGGAGATGA
ZO-1	ACTCCCACTTCCCCAAAAC	CCACAGCTGAAGGACTCACA
Occludin	CTGTCTATGCTCGTCATCG	CATTCCCAGTCTAATGACGC
Claudin-1	GTTTGCAGAGACCCCATCAC	AGAAGCCAGGATGAAACCCA

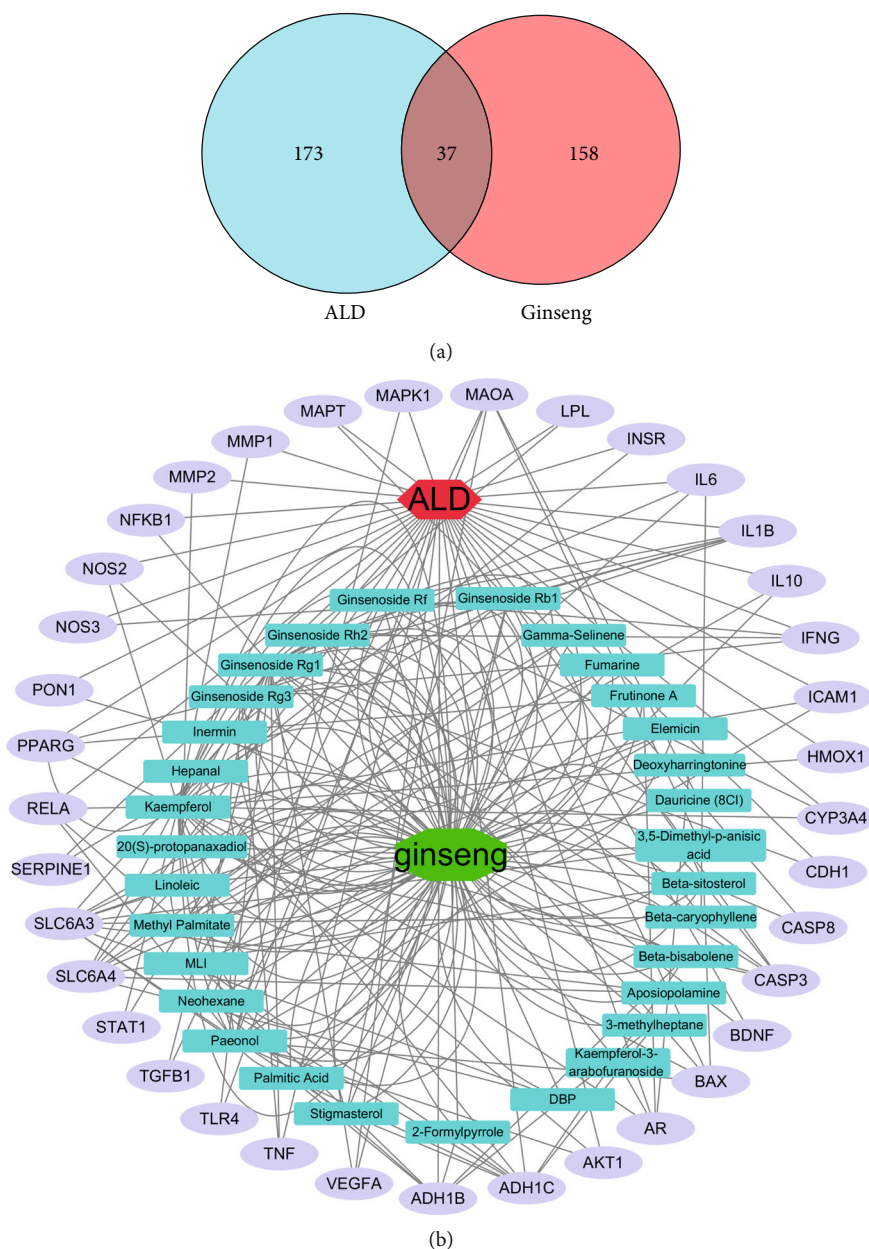


FIGURE 2: Shared targets between ginseng and ALD. (a) Venn diagram of candidate targets in ginseng and ALD. (b) Bioactive ingredients-targets-ALD network. The green octagon node represents ginseng. Cyan rectangle nodes represent the bioactive components of ginseng. The red hexagon node represents ALD. Purple ellipse nodes represent potential targets of ginseng against ALD.

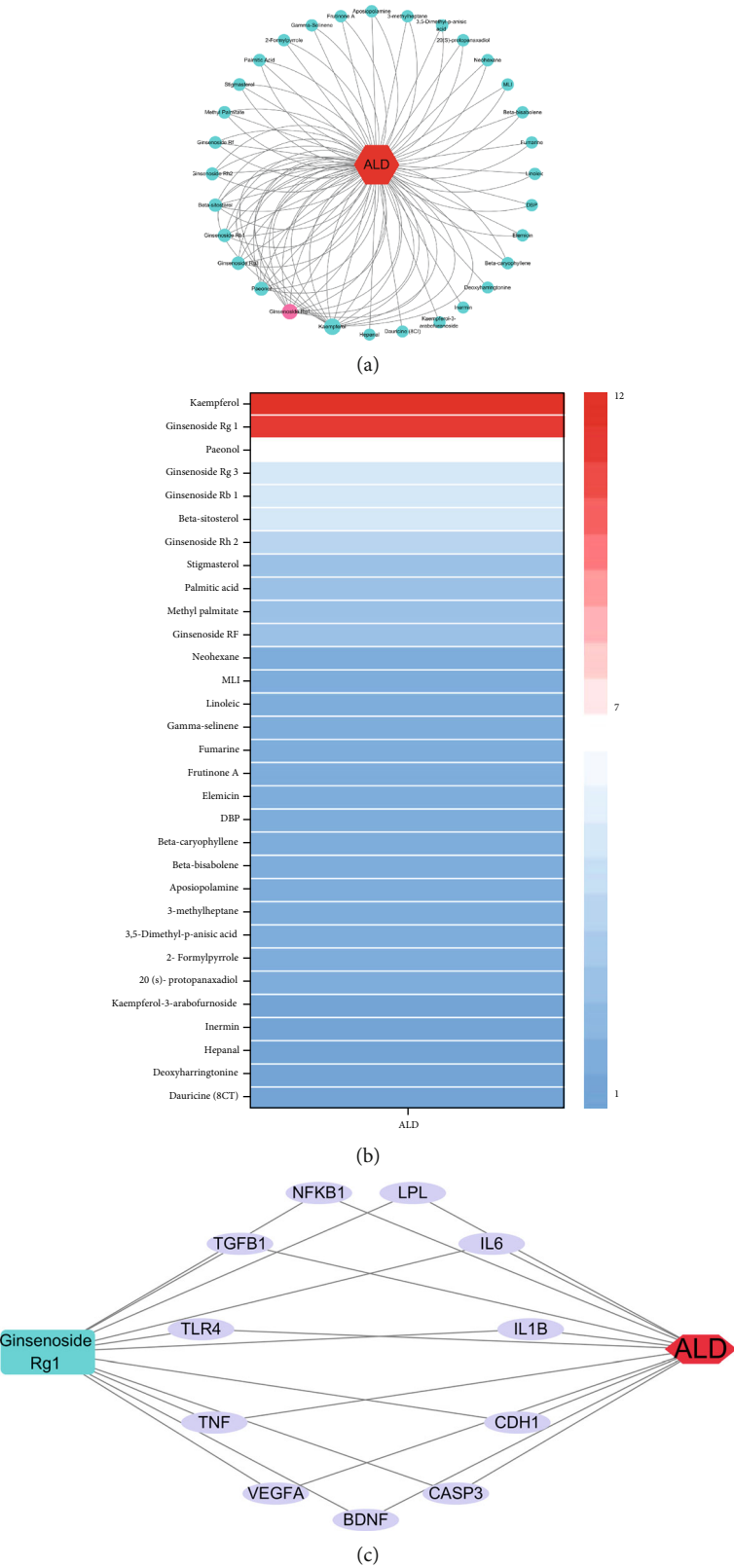


FIGURE 3: Continued.

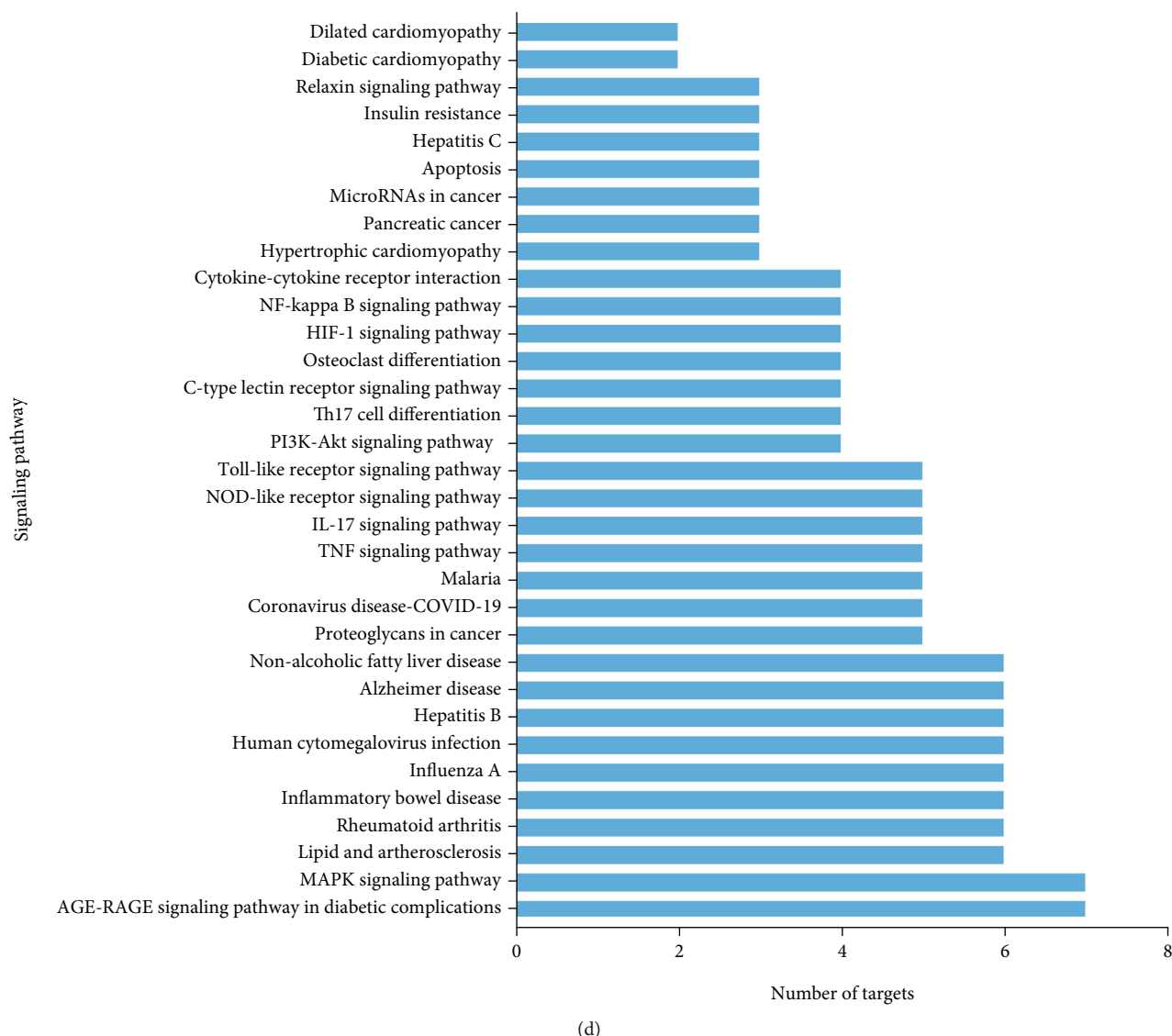


FIGURE 3: Potential targets analysis of bioactive components in ginseng against ALD. (a) Rank diagram of the degree between bioactive ingredients and ALD. The size of circle reflects the degree. (b) Heat map of the degree between bioactive ingredients and ALD. Blue and red colors indicate low and high degree value, respectively. (c) GRg1 targets ALD network. Purple ellipse nodes represent potential targets of GRg1 against ALD. (d) Enrichment diagram of KEGG pathway.

USA), and then, DNA purity was evaluated. The hypervariable region (V3-V4) of 16S rRNA was multiplied by PCR technique. The purified amplicons were quantitatively analyzed and sequenced by Illumina MiSeq platform (Illumina, San Diego, CA, USA).

2.10. Statistical Analysis. All the results in the experiment were expressed as mean \pm standard deviation (S.D.) and analyzed using GraphPad Prism 8.0. Pearson correlation coefficient and the heat map between gut microbiota and the related biomarkers were obtained on the platform of Gene-denovo Biotechnology Co. Ltd (<https://www.omicsmart.com/>). The significant difference was calculated according to the student's *t*-test. Values of $P < 0.05$ represent statistically difference.

3. Results

3.1. Shared Targets between Bioactive Ingredients in Ginseng and ALD. The bioactive ingredients of ginseng and ALD-related targets were gathered by using the corresponding database. The results showed that 195 targets corresponding to bioactive ingredients of ginseng were obtained from TCMSP, HERB, and literatures. Meanwhile, the ALD-related genes were gathered, and 210 ALD-related targets were confirmed (relevance score ≥ 40). 37 shared targets between active ingredients and ALD-related targets were identified in generating Venn diagram (Figure 2(a)). Cytoscape software was employed to construct the network of "bioactive ingredients-targets-disease" network about common targets in schematic diagram. 31 bioactive components in *Panax ginseng* were associated with 37 shared targets,

TABLE 2: The potential targets and network degrees.

Target	Description	Degree
IL-6	Interleukin-6	10
TLR4	Toll like receptor 4	10
TNF	Tumor necrosis factor	10
CASP3	Caspase 3	9
IL-1 β	Interleukin-1 beta	9
TGF- β 1	Transforming growth factor-beta 1	9
VEGFA	Vascular endothelial growth factor A	9
BDNF	Brain derived neurotrophic factor	7
CDH1	Cadherin 1	7
NF- κ B1	Nuclear factor-kappa B subunit 1	7
LPL	Lipoprotein lipase	3

which have potential preventive effects on ALD (Figure 2(b)).

3.2. Potential Target Analysis of GRg1 against ALD. To further investigate the potential anti-ALD property of 31 bioactive ingredients, the network of bioactive components in *Panax ginseng* targeted to ALD was analyzed by Cytoscape software (Figure 3(a)). The degree between bioactive ingredients and ALD was visualized in heat map (Figure 3(b)). The results showed that the degree between GRg1 and ALD was ranked the second, which showed powerful ability in preventing alcoholic liver injury (Figures 3(a) and 3(b)). Recent studies have reported that GRg1 is a major ingredient originated from *Panax ginseng*, which has the protective effect on liver disease [16, 19]. Then, GRg1-target-ALD network was established to explore the potential targets in preventing ALD. We found that 11 genes such as IL-6, TLR4, TNF, and CASP3 were interactive targets between GRg1 and ALD, suggesting that GRg1 protected alcoholic liver damage through these targets (Figure 3(c) and Table 2). Furthermore, KEGG pathway analysis was performed on these interactive targets in Figure 3(d). The results showed that GRg1 represents its protective effects against ALD were closely related to these signaling pathways including TLR signaling pathway and NF- κ B signaling pathway.

3.3. Effect of GRg1 on Alcoholic Liver Damage in Mice. To explore the potential effects of GRg1 on ALD, the hepatic tissue morphology and plasma biochemical indexes were determined in alcohol-induced liver damage mice. As shown in Figure 4(a), the liver lobule structure was clear, and the hepatocytes were arranged regularly in control group, whereas cellular swelling and inflammatory infiltration were exhibited in the alcohol group. After pretreatment with different doses of GRg1, infiltrations of inflammatory cells were gradually decreased. The improvement of histopathology in high dose-GRg1 group was similar to that in silymarin group. Meanwhile, alcohol treatment obviously elevated the activities of hepatic enzymes including ALT, AST, LDH, and AKP in the serum. However, the enzymatic activities were gradually reduced by GRg1 pretreatment. These biochemical index in high dose-GRg1 group was similar to

those in positive control group (Figures 4(b)–4(e)), indicating that the protective effect of high-dose GRg1 on alcoholic liver injury closely resembled that of silymarin. Our results demonstrate that GRg1 has protective effects on liver injury induced by alcohol.

3.4. Effect of GRg1 on Hepatic Oxidative Stress Induced Alcohol in Mice. Alcohol induces ROS generation and interferes with antioxidant defense system, which further results in oxidative stress in liver. Alcohol-induced oxidative stress demonstrated an essential role in promoting ALD development [20]. To investigate the effect of GRg1 on hepatic oxidative stress, the levels of oxidation and antioxidant parameters were detected. Alcohol administration significantly increased ROS level and oxidative products (MDA, 4-HNE, and 8-OHdG). However, these levels of oxidative indexes were gradually decreased in GRg1 group (Figures 5(a)–5(d)). Similarly, as shown in Figures 5(e) and 5(f), GRg1 pretreatment significantly alleviated the alcohol-induced decrease in antioxidant indices (SOD, GSH-Px, CAT, and GSH). Collectively, GRg1 prevents alcohol-induced oxidative stress by regulating the equilibrium between oxidation and antioxidation in the liver of mice.

3.5. GRg1 Alleviated Inflammatory Response in the Liver Treated by Alcohol. To assess the effect of GRg1 on hepatic inflammation, inflammatory indexes were measured on the basis of the network pharmacology analyses. In Table 3, LPS level was significantly elevated by alcohol. However, the elevation of LPS level in alcohol group was gradually restored by GRg1 pretreatment. Numerous studies demonstrate that low LPS concentration can activate LPS-mediated TLR4/NF- κ B pathway, which is essential to hepatic inflammation [21]. Then, the protein expression levels of TLR4 and p-NF- κ B p65 were detected through western blotting. We found that alcohol remarkably upregulated TLR4 and p-NF- κ B p65 expressions. However, these levels were gradually decreased after GRg1 pretreatment (Figures 6(a)–6(c)), suggesting that LPS-induced TLR4/NF- κ B activation is attenuated by GRg1. Furthermore, inflammatory factor levels including TNF- α , IL-1 β , IL-6, and TGF- β 1 were significantly upregulated by alcohol treatment, while GRg1 gradually decreased those levels, especially in high-dose GRg1 group (Table 3). The data imply that GRg1 inhibits LPS/TLR4/NF- κ B signaling pathway, which subsequently ameliorates liver inflammation induced by alcohol.

3.6. Effect of GRg1 on Intestinal Barrier in Alcohol-Treated Mice. To investigate the integrity of intestinal epithelial cells, anatomical and histopathological observations were performed in the colon. Histopathological examination showed that the shortened length of intestine was reversed by GRg1 pretreatment (Figure 7(a)). In addition, epithelial cells were destroyed and loosely lined, and the space of subepithelia was expanded in alcohol-treated mice, whereas those were obviously alleviated in GRg1 group (Figure 7(b)). Furthermore, the tight junction proteins (ZO-1, occludin, and claudin-1), as indicators to measure intestinal permeability,

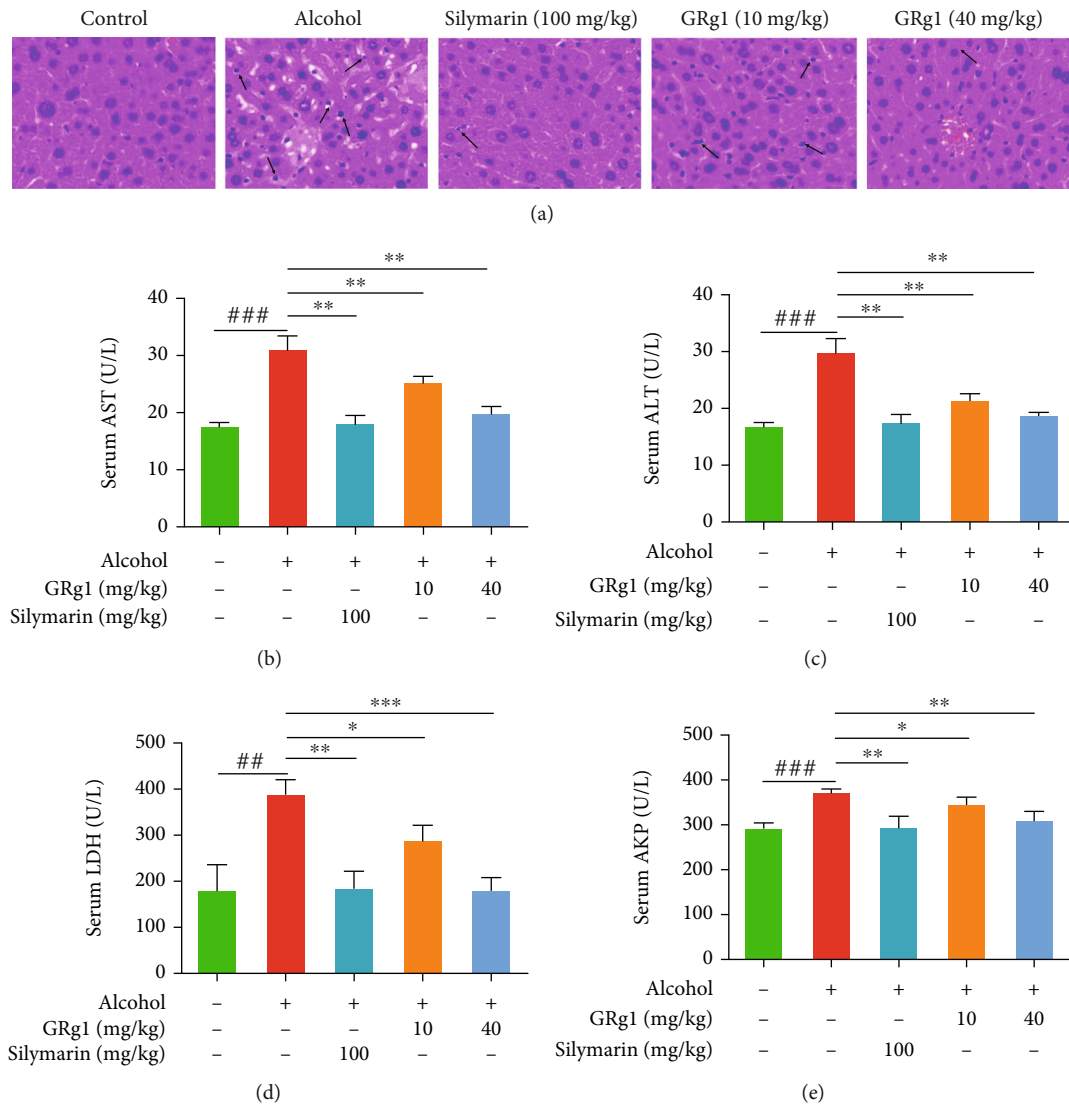


FIGURE 4: Effect of GRg1 on alcoholic liver damage *in vivo*. (a) The liver tissues were stained by hematoxylin-eosin (200 \times). The arrows indicate inflammatory cells. (b–e) The circulating levels of ALT, AST, LDH, and AKP. $^{##}P < 0.01$ and $^{###}P < 0.001$ vs. control group. $^{*}P < 0.05$, $^{**}P < 0.01$, and $^{***}P < 0.001$ vs. alcohol group.

maintain the integrity of intestinal barrier [9]. Next, the mRNA levels of colon tight junction proteins were detected by RT-qPCR. The levels of ZO-1, occludin, and claudin-1 detected by PCR in alcohol group were gradually reduced in alcohol group, which were reversed after GRg1 pretreatment (40 mg/kg b.w.) (Figure 7(c)). Meanwhile, GRg1 pretreatment gradually restored the decrease of IgA level by alcohol (Figure 7(d)). And compared with alcohol group, the intestinal and circulating levels of LPS in the GRg1 group were reduced in a form of measurement dependence (Figures 7(e) and 7(f)). The data indicate GRg1 enhances gut barrier by promoting the expressions of tight junction protein and IgA.

3.7. Effect of GRg1 on the Intestinal Microbiota Composition in Alcohol-Treated Mice. To analyze the effect of GRg1 on the GM composition in ALD mice, 16S rRNA were multiplex sequenced in the intestine. In this study, after alcohol

treatment, the indexes of Chao1 richness and Shannon diversity were gradually elevated, while GRg1 pretreatment obviously reduced the indexes of Chao1 richness and Shannon diversity compared with those in alcohol group (Figures 8(a) and 8(b)). As shown in Figure 8(c), the cluster of GM in alcohol group was obviously different with the clusters of normal mice, while those between GM in high-dose GRg1 group and control group were close to each other. Meanwhile, OTUs in each group were shared and different in the Venn diagram (Figure 8(d)).

Then, the different GM phylotypes among all groups were analyzed at different levels. The decrease of Verrucomicrobia and Bacteroidetes in alcohol group were reversed by GRg1 treatment (Figure 8(e)). In addition, *Akkermansia*, *Bacteroides*, *Lachnospiraceae_NK4A136_group*, and *Alloprevotella* were the most abundant genera (Figure 8(f)). To further investigate the specific differences of intestinal microbiota at various phylogenetic levels, LEfSe was used

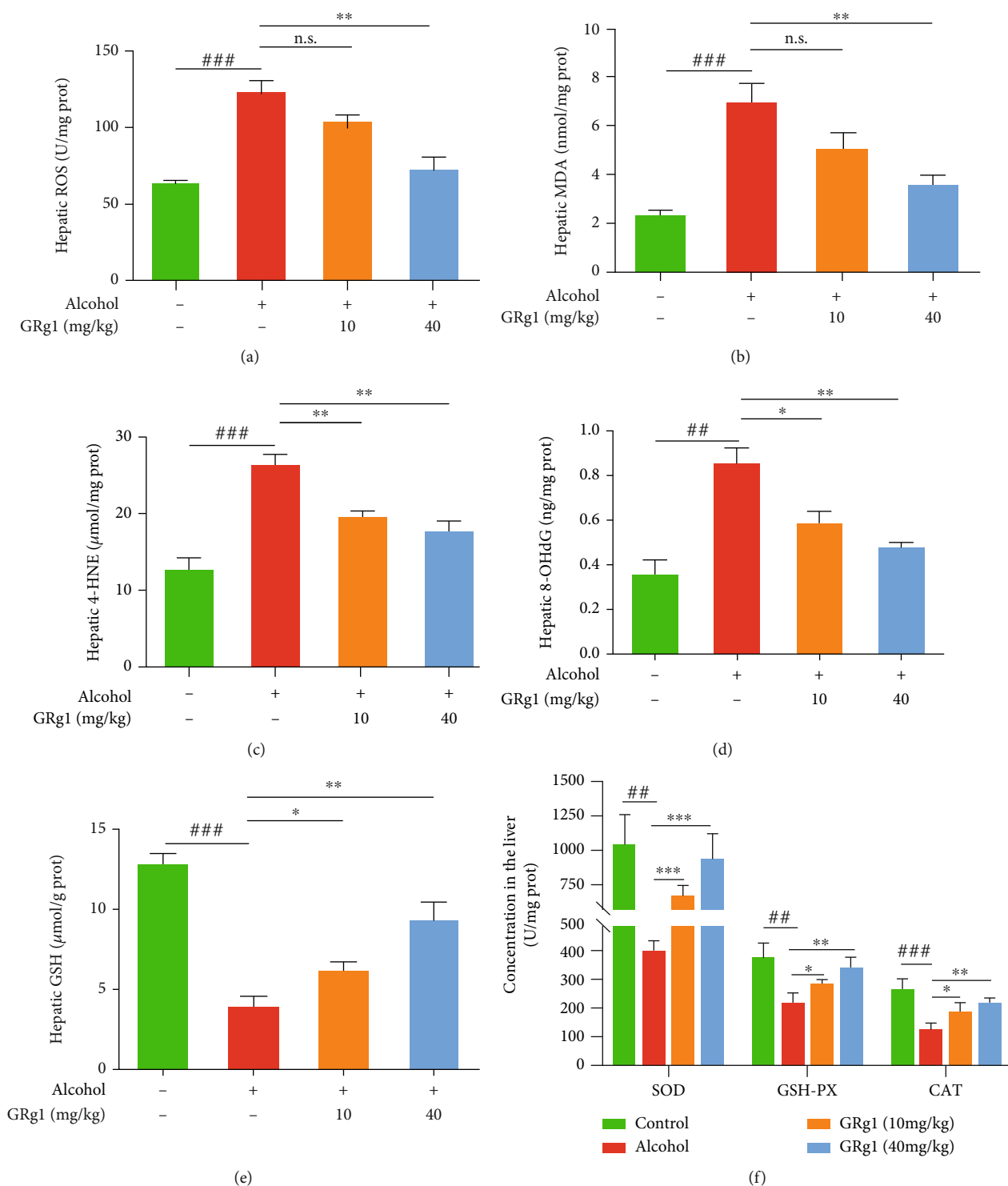


FIGURE 5: The levels of oxidative and antioxidative indexes in the liver. (a) ROS, (b) MDA, (c) 4-HNE, (d) 8-OHdG, and (e) GSH were oxidative parameters. (f) Hepatic SOD, GSH-Px, and CAT were antioxidative parameters. $##P < 0.01$ and $###P < 0.001$ vs. control group. $*P < 0.05$, $**P < 0.01$, and $***P < 0.001$ vs. alcohol group. n.s. indicates no significant difference.

to analyze the intestinal microbiota between alcohol group and GRg1 (40 mg/kg) group. As shown in Figures 8(g) and 8(h), Firmicutes phylum, two genera including *Lachnospiraceae_NK4A136_group*, and *Ruminiclostridium* were abundant in alcohol group, while Verrucomicrobia phylum and *Akkermansia* genus were predominant in GRg1

(40 mg/kg) group. These results indicate that GRg1 can regulate the composition of GM in alcohol group.

3.8. Correlations between GM and the Indexes. In order to illuminate the potential mechanisms of GRg1 on ALD, the relationship between intestinal flora and host indexes was

TABLE 3: Inflammation parameters in liver of mice.

Group	Control	Alcohol	GRg1 (10 mg per kg b.w.)	GRg1 (40 mg per kg b.w.)
LPS (EU/g prot)	129.74 ± 7.77	203.41 ± 19.61 ^{###}	198.33 ± 25.67	167.42 ± 13.56 ^{**}
TNF- α (pg/mg prot)	166.69 ± 4.58	227.81 ± 7.31 ^{###}	186.64 ± 6.93 ^{**}	171.91 ± 2.96 ^{***}
IL-1 β (pg/mg prot)	20.47 ± 1.93	29.12 ± 1.11 ^{##}	26.84 ± 1.91	24.10 ± 0.49 ^{**}
IL-6 (pg/mg prot)	20.02 ± 1.9	33.69 ± 1.71 ^{###}	28.12 ± 1.85 [*]	23.94 ± 1.24 ^{**}
TGF- β 1 (pg/mg prot)	20.24 ± 1.87	33.22 ± 1.86 ^{##}	27.52 ± 2.66 [*]	24.76 ± 1.93 ^{**}

All data are expressed as mean \pm S.D. ^{##} $P < 0.01$ and ^{###} $P < 0.001$ vs. the control group, ^{*} $P < 0.05$, ^{**} $P < 0.01$, and ^{***} $P < 0.001$ vs. the alcohol-treated group.

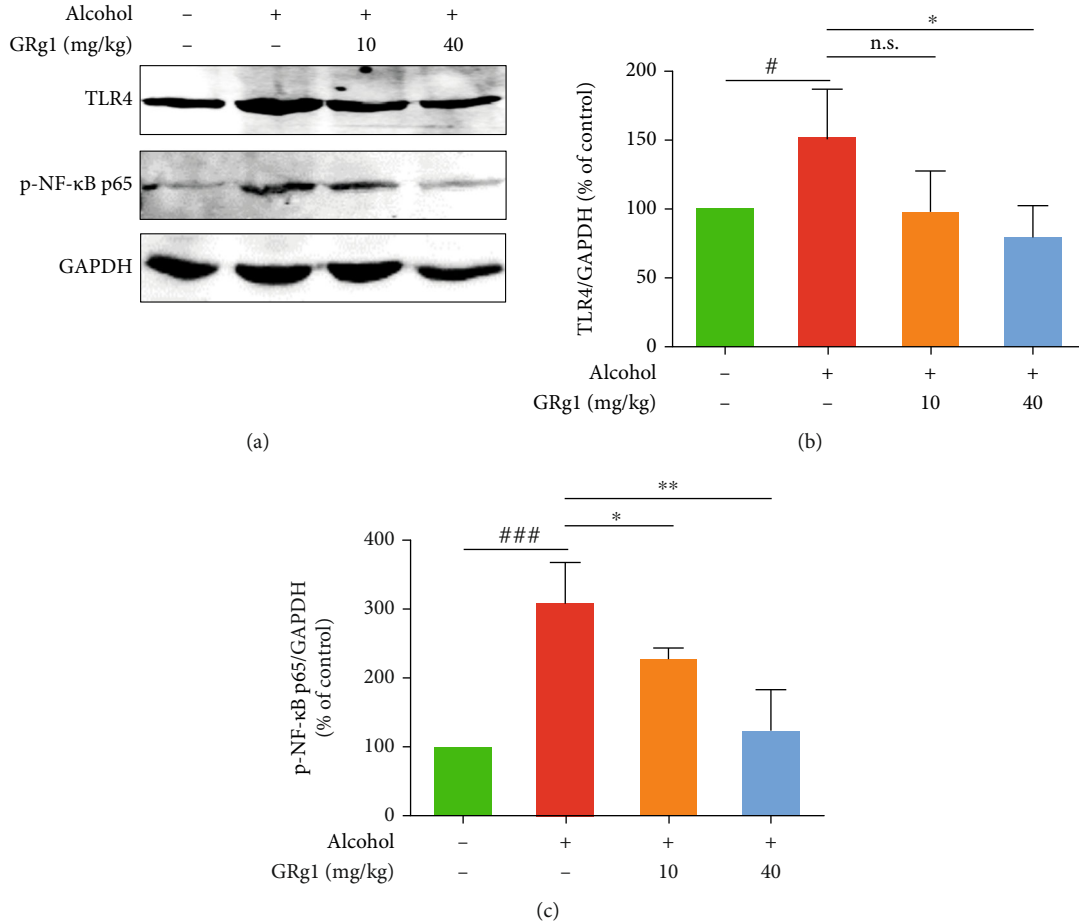


FIGURE 6: The TLR4/NF- κ B pathway in the liver. (a) The protein levels of TLR4 and p-NF- κ B p65 were detected using western blotting. Densitometric analysis of (b) TLR4 and (c) p-NF- κ B p65. [#] $P < 0.05$ and ^{###} $P < 0.001$ vs. control group. ^{*} $P < 0.05$ and ^{**} $P < 0.01$ vs. alcohol group. n.s. indicates no significant difference.

analyzed. As shown in Figure 9, the Pearson correlation analysis showed that Verrucomicrobia, Bacteroidetes, *Akkermansia*, *Bacteroides*, *Lachnospiraceae_NK4A136_group*, and *Alloprevotella* showed obvious positive correlation with intestinal integrity indexes (tight junction proteins and sIgA), while negative correlation with hepatic biomarkers (ROS, ALT, and AST), hepatic indexes of inflammation (LPS, TNF- α , IL-1 β , IL-6, and TGF- β 1) and TLR4/NF- κ B expression. In contrast, Firmicutes are positively associated with these oxidative and inflammatory parameters, whereas negatively correlated with hepatic antioxidant parameters and intestinal integrity indexes. Here, the results suggest that GRg1 causes the alter-

ation of GM population, which enhances intestinal integrity and arrests gut-derived inflammation by inhibition of LPS-mediated TLR4/NF- κ B pathway.

4. Discussion

ALD is caused by alcohol abuse, which is accompanied by the development of liver injury [22]. Oxidative stress and inflammation induced by alcohol are participated in the progression of ALD. Recent studies reported that GM participated in the evolution of alcohol-induced liver injury, which is a critical element for prevention of ALD [6, 7].

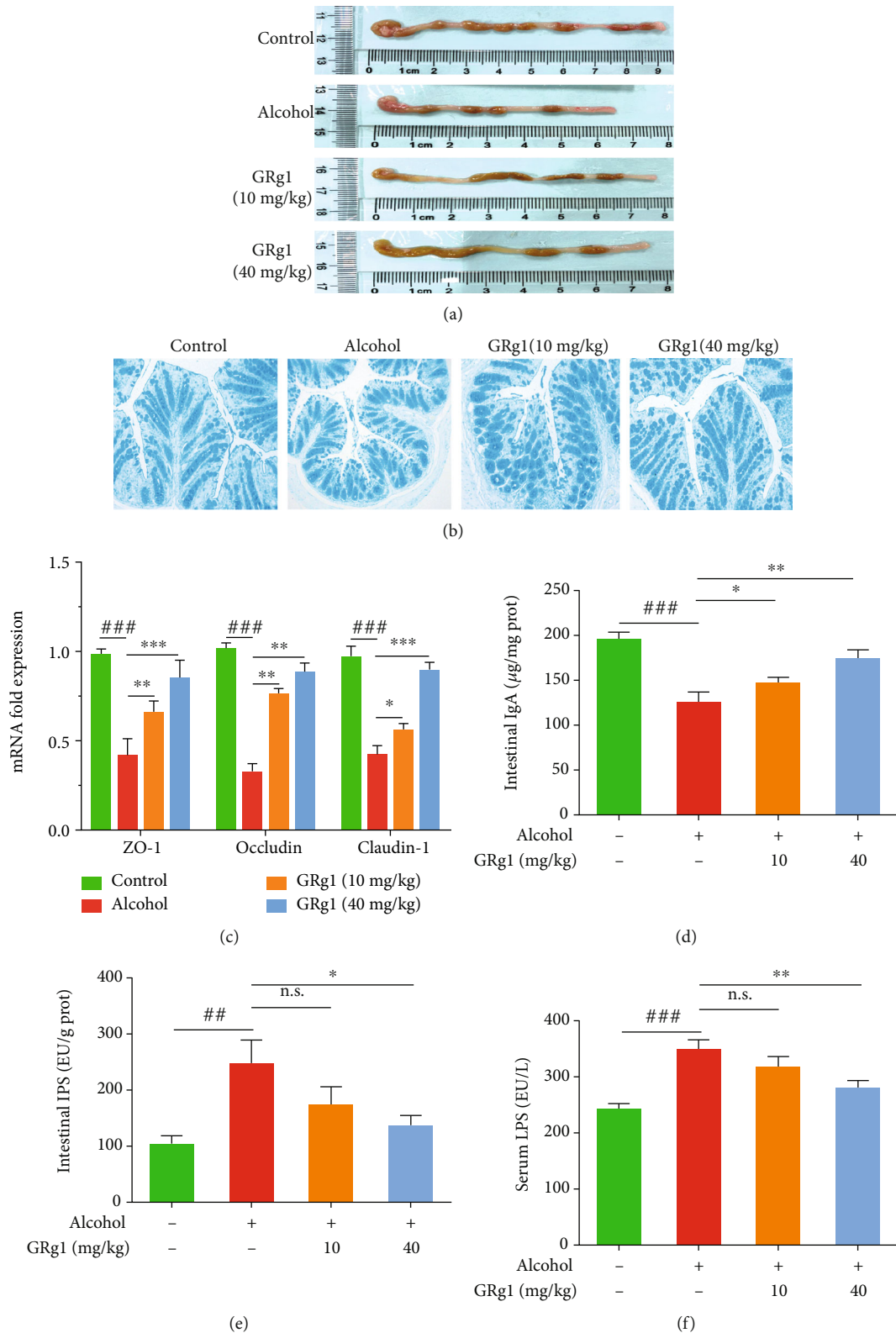


FIGURE 7: Intestinal barrier function in the colon. (a) The length of the colon. (b) The colon tissues were stained by Alcian blue (200 \times). (c) The mRNA expression levels of tight junction proteins (ZO-1, occludin, and claudin-1). (d) IgA levels, (e) intestinal LPS levels, and (f) circulating LPS levels. $##P < 0.01$ and $###P < 0.001$ vs. control group. $*P < 0.05$, $**P < 0.01$, and $***P < 0.001$ vs. alcohol group. n.s. indicates no significant difference.

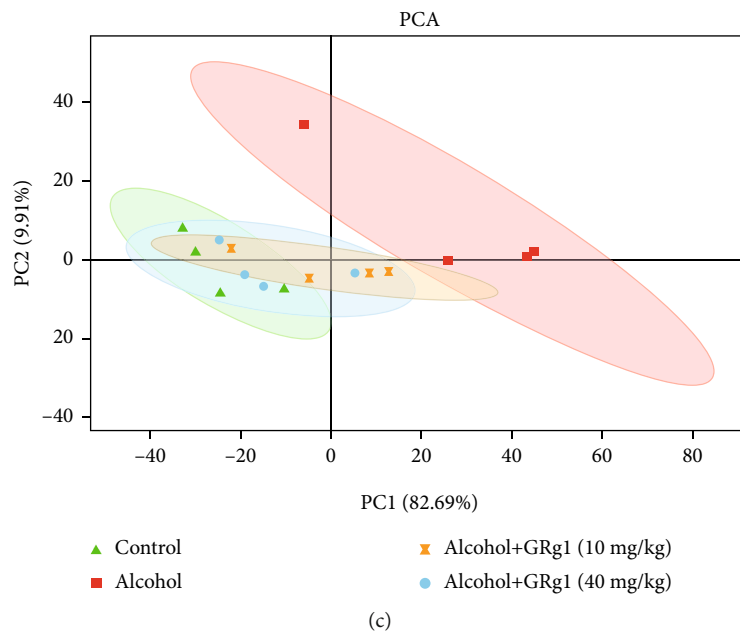
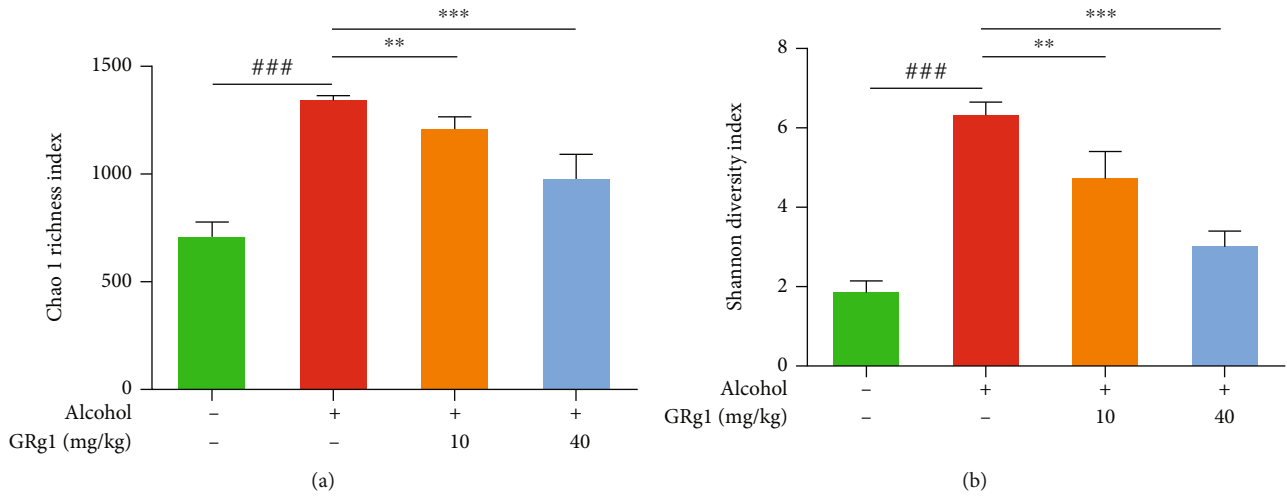


FIGURE 8: Continued.

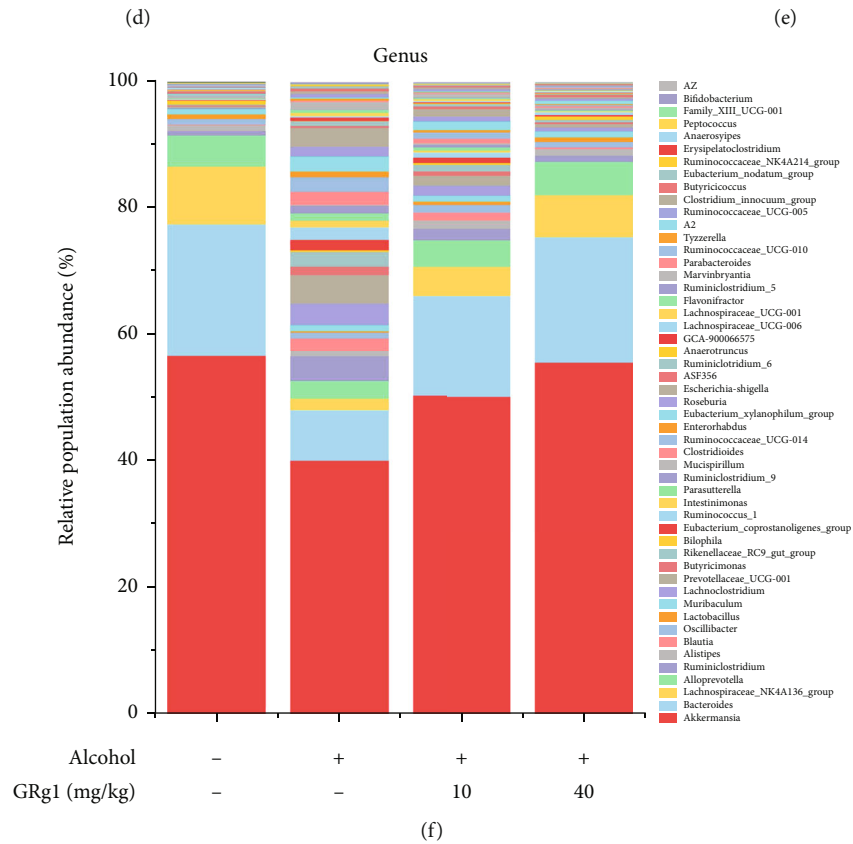
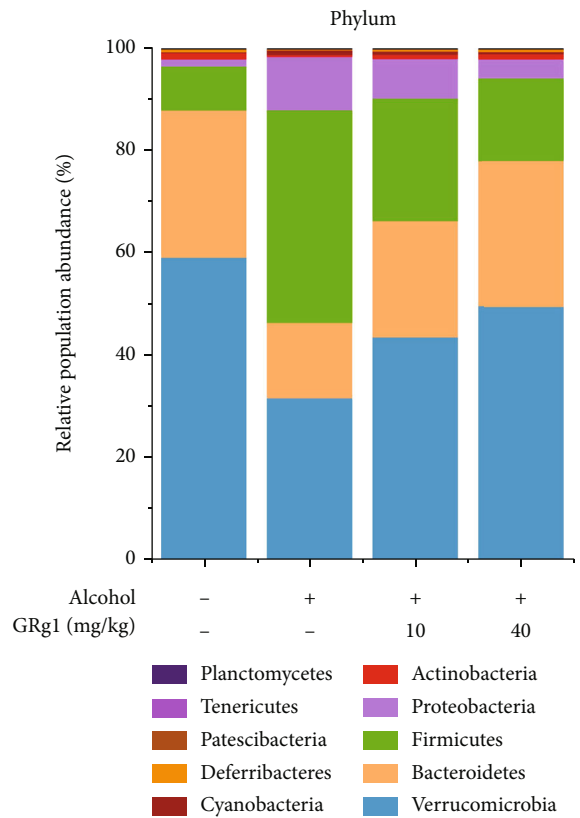
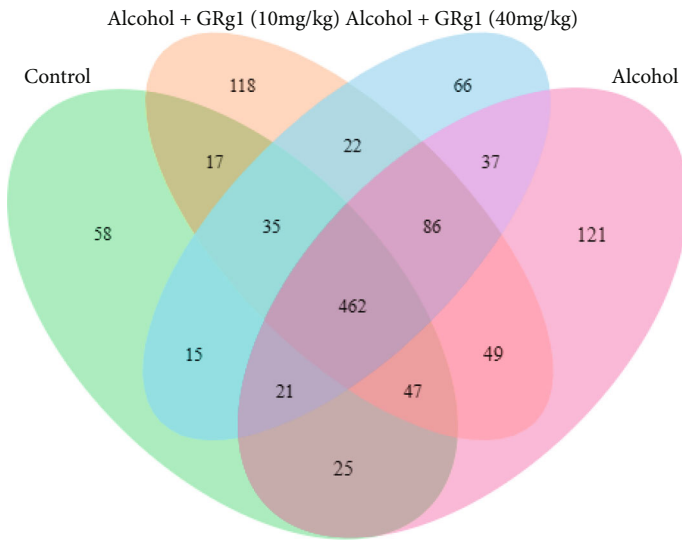


FIGURE 8: Continued.

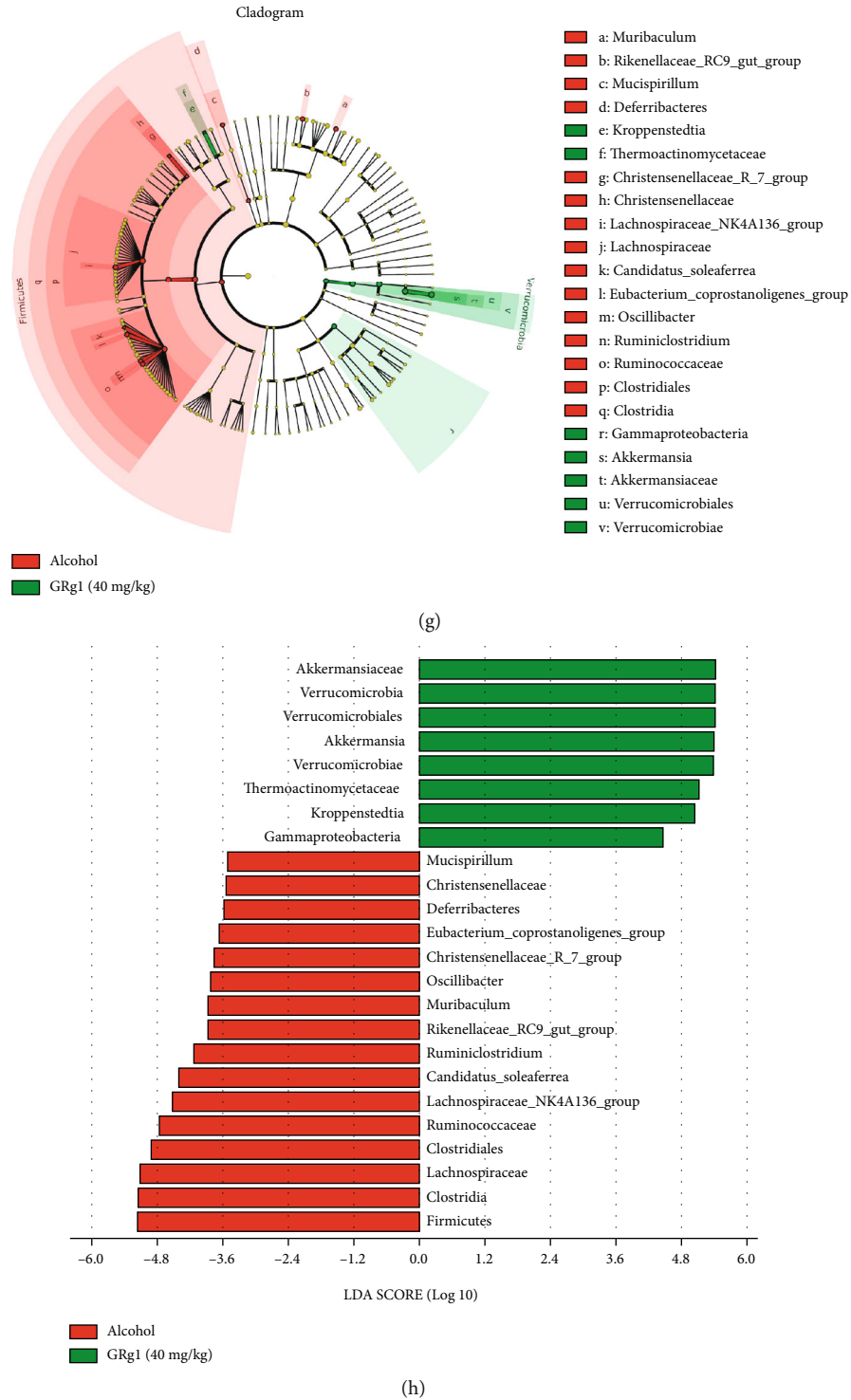


FIGURE 8: Intestinal microbiota composition in cecum. (a) Chao1 richness index. (b) Shannon diversity index. (c) PCA plot. (d) Venn diagram. (e) Relative abundances of microbial composition at phylum levels. (f) Relative abundances of microbial composition at genus levels. (g) LEfSe taxonomic cladogram between alcohol group and high-dose GRg1 group. The size of the circles is based on relative abundance. (h) LDA score diagram. $###P < 0.001$ vs. control group. $**P < 0.01$ and $***P < 0.001$ vs. alcohol group.

GRg1 extracted from ginseng can suppress oxidative stress and inflammatory responses, which exerts its pharmacological property to prevent and treat inflammation-related diseases [13, 19]. In this study, the potential targets of GRg1 against ALD were predicted through network pharmacol-

ogy, and the underlying mechanisms of GRg1 on alcoholic liver injury were investigated in mice.

Network pharmacology is an effective approach to predict the targets and pathways of drugs, which provides a way of the precise prevention and treatment of disease [15]. In this study,

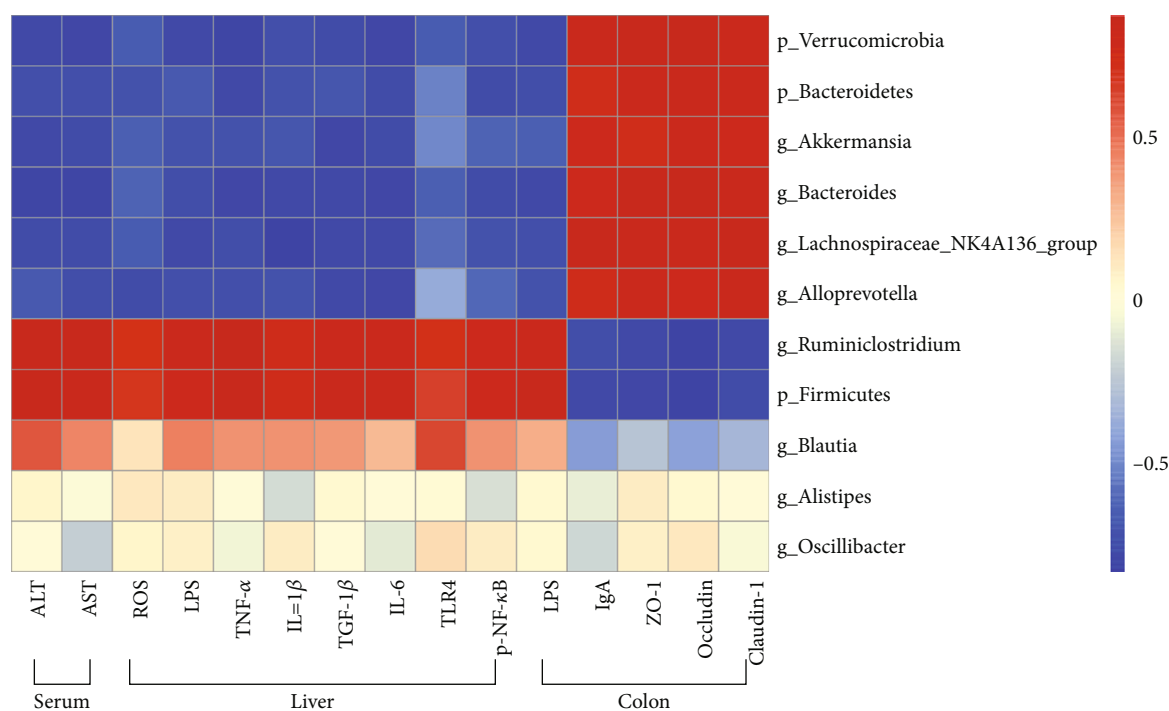


FIGURE 9: Heat map of Pearson correlation between GM and the body indexes. Blue and red colors indicate negative and positive correlation, respectively.

31 bioactive ingredients in ginseng were selected to have potential anti-ALD activity by ginseng-targets-ALD network (Figures 2(a) and 2(b)). Among these bioactive compounds, GRg1 showed the powerful pharmacology against ALD according to the degree values between bioactive ingredients and ALD (Figures 3(a) and 3(b)). Recent studies demonstrated that GRg1 can protect against some liver diseases in several animal models [23, 24]. Combined with the related references, GRg1 was chosen to perform the network of GRg1-targets-ALD. We found that 11 key genes were related to GRg1, which were strongly correlated with ALD (Figure 3(c) and Table 2). In addition, KEGG pathway analysis showed the TLR and NF- κ B signaling pathways were interrelated with GRg1 against ALD (Figure 3(d)). It has been confirmed that the activation of LPS/TLR4/NF- κ B pathway induces the secretion of inflammatory factors, which contributes to the development of ALD [9, 25]. These results indicate that LPS/TLR4/NF- κ B pathway is the potential targets of GRg1 to protect against ALD.

Excessive alcohol consumption causes histopathological changes and dysfunction in the liver [2]. The elevation of hepatic enzymes in the serum indicates the occurrence of liver injury, such as AST, ALT, and LDH [26]. It has been verified that silymarin exhibits protective effects against liver injury, which is used as a common positive control in many studies of hepatoprotective drugs [27, 28]. In the current study, it was found that GRg1 effectively alleviated histopathological changes in liver tissue and the levels of hepatic enzymes (AST, ALT, LDH, and AKP) in serum (Figure 4), indicating that GRg1 can reduce alcohol-induced liver damage. In addition, hepatoprotective effects of high dose-GRg1 were similar to silymarin, suggesting that GRg1 is a potential

agent for preventing ALD. Alcohol-induced excess ROS triggers oxidative damage of lipid and DNA and destroys equilibrium of oxidation and antioxidation, which leads to hepatic inflammation and injury [4, 29]. Our results showed that GRg1 pretreatment reversed the increase of oxidative level (ROS, MDA, 4-HNE, and 8-OHdG) and decrease of antioxidative level (SOD, CAT, GSH-Px, and GSH) (Figure 5), suggesting the alleviation of alcohol-induced oxidative stress.

Several studies indicate that alcohol and its metabolites destroy the function and structure of gut epithelial cells and result in the enlargement of gut permeability [30–32]. In this study, gross and tissue staining displayed that high-dose GRg1 pretreatment alleviated the reduction of intestinal length and histopathological changes in the colon (Figures 7(a) and 7(b)). It has been reported that tight junction proteins crosslink to the actin cytoskeleton and form the gut integrity [9]. In addition to alcohol and its metabolites, alcohol-mediated microbial proliferation and LPS have been found to disrupt tight junction proteins and increase intestinal permeability, subsequently intestinal LPS enters blood circulation through broken intestinal barrier [33, 34]. In the present study, we found that high-dose GRg1 effectively reduced the intestinal and circulating levels of LPS and increased the levels of the tight junction proteins in alcohol-treated mice (Figures 7(c), 7(e), and 7(f)). The results indicate that GRg1 pretreatment restores the expression of tight junction proteins and enhances gut barrier by reducing alcohol-induced LPS in the intestine and circulation. IgA restricts the invasion of pathogens and toxins through the mucosa and serves as the major factor of intestinal mucosal defense [35]. We found that GRg1

pretreatment improved the levels of antimicrobial peptides and IgA (Figure 7(d)). Taking together, the findings demonstrate that GRg1 enhances gut barrier function and decreases the gut permeability in alcohol-treated mice.

It is well known that LPS is a microbe-derived bacterial product, which is a crucial mediator of inflammation in ALD. Further studies have reported that alcohol intake increases intestinal permeability, and LPS is transported from intestine to liver through blood circulation, which induces inflammatory response in the liver [36, 37]. The increase of inflammatory cytokines contributes to ALD by regulating the gut-liver axis [9]. LPS-induced TLR4/NF- κ B activation builds a link between the gut permeability and liver inflammation, which aggravate liver injury [21, 38]. We found that GRg1 pretreatment reversed the elevated levels of LPS, TLR4, and p-NF- κ B in alcohol group (Figure 6 and Table 3). These findings indicate that LPS-mediated TLR4/NF- κ B activation is reduced by modulation of gut permeability in GRg1 group. Subsequently, GRg1 pretreatment alleviated the increase of inflammatory factors in the liver treated by alcohol (Table 3). Taking together, the data demonstrated that GRg1 alleviated alcohol-induced inflammatory response through suppression of LPS/TLR4/NF- κ B pathway and prevented liver damage, which further proved the target predicted by network pharmacology.

Recently, more evidences have displayed that alcohol results in imbalance of intestinal flora, and the interaction between GM and hepatic damage promotes the development of ALD [39, 40]. In this study, all the groups have unique and shared OTUs (Figure 8(d)). GRg1 pretreatment significantly decreased the values of Chao 1 richness and Shannon diversity in alcohol group, indicating the decline of α -diversity (Figures 8(a) and 8(b)). In addition, the GM cluster in high dose-GRg1 group and control group was close, indicating the similarity of β -diversity (Figure 8(c)). Our data imply that GRg1 pretreatment can alter GM profile in alcohol-treated mice. Bacteroidetes and Firmicute are the richest phyla, and changes in Firmicutes/Bacteroidetes (F/B) are often associated with health benefits [41, 42]. Our data demonstrated that GRg1 pretreatment enhanced the proportion of Bacteroidetes and Verrucomicrobia and reduced the value of F/B in alcohol group, which were consistent with previous report (Figure 8(e)). *Akkermansia muciniphila*, a gram-negative bacterium located in the mucus layer, maintains the integrity of intestinal barrier [43]. It has been demonstrated that *Bacteroides*, *Lachnospiraceae_NK4A136_group*, and *Alloprevotella* produce short-chain fatty acids, which protect intestinal barrier function and inhibit inflammatory response [44–46]. Our data showed that *Akkermansia*, *Bacteroides*, *Lachnospiraceae_NK4A136_group*, and *Alloprevotella* were the main microbiota at genus level, and GRg1 pretreatment increased these abundances (Figure 8(f)). In addition, there was specific differences of microbiota between alcohol group and high dose-GRg1 group by LEfSe analysis (Figures 8(g) and 8(h)). Collectively, these findings indicate that GRg1 can regulate GM composition to ameliorate alcoholic liver damage.

It has been demonstrated that excess ethanol intake is correlated with changes in GM composition, intestinal barrier function, and inflammatory response [47]. Some gut bacte-

ria products such as LPS reach the liver through portal vein, which activate TLR4-mediated NF- κ B pathway and produce proinflammatory cytokines in the liver [25]. Moreover, alcohol enhances gut leakiness by inhibiting tight junction protein expression and increases LPS load and liver pathology [48]. The interaction between GM alteration and gut-derived inflammation promotes a crucial effect in progression of alcoholic liver injury [9]. Our results demonstrate that inflammatory biomarkers (LPS, TLR4, NF- κ B, and cytokines) in the liver showed a negative relation with some microbiota such as Bacteroidetes, Verrucomicrobia, *Akkermansia*, and *Bacteroides* and positive association with Firmicutes after GRg1 pretreatment (Figure 9). The findings demonstrate that LPS-mediated TLR4/NF- κ B activation is decreased by alteration of GM in GRg1-treated mice. In contrast, gut barrier defense (tight junction protein expression and sIgA level) exhibited the opposite correlation with these GM. Collectively, our data imply that GRg1 alters the GM, which interacted with gut-derived inflammation, and further alleviates alcoholic liver damage.

5. Conclusion

In this study, network pharmacological analysis showed that 11 potential targets of GRg1 against ALD were obtained and implicated with TLR/NF- κ B signaling pathways. Meanwhile, GRg1 reduced liver pathological damage and the activities of hepatic enzymes in alcohol-treated mice. GRg1 alleviated alcohol-induced oxidative stress by downregulating oxidative levels and upregulating antioxidative levels. GRg1 inhibits LPS/TLR4/NF- κ B signaling pathway, which subsequently ameliorates liver inflammation induced by alcohol. Furthermore, GRg1 inhibited intestinal and circulating LPS levels and increased tight junction proteins and IgA levels, which strengthened the intestinal barrier. GRg1 regulated intestinal flora disturbance, Verrucomicrobia, Bacteroidetes, *Akkermansia*, and *Bacteroides* were positively correlated with intestinal barrier indicators and negatively associated with LPS-mediated inflammation after GRg1 treatment. Our findings proved that GRg1 as a natural product can protect against alcohol-induced liver damage *via* regulating gut-liver axis.

Abbreviations

AKP:	Alkaline phosphatase
ALD:	Alcoholic liver disease
ALT:	Alanine aminotransferase
AST:	Aspartate aminotransferase
b.w.:	Body weight
CAT:	Catalase
F/B:	Firmicutes/Bacteroidetes
GM:	Gut microbiota
GRg1:	Ginsenoside Rg1
GSH:	Glutathione
GSH-Px:	Glutathione peroxidase
IgA:	Immunoglobulin A
IL-1 β :	Interleukin-1 beta
IL-6:	Interleukin-6
LDH:	Lactate dehydrogenase

LPS:	Lipopolysaccharide
MDA:	Malondialdehyde
NF- κ B:	Nuclear factor-kappa B
p-NF- κ B p65:	Phospho-nuclear factor-kappa B p65
ROS:	Reactive oxygen species
SOD:	Superoxide dismutase
TGF- β 1:	Transforming growth factor- β 1
TLR4:	Toll-like receptor 4
TNF- α :	Tumor necrosis factor alpha
ZO-1:	Zonula occludens-1
4-HNE:	4-Hydroxynonenal
8-OHdG:	8-Hydroxy-2'-deoxyguanosin.

Data Availability

All data supporting the conclusions of this manuscript are provided in the table and figures. Please contact the authors for data requests.

Ethical Approval

All the animal procedures were performed according to the guidelines of the institutional animal ethics committee and approved by the institutional animal committee of Nankai University (SYXK2019-0001, permission date: Jan 11, 2019).

Conflicts of Interest

The authors declare no conflicts of interest.

Authors' Contributions

Ting Xia did the conceptualization and writing. Bin Fang did the writing—original draft, data curation, and formal analysis. Chaoyan Kang, Yuxuan Zhao, and Xiao Qiang did the data curation and formal analysis. Xiaodong Zhang and Yiming Wang did the methodology and investigation. Tian Zhong did the review and editing. Jianbo Xiao and Min Wang did the administrative, technical, or material support. All data were generated in-house, and no paper mill was used. All authors agree to be accountable for all aspects of work ensuring integrity and accuracy. Ting Xia and Bin Fang contributed equally to this paper.

Acknowledgments

This work was supported by National Natural Science Foundation of China (81600126). We also thank Genedenovo Biotechnology Co. Ltd. for excellent technical assistance of GM analysis.

Supplementary Materials

Figure S1: the schematic diagram of animal experimental protocol. (*Supplementary Materials*)

References

[1] D. A. Simonetto, V. H. Shah, and P. S. Kamath, "Outpatient management of alcohol-related liver disease," *Gastroenterología y Hepatología*, vol. 5, no. 5, pp. 485–493, 2020.

[2] S. Chaudhary and E. H. Forrest, "Alcohol and the liver," *Medicine*, vol. 47, no. 11, pp. 723–727, 2019.

[3] J. I. Cohen, X. C. Chen, and L. E. Nagy, "Redox signaling and the innate immune system in alcoholic liver disease," *Antioxidants & Redox Signaling*, vol. 15, no. 2, pp. 523–534, 2011.

[4] S. Li, H. Y. Tan, N. Wang et al., "The role of oxidative stress and antioxidants in liver diseases," *International Journal of Molecular Sciences*, vol. 16, no. 11, pp. 26087–26124, 2015.

[5] S. Slevin, L. Baiocchi, N. Wu et al., "Kupffer cells: inflammation pathways and cell-cell interactions in alcohol-associated liver disease," *The American Journal of Pathology*, vol. 190, no. 11, pp. 2185–2193, 2020.

[6] S. K. Sarin, A. Pande, and B. Schnabl, "Microbiome as a therapeutic target in alcohol-related liver disease," *Journal of Hepatology*, vol. 70, no. 2, pp. 260–272, 2019.

[7] M. T. Siddiqui and G. A. M. Cresci, "Microbiota reprogramming for treatment of alcohol-related liver disease," *Translational Research*, vol. 226, pp. 26–38, 2020.

[8] L. Jia, X. Chang, S. Qian et al., "Hepatocyte toll-like receptor 4 deficiency protects against alcohol-induced fatty liver disease," *Molecular Metabolism*, vol. 14, pp. 121–129, 2018.

[9] G. Szabo, "Gut-liver axis in alcoholic liver disease," *Gastroenterology*, vol. 148, no. 1, pp. 30–36, 2015.

[10] Z. A. Ratan, M. F. Haidere, Y. H. Hong et al., "Pharmacological potential of ginseng and its major component ginsenosides," *Journal of Ginseng Research*, vol. 45, no. 2, pp. 199–210, 2021.

[11] Y. T. Wang, J. Y. You, Y. Yu et al., "Analysis of ginsenosides in *Panax ginseng* in high pressure microwave-assisted extraction," *Food Chemistry*, vol. 110, no. 1, pp. 161–167, 2008.

[12] W. Xie, P. Zhou, Y. F. Sun et al., "Protective effects and target network analysis of ginsenoside Rg1 in cerebral ischemia and reperfusion injury: a comprehensive overview of experimental studies," *Cell*, vol. 7, no. 12, p. 270, 2018.

[13] Y. Xu, C. Yang, S. Zhang, J. Li, Q. Xiao, and W. Huang, "Ginsenoside Rg1 protects against non-alcoholic fatty liver disease by ameliorating lipid peroxidation, endoplasmic reticulum stress, and inflammasome activation," *Biological & Pharmaceutical Bulletin*, vol. 41, no. 11, pp. 1638–1644, 2018.

[14] C. Ning, X. Gao, C. Wang et al., "Ginsenoside Rg1 protects against acetaminophen-induced liver injury via activating Nrf2 signaling pathway *in vivo* and *in vitro*," *Regulatory Toxicology and Pharmacology*, vol. 98, pp. 58–68, 2018.

[15] A. L. Hopkins, "Network pharmacology: the next paradigm in drug discovery," *Nature Chemical Biology*, vol. 4, no. 11, pp. 682–690, 2008.

[16] M. J. Shi, X. L. Yan, B. S. Dong, W. N. Yang, S. B. Su, and H. Zhang, "A network pharmacology approach to investigating the mechanism of *tanshinone IIA* for the treatment of liver fibrosis," *Journal of Ethnopharmacology*, vol. 253, article 112689, 2020.

[17] C. Q. Ning, X. G. Gao, C. Y. Wang et al., "Hepatoprotective effect of ginsenoside Rg1 from *Panax ginseng* on carbon tetrachloride-induced acute liver injury by activating Nrf2 signaling pathway in mice," *Environmental Toxicology*, vol. 33, no. 10, pp. 1050–1060, 2018.








[18] N. Jiang, J. W. Lv, H. X. Wang et al., "Ginsenoside Rg1 ameliorates chronic social defeat stress-induced depressive-like behaviors and hippocampal neuroinflammation," *Life Sciences*, vol. 252, article 117669, 2020.

[19] J. H. Kim, Y. S. Yi, M. Y. Kim, and J. Y. Cho, "Role of ginsenosides, the main active components of *Panax ginseng*, in

- inflammatory responses and diseases," *Journal of Ginseng Research*, vol. 41, no. 4, pp. 435–443, 2017.
- [20] E. Albano, "Alcohol, oxidative stress and free radical damage," *The Proceedings of the Nutrition Society*, vol. 65, no. 3, pp. 278–290, 2006.
- [21] I. Milosevic, A. Vujovic, A. Barac et al., "Gut-liver axis, gut microbiota, and its modulation in the management of liver diseases: a review of the literature," *International Journal of Molecular Sciences*, vol. 20, no. 2, p. 395, 2019.
- [22] Y. R. Shim and W. I. Jeong, "Recent advances of sterile inflammation and inter-organ cross-talk in alcoholic liver disease," *Experimental & Molecular Medicine*, vol. 52, no. 5, pp. 772–780, 2020.
- [23] C. Yang, X. Q. He, J. Q. Zhao, and W. X. Huang, "Hepatoprotection by ginsenoside Rg1 in alcoholic liver disease," *International Immunopharmacology*, vol. 92, article 107327, 2021.
- [24] J. W. Geng, W. Peng, Y. G. Huang, H. Fan, and S. D. Li, "Ginsenoside-Rg1 from *Panax notoginseng* prevents hepatic fibrosis induced by thioacetamide in rats," *European Journal of Pharmacology*, vol. 634, no. 1-3, pp. 162–169, 2010.
- [25] B. Chassaing, L. Etienne-Mesmin, and A. T. Gewirtz, "Microbiota-liver axis in hepatic disease," *Hepatology*, vol. 59, no. 1, pp. 328–339, 2014.
- [26] M. A. Hyder, M. Hasan, and A. H. Mohieldein, "Comparative levels of ALT, AST, ALP and GGT in liver associated diseases," *European Journal of Experimental Biology*, vol. 3, pp. 280–284, 2013.
- [27] G. Testino, S. Leone, F. Ansaldi, and P. Borro, "Silymarin and S-adenosyl-L-methionine (SAME): two promising pharmacological agents in case of chronic alcoholic hepatopathy. A review and a point of view," *Minerva Gastroenterologica e Dietologica*, vol. 59, no. 4, pp. 341–356, 2013.
- [28] Z. W. Yi, Y. J. Xia, X. F. Liu, G. Q. Wang, Z. Q. Xiong, and L. Z. Ai, "Antrodin A from mycelium of *Antrodia camphorata* alleviates acute alcoholic liver injury and modulates intestinal flora dysbiosis in mice," *Journal of Ethnopharmacology*, vol. 254, article 112681, 2020.
- [29] H. Cichoż-Lach and A. Michalak, "Oxidative stress as a crucial factor in liver diseases," *World Journal of Gastroenterology*, vol. 20, no. 25, pp. 8082–8091, 2014.
- [30] T. Xia, B. Zhang, S. P. Li et al., "Vinegar extract ameliorates alcohol-induced liver damage associated with the modulation of gut microbiota in mice," *Food & Function*, vol. 11, no. 4, pp. 2898–2909, 2020.
- [31] S. Leclercq, S. Matamoros, P. D. Cani et al., "Intestinal permeability, gut-bacterial dysbiosis, and behavioral markers of alcohol-dependence severity," *Proceedings of the National Academy of Sciences of the United States of America*, vol. 111, no. 42, pp. E4485–E4493, 2014.
- [32] K. Ganesan, J. L. Quiles, M. Daglia, J. Xiao, and B. Xu, "Dietary phytochemicals modulate intestinal epithelial barrier dysfunction and autoimmune diseases," *Food Front.*, vol. 2, no. 3, pp. 357–382, 2021.
- [33] G. Szabo and S. Bala, "Alcoholic liver disease and the gut-liver axis," *World Journal of Gastroenterology*, vol. 16, no. 11, pp. 1321–1329, 2010.
- [34] G. Szabo and J. Petrasek, "Gut-liver axis and sterile signals in the development of alcoholic liver disease," *Alcohol and Alcoholism*, vol. 52, no. 4, pp. 414–424, 2017.
- [35] T. Tanikawa, T. Ishikawa, T. Maekawa, K. Kuronane, and Y. Imai, "Characterization of monoclonal immunoglobulin A and G against Shiga toxin binding subunits produced by intranasal immunization," *Scandinavian Journal of Immunology*, vol. 68, no. 4, pp. 414–422, 2008.
- [36] K. Bandow, J. Kusuyama, M. Shamoto, K. Kakimoto, T. Ohnishi, and T. Matsuguchi, "LPS-induced chemokine expression in both MyD88-dependent and -independent manners is regulated by Cot/Tpl2-ERK axis in macrophages," *FEBS Letters*, vol. 586, no. 10, pp. 1540–1546, 2012.
- [37] H. F. Liu, J. X. Liang, G. S. Xiao, L. K. Ma, and Q. Wang, "Dendrobine suppresses lipopolysaccharide-induced gut inflammation in a co-culture of intestinal epithelial Caco-2 cells and RAW264.7 macrophages," *eFood*, vol. 2, no. 2, pp. 92–99, 2021.
- [38] L. Chen, X. Y. Fan, X. J. Lin et al., "Phenolic extract from *Sonchus oleraceus* L. protects diabetes-related liver injury in rats through TLR4/NF- κ B signaling pathway," *eFood*, vol. 1, no. 1, pp. 77–84, 2020.
- [39] T. Xia, W. H. Duan, Z. J. Zhang et al., "Polyphenol-rich vinegar extract regulates intestinal microbiota and immunity and prevents alcohol-induced inflammation in mice," *Food Research International*, vol. 140, article 110064, 2021.
- [40] F. Carbonero, "Plant-based foods and the gut microbiome: a research profile of Franck Carbonero," *Food Frontiers*, vol. 2, no. 3, pp. 390–391, 2021.
- [41] R. N. Carmody, G. K. Gerber, J. M. L. Jr et al., "Diet dominates host genotype in shaping the murine gut microbiota," *Cell Host & Microbe*, vol. 17, no. 1, pp. 72–84, 2015.
- [42] L. Yang, Y. C. Gao, J. P. Gong et al., "Myricetin ameliorated prediabetes via immunomodulation and gut microbiota interaction," *Food Frontiers*, pp. 1–24, 2022.
- [43] W. Han and X. Zhuang, "Research progress on the next-generation probiotic *Akkermansia muciniphila* in the intestine," *Food Frontiers*, vol. 2, no. 4, pp. 443–448, 2021.
- [44] D. E. Campbell, L. K. Ly, J. M. Ridlon, A. Hsiao, R. J. Whitaker, and P. H. Degnan, "Infection with bacterioides phage BV01 alters the host transcriptome and bile acid metabolism in a common human gut microbe," *Cell Reports*, vol. 32, no. 11, article 108142, 2020.
- [45] S. Hu, J. Wang, Y. Xu et al., "Anti-inflammation effects of fucosylated chondroitin sulphate from *Acaudina molpadioides* by altering gut microbiota in obese mice," *Food & Function*, vol. 10, no. 3, pp. 1736–1746, 2019.
- [46] C. Kong, R. Gao, X. Yan, X. Huang, and H. Qin, "Probiotics improve gut microbiota dysbiosis in obese mice fed a high-fat or high-sucrose diet," *Nutrition*, vol. 60, pp. 175–184, 2019.
- [47] J. P. Arab, M. Arrese, and V. H. Shah, "Gut microbiota in non-alcoholic fatty liver disease and alcohol-related liver disease: current concepts and perspectives," *Hepatology Research*, vol. 50, no. 4, pp. 407–418, 2020.
- [48] S. Leclercq, P. D. Cani, A. M. Neyrinck et al., "Role of intestinal permeability and inflammation in the biological and behavioral control of alcohol-dependent subjects," *Brain, Behavior, and Immunity*, vol. 26, no. 6, pp. 911–918, 2012.

Research Article

Luteolin-Rich Extract of *Thespesia garckeana* F. Hoffm. (Snot Apple) Contains Potential Drug-Like Candidates and Modulates Glycemic and Oxidoinflammatory Aberrations in Experimental Animals

Uchenna Blessing Alozieuwa,¹ Bashir Lawal ,^{2,3} Saidu Sani,⁴ Amos Sunday Onikanni,^{5,6} Obinna Osuji,⁷ Yunusa Olatunji Ibrahim,⁸ Shukurat Bisola Babalola,⁹ Gomaa Mostafa-Hedeab ,^{10,11} Abdulrahman A. Alsayegh ,¹² Sarah Albogami,¹³ Gaber El-Saber Batiha ,¹⁴ Alexander T. H. Wu ,^{15,16,17,18} Hsu-Shan Huang ,^{2,3,19,20} and Carlos Adam Conte-Junior ²¹

¹Department of Biochemistry, Faculty of Natural and Applied Sciences, Veritas University Abuja, FCT-Abuja, Nigeria

²PhD Program for Cancer Molecular Biology and Drug Discovery, College of Medical Science and Technology, Taipei Medical University, Taipei and Academia Sinica, Taipei 11031, Taiwan

³Graduate Institute for Cancer Biology & Drug Discovery, College of Medical Science and Technology, Taipei Medical University, Taipei 11031, Taiwan

⁴Department of Biochemistry and Molecular Biology, Faculty of Science, Federal University Ndufu-Alike Ikwo, P.M., B 1010 Abakaliki, Ebonyi State., Nigeria

⁵Department of Chemical Sciences, Biochemistry Unit, Afe Babalola University, Ado-Ekiti, Ekiti State, Nigeria

⁶College of Medicine, Graduate Institute of Biomedical Science, China Medical University, Taiwan

⁷Department of Chemistry, Faculty of Physical Sciences, Alex-Ekwueme Federal University Ndufu-Alike, Ebonyi State, Nigeria

⁸Department of Biochemistry, Federal University of Technology, Minna, Nigeria

⁹Department of Chemistry, Federal University of Technology, Minna, Nigeria

¹⁰Pharmacology Department & Health Research Unit, Medical College Jouf University, Jouf, Saudi Arabia

¹¹Pharmacology Department Faculty of Medicine, Beni-Suef University, Egypt

¹²Clinical Nutrition Department, Applied Medical Sciences College, Jazan University, Jazan 82817, Saudi Arabia

¹³Department of Biotechnology, College of Science, Taif University, P.O. Box 11099, Taif 21944, Saudi Arabia

¹⁴Department of Pharmacology and Therapeutics, Faculty of Veterinary Medicine, Damanhour University, Damanhour 22511, AlBeheira, Egypt

¹⁵TMU Research Center of Cancer Translational Medicine, Taipei Medical University, Taipei 11031, Taiwan

¹⁶The PhD Program of Translational Medicine, College of Medical Science and Technology, Taipei Medical University, Taipei 11031, Taiwan

¹⁷Clinical Research Center, Taipei Medical University Hospital, Taipei Medical University, Taipei 11031, Taiwan

¹⁸Graduate Institute of Medical Sciences, National Defense Medical Center, Taipei 11490, Taiwan

¹⁹School of Pharmacy, National Defense Medical Center, Taipei 11490, Taiwan

²⁰PhD Program in Biotechnology Research and Development College of Pharmacy, Taipei Medical University, Taipei 11031, Taiwan

²¹Center for Food Analysis (NAL), Technological Development Support Laboratory (LADETEC), Federal University of Rio de Janeiro (UFRJ), Cidade Universitária, Rio de Janeiro 21941-598, Brazil

Correspondence should be addressed to Alexander T. H. Wu; chaw1211@tmu.edu.tw and Hsu-Shan Huang; huanghs99@tmu.edu.tw

Received 23 February 2022; Revised 16 June 2022; Accepted 13 July 2022; Published 30 July 2022

Academic Editor: Cassiano Felipe Gonçalves-de-Albuquerque

Copyright © 2022 Uchenna Blessing Alozieuwa et al. This is an open access article distributed under the Creative Commons Attribution License, which permits unrestricted use, distribution, and reproduction in any medium, provided the original work is properly cited.

The present study evaluated the polyphenolic contents and hypoglycemic, antioxidant, and anti-inflammatory effects of the diethyl ether fraction of *Thespesia garckeana* using various *in vitro* and *in vivo* models. Total phenol and flavonoid contents of the extract were 613.65 ± 2.38 and 152.83 ± 1.56 mg/100 g dry weight, respectively. The extract exhibited *in vitro* antioxidant activities against DPPH, FRAP, LPO, and ABTS with respective half-maximal inhibitory concentration (IC_{50}) values of 30.91 ± 0.23 , 16.81 ± 0.51 , 41.29 ± 1.82 , and 42.39 ± 2.24 μ g/mL. *In vitro* anti-inflammatory studies using membrane stabilization, protein denaturation, and proteinase activities revealed the effectiveness of the extract with respective IC_{50} values of 54.45 ± 2.89 , 93.62 ± 3.04 , and 56.60 ± 2.34 μ g/mL, while *in vitro* hypoglycemic analysis of the extract revealed inhibition of α -amylase (IC_{50} 64.59 ± 3.29 μ g/mL) and enhancement of glucose uptake by yeast cells. Interestingly, the extract demonstrated *in vivo* hypoglycemic and anti-inflammatory effects in streptozotocin- (STZ-) induced diabetic and xylene-induced ear swelling models, respectively. In addition, the extract improved insulin secretion, attenuated pancreatic tissue distortion and oxidative stress, and increased the activities of superoxide dismutase (SOD), catalase, and reduced glutathione (GSH), while reducing the concentration of LPO in the diabetic rats. A high-performance liquid chromatography (HPLC) analysis identified the presence of catechin ($6.81e-1$ ppm), rutin ($8.46e-1$ ppm), myricetin, apigenin ($4.019e-1$ ppm), and luteolin (15.09 ppm) with respective retention times (RTs) of 13.64, 24.269, 27.781, 29.58, and 32.23 min, and these were subjected to a pharmacoinformatics analysis, which revealed their drug-likeness and good pharmacokinetic properties. A docking analysis hinted at the potential of luteolin, the most abundant compound in the extract, for targeting glucose-metabolizing enzymes. Thus, the present study provides preclinical insights into the bioactive constituents of *T. garckeana*, its antioxidant and anti-inflammatory effects, and its potential for the treatment of diabetes.

1. Introduction

Diabetes mellitus (DM) is a category of metabolic disorders that affect glucose, lipid, and protein metabolism and consequently affect the overall health status [1, 2]. The prevalence of diabetes is very high, affecting millions of people globally [3]. It is characterized by the development of insulin resistance, abnormal insulin signaling, oxidative stress [4], inflammation [5], and organ dysfunction [6], leading to decreased life quality and high mortality [7]. In the past few decades, DM, particularly type 2 DM (T2DM), has become a global health problem that threatens millions of people in both developed and developing countries [2]. According to the Diabetes Atlas (10th edition) of the International Diabetes Federation (IDF) [8], there are 537 million people living with diabetes in 2021, and about 783 million cases are expected by 2045 [8], compared to 151 million sufferers in 2000 [9–11].

Although the pathogenesis and pathophysiology of T2DM are extremely complex and not fully understood, accumulating evidence has revealed that free radical generation, oxidative stress, and inflammation play critical implicative roles in the development of T2DM [12, 13]. Inflammation, a complex physiological response to injury and infection, plays a pivotal role in the development of chronic disorders, including arthritis, asthma, atherosclerosis, and cancers [14]. Experimental and clinical studies have provided evidence of the important roles of inflammation in DM [15, 16]. Reactive nitrogen species (RNS) and reactive oxygen species (ROS) were clearly implicated in the pathology of various diseases including aging, cancers, cardiovascular diseases (CVD), neuronal impairment, and diabetic complications [14, 17]. During hyperglycemia, the generation of free radicals (RNS and ROS), autooxidation of glucose, and depletion of endogenous antioxidants lead to oxidative stress and inflammatory conditions, apoptosis of pancreatic islet β cells, and impaired insulin secretion [18]. In addition, inflammation and oxidative stress also contribute to the development of diabetic complications such as hypertension, retinopathies, nephropathies, and neuropathies [19, 20].

Over the years, synthetic and chemical antioxidants and antidiabetic medications have been developed for treating diabetes and its associated complications [21]. However, their clinical applications have been limited by the loss of efficacy and more importantly by associated side effects including diarrhea, lactic acidosis, flatulence, and acute hepatitis [22, 23]. Hence, there is a need to focus on seeking new alternatives. Moreover, evidence from traditional health practice and experimental studies suggested that natural products, particularly medicinal plants, are rich sources of therapeutic agents that can offer better efficacy with minimal side effects compared to conventional therapies [24–26]. Thus, exploring bioactive metabolites from medicinal plants may offer multieffect glycemic control while modulating oxidoinflammatory aberrations and improving prognoses of diabetes and its complications.

Thespesia garckeana F. Hoffm., known as ‘snot apple’ or ‘kola of Tula,’ is a reputable medicinal plant that is widely distributed in Africa and some other tropical countries [27, 28]. As a traditional medicine, the plant is widely used for treating rheumatism, infections, diabetes, liver diseases, reproductive impairment, and other diseases [28, 29]. Several biological activities of the plant were also reported in the literature [28, 30–32]. Herein, we evaluated the hypoglycemic, antioxidant, and anti-inflammatory effects of the diethyl ether fraction of *T. garckeana* using various *in vitro* and *in vivo* models. Further characterization of the extract revealed the presence of various compounds which were subjected to a pharmacoinformatics analysis, thus unveiling their drug-likeness, good pharmacokinetics (PKs), and potential hypoglycemic properties. Altogether, our study established the preclinical efficacy of *T. garckeana* extract against inflammation, glycemic impairment, and oxidative stress, suggesting its future use for developing alternative therapies against diabetes complications.

2. Materials and Methods

2.1. Plant Collection, Extraction, and Fractionation. *Thespesia garckeana* plant was obtained from the Gombe State,

Tula Village, Kaltungo Local Government Area (Latitude 9°48'51"N and Longitude 11°18'32"E) Nigeria. Plant authentication was conducted at the Ebonyi State University, Nigeria, and a specimen voucher identification number was reported. The pulp was air-dried to a constant dry weight at 25°C for 2 weeks before being subjected to pulverization with the aid of a mechanical blending machine. Three hundred grams (300 g) of the pulverized sample was subjected to cold maceration in 1.5 L of methanol for 72 h. The resulting crude extract after concentration was further subjected to fractionation with diethyl ether, ethyl acetate, and n-butanol successively and the resulting fractions; diethyl ether (7.9% yield), ethyl acetate (3.10% yield), and n-butanol (2.45% yield) fractions were concentrated in a rotary vacuum evaporator under reduced pressure. The resulting diethyl ether fraction (diethyl-eth_ *T. garckeana*) which demonstrated the highest yield and phytochemical compositions in preliminary screening was used for subsequent analysis.

2.2. Analysis of Total Phenol and Flavonoid Contents. The total flavonoid content of the diethyl-eth fraction of *T. garckeana* was determined according to the method of Chang et al. [33], while the total phenol content was evaluated using the Folin-Ciocalteu's reagent as described by Singleton et al. [34]. Gallic acid (total phenols) and quercetin (total flavonoids) were used to prepare the calibration curves.

2.3. In Vitro Antioxidant Assays. The *in vitro* antioxidant effects of diethyl-eth_ *T. garckeana* were evaluated using the DPPH, FRAP, ABTS, and LPO assays. The DPPH assay was conducted based on the scavenge ability of the extract on DPPH radicals [35]. FRAP activity was assayed according to the method of Oyaizu [35]. The extract was incubated in K₃[Fe(CN)₆] supplemented phosphate buffer at 50°C for 20 min, after which 10% TCA was added. The resulting solution was centrifuged and color development in the presence of 0.1% ferric chloride was monitored at 700 nm. The thiobarbituric acid-reactive substance (TBARS) protocol described by Panjamurthy et al. [36] was employed for the LPO analysis, while the ABTS assay was done as reported by Re et al. [37].

2.4. In Vitro Hypoglycemic Assays. Standard analysis protocol for alpha-amylase inhibition described by Worthington [38] was employed for the *in vitro* hypoglycemic analysis of the extract. Briefly, the extract/acarbose (12.5 ~ 100 µg/mL) mixed in an enzymatic porcine pancreatic solution was incubated with a starch solution for 30 min at 37°C, followed by the addition of 10 µL of HCl (1 M) and iodine reagent for color development. In the analysis of glucose uptake by yeast cells, glucose solution (5 ~ 25 mM) was incubated (37°C for 10 min) with the extract. A yeast suspension was added to the reaction mixture and incubated for another 45-60 min, after which glucose concentration was estimated.

2.5. In Vitro Anti-Inflammatory Assays. The *in vitro* anti-inflammatory activities of the diethyl-eth_ *T. garckeana* were evaluated by using the human red blood cell (RBC and

HRBC) membrane stabilization, inhibition of protein denaturation, and proteinase inhibitory assays. The protein denaturation inhibition was assayed as described of Mizushima and Kobayashi [39], while the method of Oyedepo and Femurewa [40] was used for the proteinase inhibition assay. In the HRBC assay, a 10% human RBC suspension was incubated with the extract solution at 50-55°C for 30 min [41]. The resulting solution was centrifuged at 2500 rpm for 5 min, and the reaction changes were monitored at 560 nm.

2.6. Analysis of Toxicity and Extract Tolerated Dose. The diethyl-eth_ *T. garckeana* was subjected to an acute toxicity study to evaluate its safety and maximum tolerated dose upon oral administration according to the protocol described by Lorke [42]. Briefly, a total of eighteen (18) rats were grouped into six (6) and administered with 10, 100, 1000, 1600, 2800, and 5000 mg/kg bw of diethyl-eth_ *T. garckeana* to groups I-VI, respectively. The extract was administered once orally, after which the rats were observed for any sign of adverse toxicity and mortality within 14 days' period.

2.7. Oral Glucose Tolerance Test (OGTT). The OGTT was conducted according to the method described by Sisay et al. [43]. A total of twelve (12) overnight starved rats were grouped into 5 (3 rats per group) and treated with 2.0 mL/kg normal saline, 5 mg/kg glibenclamide, 150 mg/kg, and 300 mg/kg diethyl-eth_ *T. garckeana* for groups I-IV, respectively. After 30 minutes of treatment, 2 g/kg bw of glucose was orally administered to rats in each group. The blood glucose level was determined at 0 minutes (basal blood glucose level) and at intervals of 30 for a period of 2 hrs.

2.8. Analysis of In Vivo Antidiabetic Activities in Rats. The diethyl-eth_ *T. garckeana* was evaluated for the *in vivo* antidiabetic effects in albino rats. Experimental rats were acquired from the experimental rodent facility of AE-FUNAI, Nigeria. Animal experiments were consented by the ethical committee of the AE-FUNAI, Nigeria. Streptozotocin (STZ; 40 mg/kg) was intraperitoneally administered to overnight starved rats, and rats with FBS > 200 mg/kg were considered diabetic [44]. Rats were rationed into 4 groups and treated with the diethyl-eth_ *T. garckeana* at 150 (group 1) and 300 mg/kg (group 2), 2 mL/kg normal saline (group 3), and 200 mg/kg metformin (group 4). Healthy rats were assigned to the fifth group to serve as the control. Treatments were given on a daily basis for a period of 21 days via oral route. The fasting blood sugar concentration and animals' body weight were checked during the study period.

2.9. In Vivo Anti-Inflammatory Analysis (Xylene-Induced Ear Swelling Assay). The diethyl-eth_ *T. garckeana* was evaluated for its *in vivo* anti-inflammatory effects in mice using a xylene-induced ear edema test [45, 46]. Healthy mice were divided into five ($n = 5$) groups and administered orally with saline, diethyl-eth_ *T. garckeana* (150 and 300 mg/kg BW), or 200 mg/kg aspirin for 7 days. On the eighth day, the posterior and anterior surfaces of the rat's right ear were scrubbed with 0.02 mL aliquot of xylene. Measurement of the ear thickness was done, and the ear inflammation volume was

computed as the weight differences between the right and the left ears. Orbital blood sample was also collected and analyzed for the levels of white blood cell counts.

2.10. Collection and Processing of Samples. Experimental rats were euthanized under diethyl ether vapor for few minutes, and blood were obtained through cardiac puncture. The coagulated blood was centrifuged for 15 min ($3000 \times g$) and the separated serum were stored at 4°C [47, 48]. The rat's pancreases and liver tissues were harvested, homogenized in phosphate buffer (0.1 M, pH 7.4, 1:10 *w/v*) and centrifuged at $10,000 \times g$ for 10 min at 4°C .

2.11. Tissue Assays for Antioxidant Parameters. The *in vivo* antioxidant effects of the extract were evaluated in liver homogenate using the lipid peroxidation (LPO), superoxide dismutase (SOD), reduced glutathione (GSH), and catalase (CAT) assays. The LPO assay was conducted by measuring the tissue levels of TBARSs [49], while the modified colorimetric method of Kum-Tatt and Tan [50] was adopted for GSH assay. The activity of SOD was evaluated by using an established protocol [51]. The tissue homogenate was incubated with carbonate buffer (pH 10.2) in the presence of 0.3 mM adrenaline. The increase in absorbance at an interval of 30 s were monitored at 480 nm [51]. CAT activity was determined using a standard protocol [52]. The liver homogenate (0.1 mL) in phosphate buffer (0.01 M, pH 7.0) was incubated with 2M hydrogen peroxide (H_2O_2) for 20 min. This was followed by the addition of a dichromate acetate reagent to terminate the reaction. The changes in absorbances were monitored at the wavelength of 620 nm and the activity of CAT was expressed as a unit of $\text{H}_2\text{O}_2/\text{mg}$ protein [52].

2.12. Measurement of Insulin Levels. The Insulin ELISA kit (Calbiochem-Behring Corp, CA; catalog no. IN374S) was used for the analysis of pancreatic and serum insulin concentrations as per the manual instructions.

2.13. High-Performance Liquid Chromatography (HPLC). The dietl-eth_T. garckeana was subjected to HPLC analysis according to the method described in our previous study [20]. A hundred milligram (100 mg) of dietl-eth_T. garckeana was dissolved in five millilitres (5 mL) of an HPLC grade methanol. The extract solution was filtered and run on the HPLC (Agilent Technologies 1200) with the following chromatographic conditions: stationary phase (Hypersil BDS C18), mobile phase (acetonitrile and 0.1% formic acid), column dimension of 250 mm \times 4.0 mm, injection volume of 10 μL , a flow rate of 0.6 mL/min, detector wavelength of 280 nm, and at gradient mode of elution.

2.14. Pharmacoinformatics Analysis

2.14.1. Analysis of Drug-Likeness and ADMET-PK Properties. The most abundant compounds identified from the dietl-eth_T. garckeana were subjected to analysis of physicochemical properties, drug-likeness, PKs (ADMET), and medicinal chemistry using the ADMET-Lab, ADMET-Sar, and Swiss-ADME servers [53]. The human-intestinal

absorption and permeability by blood-brain barrier (BBB) were modeled through the BOILED-EGG and support vector machine (SVM) tools [53].

2.14.2. Analysis of Ligand Receptor Interactions Using Molecular Docking. The most abundant bioactive compound characterized from the extract was subjected to an analysis of ligand-receptor interactions using molecular docking. The crystal three-dimensional (3D) forms of the compounds were built by the Avogadro visualization tool (version 1.XX) [54], while the PDB files of the target receptors including alpha-amylase and alpha-glucosidase were downloaded from the Protein Data Bank. The mol2 files were transformed into PDB files using PyMOL software, while the PDB formats were transformed to PDBQT using AutoDock Vina [55]. Water molecules were detached, while hydrogen atoms in polar forms and Kollman charges were added to the compounds during predocking preparations [56, 57]. The version 8 of AutoDock Vina tool was used for the receptor-ligand docking as described in previous studies [56, 58, 59], while visualization was conducted using the PyMOL and Discovery studio tools [60].

2.15. Data Analysis. The GraphPad vers. 8.0 software was used for the statistical analysis of replicate data. The one-way type analysis of variance and Student's *t*-test were explored for statistical comparison between groups. Data are presented as the mean \pm standard error of the mean (SEM), and statistical annotation of "*", "**", or "***" were used to represent the statistical differences corresponding to " $p < 0.05$," " $p < 0.001$," and " $p < 0.001$," respectively.

3. Results and Discussion

3.1. Thespesia garckeana Fraction Exhibited Dose-Related In Vitro Antioxidant Activities. Plants, particularly those that are rich source of flavonoid and polyphenolic compounds, have been effective against various diseases including cancers and diabetes [61]. These phytochemicals are known to exhibit several biological activities including antioxidants, antimicrobial, anticancer, anti-inflammatory, and antidiabetic, etc. [62]. Interestingly, our results demonstrated that dietl-eth_T. garckeana contains total phenol contents of 613.65 ± 2.38 mg/100 g dry weight and total flavonoid contents of 152.83 ± 1.56 mg/100 g dry weight. The flavonoid and phenol contents reported in this study are higher than the total phenol (34.32 and 25.34 mg/100 g) and flavonoid (13.45 and 7.65 mg/100 g) contents previously reported for crude methanol and ethyl-acetate extracts of *T. garckeana* [28]. The presence of significant-high amounts of phenol and flavonoid contents in the dietl-eth_T. garckeana suggested the ability of the extract to scavenge free radicals, prevent oxidative stress and manage diabetes [62].

The formation of free radicals and oxidative stress play important roles implicated in the development of T2DM [12, 13]. Therefore, the role of antioxidants in preventing the formation of free radicals is crucial to the control of DM [61]. Our *in vitro* studies revealed significant and dose-related antioxidant activities of the dietl-eth_T.

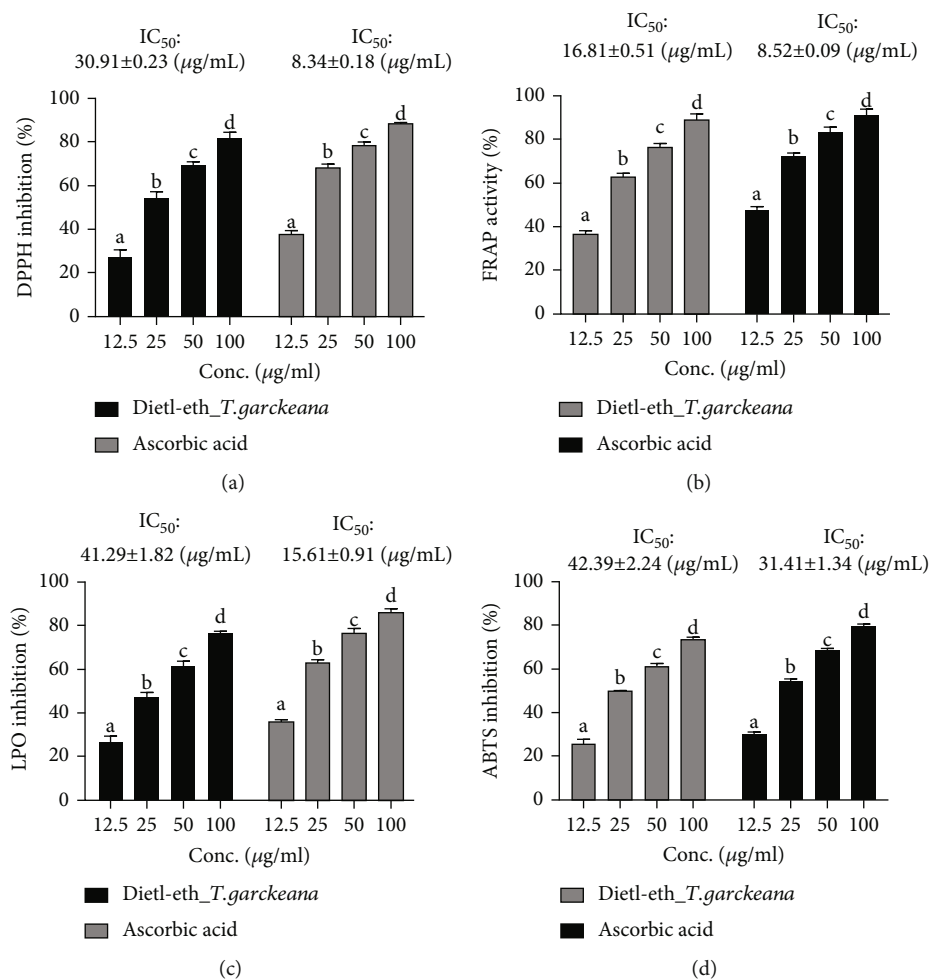


FIGURE 1: Diethyl-ether fraction of *Thespesia garckeana* (diethyl-ether fraction of *T. garckeana*) exhibited dose-related *in vitro* antioxidant activities. Bar graphs showing extract dose vs. inhibition effect of the dietl-ether fraction of *T. garckeana* on (a) 2,2-diphenyl-1-picrylhydrazyl (DPPH) radicals, (b) ferric-reducing antioxidant power (FRAP), (c) lipid peroxidation (LPO), and (d) 2,2'-azino-bis (3-ethylbenzthiazoline-6-sulphonic acid) (ABTS). Values are the mean \pm SEM ($n = 3$). Different superscript letters indicate significant differences ($p < 0.05$) between the extract doses. IC₅₀: half-maximal inhibitory concentration.

garckeana in four different *in vitro* models of antioxidant assays; DPPH, FRAP, LPO, and ABTS, with IC₅₀ values of 30.91 ± 0.23 (Figure 1(a)), 16.81 ± 0.51 (Figure 1(b)), 41.29 ± 1.82 (Figure 1(c)), and 42.39 ± 2.24 µg/mL (Figure 1(d)), respectively. Through the analysis of TBARS levels, we uncovered that the malonaldehyde (MDA) formation has been significantly compromised by dietl-ether fraction of *T. garckeana*. In addition, the hydrogen donating properties of the extract as a means of radical scavenging has been demonstrated by the DPPH assay [63]. The reduction of Fe³⁺/Fe²⁺ as suggested by the FRAP assay also confirmed the scavenging ability of dietl-ether fraction of *T. garckeana*, thereby transforming reactive radical element into a more stable product. Phenols and flavonoids were implicated in the free radical scavenging abilities and defensive properties of plants against various illnesses [64]. Consequently, the high flavonoid and phenolic contents of dietl-ether fraction of *T. garckeana* may be appraised for the antioxidants activity of the extract.

3.2. *Thespesia garckeana* Fraction Exhibited Dose-Related In Vitro Anti-Inflammatory Activities. Inflammation, a complex physiological response to injury and infection, plays a pivotal role in the development of chronic disorders, including arthritis, asthma, atherosclerosis, cancer, and DM [14]. Interestingly, *T. garckeana* exhibited dose-related anti-inflammatory activities. Our *in vitro* anti-inflammatory studies using membrane stabilization, protein denaturation, and proteinase activities revealed the effectiveness of the extract with respective IC₅₀ values of 54.45 ± 2.89 , 93.62 ± 3.04 , and 56.60 ± 2.34 µg/mL (Figures 2(a)–2(c)). The erythrocytic membrane exhibits some similarities with the lysosomal membrane and its stabilization implies that the dietl-ether fraction of *T. garckeana* may well stabilize lysosomal membranes [65]. This is important for restraining the inflammatory response by halting the lysosomal releases of active neutrophils, such as proteases and bacterial enzymes, which may induce tissue inflammation and injury upon extracellular release [66]. The dietl-ether fraction of *T. garckeana* promoting

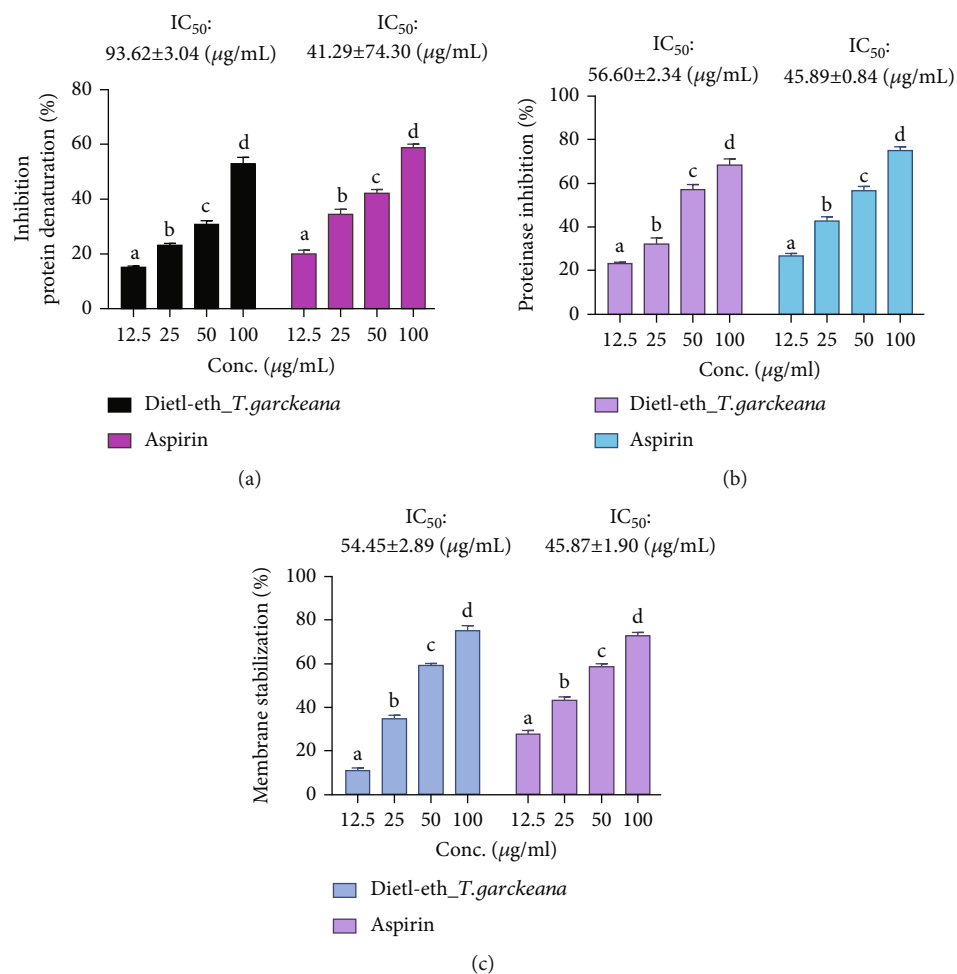


FIGURE 2: Diethyl-ether fraction of *Thespesia garckeana* (dietl-eth_*T. garckeana*) exhibited dose-related anti-inflammatory activities *in vitro*. Bar graphs showing extract dose vs. inhibition effect of the dietl-eth_*T. garckeana* on (a) inhibition of protein denaturation, (b) inhibition of proteinase activities, and (c) membrane stabilization. Values are the mean \pm SEM ($n = 3$). IC_{50} : half-maximal inhibitory concentration.

membrane stabilization also suggests its potential for mitigating phospholipases release thereby preventing the generation and activities of inflammatory mediators [67].

Proteinase inhibitory activity was studied to further explain the anti-inflammatory mechanism of dietl-eth_*T. garckeana*. Neutrophils contains high levels of serine proteinase [65] that plays a vital tissue damaging role during inflammatory events [68] and inhibitors of this proteinase protect against the damage [69]. Interestingly, the dietl-eth_*T. garckeana* exhibited dose related antiproteinase activity with IC_{50} of 56.60 \pm 2.34 $\mu\text{g/mL}$. These results provide evidence for proteinase inhibition as an additional mechanism of the anti-inflammatory effect of dietl-eth_*T. garckeana*. Altogether, these data suggest that *T. garckeana* extract would be useful for averting inflammatory complications that could be associated with diabetes.

3.3. *Thespesia garckeana* Fraction Demonstrated Safety Profile in Acute Oral Toxicity Study. According to the data obtained from this study, dietl-eth_*T. garckeana* demonstrated a good safety profile with a 50%lethal dose (LD_{50}) > 500 mg/kg bw and a safe dose of 1000 mg/kg bw (Table 1). No animal mortality was observed during the study. In addition,

rats dosed with 10, 1000, and 1000 mg/kg bw were bereft of adverse health or physiological changes, suggesting the safety of the extract at doses \leq 100 mg/kg bw. Conversely, rats treated with 1600, 2800, and 5000 mg/kg exhibited varying levels of adverse effects ranging from restlessness, hyperactivity, redness of the eyes, and profuse breathing. According to Hodge and Sterner [70], substances that demonstrate an LD_{50} of 5000 mg/kg in rats should be considered harmless substances. This result is in agreement with the findings of Iyojo et al. [71], who reported no mortality in rabbits administered different extracts of *T. garckeana* pulp at 5000 mg/kg. Altogether, dietl-eth_*T. garckeana* demonstrated high LD_{50} and is safe for use as an oral remedy at doses \leq 100 mg/kg bw. Thus, the high safety of this plant upon oral exposure justifies the widespread use of this plant for treating various ailments by traditional healers in northern Nigeria.

3.4. *Thespesia garckeana* Fraction Exhibited Dose-Related In Vitro Hypoglycemic Activities. The inhibition of carbohydrate-metabolizing enzymes and regulation of blood glucose levels are very critical to the management of DM [72]. The dietl-eth_*T. garckeana* also demonstrated a

TABLE 1: Acute oral toxicity profiles of diethyl-ether fraction of *Thespesia garckeana* in rats.

diethyl-ether fraction of <i>T. garckeana</i> (mg/kg)	Mortality	Adverse effect	Two weeks' posttreatment observation (loss of weight, sign of toxicity)
10	0/3	Nil	Nil
100	0/3	Nil	Nil
1000	0/3	Nil (MTD)	Nil
1600	0/3	Restlessness (10-15 mins)	Nil
2900	0/3	Rubbing of the mouth on the wall of the cage (about 20 mins); restlessness (about 20 mins)	Nil
5000	0/3	Rubbing of cages (20-30 mins), redness of the eye (30 mins), restlessness (30 mins), fur erection (30 mins), profuse breathing (24 h), weakness (only in day 2)	Nil

MTD: maximum tolerated dose.

hypoglycemic effect via inhibition of α -amylase (IC_{50} : $64.59 \pm 3.29 \mu\text{g/mL}$) and enhanced glucose (5, 10, and 25 mM) uptake by yeast cells in a dose-related manner (Figure 3).

Inhibitors of α -amylase, a starch-catabolizing enzyme, are widely used as oral hypoglycemic agents for the regulation of sugar levels of T2DM patient [73]. However, most of these inhibitors are synthetic with off-limit activity and associated side effects [74]. Consequently, the current results verify that the diethyl-ether fraction of *T. garckeana* exerts its hypoglycemic via the inhibition of carbohydrate-catabolizing enzymes, including the α -amylase. The inhibitory activities of the diethyl-ether fraction of *T. garckeana* on α -amylase activities suggests the attenuation of postprandial blood glucose increase by decreasing the carbohydrates flow into the bloodstream after carbohydrate intake [75].

Glucose is preferred by yeast as a primary source of fuel, and glucose absorption by yeast cells is simulate that occurring in the mammalian intestinal lumen; thus, yeast has become a commonly used model to study glucose absorption [76]. According to the present study, diethyl-ether fraction of *T. garckeana* significantly enhanced glucose uptake by yeast cells in a dose-related manner. This is important for the efficient utilization and control of glucose levels. Interestingly, a linear relationship between glucose concentration and rates of glucose uptake by the yeast cells was observed. This is in line with the finding of Keshala et al. [61] who reported a concentration-dependent increase in glucose uptake by yeast cells in the presence of plant extract. Collectively, the diethyl-ether fraction of *T. garckeana* exhibited dose-related *in vitro* hypoglycemic activities and, thus, could be regarded as a natural product with potential for the management of DM.

3.5. The diethyl-ether fraction of *T. garckeana* demonstrated hypoglycemic effect in Oral glucose tolerance test. In the present study, the evaluation of diethyl-ether fraction of *T. garckeana* for possible antidiabetic effect was also conducted using the oral glucose tolerance test. There were initial increases in glucose levels at 30 minutes of glucose dosing after which progressive decreases were observed from 30 minutes to 2 hours in all the treatment as well as the control rats. However, significant ($p < 0.05$) decreases in the glucose levels of rats treated with the 300 mg/kg diethyl-ether fraction of *T. garckeana*, as well as the standard

control group, were observed when compared with the non-treated glucose-loaded rats (Figure 4). Our result has shown that the extract can decrease postprandial blood glucose levels and improve peripheral glucose uptake and utilization in rats. The OGTT corroborate the effects of the plant extracts on insulin release by the B cells of the islets of Langerhans in diabetic rats. Postprandial elevated sugar level is with an increased risk of diabetes-associated secondary complications [77]. Therefore, the OGTT suggested the potential usefulness of diethyl-ether fraction of *T. garckeana* in T2DM subjects with insulin resistance prone to elevated postprandial sugar level [78].

3.6. The diethyl-ether fraction of *T. garckeana* Demonstrated Hypoglycemic Effect and Improved Insulin Secretion in STZ-Induced Diabetic Rats. Previous experimental studies have proved the therapeutic efficacy of medicinal plants in animal models of diabetes, inflammation, and oxidative stress-associated diseases [79–81]. The *in vivo* antidiabetic effects of the diethyl-ether fraction of *T. garckeana* was evaluated in STZ-induced diabetic rats. Interestingly, our *in vitro* findings corroborated with the data generated *in vivo*. We found that treatment of the STZ-induced diabetic rats with diethyl-ether fraction of *T. garckeana* caused significant and progressive decreases in the fasting blood sugar (FBS) levels in a dose-related manner (Figure 5(a), Table 2) and prevented the body weight loss (Figure 5(b), Table 3), while diabetic untreated rats exhibited progressive increases in FBS levels and body weight loss. At the end of the treatment duration, the extract at 150 and 300 mg/kg demonstrated 62.67% and 78.88% hypoglycemic effects, respectively, while metformin demonstrated higher hypoglycemic activity of 84.25%. Thus, the gradual decreases in FBS and improvement of body weight recorded in the *T. garckeana*-receiving animal when compared with the untreated diabetic rats presaged the ameliorative effects of the fraction on experimentally induced diabetes.

Under a physiological condition, the pancreatic cells regulate blood glucose levels by regulating β cells of Islets of Langerhans's activity through insulin secretions. Therefore, the hyperglycemia induced by STZ may be attributed to the impairment of insulin release as a consequence of the destroyed β cells of Islets of Langerhans in the pancreas

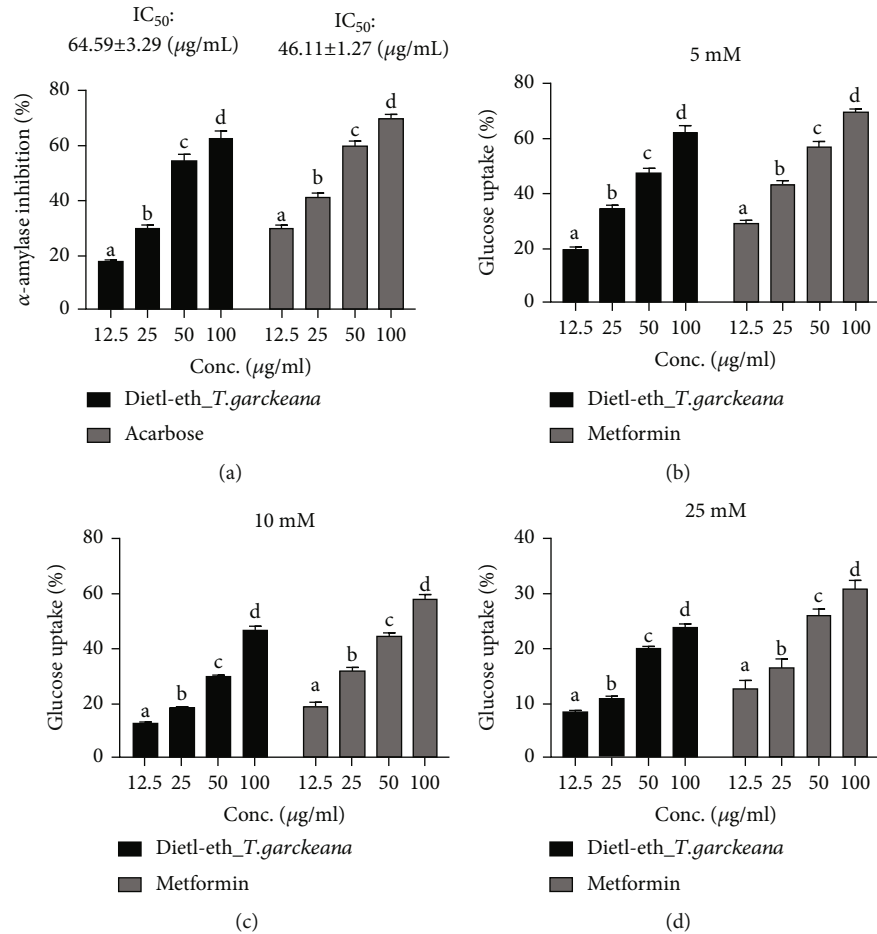


FIGURE 3: Diethyl-ether fraction of *Thespesia garckeana* (diethyl-eth_T. garckeana) demonstrated *in vitro* dose-related hypoglycemic activities. Bar graphs showing extract dose vs. inhibitory effects of the dietl-eth_T. garckeana on (a) α -amylase inhibition, and yeast glucose uptake inhibition at (b) 5, (c) 10, and (d) 25 mM concentrations of glucose. Values are the mean \pm SEM ($n = 3$). IC₅₀: half-maximal inhibitory concentration.

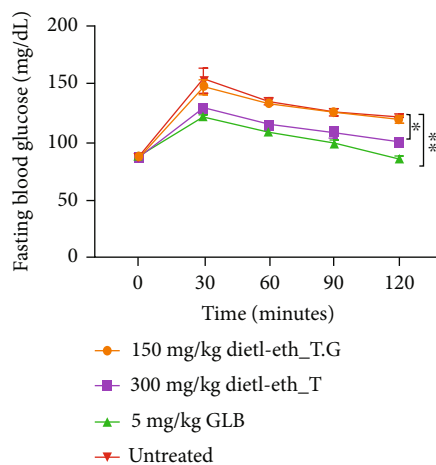


FIGURE 4: Effect of the diethyl-ether fraction of *Thespesia garckeana* (diethyl-eth_T. garckeana) on blood glucose levels in oral glucose tolerance test (OGTT). Values are the mean \pm SEM. * $p < 0.05$, ** $p < 0.01$.

[82]. Indeed, we found that the STZ-induced diabetic non-treated rats exhibited significant ($p < 0.05$) decreases in the pancreatic and serum (Figure 5(c)) insulin levels as well as histological distortion of the pancreas (Figure 5(d)) when compared with the control rats, while administrations of the dietl-eth_T. garckeana significantly ($p < 0.01$) increased the serum and pancreatic insulin levels of the 300 mg/kg-treated diabetic rats only. The serum insulin level in 150 mg/kg-treated rats was not significantly ($p > 0.05$) different from diabetic nontreated rats. Furthermore, the pancreatic section of the STZ-induced diabetic nontreated rats shows a pancreatic architecture with loose connective tissue. The parenchymatous portion of acini and islet are distorted and most enriched by adipose tissue (Figure 5(d)). However, in a similar architecture to the normal control rats, the pancreatic section of rats treated with metformin, and the 300 mg/kg extract receiving rats show the well-preserved pancreatic architectures, comprising lobules of exocrine acini separated by thin fibrous septa. Normal islets of Langerhans are seen, and there were no features of significant inflammation or damage seen. These ameliorative effects

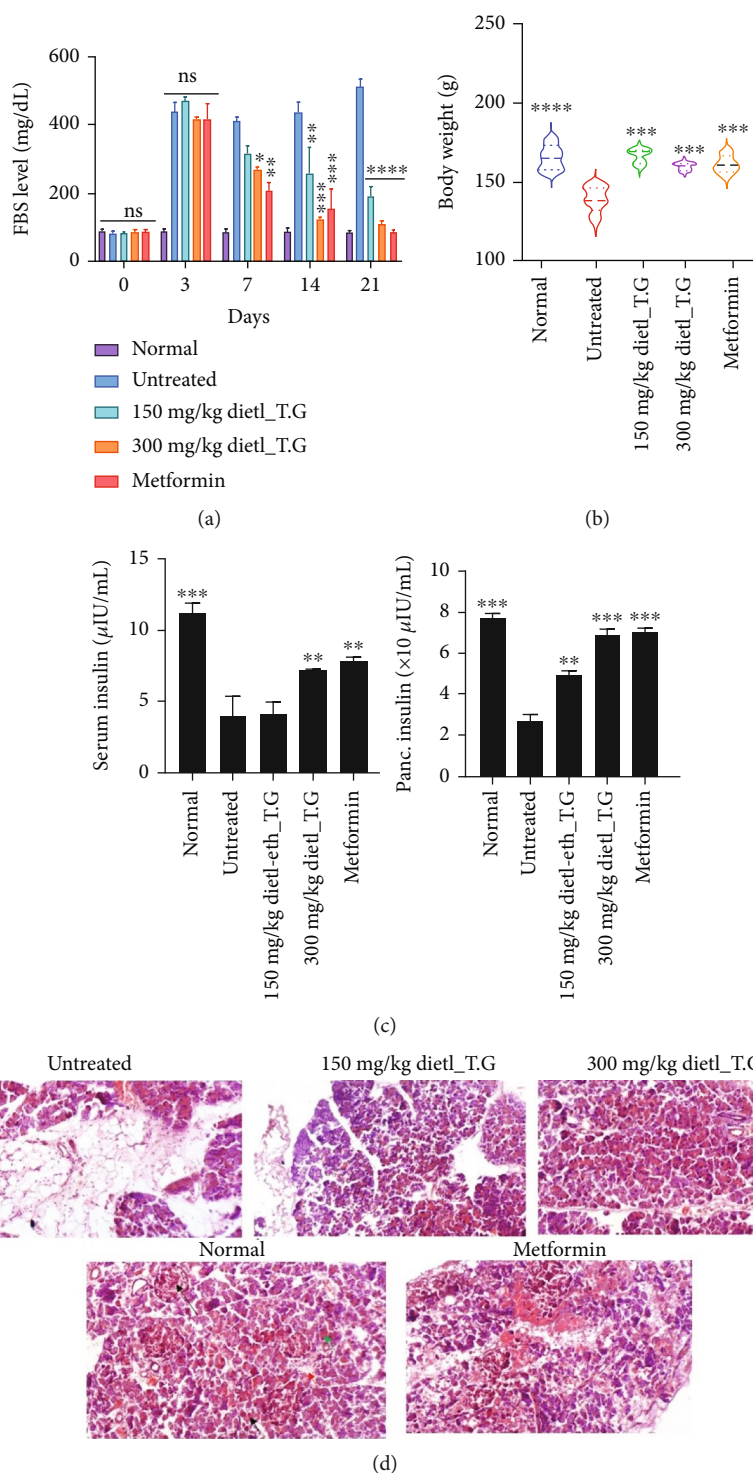


FIGURE 5: Diethyl-ether fraction of *Thespesia garckeana* (dietl-eth_ *T. garckeana*) demonstrated a hypoglycemic effect and improved insulin secretion in STZ-induced diabetic rats. Bar graph showing the effects of the dietl-eth_ *T. garckeana* on (a) fasting blood glucose, (b) body weight, and (c) pancreatic and insulin levels in diabetic rats. (d) Cross-section of the STZ-induced diabetic rat's pancreas administered dietl-eth_ *T. garckeana*. Long arrow: islet of Langerhans; short arrow: interlobular septum; red arrow: pancreatic duct; green arrow: acini. Values are the mean \pm SEM. “* $p < 0.05$,” “*** $p < 0.01$,” “**** $p < 0.001$,” and “***** $p < 0.0001$ ”.

of the extract on pancreatic architecture, activity, and insulin secretion might have promoted the effective glucose uptake and utilization [83] and thus restored the

glycemic status of the rats. Altogether, this study provides preclinical evidence supporting the potential therapeutic benefits of dietl-eth_ *T. garckeana* in stimulating insulin

TABLE 2: Effect of diethyl-ether fraction of *Thespesia garckeana* on blood glucose levels in STZ-induced diabetic rats.

Groups	0	3	7	14	21	Glucose reduction (%)
Normal	89.66 ± 1.76	88.06 ± 3.60	87.06 ± 4.58	90.66 ± 3.71	85.05 ± 1.15	—
Untreated	84.05 ± 3.00	442.50 ± 17.50	415.5 ± 5.500	441.50 ± 18.50	518.50 ± 12.50	—
150 mg/kg Dietl_T.G	82.03 ± 3.01	474.50 ± 6.50	319.50 ± 14.50	258.5 ± 54.5	193.55 ± 19.05	62.67
300 mg/kg Dietl_T.G	87.00 ± 3.00	419.50 ± 2.50	269.60 ± 4.40	125.70 ± 4.30	109.46 ± 5.87	78.88
Metformin	86.00 ± 2.08	433.33 ± 24.03	210.66 ± 15.76	169.33 ± 35.25	81.66 ± 4.25	84.25

Dietl_T.G: diethyl-ether fraction of *Thespesia garckeana*.

TABLE 3: Effect of diethyl-ether fraction of *Thespesia garckeana* on body weight gain in STZ-induced diabetic rats.

Groups	0	3	7	14	21	Weight gain (%)
Normal	157.05 ± 2.00	159.01 ± 1.54	165.22 ± 1.31	169.80 ± 1.29	176.53 ± 2.64	11.05 ± 0.19
Untreated	146.85 ± 3.86	146.03 ± 9.38	138.83 ± 8.60	136.17 ± 4.05	126.79 ± 3.30	-15.82 ± 0.03
150 mg/kg Dietl_T.G	163.26 ± 9.92	160.26 ± 8.93	169.25 ± 10.64	169.60 ± 8.61	169.33 ± 5.30	4.01 ± 2.85
300 mg/kg Dietl_T.G	158.27 ± 0.72	156.42 ± 1.34	160.63 ± 0.51	161.54 ± 0.68	162.19 ± 1.08	2.40 ± 1.09
Metformin	160.20 ± 0.88	154.37 ± 2.84	158.42 ± 4.19	163.93 ± 3.81	169.60 ± 1.49	5.53 ± 0.31

Dietl_T.G: diethyl-ether fraction of *Thespesia garckeana*.

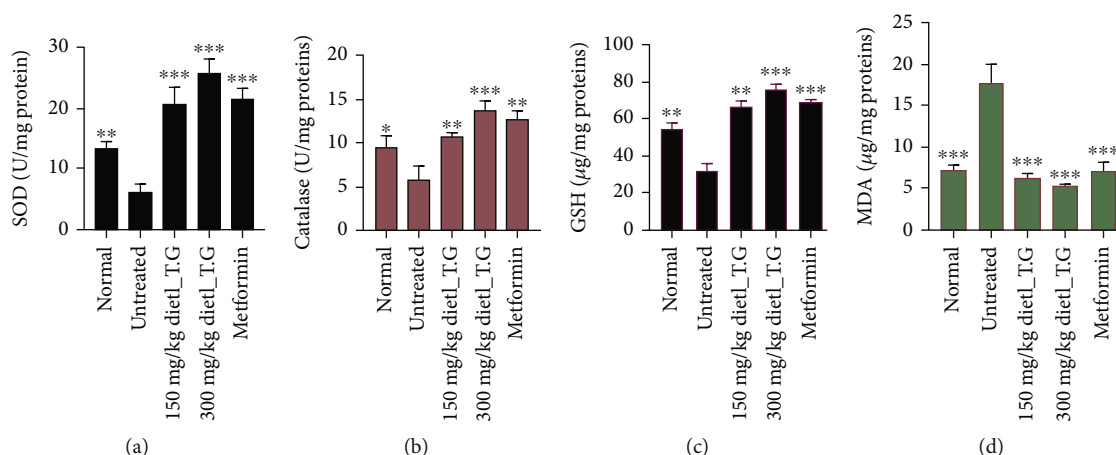


FIGURE 6: The diethyl-ether fraction of *Thespesia* (dietl-eth_T.) *garckeana* demonstrated antioxidant activities in diabetic rats. Bar graphs show the effect of the dietl-eth_T. *garckeana* on levels of (a) superoxide dismutase (SOD), (b) catalase (CAT), (c) reduced glutathione (GSH), (d), and malonaldehyde (MDA) in diabetic rats. Data = mean ± SD, $n = 3$. “*** $p < 0.001$,” “** $p < 0.01$,” and “* $p < 0.05$ ”.

secretion and attenuating hyperglycemia in streptozotocin-induced diabetic rats.

3.7. The dietl-eth_T. garckeana Exhibited Antioxidant Activities in Rats with STZ-Induced Diabetes. Inflammation and oxidative stress contribute to the development of diabetic complications such as hypertension, retinopathies, nephropathies, and neuropathies [19, 20]. The generation levels of ROS are controlled by the levels endogenous antioxidant including CAT, GSH, and SOD [84, 85]. In the present study, analysis of liver biochemical parameters of oxidative stress in rats with STZ-induced diabetes revealed significant decreases in the liver activities of antioxidant enzymes including SOD ($p < 0.01$; Figure 6(a)), CAT ($p < 0.05$;

Figure 6(b)), and GSH ($p < 0.01$; Figure 6(c)) and increased MDA levels ($p < 0.001$; Figure 6(d)) in STZ-induced diabetic rats compared to the respective normal controls.

The liver is a central detoxification organ of the body and plays a vital role in regulating glucose homeostasis [86]. As a group of insulin-sensitive tissues, the liver is among the primary organs highly susceptible to the effects of hyperglycemia-provoked oxidative stress, which may impair liver integrity [87]. Hyperglycemia, mainly caused by insulin resistance, induces the generation of free radicals by the activated Kupffer cells (phagocytic hepatic macrophages) that help in maintaining the integrity of liver cells [88]. However, these cells are highly susceptible to the effects of the free radicals generated by their own

TABLE 4: *In vitro* anti-inflammatory effects of the diethyl-ether fraction of *Thespesia* (diethyl-eth_ *T.*) *garckeana*.

Treatment	Dose (mg/kg BW)	Swelling rate	WBCs ($\times 10^9$)
diethyl-eth_ <i>T. garckeana</i>	150	16.71 \pm 1.19***	106.00 \pm 1.73***
diethyl-eth_ <i>T. garckeana</i>	300	10.41 \pm 1.56***	98.00 \pm 1.1561***
Aspirin	200	13.67 \pm 1.20***	101.00 \pm 3.46***
Untreated control	2.5 mL/normal saline	77.33 \pm 1.76	178.346 \pm 3.46
Normal control	Normal control	—	106.00 \pm 2.31***

Values are the mean \pm SD ($n = 3$). BW: body weight; WBCs: white blood cells; *** $p < 0.001$.

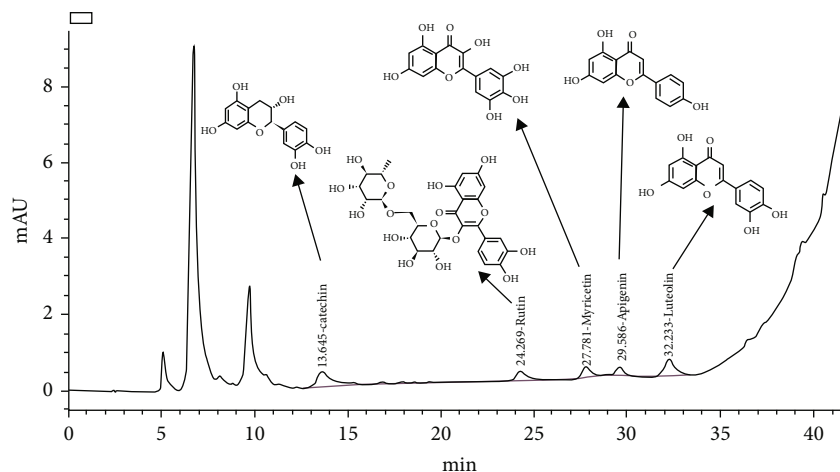


FIGURE 7: High-performance liquid chromatography (HPLC) chromatogram and chemical structures of bioactive compounds identified from the diethyl-ether fraction of *Thespesia garckeana*.

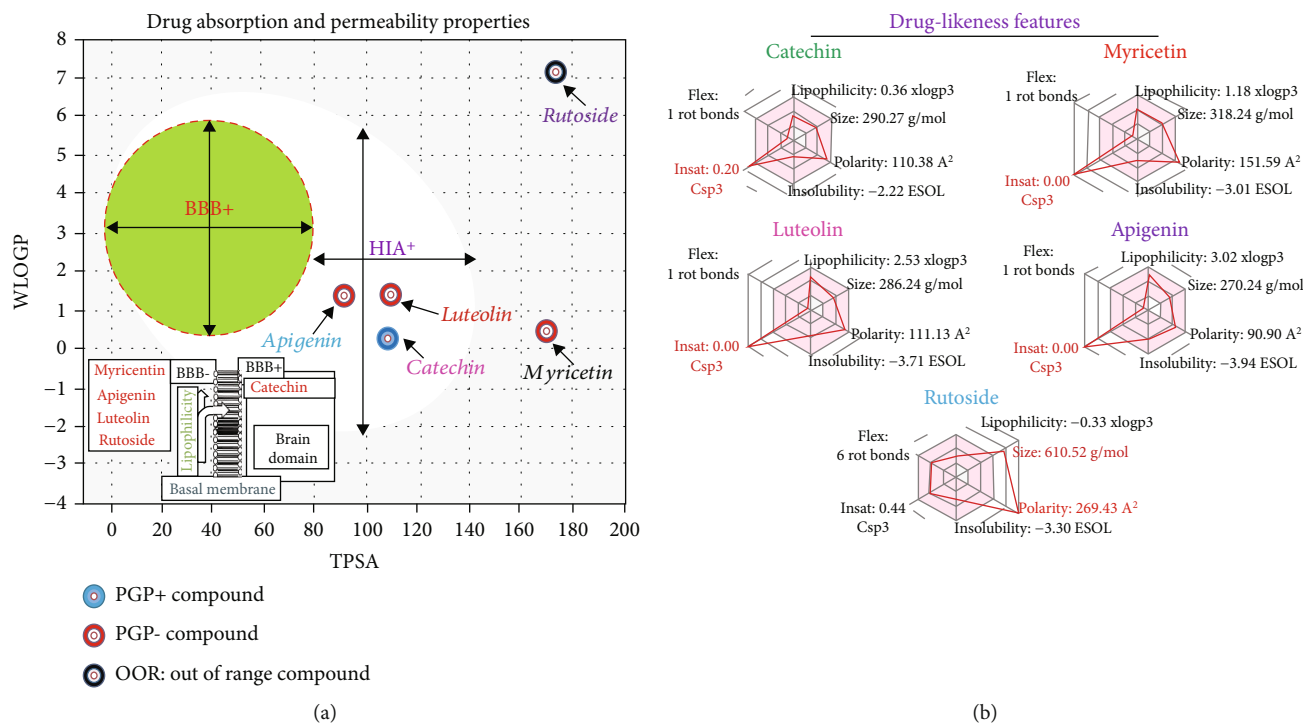


FIGURE 8: Drug-likeness and permeability simulation of compounds identified from the diethyl-eth_ *T. garckeana* (a) absorption and permeability and (b) drug-likeness modeling of compounds from the diethyl-ether fraction of *Thespesia garckeana*.

TABLE 5: Pharmacokinetic_drug-likeness characteristic of the compounds from the diethyl-ether fraction of *Thespesia garckeana*.

	Property	Rutin	Myricetin	Apigenin	Luteolin	Catechin
Physicochemical	Molecular weight	610.521	318.237	270.24	286.239	290.271
	Logp	-1.687	1.694	2.57	2.282	1.546
	HB acceptor	16	8	5	6	6
	HB donor	10	6	3	4	5
Absorption	TPSA	269.43	151.59	90.9	111.13	110.38
	LogS (solubility)	315.283 $\mu\text{g/mL}$	191.757 $\mu\text{g/mL}$	68.667 $\mu\text{g/mL}$	90.101 $\mu\text{g/mL}$	273.403 $\mu\text{g/mL}$
	LogD7.4	0.992	-0.068	0.487	0.302	0.115
	Logp	-1.687	1.694	2.577	2.282	1.546
Distribution	Papp (colorectal adenocarcinoma permeability)	-6.606 cm/s	-6.63 cm/s	-4.985 cm/s	-5.123 cm/s	-4.637 cm/s
	P-glycoprotein-inhibitor	-(0.365)	-(0.208)	-(0.328)	-(0.366)	-(0.223)
	P-glycoprotein-substrate	-(0.168)	-(0.064)	-(0.023)	-(0.038)	-(0.045)
	Intestinal absorption (HIA)	-(0.21)	+(0.438)	+(0.531)	-(0.438)	-(0.401)
Metabolism	Bioavailability	+(0.572)	+(0.557)	+(0.542)	+(0.557)	-(0.487)
	Plasma protein binding (PPB)	76.65%	76.65%	90.031%	91.796%	93.86%
	VD (L/kg)	-1.052	-1.391	-0.578	-0.934	-0.67
	Blood brain barrier	-(0.018)	-(0.369)	-(0.464)	-(0.464)	+++ (0.708)
Elimination	CYP-1A2 inhibitor	-(0.197)	+++ (0.968)	+++ (0.987)	+++ (0.968)	-(0.034)
	CYP-1A2 subst.	-(0.258)	-(0.376)	-(0.408)	-(0.412)	-(0.368)
	CYP-3A4 inhibitor	+(0.518)	-(0.459)	+++ (0.931)	++ (0.867)	-(0.221)
	CYP-3A4 subst.	-(0.418)	-(0.33)	-(0.37)	-(0.328)	-(0.398)
Toxicity/alert	CYP-2C9 inhibitor	-(0.199)	+(0.656)	-(0.12)	-(0.071)	-(0.028)
	CYP-2C9 subst.	-(0.298)	+(0.557)	+(0.631)	-(0.496)	-(0.049)
	CYP-2C19 inhibitor	-(0.072)	-(0.068)	-(0.124)	-(0.124)	-(0.431)
	CYP-2C19 subst.	-(0.49)	-(0.345)	-(0.412)	+(0.542)	-(0.476)
Toxicity/alert	CYP-2D6 inhibitor	-(0.29)	-(0.318)	+(0.611)	-(0.463)	-(0.367)
	CYP-2D6 subst.	-(0.218)	-(0.18)	-(0.488)	-(0.401)	+(0.523)
	T 1/2 (half-life time)	2.138 h	0.915 h	1.331 h	0.745 h	0.720 h
	Clearance rate (mL/min/kg)	0.641	1.709	1.885	1.919	1.914
Toxicity/alert	hERG blocker	+(0.626)	-(0.353)	+(0.598)	-(0.436)	-(0.371)
	(hepatotoxicity (H-HT))	-(0.154)	-(0.332)	+(0.6)	+(0.592)	-(0.466)
	SkinSen	-(0.235)	-(0.278)	-(0.264)	-(0.278)	-(0.329)
	50% acute toxicity (LD ₅₀ mg/kg)	419.47	648.262	858.518	737.444	860.605

TPSA: topological polar surface area; CYP: cytochrome P450; hERG: human ether-a-go-related gene.

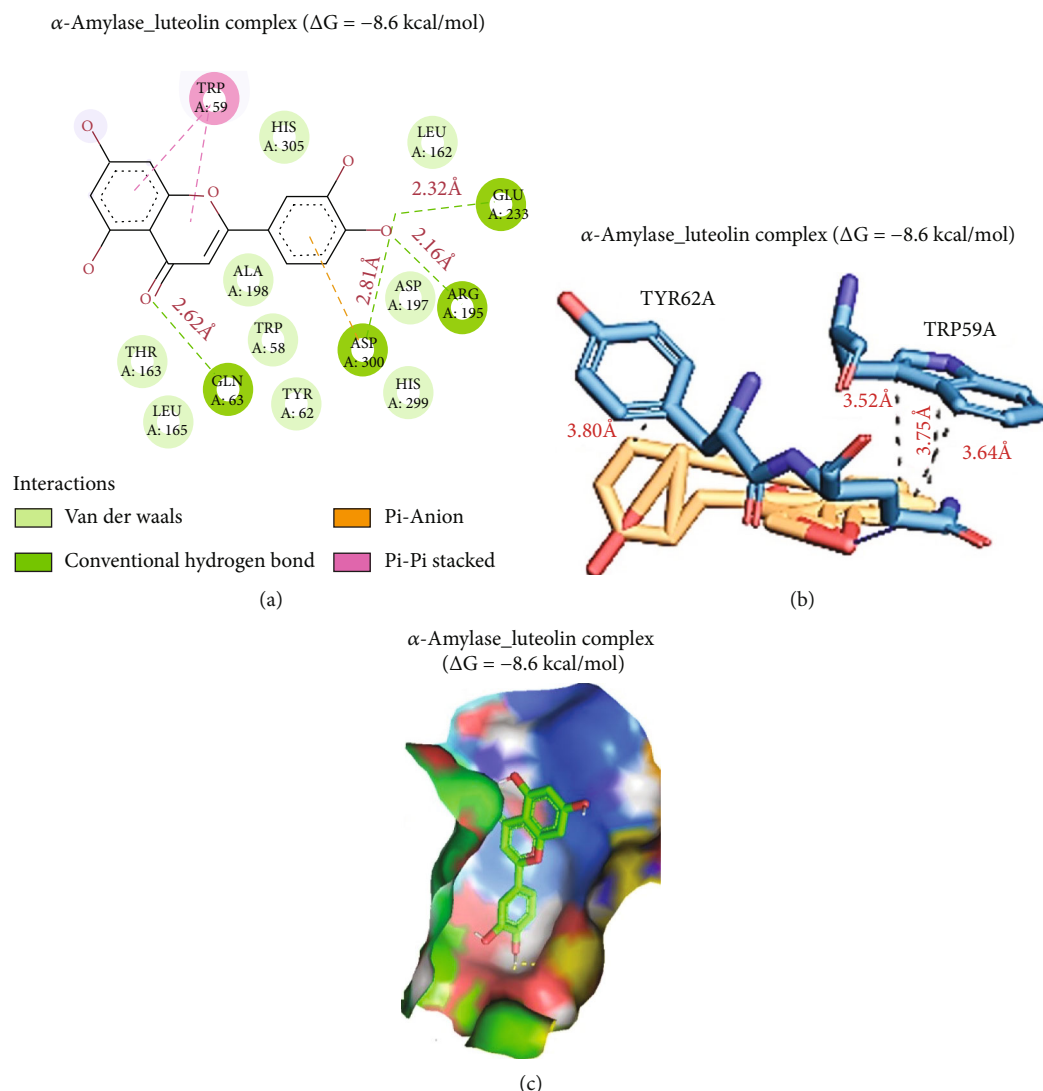


FIGURE 9: Docking of luteolin with α -amylase. (a) 2-Dimensional depiction of the luteolin complex with α -amylase, (b) 3-dimensional (3D) view of the hydrophobic interactions in the complex, and (c) surface representation of luteolin fitted within the binding cavity of the target.

immune reactions and the surrounding cells [89]. The excessive ROS production results in irreversible oxidative alterations of macromolecules including the carbohydrates, lipids, and proteins [90], thereby leading to increased oxidative stress and triggering the cascade of inflammatory events that activates the transcription of proapoptotic genes and damages hepatocytes [91, 92].

Therefore, the reduced SOD and CAT activities in the liver of STZ-induced diabetic rats may be associated with the free radical generations which inturm decreases the activities of these enzymes. GSH is a cellular defense antioxidant molecule that protects against the progressive destruction of the β cell [93]. The increases in free radicals' productions in the diabetic rat result in oxidative damage to membrane lipids and proteins and eventually causes a decrease in the levels of GSH, CAT, and SOD as recorded in rats with STZ-induced diabetes. However, our results revealed that treatment with the dietl-eth_ *T. garckeana* attenuated depleted levels of GSH, CAT, and SOD and

decreased the LPO. These observations validate the potential of dietl-eth_ *T. garckeana* in preventing free radical generation and maintaining the antioxidant status of diabetic rats [93]. This finding corroborated with literature on oxidative stress-alleviating properties of plant extracts in hyperglycemic rodent [94]. Our findings, therefore, revealed the *T. garckeana*'s ability to ameliorate oxidative impairment and restore antioxidant status of rats in hyperglycemic condition.

3.8. The dietl-eth_ *T. garckeana* Demonstrated In Vivo Anti-Inflammatory Activities in Xylene-Induced Ear Swelling of Mice. An *in vivo* analysis of the anti-inflammatory properties using a xylene-induced ear swelling model in mice revealed that the dietl-eth_ *T. garckeana* significantly ($p < 0.001$) prevented xylene-induced ear swelling compared to the untreated control. The anti-inflammatory effect demonstrated by the extract was accompanied by a significant ($p < 0.001$) decrease in WBC counts of treated mice compared to the untreated control (Table 4). Collectively, our

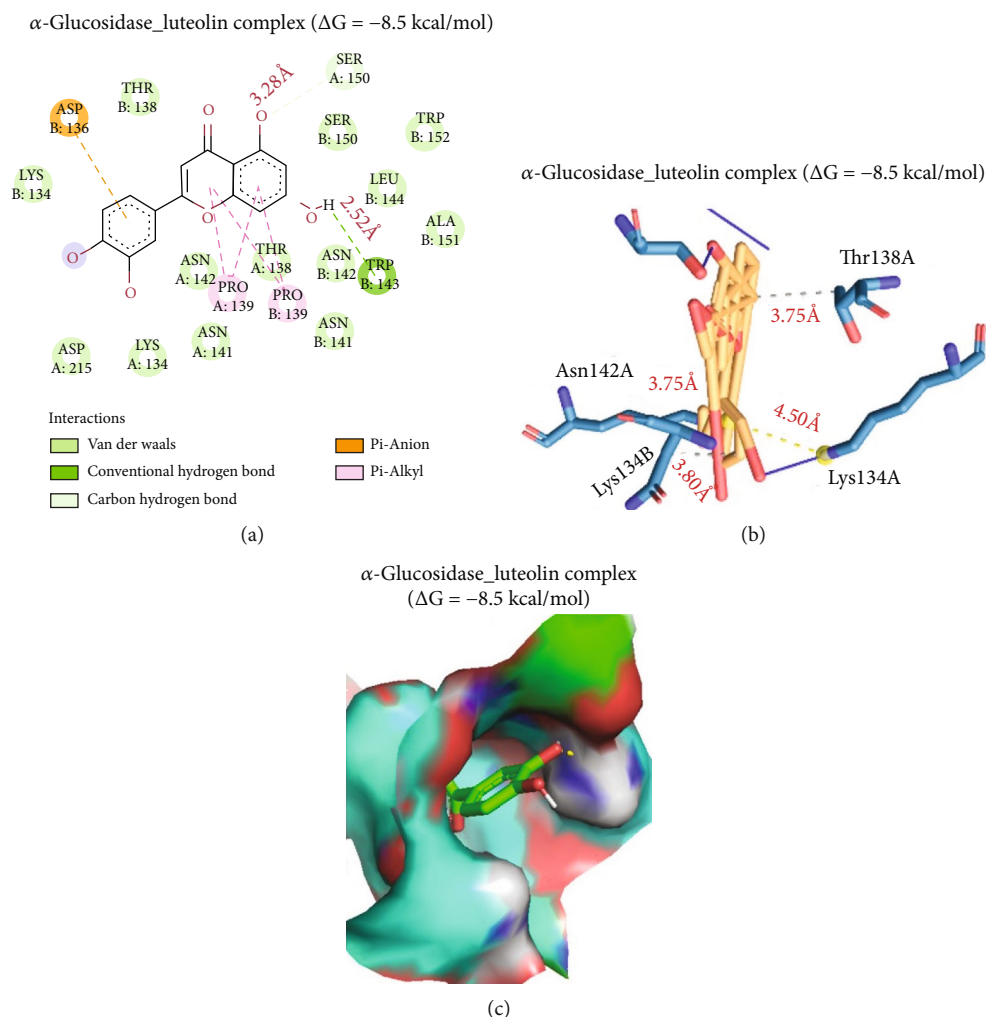


FIGURE 10: Docking of luteolin with α -glucosidase. (a) 2-Dimensional depiction of the luteolin complex with α -glucosidase, (b) 3-dimensional image of the hydrophobic links in the complex, and (c) surface representation of luteolin fitted within the binding cavity of the target.

results demonstrated that the dietl-eth_ *T. garckeana* exhibited an anti-inflammatory effect *in vivo* in addition to its *in vitro* anti-inflammatory effects.

3.9. HPLC Characterization of the dietl-eth_ *T. garckeana*. To characterize the dietl-eth_ *T. garckeana* we conducted an HPLC analysis (Figure 7) and identified the presence of catechin (6.81e-1 ppm), rutin (8.46 e-1 ppm), myricetin, apigenin (4.019 e-1 ppm), and luteolin (15.09 ppm) with respective retention times (RTs) of 13.64, 24.269, 27.781, 29.58, and 32.23 min. HPLC chromatograms and chemical structures of the compounds are displayed in Figure 7. Luteolin appeared to be the most abundant compound in the dietl-eth_ *T. garckeana*, and thus, we evaluated its prospective for targeting glucose metabolizing enzymes and an inflammatory mediator.

3.10. Drug-ADMET and Likeness Modeling of Compounds Identified from the dietl-eth_ *T. garckeana*. The goal of modern drug discovery and development is to identify a drug candidate with desirable properties within the shortest pos-

sible period of time and to avoid time- and cost-consuming approaches which in most cases produces disappointing outcome in the clinics [95, 96]. Hence, drug-likeness and PK analysis is considered an important aspect of the modern drug discovery and development. Our modeling analysis of the drug-PK, and drug-likeness revealed that apigenin, myricetin, luteolin, and catechin identified from the dietl-eth_ *T. garckeana* (Figures 8(a) and 8(b)) were potential drug-like molecules. These compounds passed the drug absorbability test and have desirable bioavailability attribute. P-glycoproteins (P-gp) are responsible for propelling compounds and drugs out of the cells [97]. The identified compounds from the dietl-eth_ *T. garckeana* are nonsubstrate or inhibitors of Pgp, thus suggesting their stability and optimal drug delivery [98]. This was also evident by their absorption and permeability record. The high volume of distribution and low binding of plasma protein by the drug further ascertain the good bioavailability and hinted at the potential good therapeutic index of the compounds but were non-BBB permeant (except for catechin) (Figure 8(b), Table 5). Cytochrome P450 (CYP450) is a

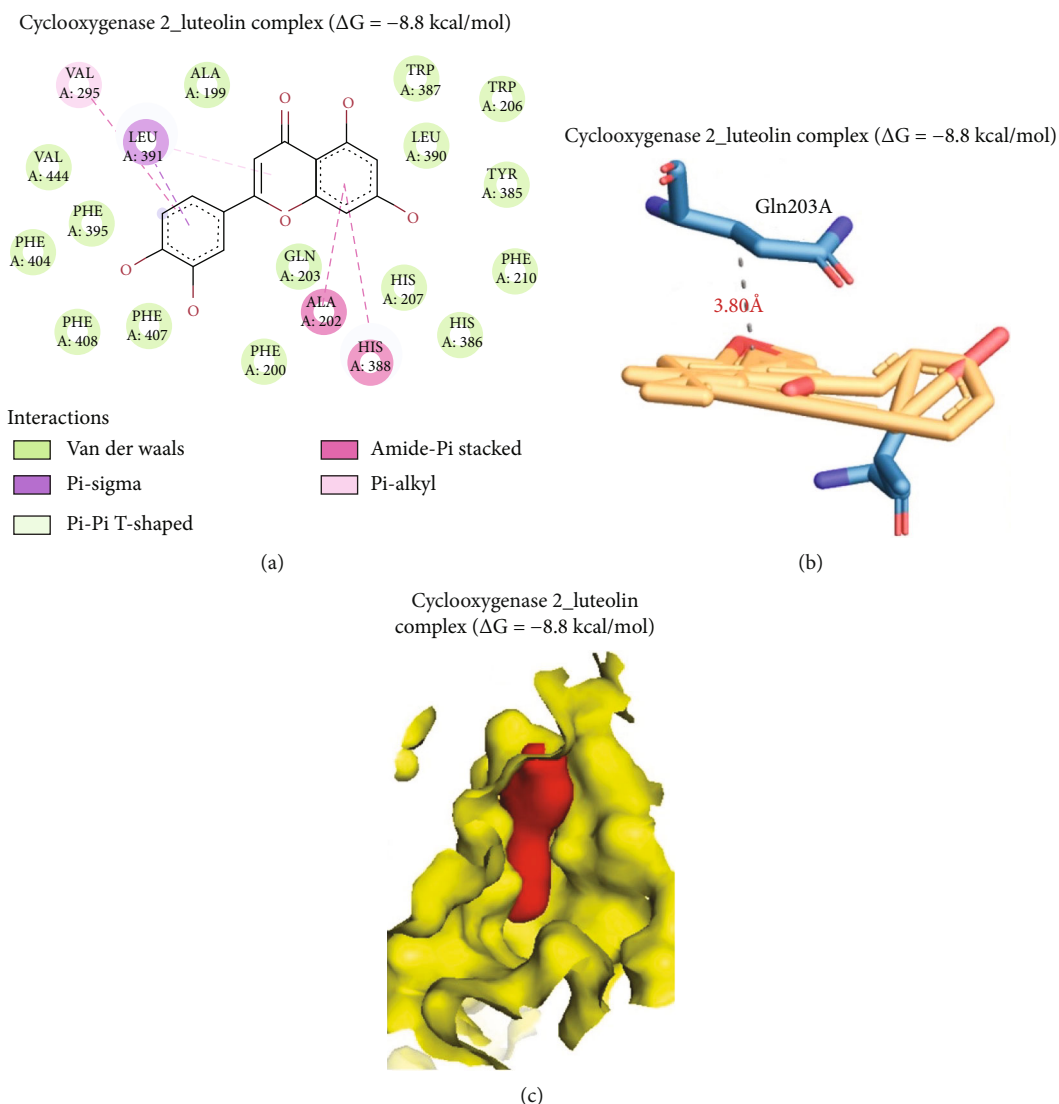


FIGURE 11: Molecular docking of luteolin with cyclooxygenase. (a) A 2-dimensional (2D) image of the luteolin complex with cyclooxygenase, (b) 3-dimensional (3D) image of the hydrophobic interactions in the complex, and (c) surface representation of luteolin fitted within the binding cavity of the target.

heme containing enzyme family that play central metabolic role on exogenous and endogenous substances [99]. Hence, impeding the activities of these enzyme isoforms may lead to deficient drug metabolism and toxic drug accumulation. Providentially, our data indicated that among the 5 isoforms analyzed, the compounds were nonsubstrate and had inhibitor tendencies for cytochrome P450 1A2 (CYP1A2) and CYP3A4. However, they were nonsubstrate nor inhibitors of CYP2C9, CYP2D6, and CYP2C19. Notwithstanding, luteolin demonstrated its ability to be a substrate for P450 CYP3A4 and CYP19, while catechin demonstrated its ability to be a substrate for CYP2D6 (Table 5). The presence of these isoforms in the liver and intestines indicates that these organs are sites of clearance of the compounds. Among the five compounds, luteolin and catechin demonstrated the best and most similar half-lives of 0.745 and 0.720 h, high clearance rates of 1.919 and 1.914 mL/min/kg, and a high safety profile with LD₅₀ values

of 737.444 and 860.605 mg/kg, respectively. Interestingly, luteolin and catechin demonstrated nontoxic attributes; non-human ether go-go-related gene (hERG) blockers, nonhepatotoxic, and were nonirritants in Skinsen assays. Collectively, our analysis revealed that among the five compounds identified, luteolin and catechin exhibited the best drug-PK and drug-likeness characteristic and, thus, were used for receptor-ligand simulation analysis.

3.11. Receptor-Ligand Simulation Analysis Revealed Luteolin's Properties for Targeting Glucose-Metabolizing Enzymes and an Inflammatory Mediator. Molecular docking is an innovative and widely approved strategies for mimicking a small-molecule interaction with a target receptor/protein [57, 100, 101]. It provides qualitative and quantitative estimation of the affinity between a compound and the corresponding protein/receptor [102]. It also gives a preamble insight into mechanistic aspect of the compound and its

behavior when in contact with the corresponding target [103–107]. Docking analysis in the present study revealed that luteolin docked efficiently to the substrate interaction domain of α -amylase with a binding affinity of -8.6 kcal/mol. The complex was bound by four hydrogen bonds to Gln63 (2.62 Å), Asp300 (2.81 Å), Arg195 (2.16 Å), and Glu233 (2.32 Å); pi-pi stacked (Trp59), pi-anion (Asp300), and several van der Waals forces including His305, Leu162, Asp197, His299, Tyr62, Trp58, Ala198, Thr163, and Leu165 (Figure 9). In addition, the complex was bound by four hydrophobic contacts with Thr62A and TRP59A with interaction distances of 3.80, 3.52, 3.75, and 3.64 Å.

Luteolin interacted with glucosidase by -8.5 kcal/mol binding efficacy. Luteolin was interposed to the cavity of glucosidase mainly by hydrogen bonds with Ser150 and TRP143 residues of glucosidase domain in respective proximity of 3.28 and 2.52 Å. The luteolin-glucosidase complex stabilization was also achieved by a pi-anion interaction with Asp136, two alkyl bonding with Pro139A and Pro139B, and several van der Waals forces, including Lys134A, Asp215, Lys134B, Asn141, Asn142A, Thr138, Asn142B, Ala151, Leu144, Ser150, and Trp152, molded at the luteolin backbone. In addition, there were three hydrophobic contacts with Thr138A (3.75 Å), Asn142A (3.75 Å), and Lys134B (3.80 Å), and the carboxylate group of luteolin formed a salt bridge interaction with the binding domain of alpha-glucosidase (Figure 10).

The luteolin-cyclooxygenase complex was stabilized by several pi interactions, including pi-alkyl (Val295), pi-sigma (Leu391), amide-pi-stacked (Ala202), and pi-pi T shape (His388), yielding a high ligand-binding affinity of -8.8 kcal/mol. In total, 13 van der Waals forces with Val444, Phe404, Phe395, Phe407, Phe200, Gln203, His207, His386, Phe210, Tyr385, Leu390, Trp387, and Thr206 residues of the cyclooxygenases were found around the luteolin backbone. In addition, hydrophobic contact of Gln203A with proximity of 3.80 Å was found in the complex (Figure 11). Overall, data presented in this study provides some scientific affirmation based on preclinical model of the anti-inflammatory, hypoglycemic, and antioxidant properties of the *T. garckeana* extract. This hinted at its potentiality for exploration in the development of alternative therapies for the management and possibly treatment of diabetes complication

4. Conclusions

The present study provides experimental evidence of the therapeutic efficacy of the diethyl-ether fraction of *Thespesia garckeana* for treating diabetes. The extract not only enhanced the activities of antioxidant enzymes but also inhibited inflammatory responses, and demonstrated *in vivo* antidiabetic effects in experimental models. The compound most abundant (luteolin) in the fraction demonstrated good drug-PK and drug-likeness and prospective for the targeting of glucose-catabolizing enzymes. Thus, the present study provides preclinical insights into the bioactive constituents of *T. garckeana*, its anti-inflammatory and antioxidant effects, and its potential for treating diabetes.

Data Availability

All data used in this study will be made available upon reasonable request.

Conflicts of Interest

The authors declare no conflict of interest.

Authors' Contributions

All authors read and approved the final version of the manuscript. Uchenna Blessing Alozieuwa and Bashir Lawal contributed equally to this work.

Acknowledgments

ATHW is funded by the Ministry of Science and Technology, Taiwan (111-2314-B-038 -142 and 111-2314-B-038 -098). The authors would like to extend their sincere appreciation to the Taif University Researchers Supporting Project number (TURSP-2020/202) Taif University, Taif, Saudi Arabia.

References

- [1] R. A. DeFronzo, "Pathogenesis of type 2 diabetes mellitus," *Medical clinics*, vol. 88, no. 4, pp. 787–835, ix, 2004.
- [2] L. M. Janssen, M. Hilgsmann, A. M. Elissen et al., "Burden of disease of type 2 diabetes mellitus: cost of illness and quality of life estimated using the Maastricht Study," *Diabetic Medicine*, vol. 2020, p. 37, 2020.
- [3] R. A. DeFronzo, E. Ferrannini, L. Groop et al., "Type 2 diabetes mellitus," *Nature reviews Disease primers*, vol. 1, pp. 1–22, 2015.
- [4] A. Maritim, R. A. Sanders, and J. B. Watkins, "Diabetes, oxidative stress, and antioxidants: a review," *Journal of Biochemical and Molecular Toxicology*, vol. 17, no. 1, pp. 24–38, 2003.
- [5] S. Tsalamandris, A. S. Antonopoulos, E. Oikonomou et al., "The role of inflammation in diabetes: current concepts and future perspectives," *European cardiology review*, vol. 14, no. 1, pp. 50–59, 2019.
- [6] Y. Wang, J. Zhai, D. Yang et al., "Antioxidant, anti-inflammatory, and antidiabetic activities of bioactive compounds from the fruits of *Livistona chinensis* based on network pharmacology prediction," *Oxidative Medicine and Cellular Longevity*, vol. 2021, 2021.
- [7] M. Piero, G. Nzaro, and J. Njagi, "Diabetes mellitus—a devastating metabolic disorder," *Asian journal of biomedical and pharmaceutical sciences*, vol. 4, no. 40, pp. 1–7, 2015.
- [8] H. Sun, P. Saeedi, S. Karuranga et al., "IDF Diabetes Atlas: global, regional and country-level diabetes prevalence estimates for 2021 and projections for 2045," *Diabetes Research and Clinical Practice*, vol. 183, p. 109119, 2022.
- [9] N. Cho, J. Shaw, S. Karuranga et al., "IDF Diabetes Atlas: global estimates of diabetes prevalence for 2017 and projections for 2045," *Diabetes Research and Clinical Practice*, vol. 138, pp. 271–281, 2018.
- [10] O. A. Ojo, M. A. Okesola, L. I. Ekakitie et al., "Gongronema latifolium Benth. leaf extract attenuates diabetes-induced neuropathy via inhibition of cognitive, oxidative stress and inflammatory response," *Journal of the Science of Food and Agriculture*, vol. 100, no. 12, pp. 4504–4511, 2020.

- [11] D. R. Whiting, L. Guariguata, C. Weil, and J. Shaw, "IDF Diabetes Atlas: global estimates of the prevalence of diabetes for 2011 and 2030," *Diabetes Research and Clinical Practice*, vol. 94, no. 3, pp. 311–321, 2011.
- [12] Z. Li, Y.-N. Geng, J.-D. Jiang, and W.-J. Kong, "Antioxidant and anti-inflammatory activities of berberine in the treatment of diabetes mellitus," *Evidence-based Complementary and Alternative Medicine*, vol. 2014, 2014.
- [13] M. Al-Zharani, A. F. Nasr, M. O. Noman, R. Conte, and E. H. E. Y. Amal, "Antioxidant, anti-inflammatory and antidiabetic properties of LC-MS/MS identified polyphenols from coriander seeds," *Molecules*, vol. 26, no. 2, p. 487, 2021.
- [14] S.-S. Huang, S.-Y. Su, J.-S. Chang et al., "Antioxidants, anti-inflammatory, and antidiabetic effects of the aqueous extracts from Glycine species and its bioactive compounds," *Botanical Studies*, vol. 57, no. 1, p. 38, 2016.
- [15] M. Y. Donath and S. E. Shoelson, "Type 2 diabetes as an inflammatory disease," *Nature Reviews Immunology*, vol. 11, no. 2, pp. 98–107, 2011.
- [16] W. Xie and L. Du, "Diabetes is an inflammatory disease: evidence from traditional Chinese medicines," *Diabetes, Obesity and Metabolism*, vol. 13, no. 4, pp. 289–301, 2011.
- [17] A. S. Onikanni, B. Lawal, A. O. Olusola et al., "*Sterculia tragacantha* Lindl leaf extract ameliorates STZ-induced diabetes, oxidative stress, inflammation and neuronal impairment," *Journal of Inflammation Research*, vol. 14, pp. 6749–6764, 2021.
- [18] J. L. Evans, I. D. Goldfine, B. A. Maddux, and G. M. Grodsky, "Are oxidative stress-activated signaling pathways mediators of insulin resistance and β -cell dysfunction?," *Diabetes*, vol. 52, no. 1, pp. 1–8, 2003.
- [19] H. Yang, X. Jin, C. W. K. Lam, and S.-K. Yan, "Oxidative stress and diabetes mellitus," *Clinical Chemistry and Laboratory Medicine*, vol. 49, no. 11, pp. 1773–1782, 2011.
- [20] A. S. Onikanni, B. Lawal, B. E. Oyinloye et al., "Therapeutic efficacy of *Clompanus pubescens* leaves fractions via downregulation of neuronal cholinesterases/ Na^+ - K^+ ATPase/ $\text{IL-1 } \beta$, and improving the neurocognitive and antioxidants status of streptozotocin-induced diabetic rats," *Biomedicine & Pharmacotherapy*, vol. 148, p. 112730, 2022.
- [21] A. Chaudhury, C. Duvoor, V. S. Reddy Dendi et al., "Clinical review of antidiabetic drugs: implications for type 2 diabetes mellitus management," *Frontiers in endocrinology*, vol. 8, p. 6, 2017.
- [22] R. F. Calson, "Miglitol and hepatotoxicity in type 2 diabetes mellitus," *American Family Physician*, vol. 62, p. 315, 2000.
- [23] R. Amoretti, C. Cicconetti, M. De Nichilo, C. Teodonio, R. Fasani, and M. Carosi, "Acarbose in the treatment of type 2 diabetes," *Minerva Dietologica e Gastroenterologica*, vol. 32, no. 1, pp. 53–59, 1986.
- [24] M. Jung, M. Park, H. C. Lee, Y.-H. Kang, E. S. Kang, and S. K. Kim, "Antidiabetic agents from medicinal plants," *Current Medicinal Chemistry*, vol. 13, no. 10, pp. 1203–1218, 2006.
- [25] N. H. Salleh, I. N. Zulklipl, H. Mohd Yasin et al., "Systematic review of medicinal plants used for treatment of diabetes in human clinical trials: an ASEAN perspective," *Evidence-based Complementary and Alternative Medicine*, vol. 2021, Article ID 5570939, 10 pages, 2021.
- [26] M. I. Yatoo, A. Saxena, A. Gopalakris, M. Alagawany, and K. Dhama, "Promising antidiabetic drugs, medicinal plants and herbs: an update," *International Journal of Pharmacology*, vol. 13, no. 7, pp. 732–745, 2017.
- [27] W. Mojeremane and S. Tshwenyane, "Azanza garckeana: a valuable edible indigenous fruit tree of Botswana," *Pakistan Journal of Nutrition*, vol. 3, no. 5, pp. 264–267, 2004.
- [28] A. A. Yusuf, B. Lawal, S. Sani et al., "Pharmacological activities of Azanza garckeana (Goron Tula) grown in Nigeria," *Clinical Phytoscience*, vol. 6, pp. 1–8, 2020.
- [29] Y. Dikko, M. Khan, T. Tor-Anyiin, J. Anyam, and U. Linus, "In vitro antimicrobial activity of fruit pulp extracts of Azanza garckeana (F. Hoffm.) Exell & Hillc. and isolation of one of its active principles, betulinic acid," *Journal of Pharmaceutical Research International*, vol. 14, no. 1, pp. 1–10, 2016.
- [30] B. B. Bukar, F. Ezeh, and S. Y. Sabo, "Methanol Extract of Azanza garckeana Fruit Pulp Protects against Formalin-Induced Reproductive Toxicity in Adult Albino Male Mice," *Journal of Advances in Medical and Pharmaceutical Sciences*, vol. 23, no. 8, pp. 38–49, 2021.
- [31] Y. Dikko, M. E. Khan, T. A. Tor-Anyiin, J. V. Anyam, and U. Linus, "In vitro Antimicrobial Activity of Fruit Pulp Extracts of Azanza garckeana (F. Hoffm.) Exell & Hillc. and Isolation of One of its Active Principles, Betulinic Acid," *British Journal of Pharmaceutical Research*, vol. 14, pp. 1–10, 2016.
- [32] B. B. Bukar, N. E. Tsokwa, and O. D. Orshi, "Ameliorative and fecundity potentials of aqueous extract of Azanza garckeana (T. Hoffm) fruit pulp in formalin-induced toxicity on male albino mice," *Journal of Pharmacy & Bioresources*, vol. 17, pp. 164–173, 2020.
- [33] C.-C. Chang, M.-H. Yang, H.-M. Wen, and J.-C. Chern, "Estimation of total flavonoid content in propolis by two complementary colorimetric methods," *Journal of Food and Drug Analysis*, vol. 10, no. 3, 2002.
- [34] V. L. Singleton, R. Orthofer, and R. M. Lamuela-Raventós, "Analysis of total phenols and other oxidation substrates and antioxidants by means of folin-ciocalteu reagent," in *Methods in enzymology 1999 Jan 1 (Vol. 299, pp. 152-178)*, vol. 299, pp. 152–178, *Methods in Enzymology*, 1999.
- [35] M. Oyaizu, "Studies on products of browning reaction antioxidative activities of products of browning reaction prepared from glucosamine," *The Japanese journal of nutrition and dietetics*, vol. 44, no. 6, pp. 307–315, 1986.
- [36] K. Panjamurthy, S. Manoharan, and C. R. Ramachandran, "Lipid peroxidation and antioxidant status in patients with periodontitis," *Cellular & Molecular Biology Letters*, vol. 10, no. 2, pp. 255–264, 2005.
- [37] R. Re, N. Pellegrini, A. Proteggente, A. Pannala, M. Yang, and C. Rice-Evans, "Antioxidant activity applying an improved ABTS radical cation decolorization assay," *Free Radical Biology and Medicine*, vol. 26, no. 9-10, pp. 1231–1237, 1999.
- [38] K. Worthington, *Alpha Amylase Worthington Enzyme Manual*, Worthington Biochemical Corporation, Lakewood, NJ, 1993.
- [39] Y. Mizushima and M. Kobayashi, "Interaction of anti-inflammatory drugs with serum proteins, especially with some biologically active proteins," *Journal of Pharmacy and Pharmacology*, vol. 20, no. 3, pp. 169–173, 1968.
- [40] O. Oyedapo and A. J. Famurewa, "Antiprotease and membrane stabilizing activities of extracts of *Fagara zanthoxyloides*, *Oxalyscorpoides* and *Tetrapleura tetraptera*," *International Journal of Pharmacognosy*, vol. 33, no. 1, pp. 65–69, 1995.
- [41] V. Thenmozhi, V. Elango, and J. Sadique, "Anti-inflammatory activity of some Indian medicinal plants," *Ancient Science of Life*, vol. 8, no. 3-4, pp. 258–261, 1989.

- [42] D. Lorke, "A new approach to practical acute toxicity testing," *Archives of Toxicology*, vol. 54, no. 4, pp. 275–287, 1983.
- [43] W. Sisay, Y. Andargie, and M. Molla, "Antidiabetic activity of hydromethanolic extract of crude *Dorstenia barnimiana* root: validation of in vitro and in vivo antidiabetic and antidyslipidemic activity," *Journal of Experimental Pharmacology*, vol. Volume 14, pp. 59–72, 2022.
- [44] E. Etuk, "Animals models for studying diabetes mellitus," *Agriculture and Biology Journal of North America*, vol. 1, pp. 130–134, 2010.
- [45] Q. Zhang, X. Li, J. Li et al., "Mechanism of anti-inflammatory and antibacterial effects of QingXiaoWuWei decoction based on network pharmacology, molecular docking and in vitro experiments," *Frontiers in Pharmacology*, vol. 12, 2021.
- [46] B. Lawal, S. Sani, A. S. Onikanni et al., "Preclinical anti-inflammatory and antioxidant effects of *Azanza garckeana* in STZ-induced glycemic-impaired rats, and pharmacoinformatics of its major phytoconstituents," *Biomedicine & Pharmacotherapy*, vol. 152, p. 113196, 2022.
- [47] O. Shittu, B. Lawal, and O. Oluyomi, "Effects of methanol extract of *Musca domestica* larvae on antioxidants enzymes in *T. Brucei* infected rats," *Nigerian Journal of Biochemistry and Molecular Biology*, vol. 29, pp. 1–10, 2014.
- [48] J. Ibrahim, A. Y. Kabiru, T. Abdulrasheed-Adeleke, B. Lawal, and A. H. Adewuyi, "Antioxidant and hepatoprotective potentials of curcuminoid isolates from turmeric (*Curcuma longa*) rhizome on CCL₄-induced hepatic damage in Wistar rats," *Journal of Taibah University for Science*, vol. 14, no. 1, pp. 908–915, 2020.
- [49] K. Shagirtha, N. Bashir, and S. MiltonPrabu, "Neuroprotective efficacy of hesperetin against cadmium induced oxidative stress in the brain of rats," *Toxicology and Industrial Health*, vol. 33, no. 5, pp. 454–468, 2017.
- [50] L. Kum-Tatt and I.-K. Tan, "A new colorimetric method for the determination of glutathione in erythrocytes," *Clinica Chimica Acta*, vol. 53, no. 2, pp. 153–161, 1974.
- [51] H. P. Misra and I. Fridovich, "The role of superoxide anion in the autoxidation of epinephrine and a simple assay for superoxide dismutase," *Journal of Biological Chemistry*, vol. 247, no. 10, pp. 3170–3175, 1972.
- [52] A. K. Sinha, "Colorimetric assay of catalase," *Analytical Biochemistry*, vol. 47, no. 2, pp. 389–394, 1972.
- [53] H. Liu, L. Wang, M. Lv et al., "AlzPlatform: an Alzheimer's disease domain-specific chemogenomics knowledgebase for polypharmacology and target identification research," *Journal of Chemical Information and Modeling*, vol. 54, no. 4, pp. 1050–1060, 2014.
- [54] M. D. Hanwell, D. E. Curtis, D. C. Lonie, T. Vandermeersch, E. Zurek, and G. R. Hutchison, "Avogadro: an advanced semantic chemical editor, visualization, and analysis platform," *Journal of Cheminformatics*, vol. 4, no. 1, p. 17, 2012.
- [55] O. Trott and A. J. Olson, "AutoDock Vina: improving the speed and accuracy of docking with a new scoring function, efficient optimization, and multithreading," *Journal of Computational Chemistry*, vol. 31, no. 2, pp. 455–461, 2010.
- [56] B. Lawal, Y.-L. Liu, N. Mokgautsi et al., "Pharmacoinformatics and preclinical studies of NSC765690 and NSC765599, potential STAT3/CDK2/4/6 inhibitors with antitumor activities against NCI60 human tumor cell lines," *Biomedicine*, vol. 9, no. 1, p. 92, 2021.
- [57] S.-Y. Wu, K.-C. Lin, B. Lawal, A. T. H. Wu, and C.-Z. Wu, "MXD3 as an onco-immunological biomarker encompassing the tumor microenvironment, disease staging, prognoses, and therapeutic responses in multiple cancer types," *Computational and Structural Biotechnology Journal*, vol. 19, pp. 4970–4983, 2021.
- [58] B. Lawal, C.-Y. Lee, N. Mokgautsi et al., "mTOR/EGFR/iNOS/MAP2K1/FGFR/TGFB1 are druggable candidates for N-(2,4-difluorophenyl)-2',4'-difluoro-4-hydroxybiphenyl-3-carboxamide (NSC765598), with consequent anticancer implications," *Frontiers in Oncology*, vol. 11, 2021.
- [59] J. O. Olugbodi, K. Samaila, B. Lawal et al., "Computational and preclinical evidence of anti-ischemic properties of L-carnitine-rich supplement via stimulation of anti-inflammatory and antioxidant events in testicular torsed rats," *Oxidative Medicine and Cellular Longevity*, vol. 2021, Article ID 5543340, 14 pages, 2021.
- [60] Visualizer, DS BIOVIA, and Dassault Systèmes, *BIOVIA Workbook, Release 2020; BIOVIA pipeline pilot, release 2020*, Dassault Systèmes, San Diego, 2020.
- [61] K. K. Keshala, A. M. P. W. Bandara, C. Padumadasa, and L. D. C. Peiris, "Bioactivities and GC-MS profiling of Malewana Madhumeha Choorna polyherbal hot infusion," *South African Journal of Botany*, vol. 140, pp. 194–203, 2021.
- [62] D. Tungmunnithum, A. Thongboonyou, A. Pholboon, and A. Yangsabai, "Flavonoids and other phenolic compounds from medicinal plants for pharmaceutical and medical aspects: an overview," *Medicine*, vol. 5, no. 3, p. 93, 2018.
- [63] D. Villaño, M. Fernández-Pachón, M. L. Moyá, A. Troncoso, and M. García-Parrilla, "Radical scavenging ability of polyphenolic compounds towards DPPH free radical," *Talanta*, vol. 71, no. 1, pp. 230–235, 2007.
- [64] S. C. Tiwari and N. Husain, "Biological activities and role of flavonoids in human health—a," *Indian Journal of Science Research*, vol. 12, pp. 193–196, 2017.
- [65] M. G. Chaudhari, B. B. Joshi, and K. N. Mistry, "In vitro anti-diabetic and anti-inflammatory activity of stem bark of *Bauhinia purpurea*," *Bulletin of Pharmaceutical and Medical Sciences (BOPAMS)*, vol. 1, pp. 139–150, 2013.
- [66] M. Govindappa, T. Sadananda, R. Channabasava, and V. B. Raghavendra, "In vitro anti-inflammatory, lipoyxygenase, xanthine oxidase and acetylcholinesterase inhibitory activity of *Tecoma stans* (L.) Juss. Ex kunth," *International Journal of Pharma and Bio Sciences*, vol. 2, pp. 275–285, 2011.
- [67] S. Rajasekaran, M. Dinesh, C. Kansrajh, and F. H. A. Baig, "Amaranthus spinosus leaf extracts and its anti-inflammatory effects on cancer," *Indian Journal of Research in Pharmacy and Biotechnology*, vol. 2, p. 1058, 2014.
- [68] S. Doumas, A. Kolokotronis, and P. Stefanopoulos, "Anti-inflammatory and antimicrobial roles of secretory leukocyte protease inhibitor," *Infection and Immunity*, vol. 73, no. 3, pp. 1271–1274, 2005.
- [69] K. Hibbetts, B. Hines, and D. Williams, "An overview of proteinase inhibitors," *Journal of Veterinary Internal Medicine*, vol. 13, no. 4, pp. 302–308, 1999.
- [70] H. C. Hodge and J. H. Sterner, "Tabulation of toxicity classes," *American Industrial Hygiene Association Quarterly*, vol. 10, no. 4, pp. 93–96, 1949.
- [71] I. J. Iyojo, R. P. Ibrahim, A. Tagang, L. Allam, and A. J. Olusegun, "Effects of different extracts of *Azanza garckeana* fruit pulp on haematological and biochemical parameters of New Zealand

- White (NZW) rabbit bucks,” *Comparative Clinical Pathology*, vol. 31, no. 3, pp. 453–463, 2022.
- [72] A. O. Owoade, A. Adetutu, O. S. Olorunnisola, and K. S. Ayinde, “The in-vitro antioxidant properties and phytochemical constituents of *Citrullus colocynthis* methanolic extract,” *Elixir Appl. Botany*, vol. 121, pp. 51556–51562, 2018.
- [73] R. Tundis, M. Loizzo, and F. Menichini, “Natural products as α -amylase and α -glucosidase inhibitors and their hypoglycaemic potential in the treatment of diabetes: an update,” *Mini Reviews in Medicinal Chemistry*, vol. 10, no. 4, pp. 315–331, 2010.
- [74] W. A. S. Chamika, T. C. Ho, V. C. Roy et al., “In vitro characterization of bioactive compounds extracted from sea urchin (*Stomopneustes variolaris*) using green and conventional techniques,” *Food Chemistry*, vol. 361, p. 129866, 2021.
- [75] N. Mahmood, “A review of α -amylase inhibitors on weight loss and glycemic control in pathological state such as obesity and diabetes,” *Comparative Clinical Pathology*, vol. 25, no. 6, pp. 1253–1264, 2016.
- [76] F. Rolland, J. Winderickx, and J. M. Thevelein, “Glucose-sensing and -signalling mechanisms in yeast,” *FEMS Yeast Research*, vol. 2, no. 2, pp. 183–201, 2002.
- [77] K. Ninomiya, Y. Yamaguchi, F. Shinmachi, H. Kumagai, and H. Kumagai, “Suppression of postprandial blood glucose elevation by buckwheat (*Fagopyrum esculentum*) albumin hydrolysate and identification of the peptide responsible to the function,” *Food Science and Human Wellness*, vol. 11, no. 4, pp. 992–998, 2022.
- [78] S. Chen, B. Lin, J. Gu et al., “Binding interaction of betulinic acid to α -glucosidase and its alleviation on postprandial hyperglycemia,” *Molecules*, vol. 27, no. 8, p. 2517, 2022.
- [79] B.-E. Van Wyk and M. Wink, *Medicinal Plants of the World*, CABI, 2017.
- [80] K. Neha, M. R. Haider, A. Pathak, and M. S. Yar, “Medicinal prospects of antioxidants: a review,” *European Journal of Medicinal Chemistry*, vol. 178, pp. 687–704, 2019.
- [81] D. Rajendiran, S. Packirisamy, and K. Gunasekaran, “A review on role of antioxidants in diabetes,” *Asian Journal of Pharmaceutical and Clinical Research*, vol. 11, no. 2, pp. 48–53, 2018.
- [82] D. M. Adams and M. T. Yakubu, “Aqueous extract of *Digitaria exilis* grains ameliorate diabetes in streptozotocin-induced diabetic male Wistar rats,” *Journal of Ethnopharmacology*, vol. 249, p. 112383, 2020.
- [83] M. C. Petersen, D. F. Vatner, and G. I. Shulman, “Regulation of hepatic glucose metabolism in health and disease,” *Nature Reviews Endocrinology*, vol. 13, no. 10, pp. 572–587, 2017.
- [84] B. Lawal, O. K. Shittu, P. C. Ossai, A. N. Abubakar, and A. M. Ibrahim, “Evaluation of antioxidant activity of giant African snail (*Achachatina maginata*) haemolymph in CCl₄-induced hepatotoxicity in albino rats,” *Journal of Pharmaceutical Research International*, vol. 6, no. 3, pp. 141–154, 2015.
- [85] O. I. Aruoma, “Free radicals, oxidative stress, and antioxidants in human health and disease,” *Journal of the American Oil Chemists’ Society*, vol. 75, no. 2, pp. 199–212, 1998.
- [86] L. Tappy, “Metabolism of sugars: a window to the regulation of glucose and lipid homeostasis by splanchnic organs,” *Clinical Nutrition*, vol. 40, no. 4, pp. 1691–1698, 2021.
- [87] J. Mohamed, A. H. Nazratun Nafizah, A. H. Zariyantey, and S. B. Budin, “Mechanisms of diabetes-induced liver damage: the role of oxidative stress and inflammation,” *Sultan Qaboos University medical journal*, vol. 16, pp. e132–e141, 2016.
- [88] M. J. Hossen, M. A. Matin, M. H. Sikder, M. S. Ahmed, and M. Rahman, “Kupffer cells and liver,” in *Recent Advancements in Microbial Diversity*, pp. 361–395, Elsevier, 2022.
- [89] H. Maeda, Y. Ishima, J. Saruwatari et al., “Nitric oxide facilitates the targeting Kupffer cells of a nano-antioxidant for the treatment of NASH,” *Journal of Controlled Release*, vol. 341, pp. 457–474, 2022.
- [90] J. S. Bhatti, A. Sehwat, J. Mishra et al., “Oxidative stress in the pathophysiology of type 2 diabetes and related complications: current therapeutics strategies and future perspectives,” *Free Radical Biology and Medicine*, vol. 184, pp. 114–134, 2022.
- [91] Y. M. Yang, Y. E. Cho, and S. Hwang, “Crosstalk between oxidative stress and inflammatory liver injury in the pathogenesis of alcoholic liver disease,” *International Journal of Molecular Sciences*, vol. 23, no. 2, p. 774, 2022.
- [92] C. Matyas, G. Haskó, L. Liaudet, E. Trojnar, and P. Pacher, “Interplay of cardiovascular mediators, oxidative stress and inflammation in liver disease and its complications,” *Nature Reviews Cardiology*, vol. 18, no. 2, pp. 117–135, 2021.
- [93] M. Kaleem, M. Asif, Q. Ahmed, and B. Bano, “Antidiabetic and antioxidant activity of *Annona squamosa* extract in streptozotocin-induced diabetic rats,” *Singapore Medical Journal*, vol. 47, no. 8, pp. 670–675, 2006.
- [94] K. O. Karigidi and C. O. Olaiya, “Antidiabetic activity of corn steep liquor extract of *Curculigo pilosa* and its solvent fractions in streptozotocin-induced diabetic rats,” *Journal of Traditional and Complementary Medicine*, vol. 10, no. 6, pp. 555–564, 2020.
- [95] D. Cao, J. Wang, R. Zhou, Y. Li, H. Yu, and T. Hou, “ADMET evaluation in drug discovery. 11. Pharmacokinetics Knowledge Base (PKKB): a comprehensive database of pharmacokinetic and toxic properties for drugs,” *Journal of Chemical Information and Modeling*, vol. 52, no. 5, pp. 1132–1137, 2012.
- [96] I. Kola and J. Landis, “Can the pharmaceutical industry reduce attrition rates?,” *Nature Reviews Drug Discovery*, vol. 3, no. 8, pp. 711–716, 2004.
- [97] M. L. Amin, “P-glycoprotein inhibition for optimal drug delivery,” *Drug target insights*, vol. 7, pp. 27–34, 2013.
- [98] J. Robert and C. Jarry, “Multidrug resistance reversal agents,” *Journal of Medicinal Chemistry*, vol. 46, no. 23, pp. 4805–4817, 2003.
- [99] K. Shankar and H. M. Mehendale, “Cytochrome P450,” in *Encyclopedia of Toxicology*, P. Wexler, Ed., pp. 1125–1127, Academic Press, Oxford, 3rd edition, 2014.
- [100] Y.-C. Yeh, B. Lawal, M. Hsiao, T.-H. Huang, C. Y. F. Huang, and C.-Y. F. Huang, “Identification of NSP3 (SH2D3C) as a prognostic biomarker of tumor progression and immune evasion for lung cancer and evaluation of organosulfur compounds from *Allium sativum* L. as therapeutic candidates,” *Biomedicine*, vol. 9, no. 11, p. 1582, 2021.
- [101] B. Lawal, Y.-C. Wang, A. T. H. Wu, and H.-S. Huang, “Pro-oncogenic c-met/EGFR, biomarker signatures of the tumor microenvironment are clinical and therapy response prognosticators in colorectal cancer, and therapeutic targets of 3-phenyl-2H-benzo[e][1,3]-oxazine-2,4(3H)-dione derivatives,” *Frontiers in Pharmacology*, vol. 12, 2021.
- [102] D. M. I. H. Dissanayake, D. D. B. D. Perera, L. R. Keerthirathna et al., “Antimicrobial activity of *Plumbago indica* and ligand screening of plumbagin against methicillin-resistant *Staphylococcus aureus*,” *Journal of Biomolecular Structure and Dynamics*, vol. 40, no. 7, pp. 3273–3284, 2022.

- [103] X.-Y. Meng, H.-X. Zhang, M. Mezei, and M. Cui, "Molecular docking: a powerful approach for structure-based drug discovery," *Current Computer-Aided Drug Design*, vol. 7, no. 2, pp. 146–157, 2011.
- [104] D. B. Kitchen, H. Decornez, J. R. Furr, and J. Bajorath, "Docking and scoring in virtual screening for drug discovery: methods and applications," *Nature Reviews Drug Discovery*, vol. 3, no. 11, pp. 935–949, 2004.
- [105] J.-H. Chen, A. T. H. Wu, B. Lawal et al., "Identification of cancer hub gene signatures associated with immune-suppressive tumor microenvironment and ovatodiolide as a potential cancer immunotherapeutic agent," *Cancers*, vol. 13, no. 15, p. 3847, 2021.
- [106] B. Lawal, Y.-C. Kuo, S.-L. Tang et al., "Transcriptomic-based identification of the immuno-oncogenic signature of cholangiocarcinoma for HLC-018 multi-target therapy exploration," *Cell*, vol. 10, no. 11, p. 2873, 2021.
- [107] B. Lawal, Y.-C. Kuo, M. R. Sumitra, A. T. Wu, and H.-S. Huang, "In vivo pharmacokinetic and anticancer studies of HH-N25, a selective inhibitor of topoisomerase I, and hormonal signaling for treating breast cancer," *Journal of Inflammation Research*, vol. 14, pp. 1–13, 2021.

Research Article

Quercetin Protects Ethanol-Induced Hepatocyte Pyroptosis via Scavenging Mitochondrial ROS and Promoting PGC-1 α -Regulated Mitochondrial Homeostasis in L02 Cells

Xingtiao Zhao ^{1,2}, Cheng Wang ^{1,2}, Shu Dai ^{1,2}, Yanfang Liu ^{1,2}, Fang Zhang ^{1,2},
Cheng Peng ^{1,2} and Yunxia Li ^{1,2}

¹State Key Laboratory of Southwestern Chinese Medicine Resources, Ministry of Education, Chengdu 611137, China

²School of Pharmacy, Chengdu University of Traditional Chinese Medicine, Chengdu 611137, China

Correspondence should be addressed to Cheng Peng; cdtcpengcheng@126.com and Yunxia Li; lyxtgyxcdutcm@163.com

Received 29 March 2022; Revised 21 June 2022; Accepted 7 July 2022; Published 16 July 2022

Academic Editor: Anderson J. Teodoro

Copyright © 2022 Xingtiao Zhao et al. This is an open access article distributed under the Creative Commons Attribution License, which permits unrestricted use, distribution, and reproduction in any medium, provided the original work is properly cited.

Alcoholic liver disease (ALD) is a multifaceted process that involves excessive lipid, reactive oxygen species (ROS) production, unbalanced mitochondrial homeostasis, and ultimate cell death. Quercetin is a dietary phytochemical presented in various fruits and vegetables, which has anti-inflammatory and antioxidant effects. According to recent advances in pharmanutritional management, the effects of quercetin on various mitochondrial processes have attracted attention. In the study, we explored whether quercetin could attenuate ethanol-induced hepatocyte pyroptosis by maintaining mitochondrial homeostasis and studied its hepatoprotective effect and the underlying mechanism. We chose L02 cells to establish an *in vitro* model with ethanol-induced hepatocyte pyroptosis. Then, the cells at approximately 80% confluence were treated with quercetin (80, 40, and 20 μ M). The cell viability (CCK-8) was used to investigate the effect of quercetin on ethanol-induced L02 cell proliferation. Relative assay kits were used to measure oxidative stress index (OSI = TOS/TAS), lipid peroxidation (LPO) release, and mitochondrial membrane potential ($\delta\Psi_m$). The morphology of mitochondria was characterized by transmission electron microscopy- (TEM-) based analysis. Mitochondrial dynamics (Mito Tracker Green), mitROS (MitoSOX Red Mitochondrial Superoxide) production, and nuclear DNA (nDNA) damage (γ H2AX) markers were detected by immunofluorescence. The mRNA levels of mitochondrial function (including mitochondrial DNA (mtDNA) transcription genes TWNK, MTCO1, and MFND) and pyroptosis-related genes were detected by RT-qPCR, and the protein levels of NLRP3, ASC, caspase1, cleaved-caspase1, IL-18, IL-1 β , and GSDMD-N were detected by western blot. The results showed that quercetin treatment downregulated redox status, lipid droplets, and LPO release, restored damaged mitochondrial membrane potential, and repaired mtDNA damage, PGC-1 α nuclear transfer, and mitochondrial dynamics. The gene and protein expressions of NLRP3, ASC, cleaved-caspase1, IL-18, IL-1 β , and GSDMD-N were decreased, which effectively inhibited cell pyroptosis. Therefore, the results indicated that quercetin protected ethanol-induced hepatocyte pyroptosis via scavenging mitROS and promoting PGC-1 α -mediated mitochondrial homeostasis in L02 cells.

1. Introduction

Excessive intake of alcohol has been considered the third largest risk factors threatening human health, and per capita alcohol consumption has increased from 5.9L to 6.5L over the past years and is estimated to rise to 7.6L by 2030 [1]. Excessive alcohol intake may result in alcoholic liver disease (ALD) which has become the leading cause of liver damage

after viral hepatitis [2] and has been reported to cause approximately 500,000 deaths per year in Europe [3].

Therefore, the prevention and treatment of ALD have far-reaching significance for maintaining human health. At present, the main treatment medication for ALD is antioxidant and anti-inflammatory drugs, such as corticosteroids, glutathione, hexanone, theobromine, colchicine, and S-adenosine methionine, but these treatments have side effects,

including kidney damage and jaundice [4, 5]. Therefore, finding a safer and more effective treatment for ALD treatments is urgently needed [6].

ALD induced by alcohol is a multifaceted process and unbalanced mitochondrial homeostasis. Mitochondria, as highly dynamic organelles, provide most ATP through oxidative phosphorylation to maintain various metabolisms and energy requirements of cells. Studies have revealed that ethanol exposure resulted in imbalance of fusion/fission balance and an immediate change in mitochondrial shape both *in vivo* and *in vitro* [7, 8]. Cytochrome P450 2E1 (CYP2E1), a unique P450 enzyme expressed in hepatocytes, has high catalytic activity for ethanol [9] and results in excessive lipid, ROS production, mitochondrial homeostasis dysfunction, and ultimate hepatocyte pyroptosis [10].

ROS are mainly produced by mitochondria and can mediate various dysfunction of mitochondria, including mitochondrial dynamics, mitochondrial dysfunction, and even pyroptosis. In addition, it is also important in all regulators of inflammatory pathways [11]. Pyroptosis is a new dissolved programmed cell death caused by inflammasome. The nod-like receptor (NLR) family pyrin domain-containing 3 (NLRP3) converts precaspase1 to cleaved-caspase1, which drives the cleavage of gasdermin D (GSDMD) at D275 (numbering after human GSDMD) into N-termini [12]. Upon cleavage, the N-terminus of GSDMD (GSDMD-N) forms a transmembrane pore that releases cytokines such as mature cytokine interleukin-1 β /18 (IL-1 β /18), eventually resulting in strong inflammation and cell death [13]. Alcohol induction has also been found to promote NLRP3 inflammasome activation in patients with alcoholic hepatitis, thereby inducing hepatocyte pyroptosis [14]. Moreover, classic caspase1 pathway-dependent hepatocyte pyroptosis has been detected in L02 cells treated with high-concentration ethanol [15]. However, the relationship between mitochondrial homeostasis and pyroptosis remains to be further studied.

Quercetin, a dietary phytochemical presented in various fruits and vegetables, has the ability to scavenge ROS and reduce lipid peroxidation due to its ion chelating and iron stabilizing effect [16]. Currently, it is considered to be related to mitochondrial biogenesis, mitochondrial membrane potential, redox states within mitochondria, and cell death. In high-fat (HF) diet-induced obese mice, quercetin protected mitochondria and counteracted different prooxidant agents [17]. Quercetin upregulated mtDNA content and enhanced the expression of mitochondrial fusion protein 1 (Mfn1) and Mfn2 proteins [18]. Moreover, quercetin possessed a protective effect on macrophage pyroptosis [19]. However, it has not been reported whether quercetin could inhibit pyroptosis in ethanol-induced hepatocyte injury.

2. Materials and Methods

2.1. Materials. All the experimental materials were shown in Table 1.

2.2. Cell Culture. L02 cells (human normal liver cells), obtained from iCell Bio-technology Co., Ltd. (iCell-h054) (Shanghai, China), were cultured in Dulbecco's modified

Eagle medium (DMEM) supplemented containing 10% Gibco fetal bovine serum (FBS) (Gibco, Grand Island, NY, United State) and 1% antibiotics (penicillin and streptomycin) at 37°C in a 5% CO₂ humidified incubator. L02 cells were randomly divided into five groups: (1) the control group, (2) the ethanol (200 mM) model group, (3) ethanol (200 mM)+quercetin (80 μ M), (4) ethanol (200 mM)+quercetin (40 μ M), and (5) ethanol (200 mM)+quercetin (20 μ M). In brief, L02 cells at approximately 80% confluence were treated with quercetin (80, 40, and 20 μ M) for 24 h after pretreated with ethanol (200 mM) for 24 h. To prevent ethanol evaporation during exposure, each culture dish was tightly wrapped with parafilm.

2.3. Cell Proliferation Assay. L02 cells were cultured in 96-well plates. Different concentrations of ethanol and quercetin were added, each group was set up with 6 duplicate wells, and a group of solvent control group was reserved. After 24 h, the cell density reached 80%, incubated with 10 μ l of CCK-8 reagent for 1 h and detected the optical density (OD) value. The absorbance of untreated cells was regarded as 100% of cell survival.

$$\text{Cell viability} = \frac{\text{Treated viable cells} - \text{blank cells}}{\text{Control viable cells} - \text{blank cells}} \times 100\%. \quad (1)$$

2.4. Oil-Red O Staining. After the experiment, the culture medium was removed, washed with phosphate-buffered saline (PBS) for 3 times, fixed with 4% paraformaldehyde for 30 min to dilute the oil red storage solution (oil red : deionized water = 3 : 2), and filtered with filter paper and heated at 37°C. After dyeing for 10 min, the added dye liquid covered the bottom, and the dye could be absorbed. Then, the dye was rinsed with 60% isopropanol for 1-2 min, and the excess dye was washed with PBS. The field of view was randomly selected under the light microscope (Leica, German) of the glycerin sealant, the dyeing situation was observed, and the image was taken for analysis by ImageJ software.

2.5. Nile Red Staining. After the experiment, the cultured cells were fixed with 4% paraformaldehyde for 20 min. After immobilization, cells were stained with Nile Red for 15 min. After wash with PBS, the nucleus was then stained with DAPI for 5 min. The field of view was randomly selected under a fluorescent inverted microscope Confocal Imaging System (Leica Microsystems).

2.6. Biochemical Index Determination. L02 cells were cultured in 96-well plates. After the experiment, the supernatant was collected to determine the subcellular redox status by TAS, TOS ELISA kits, and lipid peroxide level by the LPO ELISA kit. The final results were presented as the average of the three independent measurements.

2.7. Mitochondrial Membrane Potential ($\delta\Psi_m$) Detection. After treatments, the cells were incubated with a JC-1 staining solution for 20 min at 37°C and washed off with PBS, and the images were obtained by a fluorescent inverted

TABLE 1: Information about experimental materials.

Raw materials	Biotechnology Co., Ltd	ID
Quercetin (purity > 99.00%)	MUST, Chengdu, China	117395
Cell Counting Kit-8	G-clone, Beijing, China	CC1410-500
Ethanol and other organic reagents	Kelong, Guangdong, China	
Total antioxidant status (TAS) ELISA kit	Elabscience, Wuhan, China	E-BC-K801
Total oxidant status (TOS) ELISA kit	Elabscience, Wuhan, China	E-BC-K802
LPO ELISA kit	MeiMian, Jiangsu, China	MM-1378H1
Oil red storage solution	Solar, Wuhan, China	G1015
Nile Red staining solution	Solar, Wuhan, China	N8440
JC-1 Mitochondrial Membrane Potential Assay	Solar, Wuhan, China	G1515
γ H2AX antibody	Solar, Wuhan, China	GB111841
MitoSOX Red Mitochondrial Superoxide	Yeasen, Shanghai, China	40778ES50
DAPI staining solution	Yeasen, Shanghai, China	40728ES03
Mito Tracker Green	KeyGEN, Jiangsu, China	KGMP007
IL-18 antibody	Affinity, Cincinnati, OH, USA	DF6252
IL-1 β antibody	Affinity, Cincinnati, OH, USA	AF5103
Caspase 1 antibody	Affinity, Cincinnati, OH, USA	AF5418
Cleaved-caspase 1 (Ala317), p10 antibody	Affinity, Cincinnati, OH, USA	AF4022
NLRP3 antibody	Affinity, Cincinnati, OH, USA	DF7438
GSDMD-N-terminal antibody	Affinity, Cincinnati, OH, USA	DF12275
GAPDH antibody	Affinity, Cincinnati, OH, USA	AF0911
Cleaved-aspase3 (Asp175), p17 antibody	Affinity, Cincinnati, OH, USA	AF7022
Bcl2 antibody	Abmart, Shanghai, China	T40056
Bax antibody	Abmart, Shanghai, China	TP51006
Caspase3 antibody	Abmart, Shanghai, China	T55051
ASC/TMS1	ZEN, Chengdu, China	340097
PCG-1 α	ZEN, Chengdu, China	862041
Goat Anti-Rabbit IgG(H+L) HRP secondary antibody	Multi science, Hangzhou, China	GAR007
Goat Anti-Rabbit IgG (H+L)-Cy3 secondary antibody	ABclonal, Wuhan, China	AS040
Total RNA isolation kit	Foregene, Chengdu, China	RE-03014
Animal tissue DNA isolation kit	Foregene, Chengdu, China	DE-05011
Master Premix for first-strand cDNA synthesis	Foregene, Chengdu, China	RT-01021
Real-Time PCR EasyTM-SYBR Green I	Foregene, Chengdu, China	QP-01011

microscope Confocal Imaging System (Leica Microsystems) with randomly selected fields of vision, respectively ($n = 6$) and analyzed by ImageJ software.

2.8. Mitochondrial Dynamics and Mitochondrial ROS (MitROS) Content Detection. Cells were incubated with 150 nM Mito-Tracker green for 30 min and then stained with DAPI for 5 min at 37°C. And cells were incubated with 5 μ M MitoSOX Red in the dark for 10 min at 37°C. Afterward, cells were washed with PBS for 3 times to remove the dye. Subsequently, cells were analyzed by flow cytometry. Moreover, the images were obtained by a fluorescent inverted microscope Confocal Imaging System (Leica Microsystems) with randomly selected fields of vision, respectively ($n = 6$), and analyzed by ImageJ software.

2.9. Immunofluorescence Analysis. After the experiment, the cells were washed with PBS and fixed with 4% formaldehyde

for 5 min. Then, the cells were permeated with 0.1% Triton X-100 at room temperature for 10 min. Then, it was sealed with 5% BSA for 1 h and incubated overnight with monoclonal PGC-1 α and γ H2AX antibody solution (diluted 1 : 100) at 4°C. Then, it was diluted with Goat Anti-Rabbit IgG (H +L)-Cy3 secondary antibody (diluted 1 : 500) were incubated at room temperature for 1 h. After washing with PBS, the nucleus was then stained with DAPI for 5 min and mitochondria was then stained with Mito-Tracker green for 30 min. The images were obtained by a fluorescent inverted microscope Confocal Imaging System (Leica Microsystems) with randomly selected fields of vision.

2.10. Quantitative Real-Time PCR (RT-qPCR) Analysis. Total RNA/DNA was extracted by animal total RNA/DNA isolation kit. After the concentration measurement, Master Premix for first-strand complementary DNA (cDNA) synthesis at the conditions of 42°C for 15 min and 85°C for

TABLE 2: The gene primer sequences used for RT-qPCR.

Gene name	Forward primer (5' → 3')	Reverse primer (5' → 3')
<i>ADH1</i>	TGGGAAAAGTATCCGTACCATT	AGCTGTTGCTCCAGATCATGT
<i>ADH2</i>	GGGCAGAGAAGACAGAAACGA	TTCTCTCATCAAACCTTCTGTCA
<i>ADH3</i>	CCCAAACCTGTGGCTGACTTT	ACTCTTTCCAGAGCGAAGCA
<i>CYP2E1</i>	GAAGCCTCTCGTTGACCCAA	TGGTGGGATACAGCCAAACC
<i>ALDH2</i>	CATGGACGCATCACACAGGG	CTTGCCATTGTCCAGGGTCT
<i>COXIV</i>	GGCGGCAGGTGTACATTTTTA	AGTCTTCGCTCTTCACAACA
<i>VDAC</i>	CCCAAACCTGTGGCTGACTTT	ACTCTTTCCAGAGCGAAGCA
<i>PINK1</i>	AACCGCTTCGACTTTCTGCT	CACTTGATGAACCAGCCCCA
<i>Mfn1</i>	TGGCCACATGTAGTTTATGTTTC	TTGCACCTGCTGTAAAAAGGC
<i>Mfn2</i>	GGAAGGTGAAGCGCAATGTC	TGCATTACCTCAGCCATGT
<i>Opa1</i>	CTGTGGCCTGGATAGCAGAA	AGACTGGCAGACCTCACTCT
<i>Drp1</i>	CCGGAGACCTCTCATTCTGC	TCTGCTTCCACCCCATTTTCT
<i>Fis1</i>	TCAGCCCCATCATGTGCTTT	CAGGAGAGGACCAGGAGTGA
<i>Mff</i>	CTCTCAGCCAACCACCTCTG	GTGCTGGATTGAGAGCCACT
<i>TWINK</i>	CTGGTTGGGGGATGCCTTC	ATTGAAGCCTCCGTTCCAGGG
<i>MFND</i>	CAACTACGCAAAGGCCCA	TGATGGTAGATGTGGCGGGT
<i>MTCO1</i>	CTATCCGGAATGCCCGA	GGCATCCATATAGTCACTCCAG
IL-18	TGCAGTCTACACAGCTTCGG	GCAGCCATCTTTATTCTCTGCG
IL-1 β	TGATGGCTTATTACAGTGCGCA	CGGAGATTCTGAGCTGGATG
Caspase-1	CCTGCCGTGGTGATAATGTT	TCCACATCACAGGAACAGGC
<i>GSDMD</i>	CAGAAGGGACGTGGTGTTC	AGTTTACGGAAGTCGGCGAG
GAPDH	ACTAGGCGCTCACTGTTCT	CCAATACGACCAAATCCGTTG

5 min according to the Real-Time kit's instructions. The RT-qPCR conditions were performed at 95°C for 3 min, 40 cycles of 95°C for 10 s, and 65°C for 30 s. Each experiment was conducted with three separate biological samples and the formula of $2^{-\Delta\Delta C_t}$ was used to calculate relative mRNA expression levels of the target genes. All primer sequences were listed in Table 2.

2.11. Protein Extraction and Western Blot (WB) Analysis. Cells were lysed with RIPA lysis buffer: protein phosphatase inhibitor : PMSF : protein mixing enzyme inhibitor = 100 : 1 : 1 : 1 and crushed by ultrasonic cell crushing apparatus for 3 min and centrifuged at 13400 g for 10 min in 4°C. Then, the BCA kit was used to detect the protein concentration, and then, protein concentration was adjusted to be consistent and then probed with anti-Bcl2, Bax, caspase3, cleaved-caspase3, IL-18, IL-1 β , NLRP3, ASC, caspase1, cleaved-caspase1, and GAPDH (diluted 1 : 1000). As an internal reference, the signals were recorded using a Chemidoc imaging system (Tanon, Shanghai, China) and analyzed using ImageJ analysis software.

2.12. Transmission Electron Microscopy (TEM) Analysis. The cells after treatments were prefixed with 2% glutaraldehyde and fixed in 1% osmium tetroxide. Next, the samples were dehydrated in ethanol containing 3% uranyl acetate, embedded in epoxy resin and propylene oxide overnight, and polymerized into 70 nm thick slices and stained with lead citrate, using H-7650 transmission electron microscopy (Hitachi

H-7650) test sections independently invited two uninformed pathologists to quantify each section.

3. Statistical Analysis

All experimental data were presented by mean \pm standard deviation (S.D.) and analyzed by statistical software SPSS 25.0. $p < 0.05$ was regarded as a significant difference and differences among the groups were evaluated statistically using one-way ANOVA.

4. Results

4.1. Quercetin Inhibited CYP2E1 Activity to Alleviate High-Concentration Ethanol-Induced Hepatocyte Oxidative Stress and Lipid Peroxidation. To investigate the hepatoprotective potential of quercetin, L02 cell line, an ideal cell line widely adopted to research drug toxicity and liver function *in vitro*, was chosen in the current study. Firstly, we identified the most suitable modeling concentration of ethanol by incubating L02 cells with different concentrations of ethanol (25, 50, 100, 200, and 300 mM) for 24 h. With the increase of ethanol concentration (100-300 mM), the CCK-8 results showed that the cell viability of L02 cells decreased significantly ($p < 0.05$). When the ethanol concentration was greater than 200 mM, the cell viability was less than 70% (Figure 1(a)). In addition, with the increase of ethanol concentrations (25-100 mM) for 24 h, the mRNA expression of ADH (ADH1, ADH2, and ADH3) increased significantly

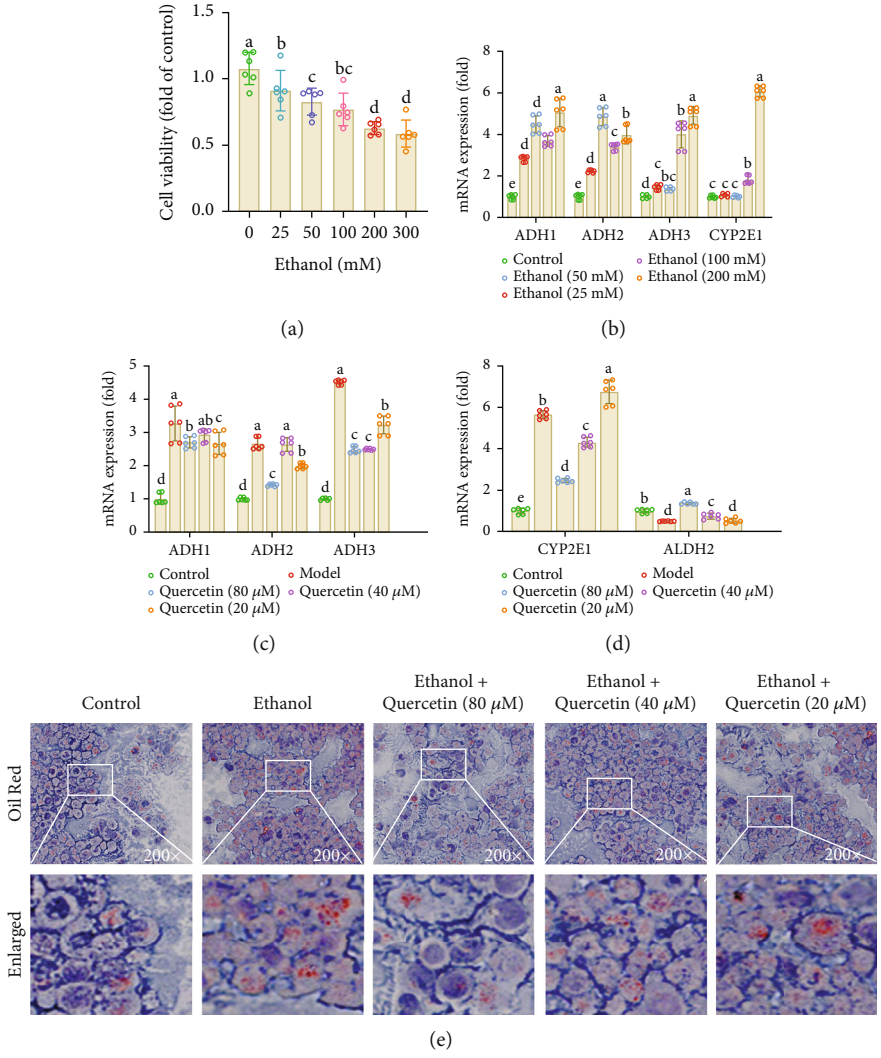


FIGURE 1: Continued.

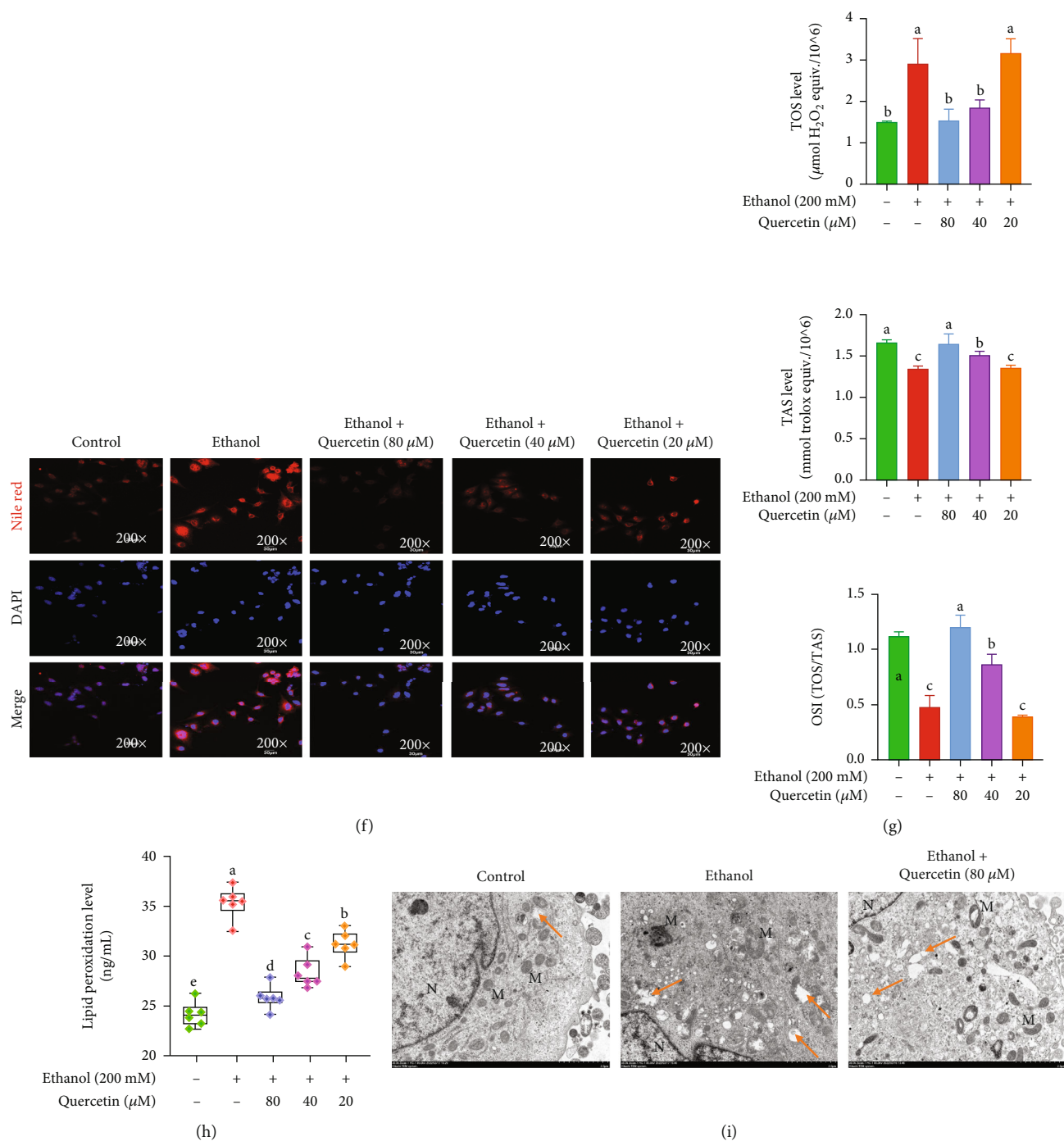


FIGURE 1: Hepatoprotective effects of quercetin against ethanol exposure. (a) Effects of different concentrations of ethanol on cell viability treated with different concentrations of ethanol for 24 h. (b) Quantitation of levels of ADH and CYP2E1 in L02 cells treated with different concentrations of ethanol for 24 h. (c, d) Quantitation of levels of ADH, CYP2E1, and ALDH2 treated with different concentrations of ethanol for 24 h. (e) Representative images of L02 cells and microphotograph of Oil-Red O staining (200x magnification). (f) Representative immunofluorescent images costained with Nile Red (red), DAPI (blue), and both channels merged. The graphs (down panel) show the fluorescence intensity profiles in two fluorescence channels along the arrow (200x magnification). (g) Determination of TAS, TOS levels, and OSI = TOS/TAS. (h) Determination of LPO level. (i) Representative TEM images of mitochondrial morphology and ultrastructure in L02 cells with boxed areas enlarged. M: mitochondria; N: nucleus; lipid drops (orange arrow) in all groups. Magnification is shown (scale bar, 2.0 μm). Data are expressed as mean \pm SD ($n = 6$). Different subscript letters indicate significant differences among the groups ($p < 0.05$).

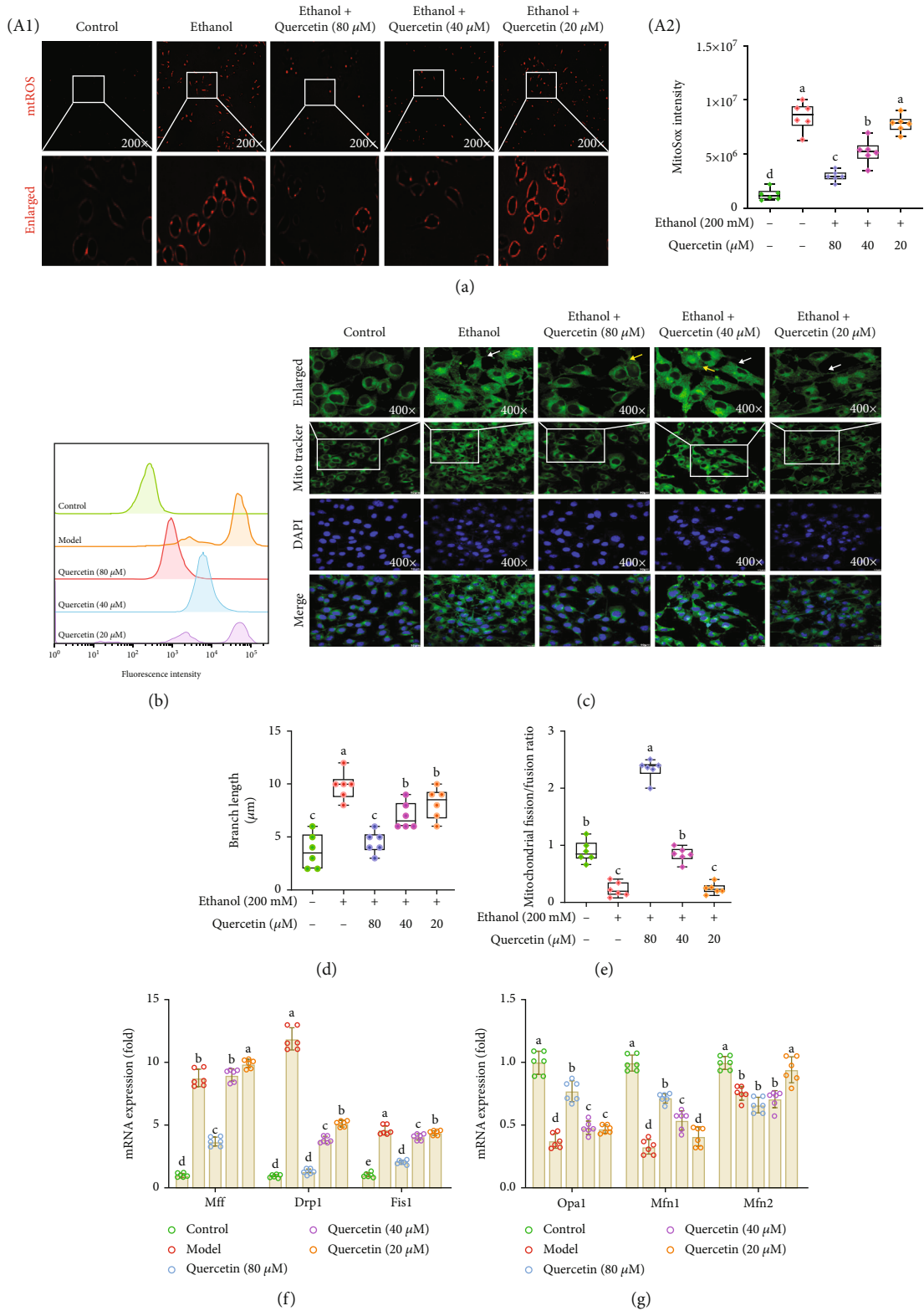


FIGURE 2: Continued.

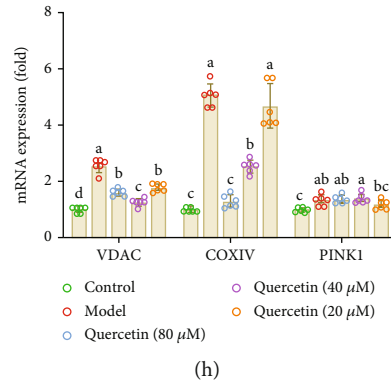


FIGURE 2: Quercetin reduced ethanol-induced mitROS generation and maintained mitochondrial dynamics. (a) Images of MitoSox Red staining for mitochondrial superoxide (200x magnification), the graphs (down panel) show the fluorescence intensity profiles in two fluorescence channels along the arrow. (b) Quantitative analysis of fluorescence intensity and mitROS generation by flow cytometry. (c) Representative immunofluorescent images co-stained with Mito-Tracker (green), DAPI (blue), and both channels merged (400x magnification). The graphs (up panel) show the fluorescence intensity profiles in two fluorescence channels along the arrow, and the white arrows represent fission; the yellow arrowheads show fusion. (d, e) Quantitative analysis of mitochondrial fission and fusion ratio and fission length. (f–h) The mRNA expression of mitochondrial function genes (VDAC, COXIV, and PINK1), mitochondrial fission genes (Mff, Drp1, and Fis1) and fusion genes (Opa1, Mfn1, and Mfn2). Data are expressed as mean \pm SD ($n = 6$). Different subscript letters indicate significant differences among the groups ($p < 0.05$).

($p < 0.05$), while the expression of CYP2E1 dominating alcohol metabolism did not change until the ethanol concentrations reached to 200 mM ($p < 0.05$) (Figure 1(b)). Interestingly, quercetin effectively reduced the activities of CYP2E1 and enhanced ALDH2 (Figures 1(b) and 1(d)), while did not change ADH significantly (Figure 1(c)), suggesting that the inhibition of CYP2E1 by quercetin may represent a novel therapeutic approach for minimizing the ethanol-induced CYP2E1 enzyme activity. Thus, 200 mM ethanol (24 h) was used in the subsequent experiments. Massive lipid droplets were dramatically reduced by quercetin in ethanol-induced hepatocytes through Oil Red O and Nile Red staining (especially 80 μ M quercetin) (Figures 1(e) and 1(f)). Moreover, the same results were also observed by TEM (Figure 1(i)). In the model group, the level of TAS was significantly decreased, whereas the levels of TOS and OSI were significantly increased (Figure 1(g)). However, quercetin treatment significantly reversed the effect of alcohol and the effect of 80 μ M quercetin was the most obvious. The release of LPO was significantly elevated in ethanol-induced hepatocyte injury. Quercetin could effectively decrease the release of LPO ($p < 0.05$), and the effect of quercetin was better with the increase of concentration (Figure 1(h)). Collectively, quercetin alleviated CYP2E1-mediated hepatic oxidative stress and lipid peroxidation, thus preventing alcoholic liver injury.

4.2. Quercetin Reduced mitROS Generation and Maintained Mitochondrial Dynamics in Ethanol-Induced Hepatocytes. Mitochondria are known for their active dynamics, and mitochondrial CYP2E1 acts as an activity generator of mitROS, whose release inhibits electron transfer along the respiratory chain, exacerbating mitochondrial dysfunction [20–22]. TEM (Figure 1(I)) was conducted to observe liver mitochondrial changes. Cells in the control group showed relatively normal mitochondria with intact membranes and cristae. However, ethanol treatment caused various degenerative

changes including abnormal shape swelling, perinuclear aggregation with a dark matrix, fragmentation, and destruction of intima. Quercetin ameliorated the damage, with slight swelling in mitochondria. Compared with the control group, massive mitROS were produced in hepatocytes after ethanol treatment, while quercetin reduced mitROS production, shown by both immunofluorescence and flow cytometry analysis ($p < 0.05$) and the effects of 80 and 40 μ M quercetin were obvious. (Figures 2(a) and 2(b)). Mitochondria are extremely dynamic organelles, constantly undergoing antagonistic processes of fission and fusion in maintaining mitochondrial function and cellular homeostasis. Recently, studies have shown that high-concentration ethanol exposure can cause mitochondrial fission and fusion imbalance in mice. We firstly detected mitochondrial fusion and fission through Mito-Tracker Green staining (Figure 2(c)), and the morphology changes of mitochondria were observed by confocal microscope. These were length or aspect ratio (AR, the ratio between the major and minor axis of the ellipse equivalent to the mitochondrion) and degree of branching or form factor (FF, defined as $(Pm2)/(4\pi Am)$, where Pm is the length of mitochondrial outline and Am is the area of mitochondrion). Since the mitochondria within a cell were often either oval or fragmented, we classified the cells as mitochondria fusion based on $FF < 1$ and the shape is more uniformly spherical, and mitochondrial fission based on $AR > 1$ and the majority (>70%) of fragmented mitochondria as previous reported [23, 24]. And our quantitative determination revealed that the length of mitochondria was significantly reduced after quercetin treatment compared with ethanol group ($p < 0.05$) (Figures 2(d) and 2(e)). In addition, the expression of related genes was determined by RT-qPCR (Figures 2(f)–2(h)), which indicated that 80 μ M quercetin increased the mRNA levels of fusion genes (Opa1 and Mfn1) and inhibited the mRNA levels of fission genes (Mff, Drp1, and Fis1) in ethanol-treated hepatocytes ($p < 0.05$). Quercetin reduced Drp1 gene expression in a

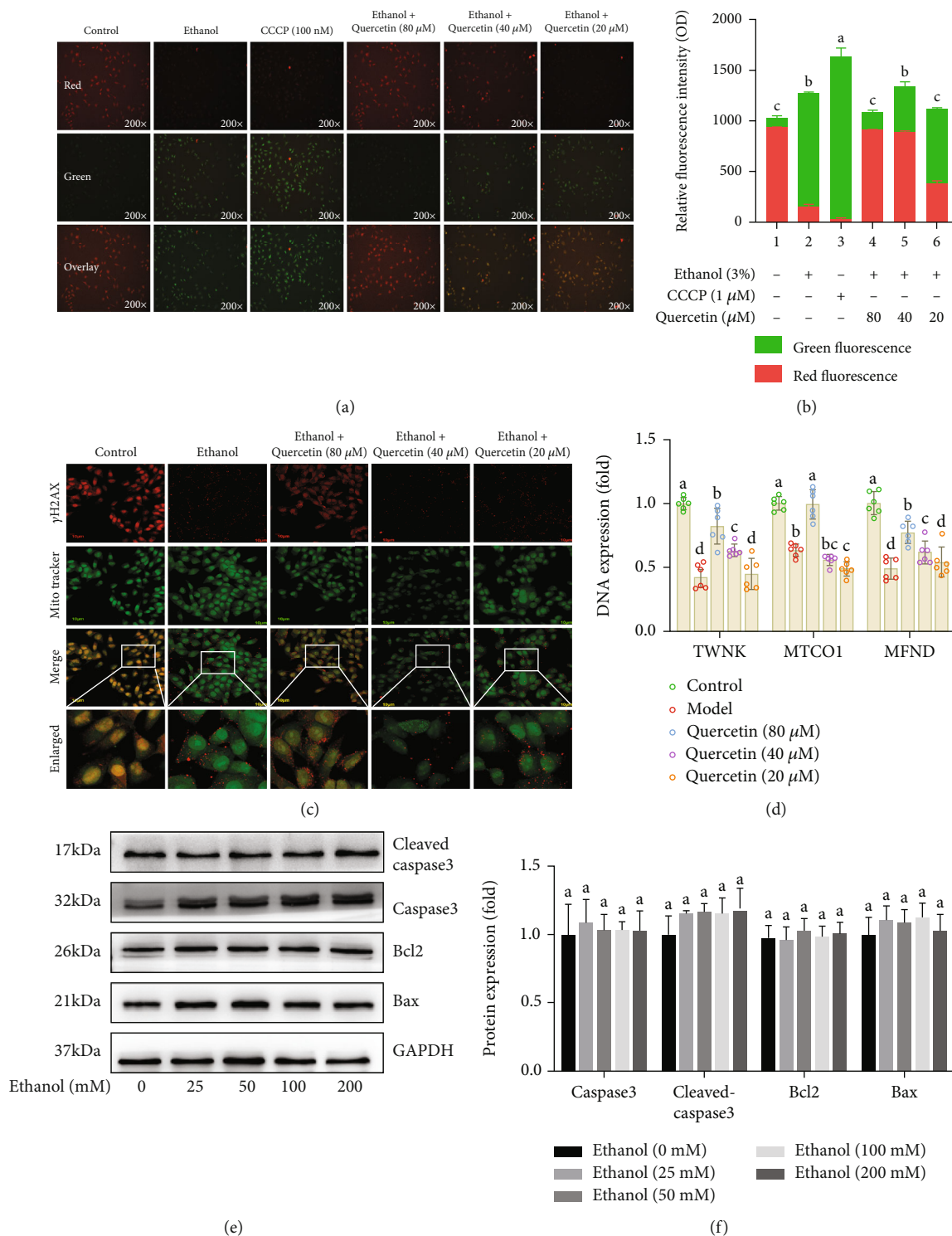


FIGURE 3: Quercetin restored ethanol-induced mitochondrial membrane potential and alleviated mtDNA damage unrelated to apoptosis (a) Representative immunofluorescent images of JC-1 is visible either as JC-1 monomers (green), JC-1 aggregates (red), and both channels merged (200x magnification), whereas more JC-1 aggregates (red) were seen in quercetin treatment while more JC-1 monomers (green) in ethanol group. **(b)** Relative fluorescence intensity calculated as red to green ratio. **(c)** Representative immunofluorescence images co-stained with γH2AX (red), Mito-Tracker (green) and both channels merged (400x magnification). The graphs (down panel) show the fluorescence intensity profiles in two fluorescence channels along the arrow, whereas a weakened fluorescence intensity of γH2AX is seen in quercetin treatment and enhanced by ethanol. **(d)** The mRNA expression that encodes the enzyme (TWNK, MTCO1, and MFND) responsible for mtDNA transcription levels. **(e)** Western blot analysis of Bax, Bcl2, caspase3, and cleaved-caspase3 protein abundance. Data are expressed as mean ± SD (n = 6). Different subscript letters indicate significant differences among the groups (p < 0.05).

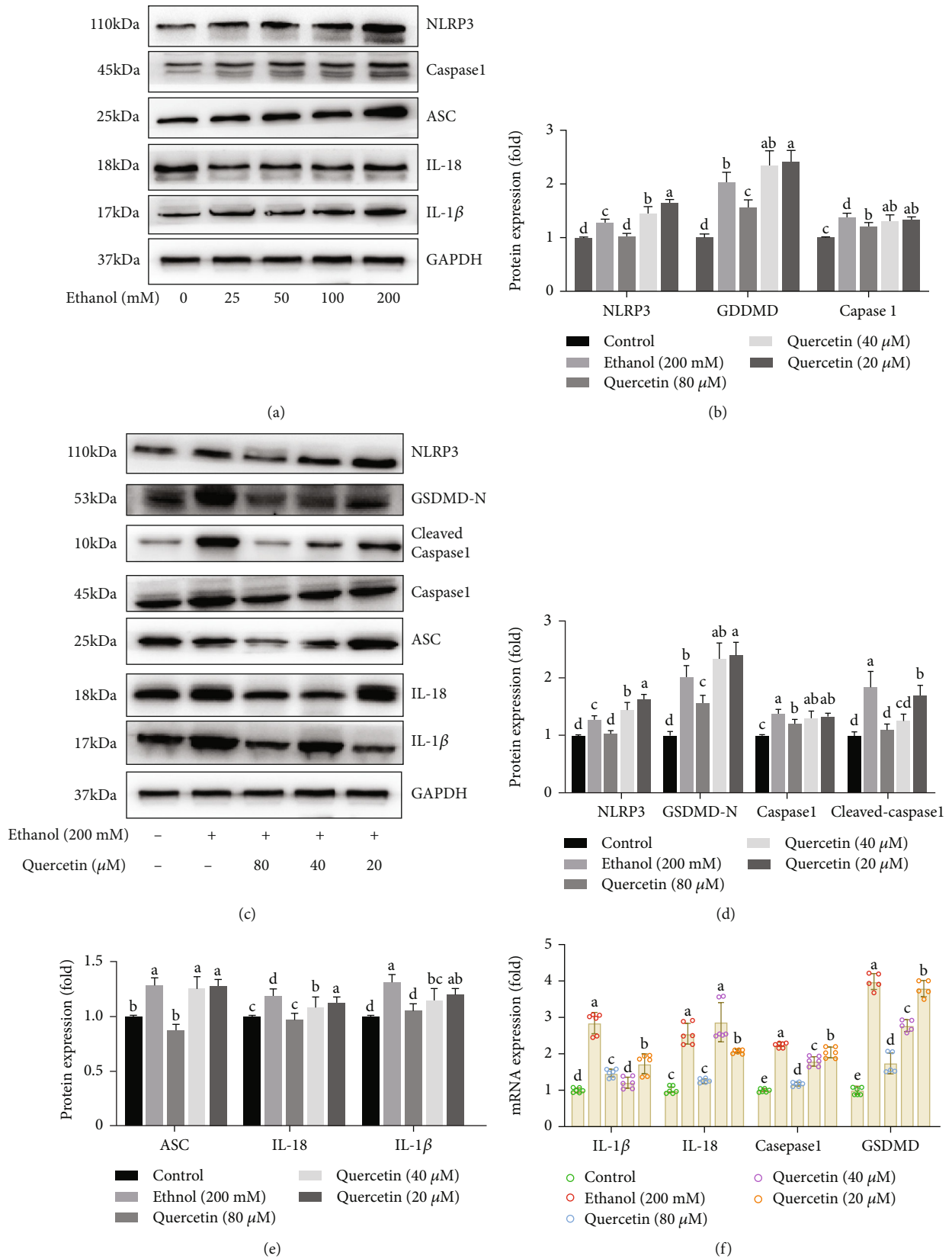


FIGURE 4: Continued.

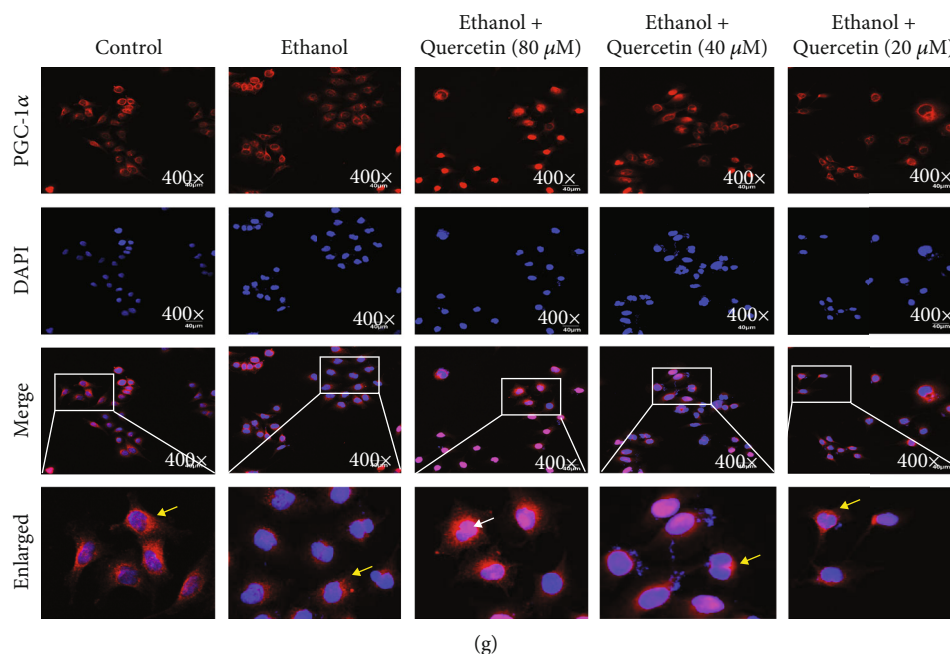


FIGURE 4: Quercetin alleviated ethanol-induced pyroptosis via the nuclear transfer of PGC1 α . (a–e) Western blot analysis of NLRP3, caspase1, cleaved-caspase1, GSDMD-N, ASC, IL-18, and IL-1 β protein abundance. (f) The mRNA expression of IL-1 β , IL-18, caspase1, and GSDMD genes. (g) Representative immunofluorescent images co-stained with PGC-1 α (red), DAPI (blue) and both channels merged (400x magnification). The graphs (down panel) show the fluorescence intensity profiles in two fluorescence channels along the arrow and the white arrows represent nucleus PGC-1 α ; the yellow arrowheads show cytoplasm PGC-1 α , whereas a clear nuclear translocation (white arrow) and shrinkage of PGC-1 α (red) is seen in quercetin treatment and inhibited by ethanol. Data are expressed as mean \pm SD ($n = 6$). Different subscript letters indicate significant differences among the groups ($p < 0.05$).

dose-dependent manner, suggesting that mitochondrial fission may play an important role.

4.3. Quercetin Restored Ethanol-Induced Mitochondrial Membrane Potential and Alleviated mtDNA Damage Unrelated to Apoptosis. Increased ROS activates the opening of mitochondrial permeability transition pores (mPTP), which creates a channel through which mtDNA can be transferred from mitochondria to the cytoplasm, disrupting mitochondrial homeostasis [25]. Mitochondrial membrane potential was detected by JC-1 kit. In normal cells, the mitochondrial membrane potential is high, and the dye aggregates into polymers in the mitochondrial matrix, forming red fluorescent aggregates (JC-1 aggregates). The change of mitochondrial membrane potential prevents the accumulation of JC-1. Therefore, the dye exists as a monomer and produces green fluorescence (JC-1 monomers), and CCCP (1 μ M) was used as a positive control to induce the decrease of mitochondrial membrane potential. The results (Figures 3(a) and 3(b)) showed that the fluorescence with ethanol treatment changed from red to green, mitochondrial membrane potential was decreased, and mitochondrial membrane were certainly damaged ($p < 0.05$). RT-qPCR results also showed the gene that encodes the enzyme (TWNK, MTCO1, and MFND) responsible for mtDNA transcription levels increased under high-concentration ethanol ($p < 0.05$), which was significantly reversed by 80 μ M quercetin (Figure 3(d)). In addition, it has been reported that mtDNA damage can induce cell death [26, 27]. Moreover, a change of mtDNA damage resulted in

mtDNA, the double-strand breaks rapidly leads to Histone-2AX (H2AX) phosphorylation (γ H2AX) [28]. Our immunofluorescence results showed that ethanol stimulated γ -H2AX formation (red fluorescence) and the spread of γ -H2AX reduced after quercetin treatment (Figure 3(c)). However, we detected apoptotic proteins (Bax, Bcl2, caspase3, and cleaved-caspase3) and found no significant changes in the related proteins with the increase of ethanol concentration (Figures 3(e) and 3(f)). These results suggested that apoptosis is not involved in ethanol-induced mitochondrial membrane potential and mtDNA damage and there may be a new pathway of cell death.

4.4. Quercetin Alleviated Ethanol-Induced Pyroptosis. Mitochondrial oxidative damage leads to a series of inflammatory responses [29]. ROS can act as a triggering factor for the activation of NLRP3 inflammasome and a bonfire or effector molecule leading to pathological processes [11]. Pyroptosis is a caspase1-dependent programmed cell death, known as the canonical inflammasome pathway. Compared with control group, various inflammasome-associated proteins (IL-1 β , IL-18, cleaved-caspase1, ASC, and GSDMD-N) as well as inflammasome sensors (NLRP3) showed higher levels in ethanol group, while quercetin decreased the activity of NLRP3, ASC, and cleaved-caspase1. And cleaved-caspase1 drives the maturation of proinflammatory cytokine IL-1 β and IL-18 and the cleavage of GSDMD at D275 (numbering after human GSDMD) into N-termini, eventually resulting in strong inflammation and cell death

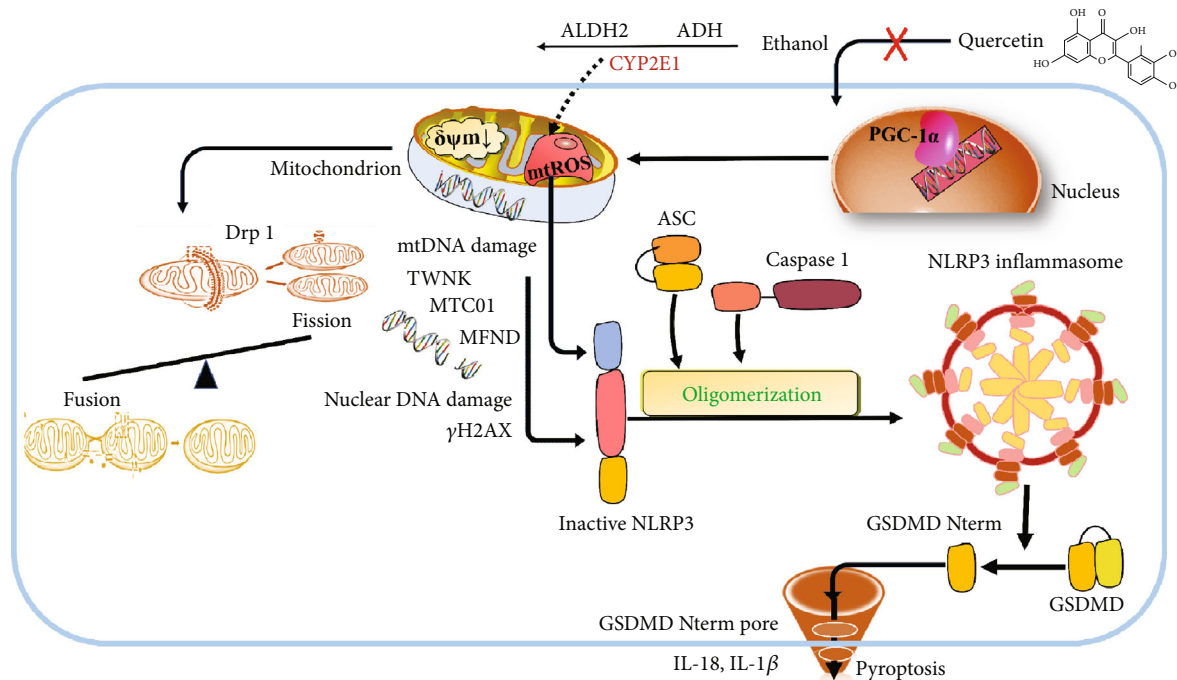


FIGURE 5: The mechanism of quercetin protected ethanol-induced hepatocyte pyroptosis.

(Figures 4(c)–4(e)). Consistently, RT-qPCR results revealed similar mRNA expression patterns of NLRP3, GSDMD, ASC, IL-1 β , and IL-18 (Figure 4(f)), suggesting quercetin protected ethanol-induced hepatocyte pyroptosis. Moreover, we next sought to determine the feasibility of alleviating ethanol-induced pyroptosis by PGC-1 α . It is a transcriptional coactivator and acts as a crucial factor in transcription of nuclear-encoded mitochondrial genes [30]. Immunofluorescence results showed that there was a substantial decline in PGC-1 α nuclear translocation when exposed to high concentration ethanol, while treatment with quercetin induced PGC-1 α nuclear translocation efficiently (Figure 4(g)), suggesting that quercetin-mediated nuclear transfer of PGC-1 α may play an important role in alcohol-induced hepatic pyroptosis.

5. Discussion and Conclusion

Quercetin, a bioactive secondary metabolite, holds incredible importance in terms of bioactivities, which has been proved by *in vivo* and *in vitro* studies [16]. Further, corresponding to the growing population and global demand for fresh fruits and vegetables, a paradigm shift and focus is laid towards exploring the mechanistic role of quercetin in hepatic pathologies. Our results indicated that quercetin protected ethanol-induced hepatocyte pyroptosis via scavenging mitROS and promoting PGC-1 α -mediated mitochondrial dynamics to alleviate hepatocyte pyroptosis in L02 cells. And it rendered quercetin an ideal phytochemical that can provide protective benefits against ALD.

Since hepatocytes are the prime liver parenchymal cells, L02 cell line, as an ideal cell line was incubated with ethanol to establish an *in vitro* model of ALD in our study [31]. In the liver, alcohol dehydrogenase (ADH) and CYP2E1 are the major oxidative pathways of alcohol metabolism, with

a secondary pathway through peroxisome catalase [20]. CYP2E1, a major contributor to ROS generation, is induced by chronic/excessive alcohol consumption and progresses to an advanced disease stage [32]. With the increase of ethanol concentrations (25–100 mM) for 24 h, the mRNA expression of ADH (ADH1, ADH2, and ADH3) increased significantly, while the expression of CYP2E1 dominating alcohol metabolism did not change until the ethanol concentration reached to 200 mM. Interestingly, quercetin effectively reduced the activities of CYP2E1 and enhanced ALDH2, while did not change ADH significantly, suggesting that the inhibition of CYP2E1 by quercetin may represent a novel therapeutic approach for minimizing the ethanol-induced CYP2E1 enzyme activity, which results the hepatotoxicity of ethanol. Thus, a large dose of ethanol (200 mM) was used to expose to L02 cells.

Prior research showed that mitochondrial CYP2E1 had very high NADPH oxidase activity, which can reduce ATP production in mitochondrial electron transport system and increase electron leakage on MRC during chronic drinking [33]. Our research also showed that mitochondrial CYP2E1 played an important role in high acute ethanol exposure. Mitochondria, as highly dynamic organelles, provide most adenosine triphosphate (ATP) production through oxidative phosphorylation (OXPHOS) for normal function [34]. The OXPHOS system consists of five polysubunit complexes in the inner mitochondrial membrane (IMM), consisting of nDNA and mtDNA coding [35]. IMM CYP2E1 acts as a ROS activity generator [33], and mtDNA is located in the inner membrane and not protected by histones, so it is more vulnerable to ROS attack than nDNA, leading to mitochondrial dysfunction [36]. mitROS can inhibit the synthesis of related protein subunits responsible for encoding mtDNA, potentially disrupting the cycle of oxidative phosphorylation, which in

turn releases more mitROS and continues to damage mtDNA, thereby creating a vicious cycle of biological energy disorders to further affect the survival of cells and tissues, and finally lead to the occurrence of cell death [37–39]. Similarly, the genes encoding the enzyme (TWNK, MTCO1, and MFND) responsible for mtDNA transcription levels were observed in our experiment. JC-1 experiment showed that the loss of mtDNA led to the change of mitochondrial membrane potential. Apparently, quercetin alleviated the collapse of the mitochondrial membrane potential to maintain mitochondrial homeostasis.

In addition, inhibition of mitochondrial dynamics also affects the elimination of irreparable mtDNA damage and the transmission of mtDNA mutations [40]. Mitochondrial dynamics is achieved through continuous crest remodeling and the fission and fusion of mitochondrial membranes. Mitochondrial fusion is a complex process involving the connection of the outer and inner membranes of mitochondria, which facilitates the communication between mitochondria and their host cell to maintain cell homeostasis. Mitochondrial outer membrane (OMM) is fused with Mfn1 and Mfn2, and then, IMM is fused with mitochondrial kinetic protein-like GTPase (OPA1) [41]. Mitochondrial fission is triggered by the contraction of endoplasmic reticulum (ER) membrane. The receptors on OMM include fission 1 protein (Fis1), mitochondrial fission factor (Mff), and dynamin-related protein 1 (Drp1), which are involved in controlling the number and distribution of mitochondria and respond to changes in cellular energy requirements [40]. Our study found that quercetin inhibited the expressions of mitochondrial fusion genes including Mfn1, Mfn2, and OPA1, as well as increased fission genes expressions, and the most significant change was Drp1, which played an important role in mediating mitophagy.

Previous studies indicated that unbalanced mitochondrial homeostasis and ROS generation are often associated with a novel type of cell fate, pyroptosis, which is different from previous apoptosis because of depending on the NLRP3/cleaved-caspase1/GSDMD-N activation [42]. In the current study, we demonstrated that it did not restore cell viability when simply reversing apoptosis in high-concentration ethanol-treated hepatocytes, which suggested that other kinds of cell fates such as pyroptosis may be involved. Therefore, we further investigated whether quercetin could alleviate ALD by inhibiting pyroptosis. As an intracellular target of ROS, NLRP3 inflammasome plays a key role in alcohol-induced acute liver injury [43]. Our results found that the inactivation of NLRP3 inflammasome was needed for quercetin to inhibit caspase1 activation in ethanol-induced hepatocytes. Here, we firstly confirmed the curative effect of quercetin to reduce NLRP3 inflammasome-cleaved-caspase1/ASC and GSDMD-N activation and decrease IL-1 β and IL-18 secretions in LO2 cells, alleviating hepatocyte pyroptosis in ALD. Similarly, PGC-1 α , a key mitochondrial biogenesis regulator, modulates NLRP3 inflammasome and attenuates hepatocyte pyroptosis in ALD [15]. In the current study, quercetin promoted the nuclear translocation of PGC-1 α . Consistent with anterior studies, our data showed that NLRP3 served as a downstream event of PGC-1 α to reduce the excessive ROS accumulation in

impaired hepatocytes, which might be the key mechanism of quercetin in relieving hepatocyte pyroptosis. However, how quercetin specifically affects PGC-1 α nuclear translocation and whether PGC-1 α directly activated transcription of GSDMD-N to induce pyroptosis remain to be further studied.

Taken together (Figure 5), it was demonstrated that quercetin protected ethanol-induced hepatocyte pyroptosis via scavenging mitochondrial ROS and maintaining mitochondrial homeostasis. Mechanistically, quercetin promoted PGC-1 α transcription and subsequently restored mitochondrial function and maintained mitochondrial dynamic balance, which ultimately protected hepatocytes from pyroptosis. The above results suggested that quercetin, as a novel phytochemical supplement, had the potential in antihepatic injury at least in part by remodeling PGC-1 α -mediated mitochondrial dynamics to alleviate hepatocyte pyroptosis.

Abbreviations

ADH:	Alcohol dehydrogenase
ALD:	Alcoholic liver disease
ALDH2:	Aldehyde dehydrogenase 2
ATP:	Adenosine triphosphate
CYP2E1:	Cytochrome P450 2E1
Drp1:	Dynamin-related protein 1
ER:	Endoplasmic reticulum
Fis1:	Fission 1 protein
GSDM:	Gasdermin
GSDMD-N:	N-terminus of GSDMD
HF:	High fat
IL-1 β /18:	Interleukin-1 β /18
IMM:	Inner mitochondrial membrane
Mff:	Mitochondrial fission factor
Mfn1:	Mitochondrial fusion protein 1
mPTP:	Mitochondrial permeability transition pores
mtDNA:	Mitochondrial DNA
nDNA:	Nuclear DNA
NLRP3:	Nod-like receptor (NLR) family pyrin domain-containing 3
OMM:	Mitochondrial outer membrane
OPA1:	Mitochondrial kinetic protein-like GTPase
OXPPOS:	Oxidative phosphorylation
ROS:	Reactive oxygen species
TEM:	Transmission electron microscopy
γ H2AX:	Histone-2AX (H2AX) phosphorylation.

Data Availability

The underlying data of the study can be obtained by contacting the authors if it is reasonable.

Additional Points

Institutional Review Board Statement. The experiments were performed under the approval of the Institutional Animal Care and Use Committee of Chengdu University of Traditional Chinese Medicine (No. SYXK (CHUAN) 2014–128).

Conflicts of Interest

All authors confirm that there is no conflict of interest.

Authors' Contributions

Conceptualization was done by X.Z. (Xingtao Zhao), Y.L. (Yunxia Li) and C.P. (Cheng Peng). Funding acquisition was done by Y.L. and C.P. Project administration was done by X.Z. Data curation was done by X.Z., C.W. (Cheng Wang), and S.D. (Shu Dai). Writing—original draft was done by X.Z. and Y.L. Writing—review and editing was done by C.W., S.D., Y.L. (Yanfang Liu), and F.Z. (Fang Zhang). All authors have read and agreed to the published version of the manuscript.

Acknowledgments

We are indebted to our alma mater, Chengdu University of Traditional Chinese Medicine for provided convenience in the collection of documents. Thanks for all the help from everyone. The National Interdisciplinary Innovation Team of Traditional Chinese Medicine (Grant No. ZYYCXTD-D-202209), National Science Foundation of China (Grant Nos. 8189101, 81891012, 8163010, and U19A2010), Sichuan Science and Technology Program (Grant No. 2021JDR0041), and Sichuan TCM Science and Technology Industry Innovation Team (No. 2022C001) supported this study.

References

- [1] J. Manthey, K. D. Shield, M. Rylett, O. S. M. Hasan, C. Probst, and J. Rehm, "Global alcohol exposure between 1990 and 2017 and forecasts until 2030: a modelling study," *The Lancet*, vol. 393, no. 10190, pp. 2493–2502, 2019.
- [2] S. Zakhari, "Overview: how is alcohol metabolized by the body?," *Alcohol Research & Health*, vol. 29, no. 4, pp. 245–254, 2006.
- [3] R. Harjumäki, C. S. Pridgeon, and M. Ingelman-Sundberg, "CYP2E1 in alcoholic and non-alcoholic liver injury. Roles of ROS, reactive intermediates and lipid overload," *International Journal of Molecular Sciences*, vol. 22, no. 15, p. 8221, 2021.
- [4] P. Burra, A. Zanetto, and G. Germani, "Liver transplantation for alcoholic liver disease and hepatocellular carcinoma," *Cancers*, vol. 10, no. 2, p. 46, 2018.
- [5] P. Mathurin and R. Bataller, "Trends in the management and burden of alcoholic liver disease," *Journal of Hepatology*, vol. 62, no. 1, pp. S38–S46, 2015.
- [6] S. A. Taylor and T. Miloh, "Adolescent alcoholic liver disease," *Clinics in Liver Disease*, vol. 23, no. 1, pp. 51–54, 2019.
- [7] Z. Zhong, V. K. Ramshesh, H. Rehman et al., "Acute ethanol causes hepatic mitochondrial depolarization in mice: role of ethanol metabolism," *PLoS One*, vol. 9, no. 3, article e91308, 2014.
- [8] J. J. Lemasters and Z. Zhong, "Mitophagy in hepatocytes: types, initiators and role in adaptive ethanol metabolism," *Liver Research*, vol. 2, no. 3, pp. 125–132, 2018.
- [9] T. M. Leung and N. Nieto, "CYP2E1 and oxidant stress in alcoholic and non-alcoholic fatty liver disease," *Journal of Hepatology*, vol. 58, no. 2, pp. 395–398, 2013.
- [10] D. Bao, J. Zhao, X. Zhou et al., "Mitochondrial fission-induced mtDNA stress promotes tumor-associated macrophage infiltration and HCC progression," *Oncogene*, vol. 38, no. 25, pp. 5007–5020, 2019.
- [11] J. M. Abais, M. Xia, Y. Zhang, K. M. Boini, and P. L. Li, "Redox regulation of NLRP3 inflammasomes: ROS as trigger or effector?," *Antioxidants & Redox Signaling*, vol. 22, no. 13, pp. 1111–1129, 2015.
- [12] B. E. Burdette, A. N. Esparza, H. Zhu, and S. Wang, "Gasdermin D in pyroptosis," *Acta pharmaceutica Sinica. B*, vol. 11, no. 9, pp. 2768–2782, 2021.
- [13] X. Huang, Z. Feng, Y. Jiang et al., "VSIG4 mediates transcriptional inhibition of Nlrp3 and Il-1 β in macrophages," *Science Advances*, vol. 5, no. 1, article eaau7426, 2019.
- [14] M. J. Heo, T. H. Kim, J. S. You, D. Blaya, P. Sancho-Bru, and S. G. Kim, "Alcohol dysregulates miR-148a in hepatocytes through FoxO1, facilitating pyroptosis via TXNIP overexpression," *Gut*, vol. 68, no. 4, pp. 708–720, 2019.
- [15] J. Kai, X. Yang, Z. Wang et al., "Oroxilin A promotes PGC-1 α /Mfn2 signaling to attenuate hepatocyte pyroptosis via blocking mitochondrial ROS in alcoholic liver disease," *Free Radical Biology & Medicine*, vol. 153, pp. 89–102, 2020.
- [16] X. Zhao, J. Wang, Y. Deng et al., "Quercetin as a protective agent for liver diseases: a comprehensive descriptive review of the molecular mechanism," *Phytotherapy Research*, vol. 35, no. 9, pp. 4727–4747, 2021.
- [17] T. M. Henagan, W. T. Cefalu, D. M. Ribnicky et al., "In vivo effects of dietary quercetin and quercetin-rich red onion extract on skeletal muscle mitochondria, metabolism, and insulin sensitivity," *Genes & Nutrition*, vol. 10, no. 1, p. 451, 2015.
- [18] M. R. de Oliveira, S. M. Nabavi, N. Braidy, W. N. Setzer, T. Ahmed, and S. F. Nabavi, "Quercetin and the mitochondria: a mechanistic view," *Biotechnology Advances*, vol. 34, no. 5, pp. 532–549, 2016.
- [19] X. Luo, X. Bao, X. Weng et al., "The protective effect of quercetin on macrophage pyroptosis via TLR2/Myd88/NF- κ B and ROS/AMPK pathway," *Life Sciences*, vol. 291, article 120064, 2022.
- [20] R. Teschke, "Alcoholic liver disease: alcohol metabolism, cascade of molecular mechanisms, cellular targets, and clinical aspects," *Biomedicine*, vol. 6, no. 4, 2018.
- [21] R. Teschke, "Microsomal ethanol-oxidizing system: success over 50 years and an encouraging future," *Alcoholism, Clinical and Experimental Research*, vol. 43, no. 3, pp. 386–400, 2019.
- [22] R. Teschke, "Alcoholic liver disease: current mechanistic aspects with focus on their clinical relevance," *Biomedicine*, vol. 7, no. 3, p. 68, 2019.
- [23] Y. Wang, M. Lu, L. Xiong et al., "Drp1-mediated mitochondrial fission promotes renal fibroblast activation and fibrogenesis," *Cell Death & Disease*, vol. 11, no. 1, p. 29, 2020.
- [24] H. Mortiboys, K. J. Thomas, W. J. Koopman et al., "Mitochondrial function and morphology are impaired in parkin-mutant fibroblasts," *Annals of Neurology*, vol. 64, no. 5, pp. 555–565, 2008.
- [25] C. A. Piantadosi, "Mitochondrial DNA, oxidants, and innate immunity," *Free Radical Biology & Medicine*, vol. 152, pp. 455–461, 2020.
- [26] Z. Zhong and J. J. Lemasters, "A unifying hypothesis linking hepatic adaptations for ethanol metabolism to the proinflammatory and profibrotic events of alcoholic liver disease,"

- Alcoholism, Clinical and Experimental Research*, vol. 42, no. 11, pp. 2072–2089, 2018.
- [27] A. Michalak, T. Lach, and H. Cichoż-Lach, “Oxidative stress—a key player in the course of alcohol-related liver disease,” *Journal of Clinical Medicine*, vol. 10, no. 14, p. 3011, 2021.
- [28] A. Sharma, K. Singh, and A. Almasan, “Histone H2AX phosphorylation: a marker for DNA damage,” *Methods in Molecular Biology*, vol. 920, pp. 613–626, 2012.
- [29] Y. R. Shim and W. I. Jeong, “Recent advances of sterile inflammation and inter-organ cross-talk in alcoholic liver disease,” *Experimental & Molecular Medicine*, vol. 52, no. 5, pp. 772–780, 2020.
- [30] S. Rius-Pérez, I. Torres-Cuevas, I. Millán, Á. L. Ortega, and S. Pérez, “PGC-1 α , inflammation, and oxidative stress: an integrative view in metabolism,” *Oxidative Medicine and Cellular Longevity*, vol. 2020, Article ID 1452696, 20 pages, 2020.
- [31] R. Pingili, A. K. Pawar, and S. R. Challa, “Quercetin reduced the formation of N-acetyl-p-benzoquinoneimine, a toxic metabolite of paracetamol in rats and isolated rat hepatocytes,” *Phytotherapy research : PTR*, vol. 33, no. 7, pp. 1770–1783, 2019.
- [32] A. Nagappan, D. Y. Jung, J. H. Kim, H. Lee, and M. H. Jung, “Gomisin N alleviates ethanol-induced liver injury through ameliorating lipid metabolism and oxidative stress,” *International Journal of Molecular Sciences*, vol. 19, no. 9, p. 2601, 2018.
- [33] L. Xu, Y. Yu, R. Sang, J. Li, B. Ge, and X. Zhang, “Protective effects of taraxasterol against ethanol-induced liver injury by regulating CYP2E1/Nrf2/HO-1 and NF- κ B signaling pathways in mice,” *Oxidative Medicine and Cellular Longevity*, vol. 2018, Article ID 8284107, 11 pages, 2018.
- [34] G. S. Gorman, P. F. Chinnery, S. DiMauro et al., “Mitochondrial diseases,” *Nature Reviews Disease Primers*, vol. 2, no. 1, article 16080, 2016.
- [35] A. Mansouri, B. Fromenty, A. Berson et al., “Multiple hepatic mitochondrial DNA deletions suggest premature oxidative aging in alcoholic patients,” *Journal of Hepatology*, vol. 27, no. 1, pp. 96–102, 1997.
- [36] D. C. Wallace, “Mitochondrial genetic medicine,” *Nature Genetics*, vol. 50, no. 12, pp. 1642–1649, 2018.
- [37] H. Cui, Y. Kong, and H. Zhang, “Oxidative stress, mitochondrial dysfunction, and aging,” *Journal of Signal Transduction*, vol. 2012, Article ID 646354, 13 pages, 2012.
- [38] M. A. Abdallah and A. K. Singal, “Mitochondrial dysfunction and alcohol-associated liver disease: a novel pathway and therapeutic target,” *Signal Transduction and Targeted Therapy*, vol. 5, no. 1, p. 26, 2020.
- [39] T. E. Müller, M. E. M. Nunes, N. R. Rodrigues et al., “Neurochemical mechanisms underlying acute and chronic ethanol-mediated responses in zebrafish: the role of mitochondrial bioenergetics,” *Neurochemistry International*, vol. 131, article 104584, 2019.
- [40] J. N. Meyer, T. C. Leuthner, and A. L. Luz, “Mitochondrial fusion, fission, and mitochondrial toxicity,” *Toxicology*, vol. 391, pp. 42–53, 2017.
- [41] H. M. Ni, J. A. Williams, and W. X. Ding, “Mitochondrial dynamics and mitochondrial quality control,” *Redox Biology*, vol. 4, pp. 6–13, 2015.
- [42] Y. Geng, Q. Ma, Y. N. Liu et al., “Heatstroke induces liver injury via IL-1 β and HMGB1-induced pyroptosis,” *Journal of Hepatology*, vol. 63, no. 3, pp. 622–633, 2015.
- [43] S. Liu, L. Tian, G. Chai, B. Wen, and B. Wang, “Targeting heme oxygenase-1 by quercetin ameliorates alcohol-induced acute liver injury via inhibiting NLRP3 inflammasome activation,” *Food & Function*, vol. 9, no. 8, pp. 4184–4193, 2018.

Research Article

Role of Inflammation, Oxidative Stress, and Mitochondrial Changes in Premenstrual Psychosomatic Behavioral Symptoms with Anti-Inflammatory, Antioxidant Herbs, and Nutritional Supplements

Arshiya Sultana ¹, Khaleequr Rahman ², Md Belal Bin Heyat ³, Sumbul ¹,
Faijan Akhtar ⁴, and Abdullah Y. Muaad ⁵

¹Department of Amraze Niswan wa Ilmul Qabalat, National Institute of Unani Medicine, Ministry of AYUSH, Bengaluru, Karnataka, India

²Department of Ilmul Saidla, National Institute of Unani Medicine, Ministry of Ayush, Bengaluru, Karnataka, India

³IoT Research Center, College of Computer Science and Software Engineering, Shenzhen University, Shenzhen, Guangdong 518060, China

⁴School of Computer Science and Engineering, University of Electronic Science and Technology of China, Chengdu, Sichuan, China

⁵IT Department, Sana'a Community College, Sana'a5695, Yemen

Correspondence should be addressed to Arshiya Sultana; drarshiya@yahoo.com, Md Belal Bin Heyat; belalheyat@gmail.com, and Abdullah Y. Muaad; abdullahmuaad9@gmail.com

Received 17 April 2022; Accepted 1 July 2022; Published 13 July 2022

Academic Editor: Chan-Yen Kuo

Copyright © 2022 Arshiya Sultana et al. This is an open access article distributed under the Creative Commons Attribution License, which permits unrestricted use, distribution, and reproduction in any medium, provided the original work is properly cited.

Premenstrual syndrome (PMS) significantly lowers the quality of life and impairs personal and social relationships in reproductive-age women. Some recommendations are that inappropriate oxidative stress and inflammatory response are involved in PMS. Various nutritional supplements and herbs showed neuro-psycho-pharmacological activity with antioxidant and anti-inflammatory properties. This study aims to determine the systematic review of randomized controlled trials (RCTs) of herbal medicine and nutritional supplements in PMS. We also comprehensively highlighted the role of oxidative stress, inflammation, and mitochondrial changes on PMS with the application of computational intelligence. We used PRISMA and research question-based techniques to collect the data for evaluation of our study on different databases such as Scopus, PubMed, and PROSPERO from 1990 to 2022. The methodological quality of the published study was assessed by the modified Jadad scale. In addition, we used network visualization and word cloud techniques to find the closest terms of the study based on previous publications. While we also used computational intelligence techniques to give the idea for the classification of experimental data from PMS. We found 25 randomized controlled studies with 1949 participants (mean \pm SD: 77.96 \pm 22.753) using the PRISMA technique, and all were high-quality studies. We also extracted the closest terms related to our study using network visualization techniques. This work has revealed the future direction and research gap on the role of oxidative stress and inflammation in PMS. In vitro and in vivo studies showed that bioactive molecules such as curcumin, allicin, anethole, thymoquinone, cyanidin 3-glucoside, gamma-linoleic acid, and various molecules not only have antioxidant and anti-inflammatory properties but also other various activities such as GABA-A receptor agonist, serotonergic, antidepressant, sedative, and analgesic. Traditional Unani Herbal medicine and nutritional supplements can effectively relieve PMS symptoms as they possess many bioactive molecules that are pharmacologically proven for the aforementioned properties. Hence, these biomolecules might influence a complex physical and psychological disease process like PMS. However, more rigorous research studies are recommended for in-depth knowledge of the efficacy of bioactive molecules on premenstrual syndrome in clinical trials.

1. Introduction

Premenstrual syndrome (PMS) is categorized by psychosomatic and behavioral symptoms that manifest repetitively in the luteal phase, a cyclic pattern, and days before menstruation. The patient is symptom-free between two luteal steps [1–3]. The global pooled prevalence of PMS is 47.8% with the highest in Asia and the lowest in Europe [4]. Eighty-five per cent of reproductive-age women experience at least one symptom of PMS, and 2.5–3% of women suffer from premenstrual dysphoric disorder (PMDD) [2]. It has been reported that women with PMS tend to have a significantly lower quality of life, legal problems, suicidal ideation, decreased work productivity, social isolation, parenting problems, increased absenteeism from work, impaired personal and social relationships, and more frequent visits to hospitals [2, 5, 6]. Additionally, PMS also leads to an increased tendency to have an accident, drug addiction, economic losses, and a decline in domestic achievement. The diagnostic criteria of the PMS for affective symptoms and somatic symptoms must be experienced during the five days before menses in three prior menstrual cycles and relieved with the menstrual flow [7]. The primary psychological range of PMS is anxiety and depression [6, 8].

Sex hormones strongly modulate the immune-inflammatory process [9]. PMS causes are still unclear and are multifactorial [10, 11] probably as a consequence of interaction and biochemical changes amid the menstrual cycle's hormonal fluctuations (imbalance like progesterone deficiency and estrogen excess) [8] with central neurotransmitters (γ -aminobutyric (GABA) and cholecystikinin serotonin) and altered brain processes [5], genetic vulnerability, and regulation of the renin-angiotensin-aldosterone system [12–14]. Previous research reported that various other factors such as high carbohydrates, fat, lack of calcium, vitamins and minerals, psychological factors (stress, depression, and anxiety), genetics, and lifestyle (alcohol consumption, smoking, lack of exercise, and eating habits) in addition to oxidative stress and inflammation are related with the incidence of PMS. Oxidative stress is higher in women who experience PMS as per the previous research [5]. Consequently, as an etiology is unclear, several possible treatments are prescribed and purchased [8]. Various therapeutic interventions have been scientifically confirmed helpful in PMS ranging from nonpharmacological management (cognitive behavioral therapy, lifestyle modification and diet, education, exercise, and complementary and herbal medications) to pharmacotherapy hormonal therapy (gonadotropin-releasing hormone (GnRH) agonists OCP, etc.) and psychotropic medications (benzodiazepines and selective serotonin reuptake inhibitors) [13]. Despite a reasonable success rate of these pharmacotherapies for PMS, each has a substantial adverse effects profile (insomnia, dysphoria, nausea, perspiration, muscle cramps, and tremor). Women with PMS symptoms are frequently hesitant to take SSRIs and other conventional medicines, partially because it causes side effects. Thus, the majority of women are turning towards complementary and alternative medicines to treat their symptoms. Many Unani herbs have been anticipated to

alleviate PMS as they are a potentially effective natural alternative for PMS symptoms [8].

In recent times, products from plants and animals that are natural sources appear to be a potential basis of emergent pharmaceutical agents and food supplements [15]. The natural products or foods have active compounds that are also established to have antioxidant property and are replacing synthetic antioxidants and antimicrobial agents due to their carcinogenicity [16]. Evidence from recent research confirmed that vitamins and supplementation (magnesium, calcium, vitamins B6, D, and E) or herbal/complementary and alternative medicine (CAM) might alter oxidative stress and the hormonal or inflammatory profile in women who experience PMS. CAMs including supplements and vitamins are preferred by women affected by PMS over conventional medical or surgical management to help cope with symptoms. It has been implicated that oxidative stress and antioxidants may affect a complex psychological and physical disease process like PMS [1]. Various Unani herbs such as polyphy, saffron, chaste berry, anise seed, black seeds, spikenard, lemon balm, borage, chamomile, ginger, fennel, and serely have been studied in premenstrual syndrome. To avert the beginning and development of neurodegeneration by amendment of pathogenic factors in neurodegenerative disorders, phytochemicals can unswervingly inhibit or promote mitochondrial apoptosis cascade and regulate mitochondrial functions, ROS/RNS production, apoptosis signaling, mitochondrial biogenesis ATP synthesis, and degradation by autophagy (mitophagy) and exhibit neuroprotection. Relatively, the vast number of compounds, including anti-inflammatory, antioxidants (vitamins C and E), inhibitors of monoamine oxidase (MAO), and coenzyme Q (bioenergetic compound agents), has been testified to be neuroprotective [17]. The “mitochondrial matrix thiol system” has a vital role in antioxidant defense [18]. In addition, bioactive food compounds of herbs and spices show both antioxidant and anti-inflammatory processes [19]. Flavonoids show anti-inflammation property through the antioxidant property and inflection of signal transduction for the amalgamation of pro-inflammatory cytokines [17].

Previously, Dante and Facchinetti [20] designed a review on herbal medicine related to PMS with 10 RCTs. They also designed a study related to herbal medicine and acupuncture for PMS in 2014 [21]. The other researchers conducted a study on the Chamomile single herb [8] and exercises for PMS [22]. However, a recent update on the systematic review of RCTs on herbal medicine and nutritional supplements alleviating PMS as per the modified Jadad scale was not available to the best of our knowledge. Hence, we aimed and intended to reconnoitre the critical appraisal and contemporary research to address the updated systematic review of RCTs as per the modified Jadad scale to provide more objective data for the effectiveness of herbal medicine and nutritional supplements in alleviating PMS symptoms.

In addition, computational intelligence has an important role in the medical areas such as detection, treatment, localization, and recommendation. Currently, some intelligence techniques such as machine learning, deep learning [23, 24], and the Internet of Things (IoT) [25] with

processing techniques such as signal processing, image processing, text processing, video processing, and audio processing are used in the medical fields. Previously, the Siddiqui group used physiological signals to detect sleep disorders [26–29]. Lai group used medical machine learning and deep learning techniques to automatic detection of bruxism sleep disorder [30–32] and cardiac diseases [33, 34]. Ali et al. [35] designed an automatic system for the detection of Parkinson's disease. Ukwuoma et al. [36] used different deep learning technique to classify and detect medical diseases. The Iqbal group applied intelligence techniques for the analysis of the experimental data [37, 38]. However, in this present study, we used the computational intelligence technique to classify the PMS experimental data.

We accumulated up-to-date research to address oxidative stress, inflammation, and mitochondrial changes and their associates. We conducted this review to address most of the information related to PMS with oxidative stress, inflammation, and mitochondrial changes. In addition, we also gave the idea about using computational techniques on PMS. Because no previous research has incorporated this type of information in the review article, this review aims to overview and analyze various issues related to inflammation, oxidative stress, and mitochondrial changes in premenstrual psychosomatic and its behavioral symptoms towards the therapeutic implication of herbal anti-inflammatory and antioxidants. Hence, this paper aims to provide a solution to the following research questions (RQs):

- (i) What is the etiopathogenesis, the role of oxidative stress, inflammation leading to mitochondrial changes in premenstrual psychosomatic, and its behavioral symptoms?
- (ii) What are the various mechanisms of action of nutritional supplements and herbal medicines with their phytochemical/bioactive constituents in premenstrual psychosomatic and its behavioral symptoms?
- (iii) Does computational intelligence have a role in PMS data analysis for future modulation of premenstrual symptoms?

We designed a comprehensive picture related to the role of inflammation and oxidative stress during symptoms based on the previous research with the recent advancement and future recommendations. We used two types of literature review: (A) systematic literature review using PRISMA guidelines on Scopus, PubMed, and PROSPERO databases [39] and (B) research questions based literature review [39, 40]. Our main contributions to this study are as follows: (a) to design a comprehensive survey on the effectiveness of herbal medicine in PMS symptoms, (b) the role of oxidative stress and inflammation on PMS symptoms, (c) to find various mechanisms of action of nutritional supplements and herbal medicine, (d) computational intelligence-based classification of the experimental data using support vector machine (SVM) and random forest model, (e) to design a network visualization and word cloud based on previously

published articles, and (f) to determine the research gaps and future directions. The present study's organization is as follows: a systematic literature review using PRISMA [41] and an answer to the RQs [39, 40] based on previous studies, network visualization [42, 43], and world clouds [44] based on keywords, discussion, research gap, future prospects, and conclusions.

2. Systematic Literature Review Based on PRISMA

2.1. Method. A comprehensive research methodology is systematically discussed, together with various data collection and analysis steps. PRISMA guidelines [39–41, 44, 45] were implemented to produce this study as it uses a guideline checklist [46]. Various steps carried out in the methods are as follows: (a) planning and developing a protocol; (b) conducting a comprehensive literature search; (c) data collection by screening titles, abstracts, and keywords; (d) developing explicit selection criteria; (e) analyzing the results; (f) synthesizing the information; and (g) reporting results [47, 48]. Additionally, a classification method for computational intelligence in an experimental study was also performed.

2.1.1. Database and Search Strategies. We retrieved online databases such as PROSPERO, PubMed, and Scopus to collect all literature from 1990 to 2022 focusing on oxidative stress, inflammation of psychosomatic and behavioral premenstrual symptoms among reproductive-age women, the therapeutic implication of antioxidants, and anti-inflammatory nutritional supplements and herbal medicines. Additionally, a classification method for computational intelligence in an experimental study was performed. To get an adequate number of studies related to our topic, we broadened MeSH search terms and categories. The keywords used for the literature search were as follows: “Premenstrual Syndrome”, “Premenstrual Dysphoric Disorders”, “Herbal medicine and the premenstrual syndrome”, “oxidative stress and PMS”, “inflammation and PMS”, “psychological symptoms and the premenstrual syndrome”, “antioxidants and the premenstrual syndrome”, and “anti-inflammatory herbal medicine and PMS”.

2.1.2. Eligibility Criteria. The selection of articles was performed in two steps. In the initial step, one of the authors screened the articles based on the titles and abstracts. Two researchers independently analyzed and extracted the data from the screened articles after reviewing them thoroughly to avoid bias, and the results were organized. Detailed records regarding age, tools for data collection, intervention type, significant results, phytoconstituents, and pharmacological activities were recorded. Irrelevant studies and insufficient quantitative data were excluded. The PRISMA and Consort Statement Checklist were used for assessing reliability, while duplicates of the studies were recognized and deleted. Table 1 summarizes the inclusion and exclusion criteria considered based on various parameters. Research articles from peer-reviewed journals and dissertations were included, and those not directly related to our framework of the study were excluded. Data from animal experiments

TABLE 1: Various inclusion and exclusion criteria.

Criteria	Inclusion	Exclusion	Justification
Subject	Patients with premenstrual symptoms	No exclusion	Included all PMSS scales
Language	English and Persian	Other languages	Probabilities of misapprehension of data in other languages may therefore disturb the accuracy
Access	Can access full text	Cannot access full text	To confirm the explanation of an article more precisely
Methodology	All	No exclusions	All methodologies were included for a holistic view
Nature of the article	Research and Survey	Observational studies, review, book, and editorial	Review articles comprehending a generalized discussion over a topic would not sufficiently answer our specific research question

and *in vitro* investigations were included for understanding the etiopathogenesis of premenstrual symptoms and pharmacological activities of herbs. In the final comparison, studies were considered reliable and were included, if they had standard criteria. All data retrieved were read and assessed by researchers and consecutively checked individually by the other authors.

2.1.3. Study and Process of Data Extraction. We studied the titles, abstracts, and keywords of all published articles to determine their eligibility and relevance to be included in our study. After a thorough examination of the full articles, final decisions on inclusion were made. To exclude duplicated publications, the complete versions and most recent articles were selected.

Figure 1 depicts the total articles retrieved from PubMed and Scopus databases. Finally, we included 25 RCTs for systematic analysis and irrelevant articles were excluded. We included one recent dissertation work and a few articles from Google Scholar. Research articles written in Chinese language were excluded. Next, these selected articles were further screened by abstracts, titles, and keywords, considering the exclusion criteria. Table 1 shows the various inclusion criteria.

2.1.4. Risk of Bias and Quality Assessment. The risk of bias and the quality of published articles included were assessed by 2 researchers (AS and S). Any kind of discrepancy was resolved by consensus among the authors. Data was successfully extracted and independently assessed for the quality assessment of the collected data from primary studies. We evaluated the methodological quality using a modified Jadad scale which includes 1 point for each domain described with a minimum score of zero and a maximum score of 8 points. The higher scores indicate better high quality (>3) and <3 signified low quality [49, 50].

2.2. Analysis and Synthesis of the Results. We used online databases, Scopus, PubMed, and PROSPERO to collect the data. All published papers were written in different languages except English and Persian in Scopus and PubMed, so we did not add those studies to our work. Few articles were included from the dissertation work and other databases. We applied “Premenstrual” AND “Herbal Medicine” “Premenstrual” AND “oxidative stress and inflammation”

to the Scopus database and collected all information about the papers. We found subject areas, year-wise publications, country-wise, and sources shared in the publications related to the premenstrual symptoms among reproductive-age women mentioned in Figures 2, 3, and 4. Figure 2 represents the publisher-wise publications of RCTs published on premenstrual syndrome and herbal medicine. The majority of papers were published by Springer (27%), followed by Hindawi (9%) and other publishers. Besides, Figure 3 represents the country-wise publications based on previous reports. The Iran researchers have a maximum of 74% contribution in the publications, followed by India (8%), Norway (7%), Denmark (6%), and others (5%). Figure 4 represents the yearly publications published from 1990 to 2022. Leading publications were found in 2020 (24%) followed by 2015 (16%). Three papers were in the Persian language, and the others were from the English language.

In Table 2, the characteristics of previously published papers using PRISMA techniques were evaluated through design, number of participants, tools, intervention type, outcomes of the study, and adverse effects of nutritional supplements and herbal medicine. Additionally, bioactive molecules and pharmacological activities were also included in the same table for ease to understand the effect of herbal medicine and nutritional supplements. PRISMA techniques only covered the given keywords on the Scopus and PubMed databases for RCT studies. We also included one dissertation work. We did not cover the other indexing, so our research questions covered most previously published articles. We found 25 randomized controlled studies with 1949 participants (mean \pm SD: 77.96 ± 22.753 ; variance: 517.71; and CI: 4.55) using the PRISMA technique. We found four RCTs, which were on nutritional supplements, and 21 RCTs where herbal medicines were used for PMS symptoms. All the studies were randomized, five were single-blind, three were triple-blind, and 17 studies were double-blind. In 25 studies, 15 studies reported the adverse effects. Most of the studies interpreted the action and pharmacological properties of herbal medicines.

2.2.1. Risk Assessment of the Data. In the 25 included studies, the risk of bias in each of the 8 domains is shown in Table 3. Most of the studies indicated a substantial quality of this systematic review with low risk for all domains. The quality of included studies was high in that 6 studies had scores of 8

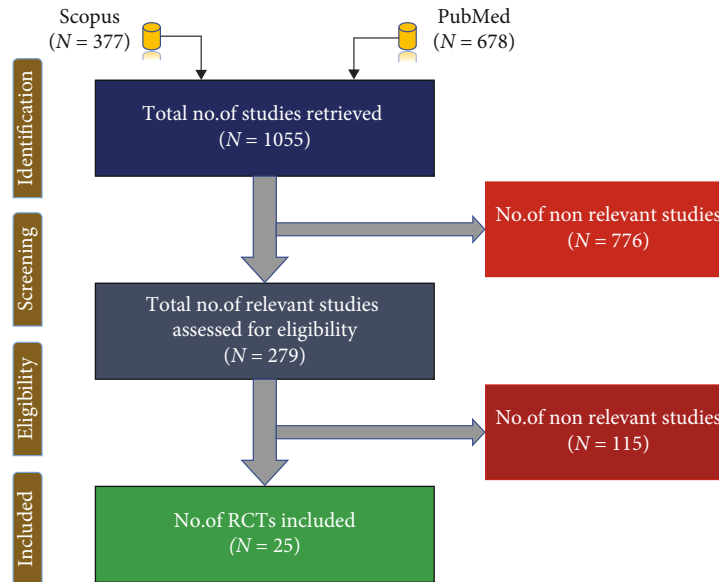


FIGURE 1: PRISMA of the proposed study.

and 19 studies had scores between 5 and 7 on the modified Jadad scale.

The systematic literature review of 25 RCTs was having low risk of bias with high quality as per the modified Jadad scale. 100 percent of studies were randomized and mentioned selection criteria, blinding process, and statistical analysis. 88% of studies reported the appropriate method of randomization, and 60% of studies have not reported the adverse effect of the drugs (see Figure 5).

3. Literature Review Based on Research Questions

Table 2 covered RCTs on nutritional supplements and herbal medicines used to alleviate premenstrual syndrome among reproductive-age women. Further, we designed research questions related to premenstrual psychosomatic and behavioral symptoms and oxidative stress, inflammation, and various mechanisms of action in nutritional supplements and Unani herbal medicines with their phytochemical constituents/bioactive molecules in premenstrual psychosomatic and its behavioral symptoms. Further, for the accuracy of data, computational intelligence has a role in RCT data analysis for future modulation of premenstrual symptoms and in designing a network visualization and word cloud based on previously published articles. Hence, the research questions were answered.

3.1. What Is the Etiopathogenesis, the Role of Oxidative Stress, Inflammation Leading to Mitochondrial Changes in Premenstrual Psychosomatic, and Its Behavioral Symptoms? PMS has a variety of stress symptoms together with psychiatric and somatic complaints, and oxidative imbalance appears to be implicated in the biochemical basis of the pathophysiologic mechanism of PMS [14]. PMS causes are still unclear and are multifactorial [10, 11]. Currently, few theories propose that there is a relationship between ovarian

hormone levels and PMS. PMS is related to ovarian hormone levels based on the fact that the absence of PMS symptoms before puberty, during pregnancy, after menopause, and during treatment with gonadotropin-releasing hormone (GnRH) analogue conditions. Nevertheless, it has been proven that there is no noteworthy difference between symptomatic and asymptomatic women concerning progesterone levels. This is explicated by the concept that some women are more sensitive to progesterone. Additionally, serotonin levels and gamma-aminobutyric acid (GABA) levels also play a role in premenstrual symptoms. Ovarian hormones, estrogen, and progesterone are influenced by estrogenic activity in the brain and are sensitive to serotonin receptors. Progesterone causes depression in an individual by increasing MOA, related to the transport of serotonin; however, estrogen produces an antidepressant effect. Consequently, high progesterone and low estrogen levels in the luteal phase trigger depressive mood. Another concept for the etiology of PMS is the relationship between GABA and progesterone. Allopregnanolone, a metabolite of progesterone, regulates the level of GABA in the blood. Before the luteal phase, allopregnanolone is in higher concentration; therefore, GABA receptors are less susceptible to allopregnanolone. Consequently, allopregnanolone's lower concentration in the luteal phase causes aggression, depression, and mood anxiety. Certainly, women suffering from PMS showed low levels of allopregnanolone levels [6].

PMS patients showed a lower 5-HT response to a 5-HT precursor, tryptophan, during the luteal phase when compared to the follicular or mid luteal phase. Currently, another possible mechanism under search is an insufficient inflammatory response to biological or physical stimuli and the manifestation of oxidative stress "an imbalance between the production of reactive oxygen species (ROS) and their inactivation by antioxidant protection mechanisms." In a healthy human, as a result of metabolic activity, not only inflammation but also oxidative stress can be seen.

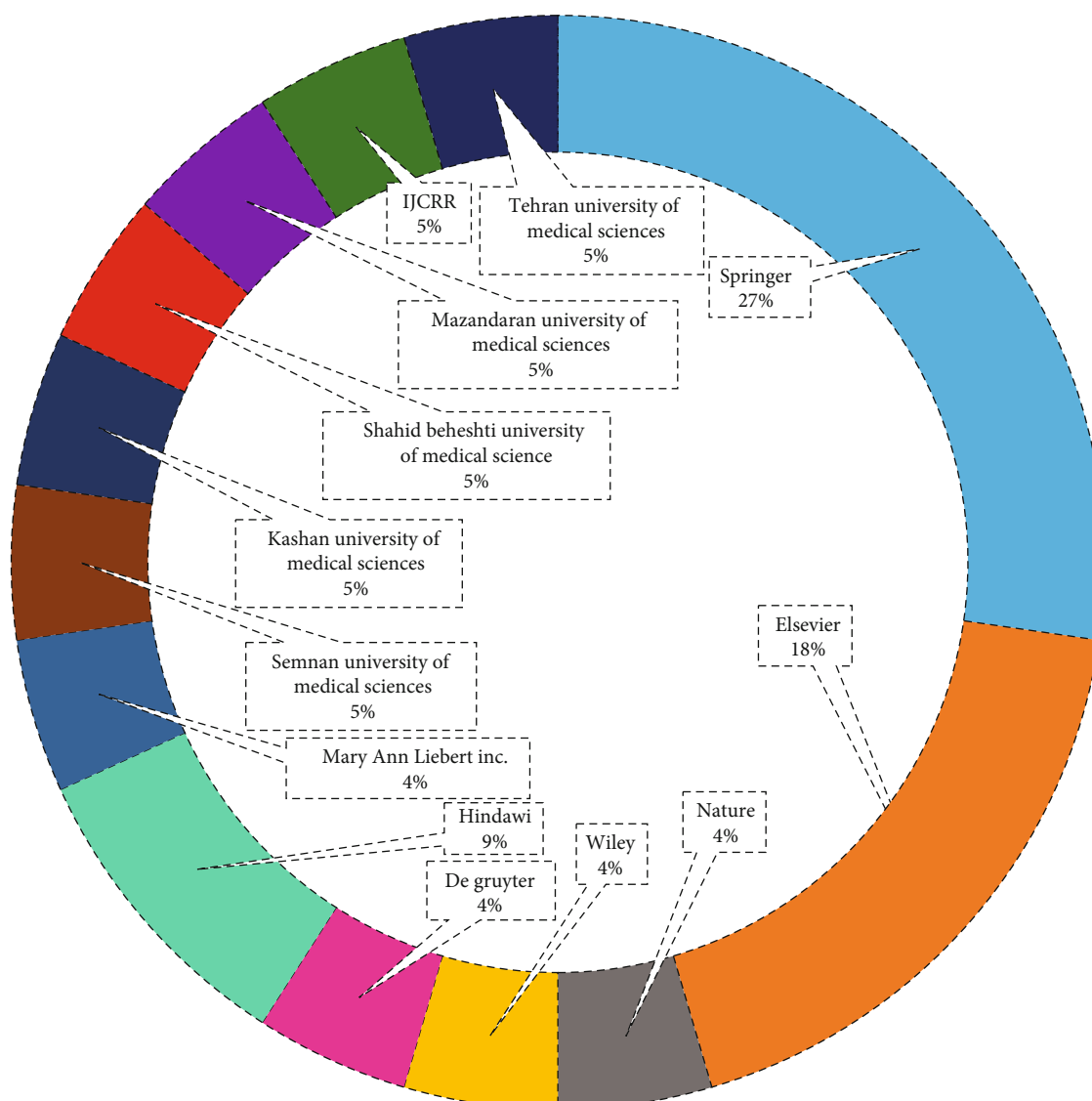


FIGURE 2: Publisher-wise previously published articles related to RCTs on PMS and herbal medicine.

Sometimes, inflammation supports cells to accustom to and subsist stress conditions. During the menstrual cycle, alternation of inflammation status is experienced by reproductive-age women. Nevertheless, oxidative stress and chronic inflammation are considered probable factors of PMS development, pre-eclampsia, endometriosis, and recurrent pregnancy loss. Biomarkers of oxidative stress and inflammation were measured in women with PMS symptoms. Another principal theory is an alternation in response to exposure or withdrawal to the progesterone metabolite, allopregnanolone, which is also a gamma-aminobutyric acid (GABA) agonist. It has been proven that premenstrual symptoms are reduced by blocking allopregnanolone production, and a serotonin re-uptake inhibitor is one of the PMS pharmacotherapies that affects allopregnanolone levels [10].

Mitochondria have a key role in cellular bioenergetics and cell survival. Oxidative stress results in chronic hypoperfusion and induces mitochondrial damage. The increased

intracellular production of oxidants and pro-oxidants is associated with mitochondrial damage [74]. Mitochondrial dysfunction possibly will initiate downstream variations in extracellular matrix proteins (EMP) such as inflammation, neuronal nitric oxide (nNOS), reelin, and finally adult hippocampal neurogenesis in oxidative stress. The reelin and mitochondrial dysfunction relationship has been studied where reelin in the periphery cooperates with the immune system; hence, a loss of reelin can amplify inflammatory markers that affect mitochondria. Additionally, some studies reported that variations in mitochondrial functions such as membrane polarity and oxidative phosphorylation, potentially increasing apoptosis, oxidative, and stress, may precede the development of depressive symptoms. Serotonin (5HT) and norepinephrine (NE) receptor activation and desensitized and dysregulated monoamine receptors result in deviations in intracellular second messenger signal transduction cascades associated with depression. These explanations are linked to mitochondrial dysfunction where the binding

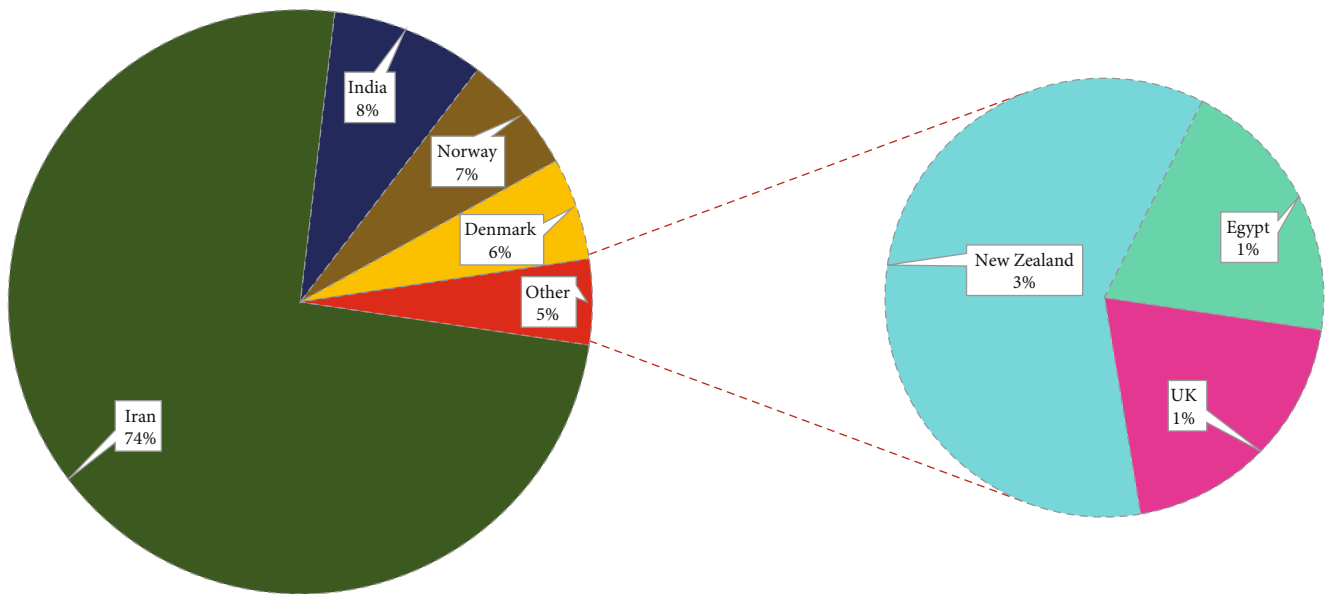


FIGURE 3: Country-wise previously published articles related to RCTs on PMS and herbal medicine.

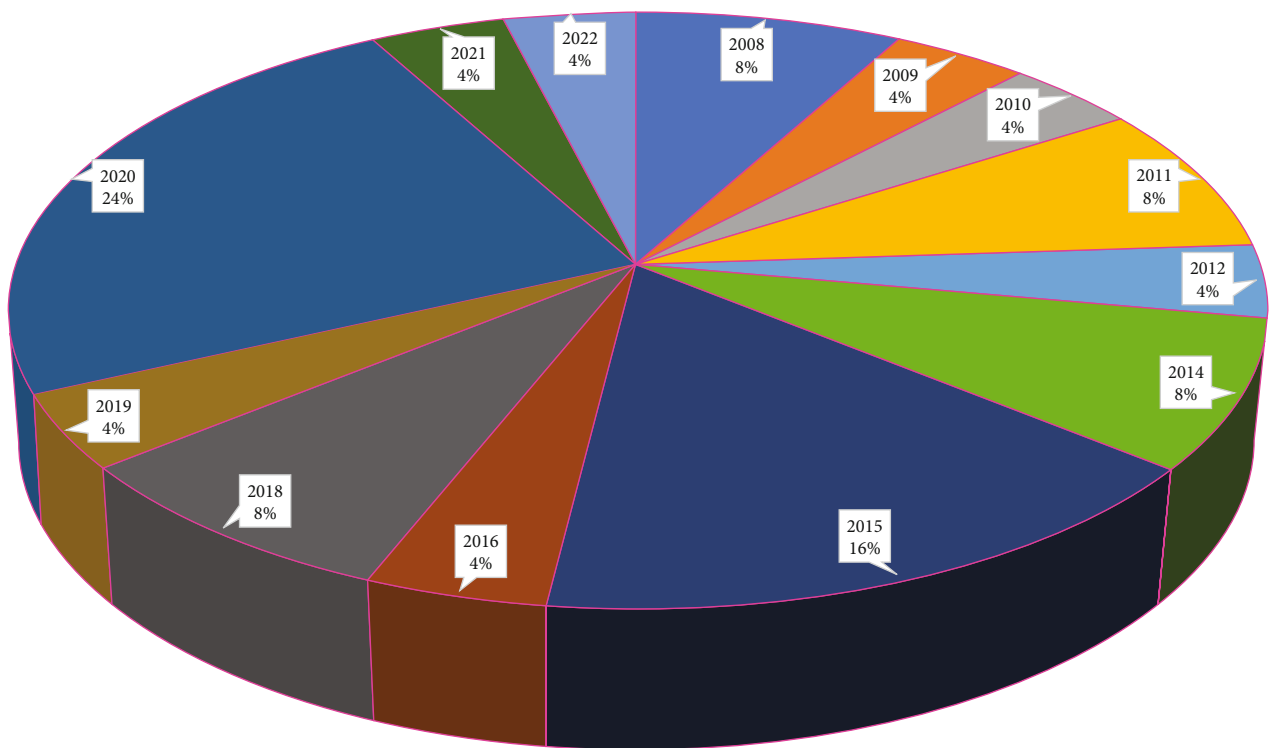


FIGURE 4: Year-wise publications related to RCTs on PMS and herbal medicine.

of neurotransmitters to receptors is required for the activation of downstream signaling of ATP. Moreover, patients with mitochondrial DNA (mtDNA) mutations or mitochondrial diseases frequently present symptoms distinctive from mood disorders. Remarkably, oxidized mtDNA triggers pro-inflammatory cytokines and increases inflammation and plays a significant role in the progression of depressive symptoms. Cognitive dysfunctions are a common symptom

related to depression, and studies reported that cognitive impairments in mice and humans are caused by variations in mtDNA. The association between mitochondrial dysfunction and psychopathology has been evidenced by a correlation found between depression rating scale scores and altered biochemistry. Indeed, depression, anxiety, autism, psychotic disorders, Alzheimer’s disease, and Huntington’s disease are connected to ATP reduction and its relation to

TABLE 2: The characteristics of the published RCTs on herbal medicines and nutritional supplements and their bioactive molecules with pharmacological activities.

Blinding in RCT	Part.	Age (years)	Tools	Exp. group	Cont. Group	Duration of Rx	Result	Adv. Event	Bioactive molecules	Pharm. Actions	Ref.
Triple-blind	76	18-24	PSST, VAS score <8 for dysmenorrhea	One capsule (500 mg of curcuminoid +5 mg piperine) (n=38)	Placebo (n=38)	Daily for 7 days before until 3 days after menstruation for 3 menstrual cycles	Curcumin significantly increased the median serum levels of vitamin D, liver function enzyme test, but did not affect blood glucose	Not reported	Curcumin	Antioxidant, anti-inflammatory, antimicrobial and anticarcinogenic	[51]
Double-blind	129	15-49	PSST	400 mg (1.1 mg allicin) (n=64)	Placebo (n=65)	One tablet daily for 3 cycles	Significant reduction in the symptoms	Reported	Allicin, inhibits MAO enzyme, acts as an antidepressant hyperforin act as SRI	Anti-depressant, anti-inflammatory antioxidant, immunomodulator	[52]
Double-blind	84	18-35	PSST	110 mg capsules of anise (n=42)	Placebo (starch) (n=42)	TID, 7 days before the start of the menstruation and first 3 days during menses for 2 consecutive menstruations	Decreased the symptoms in comparison to placebo	Reported	Anethole	Antioxidant, hypoglycemic, hypolipidemic, anticonvulsant selective moderator of estrogenic receptors	[53]
Double-blind	84	18-35	DASS 21, COPE	Oral capsules containing 500 mg of <i>Nigella sativa</i> seeds (n=42)	Placebo (n=42)	Same as above	Significant reduction in overall severity of premenstrual syndrome in the intervention group	Not reported	Thymoquinone	Increase brain GABA, anti-anxiety, antioxidant, anti-inflammatory	[54]
Double-blind	84	20-35	PSST	450 mg capsules of flowers of <i>Echium amoenum</i> (n=42)	Placebo (n=42)	TID from the 21st day to the 3rd day of their next cycle for 2 consecutive cycles	More effectively symptoms were improved in experimental group	Reported	Cyanidin 3-glucoside, (anthocyanin) GLA, ALA, pyrolozidine alkaloids, and calcium and mineral acids	Anti-inflammatory, antioxidant, analgesic, anxiolytic, sedative and anticonvulsant	[55]
Double-blind	72	>18	DRSP DASS-42	80 mg B6 (n=35)	EM Power Plus (n=35)	Four capsules BID from day 1 of menstruation of new cycle till 2 months	Both groups were effective in PMDD	Not reported	Omega fatty acid	Antioxidant	[56]

TABLE 2: Continued.

Blinding in RCT	Part.	Age (years)	Tools	Exp. group	Cont. Group	Duration of Rx	Result	Adv. Event	Bioactive molecules	Pharm. Actions	Ref.
Double-blind	60	18-30	30-item questionnaire based on DSM-VI	30-mg zinc gluconate (<i>n</i> = 30)	Placebo (<i>n</i> = 30)	12 weeks	Significant reductions in symptoms and increase in BDNF factor and total antioxidant capacity in experimental group	Not reported	Increases in BDNF Expression, inhibits GABA A receptor	Antidepressant, anti-inflammatory, antioxidant	[57]
Single-blind	60	18-45	PMSS scale HRQoL: EQ-5D-5L	1000 mg of <i>P. vulgare</i> . (<i>n</i> = 30)	Placebo (<i>n</i> = 30)	2 capsules, BID from day 16 of the menstrual cycle to day 5 of the next cycle for 3 consecutive cycles	Significant decrease in symptoms and improvement in EQ-5D-5L index value in the experimental group	Reported	Polypodin A and polypodin B bioflavonoid, tannin, phenols	Stress modulator, antidepressant, antioxidant, immunomodulator, analgesic, neuroprotective, anti-inflammatory, antioxidant properties, effects on the renin-angiotensin system, and increase 5-hydroxytryptamine in the brain	[58]
Double blind	44	18-25	BDI-S, BAI	Vitamin D3 (50,000 IU) (<i>n</i> = 22)	Placebo pearl (<i>n</i> = 22)	Every 15 days for 4 months	25(OH)D, serum IL-12 and TAC levels improved significantly in the test group	Not reported		Antidepressant, anti-inflammatory, antioxidant	[14]
Single-blind	101	20-50	PMTS-O, VAS	Pollen pistil extract serelys The tablets administered as the active treatment contained 120 mg PI 82 and 40 mg GC FEM. 2 serelys tablets (320 mg per day) (<i>n</i> = 50)	Placebo (<i>n</i> = 51)	4 months	Significant symptom reduction with serelys treatment	Not reported	Flavonoids, tannins and polyphenols		[59]

TABLE 2: Continued.

Blinding in RCT	Part.	Age (years)	Tools	Exp. group	Cont. Group	Duration of Rx	Result	Adv. Event	Bioactive molecules	Pharm. Actions	Ref.
Single-blind	60	18-45	PMTS-O, PMTS-SR, VAS score	666 mg of <i>N. jatamansi</i> (<i>n</i> = 30)	Placebo (<i>n</i> = 30)	Orally, BID for the 15 days prior to the expected date of menses for 2 cycles	Significant reductions in the test group than the placebo	Not reported	Sesquiterpene jatamansone Inhibit GABA and MAO	Anti-depressant neuroprotective activity. Preventing cognitive impairment and neurodegeneration	[60]
Double blind	70	Premenopausal women	DSM-IV	Curcumin (100 mg) (<i>n</i> = 42)	Placebo (brown sugar) (<i>n</i> = 35)	2 capsules BID daily for 7 days before and three days during menstruation for three successive cycles	Significant reduction in severity of PMS symptoms	Not reported	Curcumin	Anti-depressant due to serotonergic system, anti-inflammatory, antioxidant, neuroprotective	[61]
Double-blind	100	University students	GHQ-28, PSSST	<i>M. officinalis</i> essence (1200 mg) (<i>n</i> = 50)	Placebo (<i>n</i> = 50)	Daily for three cycles from day 1 of last day of menstrual cycle	Significant reduction of somatic, psychological and social symptoms	Not reported	Triterpenoids (ursolic and oleanolic acids) accountable for the inhibition of rat brain GABA transaminase.	Anxiolytic, anti-depressant spasmolytic, sedative, antioxidant, immunomodulatory antiviral and antispasmodic	[62]
Triple-blind	100	20-45	DSR, BDI	Wheat germ extract (400 mg capsules)	Placebo (<i>n</i> = 50)	TID a day between the 16th day of the menstrual cycle to the 5th day of the next menstrual period for two cycles	Significant reduction in symptoms	Not reported	Magnesium, zinc, calcium, antioxidants including beta-carotene (for vitamin A), thiamin, folic acid, vit E, C, B12, B6, riboflavin, niacin, iron, amino acids, and enzymes. Linoleic acid	Antioxidant, anti-inflammatory	[63]
Double-blind	70	Students	DSM-IV Fasting serum BDNF level	100 mg/12 h. curcumin capsules (<i>n</i> = 35)	Placebo (<i>n</i> = 35)	3 successive menstrual cycles and each cycle ran 10 days (in each menstrual cycle 7 days before and 3 days after onset of menstrual bleeding)	Significantly increase in BDNF levels and PMS symptoms were significantly reduced in the test than placebo group	Not reported	Curcumin	Modulating level of BDNF, anti-depressant	[64]

TABLE 2: Continued.

Blinding in RCT	Part.	Age (years)	Tools	Exp. group	Cont. Group	Duration of Rx	Result	Adv. Event	Bioactive molecules	Pharm. Actions	Ref.
Triple-blind	80	18-30	DSM IV-TR	1500 mg primrose oil (<i>Oenothera biennis</i>) (n = 40)	Placebo (n = 40)	TID for three months	Reduction of symptom severity in both primrose and placebo group	Not reported	Linoleic acid and gamma linoleic acid	Antioxidant, anti-inflammatory	[65]
Double-blind	70	18-35	DSM-IV	Two ginger capsules 250 mg (n = 35)	Placebo (n = 35)	BID (7days) before menstruation to three days after menstruation for three cycles	Reduction in symptoms	Reported	Sesquiterpenoids, with (-)-zingiberene. Sesquiterpene lactones (SLs) are responsible for their anti-inflammatory activity	Immunomodulatory, anti-tumorigenic, anti-inflammatory, anti-apoptotic, anti-hyperglycemic, anti-lipidemic, and anti-emetic actions (Rehman et al. 2011)	[66]
Single-blind	60	13-40	PMTS-SR, PMTS-O	<i>Vitex agnus castus</i> seed 1 gm and <i>Mentha pipperita</i> distillate (Arq Pudina) 36 ml (n = 30)	Placebo (n = 30)	BID daily, 10 days before menstruation in every cycle for 3 cycles	A significant reduction in scores was observed in the test group than placebo (p < 0.01)	Not reported	Flavonoid casticin phenols, tannin, α -pinene, limonene, β -caryophyllene, sabinene, and β -farnesene	chemopreventive, immunomodulatory and cytotoxicity, antimicrobial, antifungal, antinociceptive, opioidergic, antiepileptic neuroprotective	[67]
Double-blind	128	Child bearing age	DSR	<i>Vitex agnus</i> (40 drops of in a glass of fruit juice) (n = 62)	Placebo (n = 66)	Orally in the morning from the 6th day prior menses until menstruation, for 6 consecutive cycles	Significant relief of mild and moderate PMS symptoms	Not reported	Flavonoid casticin phenols, tannin, α -pinene, limonene, β -caryophyllene, sabinene, and β -farnesene	Antioxidant, chemo preventive, immunomodulatory and cytotoxicity, antimicrobial, antifungal, antinociceptive, opioidergic, antiepileptic neuroprotective	[68]
Double blind	80	18-30	DSM-IV	10 drops of citrus essence (n = 40)	Placebo (n = 40)	TID during the luteal phase for two cycles	Reduction in the severity of premenstrual syndrome in the experimental group	Not reported	β -Pinene, limonene, terpinolene, α - and γ -terpinene, 1,8-cineol, α -pinene	Enhancing mood and effects sedation, antispasmodic, anti-inflammatory, antioxidant (Hsouna 2017)	[69]

TABLE 2: Continued.

Blinding in RCT	Part.	Age (years)	Tools	Exp. group	Cont. Group	Duration of Rx	Result	Adv. Event	Bioactive molecules	Pharm. Actions	Ref.
Double blind	60	—	DRSP-Q	30 drops of fennel extract ($n = 30$)	Placebo ($n = 30$)	Every 8 hours for 3 days during menses for three months	Significantly greater improvement with the fennel extract than placebo	Reported	Anethole, estragole	Prostaglandin inhibitor, antioxidant, anti-inflammatory, analgesic (Korinek et al., 2021)	[70]
Double-blind	36	18-45	DSR	<i>Hypericum perforatum</i> 450 mg ($n = 19$)	Placebo ($n = 17$)	BID for cycle 4-10 months	Significantly benefit on symptoms	Reported	Hypericin inhibits MAO enzyme and acts as an antidepressant Hyperforin acts as SRI	Neuroprotective, anti-depressant, antiangiogenic Anti-inflammatory wound healing and anti-nociceptive effect. Antioxidant	[71]
Single-blind	90	18-30	DSM-IV, BDI	<i>G. biloba</i> L. tablets (containing 40 mg leaf extracts) ($n = 45$)	Placebo ($n = 45$)	TID from the 16th day of the menstrual cycle to the 5th day of the next cycle for 2 cycles	Significant decrease in the overall severity of symptoms in the experiment group	Reported	Quercetin is an effective inhibitor of histamine release Bioflavonoids are stress modulator	Anti-inflammatory, anxiolytic, anti-depression	[13]
Double blind	50	20-45	Premenstrual daily symptoms score Steiner premenstrual tension syndrome and VAS	Capsule saffron 30 mg/day ($n = 25$)	Capsule placebo ($n = 25$)	15 mg BID for a two menstrual cycles	Significant difference in the total PMS and HDRS scores	Reported	Crocin and safranal of saffron inhibit the reuptake of dopamine, norepinephrine and serotonin	Antioxidant, anti-depressant, antispasmodic, anticancer agent and memory enhancer	[72]
Double blind	101	20-50	Steiner premenstrual tension syndrome and VAS	Femal, 160 mg ($n = 50$)	Placebo ($n = 51$)	BID for four menstrual cycles	Significant reduction in PSF and PMTS scale	Reported	Thymol, camphor	Serotonin reuptake inhibitors	[73]

Total participants: 1949 with mean \pm SD: 77.96 \pm 22.753, variance: 517.71; and CI: 4.55. BAI: Beck Anxiety Inventory, BDI: Beck Depression Inventory; BDI-SL: Beck Depression Short Inventory; COPE: calendar of premenstrual experience; DSR: daily symptom report; DRSP-Q: daily record of severity of problem questionnaire; daily premenstrual syndrome questionnaire with DSM-IV; HDRS: Hamilton Depression Rating Scale; PMTS-O: Steiner premenstrual tension observer questionnaire; PMTS-SR: Steiner premenstrual tension self-rating questionnaire; PSST: Premenstrual Symptoms Screening Tool questionnaire; SD: standard deviation; CI: confidence interval.

TABLE 3: Randomized controlled studies showing risk of bias.

Study	Randomization	Approach of randomization appropriate	Blinding	Approach of blinding appropriate	Presentation of withdrawals and dropouts	Presentation of the inclusion/exclusion criteria	Adverse effects described	Statistical analysis described	Modified Jadad scale
Ozgoli et al., 2009 [13]	1	1	0.5	1	1	1	1	1	7.5
Heidari et al., 2019 [14]	1	1	1	1	1	1	0	1	7
Arabnezhad et al., 2022 [51]	1	1	1	1	1	1	0	1	7
Jafari et al., 2021 [52]	1	1	1	1	1	1	1	1	8
Farahmand et al., 2020 [53]	1	1	1	1	1	1	1	1	8
Maskani et al., 2020 [54]	1	1	1	1	1	1	0	1	7
Farahmand et al., 2020 [55]	1	1	1	1	1	1	1	1	8
Brown et al., 2020 [56]	1	1	1	1	1	1	0	1	7
Jafari et al., 2020 [57]	1	1	1	1	1	1	0	1	7
Khanam and Sultana, 2020 [58]	1	1	0.5	1	1	1	1	1	7.5
Winther et al., 2018 [59]	1	1	1	1	1	1	0	1	7
Malik et al., 2018 [60]	1	1	0.5	1	1	1	0	1	6.5
Khayat et al., 2015 [61]	1	1	1	1	1	1	0	1	7
Akbarzadeh et al., 2015 [62]	1	0	1	1	0	1	0	1	5
Ataollahi et al., 2015 [63]	1	1	1	0	0	1	0	1	5
Fanaei et al., 2016 [64]	1	1	1	1	1	1	0	1	7
Saki et al., 2015 [65]	1	1	1	0	0	1	0	1	5
Khayat et al., 2014 [66]	1	0	1	1	1	1	1	1	7

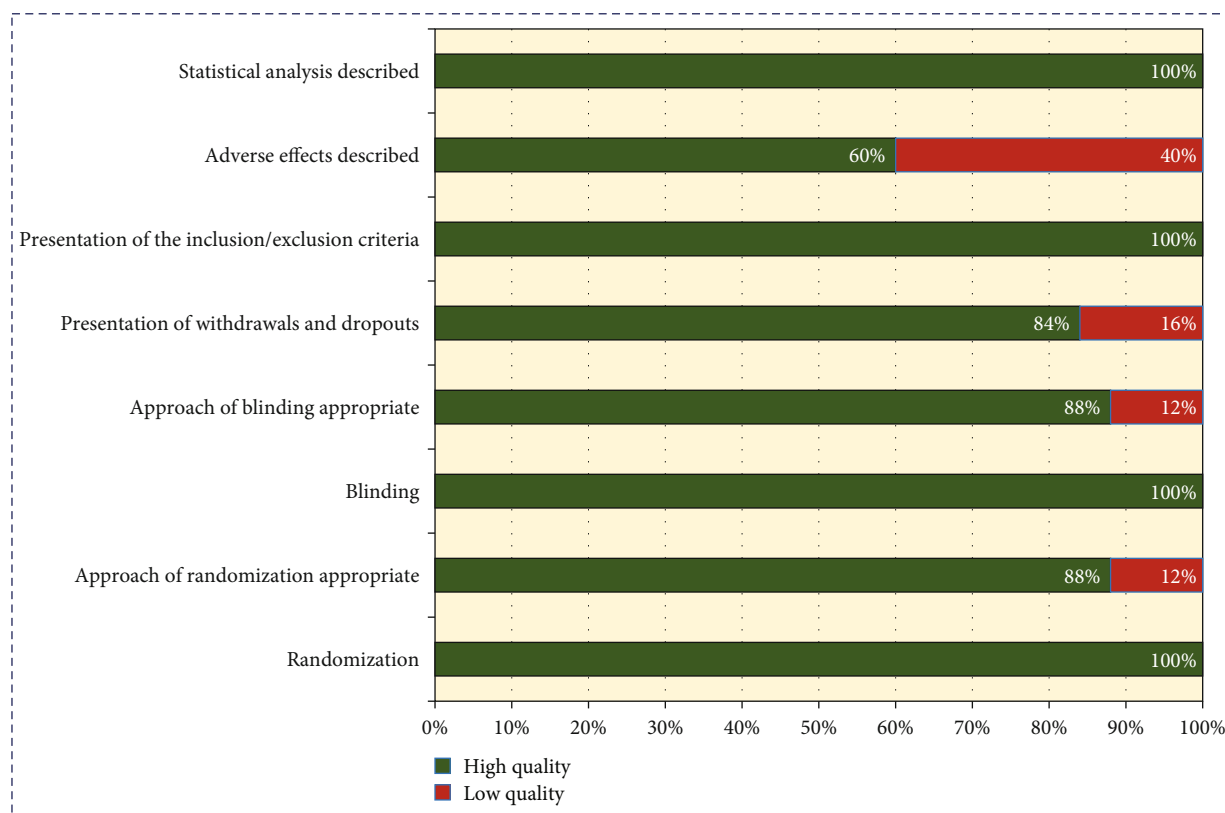


FIGURE 5: Quality assessment of randomized controlled trials.

oxidative stress [18, 75]. Hence, the expression of NOS enzymes is excited by hypoperfusion in the brain tissues caused by prolonged oxidative stress, which accelerates the development of ROS and RNS. ROS and RNS together contribute to the blood-brain barrier (BBB) dysfunction and brain parenchymal cell damage [74]. Studies showed that small increases in the immune mediator C4 and lowered antioxidant defenses (PON1 and AREase) are related to an increase in premenstrual symptoms during the menstrual cycle. Moreover, estradiol and progesterone possibly have a protective role to counter oxidative stress [76].

The common features of PMS are psychiatric (depression, anxiety, etc.) and somatic disorders that involve the etiology of chronic inflammation, which ensues when cytokine-producing cells remain activated. A prevalence study on PMS women reported a correlation between inflammatory factors elevated levels (IL-2, IL-4, IL-10, and IL-12) and the total symptom score in PMS, and further, higher correlations were noted for IL-12, IL-10, and PMS symptoms [14]. P21-activated kinase 1 (PAK1) plays a critical role and contributes to various diseases including inflammation, immunosuppression, cancer, viral infection, ageing, and diabetes [77]. Zeinolabediny et al. [78] discussed the inflammatory disease associated with cardiovascular complications. TNF- α , CRP, and IL-6, the inflammatory markers, are related to migraine headache, a usual symptom of PMS. Johnson et al. [79] reported that there was the strongest correlation between IL-10 and IL-12 levels among inflammatory indices and the total score of symptoms in PMS women. One of the studies showed the relationship

between anxiety and IL-10 and a positive relationship in female soccer players with PMS post-game in the luteal phase [80].

3.2. What Are the Various Mechanisms of Action in Nutritional Supplements and Herbal Medicines with their Bioactive Molecules in Premenstrual Psychosomatic and Behavioral Symptoms? As per the suggestions, PMS management needs a progressively multidisciplinary team that has embraced an integrated holistic method. Similarly, a personalized therapy and management plan for an individual would be practical as the type, number, and severity of PMS symptoms vary from individual to individual. For example, if premenstrual symptoms are mild to moderate, diet and lifestyle changes cause a cure. Pharmacological treatment is suggested if the symptoms start to have an adversarial effect on daily life. The initial step in PMS management is to make awareness regarding education and consultancy, self-care, and self-screening practices. Next, treatment includes nonpharmacological and pharmacological approaches. Lastly, the option is surgical methods.

Many plant products are useful for the alleviation of PMS symptoms. In a RCT, *Polypodium vulgare* showed a significant reduction in the premenstrual symptoms scale (PMSS) and HRQoL [58]. *Polypodium vulgare* Linn. (*Bisfayej*) is indicated for various ailments such as melancholia, epilepsy, dementia, arthritis [81, 82], abdominal pain, and other neurological diseases as it possesses brain and heart exhilarant properties [82]. Herbal medicines are pharmacologically proven for various properties such as tranquillizing

effect, memory retention improvement, analgesic, aldosterone antagonists, immune-modulator, antioxidant, anti-inflammatory, cholinesterase inhibitory activity, smooth muscle relaxant, CNS depressant, and dopamine effect [83–86] (see Table 2). *P. vulgare*, *C. sativus*, *Vitex agnus castus*, anise seed, *Nigella sativa*, *N. jatamansi*, *M. officinalis*, *Echium amoenum*, chamomile, *H. perforatum*, *G. biloba*, *Z. officinalis*, fennel, and serelys consist of various inorganic constituents and organic constituents (flavonoids, resins, tannins, steroids, and protein) (see Table 2) that have antioxidant and anti-inflammatory properties. Flavonoids exhibit anti-inflammation activity through antioxidant property and inflection of signal transduction for the pro-inflammatory cytokines synthesis [17]. Randomized controlled studies carried out with herbal medicines and nutritional supplements to treat the symptoms of PMS are summarized in Table 2. The placebo group in this study also had amelioration in the severity of somatic and psychological symptoms that probably accredited to the psychological effect of the placebo. In various studies, the significant response to placebo and the usefulness of herbal medicines in PMS management was pragmatic as a usual finding. This might be clarified by the circumstances that using beneficial methods give women a sensation of augmented self-control over their lives. Hence, minor interventions like placebo perhaps lead to required effects [13]. An observational analytical study on 90 students aimed to determine the association between mental status, levels of 8-OhdG, and nutritional intake in urine with PMS events [5].

PMS symptoms are linked to the increased inflammatory reactions and oxidative stress as well as super activation of the renin-angiotensin-aldosterone system [87]. The literature demonstrates the relationship between diverse symptoms connected to the menstrual cycle and a multitude of other psychological and physical diseases and sustenance for the practice of antioxidants in managing them. Nevertheless, the precise mechanisms are unclear; we theorized that oxidative stress and antioxidants might also probably affect a complex psychological and physical disease process such as PMS. A research [1] described that women with PMS had higher concentrations of oxidative stress markers. The positive relations between F2-isoprostane with psychological symptoms (anger, tension, and crying) may perhaps be explicated by an original disturbance in the neurotransmitter GABAergic neuroendocrine system by reactive oxygen species (ROS). ROS causes variations in these neurotransmitter levels and may probably cause neuronal cell damage, producing behavior changes (increased appetite and obesity) and mood and the progress of depression and anxiety symptoms [1]. Estrogen and progesterone in healthy women act as antioxidants, whereas in PMS women the inappropriate increase in pro-oxidant activity may lead to oxidative damage to the polyunsaturated fatty acid-rich neuronal membrane (Figure 6). Consequently, dysfunction of the GABAergic system perhaps leads to the PMS symptom development. Catechol estrogens, which produce oxygen radicals, are an additional cause of oxidative damage occurring in the neuronal membrane [10]. A protective role of estradiol in mitochondria has been reported in some studies. It possibly inhibits the ROS passage in the mitochondria and

increases the rate of ATP synthesis and prevents mitochondrial collapse. Mitochondrial functions such as ROS production and apoptosis are affected by the biosynthesis of OXPHOS enzymes. It appears that mitochondrial estrogen and glucocorticoid receptors (GRs) in lung tissue are intricately in oxidative stress and mitochondria are receptive to changing levels of estradiol and stress hormones. Dysfunctional mitochondria cause a negative cascade that might eventually increase inflammatory responses, oxidative stress, and proapoptotic events; a few of them intricately in the pathogenesis of depression [18].

The antioxidant is currently any chemical that prevents, slows, or reverses oxidative damage in the target molecule [81]. It is widely known that flavonoids have a higher antioxidant capacity due to their capacity to scavenge free radicals [81]. Flavonoids are direct scavengers of ROS and RNS downregulation of radical-producing ones and upregulation of ROS-removing enzymes, hence acting as strong antioxidants. Flavonoids produce a hydrogen molecule, a phenoxy radical, which scavenges single oxygen, hydroxyl, peroxy, and superoxide radicals by releasing another hydrogen. The diol group suppresses ROS generation by forming a composite with copper, ferric iron, and other transition metal ions. Superoxide dismutase, glutathione S-transferases, catalase, glutathione reductase, glutathione peroxidase, and NAD (P)H: quinone oxidoreductase (NQO1) are all upregulated by polyphenols. “The production of inflammatory signal molecule peroxiredoxin 2 (PRDX2) and the activation of macrophages to generate IL-6 are both important roles for ROS in inflammation.” Flavonoids inhibited the synthesis and release of inducible nitric oxide synthase, inflammatory IL-6, TNF- α , and MCP-1 by inhibiting NF- κ B, AP-1, and other pro-inflammatory transcription factors. Through the second messenger modulation (cGMP, cAMP, calcium, and protein kinases), flavonoids suppress the formation of inflammation mediators such as prostaglandins, leukotrienes, and arachidonic acid and inhibit the activity of COX and lipoxygenase and arachidonic acid-metabolizing enzymes [17].

Polypody rhizome contains various organic compounds like resins, tannins, steroids, flavonoids, glycosides, proteins, and reducing sugars and various inorganic compounds like iron, calcium, magnesium, potassium, sulphur, and chloride. Its ash contains a large amount of carbonate of potassium. Polypody rhizome contains active constituents phytoecdysteroids, identified as “20-hydroxyecdysone and polypodine B.” Numerous researches reported the antioxidant and neuroprotective effects of 20-hydroxyecdysone. Polypody rhizome contains flavonoids that have been proven for their antioxidant property [85]. They probably act as antioxidants to inhibit lipid peroxidation and free-radical-mediated cytotoxicity, or as weak estrogenic agonists or antagonists to modulate endogenous hormone activity. They contain conjugated ring structures and hydroxyl groups which might probably function as antioxidants, *in vitro*, or in cell-free systems by scavenging superoxide anions, chelating redox-active metals, and singlet oxygen or complexing with oxidizing species. The contents of flavonoids in the extracts of *Rhizome polypodii* as per HPLC-DAD are catechin,

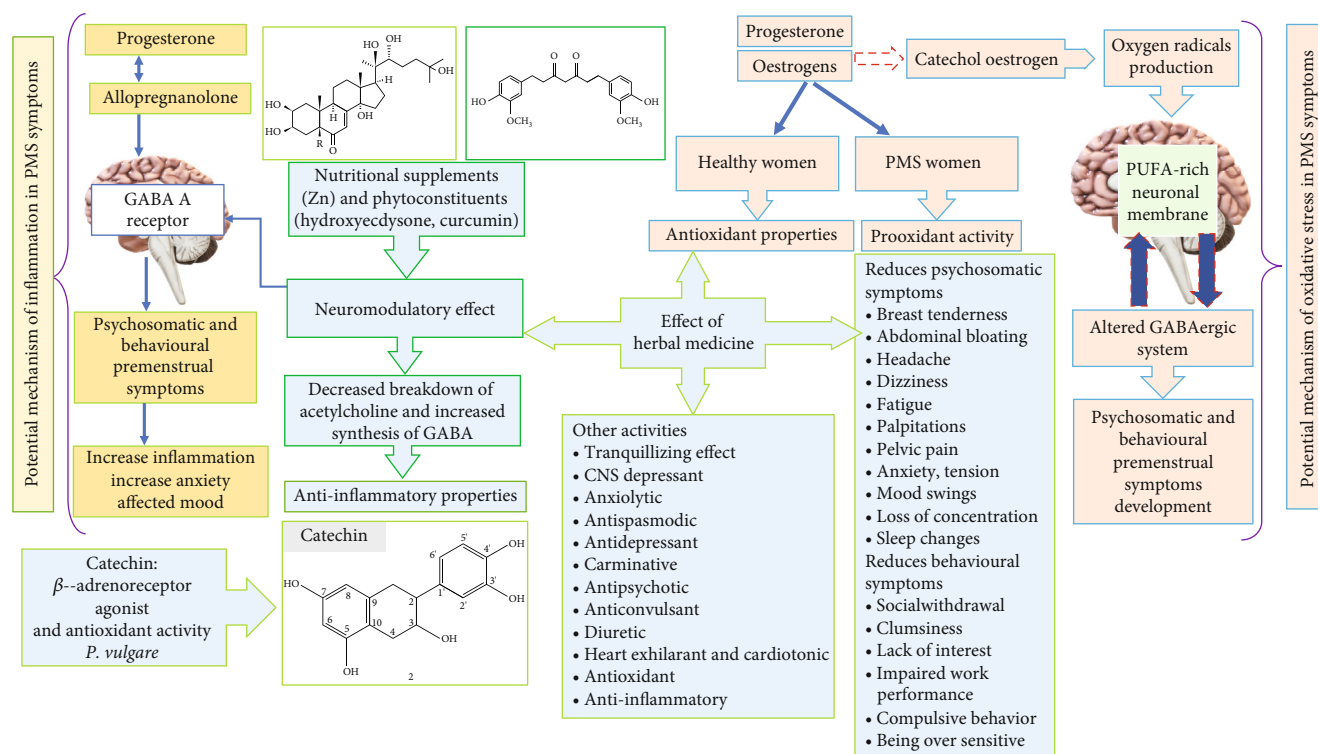


FIGURE 6: Potential mechanisms of inflammation and oxidative stress in PMS. Antioxidant and anti-inflammatory effects of nutritional supplements and herbal medicines.

naringenin, resveratrol, and quercetin. Low concentrations of quercetin scavenged free radicals, however, inhibiting oxidative DNA breakage [88]. Another study result demonstrated that the methanolic extract of *P. vulgare* contains significant amounts of flavonoids such as epicatechin, catechin, shikimic acid, and caffeoylquinic acid derivatives showing cellular repair and cytoprotective activities. The high content of polyphenolic compounds may be responsible for this biological activity [88]. Monoamine oxidase (MAO) functions as a modulator of signal pathways involved in neuronal survival and death. It is found on the outer membrane of mitochondria and helps to maintain monoamine neurotransmitter homeostasis in the brain. Antidepressants are made up of MAO inhibitors of type A (MAO-A). MAO is inhibited by flavonoids like catechin and quercetin. Quercetin, a flavonoid, inhibits MAO-A. "Flavonoids activated upstream MAPK-kinase-kinase, inhibited oxidative stress-induced apoptosis, and prevented Jun N-terminal kinase activation." Catechin raises serum brain-derived neurotrophic factor in humans (BDNF). Tropomyosin-related kinase B (TrkB) and tropomyosin-related kinase A (TrkA) expression and neurogenesis are increased by polyphenols, resulting in neuroprotection and antidepressant activity [17]. Tannins may work as antioxidants to scavenge free radicals and stop such damaging reactions [85]. It is advocated that mitochondrial energy metabolism may perhaps have an antidepressant mechanism of action [18]. Moreover, the bioflavonoids present in *P. vulgare* are primarily known as stress modulators. It is recommended that the serotonergic mechanism is involved in the antidepressant effect [72]. *P. vulgare* is one of the

constituents of *Sharbat-e-Ahmed Shah*, a compound formulation useful in depression and insomnia in traditional medicine since antiquity as an antidepressant activity [89]. Researchers reported that this compound was able to increase the availability of tryptophan, a 5HT precursor in the blood and brain, and hence increase 5-hydroxytryptamine (serotonin: 5HT) in the brain, thus causing anxiolytic and antidepressant activities in experimental rats [89]. In our study, polyphy was able to reduce the psychological symptoms as it has antidepressant properties and increases the availability of tryptophan as studies have proved that PMS patients show a lower 5-HT response to tryptophan during the luteal phase. An animal study in anaesthetized dogs that showed *P. vulgare* extract showed hypotensive activity due to β -adrenoreceptor agonist activity and vasodilation effect that was caused due to phytochemical catechins [83, 89].

It is hypothesized that sex steroids and allopregnanolone (a derivative of progesterone) may influence the PMS symptoms as their receptors are prevailing in the hypothalamus or amygdala of the brain and they easily pass the blood-brain barrier. Allopregnanolone (a progesterone metabolite) is an agonist of GABA A and depending upon its concentration has different actions. For example, it has anxiolytic and sedative effects at high concentration, whereas it may cause depression and negative mood at a lower concentration. As in the luteal phase, GABA A receptors turn out to be less sensitive to allopregnanolone after exposure to its high concentrations, resulting in increased premenstrual symptoms. The relation between inflammation and allopregnanolone is relatively complex: Animal study results specify that "agonists of GABA A receptors attenuate the impact of

inflammation, while the inhibition of GABA A receptor activity increases proinflammatory effects.” Allopregnanolone decreases anxiety and improves mood (Figure 6) [10].

Typical ecdysteroids present in *P. vulgare* are “20-hydroxyecdysone (20E) and polypodine B (polB).” A research report showed that phytoecdysteroids present in *P. vulgare* probably impact the activity of the CNS not only because of neuromodulatory effects on the GABA A receptor as well as partly due to neurotransmitter metabolism (decreased breakdown of acetylcholine and increased synthesis of GABA) and enhanced activity of the immunologic system, antioxidant, antimicrobial, and antiproliferative properties [90]. Furthermore, the rhizome of *P. vulgare* L. has been found to possess a protective effect in drug-induced catalepsy, thus suggesting that it enhances the transmission of dopamine in the CNS and has been explored for various psycho-neurological disorders. The rhizome extract possesses a tranquillizing effect, memory retention improvement [83], cholinesterase inhibitory activity [84], anticonvulsant, CNS depressant, and antiepileptic [83] activities. *P. vulgare* showed neuro-psycho-pharmacological activity. Hence, the significant reduction of neuropsychological symptoms such as tension, anxiety, irritability, depression, mood swings [91], sleep changes [92–94], forgetfulness, and confusion could be justified because of the aforementioned properties of polypody rhizome. Female was able to significantly reduce premenstrual sleep disturbance [95] and irritability in PMS women. The authors reported that it could have central effects, perhaps by altering the serotonergic mechanism that regulates sleep [73].

Micronutrients improve quality of life, and nutrients have been used in the PMS symptoms alleviation for decades, but studies into their efficacy are rare. Research has documented the optimistic effects of micronutrients to treat various mental health concerns from stress to insomnia [56]. Furthermore, nutrition and dietary supplements are not only important in premenstrual syndrome and chronic diseases including diabetes and cancer [96]. Currently, ACOG has only recommended calcium (for the diminution of both mood symptoms and physical discomfort), and magnesium (to reduce breast tenderness, mood symptoms, and water retention) only supplements for PMS symptoms. Recent research showed evidence of the efficacy of herbs or dietary supplementation with other vitamins such as A, C, E, B6, and magnesium, as they might modify the hormonal or oxidative stress or anti-inflammatory profile of women experiencing PMS. Some studies support the relation between vitamin intake and symptom reduction in PMS. A study has shown the optimistic effect of calcium and vitamin E in PMS symptoms [97]. Retallick-Brown et al. [56] reported that vitamin B6 is used as an effective management for PM. They also suggested that nutritional treatment through micronutrients is also beneficial in PMS. In addition, they recommended that multiple micronutrients perhaps have better usefulness than vitamin B6 with severe symptoms. Initial evidence proposes that omega-3 has a useful action on the premenstrual physical and psychological symptoms. Omega-3 controls inflammation and tissue homeostasis [98].

A study reported that serum brain-derived neurotrophic factor (BDNF) levels in the luteal phase were lower in women with PMS. Zinc supplement administration in PMS caused a significant surge in BDNF than placebo. Zinc has antioxidant, anti-inflammatory, and antidepressant activities. This function is probably because of its contribution to increasing BDNF gene expression. It might influence inflammatory markers, viz., high sensitivity C-reactive protein (hs-CRP), and, thus, improve PMS symptoms [52]. Additionally, Zn^{2+} has an inhibitory role at neurosteroid sensitive extra synaptic GABA-A receptors [99]. A study found that in the hippocampus, zinc increases the BDNF protein and mRNA. It induces the matrix metalloproteinase (MMP) that triggers tropomyosin-related kinase proteinase, subsequently leading to pro-BDNF release from cells and converting to BDNF. BDNF supports the differentiation and survival of serotonin in neuron. In addition, zinc is thought to counteract the excess ROS in the body and inhibits NADPH oxidase [57].

The mechanism of how vitamin D decreases inflammation is based on findings that the action of 1, α , 25-dihydroxy vitamin D3 (1, α , 25 (OH)2D3) is mediated through Interleukins. Vitamin D3 inhibits IL-12 production in activated macrophages. However, no functional vitamin D response elements (VDREs) have been established in the genes IL-12A or IL-12B23. The initial effect of 1, α , 25 (OH)2D3 is a cyclical down regulation of IL-12B expression at the onset of inflammation, until sustaining the immune response with a possible level. Furthermore, a secondary effect of IL-10 occurs that turns off the IL-12B gene. In addition, IL-10 has an anti-inflammatory immune function and has effects on the brain and behavior, taking part in anxiety, modulation of mood, and depression symptoms. Thus, a study reported that the mean score of the total PMS symptoms significantly improved along with a significant improvement in inflammation marker. Based on their results, after treatment with vitamin D, increased serum levels of vitamin D ensued a noteworthy increase in serum TAC levels, imitating an enhancement in antioxidant status in PMS women [14].

Mostly, flowers and leaves are the most important parts of medicinal plants. The plant contains alpha-linolenic acid (ALA), delta6-fatty acyl desaturase, gamma-linolenic acid (GLA), pyrrolizidine alkaloids, delta8-sphingolipid desaturase, mucilage, potassium nitrate, calcium, resin, and mineral acids. *Echium amoenum* has anxiolytic, anti-inflammatory, antidepressant, anti-anxiety, antioxidant, analgesic, and anti-obsessive-compulsive properties. Probably, the functional mechanism of *Echium Amoenum* (EA) depends on γ linolenic acid [55]. Flowers have GLA. GLA perhaps have anti-inflammatory and antioxidant properties. Various research studies have confirmed the beneficial effects of GLA on the severity and duration of PMS symptoms. Evening primrose oil is also one of the rich sources of GLA, and a review study approved its efficacy to decrease the severity of PMS symptoms after 4 to 6 months of treatment [100]. Indeed, the conversion of inflammation from a physiologic to a pathologic state can intensify PMS symptoms among individuals with PMS [79, 101, 102]. Additionally, PMS perhaps causes

increased oxidative stress and decrease antioxidant capacity [103]. Furthermore, the most common anthocyanin, cyanidin 3-glucoside present in the petals of EA, has had neuroprotective effects and has customarily been used as an antidepressant and anxiolytic medicine in Asia [53].

Arabnezhad et al. [51] reported that curcumin improves serum vitamin D levels. Xin et al. [104] described that curcumin induces overexpression of vitamin D receptor (VDR) in osteoblasts and femurs probably involved in the protective effect of curcumin on bone loss created by microgravity although curcumin administration has no considerable effect on serum 1,25-(OH)₂D₃ concentration. VDR has an important effect on calcium absorption, bone mineralization rate, and regeneration, as it is a nuclear transcription factor that can modulate the activity of 1,25-(OH)₂ [105]. VDR is also expressed in the ovarian tissue, placenta, endometrium, and fallopian tube epithelial cells. The VDR target genes such as CYP24, cytochrome P450 (CYP) 3A4, and TRPV6 can be stimulated and directly bound to curcumin and get triggered [106]. The role of vitamin D regarding the etiopathology of PMS and dysmenorrhea and its augmentation by curcumin might signify a reasonable mechanism for the useful therapeutic effect of curcumin in menstrual-associated symptoms. In addition, curcumin decreases gene expression of pro-inflammatory cytokines and suppresses nuclear factor kappa B (NF- κ B) induction and high mobility group box 1 (HMGB1), cyclooxygenase-2, downregulation of ICAM-1 and MCP-1, procollagen type I, CD11b, and tissue inhibitor of metalloproteinase-1 and induction of peroxisome proliferator-activated receptor-gamma (PPAR- γ) causing the amelioration of the development and enhancement of inflammation [107]. Furthermore, the antioxidant activity of curcumin is interrelated with triggering many antioxidant enzyme activities such as catalase, glutathione transferase, and heme-oxygenase-1 [108].

The polyphy rhizome showed a significant reduction in PMS symptoms as it contains calcium and magnesium. Iron also plays a role in the metabolism of GABA and serotonin and is an essential cofactor for the tryptophan hydroxylase. The iron deficiency symptoms include cognitive problems, depression, and physical activity disorders. Few studies have reported a reduction in PMS symptom association after receiving iron. Polyphy rhizome also contains iron, hence able to reduce PMS symptoms, similarly, has been reported in the wheat germ study [63].

Curcumin has anti-inflammatory, antioxidant, and neuroprotective activities. During the past decade, various scientific studies established that curcumin can curb the levels of neurotransmitters (dopamine, BDNF, norepinephrine, and serotonin) that are responsible for mood and behavior regulation [64, 109]. In stressed animals, curcumin prevented a diminution in hippocampal BDNF levels to levels comparable to imipramine. Furthermore, its treatment exerts strong antidepressant effects that are similar to the SSRIs (fluoxetine and imipramine), well-known antidepressant drugs [64]. Various physiological processes in the brain such as emotions, sleeping, attention, dreaming, and learning are controlled by norepinephrine. In an animal trial, curcumin increases dopamine levels in rodents and even noticeably

decreases the effects of agents that induce reductions in the concentration of dopamine and adrenaline in the brain. In addition, the cyclooxygenase-2 enzyme (COX-2) produces prostaglandin E₂, recognized to contribute a significant role in the premenstrual symptom's pathophysiology. It can downregulate the gene expression of the COX-2 enzyme and thus inhibits prostaglandin synthesis as per experimental research in animals. Khayat et al. [61] reported that levels of neurotransmitters were augmented by curcumin that improved mood and behavioral symptoms of PMS and through inhibition of COX-2 enzyme reduced physical symptoms of menstruation.

Chamomile tea is useful to reduce the severity of premenstrual symptoms as possessing anti-inflammatory, antioxidant, anti-anxiety, antihistamine, antispasmodic, analgesic, and antidepressant activities. Apigenin compound present in chamomile tea reduces the impact of hormones on the body and mind and excitation neurotransmitters, thereby soothing the hyperactive sympathetic nervous system. It modulates dopamine and serotonin activity and reduces the impact of depressive symptoms. Additionally, it reduces pain sensation by inhibiting the COX enzyme and reducing the inflammatory response of the immune system. Furthermore, its essential oil has antispasmodic and relaxing activities and is beneficial to calm the symptoms associated with PMS. A study compared the efficacy of the well-known anti-inflammatory medications, mefenamic acid, and ibuprofen with chamomile extract for relieving PMS. It is also effective for stress and anxiety relief as apigenin, Luteolin, glycine, and flavonoid since CNS stimulating molecule is a nerve relaxant. It is considered generally safe [8].

N. sativa has antioxidant, immunomodulatory, anti-inflammatory, and anticancer activities. Fresh extracted oil of *N. sativa* contains more thymoquinone that reduced IL-6 levels significantly, whereas stored extracted oil inhibits IL-1 β and had a higher antioxidant activity. Thymoquinone reduces IL-6 levels significantly [110]. Fennel significantly reduces calcium influx recovery time and suppresses MAPK's phosphorylation as well as JNK, ERK, and p38 phosphorylation, with downstream signaling leading to degranulation and activation of respiratory bursts and in human neutrophils. Fascinatingly, fennel inhibiting protein kinase (PKA) inhibitor H89 partly restores the superoxide anion generation, along with the inhibitory effect on calcium influx recovery time, and indicates a role of the cAMP/PKA pathway in the anti-inflammatory effects of fennel. Fennel estragole exhibited anti-inflammatory effects *in vitro* by suppressing Nrf-2 and NF- κ B pathways and *in vivo* (30 mg/kg) reduction of paw edema and leukocyte emigration in the peritoneal fluid [111]. The mechanism of action of *Allium sativum* is immuno-regulation and modulation of secretion of cytokines with therapeutic effects for metabolic syndrome such as anti-hypertensive, antidiabetic, and hypolipidemic properties. Persuasive evidence confirms the ability of garlic extract (AGE) to protect against oxidant-induced diseases, i.e., reduced risk of cancer, cardiovascular (CVD) disease, ageing, and stroke. In addition, it is effective in neurodegenerative disorders caused by oxidant-mediated brain cell damage, particularly

Alzheimer's disease (AD) [52]. Several studies reported that garlic intake probably inhibits β -amyloid protein ($A\beta$) aggregation in the human brain. An experimental study in ovariectomized rats showed noteworthy antidepressant-like properties of a diet supplement containing garlic and black sesame [112]. Garlic, perhaps by reducing brain oxidative stress, reduces anxiety and depression behaviors in diabetic rats [113]. AGE possibly improves memory by affecting the glutamatergic, cholinergic, and GABAergic systems regarding cognitive impairment in $A\beta$ -induced rats. An experiment in mice showed that garlic extract inhibits monoaminoxidase-A and monoaminoxidase-B, proving its antidepressant-like activity [114]. Research also showed that the administration of garlic in rats increases brain serotonin (5-hydroxytryptamine) levels [52]. Studies have shown that saffron has antioxidant properties. The phytoconstituent crocetin has stronger antioxidant activity than safranal, and the potential of crocetin was equivalent to that of Trolox and butyl hydroxyl toluene (BHT) [115].

The mechanisms of action for phytoestrogen effects are unclear in PMS; however, there is indicative evidence that phytoestrogens may act through an estrogen receptor-independent. Various studies confirmed that phytoestrogens bind to estrogen receptors and show significant estrogenic-like effects [116]. The mechanism of anise is comparable to the selective moderators of estrogenic receptors that have agonistic effects as well as antagonistic effects on the estrogenic receptors. Anethole present in anise is considered the active estrogenic agent, and these herbs are considered phytoestrogens [53]. *N. sativa* may probably act directly as well as indirectly on the estrogen receptors and lead to substantial changes in the level of estrogen. Its estrogenic activity may perhaps be accredited to the presence of unsaturated fatty acids, which are established to possess estrogenic effects in animals, man, and cell cultures (Figure 7) [18, 116].

3.3. Does Computational Intelligence Have a Role in PMS Data Analysis for Future Modulation of Premenstrual Symptoms? For example, we have applied computational intelligence techniques such as RF and SVM-radial basis function (SVM-RBF) to the experimental and placebo group. This study would be helpful for researchers, scientists, and doctors to understand the computational intelligence in this area.

In the experimental group, polypody dried rhizome, 2000 mg fine powdered, was administered in two capsules of 1 gm per oral twice a day from day 16 of the menstrual cycle to day 5 of the next cycle for three consecutive cycles. In the placebo group, edible cellulose powder (placebo), 2000 mg, was administered in two capsules of 1 gm per oral twice a day from day 16 of the menstrual cycle to day 5 of the next cycle for three consecutive cycles. The primary outcomes were changes in the total and subtotal score of PMSS for the occurrence and severity of PMS symptoms, and change in duration was assessed by the premenstrual tracker sheet. The secondary outcome was a change in EQ-5D-5L HRQoL. We have added the methods and results of the computational intelligence as shown in the following sections below.

3.3.1. Computational Intelligence Methods

- (i) RF classifier: Ensemble techniques are used to anticipate the final results of RF. A decision node, a leaf node, and a root node are all present in each of the decision trees. The leaf node is the output of each decision tree, and a majority voting process determines the ultimate conclusion [117–119]. If we have attributes Θ of a vector x and the decision tree based on these attributes is $h(x, \Theta)$, then the RF classifier can be defined:

$$R_F = [h(x, \Theta_l)], l = 1, 2, \dots, L \quad (1)$$

- (ii) SVM classifier: It is utilized in the classification and regression methods of data analysis. For data prediction, SVM creates a hyperplane in infinite-dimensional space. The hyperplane with the greatest distance to the nearest training point of the class achieves the maximum accuracy. SVM was initially established in 1963 by prominent scientists Alexey Ya Chervonenkis and Vladimir N Vapnik. After 29 years, Vapnik's team created SVM for nonlinear data using a kernel method to boost the hyperplanes' maximum margin [120]
- (iii) Performance measures: We used SVM-RBF kernel and RF classifiers for the classification of control and Polypody in terms of accuracy, precision, sensitivity, specificity, and area under the curve (AUC) [25, 30–32, 35, 121] with leave-one-out and cross-validation (CV) 5-fold models:

$$\text{Accuracy} = \left(\frac{(TP + TN)}{(TP + TN + FP + FN)} \right), \quad (2)$$

$$\text{Sensitivity} = \left(\frac{TP}{(FN + TP)} \right), \quad (3)$$

$$\text{Specificity} = \left(\frac{TN}{(FP + TN)} \right), \quad (4)$$

$$\text{precision} = \left(\frac{TP}{(TP + FP)} \right), \quad (5)$$

where TP is true positive, FP is false positive, TN is true negative, and FN is false negative.

3.3.2. Computational Intelligence Results. We have designed the heat map of the experimental data related to the premenstrual syndrome mentioned in Figure 8. It showed the relationship between control and polypody experimental data. The leave-one-one-out classification model of the RF classifier achieved maximum accuracy in terms of accuracy (90%), recall (90%), specificity (90%), and precision (90.20%). Moreover, the CV-5 classification model of the RF classifier

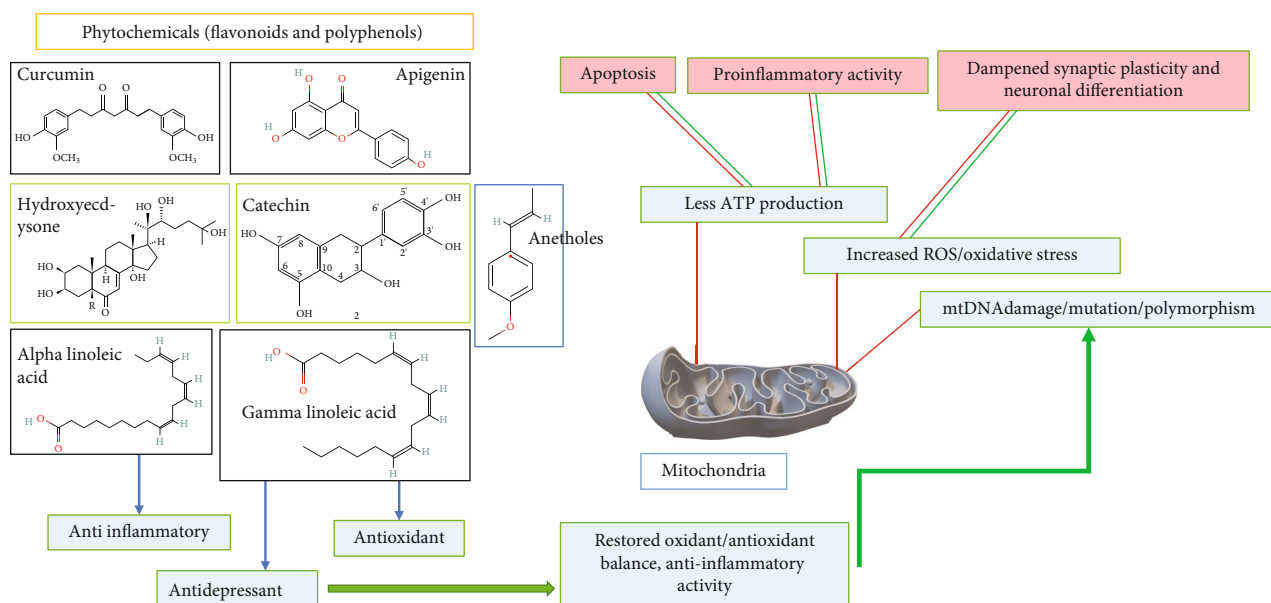


FIGURE 7: Antioxidant and anti-inflammatory effects of phytoconstituents in herbal medicine and nutritional supplements.

achieved maximum accuracy in terms of accuracy (88.30%), recall (88.30%), specificity (88.30%), and precision (88.40%).

However, our RF leave-one-one-out models are more suitable for the classification of the experimental data related to premenstrual psychosomatic and its behavioral symptoms shown in Table 4. Furthermore, the random forest classifier achieved maximum accuracy in terms of accuracy, recall, specificity, and precision.

4. Discussion

In this review, comprehensively, we highlighted the low risk and high quality of 25 RCTs, etiopathogenesis, the contribution of oxidative stress, inflammation leading to mitochondrial changes, and the role of phytochemical constituents in premenstrual psychosomatic and its behavioral symptoms. Additionally, as per our knowledge, it is the first time that computational intelligence technique has been applied to detect premenstrual psychosomatic and its behavioral symptoms assessed by PMSS questionnaire in women who used *Polypodium vulgare* L. herb vs placebo towards future modulation of computational intelligence in clinical trials.

This study covered the required details for the up-to-date research work on premenstrual psychosomatic and its behavioral symptoms. We found that in previous work various tools were used to assess PMS symptoms. We reviewed twenty-five articles with 1949 participants (mean \pm SD: 77.96 ± 22.753) using PRISMA techniques. Besides, our research questions covered mitochondrial changes, oxidative stress and antioxidants, inflammation, anti-inflammatory herbal medicine, and nutritional supplements in PMS. In addition, bioactive molecules and pharmacological activities of herbs effective in PMS symptoms and the mechanism of action have been highlighted.

We also designed the word cloud and network visualization of the current review mentioned in Figure 9 [39, 40, 122, 123]. A word cloud is advantageous to cover all valuable key-

words of the present study in a single diagram. Additionally, we have designed a brief description of the proposed RQs based on MeSH terms using network visualization techniques [123], shown in Table 5. This technique is valuable to get the exact MeSH keywords related to a particular disease, and it is a new tool to analyze many previously published data. Additionally, manually, it is tough to determine the closest terms for any big database. These tools will upwhirl a new way to envisage the dataset through software. It easily divides the previously published articles based on terms in the cluster. For better comprehension, previous studies on the role of oxidative and inflammation in premenstrual symptoms, nutritional supplements, and herbal medicine were retrieved from Scopus, PubMed, and PROSPERO databases were retrieved.

Previously, the researchers reviewed inflammation, oxidative stress in PMS, various nutritional supplements, and herbal medicines in PMS. In [1], a prospective cohort study examined the serum antioxidant vitamin concentrations and oxidative stress markers in PMS. Granda et al. determined oxidative stress, inflammation markers, and antioxidant status in PMS women. They used to update the data until January 2021 from PubMed and Scopus to cover the literature of the study. Koohpayeh et al. [124] investigated the effects of *Rosa damascena* on menstruation-related pain, anxiety, fatigue, headache, and bloating. In [8], the authors investigated chamomile for the treatment of PMS syndrome and collected literature reviews from various databases from 1990 to 2019. They included eight studies. Verkaik et al. [125] investigated for *Vitex agnus castus*, collected data up to January 2016 from various databases, and included 17 studies. Csupor et al. [126] collected data from three clinical trials from 21 clinical trials to compare the efficacy of Ze 440 and BNO 1095 with placebo for the management of PMS. The effectiveness and safety of Iranian herbal medicines for PMS investigators collected data up to 2017 and included 18 RCTs [127]; it included 10 RCTs from 17 RCTs for herbal

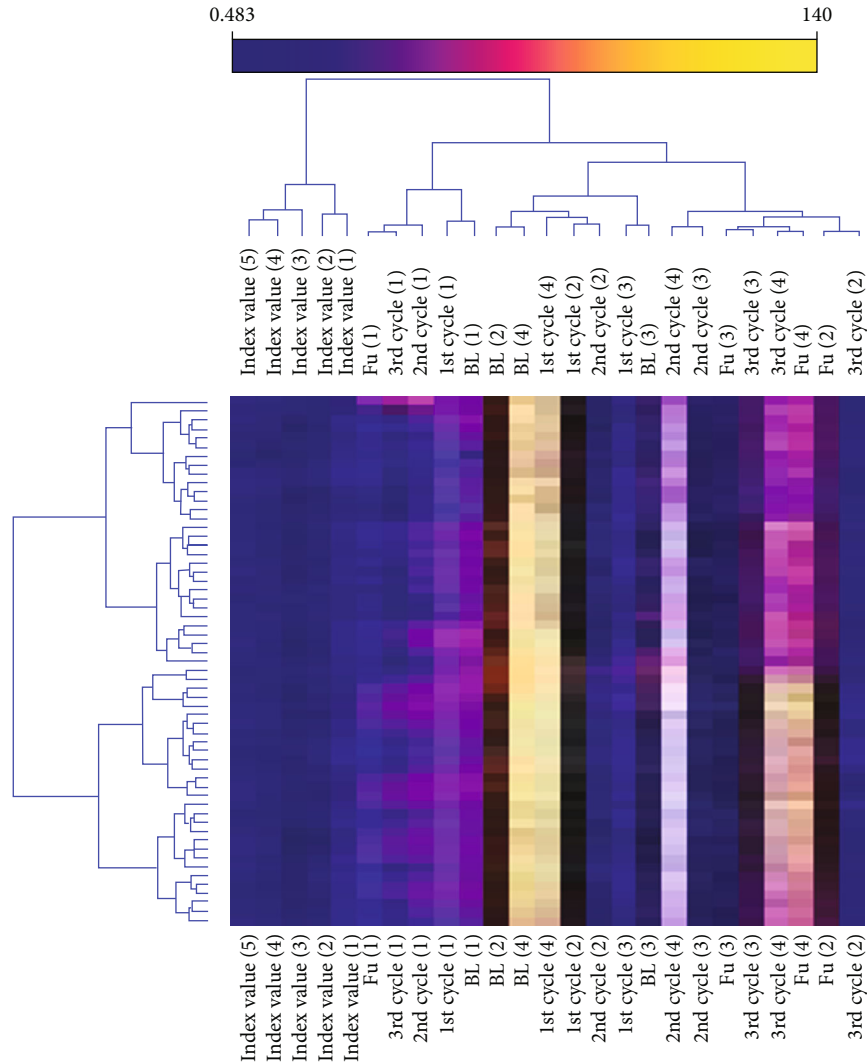


FIGURE 8: Heat map of the experimental and placebo group of the PMS. It showed the relation between premenstrual scale score, health-related quality of life index value related to the premenstrual psychosomatic and its behavioral symptoms of baseline (BL), three cycles with treatments, and one follow-up (FU) without treatment.

TABLE 4: Performance of the system is based on control and Polytypy classification using computational intelligence techniques such as SVM-RBF and RF classifiers.

Classifier	Model	Accuracy (%)	Recall (%)	Specificity (%)	Precision (%)	AUC (%)
SVM-RBF	Leave one out	88.30	88.30	88.30	88.40	91.30
RF		90.00	90.00	90.00	90.20	89.10
SVM-RBF	CV-5	86.70	86.70	86.70	86.70	91.60
RF		88.30	88.30	88.30	88.40	89.30
Mean		88.325	88.325	88.425	90.325	88.325
±Standard deviation		1.166	1.166	1.237	1.132	1.166
Variance		1.361	1.361	1.531	1.281	1.361

treatment for PMS [20]. Canning et al. [71] investigated dietary supplements and herbal medicines for PMS. Tu et al. [128] recommended that education and communication with parents might reduce parental stress and anxiety. Lai group designed a comprehensive survey on insomnia and

bruxism sleep disorders based on PRISMA, RQs, and network visualization techniques. As per our knowledge, researcher used these methods on the PMS, oxidative stress, and inflammation with world clouds and computational intelligence techniques.

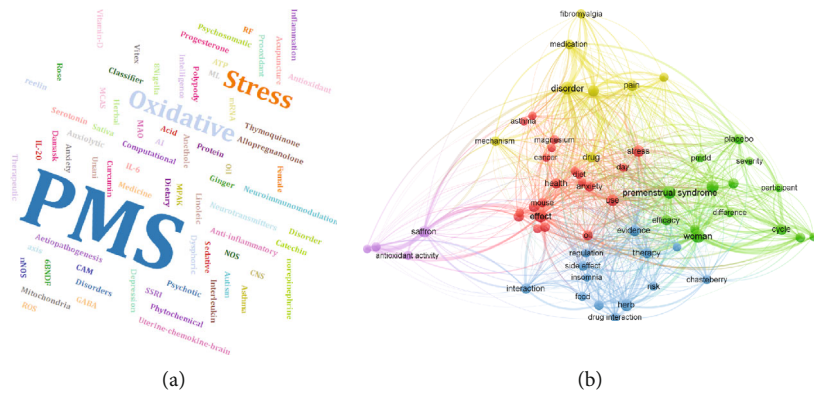


FIGURE 9: Closest terms of the present study based on (a) word cloud and (b) network visualization.

TABLE 5: Description of the proposed research questions based on closest terms using the network visualization model.

S. No.	Research questions	Closest terms
1.	What is etiopathogenesis and the role of oxidative stress, inflammation leading to mitochondrial changes in premenstrual psychosomatic, and its behavioral symptoms?	Anxiety, depression, disorder, menstrual cycle, pain, patient, placebo, PMS, premenstrual symptoms, premenstrual syndrome, relationship, role, severity, symptom, behavioral, and woman
2.	What are the various mechanisms of action in nutritional supplements and herbal medicines with their phytochemical constituents in premenstrual psychosomatic and its behavioral symptoms?	Anxiety, antioxidants, biomarkers, calcium, clinical trials, depression, inflammation, infection, menstrual cycle, patients, premenstrual syndrome, roots, superoxide, symptom, woman, BDR, brain, herbal medicine, nutrition, phytochemicals, symptom, PMS, protein, ROS, and woman
3.	Does computational intelligence have a role in PMS data analysis for future modulation of premenstrual symptoms?	AI, analysis, data, classification, classifier, recognition, computational intelligence, machine learning, PMS, prediction, RF, and SVM

However, our study is different from others regarding details related to etiopathogenesis, the contribution of oxidative stress and inflammation leading to mitochondrial changes in premenstrual symptoms, the therapeutic implication of herbal medicines and nutritional supplements, and the mechanisms of action of these herbal medicines and nutritional supplements. Additionally, we applied computational intelligence techniques to the experimental and placebo groups. These techniques would be helpful for the detection, treatment, and localization-related to our studies. Furthermore, network visualization for retrieval of a literature review from the Scopus database was also performed. This study will benefit academicians, researchers, and scientists to work in this area and use artificial intelligence for data retrieval from various databases. In addition, our closest terms would be helpful for the researchers, scientists, students, doctors, and academicians to find the closest article related to our study.

5. Research Gap and Future Recommendations

The prerequisite of additional information that replicates the effect of premenstrual psychosomatic and its behavioral symptoms to appropriately reply to the self-reported questionnaire and questions on instinct decisions on the physical and mental health of an individual with specific criteria would give a further and definite reason for PMS. The mea-

surement limitation might be present in those questions that are inclusive of the self-reported questionnaire as there could be personal questions that some participants may find challenging to answer. In this paper, that gap is apparent and thus would need further exploration. More research, including a larger sample of subjects, would allow evidence to support a relationship between oxidative stress, inflammation, and PMS and the therapeutic implication of herbal medicine and nutritional supplements in premenstrual psychosomatic and its behavioral symptoms.

In literature research, oxidative stress and inflammation are still not very comprehensively discussed, so what is recommended is more in-depth qualitative and quantitative studies with more significant sample sizes. Indeed, further investigation is essential to explore the relationship between a given mechanism of action of herbal medicine and nutritional supplements in human trials, although few animal studies have proven anti-inflammatory and antioxidant properties of herbal medicine and nutritional supplements beneficial in premenstrual psychosomatic and its behavioral symptoms. More analysis is needed at the molecular and cellular level to further guide. Future studies must be started to better identify possible mitochondrial dysfunction linked to PMS and the molecular mechanisms and software development for the automatic detection related to mitochondrial dysfunction targeting the cognitive, psychomotor, and affective domains in PMS. Researchers would develop more

specific scales to define PMS and causal connections between inflammatory and marker markers. Emerging technologies like machine learning, brain network, quantum techniques, computer vision, and block-chain technology help to analyze experimental RCTs data.

6. Conclusion

This review can be a milestone towards experimenting with herbal medicines and nutritional supplements that are potentially effective natural alternatives to relieve PMS symptoms as they possess bioactive molecules such as curcumin, allicin, anethole, thymoquinone, cyanidin 3-glucoside, pyrrolizidine alkaloids, omega fatty acid, polypodin A and polypodin B, sesquiterpene, jatamansone, ursolic and oleonic acids, magnesium, zinc, calcium, beta-carotene, linoleic acid, and gamma linoleic acid not only have antioxidants and anti-inflammatory properties but also other various activities (GABAA receptor agonist, MAO inhibitors, serotonergic, antidepressant, sedative, and analgesic). Further, computational intelligence analyses of the experimental data of one of the RCTs using computational intelligence techniques showed the accuracy of the data. Hence, it is recommended that machine learning techniques have potential and are useful in clinical trials. However, more rigorous research studies are recommended for in-depth knowledge of the efficacy of bioactive molecules on premenstrual syndrome in clinical trials.

Data Availability

The data used to support the findings of this study are included within the article.

Conflicts of Interest

The authors declare that there are no conflicts of interest regarding the publication of this study.

Authors' Contributions

A.S., K.R., M.B.B.H., S., and F.A. were assigned in the drafting, conceptualization, designing, validation, critically reviewing, revision, and proofreading; AYM was assigned in the guidance and proofreading. All authors have read and agreed to the published version of the manuscript. Dr. Arshiya Sultana, Dr. Khaleequr Rahman, Md Belal Bin Heyat, and Faijan Akhtar contributed equally to this work.

Acknowledgments

We are thankful to Prof. Wu, Prof. Naseem, Prof. Siddiqui, Dr. Ijaz Gul, Dr. Nasir Ilyas, and Dr. Abdullah Aaman Khan for their motivation and support. We also acknowledge to the United Nations for the support of this publication. This work was supported by the China NSFC (U2001207, 61872248, and U21A20146), Guangdong NSF (2017A030312008), Shenzhen Science and Technology Foundation (ZDSYS20190902092853047 and R2020A045), Project of DEGP (2019KCXTD005), and the Guangdong

“Pearl River Talent Recruitment Program” (2019ZT08X603). We would like to thank the UN for the Research4Life program to support the publication.

References

- [1] R. A. Frankel, K. A. Michels, K. Kim et al., “Serum antioxidant vitamin concentrations and oxidative stress markers associated with symptoms and severity of premenstrual syndrome: a prospective cohort study,” *BMC Women's Health*, vol. 21, no. 1, p. 49, 2021.
- [2] S. Z. Masoumi, M. Ataollahi, and K. Oshvandi, “Effect of combined use of calcium and vitamin B6 on premenstrual syndrome symptoms: a randomized clinical trial,” *Journal of Caring Sciences*, vol. 5, no. 1, pp. 67–73, 2016.
- [3] E. A. da Silva and D. A. Pires, “Prevalence of premenstrual syndrome and its psychological effects among university students who participate and do not participate in resistance training,” *Revista Brasileira de Ciências do Esporte*, vol. 43, 2021.
- [4] K. Sattar, “Epidemiology of premenstrual syndrome, a systematic review and meta-analysis study,” *Journal of Clinical And Diagnostic Research: JCDR*, vol. 8, no. 2, pp. 106–109, 2014.
- [5] J. Purnawati, A. W. Sinrang, E. C. Jusuf, E. Limoa, M. Ahmad, and A. N. Usman, “Nutrition, mental status and level of 8-hydroxy-2-deoxyguanosine (OHDG) urine as predictors of premenstrual syndrome (PMS) in adolescent girls,” *Int. J. Curr. Res. Rev.*, vol. 12, no. 23, pp. 7–13, 2020.
- [6] H. Abay and S. Kaplan, “Current approaches in premenstrual syndrome management,” *Bezmialem Science*, vol. 7, no. 2, pp. 150–156, 2019.
- [7] E. W. Freeman and U. Halbreich, “Premenstrual syndromes,” *Psychopharmacology Bulletin*, vol. 34, no. 3, pp. 291–295, 1998.
- [8] Z. B. Khalesi, S. P. Beiranvand, and M. Bokaie, “Efficacy of chamomile in the treatment of premenstrual syndrome: a systematic review,” *Journal of Pharmacopuncture*, vol. 22, no. 4, pp. 204–209, 2019.
- [9] C. Roomruangwong and M. Maes, “Biomarker validation of a new case definition of menstrual cycle-associated syndrome (MCAS) opinion paper,” *CNS & Neurological Disorders-Drug Targets (Formerly Current Drug Targets-CNS & Neurological Disorders)*, vol. 20, pp. 105–111, 2021.
- [10] D. Granda, M. K. Szmidt, and J. Kaluza, “Is premenstrual syndrome associated with inflammation, oxidative stress and antioxidant status? A Systematic Review of Case-Control and Cross-Sectional Studies,” *Antioxidants*, vol. 10, no. 4, p. 604, 2021.
- [11] S. Hofmeister and S. Bodden, “Premenstrual syndrome and premenstrual dysphoric disorder,” *American Family Physician*, vol. 94, no. 3, pp. 236–240, 2009.
- [12] J. Zheng, X. Chen, K. Ismail, and T. Wu, “Herbal treatment for premenstrual syndrome,” in *Cochrane Database of Systematic Reviews*, T. Wu, Ed., John Wiley & Sons, Ltd, Chichester, UK, 2007.
- [13] G. Ozgoli, E. A. Selselei, F. Mojab, H. A. Majd, and A. Randomized, “A randomized, placebo-controlled trial of Ginkgo biloba L. in treatment of premenstrual syndrome,” *Journal of Alternative and Complementary Medicine*, vol. 15, no. 8, pp. 845–851, 2009.

- [14] H. Heidari, R. Amani, A. Feizi, G. Askari, S. Kohan, and P. Tavasoli, "Vitamin D supplementation for premenstrual syndrome-related inflammation and antioxidant markers in students with vitamin D deficient: a randomized clinical trial," *Scientific Reports*, vol. 9, no. 1, pp. 1–8, 2019.
- [15] C. Y. Kuo, Y. T. Cheng, S. T. Ho, C. C. Yu, and M. J. Chen, "Comparison of anti-inflammatory effect and protein profile between the water extracts from Formosan sambar deer and red deer," *Journal of Food and Drug Analysis*, vol. 26, no. 4, pp. 1275–1282, 2018.
- [16] K. Rashed and M. Butnariu, "Antimicrobial and antioxidant effects of cichorium intybus aerial parts and chemical profile," *Egyptian Journal of Chemistry*, vol. 64, pp. 4689–4696, 2021.
- [17] M. Naoi, M. Shamoto-Nagai, and W. Maruyama, "Neuroprotection of multifunctional phytochemicals as novel therapeutic strategy for neurodegenerative disorders: antiapoptotic and antiamyloidogenic activities by modulation of cellular signal pathways," *Future Neurology*, vol. 14, no. 1, p. FNL9, 2019.
- [18] J. Allen, R. Romay-Tallon, K. J. Brymer, H. J. Caruncho, and L. E. Kalynchuk, "Mitochondria and mood: mitochondrial dysfunction as a key player in the manifestation of depression," *Frontiers in Neuroscience*, vol. 12, pp. 1–13, 2018.
- [19] A. J. Teodoro, "Bioactive compounds of food: their role in the prevention and treatment of diseases," *Oxidative Medicine and Cellular Longevity*, vol. 2019, 4 pages, 2019.
- [20] G. Dante and F. Facchinetti, "Herbal treatments for alleviating premenstrual symptoms: a systematic review," *Journal of Psychosomatic Obstetrics and Gynecology*, vol. 32, no. 1, pp. 42–51, 2011.
- [21] S. H. Jang, D. I. Kim, and M. S. Choi, "Effects and treatment methods of acupuncture and herbal medicine for premenstrual syndrome/premenstrual dysphoric disorder: systematic review," *BMC Complementary and Alternative Medicine*, vol. 14, no. 1, 2014.
- [22] E. Pearce, K. Jolly, L. L. Jones, G. Matthewman, M. Zanganeh, and A. Daley, "Exercise for premenstrual syndrome: a systematic review and meta-analysis of randomised controlled trials," *BJGP Open*, vol. 4, no. 3, pp. 1–11, 2020.
- [23] B. Guragai, O. AlShorman, M. Masadeh, and M. B. Bin Heyat, "A survey on deep learning classification algorithms for motor imagery," in *In 2020 32nd international conference on microelectronics (ICM)*, pp. 1–4, Aqaba, Jordan, 2020.
- [24] C. C. Ukwuoma, Q. Zhiguang, M. B. Bin Heyat, L. Ali, Z. Almaspoor, and H. N. Monday, "Recent advancements in fruit detection and classification using deep learning techniques," *Mathematical Problems in Engineering*, vol. 2022, 29 pages, 2022.
- [25] C. Chola, M. B. Bin Heyat, F. Akhtar et al., "IoT based intelligent computer-aided diagnosis and decision making system for health care," in *In 2021 International Conference on Information Technology (ICIT)*, pp. 184–189, Amman, Jordan, 2021.
- [26] M. B. Bin Heyat, F. Akhtar, M. A. Bin Hayat, and S. Azad, "Power Spectral Density Are Used in the Investigation of Insomnia Neurological Disorder," in *In XL-Pre Congress Symposium*, pp. 45–50, King George Medical University & State Takmeelut-Tib College and Hospital, Lucknow, Uttar Pradesh, India, Lucknow, UP, India, 2016.
- [27] H. Bb, F. Akhtar, A. Mehdi, S. Azad, S. Azad, and S. Azad, "Normalized power are used in the diagnosis of insomnia medical sleep syndrome through EMG1-EMG2 channel," *Austin J. Sleep Disorders*, vol. 4, pp. 2–4, 2017.
- [28] M. B. Bin Heyat, F. Akhtar, M. Sikandar, H. Siddiqui, and S. Azad, "An overview of Dalk therapy and treatment of insomnia by Dalk therapy," in *In National Seminar on Research Methodology in Ilaj-Bit-Tadbeer, organized by State Takmeel-ut-Tib-College & Hospital, Lucknow, State Takmeel-ut-Tib-College & Hospital, Lucknow, UP, India*, 2015.
- [29] B. Bin Heyat, F. Akhtar, S. K. Singh, and M. M. Siddiqui, "Hamming Window Are Used in the Prognostic of Insomnia," in *In International Seminar Present Scenario Future Prospectives Res. Eng. Sci.(ISPSFPRES)*, pp. 65–71, Integral University, Lucknow, Uttar Pradesh, India, Lucknow, Uttar Pradesh, India, 2017.
- [30] M. B. Bin Heyat, D. Lai, F. I. Khan, and Y. Zhang, "Sleep bruxism detection using decision tree method by the combination of C4-P4 and C4-A1 channels of scalp EEG, IEEE," *Access*, vol. 7, pp. 102542–102553, 2019.
- [31] M. B. Bin Heyat, F. Akhtar, A. Khan et al., "A novel hybrid machine learning classification for the detection of bruxism patients using physiological signals," *Applied Sciences*, vol. 10, no. 21, p. 7410, 2020.
- [32] D. Lai, M. B. Bin Heyat, F. I. Khan, and Y. Zhang, "Prognosis of sleep bruxism using power spectral density approach applied on EEG signal of both EMG1-EMG2 and ECG1-ECG2 channels," *Access*, vol. 7, pp. 82553–82562, 2019.
- [33] D. Lai, X. Zhang, Y. Zhang, and M. B. Bin Heyat, "Convolutional Neural Network Based Detection of Atrial Fibrillation Combing R-R Intervals and F-Wave Frequency Spectrum," in *In 2019 41st Annual International Conference of the IEEE Engineering in Medicine and Biology Society (EMBC)*, Berlin, Germany, 2019.
- [34] D. Lai, Y. Zhang, X. Zhang, Y. Su, and M. B. Bin Heyat, "An automated strategy for early risk identification of sudden cardiac death by using machine learning approach on measurable arrhythmic risk markers, IEEE," *Access*, vol. 7, pp. 94701–94716, 2019.
- [35] L. Ali, Z. He, W. Cao, H. T. Rauf, Y. Imrana, and M. B. B. Heyat, "MMDD-Ensemble: a multimodal data-driven ensemble approach for Parkinson's disease detection," *Frontiers in Neuroscience*, vol. 15, pp. 1–11, 2021.
- [36] C. C. Ukwuoma, M. B. B. Heyat, M. Masadeh et al., "Image in painting and classification agent training based on reinforcement learning and generative models with attention mechanism," in *In 2021 International conference on microelectronics (ICM)*, pp. 96–101, New Cairo City, Egypt, 2021.
- [37] A. K. Nawabi, S. Jinfang, R. Abbasi et al., "Segmentation of drug-treated cell image and mitochondrial-oxidative stress using deep convolutional neural network," *Oxidative Medicine and Cellular Longevity*, vol. 2022, 14 pages, 2022.
- [38] M. S. Iqbal, R. Abbasi, M. B. Bin Heyat et al., "Recognition of mRNA N4 acetylcytidine (ac4C) by using non-deep vs. deep learning," *Applied Sciences*, vol. 12, no. 3, pp. 1316–1344, 2022.
- [39] M. B. Bin Heyat, F. Akhtar, M. H. Khan et al., "Detection, treatment planning, and genetic predisposition of bruxism: a systematic mapping process and network visualization technique," *CNS & Neurological Disorders-Drug Targets (Formerly Current Drug Targets-CNS & Neurological Disorders)*, vol. 20, no. 8, pp. 755–775, 2021.
- [40] M. B. Bin Heyat, F. Akhtar, M. A. Ansari et al., "Progress in detection of insomnia sleep disorder: a comprehensive

- review,” *Current Drug Targets*, vol. 22, no. 6, pp. 672–684, 2021.
- [41] M. J. Page, J. E. McKenzie, P. M. Bossuyt et al., “The PRISMA 2020 statement: an updated guideline for reporting systematic reviews,” *BMJ*, vol. 372, 2021.
- [42] F. Akhtar, M. B. Bin Heyat, J. P. Li, P. K. Patel, and B. G. Rishipal, “Role of machine learning in human stress: a review,” in *In 2020 17th International Computer Conference on Wavelet Active Media Technology and Information Processing (ICCWAMTIP)*, pp. 170–174, Chengdu, China, 2020.
- [43] F. Akhtar, J. P. Li, M. B. Bin Heyat et al., “Potential of blockchain technology in digital currency: a review,” in *In 2019 16th International Computer Conference on Wavelet Active Media Technology and Information Processing*, pp. 85–91, Chengdu, Sichuan, China, 2019.
- [44] B. N. Teelhawod, F. Akhtar, M. B. Bin Heyat et al., “Machine learning in E-health: a comprehensive survey of anxiety,” in *In 2021 International Conference on Data Analytics for Business and Industry (ICDABI)*, pp. 167–172, Sakheer, Bahrain, 2021.
- [45] F. Akhtar, P. K. Patel, M. B. Bin Heyat et al., “Smartphone addiction among students and its harmful effects on mental health, oxidative stress, and neurodegeneration towards future modulation of anti-addiction therapies: a comprehensive survey based on SLR, research questions, and network visualization techniques,” *CNS & Neurological Disorders Drug Targets*, vol. 21, 2022.
- [46] K. Hussain, M. N. Mohd Salleh, S. Cheng, and Y. Shi, “Meta-heuristic research: a comprehensive survey,” *Artificial Intelligence Review*, vol. 52, no. 4, pp. 2191–2233, 2019.
- [47] M. Abelha, S. Fernandes, D. Mesquita, F. Seabra, and A. T. Ferreira-Oliveira, “Graduate employability and competence development in higher education—a systematic literature review using PRISMA,” *Sustainability*, vol. 12, no. 15, p. 5900, 2020.
- [48] S. Singh and K. Kumar, “Review of literature of lean construction and lean tools using systematic literature review technique (2008–2018),” *Ain Shams Engineering Journal*, vol. 11, no. 2, pp. 465–471, 2020.
- [49] T. J. Chien, C. Y. Liu, C. J. Fang, and C. Y. Kuo, “The efficacy of acupuncture in chemotherapy-induced peripheral neuropathy: systematic review and meta-analysis,” *Integrative Cancer Therapies*, vol. 18, p. 153473541988666, 2019.
- [50] P. L. Wu, M. Lee, and T. T. Huang, “Effectiveness of physical activity on patients with depression and Parkinson’s disease: a systematic review,” *PLoS One*, vol. 12, no. 7, pp. 1–14, 2017.
- [51] L. Arabnezhad, M. Mohammadifard, L. Rahmani, Z. Majidi, G. A. Ferns, and A. Bahrami, “Effects of curcumin supplementation on vitamin D levels in women with premenstrual syndrome and dysmenorrhea: a randomized controlled study,” *BMC Complementary Medicine and Therapies*, vol. 22, no. 1, pp. 11–19, 2022.
- [52] F. Jafari, M. Tabarraei, A. Abbassian, F. Jafari, and M. H. Ayati, “Effect of garlic (*Allium sativum*) supplementation on premenstrual disorders: a randomized, double-blind, placebo-controlled trial,” *Evidence-Based Complementary and Alternative Medicine*, vol. 2021, 9 pages, 2021.
- [53] M. Farahmand, D. Khalili, F. Ramezani Tehrani, G. Amin, and R. Negarandeh, “Could Anise decrease the intensity of premenstrual syndrome symptoms in comparison to placebo? A double-blind randomized clinical trial,” *Journal of Complementary and Integrative Medicine*, vol. 17, pp. 1–10, 2020.
- [54] H. E. Samaneh Maskani, M. Tafazoli, and H. Rakhshandeh, “Effect of *Nigella sativa* seeds on the severity of symptoms of premenstrual syndrome: a randomized clinical trial,” *Koomeh*, vol. 22, pp. 33–40, 2020.
- [55] M. Farahmand, D. Khalili, F. Ramezani Tehrani, G. Amin, and R. Negarandeh, “Effectiveness of Echinium amoenum on premenstrual syndrome: a randomized, double-blind, controlled trial,” *BMC Complementary Medicine and Therapies*, vol. 20, no. 1, pp. 295–299, 2020.
- [56] H. Retallick-Brown, N. Blampied, and J. J. Rucklidge, “A pilot randomized treatment-controlled trial comparing vitamin B6 with broad-spectrum micronutrients for premenstrual syndrome,” *Journal of Alternative and Complementary Medicine*, vol. 26, no. 2, pp. 88–97, 2020.
- [57] F. Jafari, R. Amani, and M. J. Tarrahi, “Effect of zinc supplementation on physical and psychological symptoms, biomarkers of inflammation, oxidative stress, and brain-derived neurotrophic factor in young women with premenstrual syndrome: a randomized, double-blind, placebo-controlled trial,” *Biological Trace Element Research*, vol. 194, no. 1, pp. 89–95, 2020.
- [58] A. Sultana, *Effect of Bisfayej in premenstrual syndrome: a randomised controlled study*, Rajiv Gandhi University of Health Science, 2020.
- [59] K. Winther, J. Campbell-Tofte, A. M. Motawei et al., “A double-blinded, randomized, placebo controlled, parallel study of pollen pistil extract (Sèrèlys) on women reporting irritability as predominant PMS symptom,” *Journal of Herbal Medicine*, vol. 12, pp. 23–32, 2018.
- [60] R. Malik, K. F. Firdose, and M. D. A. Bhat, “Efficacy of *Nardostachys jatamansi* DC. in the management of premenstrual syndrome: a randomized controlled study,” *Journal of Herbal Medicine*, vol. 14, pp. 17–21, 2018.
- [61] S. Khayat, H. Fanaei, M. Kheirkhah, Z. B. Moghadam, A. Kasaeian, and M. Javadimehr, “Curcumin attenuates severity of premenstrual syndrome symptoms: a randomized, double-blind, placebo-controlled trial,” *Complementary Therapies in Medicine*, vol. 23, no. 3, pp. 318–324, 2015.
- [62] M. Akbarzadeh, M. Deghani, Z. Moshfeghy, M. Emamghoreishi, P. Tavakoli, and N. Zare, “Effect of *Melissa officinalis* capsule on the intensity of premenstrual syndrome symptoms in high school girl students,” *Nursing And Midwifery Studies*, vol. 4, no. 2, p. e27001, 2015.
- [63] M. Ataollahi, S. A. A. Akbari, F. Mojab, and H. A. Majd, “The effect of wheat germ extract on premenstrual syndrome symptoms,” *Iranian Journal of Pharmaceutical Research: IJPR*, vol. 14, pp. 159–166, 2015.
- [64] H. Fanaei, S. Khayat, A. Kasaeian, and M. Javadimehr, “Effect of curcumin on serum brain-derived neurotrophic factor levels in women with premenstrual syndrome: a randomized, double-blind, placebo-controlled trial,” *Neuropeptides*, vol. 56, pp. 25–31, 2016.
- [65] M. Saki, S. Akbari, M. Saki, M. Tarrahi, M. Gholami, and S. Pirdadeh, “The effect of primrose oil on the premenstrual syndrome among the female students in Lorestan University of Medical Sciences: a triple blind study,” *Journal of Nursing and Midwifery Sciences*, vol. 2, no. 1, p. 20, 2015.
- [66] S. Khayat, M. Kheirkhah, Z. Behboodi Moghadam, H. Fanaei, A. Kasaeian, and M. Javadimehr, “Effect of treatment with

- ginger on the severity of premenstrual syndrome symptoms, ISRN,” *Obstetrics and Gynecology*, vol. 2014, pp. 1–5, 2014.
- [67] W. Naveed, I. Shameem, and K. Tabassum, “Clinical study of Mutlazima Qabl Haiz (premenstrual syndrome) and its management with Unani formulation - a randomized controlled trial,” *International Journal of Current Research and Review*, vol. 6, pp. 51–57, 2014.
- [68] M. Zamani, N. Neghab, and S. Torabian, “Therapeutic effect of Vitex agnus castus in patients with premenstrual syndrome,” *Acta Med.*, *Iran*, vol. 50, pp. 101–106, 2012.
- [69] N. N. G. Ozgoli, M. Shahveh, and S. Esmaili, “Essential oil of Citrus sinensis for the treatment of premenstrual syndrome; a randomized double-blind placebo-controlled trial,” *Journal of Reproduction & Infertility*, vol. 12, pp. 123–129, 2011.
- [70] M. S. H. M. Delaram, “Herbal remedy for premenstrual syndrome with fennel (*Foeniculum vulgare*) – randomized, placebo-controlled study,” *Advanced Clinical and Experimental Medicine*, vol. 20, pp. 509–512, 2011.
- [71] S. Canning, M. Waterman, N. Orsi, J. Ayres, N. Simpson, and L. Dye, “The efficacy of hypericum perforatum (St John’s wort) for the treatment of premenstrual syndrome: a randomized, double-blind, placebo-controlled trial,” *CNS Drugs*, vol. 24, no. 3, pp. 207–225, 2010.
- [72] M. Agha-Hosseini, L. Kashani, A. Aleyaseen et al., “Crocus sativus L. (saffron) in the treatment of premenstrual syndrome: a double-blind, randomised and placebo-controlled trial, BJOG An Int,” *Journal of Obstetrics and Gynaecology*, vol. 115, no. 4, pp. 515–519, 2008.
- [73] G. Gerhardsen, A. V. Hansen, M. Killi, G. G. Fornitz, F. Pedersen, and S. B. Roos, “The efficacy of Femal in women with premenstrual syndrome: a randomised, double-blind, parallel-group, placebo-controlled, multicentre study,” *Advances in Therapy*, vol. 25, no. 6, pp. 595–607, 2008.
- [74] S. O. Aliev, M. Priyadarshini, V. Reddy et al., “Oxidative stress mediated mitochondrial and vascular lesions as markers in the pathogenesis of Alzheimer disease,” *Current Medicinal Chemistry*, vol. 21, no. 19, pp. 2208–2217, 2014.
- [75] M. Zhu, X. Huang, H. Shan, and M. Zhang, “Mitophagy in traumatic brain injury: a new target for therapeutic intervention,” *Review Article Mitophagy in Traumatic Brain Injury: A New Target for Therapeutic Intervention*, vol. 2022, pp. 1–10, 2022.
- [76] C. Roomruangwong, A. K. Matsumoto, A. P. Michelin et al., “The role of immune and oxidative pathways in menstrual cycle associated depressive, physio-somatic, breast and anxiety symptoms: modulation by sex hormones,” *Journal of Psychosomatic Research*, vol. 135, article 110158, 2020.
- [77] W. L. Cheng, Q. Zhang, B. Li et al., “PAK1 silencing attenuated proinflammatory macrophage activation and foam cell formation by increasing PPAR γ expression,” *Oxidative Medicine and Cellular Longevity*, vol. 2021, 13 pages, 2021.
- [78] Y. Zeinolabediny, S. Kumar, and M. Slevin, “Monomeric C-reactive protein - a feature of inflammatory disease associated with cardiovascular pathophysiological complications?,” *In Vivo (Brooklyn)*, vol. 35, no. 2, pp. 693–697, 2021.
- [79] E. R. Bertone-Johnson, A. G. Ronnenberg, S. C. Houghton et al., “Association of inflammation markers with menstrual symptom severity and premenstrual syndrome in young women,” *Human Reproduction*, vol. 29, no. 9, pp. 1987–1994, 2014.
- [80] R. Foster, M. Vaisberg, M. P. D. Araújo et al., “Relationship between anxiety and interleukin 10 in female soccer players with and without premenstrual syndrome (PMS),” *Revista Brasileira de Ginecologia e Obstetrícia*, vol. 39, no. 11, pp. 602–607, 2017.
- [81] A. Farràs, M. Mitjans, F. Maggi, G. Caprioli, M. P. Vinardell, and V. López, “Polypodium vulgare L. (Polypodiaceae) as a source of bioactive compounds: polyphenolic profile, cytotoxicity and cytoprotective properties in different cell lines,” *Frontiers in Pharmacology*, vol. 12, 2021.
- [82] P. A. Dar, G. Sofi, and M. A. Jafri, “Polypodium vulgare linn. A versatile herbal medicine: A review,” *Int. J. Pharm. Sci. Res.*, vol. 3, pp. 1616–1620, 2012.
- [83] A. Mannan, R. A. Khan, and M. Asif, “Pharmacodynamic studies on Polypodium vulgare (Linn.),” *Indian Journal of Experimental Biology*, vol. 27, no. 6, pp. 556–560, 1989.
- [84] M. Saeedi, K. Babaie, E. Karimpour-Razkenari et al., “In vitro cholinesterase inhibitory activity of some plants used in Iranian traditional medicine,” *Natural Product Research*, vol. 31, no. 22, pp. 2690–2694, 2017.
- [85] G. Sofiane, N. Wafa, and D. Ouarda, “Antioxidant, antimicrobial and anti-inflammatory activities of flavonoids and tannins extracted from Polypodium vulgare L,” *Asian J. Biochem Pharmaceutical Research*, vol. 5, pp. 114–122, 2015.
- [86] S. B. Naz, M. A. Chaudhry, and M. S. Ur Rahaman, “Dual receptors blocked mechanism arbitrates smooth muscles relaxant effect of Polypodium vulgare, Bangladesh,” *Journal de Pharmacologie*, vol. 11, no. 2, pp. 414–420, 2016.
- [87] P. Tacani, D. de Oliveira Ribeiro, B. E. Barros Guimarães, A. F. Perez Machado, and R. E. Tacani, “Characterization of symptoms and edema distribution in premenstrual syndrome,” *International Journal of Women’s Health*, vol. 7, pp. 297–303, 2015.
- [88] H. Akkaya and O. Yilmaz, “The Rhizoma Polypodii Extract Prevents Lipid Peroxidation and Protects the Unsaturated Fatty Acids in the Environment with Radical Sourced Oxidations,” *Gazi University Journal of Science*, vol. 28, no. 2, pp. 201–207, 2015.
- [89] M. Ahmed and A. Azmat, “Decreased brain serotonin turnover rate following administration of Sharbat-e-Ahmed Shah produces antidepressant and anxiolytic effect in rats,” *Metabolic Brain Disease*, vol. 32, no. 6, pp. 1785–1790, 2017.
- [90] B. Thiem, M. Kikowska, M. P. Maliński, D. Kruszka, M. Napierała, and E. Florek, “Ecdysteroids: production in plant in vitro cultures,” *Phytochemistry Reviews*, vol. 16, no. 4, pp. 603–622, 2017.
- [91] O. AlShorman, M. Masadeh, A. Alzyoud, M. B. B. Heyat, and F. Akhtar, “The effects of emotional stress on learning and memory cognitive functions: an EEG review study in education,” in *In 2020 Sixth International Conference on e-Learning (econf)*, pp. 177–182, Sakheer, Bahrain, 2020.
- [92] M. B. Bin Heyat, *Insomnia: Medical Sleep Disorder & Diagnosis*, Anchor Academic Publishing, Hamburg, Germany, 1st edition, 2016.
- [93] M. B. Bin Heyat, D. Lai, F. Akhtar, M. A. Bin Hayat, and S. Azad, “Short Time Frequency Analysis of Theta Activity for the Diagnosis of Bruxism on EEG Sleep Record,” in *In Advanced Computational Intelligence Techniques for Virtual Reality in Healthcare*, K. Gupta and A. Hassanien, Eds., pp. 63–83, Springer, Cham, 2020.

- [94] Y. M. Hasan, B. Bin Heyat, M. M. Siddiqui, S. Azad, and F. Akhtar, "An overview of sleep and stages of sleep," *Sleep*, vol. 4, no. 8, pp. 505–509, 2015.
- [95] M. B. Bin Heyat, D. Lai, F. Akhtar et al., "Bruxism Detection Using Single-Channel C4-A1 on Human Sleep S2 Stage Recording," in *Intelligent Data Analysis: From Data Gathering To Data Comprehension*, Wiley Online Library, 2020.
- [96] M. Cong, W. Zhu, C. Wang et al., "Nutritional status and survival of 8247 cancer patients with or without diabetes mellitus—results from a prospective cohort study," *Cancer Medicine*, vol. 9, no. 20, pp. 7428–7439, 2020.
- [97] K. A. Masoumeh Pourmohsen, S.-T. Zoneamat, and A. F. Hossweini, "Effect of Combined Calcium and Vitamin E Consumption on Premenstrual Syndrome [Article in Persian] [Request PDF]," *Iran Journal of Nursing*, vol. 23, no. 65, pp. 8–14, 2010.
- [98] A. R. Silva, B. P. T. Moraes, and C. F. Gonçalves-De-albuquerque, "Mediterranean diet: lipids, inflammation, and malaria infection," *International Journal of Molecular Sciences*, vol. 21, no. 12, pp. 1–22, 2020.
- [99] C. M. Carver, S. H. Chuang, and D. S. Reddy, "Zinc selectively blocks neurosteroid-sensitive extrasynaptic δ GABAA receptors in the hippocampus," *The Journal of Neuroscience*, vol. 36, no. 31, pp. 8070–8077, 2016.
- [100] M. Mahboubi, "Evening primrose (*Oenothera biennis*) oil in management of female ailments," *Journal of Menopausal Medicine*, vol. 25, no. 2, pp. 74–82, 2019.
- [101] E. B. Gold, C. Wells, and M. O. N. Rasor, "The association of inflammation with premenstrual symptoms," *Journal Of Women's Health*, vol. 25, no. 9, pp. 865–874, 2016.
- [102] A. Graziottin and P. P. Zanello, "Menstruation, inflammation and comorbidities: implications for woman health," *Minerva Ginecologica*, vol. 67, pp. 21–34, 2015.
- [103] C. I. Duvan, A. Cumaoglu, N. O. Turhan, C. Karasu, and H. Kafali, "Oxidant/antioxidant status in premenstrual syndrome," *Archives of Gynecology and Obstetrics*, vol. 283, no. 2, pp. 299–304, 2011.
- [104] M. Xin, Y. Yang, D. Zhang, J. Wang, S. Chen, and D. Zhou, "Attenuation of hind-limb suspension-induced bone loss by curcumin is associated with reduced oxidative stress and increased vitamin D receptor expression," *Osteoporosis International*, vol. 26, no. 11, pp. 2665–2676, 2015.
- [105] J. W. Pike, H. Yamamoto, and N. K. Shevde, "Vitamin D receptor-mediated gene regulation mechanisms and current concepts of vitamin D analog selectivity," *Advances in Renal Replacement Therapy*, vol. 9, no. 3, pp. 168–174, 2002.
- [106] L. Bartik, G. K. Whitfield, M. Kaczmarska et al., "Curcumin: a novel nutritionally derived ligand of the vitamin D receptor with implications for colon cancer chemoprevention," *The Journal Of Nutritional Biochemistry*, vol. 21, no. 12, pp. 1153–1161, 2010.
- [107] Y. Wang, J. Li, L. Zhuge et al., "Comparison between the efficacies of curcumin and puerarin in C57BL/6 mice with steatohepatitis induced by a methionine-and choline-deficient diet," *Experimental and Therapeutic Medicine*, vol. 7, no. 3, pp. 663–668, 2014.
- [108] M. Iqbal, S. D. Sharma, Y. Okazaki, M. Fujisawa, and S. Okada, "Dietary supplementation of curcumin enhances antioxidant and phase II metabolizing enzymes in ddY male mice: possible role in protection against chemical carcinogenesis and toxicity," *Pharmacology & Toxicology*, vol. 92, no. 1, pp. 33–38, 2003.
- [109] A. L. Lopresti, S. D. Hood, and P. D. Drummond, "Multiple antidepressant potential modes of action of curcumin: a review of its anti-inflammatory, monoaminergic, antioxidant, immunomodulating and neuroprotective effects," *Journal of Psychopharmacology*, vol. 26, pp. 1512–1524, 2012.
- [110] L. Bordoni, D. Fedeli, C. Nasuti et al., "Antioxidant and anti-inflammatory properties of nigella sativa oil in human preadipocytes," *Antioxidants*, vol. 8, no. 2, p. 51, 2019.
- [111] M. Korinek, H. Handoussa, Y. H. Tsai et al., "Anti-inflammatory and antimicrobial volatile oils: fennel and cumin inhibit neutrophilic inflammation via regulating calcium and MAPKs," *Frontiers in Pharmacology*, vol. 12, pp. 1–20, 2021.
- [112] S. Bhandare and S. Tembhurne, "Antidepressant effects of dietary supplements garlic and black sesame extracts in ovariectomized rats: involving possible estrogenic and antioxidant mechanism," *International Journal Pharmtech Research*, vol. 6, pp. 168–173, 2014.
- [113] H. E. G. Rahmani, F. Farajdokht, G. Mohaddes, S. Babri, V. Ebrahimi, and H. Ebrahimi, "Garlic (*Allium sativum*) improves anxiety-and depressive-related behaviors and brain oxidative stress in diabetic rats," *Archives of Physiology and Biochemistry*, vol. 126, no. 2, pp. 95–100, 2020.
- [114] D. Dhingra and V. Kumar, "Evidences for the involvement of monoaminergic and GABAergic systems in antidepressant-like activity of garlic extract in mice," *Indian Journal of Pharmacology*, vol. 40, no. 4, pp. 175–179, 2008.
- [115] M. Butnariu, C. Quispe, J. Herrera-Bravo et al., "The pharmacological activities of *Crocus sativus* L.: a review based on the mechanisms and therapeutic opportunities of its phytoconstituents," *Oxidative Medicine and Cellular Longevity*, vol. 2022, 29 pages, 2022.
- [116] S. Parhizkar, L. A. Latiff, S. A. Rahman, M. A. Dollah, and H. Parichehr, "Assessing estrogenic activity of nigella sativa in ovariectomized rats using vaginal cornification assay," *The Journal of Pharmacy and Pharmacology*, vol. 5, no. 2, pp. 137–142, 2011.
- [117] M. B. Bin Heyat, F. Akhtar, S. J. Abbas et al., "Wearable flexible electronics based cardiac electrode for researcher mental stress detection system using machine learning models on single lead electrocardiogram signal," *Biosensors*, vol. 12, no. 6, p. 427, 2022.
- [118] T. K. Ho, "The random subspace method for constructing decision forests," *IEEE Transactions on Pattern Analysis and Machine Intelligence*, vol. 20, no. 8, pp. 832–844, 1998.
- [119] T. K. Ho, "A data complexity analysis of comparative advantages of decision forest constructors," *Pattern Analysis & Applications*, vol. 5, no. 2, pp. 102–112, 2002.
- [120] B. E. Boser, I. M. Guyon, and V. N. Vapnik, "Training Algorithm for Optimal Margin Classifiers," in *In Proceedings of the fifth annual workshop on Computational learning theory*, New York, 1992.
- [121] Z. H. Q. Liu, C. Chen, Y. Zhang, and Z. Hu, "Feature Selection for Support Vector Machines with RBF Kernel," *Artificial Intelligence Review*, vol. 36, no. 2, pp. 99–115, 2011.
- [122] N. J. van Eck and L. Waltman, "Visualizing bibliometric networks," in *In Measuring scholarly impact*, Springer, Cham, 2014.
- [123] S. Sheikh, M. B. Bin Heyat, O. AlShorman, M. Masadeh, and F. Alkhatni, "A review of usability evaluation techniques for

- augmented reality systems in education,” in *In 2021 Innovation and New Trends in Engineering, Science and Technology Education Conference (IETSEC)*, pp. 1–6, Amman, Jordan, 2021.
- [124] S. A. Koohpayeh, M. Hosseini, M. Nasiri, and M. Rezaei, “Effects of *Rosa damascena* (damask rose) on menstruation-related pain, headache, fatigue, anxiety, and bloating: a systematic review and meta-analysis of randomized controlled trials,” *Journal of Education and Health Promotion*, vol. 30, p. 272, 2021.
- [125] S. Verkaik, A. M. Kamperman, R. van Westrhenen, and P. F. J. Schulte, “The treatment of premenstrual syndrome with preparations of *Vitex agnus castus*: a systematic review and meta-analysis,” *American Journal of Obstetrics and Gynecology*, vol. 217, no. 2, pp. 150–166, 2017.
- [126] D. Csupor, T. Lantos, P. Hegyi et al., “*Vitex agnus-castus* in premenstrual syndrome: a meta-analysis of double-blind randomised controlled trials,” *Complementary Therapies in Medicine*, vol. 47, p. 102190, 2019.
- [127] N. Maleki-Saghooni, F. Z. Karimi, Z. Behboodi Moghadam, and K. M. Najmabadi, “The effectiveness and safety of Iranian herbal medicines for treatment of premenstrual syndrome: a systematic review., *Avicenna*,” *Avicenna Journal of Phytomedicine*, vol. 8, pp. 96–113, 2018.
- [128] W. J. Tu, J. He, H. Chen, X. D. Shi, and Y. Li, “Psychological effects of false-positive results in expanded newborn screening in China,” *PLoS One*, vol. 7, no. 4, 2012.

Research Article

Theaflavin-3,3'-Digallate Protects Cartilage from Degradation by Modulating Inflammation and Antioxidant Pathways

Yun Teng,¹ Zheyu Jin,¹ Weizhi Ren,² Minghao Lu,³ Mingzhuang Hou,¹ Quan Zhou,¹ Wenhao Wang,¹ Huilin Yang^{ID},¹ and Jun Zou^{ID}¹

¹Department of Orthopaedic Surgery, The First Affiliated Hospital of Soochow University, Suzhou, Jiangsu, China

²Department of Orthopaedic Surgery, The Second Affiliated Hospital of Soochow University, Suzhou, Jiangsu, China

³Department of Orthopaedic Surgery, The Second People's Hospital of Changshu, Suzhou, Jiangsu, China

Correspondence should be addressed to Huilin Yang; hlyang@suda.edu.cn and Jun Zou; jzou@suda.edu.cn

Received 10 March 2022; Accepted 15 June 2022; Published 8 July 2022

Academic Editor: Alin Ciobica

Copyright © 2022 Yun Teng et al. This is an open access article distributed under the Creative Commons Attribution License, which permits unrestricted use, distribution, and reproduction in any medium, provided the original work is properly cited.

Background. Osteoarthritis (OA) is a common degenerative joint disease that may be closely linked to inflammation and oxidative stress destroying the balance of cartilage matrix. Theaflavin-3,3'-digallate (TFDG), a natural substance derived from black tea, has been reported to restrict the activity of inflammatory cytokines and effectively eliminate reactive oxygen species (ROS) in various diseases. However, it is not clear whether TFDG can improve OA. **Methods.** Chondrocytes were treated with or without IL-1 β and 20 μ M and 40 μ M TFDG. The effect of TFDG on the proliferation of chondrocytes was detected by CCK8. RT-qPCR was used to detect the gene expression of inflammatory factors, extracellular matrix synthesis, and degradation genes. Western blot and immunofluorescence assays were used to detect the protein expression. The fluorescence intensity of reactive oxygen species labeled by DCFH-DA was detected by flow cytometry. We established an OA rat model by performing destabilized medial meniscus (DMM) surgery to observe whether TFDG can protect chondrocytes under arthritis in vivo. **Results.** TFDG was found to inhibit proinflammatory factors (IL-6, TNF- α , iNOS, and PGE) and matrix-degrading enzymes (MMP13, MMP3, and ADAMTS5) expression and protected extracellular matrix components of chondrocytes (ACAN, COL2, and SOX9). TFDG accelerated the scavenging of ROS caused by IL-1 β according to the Nrf2 signaling pathway activation. At the same time, TFDG suppressed the PI3K/AKT/NF- κ B and MAPK signaling pathways to delay the inflammatory process. The cartilage of DMM rats receiving TFDG showed lower Osteoarthritis Research Society International (OARSI) scores and expressed higher levels of COL2 and Nrf2 compared with those of rats in the DMM group. **Conclusion.** TFDG could protect cartilage from degradation and alleviate osteoarthritis in rats, which suggests that TFDG has potential as a drug candidate for OA therapy.

1. Introduction

A chronic degenerative disease of total joints, osteoarthritis (OA) affects most easily the knee joint, and in second instance the hand and hip joints [1]. Its clinical symptoms include joint swelling and pain, joint stiffness and limited movement, atrophy of the muscles around the joint, and frictional sounds during movement, which eventually leads to joint deformity in the late stage of the disease [2]. There are many risk factors for OA, including age, obesity, being female, and history of knee joint injury; among these, age is the most relevant [3, 4]. Therefore, along with the increasing incidence of obesity due to population aging and dietary

changes, the global prevalence of OA is also increasing. It is estimated that 242 million people are affected by OA worldwide [5]. The high incidence of OA, combined with the irreversibility of disease progression, ranks it alongside diabetes as one of the fastest-growing causes of disability worldwide; in particular, OA is expected to become the fourth leading cause of disability by 2020 [6–8]. At present, because of its pathogenesis, OA is difficult to cure. Therefore, the corresponding treatment plan is provided according to the situation of the patient and disease stage. In general, for early lesions, OA patients with no obvious symptoms usually adopt preventive nondrug treatment [9]. Furthermore, loss of weight, avoidance of daily activities that exert pressure

on the joints for a long time, moderate movement to enhance joint stability, and physical therapy can help delay the progression of OA as much as possible [10]. Conversely, OA patients with obvious clinical symptoms may require nondrug therapy, nonsteroidal anti-inflammatory drugs, analgesic drugs, antianxiety drugs, or proprietary Chinese medicine to relieve pain caused by OA [11, 12]. In particular, intra-articular injection of the drug will relieve pain more quickly and effectively. However, conventional drugs and physical therapy are no longer effective when the disease is in its final stages, and surgery is the only option to relieve pain and correct deformities [13]. Surgery practices mainly consist in articular cartilage repair, arthroscopic debridement, osteotomy, and joint replacement. The latter is currently the most widely used method worldwide, but its postoperative complications are still difficult to resolve completely [14, 15]. Therefore, it is urgent to deepen current knowledge of OA pathogenesis in order to find better therapeutic options for this disease.

Previous studies have explored the pathogenesis of OA, but the exact mechanism remains unclear. A large number of cytokines and signaling pathways play a synergistic role in the pathogenesis of OA, and the related inflammatory responses and oxidative stress have been widely studied [16, 17]. Cytokines that trigger inflammatory responses, such as interleukin 1 (IL-1) and tumor necrosis factor (TNF), are the most crucial molecules supporting OA pathogenesis [18]. Previous clinical studies have found the synovial fluid of OA patients have escalated IL-1 β secretion [19]. Moreover, Tesche and Miosge reported IL-1 β overexpression in osteoarthritic cartilage [20]. These findings implied that IL-1 β plays a relevant role in OA. Inflammatory factors such as IL-1 β can either directly promote the synthesis of matrix-degrading enzymes in chondrocytes, thereby promoting extracellular matrix degradation, or amplify the inflammatory response and accelerate chondrocytes apoptosis by activating downstream signaling pathways or other inflammatory factors [21, 22]. For example, IL-1 β can activate the ERK, p38, and JNK, NF- κ B, and PI3K pathways or other cytokines to accelerate the progression of arthritis [23–25]. Oxidative stress also plays a major role in OA progression [26]. In chondrocytes, mitochondrial electron transfer generated mostly reactive oxygen species (ROS). Upon normal mitochondrial function, the production and clearance of ROS are maintained in a dynamic balance [27]. However, when mitochondria are dysfunctional and ROS generation exceeds the mitochondrial clearance capacity, such balance is disrupted, and excessive ROS accumulation lead to cell damage [28, 29]. Excess ROS, when released in chondrocytes, damage DNA and proteins, induce mitochondrial dysfunction, and activate proinflammatory mediators and matrix-degrading enzymes. Conversely, the application of antioxidants can significantly improve the condition of chondrocytes [30]. In summary, both inflammation and oxidative stress are involved in the pathogenesis of OA and can mutually reinforce. Therefore, inhibiting inflammation and oxidative stress is believed to be an effective approach to treat OA.

Many natural active substances in herbs and plants have been proven to exert beneficial biological effects as they can play anti-inflammatory and antioxidant roles both *in vitro* and *in vivo* [31]. Therefore, further research on these substances may yield new antiarthritic drugs. In particular, theaflavin-3-3'-digallate (TFDG), the active substances extracted from black tea, have been shown to exert a variety of biological effects. For instance, TFDG have been reported to alleviate cardiomyocyte reperfusion through the inhibition of autophagy [32]. These molecules can also improve lipopolysaccharide-induced bronchitis in rats by suppressing the release of inflammatory factors [33]. As for the skeletal system, previous studies have found that theaflavins can inhibit the activation of osteoclasts and prevent bone loss in castrated mice, thereby preventing osteoporosis [34]. Finally, Liu and Li reported that TFDG alleviates rheumatoid arthritis by inhibiting the NF- κ B and MAPK pathways in mice model [35]. Therefore, we aimed to investigate whether TFDG can bring into play anti-inflammatory and antioxidant function in OA models, verify whether TFDG treatment can retard OA progression, and further study its mechanism of action.

2. Materials and Methods

2.1. Regents and Antibodies. TFDG (CSN20910) was obtained from CNS Pharmaceuticals (Chicago, IL, USA), configured with ethyl alcohol (Sigma-Aldrich, USA), and diluted to a concentration of 10 mM. Recombinant IL-1 β of rats was offered by PeproTech Inc. (East Windsor, NJ, USA) and dissolved in a 5% trehalose solution. Primary antibodies against collagen II (ab188570), COX-2 (ab179800), MMP3 (ab52915), ADAMTS5 (ab41037), SOX9 (ab185230), iNOS (ab178945), and SOD2 (ab68155) were acquired from Abcam (Cambridge, UK). Antibodies against p85 (#4257), p110 (#4255), AKT (#9272), phospho-AKT (#4060), ERK1/2 (#9102), phospho-JNK (#4668), p38 (#8690), phospho-p38 (#4511), phospho-ERK1/2(#4370), phospho-p65 (#3033), p65 (#8242), phospho-I κ B α (#2859), I κ B α (#9242), and JNK (#9252) were supplied by CST (Beverly, USA). Anti-Nrf2 (16396-1-AP), anti-ACAN (13880-1-AP), anti-MMP13 (18165-1-AP), anti- β -actin (20536-1-AP), and anti-HO-1 (10701-1-AP) antibodies were taken from Proteintech (Wuhan, China).

2.2. Extraction and Culture of Rat Chondrocytes. 6–8-week-old Sprague-Dawley (SD) rats supplied by the Experimental Animal Center of Soochow University were used for primary chondrocytes isolation. SD rats were sacrificed and then confirmed dead according to their lack of respiration and heartbeat. The articular cartilages were exposed and separated from their subchondral bone. The cartilage was chopped into little pieces, placed in cell culture dishes, and digested using type II collagenase (0.2%, Thermo Fisher Scientific) for 6 h at 37°C. DMEM/F12 containing 100 U antibiotics and 10% fetal bovine serum (FBS) (Thermo Fisher Scientific) were used for collected chondrocytes culturing at 37°C and 5% CO₂. The medium was replaced every 3 days and chondrocytes were passaged with 0.25% trypsin/

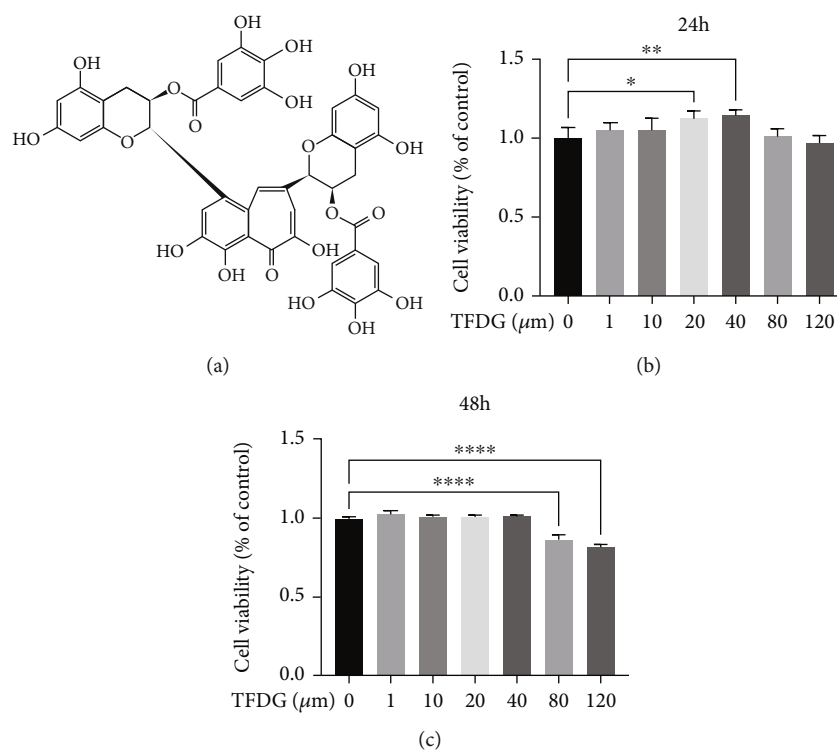


FIGURE 1: The structure of TFDG and effect of TFDG on cell viability. (a) The molecular structure of TFDG. (b, c) Different concentrations of TFDG (1, 10, 20, 40, 80, or 120 μM) to determine its cytotoxicity at 24 h and 48 h. The bar graph shows the mean ± SD of data ($n = 6$). * $p < .05$, ** $p < .01$, *** $p < .001$, and **** $p < .0001$.

ethylenediaminetetraacetate (Thermo Fisher) at 90% cell density. Chondrocytes from the first and second passages were used for study.

2.3. Cell Proliferation Analysis. The effects of TFDG on cell viability were monitored by CCK-8 KIT (Beyotime, Shanghai, China). Chondrocytes in 96-well plates (5000 cells/well) were cocultured with multiple concentration of TFDG after adhering to the wells; untreated cells were set for negative control. After discarding the original culture medium and washing the wells twice, the chondrocytes were handled with CCK-8 solution (10%) at 37°C for 1 h. Microplate reader (BioTek, USA) was used for measuring the optical density (OD) of the cell cultures at 450 nm. The cell viability was calculated according to the following formula. Cell viability = $[(\text{OD}_{\text{experimental well}} - \text{OD}_{\text{blank well}}) / (\text{OD}_{\text{control well}} - \text{OD}_{\text{blank well}})] * 100\%$.

2.4. Detection of Intracellular Reactive Oxygen Species. After treatment with IL-1β and TFDG for 24 h, chondrocytes cultured in six-well plates were collected and cocultured with 10 μM 2',7'-dichlorofluorescein diacetate (DCFH-DA) at 37°C for 20 min. The mean fluorescence intensity was measured by flow cytometry (Thermo Fisher Scientific), and FlowJo software 10.7 (BD Life Sciences, Franklin Lakes, NJ, USA) was employed for dealing with data.

2.5. RNA Isolation and Quantitative Real-Time PCR. TRIzol® (Thermo Fisher Scientific) was applied for total RNA extracting from chondrocytes, and RNA reverse transcrip-

tion was performed using the PrimeScript RT Reagent Kit (Takara, Tokyo, Japan) to obtain complementary DNA (cDNA). Real-time reverse transcription quantitative PCR (RT-qPCR) was carried out on a Real-Time PCR System (Bio-Rad, USA) using iTaq™ Universal SYBR® Green Super Mix with 1 μg of cDNA and primers. *Gapdh* as an internal reference was used to normalize gene expression, which was calculated using the $2^{-\Delta\Delta Ct}$ method. Supplementary Table 1 shows the primer sequences used to detect target genes.

2.6. Western Blotting. Chondrocytes cultured in six-well plates were washed twice, and RIPA lysis buffer was utilized for total protein isolation. Nuclear and Cytoplasmic Protein Extraction Kit (Beyotime) was used for separating proteins from nuclei and cytoplasm. Quantified protein concentration was detected using a Pierce™ BCA Kit (Thermo Fisher Scientific); equal proteins diluted in loading buffer were isolated by 10% SDS-PAGE and then delivered to nitrocellulose membranes. Western blocking buffer (Beyotime) was utilized for membranes blocking which then was incubated with the corresponding primary antibodies overnight at 4°C. Next, at room temperature, incubation with horseradish peroxidase- (HRP-) conjugated secondary antibodies was performed for 1 h. Membranes were exposed using ECL (Thermo Fisher Scientific) and visualized using a GS-800 scanner (Bio-Rad). ImageJ software (National Institutes of Health, Bethesda, MD, USA) was used for analyzing the density of band.

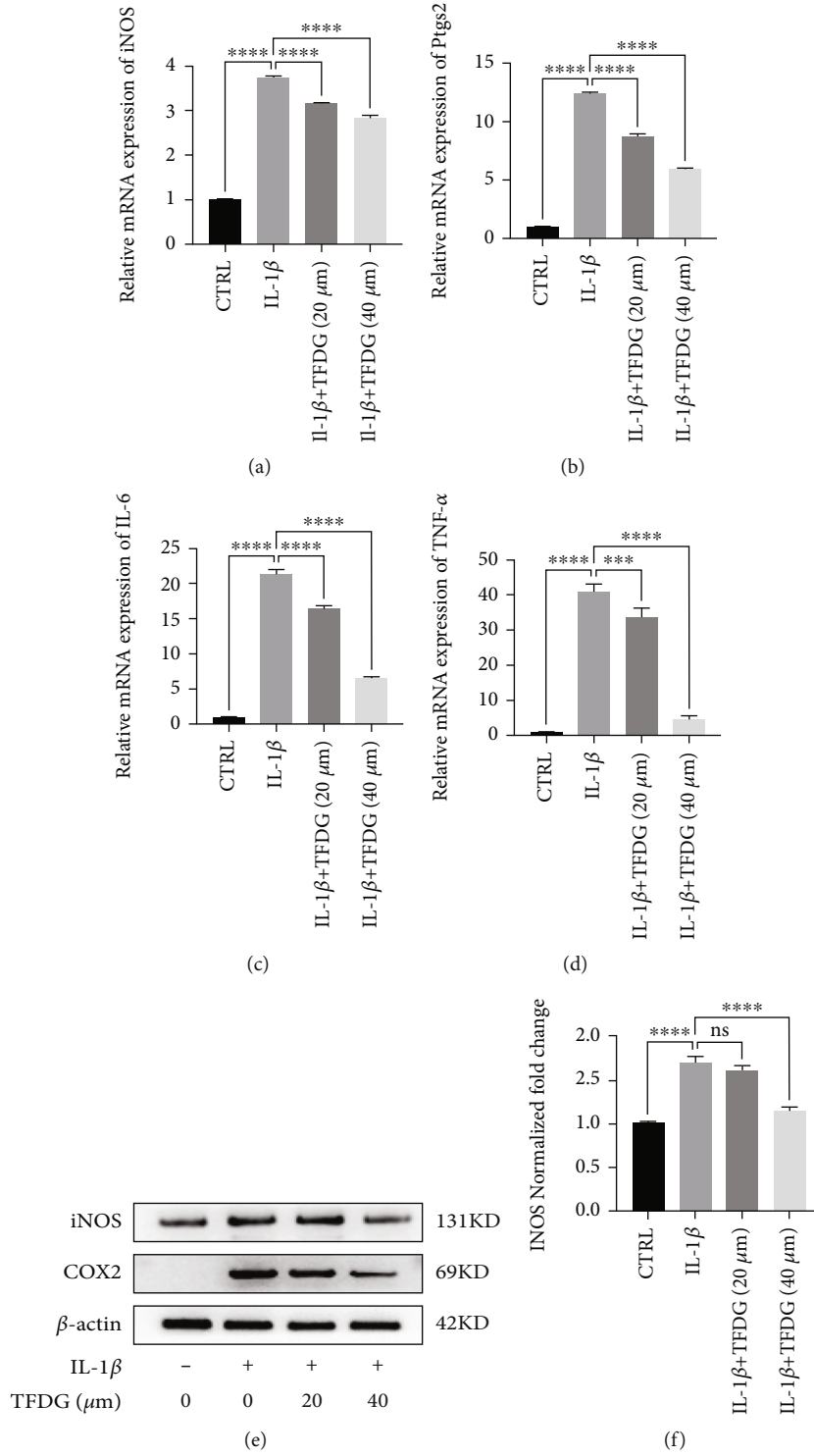


FIGURE 2: Continued.

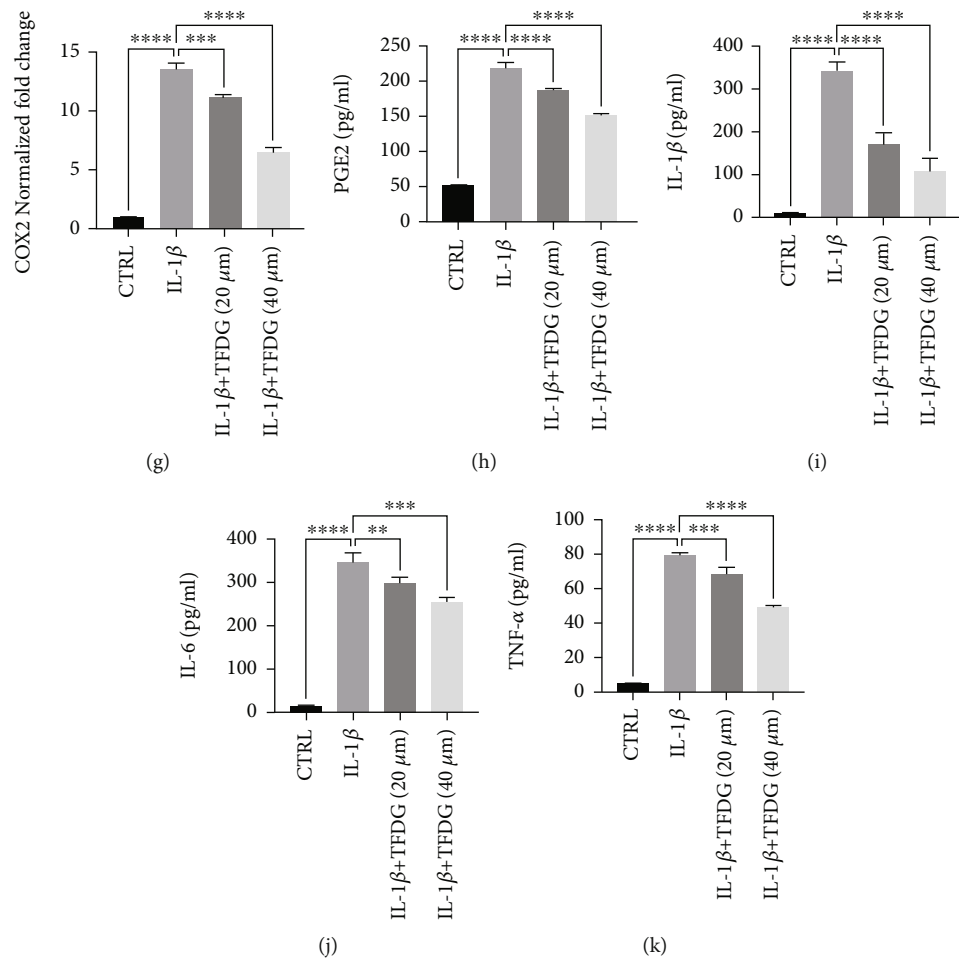


FIGURE 2: TFDG alleviates inflammatory responses in chondrocytes. (a–d) The transcription levels of iNOS, Ptg2, TNF- α , and IL-6 were determined by RT-qPCR. (e–g) The protein expressions of iNOS and COX2 were analyzed by western blotting. The grey values normalized with β -actin and control group were quantified by ImageJ. (h–k) Proinflammatory cytokines such as PGE2, IL-1 β , IL-6, and TNF- α from chondrocytes in different groups detected by ELISA. The bar graph shows the mean \pm SD of data ($n = 4$). * $p < .05$, ** $p < .01$, *** $p < .001$, and **** $p < .0001$.

2.7. Immunofluorescence. 24-well plates were applied for culture of chondrocytes treated with IL-1 β or TFDG. After cells reaching 50% density, the medium was replaced with PBS for rinsing cells twice, subsequently experienced fixation for 4% paraformaldehyde for 10 min, and then 0.25% Triton X-100 was used for cells permeabilization for 15 min and then blocked for 1 h. Cells were then soaked into diluted antibodies solution at 4°C overnight, and at room temperature, cells were incubated with fluorescent secondary antibodies for 1 h. 4',6-Diamidino-2-phenylindole (DAPI, Abcam) was used to counterstain nuclei via incubation for 10 min. Fluorescence microscope (Zeiss, Germany) was used for obtaining pictures.

2.8. siRNA Transfection. After reaching 50% confluence, chondrocytes cultured in six-well plates were transfected with siNrf2 and siNC, which were provided by RiboBio (Guangzhou, China), using Lipofectamine 3000 transfection

reagent on the base of the instruction for 6 h at 37°C. Transfected cells were used for subsequent experiments.

2.9. Animal Surgical Model and Treatments. All animal experiments were checked by the Ethics Committee for Animal Experiments at the First Affiliated Hospital of Soochow University. Thirty 6–8-week-old SD rats provided by the Experimental Animal Center of Soochow University were randomly assigned to three groups: the sham, OA, and OA +TFDG. A knee OA model was established according to giving rise to surgical destabilization of the medial meniscus (DMM). After all rats were anesthetized inhaling 2% isoflurane, a medial parapatellar incision in the right knee joint was performed to disclose the medial meniscotibial ligaments (MML). Rats in the OA and TFDG-injected groups underwent excision of MML, while the sham group retained intact MML. Intra-articular injections were performed 2 weeks after modeling. 100 μ L of this saline solution, containing 4 mM TFDG, was infused into the right knee joint of rats

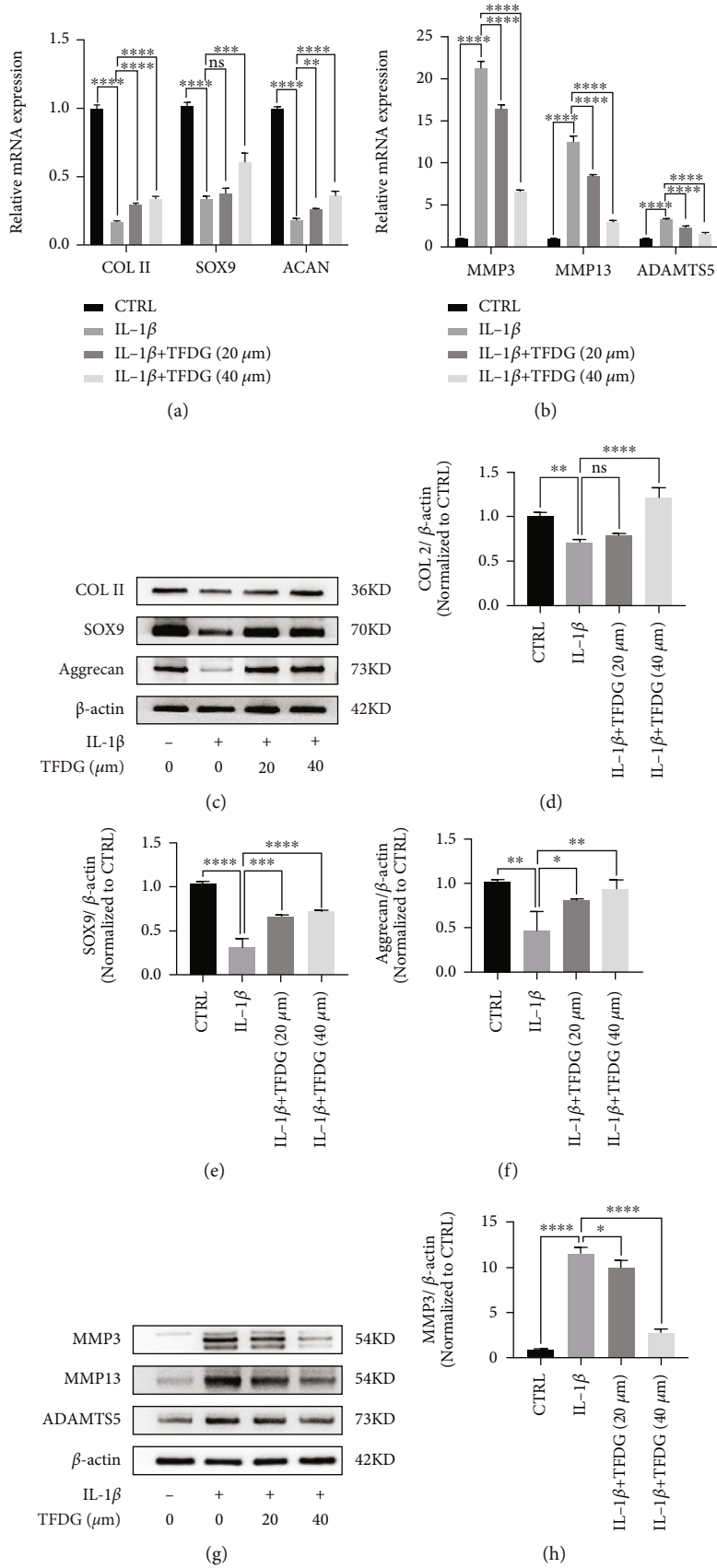


FIGURE 3: Continued.

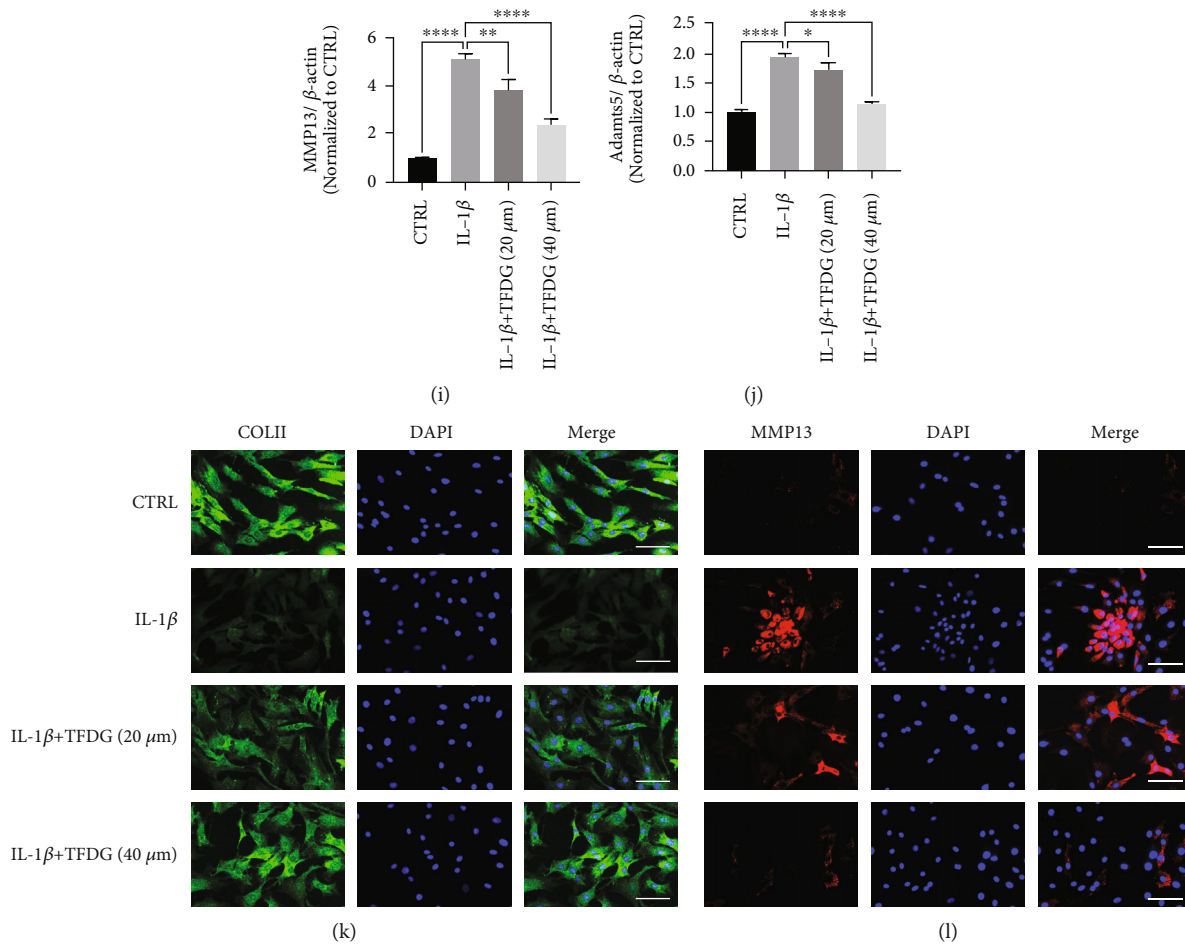


FIGURE 3: TFDG protects the cartilage matrix of chondrocytes. (a and b) The gene levels of *Mmp3*, *Mmp13*, and *Adamts5* and *Col2a1*, *Sox9*, and *ACAN* were analyzed by RT-qPCR. (c–j) The protein expressions of COL2, SOX9, aggrecan, MMP13, MMP3, and ADAMTS5 were analyzed by western blotting. The grey values normalized with β -actin and control group were quantified by ImageJ. The bar graph shows the mean \pm SD of data ($n = 4$). * $p < .05$, ** $p < .01$, *** $p < .001$, and **** $p < .0001$. (k and l) COL2 and MMP13 protein expressions were detected by immunofluorescence. Scale bar: 100 μ m.

in the TFDG group every 2 days for 6 weeks. Rats in other two groups received the same volume of saline solution in the knee joint.

2.10. Histology and Immunohistochemistry. All groups of rats raised for 8 weeks were sacrificed for collecting the right knee joints and 4% paraformaldehyde-fixed tissue underwent decalcification in 10% EDTA for 1 month. The specimens wrapped in wax were cut into 6 μ m thick slices for hematoxylin-eosin (HE) and safranin O/fast green (SO) staining, and the severity of cartilage degradation was estimated according to the Osteoarthritis Research Society International (OARSI) scoring system. Immunohistochemistry was performed as follows: xylene and gradient alcohol were used for dewaxing and dehydrating slices. After removal of endogenous peroxidase, the slices were incubated with 0.25% tyrisin for 60 min to restore the masked epitope, and then, goat serum was used for blocking slices for 20 min. Slices were then covered with anti-nrf2 and anti-COLII antibodies overnight at 4°C, and after that, secondary antibodies were used for 1 h at room temperature. Finally, a diamino-

benzidine (DAB) substrate kit was used to visualize the antigens, and hematoxylin was used for nuclear counterstaining. The calculation method of the staining ratio of positive cells is the number of stained cells/total number of cells in limited area, and the number of positive cells was marked and analyzed using ImageJ. All images were photoed under a Zeiss Axiovert 40CFL microscope.

2.11. Enzyme-Linked Immunosorbent Assay (ELISA). The medium of cells treated with various concentrations of TFDG was collected and added to appropriate 96-well plates included in the ELISA kit (MultiSciences, China). TNF- α , PEG2, and IL-1 β cytokine concentrations in the medium were quantified according to the detection of stop buffer absorbance at 450 nm and calculated through the standard curve.

2.12. Statistical Analysis. GraphPad Prism 8.0 software (San Diego, CA, USA) was used for performing all data processing. One-way analysis of variance (ANOVA) and Tukey's test were used for multiple comparisons. Comparison

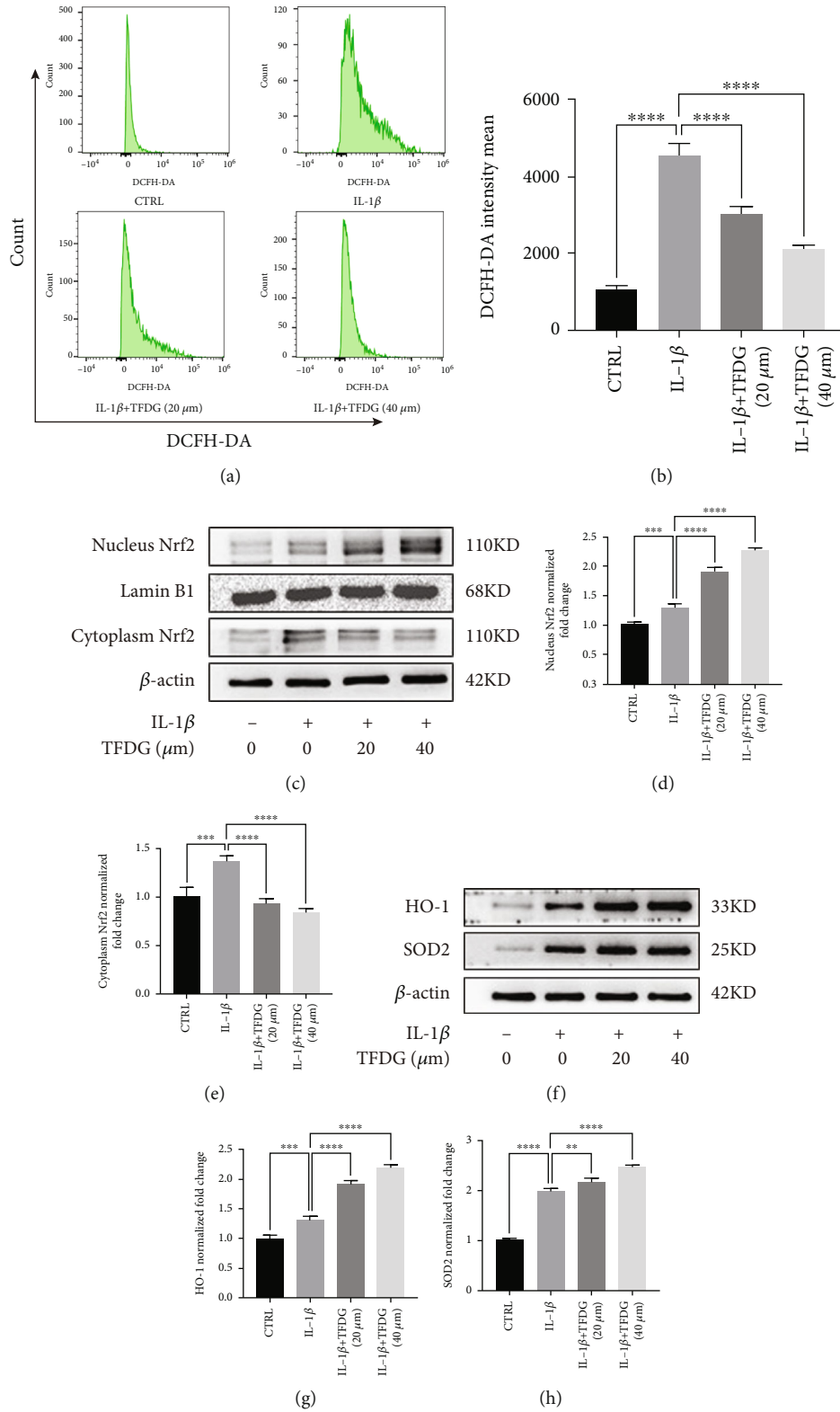


FIGURE 4: Continued.

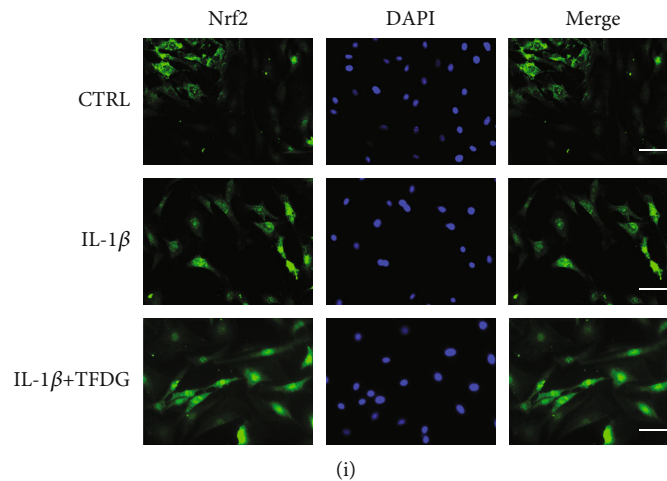


FIGURE 4: TFDG reduces IL-1 β -induced ROS accumulation by activating the Nrf2 pathway. (a and b) The intensity mean of ROS marked by DCFH-DA was quantified by flow cytometry. (c–h) The protein expressions of Nrf2 in nucleus and cytoplasm, HO-1, and SOD2 were analyzed by western blotting. The grey values of Nrf2 protein in nucleus normalized with Lamin B and other protein normalized with β -actin and control group were quantified by ImageJ. The bar graph shows the mean \pm SD of data ($n = 4$). * $p < .05$, ** $p < .01$, *** $p < .001$, and **** $p < .0001$. (i) Nrf2 protein expressions were detected by immunofluorescence. Scale bar: 100 μ m.

between two groups was evaluated using Student's t -test. All experiments were performed at least three times, and $p < 0.05$ was regarded as statistical significance.

3. Results

3.1. Effect of TFDG on Cell Viability. The molecular structure of TFDG is shown in Figure 1(a). Various concentrations of TFDG (1, 10, 20, 40, 80, or 120 μ M) were added to the cell culture medium to determine its cytotoxicity. Chondrocytes treated with TFDG at concentrations lower than 80 μ M showed increased viability with respect to control cells; in particular, treatment with 20 μ M and 40 μ M TFDG significantly promoted cell proliferation at 24 h ($p < 0.05$), although this effect was not apparent at 48 h. When the concentration of TFDG exceeded 80 μ M, its toxicity was not obvious at 24 h, but it significantly inhibited cell proliferation at 48 h (Figures 1(b) and 1(c)). Based on the above results, TFDG concentrations of 20 μ M and 40 μ M were used in the following experiments.

3.2. TFDG Alleviates Inflammatory Responses in Chondrocytes. IL-1 β (10 ng/mL) was used to simulate the environment where chondrocytes were affected by inflammation. Compared to the control group, the transcription levels of *iNOS*, *ptgs2*, *Tnf- α* , and *Il-6* were significantly upregulated in chondrocytes treated with IL-1 β which also led to elevating *iNOS* and *COX-2* protein expression. However, TFDG reversed the effect of IL-1 β on chondrocytes as it downregulated the expression of the above-mentioned inflammation-related factors at both the gene and protein expression (Figures 2(a)–2(d)). ELISA results also suggested that TFDG inhibits IL-1 β -induced secretion of IL-1 β , PGE₂, IL-6, and TNF- α from chondrocytes (Figures 2(h)–2(k)).

3.3. TFDG Protects the Cartilage Matrix of Chondrocytes. IL-1 β treatment suppressed *Col2a1*, *Sox9*, and *ACAN* expres-

sions in chondrocytes, while treatment with TFDG partly restored the expression of these genes associated with matrix synthesis (Figure 3(a)). At the same time, RT-qPCR revealed that IL-1 β remarkably promoted the transcription of *Adamts5*, *Mmp3*, and *Mmp13* which was prevented by TFDG treatment (Figure 3(b)). Western blotting results also confirmed that IL-1 β dramatically downregulated COLII, SOX9, and aggrecan expression while upregulating matrix-degrading enzymes expression, including MMP3, MMP13, and ADAMTS5 at the protein level; however, TFDG blocked this effect (Figures 3(c)–3(j)). Consistently, an immunofluorescence assay confirmed that TFDG promoted COLII synthesis but suppressed IL-1 β -induced MMP13 expression (Figures 3(k) and 3(l)).

3.4. TFDG Reduces IL-1 β -Induced ROS Accumulation by Activating the Nrf2 Pathway. The production of intracellular ROS stimulated by IL-1 β was measured by inspecting changes in DCFH-DA fluorescence. After being treated with IL-1 β and/or TFDG, chondrocytes were collected and incubated with DCFH-DA. Subsequently, DCFH-DA fluorescence was measured by flow cytometry, and stronger green fluorescence intensity indicated greater ROS accumulation in chondrocytes. Flow cytometric analysis suggested that IL-1 β treatment resulted in a robust production of ROS in cells, whereas TFDG treatment assisted chondrocytes in scavenging ROS and reduced their accumulation (Figures 4(a) and 4(b)). To determine the mechanism by which TFDG inhibits ROS accumulation, the activity status of the Nrf2/HO-1 signaling pathway, which plays an important role in ROS detoxification, was further investigated. Western blotting results demonstrated that the Nrf2/HO-1 signaling pathway is involved in the ROS-scavenging activity of TFDG. In fact, TFDG significantly promoted the expression of Nrf2 in the nucleus, where it binds to ARE elements, as well as HO-1 and SOD2 expression. Conversely, IL-1 β upregulated Nrf2 expression mainly in the cytoplasm;

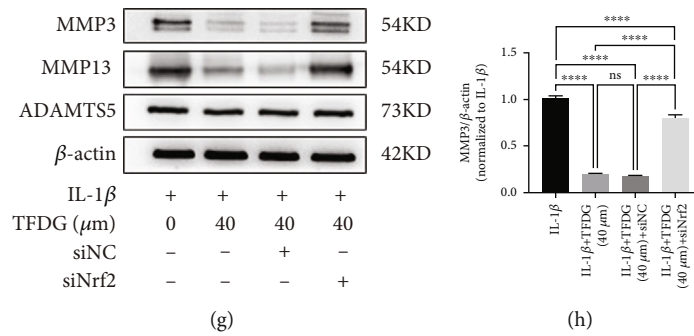
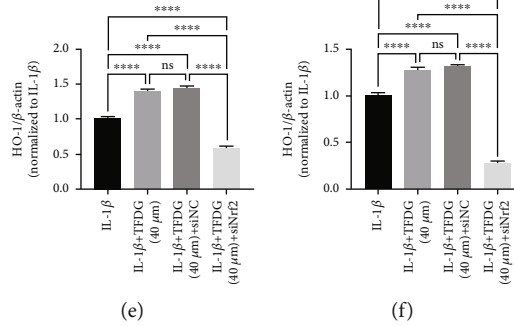
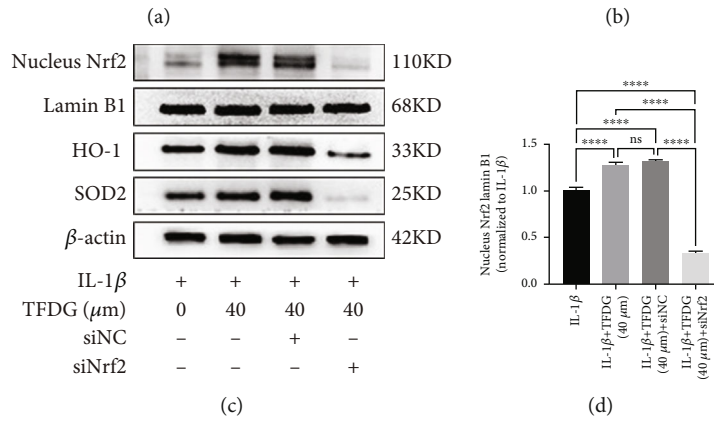
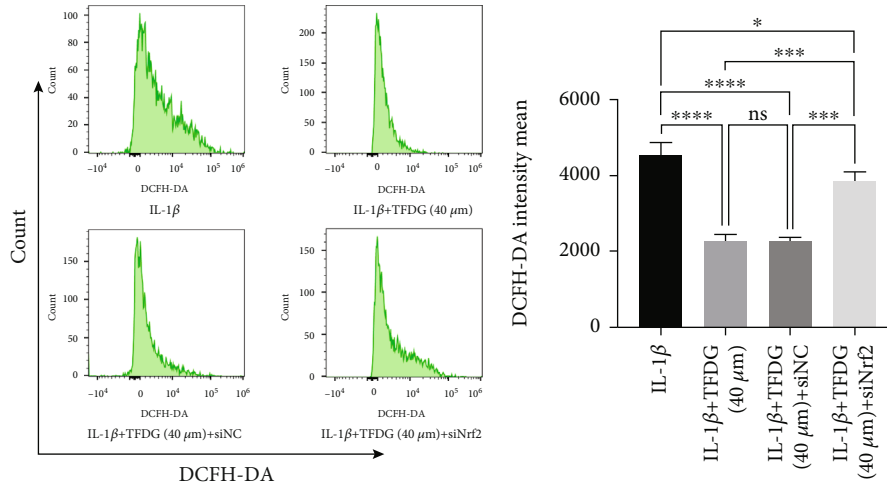


FIGURE 5: Continued.

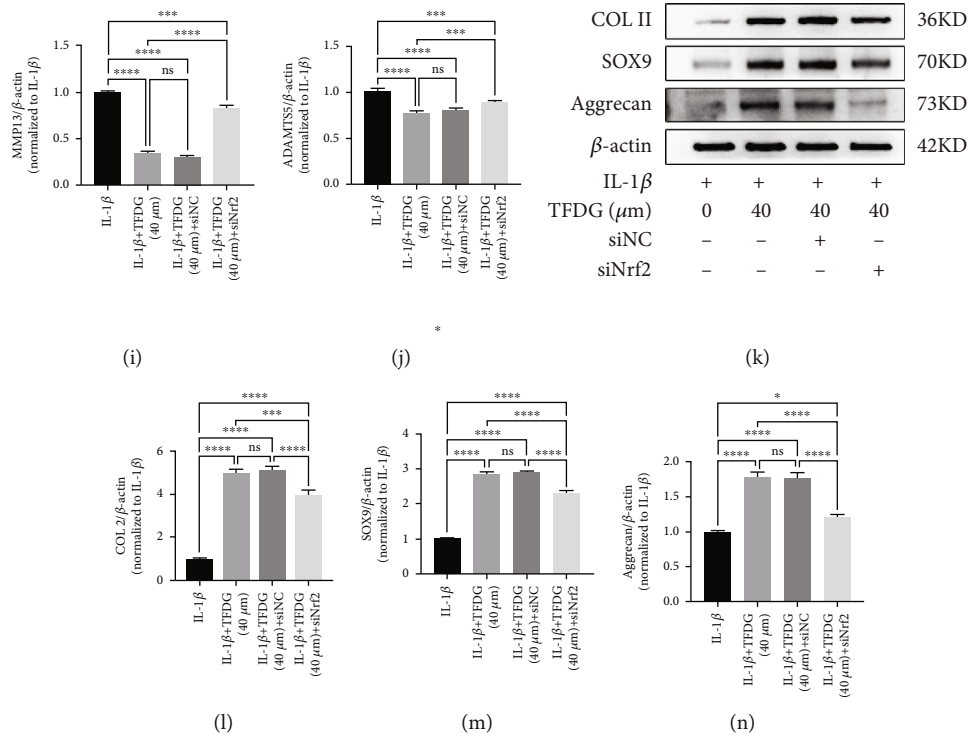


FIGURE 5: The blockade of Nrf2/HO-1 signaling partly reverses the protective effect of TFDG. (a and b) The intensity mean of ROS marked by DCFH-DA was quantified by flow cytometry. (c–n) The protein expressions of Nrf2 in nucleus, HO-1, SOD2, COL2, SOX9, aggrecan, MMP13, MMP3, and ADAMTS5 were analyzed by western blotting. The grey values of Nrf2 protein in nucleus normalized with Lamin B and other protein normalized with β -actin and control group were quantified by ImageJ. The bar graph shows the mean \pm SD of data ($n = 4$). * $p < .05$, ** $p < .01$, *** $p < .001$, and **** $p < .0001$.

moreover, HO-1 and SOD2 expressions were upregulated only slightly compared to that of the control (Figures 4(c)–4(h)). Similarly, immunofluorescence also revealed that Nrf2 mainly accumulated in the nuclei, confirming that TFDG can enhance Nrf2 translocation into the nucleus (Figure 4(i)).

3.5. The Blockade of Nrf2/HO-1 Signaling Partly Reverses the Protection of TFDG. To verify that the Nrf2/HO-1 signaling pathway participates in the protection against OA offered by TFDG, chondrocytes were transfected with siNrf2 to knock down Nrf2 expression; siNC was used as a negative control to account for the effects of the transfection process. According to flow cytometric analysis, green fluorescence intensity remained elevated in siNrf2-transfected cells, indicating that the inhibition of the Nrf2 weakened the clearance effect of TFDG on ROS and thus led to ROS accumulation (Figures 5(a) and 5(b)). Western blot analysis indicated that Nrf2 expression in the nucleus decreased significantly upon siNrf2; in turn, this suppression also resulted in HO-1 and SOD2 protein expression decreasing (Figures 5(c)–5(f)). The blockade of the Nrf2/HO-1 pathway also interfered with the defendant of the cartilage matrix caused by TFDG. In fact, compared to those of the TFDG group and the TFDG + siNC group, the expression of COL2A1, SOX9, and aggrecan in chondrocytes was decreased in the TFDG+siNrf2 group, although it remained higher than that of the IL-1 β group. The opposite was observed for MMP3, MMP13,

and ADAMTS5 protein expressions in the TFDG+siNrf2 group, which was higher than that of the TFDG group and the TFDG+siNC group but lower than that of the IL-1 β group (Figures 5(g)–5(n)).

3.6. TFDG Inhibits Inflammation-Related Pathways Induced by IL-1 β . The MAPK and PI3K/AKT/NF- κ B signaling pathways are believed to hasten OA, and some article showed that TFDG can inhibit these pathways in other diseases. To confirm that TFDG can repress these two pathways, western blotting assays were carried out. In IL-1 β -treated chondrocytes, the expression of phosphorylated PI3K, AKT, p65, I κ B α , ERK, JNK, and p38 was significantly upregulated, whereas I κ B α expression was downregulated, which represents the activation of the inflammation-related axis. Nevertheless, the expression of phosphorylated PI3K, AKT, p65, I κ B α , ERK, JNK, and p38 was reduced, while I κ B α expression was increased in the presence of TFDG, which hindered the activation of these pathways (Figures 6(a)–6(i)). An immunofluorescence assay was performed to observe changes in p65 expression and localization: the results demonstrated that the in control group p65 protein was mostly in the cytoplasm, while IL-1 β treatment caused p65 transfer into the nucleus. However, in TFDG-treated group, p65 expression restored in the cytoplasm (Figure 6(j)).

3.7. TFDG Prevented DMM-Induced Cartilage from Degradation. To explore the effects of TFDG *in vivo*, rats

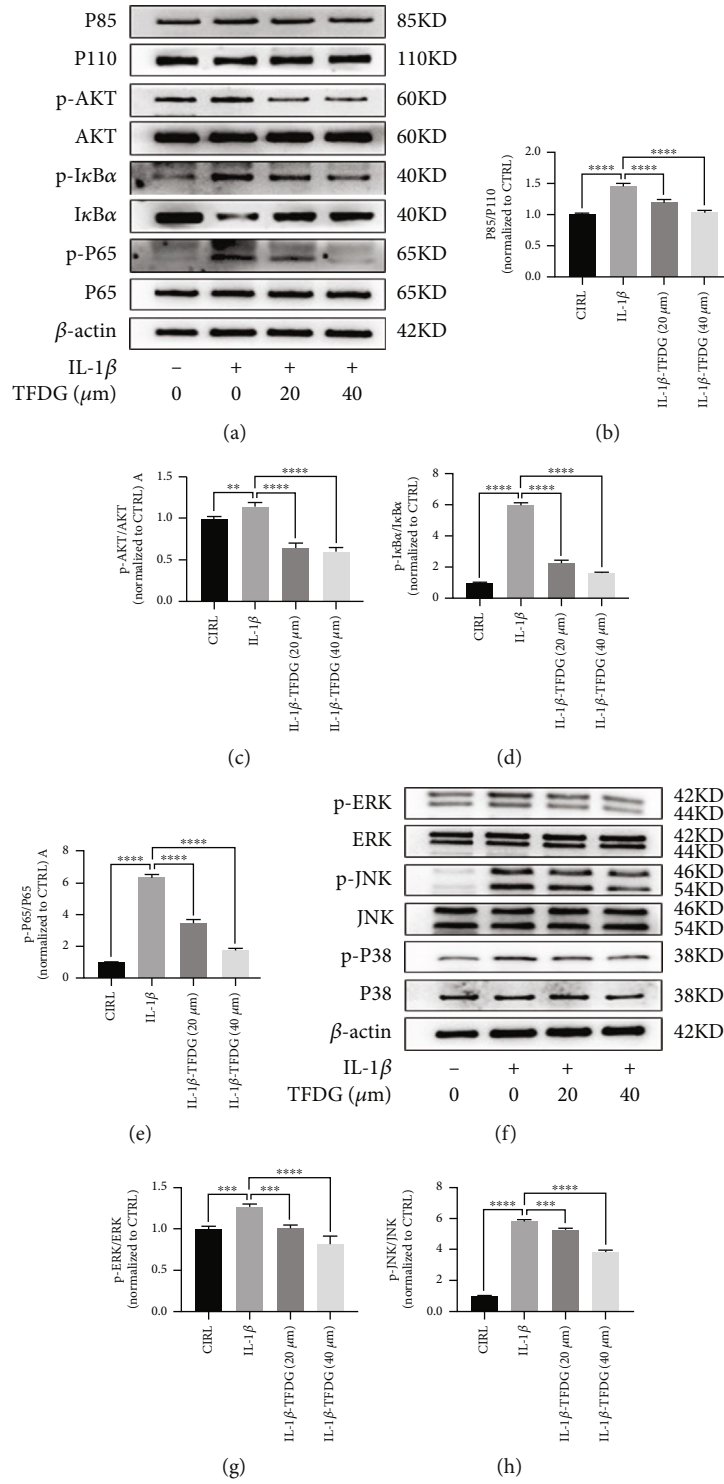


FIGURE 6: Continued.

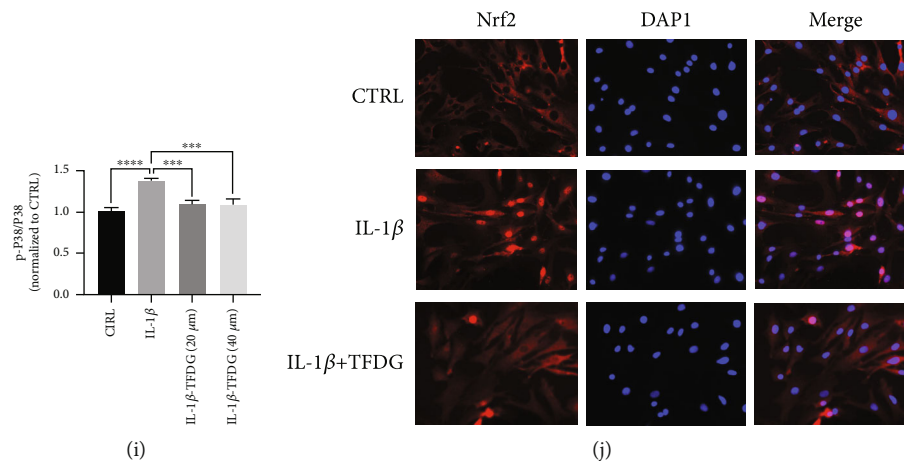


FIGURE 6: TFDG inhibits inflammation-related pathways induced by IL-1 β . (a-i) The protein expressions of phosphorylated PI3K, AKT, p65, I κ B α , ERK, JNK, and p38 were analyzed by western blotting. The grey values normalized with control group were quantified by ImageJ. The bar graph shows the mean \pm SD of data ($n = 4$). * $p < .05$, ** $p < .01$, *** $p < .001$, and **** $p < .0001$. (j) P65 protein expressions were detected by immunofluorescence. Scale bar: 100 μ m.

in the OA and TFDG-injected groups underwent DMM surgery accompanied or not by TFDG treatment. All rats were sacrificed 8 weeks after surgery, and the extracted knee joints were sliced into sections. To analyze the degree of cartilage destruction, the sections were stained by HE and safranin O/fast green. The articular surface from the control group was complete, and the cartilage could secrete abundant glycosaminoglycans. However, OA induced severe joint wear and loss of glycosaminoglycans in the cartilage. Conversely, the cartilage of rats that had received TFDG injection for 6 weeks after surgery was protected from degradation and could accumulate more glycosaminoglycans (Figures 7(a) and 7(b)). The severity of OA was quantified according to the OARSI scoring system: rats in the TFDG group exhibited higher scores than those in the OA group (Figure 7(e)). Immunohistochemistry assays revealed a higher number of cells positive for COLII and Nrf2 expression in the TFDG-injected group than in the OA group; this suggests that TFDG can protect the cartilage matrix from inflammation via activation of Nrf2 (Figures 7(c), 7(d), 7(f), and 7(g)).

4. Discussion

According to the literature, the occurrence of OA depends on a variety of mechanisms. In addition to inflammatory responses, mechanical load, oxidative stress, and cell senescence may all promote the degradation and inhibit the synthesis of the extracellular matrix, resulting in cartilage damage and ultimately OA [36–39]. Therefore, early suppression of inflammatory responses in chondrocytes and mitigation of oxidative stress levels may delay the onset of OA. Many natural compounds with antioxidant and anti-inflammatory properties have been explored as candidates for delaying the progression of OA [40]. TFDG is a characteristic compound of black tea, and its excellent anti-inflammatory and antioxidant properties have been demonstrated in a variety of diseases [41]. For example, Ai et al. found that TFDG treatment could reduce RANKL-induced

intracellular ROS accumulation in RAW cells and inhibit osteoclast formation, thereby promoting osteogenesis and alleviating bone loss in immunized mice [34]. Similarly, San Cheang et al. found that TFDG can delay hypertension-induced apoptosis of endothelial cells through their antioxidant properties [41]. Therefore, we aimed to investigate whether TFDG can exert anti-inflammatory and antioxidant effects in chondrocytes to delay the progression of arthritis. To determine the appropriate dose of TFDG for chondrocytes in an inflammatory environment *in vitro*, we selected six gradually increasing concentrations (1, 10, 20, 40, 80, and 120 μ M) by referring to the application of TFDG in other diseases. Then, the CCK-8 assay was used to measure the effect of TFDG at these six concentrations on chondrocyte proliferation, to facilitate the selection of a low concentration and a high concentration for subsequent experiments. According to the results of the CCK-8 assay, TFDG is safe for chondrocytes when administered at a concentration below 40 μ M but can significantly inhibit the growth of chondrocytes after treatment at a higher dose. At the same time, TFDG was found to promote the growth of chondrocytes within 24 h, especially at a concentration of 40 μ M, but this effect was no longer obvious after 48 h. Therefore, the treatment duration was 24 h, and 20 μ M TFDG was used for the low-concentration treatment group, while 40 μ M TFDG was used for the high-concentration treatment group. After determining the working dose of TFDG, we treated chondrocytes with IL-1 β and/or TFDG and observed changes in inflammatory indexes, matrix synthesis, and degradation indexes. We found that IL-1 β -mediated inhibition of chondrocyte proliferation was alleviated by combined IL-1 β /TFDG treatment. TFDG was found to exert a dose-dependent effect on decreasing inflammatory indicators in chondrocytes and to significantly downregulate IL-1 β and TNF- α expression; similarly, the expression levels of COX-2 and iNOS, two landmark inflammatory proteins, were significantly reduced, especially in the high-concentration TFDG-treated group; all other indicators were

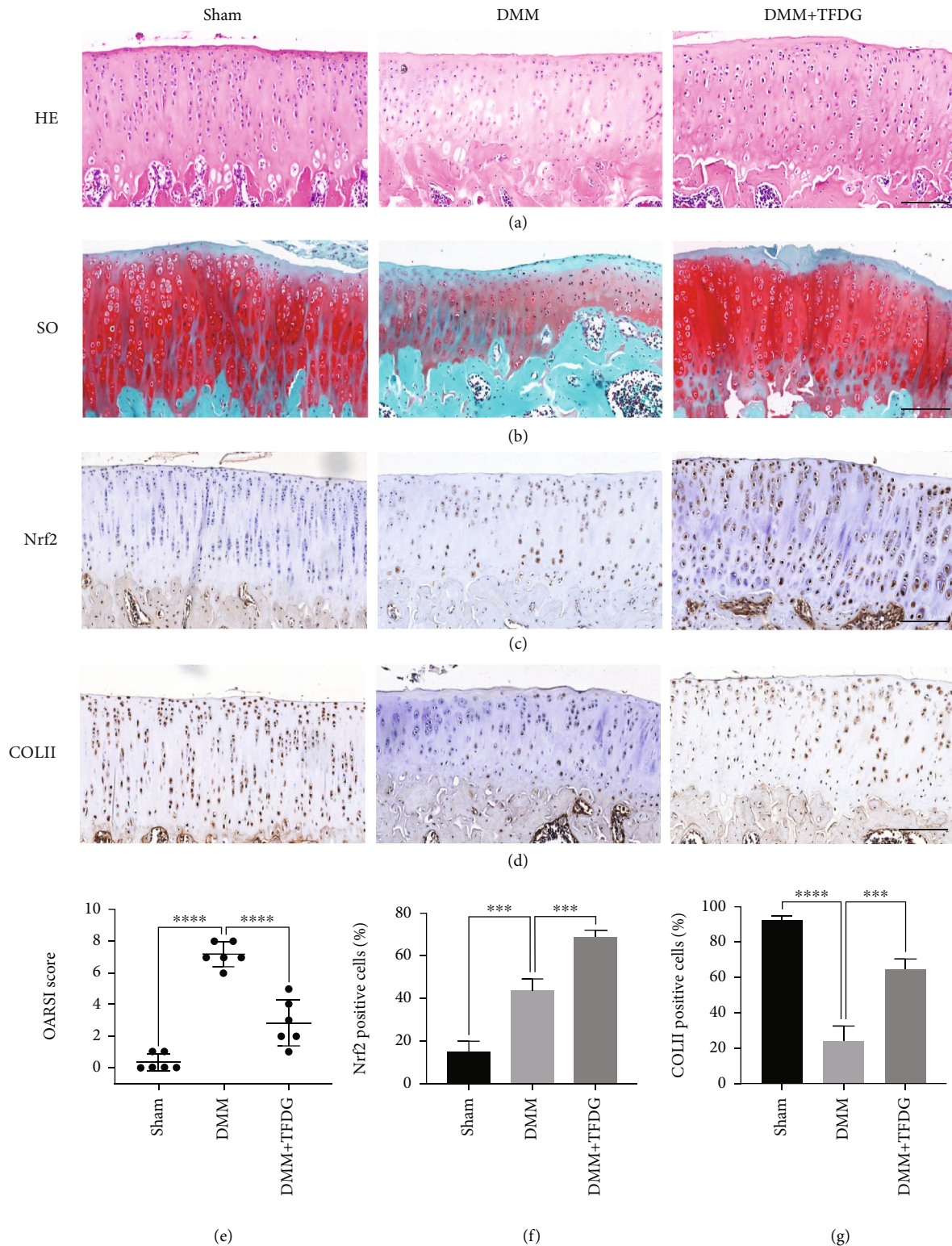


FIGURE 7: TFDG protects DMM-induced cartilage from degradation. (a and b) The rats of joint sections were stained by HE and safranin O/fast green. (c and d) The COLII and Nrf2 protein expressions in cartilage were determined by immunohistochemistry staining. (e) The OARSI scores of cartilages in different groups. (f and g) The Nrf2 and COLII positive cells were quantified. The bar graph shows the mean \pm SD of data ($n = 4$). $*p < .05$, $**p < .01$, $***p < .001$, and $****p < .0001$. Scale bar: 100 μm .

close to normal levels. When measuring matrix synthesis and degradation indexes, we found that the expression of type II collagen and proteoglycans at both the gene and pro-

tein levels increased with increasing TFDG concentrations, while the expression of *Mmp3*, *Mmp13*, and *Adamts5* decreased with increasing TFDG concentrations.

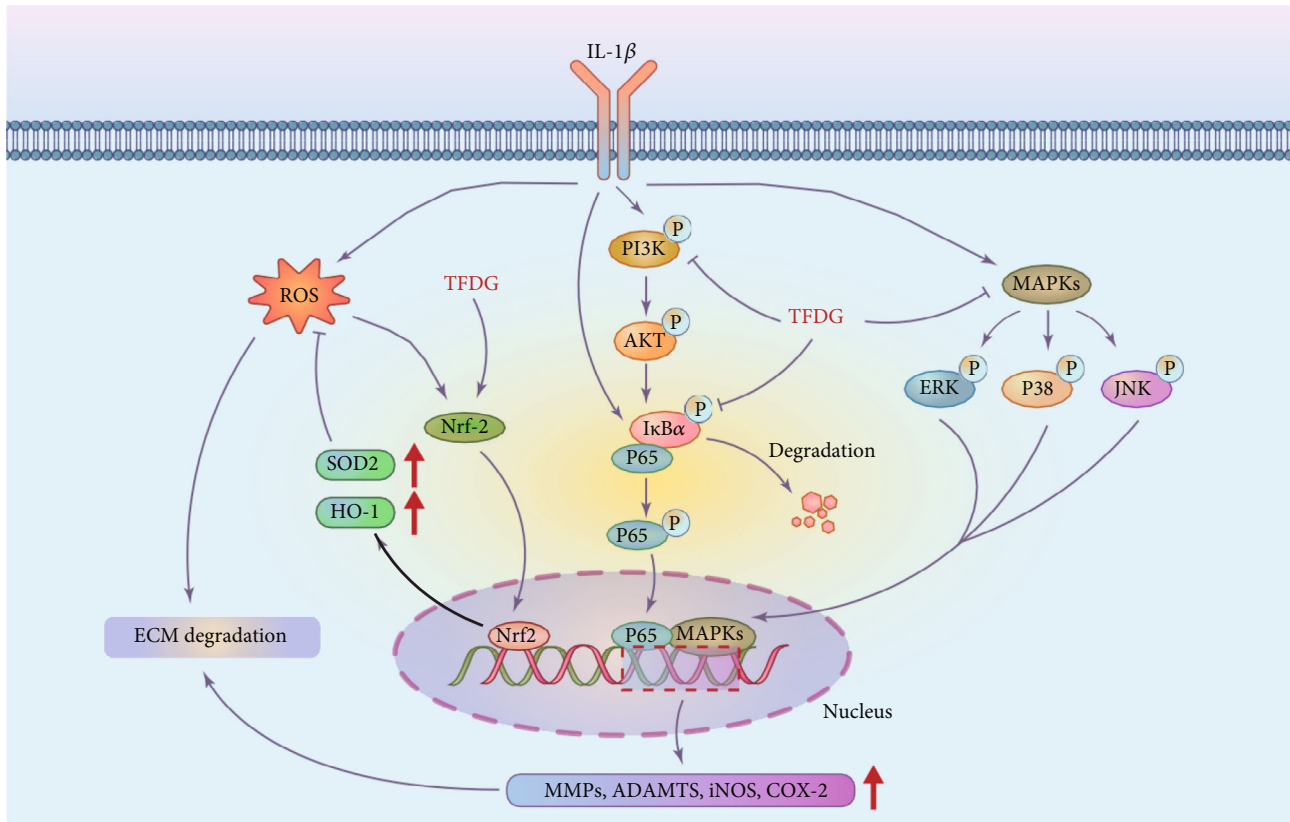


FIGURE 8: The mechanism of TFDG delaying cartilage degradation involves the activation of Nrf2/HO-1 signal pathway and the inhibition of PI3K/AKT/NF- κ B and MAPK pathways.

Previous studies have found that oxidative stress promotes the onset of OA and plays a key role in its progression [42, 43]. On the other hand, TFDG has been reported to be an effective antioxidant. Consistent with this background, the results of our flow cytometry assay using the fluorescent probe DCFH-DA, a marker of ROS in cartilage cells, aiming to quantify the indirect fluorescence intensity of intracellular ROS, showed that IL-1 β can induce the production of intracellular ROS, but TFDG treatment can counteract such accumulation. Keap1/Nrf2, as a classical antioxidant pathway, is expressed in multiple organs where it plays an important role [44]. Under normal conditions, the DGR region of Keap1 binds to the DLG and ETGE sequences of Nrf2, which stabilizes Nrf2 in the cytoplasm and induces Nrf2 degradation through the ubiquitination system to inhibit its activity [45]. Keap1 transforms its connection with Nrf2 by sensing changes in electrons and ROS which reduces the degradation of Nrf2 through ubiquitination, accelerating the accumulation of nucleus Nrf2 binding with the promoter ARE to promote transcription and translation of downstream antioxidant proteases. Therefore, the imbalance or deletion of Keap1/Nrf2 pathway often leads to the damage of the organ and the progression of the corresponding disease [46]. On the contrary, upregulating Keap1/Nrf2 expression can effectively resist chronic inflammation, degenerative changes, and even cancer caused by oxidative stress [47–49]. Adeel Safdar found that Keap1/Nrf2 pathway is also involved in the musculoskeletal diseases. The ROS

generation rate and Nrf2 expression level are both low in young individuals. However, with the aging of individuals, at first, the increased Nrf2 expression is consistent with the increased ROS level. Thus, cells can still maintain oxidative stress balance, however, which is transient. With aging, transcription of Nrf2 regulated by ARE will be destroyed eventually, resulting in the decrease of Nrf2 expression, and the accumulation of ROS is difficult to clear, leading to cell apoptosis and musculoskeletal degeneration [50]. Cai et al. found that after the onset of OA in a murine model of DMM, the expression of Nrf2 and its downstream antioxidant enzymes significantly increased to limit OA progression, while Nrf2-KO mice lost the ability to activate Nrf2 to reduce MMPs and protect cartilage [51]. Therefore, the spontaneous increase of Nrf2 expression in the aged population after the occurrence of OA is insufficient to remove the intracellular ROS, and further stimulation of Nrf2 expression through exogenous intervention may be an effective means to treat OA and protect cartilage. Our study found that after the chondrocytes were stimulated by IL-1 β , the expressions of Nrf2 in the nucleus and the downstream antioxidant proteases SOD2 and HO-1 were slightly increased, so the intracellular ROS still maintained a high level. After TFDG intervention, the expression of Nrf2 in the nucleus, SOD2, and HO-1 was significantly increased, and the scavenging of ROS was accelerated. To confirm that the activation of Nrf2 pathway is an important way for TFDG to protect articular cartilage, we used siRNA to interfere with

Nrf2 transcription and found that the effect of TFDG was reversed and the levels of Nrf2 in the nucleus as well as SOD2 and HO-1 in the cytoplasm decreased, while intracellular ROS increased again. These results indicated that TFDG reduced ROS in the articular chondrocytes relying on Nrf2 mediated and the protective effect of TFDG on the extracellular matrix of chondrocytes was also weakened. In vivo immunohistochemical results also showed Nrf2 activation in OA group, but Nrf2 activation was more significant after TFDG injection, which was conducive to maintaining the homeostasis of the joint environment.

Previous studies found that after Nrf2/HO-1 pathway was inhibited, the protective effect of TFDG on chondrocytes was not completely lost, which may depend on the anti-inflammatory effect of TFDG. Therefore, PI3K/AKT/NF- κ B and MAPK pathways were investigated successively. The NF- κ B signaling pathway is responsible for the transmission and amplification of inflammatory signals and activated NF- κ B was seen in the synovium of both osteoarthritis and rheumatoid arthritis patients [52]. In response to endogenous or exogenous inflammatory cytokines (IL-1 β and TNF- α), IKK β is activated first, leading to phosphorylation of I κ B α protein which degraded through ubiquitination which releases NF- κ B dimer into the nucleus binding to specific DNA sequences and promote transcription of inflammatory factors, chemokines, and metalloproteinases promoting the progression of osteoarthritis [53, 54]. Phosphoinositide-3 kinase (PI3K) consists of two subunits, p85 and P110, which regulate and catalyze the phosphorylation of the downstream Serine/threonine kinase AKT through lipid secondary messengers and regulate immune and inflammatory responses [55, 56]. More studies have shown that activation of NF- κ B pathway is often accompanied by activation of AKT. Inhibition of phosphorylation of PI3K/AKT pathway can partially block NF- κ B pathway and reduce transcription of downstream cytokines and protein-degrading enzymes [57, 58]. Our study also found that IL-1 β stimulated chondrocytes increased the phosphorylation of PI3K and AKT and activated the NF- κ B pathway, while TFDG significantly inhibited the PI3K/AKT/NF- κ B pathway, thereby reducing the transcription of downstream inflammatory factors and metalloproteinases. Mitogen-activated protein kinase (MAPK) has three forms: C-Jun N-terminal kinases, P38 MAPKs, and ERKs. Among them, JNK and P38 MAPK pathways are activated mainly by receiving stimulation of inflammatory factors and signals of extracellular pressure [59, 60]. Many growth factors, cytokines, and bacterial metabolites can activate the ERKs pathway. Significantly increased IL-1 β in synovium of patients with osteoarthritis can strongly activate C-Jun, P38 MAPKs, and ERKs through IL-1R. Previous studies have found that activation of MAPK pathway can increase the transcription of MMPs and ADAMTs and accelerate the degradation of extracellular matrix, while inhibitors of MAPK pathway can effectively protect the extracellular matrix and reduce chondrocyte apoptosis in vivo and in vitro [61, 62]. Similarly, we found that TFDG can effectively inhibit IL-1 β -induced MAPK pathway activation by reduc-

ing c-Jun, P38 MAPKs, and ERKs phosphorylated proteins in chondrocytes.

Our study found that TFDG could protect cartilage from degradation via its anti-inflammatory and antioxidant properties involving the enhancement of Nrf2/HO-1 signal pathway and the inhibition of PI3K/AKT/NF- κ B and MAPK pathways (Figure 8). However, our research has some limitations. Firstly, anti-inflammatory and antioxidant signal pathway may have crosstalk and we cannot separate them to analyze their function [63]. On the one hand, declined ROS which mediated by antioxidant enzymes can also reduce iNOS or COX2 protein expression and lessen the inflammatory reactions by decreased stimulation of NF- κ B pathway. HO-1, a downstream target gene of Nrf2, can even directly inhibited p65 nuclear translocation and NF- κ B mediated transcription including MMPs [64, 65]. On the other hand, the reduction of endogenous inflammatory factors due to the suppression of PI3K/AKT/NF- κ B and MAPK pathways decreased the production of ROS according to NOX4 complex, which also contributes to maintain redox homeostasis [66]. Secondly, we were unable to find specific agonist activating PI3K/AKT/NF- κ B and MAPK pathways to reverse the therapeutic effects of TFDG; thus, we cannot rule out interference between the pathways. Thirdly, we did not verify the inhibition of PI3K/AKT/NF- κ B and MAPK pathways in vivo via immunohistochemistry detection.

5. Conclusions

In conclusion, TFDG was found for the first time to exert anti-inflammatory effects in chondrocytes in vivo and vitro through the PI3K/AKT/NF- κ B and MAPK pathways and promote the antioxidant ability of chondrocytes through the Nrf2/HO-1 pathway. These results suggest a novel therapeutic approach for the treatment of OA.

Abbreviations

OA:	Osteoarthritis
IL-1:	Interleukin 1
TNF:	Tumor necrosis factor
ERK:	Extracellular signal-regulated kinase
MAPK:	Mitogen-activated protein kinase
JNK:	C-Jun N-terminal kinase
NF- κ B:	Nuclear factor kappa-B
I κ B α :	Inhibitor kappa B alpha
PI3K:	Phosphoinositide-3 kinase
AKT:	Protein kinase B
ROS:	Reactive oxygen species
TFDG:	Theaflavin-3-3'-digallate
SOX9:	SRY-related HMG box 9
COL-II:	Type II collagen
ACAN:	Aggrecan
MMP13:	Matrixmetalloproteinase13
MMP3:	Matrixmetalloproteinase3
ADAMTS5:	A disintegrin and metalloproteinase with thrombospondin motifs5
Nrf2:	Nuclear factor erythroid 2-related factor 2

HO-1: Heme oxygenase-1
 SOD2: Superoxide dismutase2
 CCK-8: Cell Counting Kit-8
 PGE2: Prostaglandin E2
 iNOS: Inducible nitric oxide synthase
 COX2: Cyclooxygenase-2
 ARE: Antioxidant response element.

Data Availability

All data supporting the finding are available within the study.

Ethical Approval

All animal experiments were approved by the Ethics Committee for Animal Experiments at the First Affiliated Hospital of Soochow University.

Conflicts of Interest

The authors declare that no competing interests exist.

Authors' Contributions

J.Z. and Y.T. designed the experiment. Y.T., Z.J., W.R., M.L., M.H., Q.Z., and W.W. performed the study and prepared the manuscript. Y.T., Z.J., M.L., H.Y., and J.Z. analyzed the data. Y.T., W.R., M.H., and W.W. built the animal model and were responsible for animal experiments. H.Y. and J.Z. provided funding support and supervised the experiment. Y.T., Z.J., and W.R. contributed equally to this work.

Acknowledgments

This work was supported by the National Natural Science Foundation of China (82030068 and 82172506).

Supplementary Materials

Supplementary Table 1: the sequences used to detect target genes in the study were shown in the table. (*Supplementary Materials*)

References

- [1] A. Powell, A. J. Teichtahl, A. E. Wluka, and F. M. Cicuttini, "Obesity: a preventable risk factor for large joint osteoarthritis which may act through biomechanical factors," *British Journal of Sports Medicine*, vol. 39, no. 1, pp. 4-5, 2005.
- [2] D. J. Hunter and S. Bierma-Zeinstra, "Osteoarthritis," *The Lancet*, vol. 393, no. 10182, pp. 1745-1759, 2019.
- [3] N. C. Butterfield, K. F. Curry, J. Steinberg et al., "Accelerating functional gene discovery in osteoarthritis," *Nature Communications*, vol. 12, no. 1, p. 467, 2021.
- [4] P. R. Coryell, B. O. Diekman, and R. F. Loeser, "Mechanisms and therapeutic implications of cellular senescence in osteoarthritis," *Nature Reviews Rheumatology*, vol. 17, no. 1, pp. 47-57, 2021.
- [5] A. Ghouri and P. G. Conaghan, "Update on novel pharmacological therapies for osteoarthritis," *Therapeutic advances in musculoskeletal disease*, vol. 11, p. 1759720X1986449, 2019.
- [6] X. Tang, S. Wang, S. Zhan et al., "The prevalence of symptomatic knee osteoarthritis in China: results from the China health and retirement longitudinal study," *Arthritis & Rheumatology*, vol. 68, no. 3, pp. 648-653, 2016.
- [7] S. Jiang, Y. Liu, B. Xu, Y. Zhang, and M. Yang, "Noncoding RNAs: New regulatory code in chondrocyte apoptosis and autophagy," *Wiley Interdisciplinary Reviews: RNA*, vol. 11, no. 4, p. e1584, 2020.
- [8] V. Francisco, J. Pino, M. A. Gonzalez-Gay et al., "A new immunometabolic perspective of intervertebral disc degeneration," *Nature Reviews Rheumatology*, vol. 18, no. 1, pp. 47-60, 2022.
- [9] M. DeRogatis, H. K. Anis, N. Sodhi et al., "Non-operative treatment options for knee osteoarthritis," *Annals of translational medicine*, vol. 7, Supplement 7, p. S245, 2019.
- [10] B. Zampogna, R. Papalia, G. F. Papalia et al., "The role of physical activity as conservative treatment for hip and knee osteoarthritis in older people: a systematic review and meta-analysis," *Journal of Clinical Medicine*, vol. 9, no. 4, p. 1167, 2020.
- [11] C. Cadet, E. Maheu, and A. G. The French, "Non-steroidal anti-inflammatory drugs in the pharmacological management of osteoarthritis in the very old: prescribe or proscribe?," *Therapeutic advances in musculoskeletal disease*, vol. 13, 2021.
- [12] H. L. Kim, H. J. Lee, D. R. Lee, B. K. Choi, and S. H. Yang, "Herbal composition LI73014F2 alleviates articular cartilage damage and inflammatory response in monosodium iodoacetate-induced osteoarthritis in rats," *Molecules*, vol. 25, no. 22, p. 5467, 2020.
- [13] Y. F. Lai, P. C. Lin, C. H. Chen, J. L. Chen, and H. T. Hsu, "Current status and changes in pain and activities of daily living in elderly patients with osteoarthritis before and after unilateral total knee replacement surgery," *Journal of Clinical Medicine*, vol. 8, no. 2, p. 221, 2019.
- [14] Y. Wu, Y. Teng, C. Zhang et al., "The ketone body β -hydroxybutyrate alleviates CoCrMo alloy particles induced osteolysis by regulating NLRP3 inflammasome and osteoclast differentiation," *Journal of Nanobiotechnology*, vol. 20, no. 1, p. 120, 2022.
- [15] Y. Wu, F. He, C. Zhang et al., "Melatonin alleviates titanium nanoparticles induced osteolysis via activation of butyrate/GPR109A signaling pathway," *Journal of nanobiotechnology*, vol. 19, no. 1, p. 170, 2021.
- [16] Y. Dai, S. Liu, J. Li et al., "SIRT4 suppresses the inflammatory response and oxidative stress in osteoarthritis," *American Journal of Translational Research*, vol. 12, no. 5, pp. 1965-1975, 2020.
- [17] D. Kang, J. Lee, J. Jung et al., "Selenophosphate synthetase 1 deficiency exacerbates osteoarthritis by dysregulating redox homeostasis," *Nature Communications*, vol. 13, no. 1, p. 779, 2022.
- [18] T. Ohtsuki, O. F. Hatipoglu, K. Asano, J. Inagaki, K. Nishida, and S. Hirohata, "Induction of CEMIP in chondrocytes by inflammatory cytokines: underlying mechanisms and potential involvement in osteoarthritis," *International Journal of Molecular Sciences*, vol. 21, no. 9, p. 3140, 2020.
- [19] F. Liote, R. Champy, M. Moenner, B. Boval-Boizard, and J. Badet, "Elevated angiogenin levels in synovial fluid from patients with inflammatory arthritis and secretion of

- angiogenin by cultured synovial fibroblasts," *Clinical and Experimental Immunology*, vol. 132, no. 1, pp. 163–168, 2003.
- [20] F. Tesche and N. Miosge, "Perlecan in late stages of osteoarthritis of the human knee joint," *Osteoarthritis and Cartilage*, vol. 12, no. 11, pp. 852–862, 2004.
- [21] P. Kongdang, C. Chokchaitaweesuk, S. Tangyuenyong, and S. Ongchai, "Proinflammatory effects of IL-1 β combined with IL-17A promoted cartilage degradation and suppressed genes associated with cartilage matrix synthesis in vitro," *Molecules*, vol. 24, no. 20, p. 3682, 2019.
- [22] Y. Cao, S. Tang, X. Nie et al., "Decreased miR-214-3p activates NF- κ B pathway and aggravates osteoarthritis progression," *eBioMedicine*, vol. 65, p. 103283, 2021.
- [23] M. A. Hossain, M. J. Alam, B. Kim, C. W. Kang, and J. H. Kim, "Ginsenoside-Rb1 prevents bone cartilage destruction through down-regulation of p-Akt, p-P38, and p-P65 signaling in rabbit," *Phytomedicine*, vol. 100, p. 154039, 2022.
- [24] Z. L. Zou, M. H. Sun, W. F. Yin, L. Yang, and L. Y. Kong, "Avascularin suppresses cartilage extracellular matrix degradation and inflammation via TRAF6/MAPK activation," *Phytomedicine*, vol. 91, p. 153657, 2021.
- [25] S. Ni, D. Li, H. Wei, K. S. Miao, and C. Zhuang, "PPAR γ attenuates interleukin-1 β -induced cell apoptosis by inhibiting NOX2/ROS/p38MAPK activation in osteoarthritis chondrocytes," *Oxidative Medicine and Cellular Longevity*, vol. 2021, Article ID 5551338, 15 pages, 2021.
- [26] Y. Yang, P. Shen, T. Yao et al., "Novel role of circRSU1 in the progression of osteoarthritis by adjusting oxidative stress," *Theranostics*, vol. 11, no. 4, pp. 1877–1900, 2021.
- [27] Y. Ohashi, N. Takahashi, K. Terabe et al., "Metabolic reprogramming in chondrocytes to promote mitochondrial respiration reduces downstream features of osteoarthritis," *Scientific Reports*, vol. 11, no. 1, p. 15131, 2021.
- [28] X. Mao, P. Fu, L. Wang, and C. Xiang, "Mitochondria: potential targets for osteoarthritis," *Frontiers in Medicine*, vol. 7, p. 581402, 2020.
- [29] J. A. Bolduc, J. A. Collins, and R. F. Loeser, "Reactive oxygen species, aging and articular cartilage homeostasis," *Free Radical Biology & Medicine*, vol. 132, pp. 73–82, 2019.
- [30] N. B. Tudorachi, E. E. Totu, A. Fiferu et al., "The implication of reactive oxygen species and antioxidants in knee osteoarthritis," *Antioxidants*, vol. 10, no. 6, p. 985, 2021.
- [31] T. Jayakumar, P. Saravana Bhavan, and J. R. Sheu, "Molecular targets of natural products for chondroprotection in destructive joint diseases," *International Journal of Molecular Sciences*, vol. 21, no. 14, p. 4931, 2020.
- [32] Z. Shen, Q. Chen, T. Jin et al., "Theaflavin 3,3'-digallate reverses the downregulation of connexin 43 and autophagy induced by high glucose via AMPK activation in cardiomyocytes," *Journal of Cellular Physiology*, vol. 234, no. 10, pp. 17999–18016, 2019.
- [33] Y. Wu, F. Jin, Y. Wang et al., "In vitro and in vivo anti-inflammatory effects of theaflavin-3, 3'-digallate on lipopolysaccharide-induced inflammation," *European Journal of Pharmacology*, vol. 794, pp. 52–60, 2017.
- [34] Z. Ai, Y. Wu, M. Yu, J. Li, and S. Li, "Theaflavin-3, 3'-digallate suppresses RANKL-induced osteoclastogenesis and attenuates ovariectomy-induced bone loss in mice," *Frontiers in Pharmacology*, vol. 11, p. 803, 2020.
- [35] W. Liu and J. Li, "Theaflavin-3, 3'-digallate attenuates rheumatoid inflammation in mice through the nuclear factor- κ B and MAPK pathways," *Archivum Immunologiae et Therapiae Experimentalis (Warsz)*, vol. 67, no. 3, pp. 153–160, 2019.
- [36] R. Wang, J. Li, X. Xu et al., "Andrographolide attenuates synovial inflammation of osteoarthritis by interacting with tumor necrosis factor receptor 2 trafficking in a rat model," *J Orthop Translat.*, vol. 29, pp. 89–99, 2021.
- [37] L. Zhang and C. Wen, "Osteocyte dysfunction in joint homeostasis and osteoarthritis," *International Journal of Molecular Sciences*, vol. 22, no. 12, p. 6522, 2021.
- [38] C. Ruiz-Fernandez, M. Gonzalez-Rodriguez, V. Francisco et al., "Monomeric C reactive protein (mCRP) regulates inflammatory responses in human and mouse chondrocytes," *Laboratory Investigation*, vol. 101, no. 12, pp. 1550–1560, 2021.
- [39] T. S. Ramasamy, Y. M. Yee, and I. M. Khan, "Chondrocyte aging: the molecular determinants and therapeutic opportunities," *Frontiers in Cell and Development Biology*, vol. 9, p. 625497, 2021.
- [40] H. Lee, X. Zhao, Y. O. Son, and S. Yang, "Therapeutic single compounds for osteoarthritis treatment," *Pharmaceuticals (Basel)*, vol. 14, no. 2, p. 131, 2021.
- [41] W. San Cheang, C. Yuen Ngai, Y. Yen Tam et al., "Black tea protects against hypertension-associated endothelial dysfunction through alleviation of endoplasmic reticulum stress," *Scientific Reports*, vol. 5, no. 1, p. 10340, 2015.
- [42] K. N. Reed, G. Wilson, A. Pearsall, and V. I. Grishko, "The role of mitochondrial reactive oxygen species in cartilage matrix destruction," *Molecular and Cellular Biochemistry*, vol. 397, no. 1-2, pp. 195–201, 2014.
- [43] F. J. Blanco, I. Rego, and C. Ruiz-Romero, "The role of mitochondria in osteoarthritis," *Nature Reviews Rheumatology*, vol. 7, no. 3, pp. 161–169, 2011.
- [44] M. Yamamoto, T. W. Kensler, and H. Motohashi, "The KEAP1-NRF2 system: a thiol-based sensor-effector apparatus for maintaining redox homeostasis," *Physiological Reviews*, vol. 98, no. 3, pp. 1169–1203, 2018.
- [45] A. S. Marchev, P. A. Dimitrova, A. J. Burns, R. V. Kostov, A. T. Dinkova-Kostova, and M. I. Georgiev, "Oxidative stress and chronic inflammation in osteoarthritis: can NRF2 counteract these partners in crime?," *Annals of the New York Academy of Sciences*, vol. 1401, no. 1, pp. 114–135, 2017.
- [46] T. Suzuki and M. Yamamoto, "Molecular basis of the Keap1-Nrf2 system," *Free Radical Biology & Medicine*, vol. 88, pp. 93–100, 2015.
- [47] K. Taguchi and M. Yamamoto, "The KEAP1-NRF2 system as a molecular target of cancer treatment," *Cancers*, vol. 13, no. 1, 2021.
- [48] M. Schafer and S. Werner, "Transcriptional control of wound repair," *Annual Review of Cell and Developmental Biology*, vol. 23, no. 1, pp. 69–92, 2007.
- [49] H. Wang, X. M. Zhou, L. Y. Wu et al., "Aucubin alleviates oxidative stress and inflammation via Nrf2-mediated signaling activity in experimental traumatic brain injury," *Journal of Neuroinflammation*, vol. 17, no. 1, p. 188, 2020.
- [50] M. C. Lu, J. A. Ji, Z. Y. Jiang, and Q. D. You, "The Keap1-Nrf2-ARE pathway as a potential preventive and therapeutic target: an update," *Medicinal Research Reviews*, vol. 36, no. 5, pp. 924–963, 2016.
- [51] D. Cai, S. Yin, J. Yang, Q. Jiang, and W. Cao, "Histone deacetylase inhibition activates Nrf 2 and protects against

- osteoarthritis,” *Arthritis Research & Therapy*, vol. 17, no. 1, p. 269, 2015.
- [52] T. N. Crotti, M. D. Smith, H. Weedon et al., “Receptor activator NF-kappaB ligand (RANKL) expression in synovial tissue from patients with rheumatoid arthritis, spondyloarthropathy, osteoarthritis, and from normal patients: semiquantitative and quantitative analysis,” *Annals of the Rheumatic Diseases*, vol. 61, no. 12, pp. 1047–1054, 2002.
- [53] A. K. Roshak, J. F. Callahan, and S. M. Blake, “Small-molecule inhibitors of NF-kappa B for the treatment of inflammatory joint disease,” *Current Opinion in Pharmacology*, vol. 2, no. 3, pp. 316–321, 2002.
- [54] I. E. Wertz and V. M. Dixit, “Signaling to NF-kappaB: regulation by ubiquitination,” *Cold Spring Harbor Perspectives in Biology*, vol. 2, no. 3, article a003350, 2010.
- [55] L. W. Huang, T. C. Huang, Y. C. Hu et al., “S-equol protects chondrocytes against sodium nitroprusside-caused matrix loss and apoptosis through activating PI3K/Akt pathway,” *International Journal of Molecular Sciences*, vol. 22, no. 13, p. 7054, 2021.
- [56] K. Xu, Y. He, S. A. A. Moqbel, X. Zhou, L. Wu, and J. Bao, “SIRT3 ameliorates osteoarthritis via regulating chondrocyte autophagy and apoptosis through the PI3K/Akt/mTOR pathway,” *International Journal of Biological Macromolecules*, vol. 175, pp. 351–360, 2021.
- [57] H. Lu, C. Fu, S. Kong et al., “Maltol prevents the progression of osteoarthritis by targeting PI3K/Akt/NF- κ B pathway: in vitro and in vivo studies,” *Journal of Cellular and Molecular Medicine*, vol. 25, no. 1, pp. 499–509, 2021.
- [58] Y. Q. Qian, Z. H. Feng, X. B. Li et al., “Downregulating PI3K/Akt/NF- κ B signaling with allicin for ameliorating the progression of osteoarthritis: in vitro and vivo studies,” *Food & Function*, vol. 9, no. 9, pp. 4865–4875, 2018.
- [59] Y. Guo, Z. Min, C. Jiang et al., “Downregulation of HS6ST2 by miR-23b-3p enhances matrix degradation through p38 MAPK pathway in osteoarthritis,” *Cell Death & Disease*, vol. 9, no. 6, p. 699, 2018.
- [60] D. H. Rosenzweig, T. M. Quinn, and L. Haglund, “Low-frequency high-magnitude mechanical strain of articular chondrocytes activates p 38 MAPK and induces phenotypic changes associated with osteoarthritis and pain,” *International Journal of Molecular Sciences*, vol. 15, no. 8, pp. 14427–14441, 2014.
- [61] Y. Xu, Y. Gu, W. Ji, and Q. Dong, “Activation of the extracellular-signal-regulated kinase (ERK)/c-Jun N-terminal kinase (JNK) signal pathway and osteogenic factors in subchondral bone of patients with knee osteoarthritis,” *Annals of Translational Medicine*, vol. 9, no. 8, p. 663, 2021.
- [62] S. M. Hou, P. C. Chen, C. M. Lin, M. L. Fang, M. C. Chi, and J. F. Liu, “CXCL1 contributes to IL-6 expression in osteoarthritis and rheumatoid arthritis synovial fibroblasts by CXCR2, c-Raf, MAPK, and AP-1 pathway,” *Arthritis Research & Therapy*, vol. 22, no. 1, p. 251, 2020.
- [63] P. Lepetsos, K. A. Papavassiliou, and A. G. Papavassiliou, “Redox and NF- κ B signaling in osteoarthritis,” *Free Radical Biology & Medicine*, vol. 132, pp. 90–100, 2019.
- [64] J. D. Wardyn, A. H. Ponsford, and C. M. Sanderson, “Dissecting molecular cross-talk between Nrf2 and NF- κ B response pathways,” *Biochemical Society Transactions*, vol. 43, no. 4, pp. 621–626, 2015.
- [65] M. J. Alcaraz and M. L. Ferrandiz, “Relevance of Nrf2 and heme oxygenase-1 in articular diseases,” *Free Radical Biology & Medicine*, vol. 157, pp. 83–93, 2020.
- [66] F. Rousset, F. Hazane-Puch, C. Pinosa et al., “IL-1beta mediates MMP secretion and IL-1beta neosynthesis via upregulation of p22^{phox} and NOX4 activity in human articular chondrocytes,” *Osteoarthritis and Cartilage*, vol. 23, no. 11, pp. 1972–1980, 2015.

Research Article

Mulberrin Confers Protection against Doxorubicin-Induced Cardiotoxicity via Regulating AKT Signaling Pathways in Mice

Peng Ye ¹, Wen-Lan Li ², Long-Tang Bao ³, and Wei Ke ⁴

¹Department of Pharmacy, Renmin Hospital of Wuhan University, Wuhan 430060, China

²Department of Anesthesiology, Renmin Hospital of Wuhan University, Wuhan, Hubei 430060, China

³Day-Care Unit, The Affiliated Hospital of Inner Mongolia Medical University, Hohhot 010050, China

⁴Department of Neurology, Renmin Hospital of Wuhan University, Wuhan 430060, China

Correspondence should be addressed to Long-Tang Bao; fyblt@163.com and Wei Ke; vigarmale2021@126.com

Received 29 March 2022; Accepted 13 June 2022; Published 7 July 2022

Academic Editor: Felipe L. de Oliveira

Copyright © 2022 Peng Ye et al. This is an open access article distributed under the Creative Commons Attribution License, which permits unrestricted use, distribution, and reproduction in any medium, provided the original work is properly cited.

Doxorubicin (DOX) is an antitumor anthracycline, but its clinical use was largely limited by its cardiac toxicity. DOX-induced oxidative damage and cardiomyocyte loss have been recognized as the potential causative mechanisms of this cardiac toxicity. Growing interests are raised on mulberrin (Mul) for its wide spectrum of biological activities, including antioxidative and anti-inflammatory properties. The aim of this study was to investigate the effect of Mul on DOX-induced heart injury and to clarify the underlying mechanism. Mice were given daily 60 mg/kg of Mul via gavage for 10 days. Mice received an intraperitoneal injection of DOX to mimic the model of DOX-related acute cardiac injury at the seventh day of Mul treatment. Mul-treated mice had an attenuated cardiac injured response and improved cardiac function after DOX injection. DOX-induced oxidative damage, inflammation accumulation, and myocardial apoptosis were largely attenuated by the treatment of Mul. Activated protein kinase B (AKT) activation was essential for the protective effects of Mul against DOX-induced cardiac toxicity, and AKT inactivation abolished Mul-mediated protective effects against DOX cardiotoxicity. In conclusion, Mul treatment attenuated DOX-induced cardiac toxicity via activation of the AKT signaling pathway. Mul might be a promising therapeutic agent against DOX-induced cardiac toxicity.

1. Introduction

Doxorubicin (DOX) is a widely used chemotherapy drug. This drug results in cardiotoxicity, which is manifested as a progressive and irreversible cardiomyopathy [1]. The incidence of DOX-induced cardiac injury ranges from 11% to 18%, as estimated by previous studies [2, 3]. The onset of DOX-induced cardiotoxicity can be acute, occurring within 2-3 days or be chronic until several months after the end of chemotherapy [3]. Current studies pay more attention to DOX-related chronic cardiomyopathy but lose sight of the clinical importance of DOX-induced acute cardiotoxicity. Several mechanisms are involved in the process of DOX-related toxicities including mitochondrial dysfunction, oxidative stress, inhibition of autophagy, and myocardial apoptosis [4]. Currently, there are no molecules with an actual cardioprotective effect on DOX-induced acute cardio-

toxicity. It is therefore important to find an approach for preventing DOX-induced cardiotoxicity in the clinic.

DOX treatment leads to the production of free oxygen radicals and antioxidant deficiency, which causes oxidative stress in the heart [1, 4]. Oxidative stress has been established as a potential causative mechanism [5, 6]. Overexpression of antioxidant enzymes can ameliorate DOX-induced cardiotoxicity in mice [7, 8]. DOX-dependent oxidative damage induced the release of cytochrome C and subsequent activation of caspase 3, causing myocardial apoptosis [9]. The attenuation of DOX-induced myocardial apoptosis could protect against DOX-induced cardiotoxicity [10]. These findings highlighted the importance of finding a promising therapeutic strategy to inhibit oxidative damage and apoptotic cell death in DOX-related cardiotoxicity.

Mulberrin (Mul) is a natural product of *Ramulus mori* and has potent biological abilities, including antioxidant,

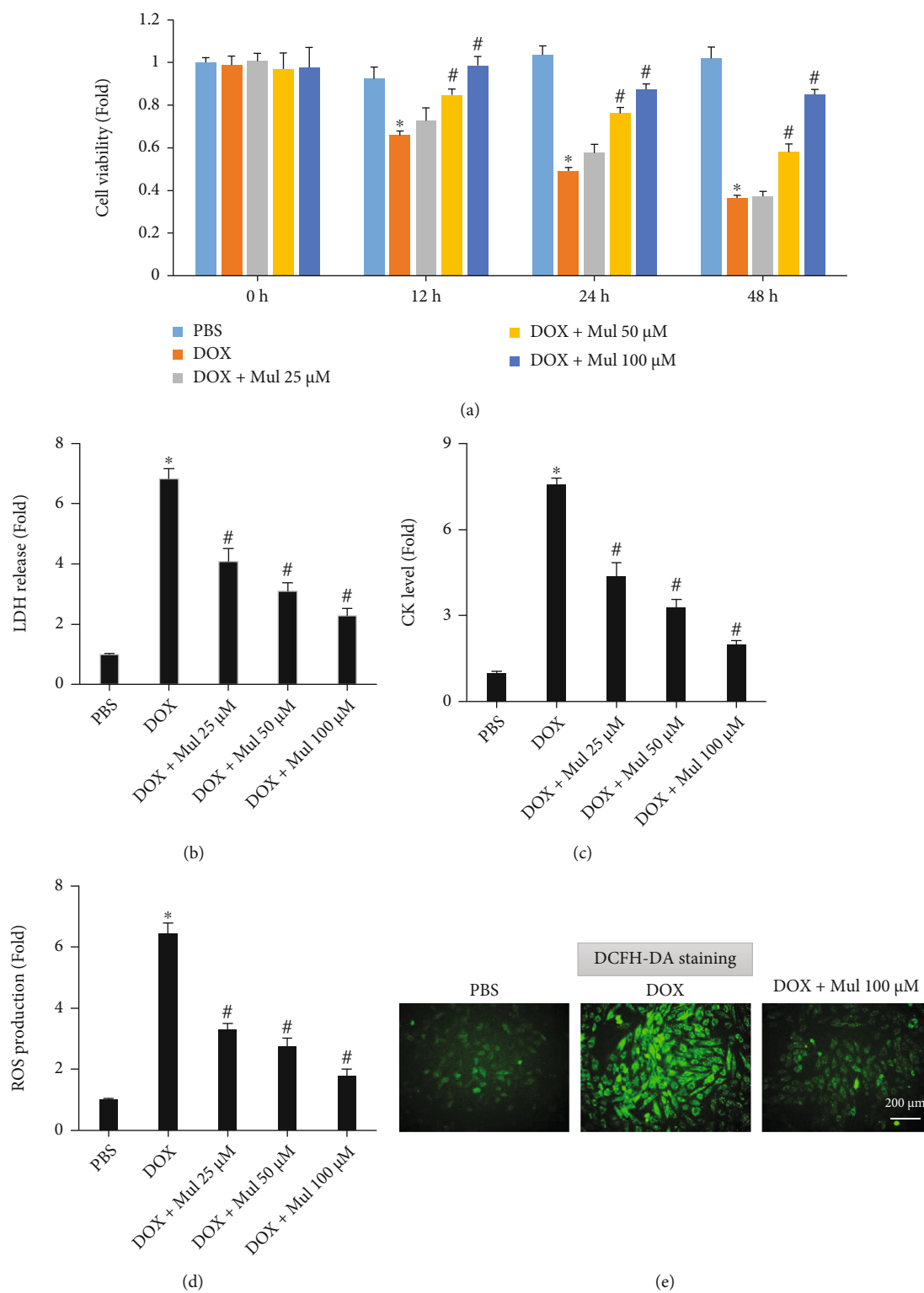


FIGURE 1: Continued.

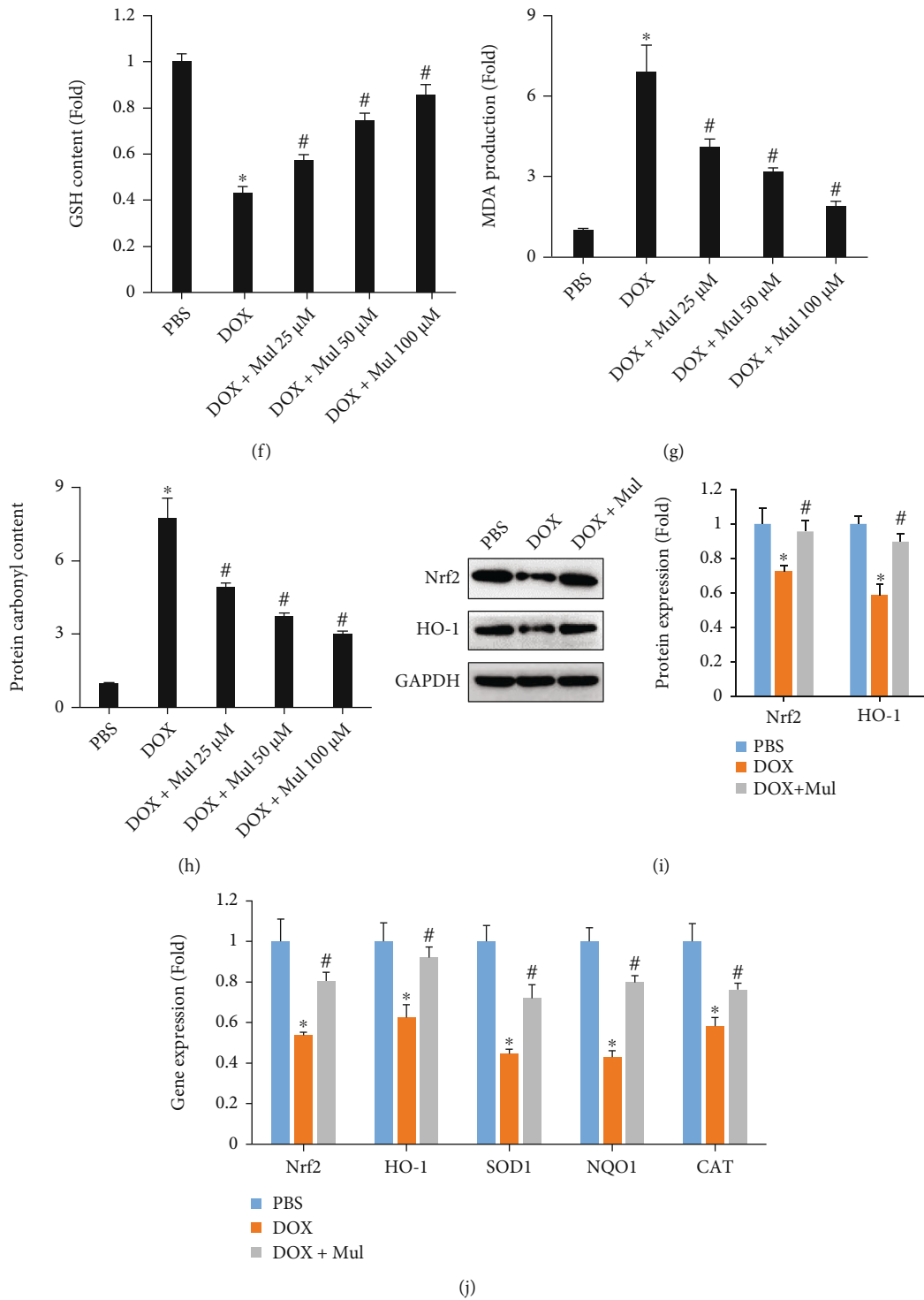


FIGURE 1: Mulberrin-suppressed DOX-induced ROS generation and oxidative stress in cardiomyocytes. Cell viability (a) and the release of LDH (b) and CK (c) were performed to estimate the toxic effects on cells in response to DOX. The ROS level (d, e), GSH content (f), MDA content (g), and protein carbonyl content (h) in the DOX-treated cells were detected to reflect oxidative damage caused by DOX. Nrf2 and HO-1 protein (i) were detected in the indicated groups. The mRNA levels of Nrf2 downstream gene products (j) were also quantified. Data are presented as mean \pm SEM. $n = 5 - 6$ for each group at each time point. * $P < 0.05$ compared with the PBS group; # $P < 0.05$ compared with DOX alone.

anti-inflammatory, antifibrotic effects [11, 12]. Cao et al. found that Mul attenuated Parkinson's disease by activating the β -catenin signaling pathway in mice [13]. Mul reduced

spinal cord injury-induced apoptosis and inflammation and attenuated hepatic fibrosis by targeting nuclear factor E2-related factor 2 (Nrf2) in mice [11, 12]. Mul significantly

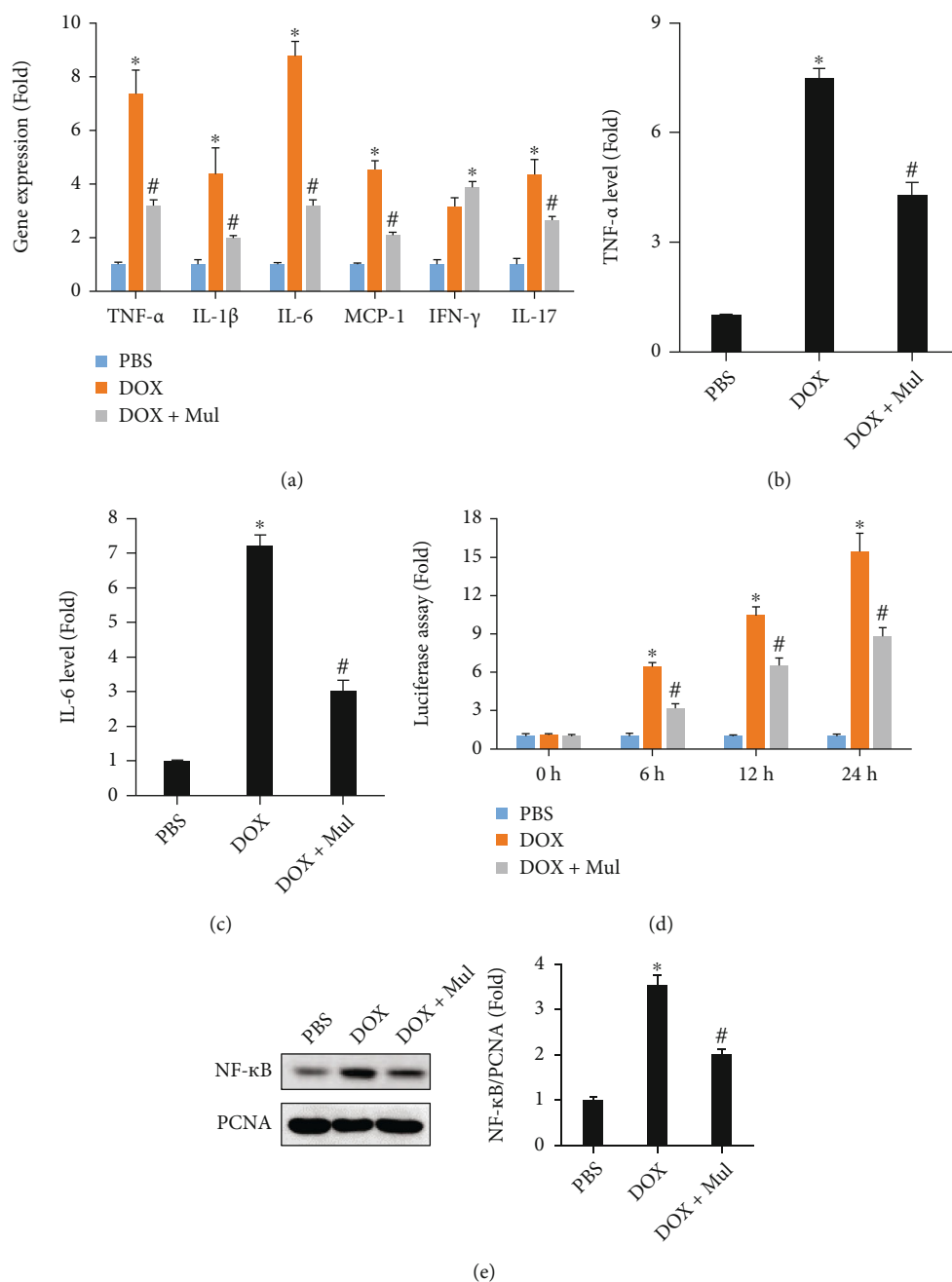


FIGURE 2: Mulberrin at the dose of 100 μ M attenuated the upregulation of inflammatory cytokines induced by DOX in vitro. The mRNA levels of inflammatory factors (a) were examined by qRT-PCR. The protein expression of TNF- α (b) and IL-6 (c) were detected by ELISA. Luciferase assay (d) was used to reflect NF- κ B transactivation in vitro. The nuclear accumulation of NF- κ B protein (e) was detected in the indicated groups. Data are presented as mean \pm SEM. $n = 5$ for each group. * $P < 0.05$ compared with the PBS group; # $P < 0.05$ compared with DOX alone.

reduced blood glucose and alleviated the metabolic syndrome in rodents [14]. Based on these reports, we speculated that Mul might protect against DOX-related cardiac injury in mice. Therefore, we designed this study to explore the effect of Mul treatment on DOX-derived cardiotoxicity.

2. Materials and Methods

2.1. Materials. Mul (#62949-79-5, purity $\geq 95\%$ as detected by HPLC) was provided by MedChemExpress (Shanghai,

China), and this reagent was dissolved into 0.1% dimethyl sulfoxide (DMSO). DOX and the protein kinase B (AKT) inhibitor were purchased from Sigma-Aldrich (St. Louis, USA). DMEM and fetal bovine serum (FBS) were provided by Thermo Fisher (Shanghai, China).

2.2. Animals. All animal experimental procedures were approved by the Institutional Animal Care and Use Committee at Renmin Hospital of Wuhan University (Wuhan, China). C57BL/6 male mice with 8-9 weeks of age (body

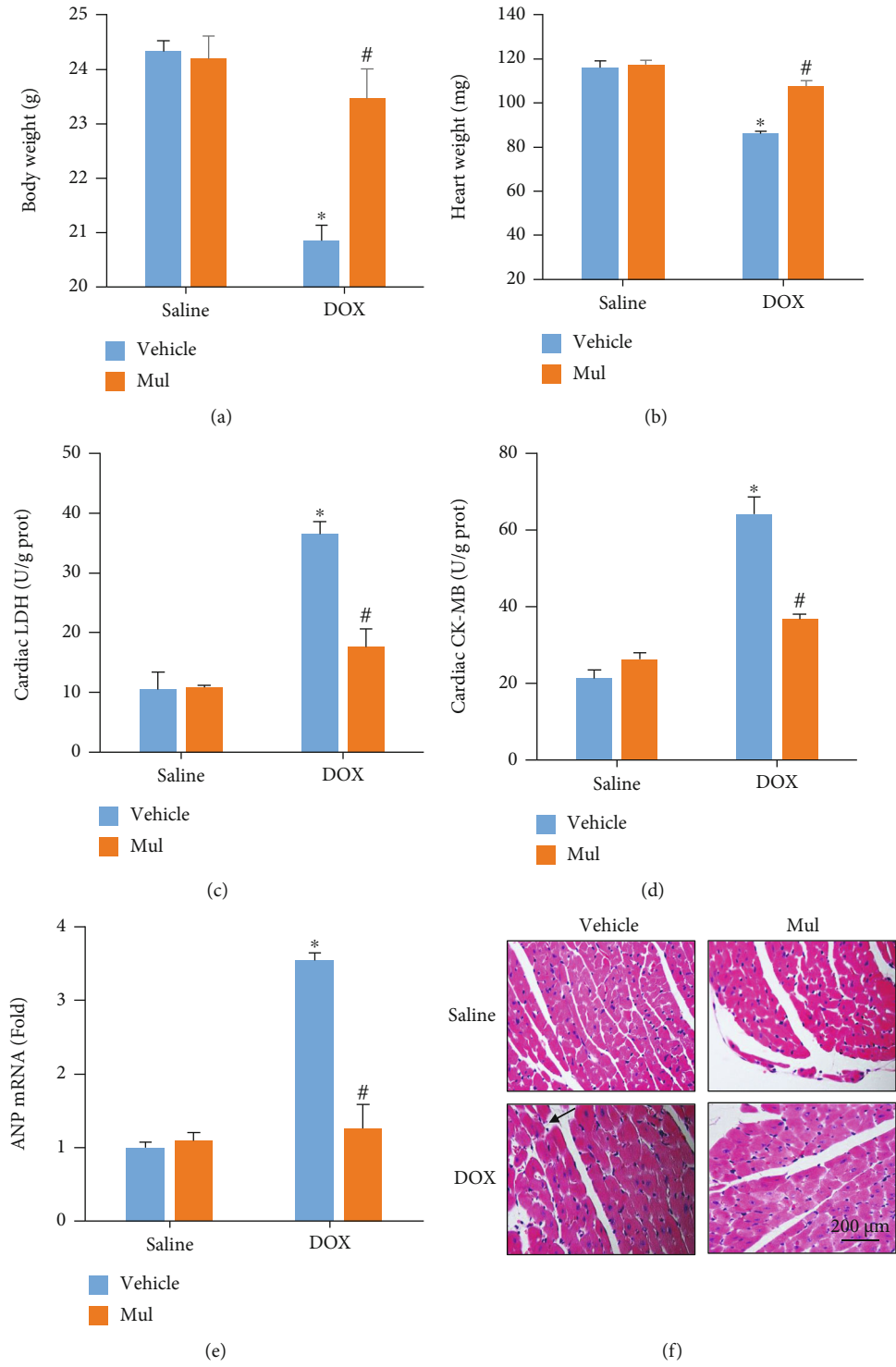


FIGURE 3: Continued.

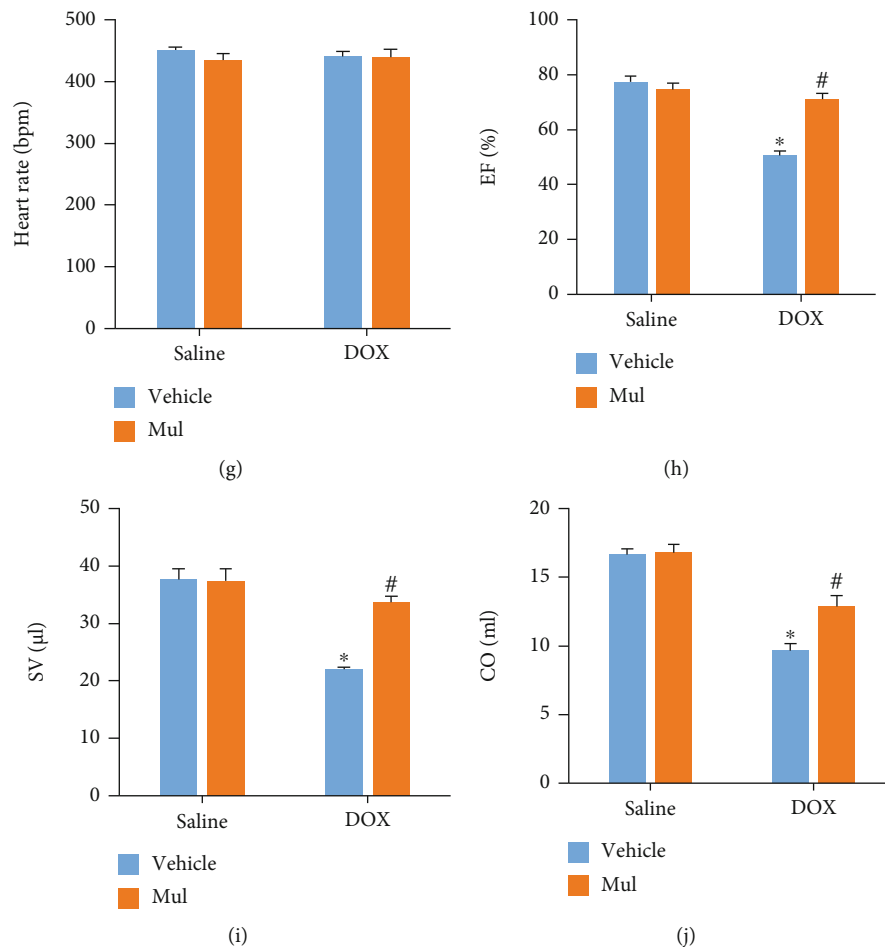


FIGURE 3: Mulberrin treatment prevented the DOX-induced cardiac dysfunction in mice. Body weight (a), heart weight (b), and myocardial LDH and CK (c, d) content were detected to evaluate DOX-induced cardiac injury. The mRNA level of ANP (e) was examined by qRT-PCR. H&E staining (f). Black line indicates myofibrillar disarrangement. Cardiac function including heart rate (g), ejection fraction (h), stroke volume (i), and cardiac output (j) was detected using an invasive hemodynamic monitoring. Data are presented as mean \pm SEM. For (a, b), $n = 10$ each group; for (c–j), $n = 6$ each group. * $P < 0.05$ compared with the saline group; # $P < 0.05$ compared with DOX alone.

weight: 21–24 g) were purchased from HFK Bioscience (Beijing, China) and housed at a standard temperature ($24 \pm 2^\circ\text{C}$) and humidity (50–60%) under a 12 h/12 h photoperiod. Mice were orally given 60 mg/kg Mul by gavage for 10 days. At the seventh day of Mul treatment, mice received an intraperitoneal injection of DOX (20 mg/kg) to mimic the model of DOX-related acute cardiac injury. The dose of Mul was selected according to a previous study [11]. Normal saline was used instead of Mul in control groups. Three days after DOX or normal saline injection, mice were anaesthetized and sacrificed to evaluate DOX-related cardiac injury.

The adeno-associated virus 9 (AAV9) vectors carrying protein kinase B- (AKT-) dominant negative mutant (dnAKT) and GFP were provided by Hanbio Biotechnology Co. (Shanghai, China). To overexpress this mutant in the heart, mice were given a single injection of AAV9-dnAKT at a dose of 1×10^{11} particles per mouse via tail vein [15]. All mice were divided into 6 groups: saline+Con, DOX+Con, DOX+Mul+Con, saline+dnAKT, DOX+dnAKT, and DOX+Mul+dnAKT groups ($n = 8$ for each group). Four weeks after AAV9-dnAKT infection, these mice received

20 mg/kg DOX to mimic DOX-related acute cardiac injury. Three days after DOX or normal saline injection, all mice were sacrificed to the phenotypes.

2.3. Invasive Hemodynamics. Invasive hemodynamic monitoring was conducted in mice anesthetized with 2% isoflurane by a 1.0F microtip catheter (PVR 1045), which was connected to a Millar Pressure-Volume System (MPVS-400; Millar Instruments). These data were recorded and analyzed by a PVAN analysis software.

2.4. Cell Culture and Treatment. H9c2 cardiomyocytes were purchased from the American Type Culture Collection (ATCC) and cultured in DMEM supplemented with 10% FBS. Only H9c2 cells at 3–5 passages were used for this experiment. At approximately 75% confluence, these cells were starved with a serum-free DMEM medium for 24 hours. After that, H9c2 cardiomyocytes were incubated in DMEM medium containing PBS, DOX ($1 \mu\text{M}$), DOX ($1 \mu\text{M}$) plus $25 \mu\text{M}$ Mul, DOX ($1 \mu\text{M}$) plus $50 \mu\text{M}$ Mul, and DOX ($1 \mu\text{M}$) plus $100 \mu\text{M}$ Mul. Cells were harvested at 0 h,

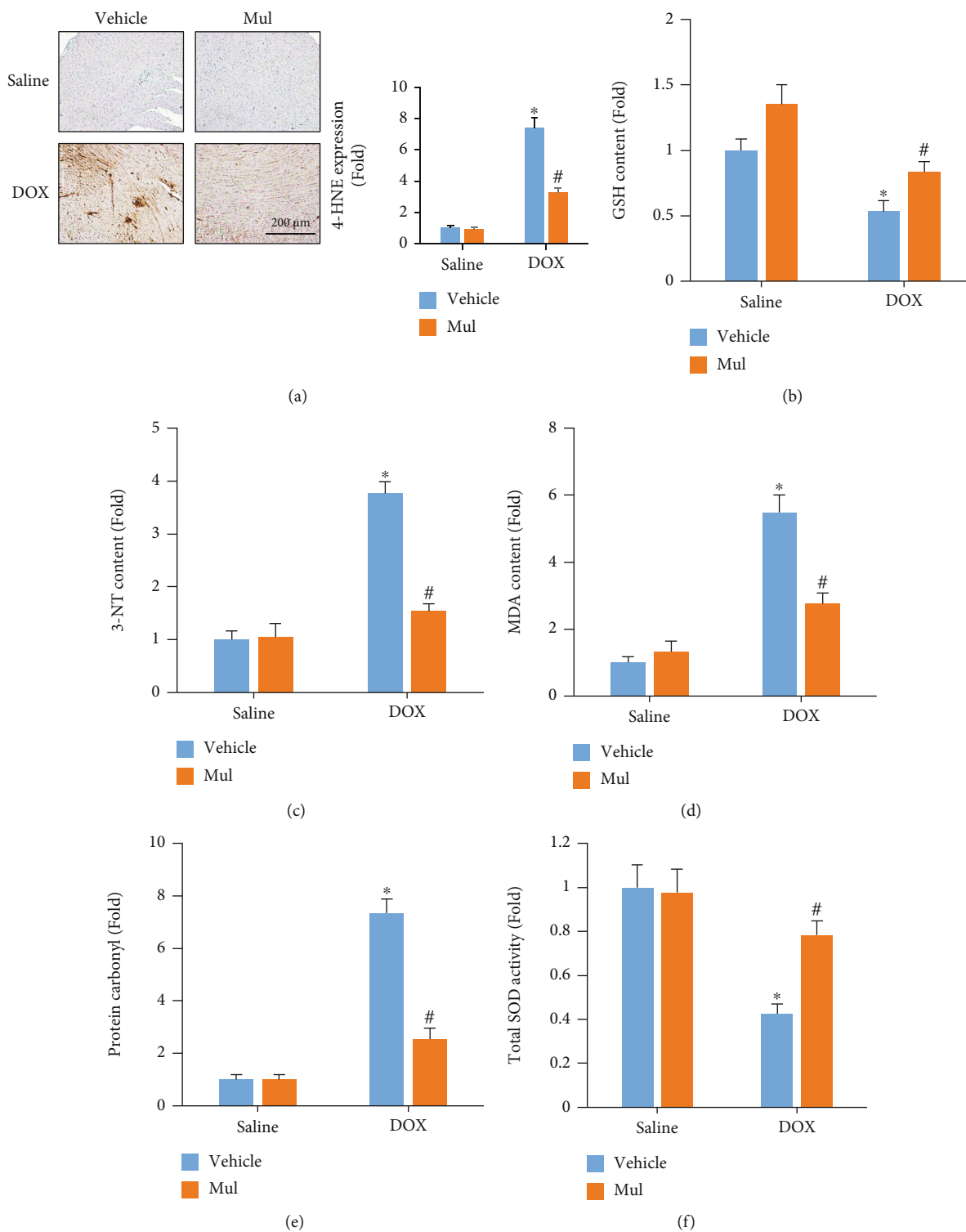


FIGURE 4: Continued.

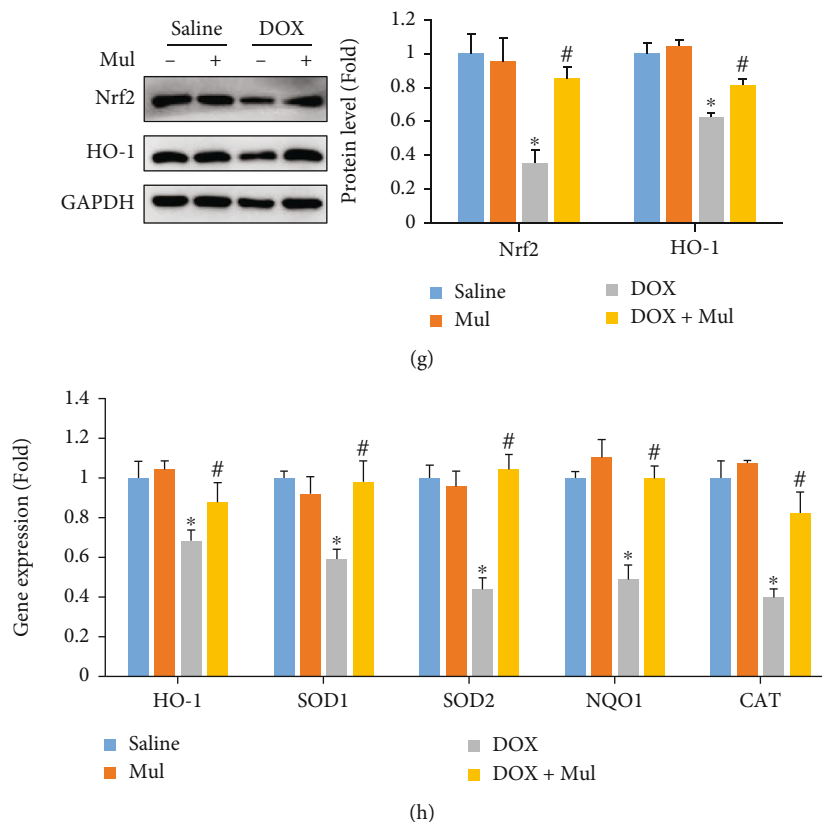


FIGURE 4: Mulberrin treatment prevented the DOX-induced oxidative damage in mice. 4-Hydroxynonenal (4-HNE) immunohistochemistry of indicated groups (a). Accumulation of the oxidative stress markers, including GSH content (b), 3-NT (c), MDA content (d), and protein carbonyl content (e), was quantified by the commercial kits. Total SOD activity (f) was also detected in DOX-treated mice. Nrf2 and HO-1 protein (g) were detected in the indicated groups. The mRNA levels of Nrf2 downstream gene products (h) were also quantified. Data are presented as mean \pm SEM. $n = 6$ for each group. * $P < 0.05$ compared with the saline group; # $P < 0.05$ compared with DOX alone.

12 h, 24 h, and 48 h. Cell viability was examined using the Cell Counting Kit-8 assay (CCK-8, #HY-K0301, MedChem-Express) according to the manufacturer's instructions. To inhibit the activation of AKT, H9c2 cardiomyocytes were pretreated with a specific AKT inhibitor ($1 \mu\text{M}$) for 24 h.

H9c2 cardiomyocytes were cultured in a six-well plate. After serum starvation for 24 h, H9c2 cells were electrotransfected with nuclear factor kappa-B- (NF- κB -) luc ($0.03 \mu\text{g}$) with a Neon[®] Transfection System (pulse width: 20 ms, pulse voltage: 1700 V). After that, these cells were treated with DOX and Mul ($100 \mu\text{M}$) for 48 h. At the end of this experiment, cells were lysed in $100 \mu\text{l}$ of a cell lysis reagent (Promega, Madison, USA). Luciferase activity was detected with a Promega Luciferase assay reagent (#E1500).

2.5. Western Blotting and Quantitative Real-Time PCR. Total protein was extracted from mouse hearts and cultured cells using the RIPA Lysis Buffer [10]. NE-PER[™] Nuclear and Cytoplasmic Extraction Reagent (#78833, Invitrogen, Carlsbad, CA, USA) was used to separate nuclear proteins. These proteins were separated by electrophoresis and transferred to nitrocellulose membranes and incubated with several primary antibodies against Nrf2 (#ab62352, 1:1000, Abcam, Cambridge, MA, USA), heme oxygenase-1 (HO-1, Abcam, #ab52947, 1:1000), GAPDH (Abcam, #ab9485, 1:1000),

NF- κB p65 (Abcam, #ab207297, 1:1000), anti-NF- κB p65 phospho S536 (Abcam, #ab239882, 1:1000), inhibitor of kappa B alpha ($\text{I}\kappa\text{B}\alpha$, Abcam, #ab76429, 1:2000), phosphorylated- $\text{I}\kappa\text{B}\alpha$ (Abcam, #ab133462, 1:2000), glycogen synthase kinase 3β (GSK3 β , Abcam, #ab32391, 1:1000), phosphorylated-GSK3 β (Abcam, #ab75814, 1:1000), Bax (Abcam, #ab32503, 1:1000), Bcl-2 (Abcam, #ab182858, 1:1000), mammalian target of rapamycin (mTOR Abcam, #ab32028, 1:1000), and phosphorylated-mTOR (Abcam, #ab109268, 1:1000). After that, the membranes were then hybridized with HRP-conjugated secondary antibodies (Proteintech; 1:5000) for 2 h at room temperature. The membranes were scanned with the Quant LAS 500 system.

Total mRNA was extracted from heart tissues with a TRIzol reagent (Invitrogen, Carlsbad, USA). The isolated RNA was reversely transcribed into complementary DNA using Advantage[®] RT-for-PCR Kit (#639505, Takara Bio, Kusatsu, Shiga, Japan). Quantitative PCR was conducted with an iQ5 Multi-Color Real-Time PCR Detection System (Bio-Rad, CA, USA) using the SYBR Green Real-Time PCR Master Mix kit (#QPK-201, Takara, Dalian, China).

2.6. Biochemical Analyses. Heart tissues were homogenized in iced PBS, and homogenates were centrifuged at 4800 g for 20 minutes to isolate the supernatant. Myocardial lactate

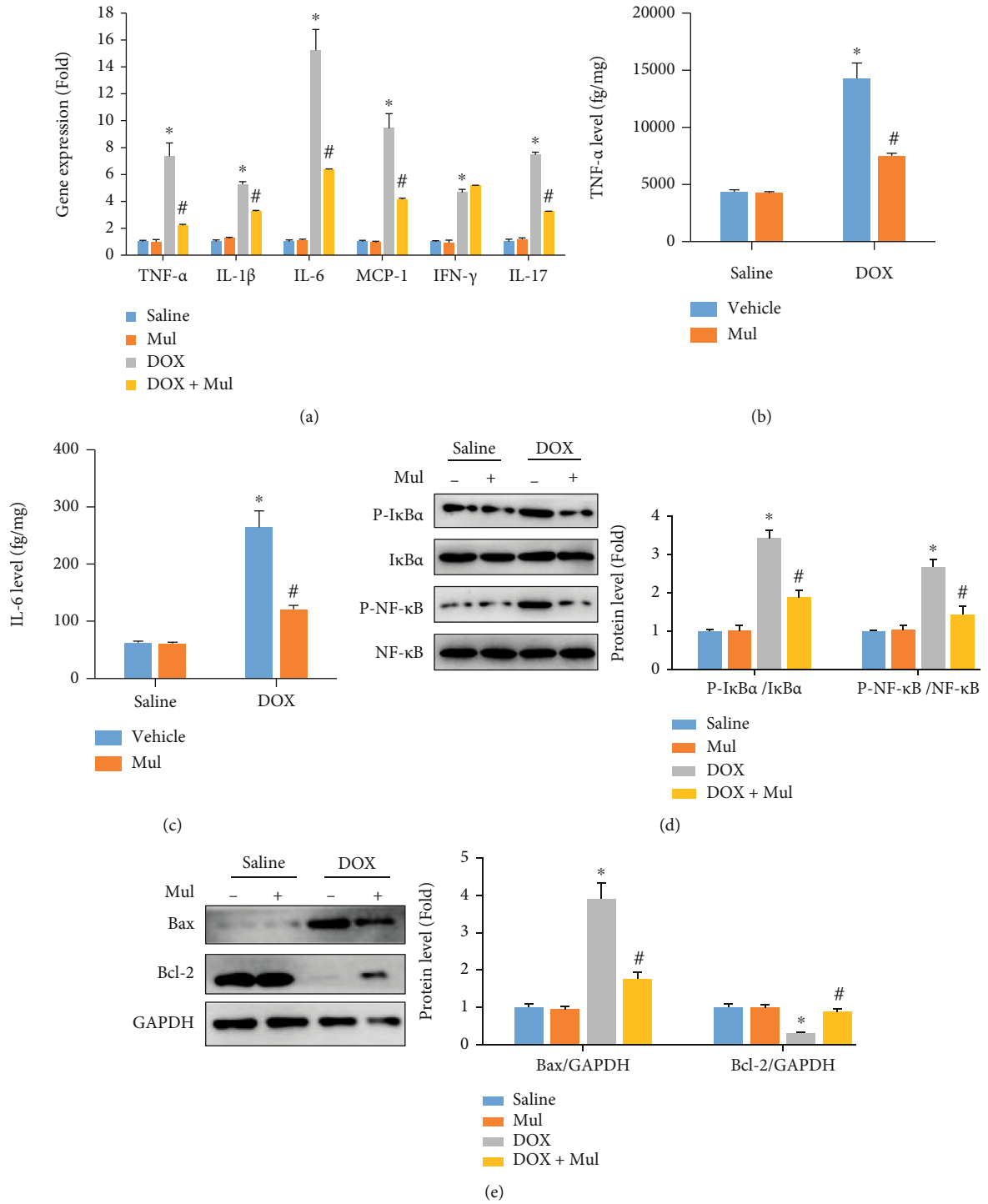


FIGURE 5: Continued.

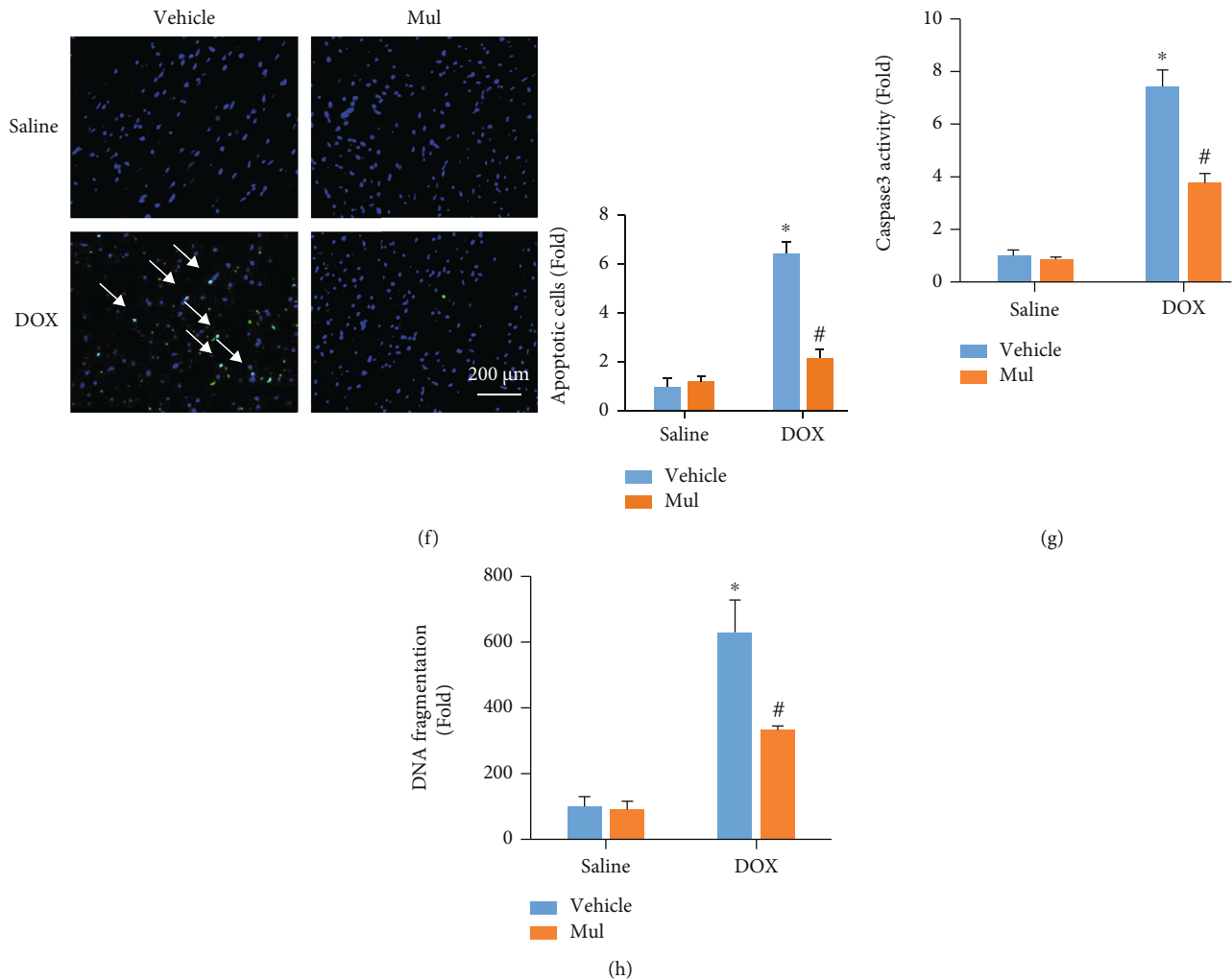


FIGURE 5: Mulberrin attenuated the expression of inflammatory cytokines in DOX-treated mice. The mRNA levels of inflammatory factors (a) were also quantified. The protein expression of TNF- α (b) and IL-6 (c) were detected by ELISA. The phosphorylation of NF- κ B and I κ B α (d) was detected in the indicated groups. The protein expression of Bax and Bcl-2 (e) was detected by western blotting. Myocardial apoptosis were evaluated by the TUNEL staining (f), caspase 3 activity (g), and DNA fragmentation test (h). Data are presented as mean \pm SEM. $n = 6$ for each group. * $P < 0.05$ compared with the saline group; # $P < 0.05$ compared with DOX alone.

dehydrogenase (LDH) and creatine kinase- (CK-) MB were detected by using the commercial kits. The mouse LDH ELISA kit was provided by CUSABIO (#CSB-E17733m, Wuhan, China). The CK-MB assay kit (#A032-1-1) was obtained from the Nanjing Jiancheng Biological Engineering Research Institute.

The levels of glutathione (GSH), malondialdehyde (MDA), 3-nitrotyrosine (3-NT), protein carbonyl, total SOD activity, tumor necrosis factor- α (TNF- α) level, and interleukin- (IL-) 6 level were determined using commercial kits based on the manufacturer's instructions. GSH assay kit (#A061), MDA assay kit (A003-1-2), and the total SOD activity (A001-3-2) were provided by the Nanjing Jiancheng Institute of Biotechnology (Nanjing, China). 3-NT competitive ELISA (#ab113848) was obtained from Abcam. The protein carbonyl ELISA kit was provided by Abnova (#KA6397, Taipei, Taiwan). The TNF- α Mouse ELISA kit (#BMS607-3TEN) was provided by Invitrogen, and the IL-6 (mouse)

ELISA kit was provided by Biovision (#K4795). All assays were performed in triplicate.

2.7. Reactive Oxygen Species Production Measurements and Immunohistochemistry. The reactive oxygen species (ROS) was measured with 2',7'-dichlorofluorescein-diacetate (DCFH-DA, Beyotime Institute) staining. H9c2 cells were incubated with DCFH-DA (10 μ M) for 60 min in 37°C, and immunofluorescence was detected via a fluorescence microplate reader and an Olympus IX53 fluorescence microscope. To detect myocardial lipid peroxidation products, 4-hydroxynonenal (4-HNE) immunohistochemistry was performed. Prepared heart sections were incubated with an anti-4-HNE antibody (1:200, #ab48506, Abcam) at 4°C overnight, then with secondary antibodies at 37°C for 1 h, and detected with 3,3'-diaminobenzidine, and sections were counterstained with hematoxylin. Immunohistochemistry images were captured via Aperio VERSA 8 (Leica

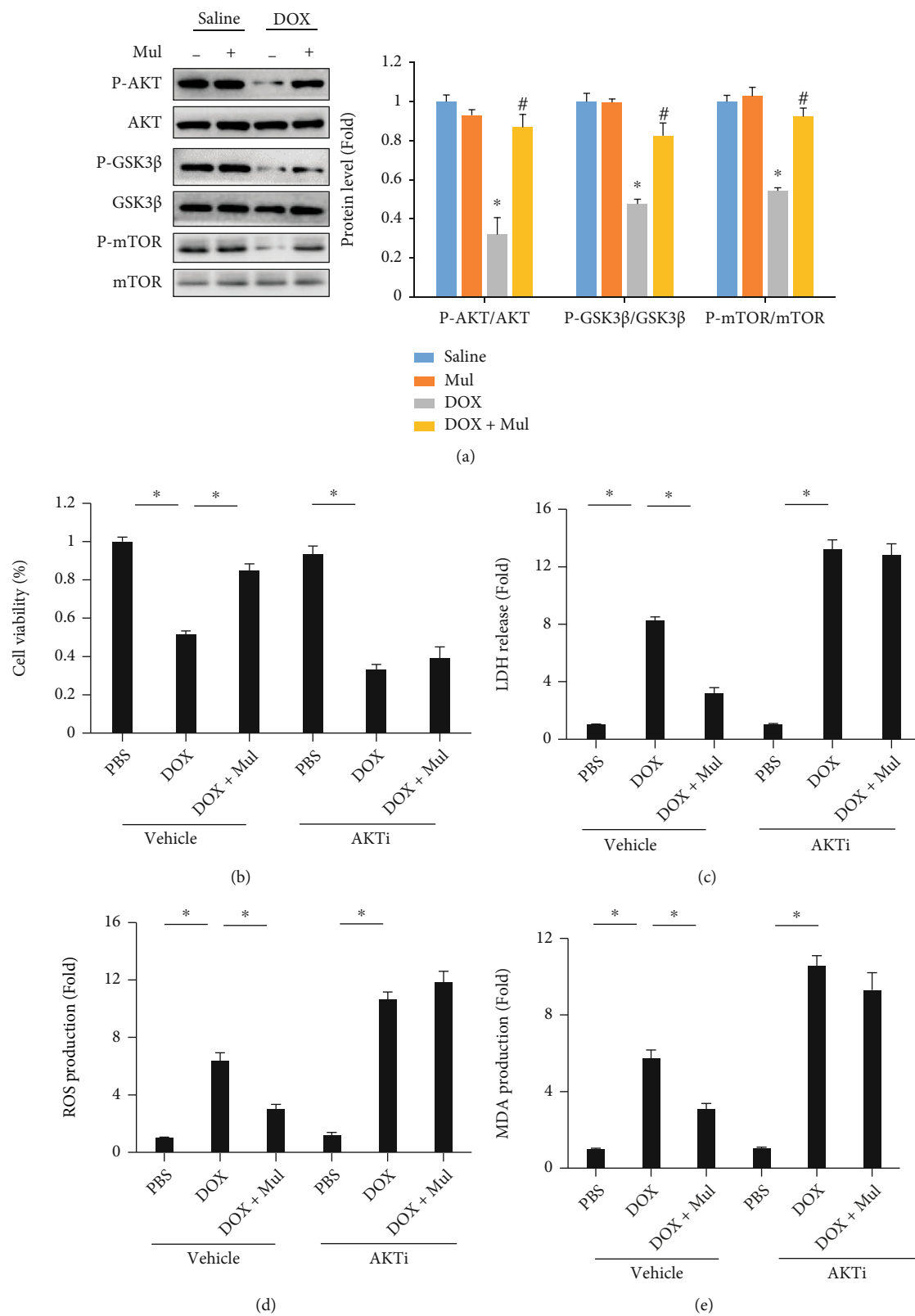


FIGURE 6: Continued.

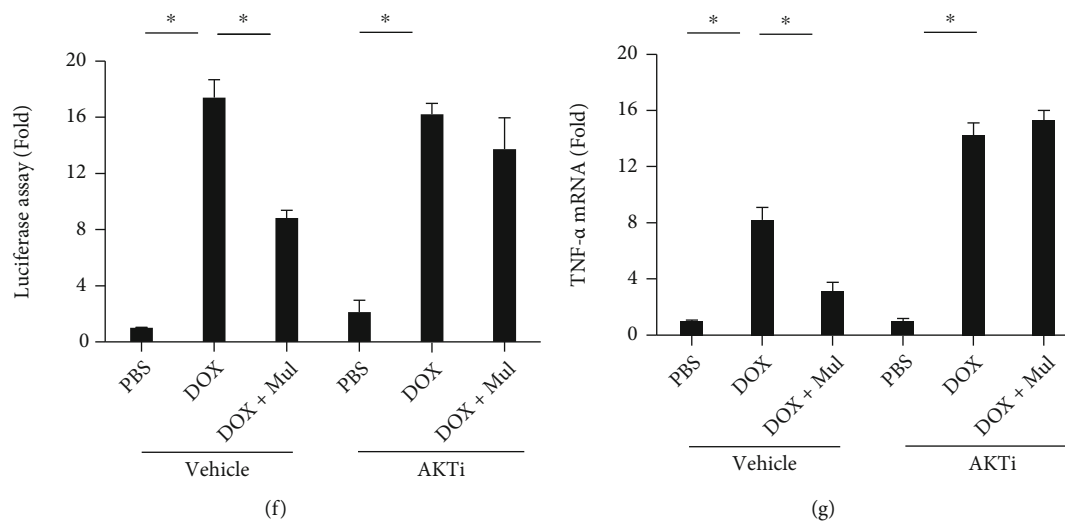


FIGURE 6: AKT inhibition abolished the anti-inflammatory and antioxidative activities of mulberrin in DOX-stimulated cells. The phosphorylation of AKT, GSK3 β , and mTOR (a) was detected in the indicated groups. Cell viability was detected in cells treated with an AKT inhibitor (b). Cardiomyocyte injury was assayed by the release of LDH (c). The ROS level (d) and MDA content (e) were detected to reflect oxidative damage caused by DOX in cells incubated with an AKT inhibitor. Luciferase assay (f) was used to reflect NF- κ B transactivation in vitro. The mRNA level of TNF- α (g) in cells incubated with an AKT inhibitor. Data are presented as mean \pm SEM. $n = 6$ for each group. For (a), * $P < 0.05$ compared with the saline group; # $P < 0.05$ compared with DOX alone. For others, * $P < 0.05$ compared with the control groups.

Biosystems). All images were analyzed by a person blinded to the treatment by using Image-Pro Plus 6.0.

2.8. Apoptotic Detection. Frozen heart tissues were cut into sections and fixed in 4% neutral paraformaldehyde. TUNEL assay was conducted with the in situ apoptosis detection kit (Takara Bio Inc., Shiga, Japan), and these slides were observed under a fluorescence microscope. This evaluation was performed by one person who was blinded to the treatment group. Heart tissues were homogenized in iced PBS. Cardiac caspase 3 levels were detected using a Caspase-3 Colorimetric Assay Kit (Clontech, USA). DNA fragmentation assay was detected using the DNA Fragmentation Detection Kit (#AS20-4459, Agrisera) according to the manufacturer's instructions.

2.9. Statistical Analysis. Data are represented as mean \pm standard error of mean (SEM). Statistical analysis between two groups was determined via unpaired Student's t -test. We used one-way analysis of variance followed by Tukey's test to compare differences between multiple groups. Differences were considered as statistically significant at $P < 0.05$.

3. Result

3.1. Mul Treatment-Attenuated DOX-Induced Oxidative Stress In Vitro. We first used a CCK-8 assay to determine the viability of DOX-treated cells. Compared with the PBS group, DOX time-dependently decreased the viability of cardiomyocytes. However, this pathological reduction was markedly attenuated by Mul treatment at either 50 or 100 μ M (Figure 1(a)). However, Mul at the dose of 25 μ M did not improve the viability of DOX-treated cells. The levels

of LDH and CK in DOX-treated cells were higher than with those in the PBS-treated group. However, Mul treatment significantly inhibited the release of LDH and CK in response to DOX administration (Figures 1(b) and 1(c)). It also showed that the ROS level in DOX-treated H9c2 cells was increased. And Mul treatment dose-dependently decreased the cellular ROS level in DOX-treated cells (Figure 1(d)). DCFH-DA immunofluorescence also revealed that Mul significantly decreased DOX-induced ROS production in vitro (Figure 1(e)). In addition, Mul treatment also dose-dependently increased GSH content and decreased MDA and protein carbonyl levels in DOX-exposed cells (Figures 1(f)–1(h)). The protein expression of Nrf2 and HO-1 was significantly lower in cardiomyocytes exposed to DOX than in those exposed to PBS. The expression of Nrf2 and HO-1 exposure to DOX was higher in cardiomyocytes treated with Mul than in those treated with DOX only (Figure 1(i)). We also determined the mRNA levels of Nrf2-regulated downstream targets. The decreased mRNA levels of HO-1, SOD1, SOD2, NQO1, and CAT were obviously restored after Mul treatment (Figure 1(j)).

3.2. Mul Treatment-Suppressed Inflammatory Response in DOX-Incubated Cells. The mRNA levels of several inflammatory factors, including TNF- α , IL-1 β , IL-6, monocyte chemoattractant protein-1 (MCP-1), interferon γ (IFN- γ), and IL-17, in cardiomyocytes were greater in the DOX group than in the PBS group. Mul treatment (100 μ M) attenuated all these pathological elevations except IFN- γ (Figure 2(a)). Further detection the protein expression of TNF- α and IL-6 also reveal that Mul at the dose of 100 μ M suppressed the inflammatory response induced by DOX (Figures 2(b) and 2(c)). The luciferase assay also revealed that DOX

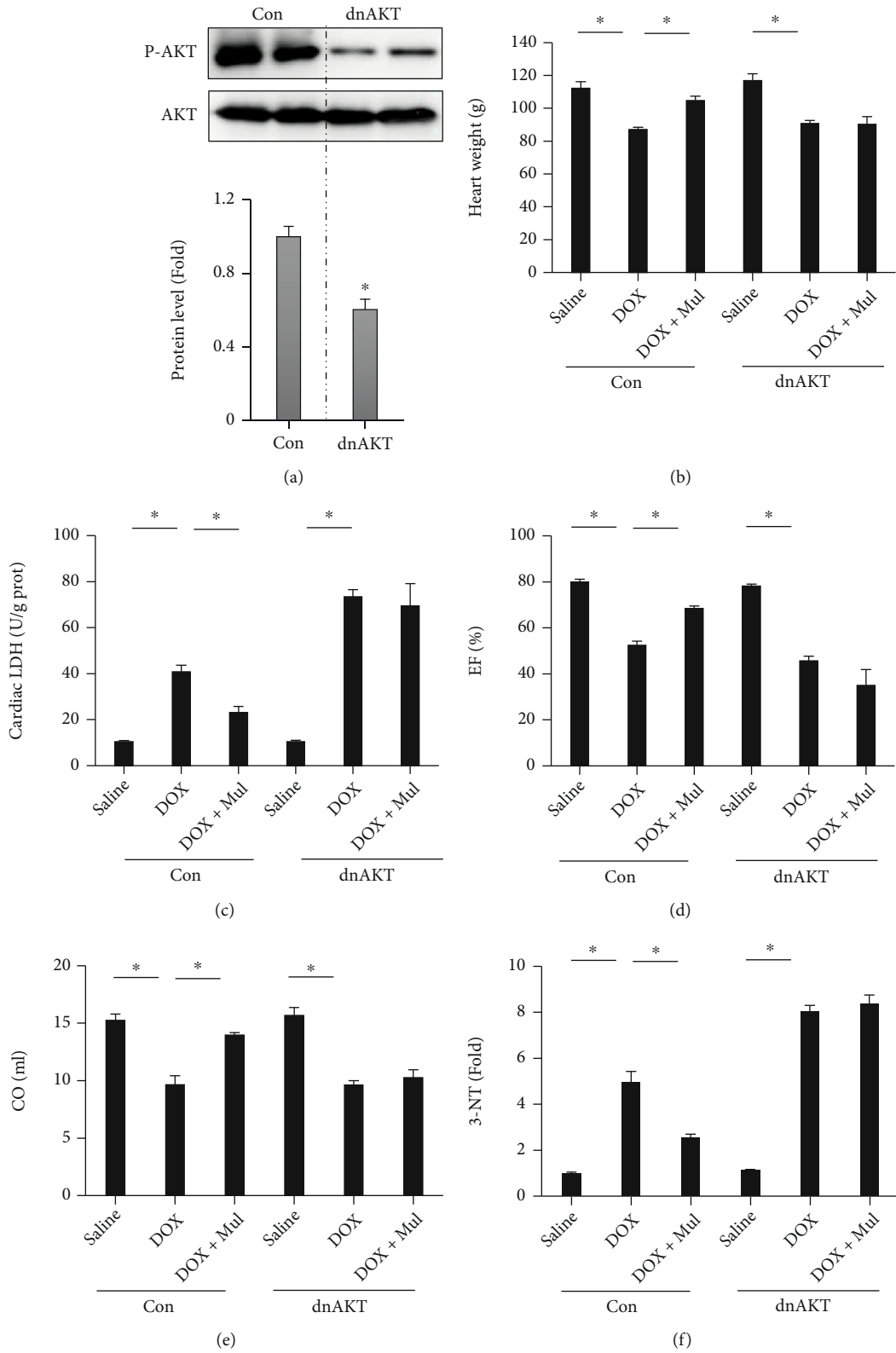


FIGURE 7: Continued.

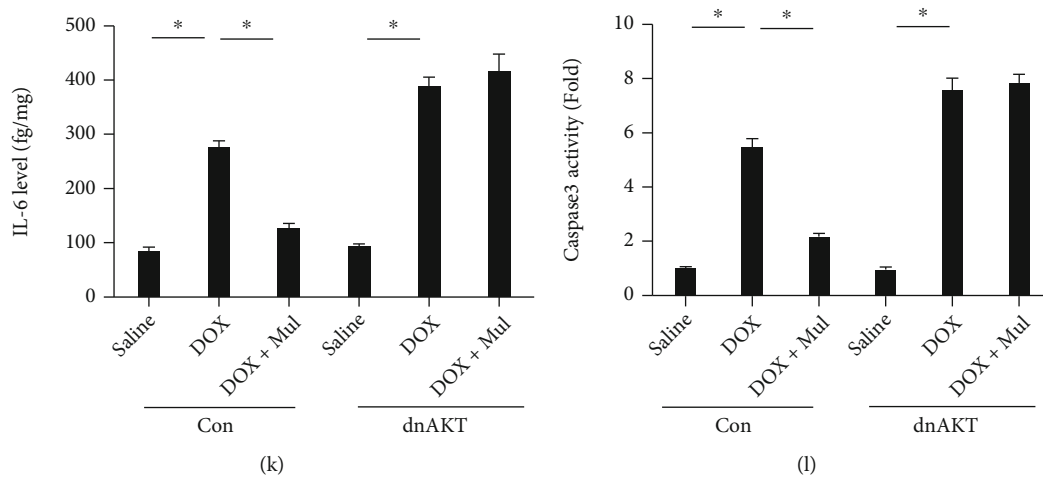
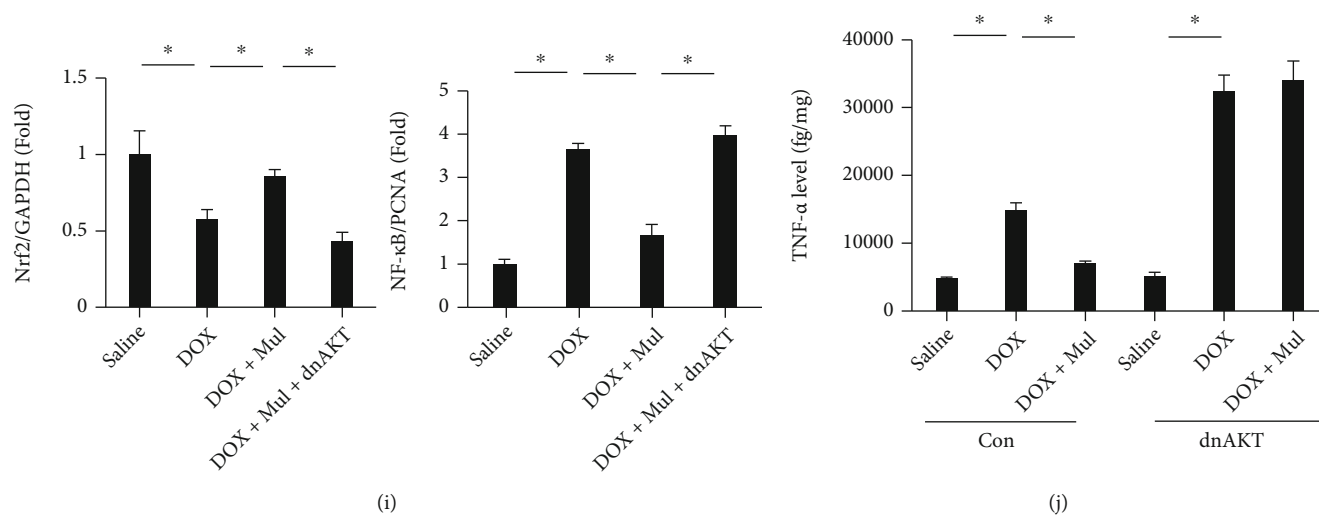
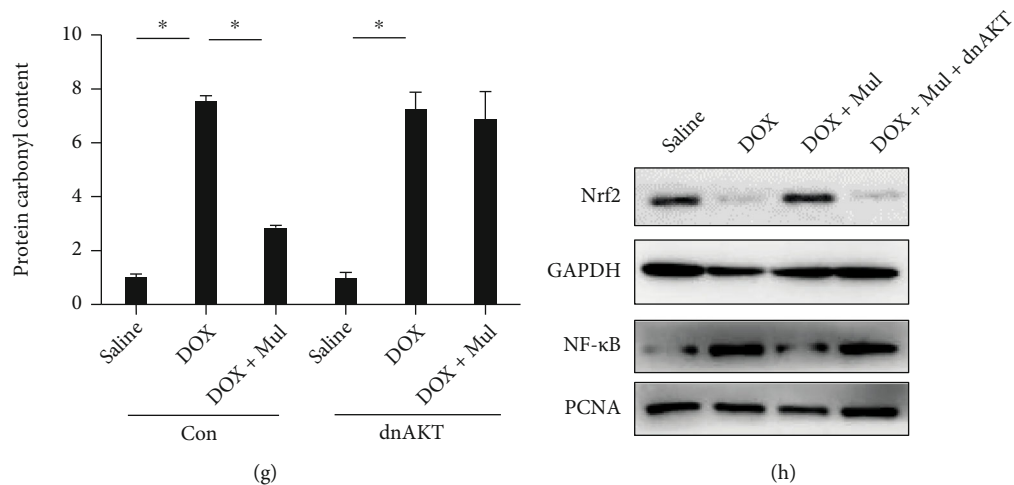


FIGURE 7: Continued.

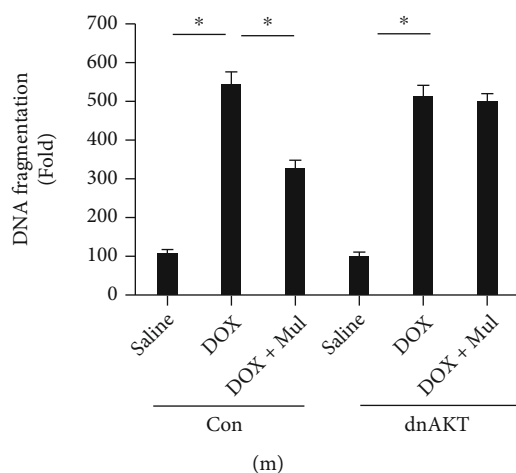


FIGURE 7: Infection of AKT-dominant negative mutant blocked the protection of mulberrin against DOX-induced cardiac injury in vivo. The phosphorylation of AKT (a) was detected via western blotting in mice at 4 weeks after AAV9-dnAKT or AAV9-Con injection. Heart weight (b) and myocardial LDH (c) were detected to evaluate DOX-induced cardiac injury. Cardiac function including ejection fraction (d) and cardiac output (e) were detected using an invasive hemodynamic monitoring. Oxidative stress markers, 3-NT (f) and protein carbonyl content (g), were quantified by the commercial kits. Nrf2 protein expression (h, i) was detected via western blotting. The nuclear accumulation of NF- κ B protein (h, i) was detected in an isolated nuclear fraction. The levels of inflammatory factors (j, k) were also quantified. Myocardial apoptosis was evaluated by caspase 3 activity (l) and DNA fragmentation test (m). Data are presented as mean \pm SEM. $n = 8$ for each group. * $P < 0.05$ compared with the control groups.

induced NF- κ B transactivation in a time-dependent manner. And Mul at the dose of 100 μ M largely suppressed this activation of NF- κ B after DOX incubation in a time-dependent manner (Figure 2(d)). Detection of nuclear NF- κ B found that Mul at the dose of 100 μ M suppressed nuclear NF- κ B accumulation in DOX-treated cardiomyocytes (Figure 2(e)).

3.3. Mul Treatment-Attenuated Acute Cardiac Injury in DOX-Injected Mice. As shown in Figures 3(a) and 3(b), body weight and heart weight declined in response to DOX injection. And these declines in DOX-treated mice were largely blocked by the treatment of Mul (Figures 3(a) and 3(b)). The release of LDH and CK-MB can reflect the severity of cardiac injury. DOX significantly upregulated LDH and CK-MB levels in heart tissues, which were alleviated by Mul treatment (Figures 3(c) and 3(d)). The detection of the mRNA level of ANP also revealed that Mul treatment significantly decreased the elevated ANP mRNA level in DOX-treated mice (Figure 3(e)). Histological detection revealed that myofibrillar disarrangement in DOX-injected mice was attenuated by Mul treatment (Figure 3(f)). Unexpectedly, DOX injection did not decrease the heart rate in mice (Figure 3(g)). Compared to those in the saline group, ejection fraction (EF), stroke volume (SV), and cardiac output (CO) were significantly reduced in the DOX group (Figures 3(h)–3(j)). Conversely, these parameters were significantly restored by treatment with Mul (Figures 3(h)–3(j)).

3.4. Mul Treatment-Alleviated DOX-Induced Oxidative Damage in Mice. As oxidative damage was a fundamental feature of acute cardiac injury induced by DOX, the effect of Mul on oxidative status was evaluated. Mul treatment also suppressed the production of myocardial lipid peroxidation

in DOX-injected mice (Figure 4(a)). Upon DOX injection, GSH levels in cardiac tissues were decreased, and treatment with Mul administration almost restored the level of GSH in the hearts (Figure 4(b)). In addition, compared with the saline group, all oxidative damage markers, including 3-NT, MDA, and protein carbonyl, in heart tissues were significantly increased (Figures 4(c)–4(e)). Conversely, Mul treatment largely suppressed the elevations in these markers. We also found that the impaired SOD activity in DOX-treated hearts was improved via the treatment of Mul (Figure 4(f)). As shown in Figure 4(g), Nrf2 protein expression and the downstream HO-1 of DOX mice were assessed via western blotting, and we found that Nrf2 and HO-1 protein expressions were significantly decreased via DOX injection compared with the saline group. However, compared with the DOX group, Mul treatment significantly increased Nrf2 and HO-1 protein expression (Figure 4(g)). Further detection of the mRNA levels of Nrf2-regulated genes also suggested that Mul treatment significantly increased the mRNA expression of HO-1, SOD1, SOD2, NQO1, and CAT in DOX-treated mice (Figure 4(h)).

3.5. Mul Treatment-Alleviated Inflammation and Apoptosis in DOX-Treated Cardiac Tissues. The mRNA levels of several cytokines in heart samples were measured, and the results demonstrated that the expression of these cytokines in the hearts was significantly increased after exposure to DOX (Figure 5(a)). Treatment with Mul largely alleviated the DOX-induced inflammatory response in mice (Figure 5(a)). Further detection revealed that Mul treatment prevented the production of cardiac TNF- α and IL-6 in DOX-treated mice (Figures 5(b) and 5(c)). DOX induced the transactivation of NF- κ B, which played a key role in DOX-associated inflammation [16]. In response to DOX

injection, the activated IKK complex phosphorylates I κ B α , thereby leading to nuclear accumulation of NF- κ B to regulate inflammatory gene expression. As indicated in Figure 5(d), the phosphorylation of I κ B α and NF- κ B was increased in DOX-injected hearts; these pathological alterations were not observed in Mul-treated hearts. In view of the anti-inflammatory effects of Mul, we hypothesized that Mul treatment might suppress cardiomyocyte apoptosis in mice with DOX injection. As expected, DOX increased the proapoptotic protein Bax but decreased the antiapoptotic protein Bcl-2. However, these abnormal alterations were prevented by Mul (Figure 5(e)). The number of TUNEL-positive cells was much higher in the DOX group than in the control group, and Mul largely decreased the number of these apoptotic cells (Figure 5(f)). Caspase 3 activation and DNA fragmentations in DOX hearts were increased compared with the saline group, and these effects were reduced via Mul treatment (Figures 5(g) and 5(h)).

3.6. Mul-Enhanced AKT Signaling Pathway in the Hearts of DOX-Treated Mice. Given that AKT was responsible for the activation of Nrf2 and that AKT activation could provide benefit against DOX-induced cardiomyocyte apoptosis [17], we asked whether Mul exerted its protective effects on DOX-induced injury through an AKT-dependent manner. DOX caused a significant decrease in the phosphorylation of AKT and downstream kinase GSK3 β and mTOR in the heart tissues (Figure 6(a)). Mul treatment prevented the DOX-induced inactivation of the two kinases (Figure 6(a)). To test the role of AKT in the protection provided by Mul, we used a specific AKT inhibitor. As expected, AKT inhibition blocked the beneficial effect of Mul on cell viability and LDH release (Figures 6(b) and 6(c)). DOX-induced oxidative stress which was reflected by ROS and MDA production was suppressed by the treatment of Mul, and these protective effects were offset by the use of this AKT inhibitor (Figures 6(d)–6(e)). AKT inhibition blocked the beneficial effects of Mul on inflammatory response, as reflected by the luciferase assay of NF- κ B transactivation and TNF- α mRNA expression (Figures 6(f) and 6(g)).

3.7. AKT Signaling Was Responsible for Mul-Mediated Protective Role in the Hearts. To further verify the effect of AKT in Mul-mediated protective actions, we used an AKT-dominant negative mutant to alter the activation of AKT in the hearts. As shown in Figure 7(a), this dominant negative mutant significantly reduced myocardial AKT activation at 4 weeks after AAV9-dnAKT or AAV9-Con injection. AKT-dominant negative mutant infection almost completely abolished the Mul-mediated protective role in the hearts, as indicated by the alterations in heart weight, cardiac LDH release, and cardiac function (EF and CO) (Figures 7(b)–7(e)). DOX-induced oxidative stress, as reflected by the 3-NT content and protein carbonyl, was suppressed by the treatment of Mul. And these effects were abolished by the AKT-dominant negative mutant infection (Figures 7(f) and 7(g)). Nrf2 protein expression was decreased in response to DOX exposure but restored by the treatment of Mul. This restoration of Nrf2 was blocked

by this AKT-dominant negative mutant infection (Figures 7(h) and 7(i)). Mul treatment lost its anti-inflammatory effects, as detected by the alteration of NF- κ B, TNF- α , and IL-6 levels (Figures 7(h)–7(k)). The protective effects of Mul treatment on caspase 3 activity and DNA fragmentations were also blocked by this AKT-dominant negative mutant infection (Figures 7(l) and 7(m)).

4. Discussion

Previous studies have confirmed a high affinity of DOX to the heart, and DOX could be accumulated in the cardiomyocytes, thus causing myocardial apoptotic loss and congestive heart failure [10]. Dexrazoxane was the only drug that was approved by FDA for the treatment of DOX-induced cardiotoxicity [18]. However, this drug had life-threatening side effects, including myelosuppression and coagulation disorder. Clearly, finding an effective approach to treat DOX-induced cardiac injury would be of great clinical significance. Actually, several scavengers of ROS were capable of attenuating DOX-related cardiotoxicity in animal experiments [19, 20]. The reasons for their failure in clinical practice included low bioavailability and secondary reactions with other molecules [21]. Here, we observed that Mul treatment could attenuate DOX-induced cardiac damage and inhibit DOX-induced inflammatory response, oxidative damage, and myocardial apoptosis in mice. Supplementation of Mul might serve as a novel therapy for DOX-induced cardiotoxicity.

Emerging evidence suggested that oxidative stress and inflammatory response were the major mediators of DOX-related cardiotoxicity [22]. DOX was rapidly reduced to a semiquinone through one-electron reduction of the quinone moiety, semiquinone autoxidized, and produced superoxide anions [23, 24]. Excessive ROS production provoked oxidative damage to the lipid and protein, thus causing cardiac dysfunction [25]. In our study, multiple lines of findings suggested that DOX-induced ROS generation and oxidative damage in cardiac tissues were prevented by Mul treatment. In addition, heart samples had lower levels of endogenous antioxidant enzymes. What was more serious was that DOX significantly reduced the endogenous antioxidant, rendering the heart more vulnerable to DOX-induced oxidative stimuli. In this aspect, the restoration of antioxidant systems via the treatment of Mul might also contribute the protection of Mul against cardiotoxicity. It has been reported that Nrf2, a basic leucine zipper bZIP protein, was closely involved into DOX-induced cardiomyopathy. Nrf2 deficiency aggravated DOX-related cardiotoxicity and cardiac dysfunction in mice [26]. Conversely, activation of Nrf2 via a pharmacological agent protected against DOX toxicity through upregulation of antioxidant and antielectrophile enzyme expression in mice [27]. In our study, the expression of Nrf2 and its downstream targets was found to be decreased after DOX exposure, and treatment of Mul significantly blocked these pathological alterations, suggesting that Mul might improve antioxidant capacity in DOX-related hearts via activation of Nrf2.

Proinflammatory factors were closely involved into DOX-induced heart dysfunction [28]. Surprisingly, we demonstrated that treatment with Mul not only attenuated the DOX-induced upregulation of inflammatory factors but also inhibited the phosphorylation of $\text{I}\kappa\text{B}\alpha$ and transactivation of NF- κB . However, there sounds a different voice about alteration of NF- κB in DOX-induced acute cardiac injury. Riad et al. reported that DOX treatment did not induce a significant alteration of NF- κB binding activity [29]. This finding could not compromise the fundamental functions of NF- κB and NF- κB -dependent inflammation in cardiac injury caused by DOX injection. Taken together, these data indicated that the protection of Mul against DOX-related cardiac injury might partly be attributed to the inhibitory effects on $\text{I}\kappa\text{B}\alpha$ /NF- κB association and subsequent transcription of inflammatory factors.

The increase in myocardial apoptosis was another landmark of DOX-induced cardiac injury [30]. Attenuation of p53-dependent apoptosis improved cardiac function in DOX-injected mice [31]. In agreement with these findings, we observed a marked elevation in myocardial apoptosis and caspase 3 activity after DOX injection. After Mul treatment, TUNEL-positive cells, DNA fragmentation, and the Bax/Bcl-2 ratio were all decreased in DOX-injected mice. The results indicated that Mul treatment could suppress DOX-induced these apoptotic alterations in mice.

AKT inactivation played a critical role in DOX-induced cardiac injury, and restoration of AKT activity protected against cardiac apoptosis and prevented DOX-induced cardiac dysfunction [32]. Here, for the first time, we showed that Mul treatment activated the AKT signaling pathway and provided benefits against DOX-induced cardiac injury. This finding was in line with a study that reported that AKT inactivation was closely involved in the process of DOX-induced cardiotoxicity [33]. AKT inactivation resulted in GSK3 β /FYN activation, thus promoting the nuclear exclusion of Nrf2 and its degradation in cytoplasm [34]. Here, we also reported that DOX decreased Nrf2 expression, and Mul treatment restored Nrf2 protein expression. And this restoration was blocked by the use of AKT-dominant negative mutant infection, suggesting that Mul treatment regulated Nrf2 activation through an AKT-dependent manner in DOX-treated mice.

In conclusion, these data suggested that Mul treatment attenuated DOX-induced acute cardiotoxicity via the AKT-dependent attenuation of oxidative damage, inflammation accumulation, and myocardial apoptosis. Our present findings suggest that Mul could be useful in the therapy of DOX-induced acute cardiotoxicity.

Data Availability

The data that support the findings of this study are available from the corresponding authors upon reasonable request.

Conflicts of Interest

The authors declare that they have no conflicts of interest.

Authors' Contributions

Peng Ye and Wen-Lan Li contributed equally to this work.

Acknowledgments

This project was supported by grants from the National Natural Science Foundation of China (Nos: 81600734 and 81600290) and supported by the Natural Science Foundation of Inner Mongolia (2018MS08089).

References

- [1] J. J. Bartlett, P. C. Trivedi, and T. Pulinilkunnil, "Autophagic dysregulation in doxorubicin cardiomyopathy," *Journal of Molecular and Cellular Cardiology*, vol. 104, pp. 1–8, 2017.
- [2] J. Sabatino, S. De Rosa, L. Tammè et al., "Empagliflozin prevents doxorubicin-induced myocardial dysfunction," *Cardiovascular Diabetology*, vol. 19, no. 1, p. 66, 2020.
- [3] M. Nicol, M. Sadoune, E. Polidano et al., "Doxorubicin-induced and trastuzumab-induced cardiotoxicity in mice is not prevented by metoprolol," *ESC Heart Failure*, vol. 8, no. 2, pp. 928–937, 2021.
- [4] M. Songbo, H. Lang, C. Xinyong, X. Bin, Z. Ping, and S. Liang, "Oxidative stress injury in doxorubicin-induced cardiotoxicity," *Toxicology Letters*, vol. 307, pp. 41–48, 2019.
- [5] N. Wenningmann, M. Knapp, A. Ande, T. R. Vaidya, and S. Ait-Oudhia, "Insights into doxorubicin-induced cardiotoxicity: molecular mechanisms, preventive strategies, and early monitoring," *Molecular Pharmacology*, vol. 96, no. 2, pp. 219–232, 2019.
- [6] D. Li, Y. Yang, S. Wang et al., "Role of acetylation in doxorubicin-induced cardiotoxicity," *Redox Biology*, vol. 46, article 102089, 2021.
- [7] Y. Xiong, X. Liu, C. P. Lee, B. H. Chua, and Y. S. Ho, "Attenuation of doxorubicin-induced contractile and mitochondrial dysfunction in mouse heart by cellular glutathione peroxidase," *Free Radical Biology & Medicine*, vol. 41, no. 1, pp. 46–55, 2006.
- [8] H. C. Yen, T. D. Oberley, S. Vichitbandha, Y. S. Ho, and C. D. St. St., "The protective role of manganese superoxide dismutase against adriamycin-induced acute cardiac toxicity in transgenic mice," *The Journal of Clinical Investigation*, vol. 98, no. 5, pp. 1253–1260, 1996.
- [9] L. He, F. Liu, and J. Li, "Mitochondrial sirtuins and doxorubicin-induced cardiotoxicity," *Cardiovascular Toxicology*, vol. 21, no. 3, pp. 179–191, 2021.
- [10] X. Zhang, C. Hu, C. Y. Kong et al., "FNDC5 alleviates oxidative stress and cardiomyocyte apoptosis in doxorubicin-induced cardiotoxicity via activating AKT," *Cell Death and Differentiation*, vol. 27, no. 2, pp. 540–555, 2020.
- [11] C. Ge, J. Tan, D. Lou et al., "Mulberrin confers protection against hepatic fibrosis by Trim31/Nrf2 signaling," *Redox Biology*, vol. 51, article 102274, 2022.
- [12] P. Xia, X. Gao, L. Duan, W. Zhang, and Y. F. Sun, "Mulberrin (Mul) reduces spinal cord injury (SCI)-induced apoptosis, inflammation and oxidative stress in rats via miRNA-337 by targeting Nrf-2," *Biomedicine & Pharmacotherapy*, vol. 107, pp. 1480–1487, 2018.
- [13] W. Cao, Y. Dong, W. Zhao, X. Lu, and L. Sun, "Mulberrin attenuates 1-methyl-4-phenyl-1,2,3,6-tetrahydropyridine

- (MPTP)-induced Parkinson's disease by promoting Wnt/ β -catenin signaling pathway," *Journal of Chemical Neuroanatomy*, vol. 98, pp. 63–70, 2019.
- [14] V. Ambros, "The functions of animal microRNAs," *Nature*, vol. 431, no. 7006, pp. 350–355, 2004.
- [15] Z. G. Ma, Y. P. Yuan, X. Zhang et al., "C1q-tumour necrosis factor-related protein-3 exacerbates cardiac hypertrophy in mice," *Cardiovascular Research*, vol. 115, no. 6, pp. 1067–1077, 2019.
- [16] R. Dhingra, M. Guberman, I. Rabinovich-Nikitin et al., "Impaired NF- κ B signalling underlies cyclophilin D-mediated mitochondrial permeability transition pore opening in doxorubicin cardiomyopathy," *Cardiovascular Research*, vol. 116, no. 6, pp. 1161–1174, 2020.
- [17] Y. Zeng, W. W. Du, Y. Wu et al., "A circular RNA binds to and activates AKT phosphorylation and nuclear localization reducing apoptosis and enhancing cardiac repair," *Theranostics*, vol. 7, no. 16, pp. 3842–3855, 2017.
- [18] S. E. Lipshultz, N. Rifai, V. M. Dalton et al., "The effect of dexrazoxane on myocardial injury in doxorubicin-treated children with acute lymphoblastic leukemia," *The New England Journal of Medicine*, vol. 351, no. 2, pp. 145–153, 2004.
- [19] Y. Zhao, J. Sun, W. Zhang et al., "Follistatin-like 1 protects against doxorubicin-induced cardiomyopathy through upregulation of Nrf2," *Oxidative Medicine and Cellular Longevity*, vol. 2020, Article ID 3598715, 11 pages, 2020.
- [20] Y. Liu, L. Zhou, B. Du et al., "Protection against doxorubicin-related cardiotoxicity by jaceosidin involves the Sirt1 signaling pathway," *Oxidative Medicine and Cellular Longevity*, vol. 2021, Article ID 9984330, 18 pages, 2021.
- [21] H. J. Forman, K. J. Davies, and F. Ursini, "How do nutritional antioxidants really work: nucleophilic tone and para-hormesis versus free radical scavenging in vivo," *Free Radical Biology & Medicine*, vol. 66, pp. 24–35, 2014.
- [22] P. Wang, L. Wang, J. Lu et al., "SESN2 protects against doxorubicin-induced cardiomyopathy via rescuing mitophagy and improving mitochondrial function," *Journal of Molecular and Cellular Cardiology*, vol. 133, pp. 125–137, 2019.
- [23] S. Deng, A. Kruger, A. L. Kleschyov, L. Kalinowski, A. Daiber, and L. Wojnowski, "Gp91phox-containing NAD(P)H oxidase increases superoxide formation by doxorubicin and NADPH," *Free Radical Biology & Medicine*, vol. 42, no. 4, pp. 466–473, 2007.
- [24] R. Nithipongvanitch, W. Ittarat, M. P. Cole, J. Tangpong, D. K. Clair, and T. D. Oberley, "Mitochondrial and nuclear p53 localization in cardiomyocytes: redox modulation by doxorubicin (adriamycin)," *Antioxidants & Redox Signaling*, vol. 9, no. 7, pp. 1001–1008, 2007.
- [25] Y. P. Yuan, Z. G. Ma, X. Zhang et al., "CTRP3 protected against doxorubicin-induced cardiac dysfunction, inflammation and cell death via activation of Sirt1," *Journal of Molecular and Cellular Cardiology*, vol. 114, pp. 38–47, 2018.
- [26] S. Li, W. Wang, T. Niu et al., "Nrf2 deficiency exaggerates doxorubicin-induced cardiotoxicity and cardiac dysfunction," *Oxidative Medicine and Cellular Longevity*, vol. 2014, Article ID 748524, 15 pages, 2014.
- [27] P. Singh, R. Sharma, K. McElhanon et al., "Sulforaphane protects the heart from doxorubicin-induced toxicity," *Free Radical Biology & Medicine*, vol. 86, pp. 90–101, 2015.
- [28] J. Ye, Y. Huang, B. Que et al., "Interleukin-12p35 knock out aggravates doxorubicin-induced cardiac injury and dysfunction by aggravating the inflammatory response, oxidative stress, apoptosis and autophagy in mice," *Apoptosis and Autophagy in Mice. Ebiomedicine*, vol. 35, pp. 29–39, 2018.
- [29] A. Riad, S. Bien, M. Gratz et al., "Toll-like receptor-4 deficiency attenuates doxorubicin-induced cardiomyopathy in mice," *European Journal of Heart Failure*, vol. 10, no. 3, pp. 233–243, 2008.
- [30] Y. Wang, T. Lei, J. Yuan et al., "GCN2 deficiency ameliorates doxorubicin-induced cardiotoxicity by decreasing cardiomyocyte apoptosis and myocardial oxidative stress," *Redox Biology*, vol. 17, pp. 25–34, 2018.
- [31] Y. Shizukuda, S. Matoba, O. Y. Mian, T. Nguyen, and P. M. Hwang, "Targeted disruption of p53 attenuates doxorubicin-induced cardiac toxicity in mice," *Molecular and Cellular Biochemistry*, vol. 273, no. 1–2, pp. 25–32, 2005.
- [32] G. C. Fan, X. Zhou, X. Wang et al., "Heat shock protein 20 interacting with phosphorylated Akt reduces doxorubicin-triggered oxidative stress and cardiotoxicity," *Circulation Research*, vol. 103, no. 11, pp. 1270–1279, 2008.
- [33] S. Maruyama, R. Shibata, K. Ohashi et al., "Adiponectin ameliorates doxorubicin-induced cardiotoxicity through Akt protein-dependent mechanism*," *The Journal of Biological Chemistry*, vol. 286, no. 37, pp. 32790–32800, 2011.
- [34] D. Dong, Y. Zhang, H. He, Y. Zhu, and H. Ou, "Alpinetin inhibits macrophage infiltration and atherosclerosis by improving the thiol redox state: requirement of GSK3 β /Fyn-dependent Nrf2 activation," *The FASEB Journal*, vol. 36, no. 4, article e22261, 2022.

Research Article

Vitexin Mitigates *Staphylococcus aureus*-Induced Mastitis via Regulation of ROS/ER Stress/NF- κ B/MAPK Pathway

Yu Chen ¹, Jing Yang ¹, Zhi Huang ¹, Baoyi Yin ¹, Talha Umar ¹, Cheng Yang ¹,
Xiangqian Zhang ¹, Hongyuan Jing ¹, Shuai Guo ¹, Mengyao Guo ²,
Ganzhen Deng ¹ and Changwei Qiu ¹

¹Department of Clinical Veterinary Medicine, College of Veterinary Medicine, Huazhong Agricultural University, Wuhan 430070, China

²Department of Clinical Veterinary Medicine, College of Veterinary Medicine, Northeast Agricultural University, Harbin 150030, China

Correspondence should be addressed to Changwei Qiu; sdqiu2001@mail.hzau.edu.cn

Received 11 March 2022; Revised 2 June 2022; Accepted 14 June 2022; Published 27 June 2022

Academic Editor: Cassiano Felipe Gonçalves-de-Albuquerque

Copyright © 2022 Yu Chen et al. This is an open access article distributed under the Creative Commons Attribution License, which permits unrestricted use, distribution, and reproduction in any medium, provided the original work is properly cited.

Mastitis, caused by a variety of pathogenic microorganisms, seriously threatens the safety and economic benefits of the dairy industry. Vitexin, a flavone glucoside found in many plant species, has been widely reported to have antioxidant, anti-inflammatory, antiviral, anticancer, neuroprotective, and cardioprotective effects. However, few studies have explored the effect of vitexin on mastitis. This study is aimed at exploring whether the antioxidant and anti-inflammatory functions of vitexin can improve *Staphylococcus aureus*-induced mastitis and its possible molecular mechanism. The expression profiles of *S. aureus*-infected bovine mammary epithelial cells and gland tissues from the GEO data set (GSE94056 and GSE139612) were analyzed and found that DEGs were mainly involved in immune signaling pathways, apoptosis, and ER stress through GO and KEGG enrichment. Vitexin blocked the production of ROS and increased the activity of antioxidant enzymes (SOD, GSH-PX, and CAT) via activation of PPAR γ *in vivo* and *in vitro*. In addition, vitexin reduced the production of inflammatory cytokines (TNF- α , IL-1 β , and IL-6) and inhibited apoptosis in MAC-T cells and mouse mammary tissues infected with *Staphylococcus aureus*. Moreover, vitexin decreased the expression of PDI, Ero1-L α , p-IRE1 α , PERK, p-eIF2 α , and CHOP protein but increased BiP in both mammary gland cells and tissues challenged by *S. aureus*. Western blot results also found that the phosphorylation levels of JNK, ERK, p38, and p65 were reduced in vitexin-treated tissues and cells. Vitexin inhibited the production of ROS through promoting PPAR γ , increased the activity of antioxidant enzymes, and reduced inflammatory cytokines and apoptosis by alleviating ER stress and inactivation MAPKs and NF- κ B signaling pathway. Vitexin maybe have great potential to be a preventive and therapeutic agent for mastitis.

1. Introduction

Staphylococcus aureus (*S. aureus*) is an important pathogenic microorganism that causes food-borne infections, and it is also the main pathogen that causes mastitis in ruminants [1, 2]. Milk produced by cows suffering from *S. aureus* mastitis is one of the most important sources of milk contamination, whereas raw milk and dairy products are the natural medium for the growth of *S. aureus* [3]. *S. aureus* is a common opportunistic pathogen in the farm environment. Lactating dairy cows are highly susceptible to infec-

tion and transmission of *S. aureus* due to open lactation passages and exposure to contaminants such as milking equipment. The exotoxin produced by *S. aureus* can easily cause food poisoning [4]. Once exotoxin enters the gut, the T-cell inflammatory cytokine storm is triggered in the host [5, 6]. *S. aureus* is a common pathogen of dairy cow mastitis, which seriously affects milk production and quality and causes huge economic losses to the dairy industry [7, 8]. The mechanisms by which *S. aureus* challenge the host immune response are complicated. During the colonization and invasion of *S. aureus*, white blood cells are recruited to

the site of infection, and white blood cells produce a series of reactive substances (including superoxide, hydrogen peroxide, nitric oxide, and hypochlorous acid), which can modify and inactivate cells large molecules, even lead to growth defects or death [9]. Oxidative stress caused by *S. aureus* produces oxidants that react with cell macromolecules [10]. The accumulation of a large number of reactive oxygen species (ROS) attacked oxidized proteins, lipids, and DNA to cause oxidative damage is a characteristic of many inflammatory diseases [11]. ROS causes endoplasmic reticulum (ER) stress, which breaks the ER redox environment and induces protein folding errors [12, 13]. Persistent ER stress can also trigger an inflammatory response through the unfolded protein response (UPR) pathway [14]. ER participates in the modification (including disulfide bonds, aminoglycosylation, and folding) of secreted proteins and transmembrane proteins. Immunoglobulin heavy chain binding protein (BiP) and protein disulfide isomerase (PDI), molecular chaperone proteins in the ER, play an important role in protein folding and oxidation [15]. Protein kinase R- (PKR-) like endoplasmic reticulum kinase (PERK) and inositol-requiring enzyme 1 α (IRE1 α) serve as a quality controller for protein synthesis in the endoplasmic reticulum [16–18]. Once UPR is activated in the context of ER stress, BiP will separate from PERK and IRE1 α and cause their activation, promoting the transcription of ER stress response genes [16, 19]. PERK directly phosphorylates eIF2 α after autophosphorylation, thereby reducing protein translation and promoting the production of C/EBP homologous protein (CHOP) [20]. Elevated CHOP plays an important role in apoptosis induced by ER stress [21]. *S. aureus* also induced a cell-mediated immune response in the mouse mammary gland, which significantly promoted the production of IFN- γ and increased the percentage of CD4⁺ and CD8⁺ T cells [22]. The treatment of dairy cow mastitis usually uses antibiotics including penicillin, sulfonamides, tetracyclines, and glycopeptides [23]. However, the emergence of antibiotic resistance to *S. aureus* (such as methicillin-resistant *S. aureus*) complicates the treatment [24, 25]. Natural compounds have a variety of biological activities (anti-inflammatory, antioxidant, anticancer, etc.), which is a huge treasure house for screening potential mastitis treatment drugs.

Vitexin (8-beta-D-glucopyranosyl-apigenin) is an apigenin flavonoid glycoside found in food and medicinal plants, which has a variety of pharmacological effects, including anti-inflammatory, anticancer, antioxidant, analgesic, and neuroprotective effects [26, 27]. Vitexin inhibited the recruitment of neutrophils and also regulated the transcription factors of proinflammatory mediators and reduced the expression of p-p38, p-ERK1/2, and p-JNK in LPS-induced cells [28]. Studies have reported that vitexin repressed the activation of TLR4/NF- κ B signaling pathway in colitis liver injury [29]. Many studies have also found that vitexin exerts anti-inflammatory effects on endothelial cell damage [30], acute lung injury [31], allergic asthma [32], and neuroinflammation [33]. Both *in vitro* and *in vivo* data show that vitexin can enhance the body's antioxidant capacity and reduce the occurrence of oxidative stress [34].

Vitexin has been proven to produce a powerful antioxidant defense by acting as an effective oxygen free radical scavenger to increase the activity of antioxidant enzymes and upregulate the protein of antioxidant reactions [35]. Based on the various biological activity properties of vitexin, we hypothesized that vitexin could improve the oxidative stress and inflammation induced by *S. aureus*.

In this study, to confirm the therapeutic effect of vitexin on mastitis stimulated by *S. aureus*, we simulated mastitis on cow mammary epithelial cells and mouse mammary glands *in vitro* and *in vivo* and explored the possible molecular mechanisms of vitexin exerting antioxidant and anti-inflammation.

2. Materials and Methods

2.1. High Pressure Liquid Chromatography (HPLC). HPLC was performed to measure vitexin purity. Briefly, vitexin was diluted to 0.5 mg/mL by the solution (methanol : DMSO : water = 6 : 2 : 2). 20 μ L vitexin was added to a SinoChrom ODS-BP chromatographic column (4.6 mm \times 250 mm, 5 μ m). Hereafter, the 0.1% phosphate water/acetonitrile mobile phase was used to elute. The flow rate was 1.0 mL/min, and the detection wavelength was 335 nm.

2.2. Cell Culture and Treatment. The cow mammary epithelial cell line MAC-T was purchased from the American Type Culture Collection (ATCC, USA). The cell culture method was referred to previous studies [36]. Briefly, cells were grown in DMEM/F-12 (1 : 1) medium (Gibco, USA) supplemented with 10% fetal bovine serum (FBS; AUSGENEX, AUS), 5 μ g/mL insulin (Biosharp, China), 5 mmol/L L-glutamine (Biosharp, China), 1 μ g/mL hydrocortisone (Sigma-Aldrich, USA), and 100 U/mL penicillin and 100 μ g/mL streptomycin (Invitrogen, USA) at 37°C incubator with 5% CO₂. *S. aureus* CVCC3051 strain was available at China Veterinary Culture Collection (CVCC, China), which was cultured with lysogeny broth (LB) and its colony forming unit (CFU) was calculated using the LB plate counting method. *S. aureus* was inactivated in a water bath at 85°C for 15 min and then diluted it with DMEM/F-12 medium according to CFU. MAC-T cells were seeded into a six-well plate at 5 \times 10⁵ cells/well. When the degree of cell fusion reached 60%-70%, *S. aureus* was added to the four wells of the six-well plate at a multiplicity of infection (MOI) of 100. After infected for 6 h, different concentrations of vitexin were added to the four wells, respectively. The six groups are (1) Control, (2) *S. aureus*, (3) *S. aureus*+10 μ M vitexin, (4) *S. aureus*+20 μ M vitexin, (5) *S. aureus*+40 μ M vitexin, and (6) 40 μ M vitexin. After incubating for another 24 h, cell samples were harvested for RNA or protein extraction.

2.3. Cell Counting Kit-8 (CCK-8) Assay. The effect of vitexin on the viability of MAC-T cells was analyzed by CCK-8. Detailed methods referred to previous research [37]. In short, MAC-T cells were planted into 96-well plates at a density of 1 \times 10⁴ cells/well, and then, the cells were treated with different concentrations of vitexin (0, 10, 20, and 40 μ M) for 24 h. 10 μ L CCK-8 reagent (Yeasen, Shanghai, China) was

TABLE 1: Primers used for qPCR.

Species	Gene name	Primer sequence (5'-3')	GenBank accession number	Product size (bp)
Bos taurus	IL-1 β	Sense: GGCAACCGTACCTGAACCCA Antisense: CCACGATGACCGACACCACC	NM_174093.1	206
	IL-6	Sense: ATGCTTCCAATCTGGGTTCA Antisense: GAGGATAATCTTTGCGTTCTTT	NM_173923.2	268
	TNF- α	Sense: ACGGGCTTTACCTCATCTACTCA Antisense: GGCTCTTGATGGCAGACAGG	NM_173966.3	141
	GAPDH	Sense: TGCTGGTGCTGAGTATGTGGTG Antisense: CAGTCTTCTGGGTGGCAGTGAT	NM_001034034.2	296
Mus musculus	IL-1 β	Sense: TGCCACCTTTTGACAGTGATG Antisense: AAGGTCCACGGGAAAGACAC	NM_008361.4	220
	IL-6	Sense: TCTTGGGACTGATGCTGGTG Antisense: TTGCCATTGCACAACCTCTTTTC	NM_031168.2	178
	TNF- α	Sense: GGTCCCCAAAGGGATGAGAAGT Antisense: TTGCTACGACGTGGGCTACA	NM_013693.3	124
	GAPDH	Sense: AAGAGGGATGCTGCCCTTAC Antisense: CCAATACGGCCAAATCCGTTC	NM_001289726.1	123

added to each well and incubated at 37°C for 4 h. The microplate reader measured the OD value at 450 nm.

2.4. Flow Cytometry Analysis. Apoptosis was examined with Annexin V-FITC/PI Double Stain Apoptosis Detection Kit (BestBio, China). MAC-T cells were treated with *S. aureus* and/or vitexin, and then, the cells were digested and centrifuged to collect suspended cells. 400 μ L 1 \times Annexin V binding solution was used to resuspend the cells at a concentration of approximately 1×10^6 cells/mL. Then, 5 μ L Annexin V-FITC solution was added to the cell suspension, mixed gently, and incubated for 15 min at 4°C in the dark. Then, 5 μ L PI was added and incubated for 5 min at 4°C in the dark. Finally, the flow cytometer was hired immediately to obtain the results.

2.5. Mouse and Mastitis Animal Models. A total of 60 KM female mice (6-7 weeks old, 32-34 g weight) were gained and fed in Huazhong Agricultural University Laboratory Animal Research Center (Wuhan, China). All mice were allowed to obtain food and water ad libitum in the environment maintained at 25°C \pm 1°C and 65% humidity. All procedures of this study were carried out in accordance with standards provided by the Ethical Committee on Animal Research at Huazhong Agricultural University.

All mice were randomly divided into 6 groups: control group, *S. aureus* group, *S. aureus* + vitexin (15, 30, and 60 mg/kg) groups, and vitexin (60 mg/kg) group. *S. aureus* was injected into the mammary ducts of mice to produce mastitis in mice according to previous studies [7]. Vitexin was diluted with sterile PBS to 20 mg/mL. After mouse mammary gland infection with *S. aureus* for 24 h, the control group was intraperitoneally injected with sterile PBS. As the previous study described the dosage of vitexin [38, 39], the *S. aureus* + vitexin (15, 30, and 60 mg/kg) groups were intraperitoneally injected with vitexin at different doses (15, 30, and 60 mg/kg); the vitexin (60 mg/kg) group was

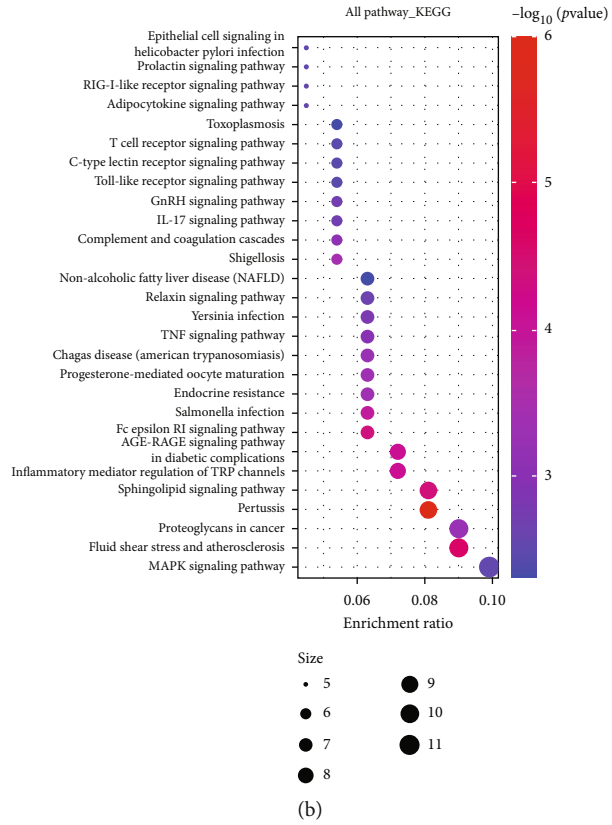
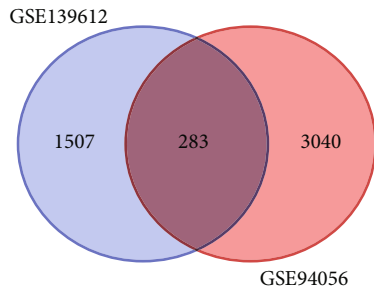
intraperitoneally injected with vitexin at 60 mg/kg. All groups were injected three times with an interval of 8 h. Then, the mice were euthanized at 8 h after the last drug treatment, and breast tissues were harvested and stored at -80°C refrigerator.

2.6. Hematoxylin and Eosin (H&E) Staining. H&E staining was used to evaluate the histopathology of *S. aureus* infection in mouse breast tissue. The experimental method was in accordance with the previous research [40]. In short, the collected fresh mouse breast tissue was immediately fixed in 4% paraformaldehyde solution, paraffin embedded, sectioned, transparent, dehydrated, and H&E stained. Finally, the histopathological changes were checked by an optical microscope.

2.7. Myeloperoxidase (MPO) Activity. MPO Assay Kit (Nanjing Jiancheng Bioengineering Institute, China) was bought to detect MPO activity. The mouse mammary gland tissue was accurately weighed, and the homogenization medium ($w : v = 1 : 19$) was added to prepare a 5% tissue homogenate.

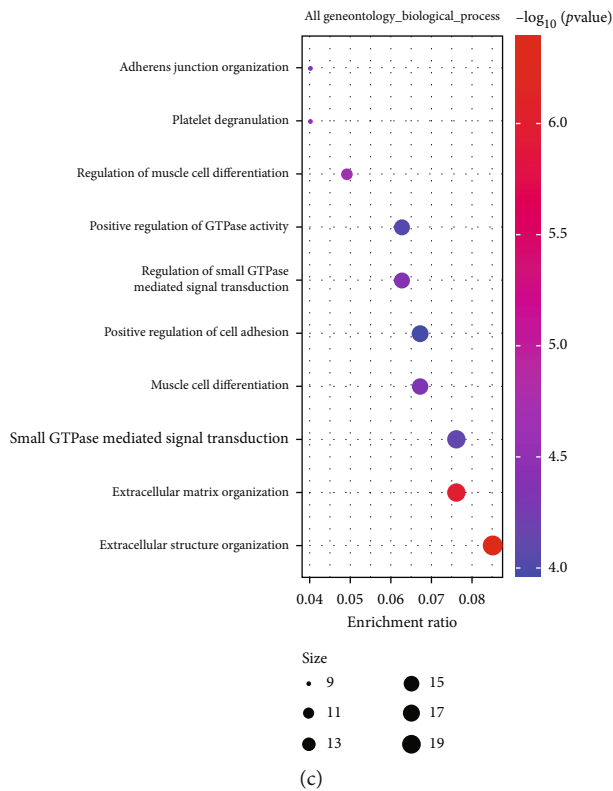
2.8. Enzyme-Linked Immunosorbent Assay (ELISA). The effect of vitexin on proinflammatory cytokine production was examined in *S. aureus* challenge-MAC-T cells and mouse breast tissues. The concentration of TNF- α , IL-1 β , and IL-6 was detected by ELISA kits (BioLegend, San Diego, CA, USA) following the manufacturer's instructions.

2.9. ROS Detection. Intracellular ROS level was measured with DHE-ROS Detection Kit (BestBio, Shanghai, China) according to the manufacturer's manual. Briefly, MAC-T cells were pretreated for 30 min with GW9662 (10 μ M) or GW1929 (10 μ M) to downregulate or upregulate the expression of PPAR γ , respectively. Cells were stimulated with *S. aureus* to mimic inflammatory stimulation and then treated with vitexin (40 μ M) for 24 h. The DHE probe was diluted

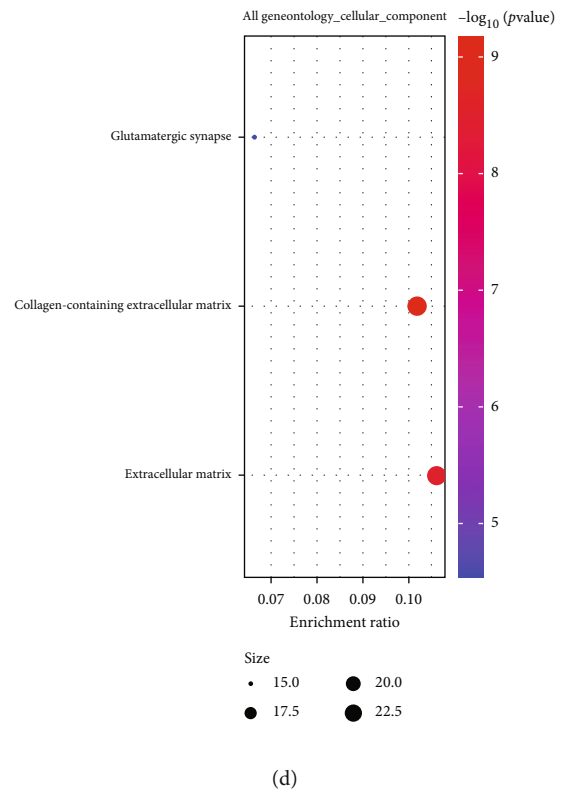


(a)

(b)



(c)



(d)

FIGURE 1: Continued.

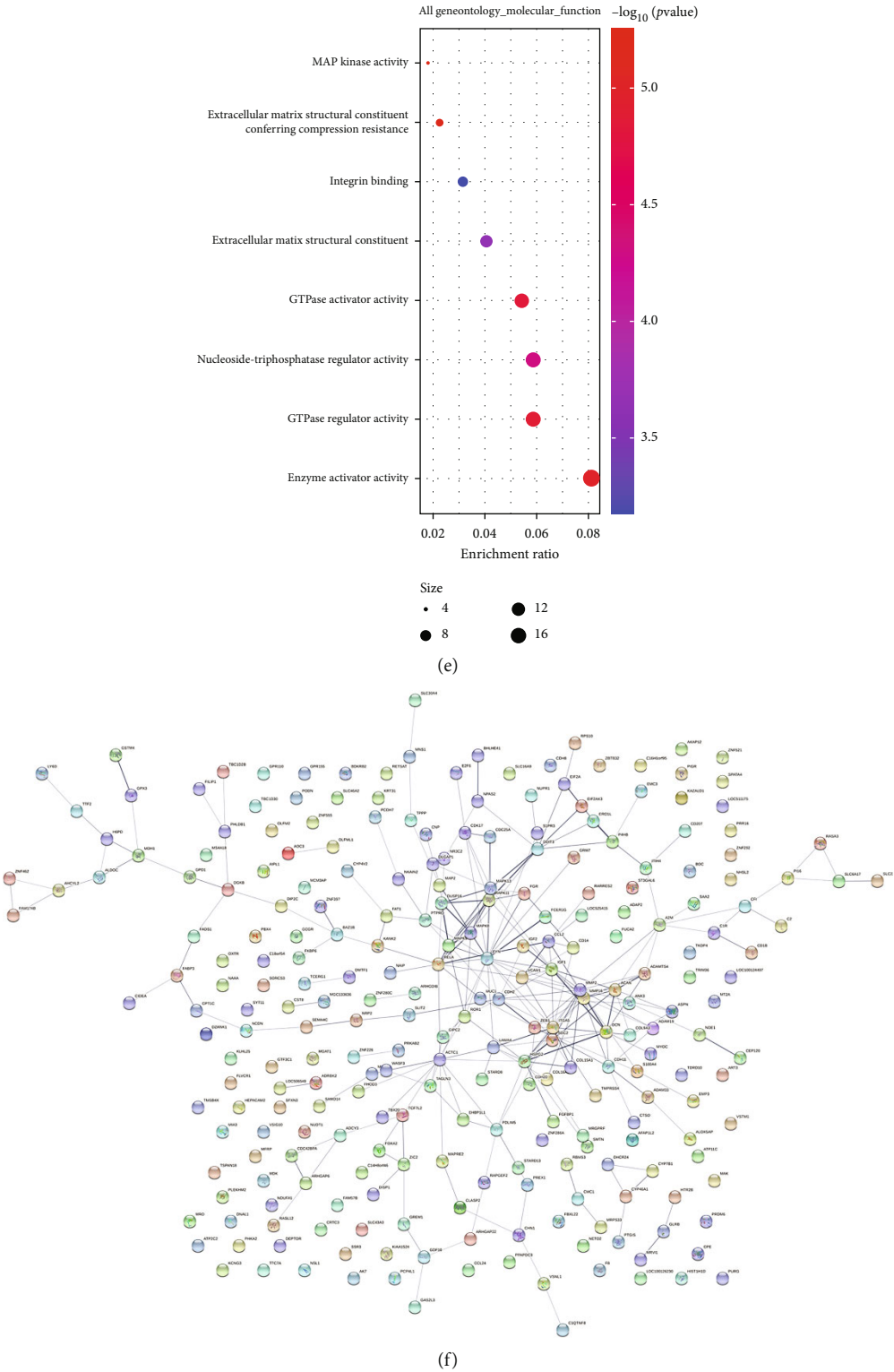


FIGURE 1: Continued.

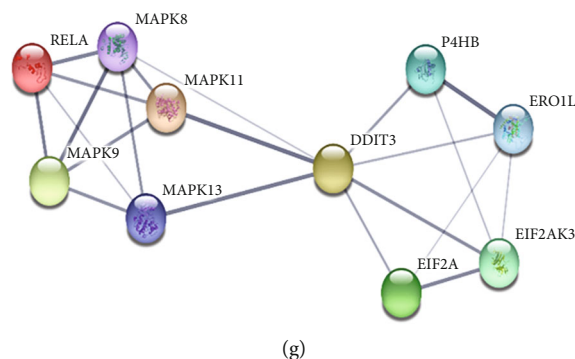


FIGURE 1: DEG analysis of *S. aureus*-induced mastitis from GEO database. (a) The Venn diagram displayed the distribution of DEGs in two GEO datasets (GSE94056 and GSE139612). (b) KEGG enriched these common DEG pathways. (c–e) GO enrichment analysis on 283 DEGs, including biological process, cellular components, and molecular functions. (f) The interaction between 283 DEGs was analyzed through the STRING database. (g) Emphasized the interaction relationship with CHOP- (DDIT3-) related DEGs.

1000 times with DMEM/F-12 medium and then added to the cells to continue to incubate in the dark for 30 min at 37°C. The cells were washed with PBS to remove the DHE probe and finally observed with a fluorescence microscope at the excitation wavelength (Ex) of 535 nm and the emission wavelength (Em) of 610 nm.

Tissue ROS Detection Kit (BBoxiProbe O13®) was obtained from BestBio (Shanghai, China). The harvested fresh mouse mammary gland tissue was accurately weighed and then prepared into a homogenizer with a glass homogenizer. The homogenate supernatant was collected by centrifugation and added into 96-well plate with 2 μ L probe O13. After incubating for 30 min at 37°C in the dark, the fluorescence intensity was detected with a fluorescence microplate reader at Ex/Em = 535/610 nm.

2.10. Antioxidant Biochemical Indicators. Total antioxidant capacity (T-AOC), superoxide dismutase (SOD), glutathione peroxidase (GSH-PX), catalase (CAT), and malondialdehyde (MDA) were determined to assess antioxidant capacity. T-AOC assay kit, SOD assay kit (WST-1 method), GSH-PX assay kit, CAT assay kit (visible light), and MDA assay kit (TBA method) were bought from Nanjing Jiancheng Bioengineering Institute (Nanjing, China), and the inspection process was carried out in accordance with the instructions.

2.11. Real Time-Quantitative Polymerase Chain Reaction (RT-qPCR). The total RNA of mouse mammary gland tissue and MAC-T cells was extracted with TRIzol reagent (Solarbio, Beijing). Q5000 ultramicro spectrophotometer (Quawell, USA) was used to evaluate RNA purity and measure RNA concentration. Hifair® III 1st Strand cDNA Synthesis SuperMix for qPCR (gDNA digester plus) and Hieff® qPCR SYBR® Green Master Mix were acquired from Yeasen (Shanghai, China) and used to examine target gene expression by qPCR with $2^{-\Delta\Delta C_q}$ method. The primers used in this study are shown in Table 1.

2.12. Western Blot. The total protein of mouse breast tissues and MAC-T cells was separated by RIPA reagent (Biosharp, China). The BCA Protein Assay Kit (Thermo Scientific, MA,

USA) was performed to detect protein concentration. The protein was separated by sodium dodecyl sulfate-polyacrylamide gel electrophoresis (SDS-PAGE); then, polyvinylidene difluoride (PVDF) membranes were used to receive the transferred protein from the gel. The membranes were blocked with 5% skimmed milk for 2 h; then, the primary antibodies (BiP, Ero1-L α , PDI, IRE1 α , PERK, CHOP, JNK, ERK, p38, p65, and β -actin from Cell Signaling Technology, USA; PPAR γ from Abcam, UK) were incubated at 4°C overnight, and then, the secondary antibody (anti-rabbit IgG and HRP-linked antibody from Cell Signaling Technology, USA) was incubated at 37°C for 1 h. Finally, the immunoblot signal was displayed with ECL ultrasensitive chemiluminescent solution with chemiluminescence imaging system.

2.13. Bioinformatics Analysis. Expression profiles of *S. aureus*-infected bovine mammary epithelial cells and glandular cistern (GSE94056 and GSE139612) were downloaded from the GEO dataset (<https://www.ncbi.nlm.nih.gov/gds/?term=>). Differentially expressed genes (DEGs) were screened from these two datasets, and common DEGs were further analyzed by the online tool Draw Venn Diagrams (<http://bioinformatics.psb.ugent.be/webtools/Venn/>). Gene Ontology Resource (GO, <http://geneontology.org/>) and Kyoto Encyclopedia of Genes and Genomes (KEGG, <https://www.kegg.jp/>) were used to analyze GO and KEGG enrichment of common DEGs. In addition, protein-protein interaction (PPI) network was built by STRING database (<https://string-db.org/>).

The druggability of vitexin was assessed by the Traditional Chinese Medicine System Pharmacology Database (TCMSP, <https://tcmsp.com/>), and the potential targets of vitexin were identified using SwissTarget Prediction (<http://www.swisstargetprediction.ch/>).

2.14. Statistical Analysis. Statistical analysis was processed with the GraphPad Prism 9.00 software. Statistical data were expressed as mean \pm SEM of three individual experiments. After the normality test, differences between groups were analyzed by one-way ANOVA or Student's *t*-tests. #*p* < 0.01 vs. the control group, **p* < 0.05 vs. the *S. aureus* group, and ***p* < 0.01 vs. the *S. aureus* group.

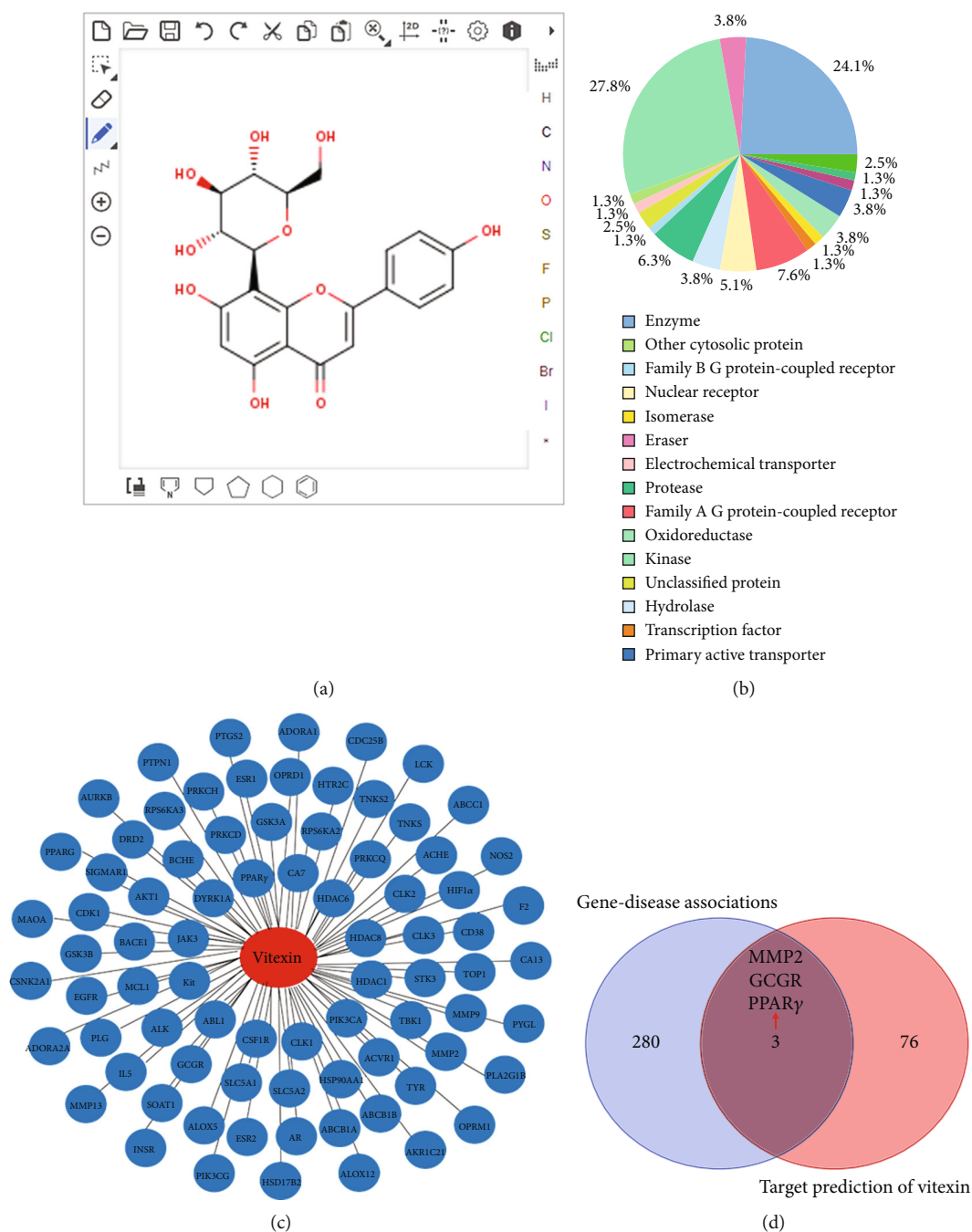


FIGURE 2: Network pharmacology analysis of vitexin. (a) The chemical structural formula of the searched molecule. (b) The target classes of vitexin. (c) The potential targets of vitexin were predicted on the SwissTarget Prediction. (d) The common target genes of vitexin and *S. aureus*-induced mastitis.

3. Results

3.1. DEG Analysis of *S. aureus*-Induced Mastitis from GEO Database. Given that the host infection event usually undergoes a large number of complex gene expression changes, we analyzed the expression profiles of bovine mammary epithelial cell and gland cistern infected with *S. aureus* from the GEO dataset (GSE94056 and GSE139612) [41, 42]. In these two GEO datasets, GEO2R was used to analyze the DEGs [43, 44]. Furthermore, the intersection of these DEGs

was calculated through drawing Venn diagrams. The DEGs of two GEO datasets contained 283 identical DEGs (Figure 1(a)). These 283 DEGs were further analyzed by KEGG and GO enrichment. We found that these DEGs mainly involve innate immunity and apoptosis signaling pathways (MAPK signaling pathway, TNF signaling pathway, Toll-like receptor signaling pathway, RIG-I-like receptor signaling pathway, etc.) (Figure 1(b)). The biological process that DEGs participated in included extracellular structure organization, extracellular matrix organization,

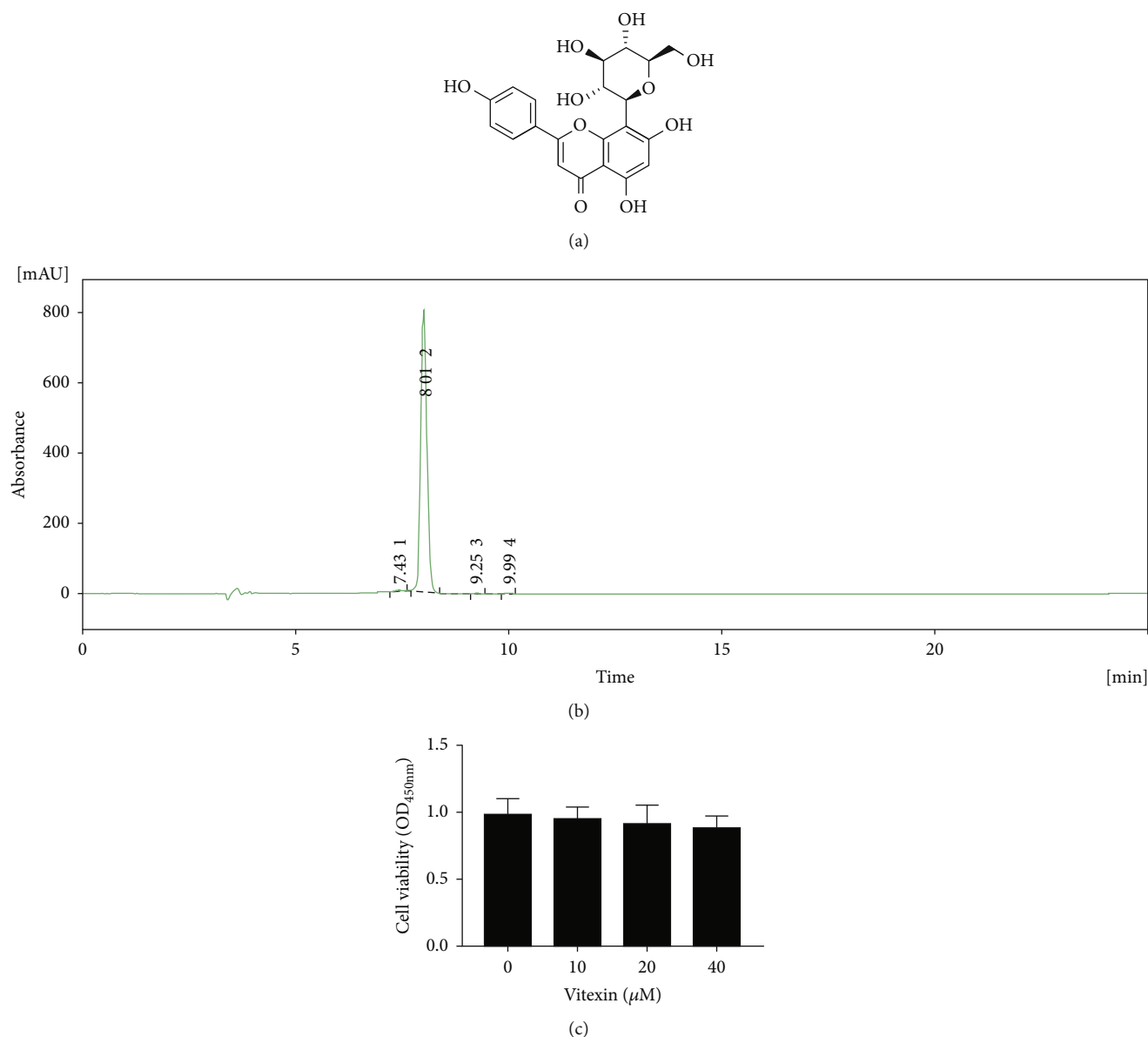


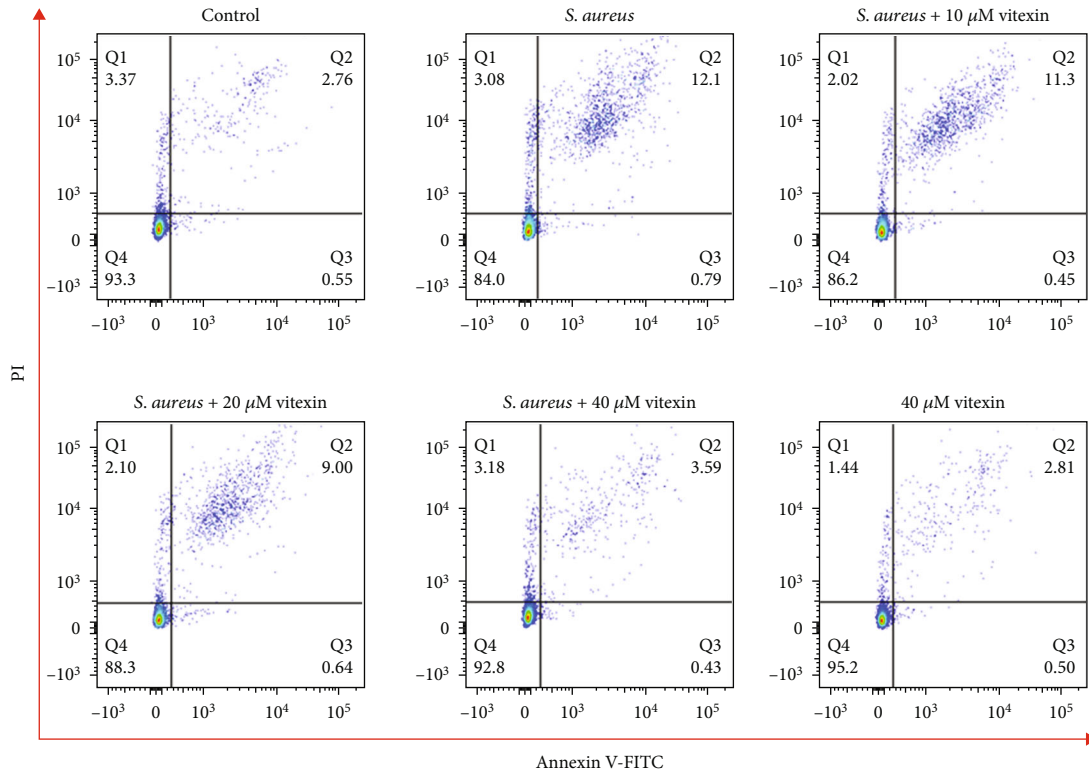
FIGURE 3: The purified substance vitexin had no effect on the viability of MAC-T cells. (a) The chemical structure of vitexin. (b) HPLC for purity inspection of vitexin. (c) CCK-8 assessed the effect of vitexin on the viability of MAC-T cells.

small GTPase-mediated signal transduction, muscle cell differentiation, positive regulation of cell adhesion, regulation of small GTPase-mediated signal transduction, positive regulation of GTPase activity, regulation of muscle cell differentiation, platelet degranulation, and adherens junction organization (Figure 1(c)). These DEGs were involved in the extracellular matrix, collagen-containing extracellular matrix and glutamatergic synapses in cellular components term (Figure 1(d)). The molecular functions of these DEGs were enzyme activator activity, GTPase regulator activity, nucleoside-triphosphatase regulator activity, GTPase activator activity, extracellular matrix structural constituent, integrin binding, extracellular matrix structural constituent, conferring compression resistance, and MAP kinase activity (Figure 1(e)). To further explore the interaction between these DEGs, we used the STRING database to build an inter-

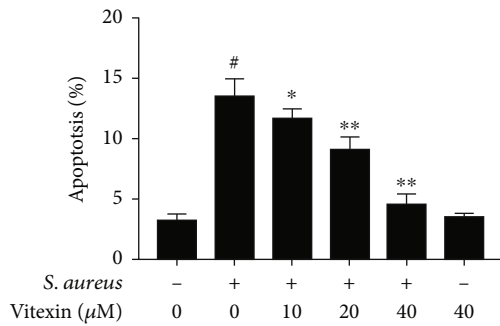
action network diagram (Figure 1(f)) and built an interaction network diagram for the extremely significant DEGs separately (Figure 1(g)).

3.2. Network Pharmacology Analysis of Vitexin. As displayed in Figure 2, our results showed that vitexin has good druggability with 79 potential target genes. There were three target genes (PPAR γ , MMP2, and GCGR) that intersect with common DEGs, among which PPAR γ was involved in oxidative stress.

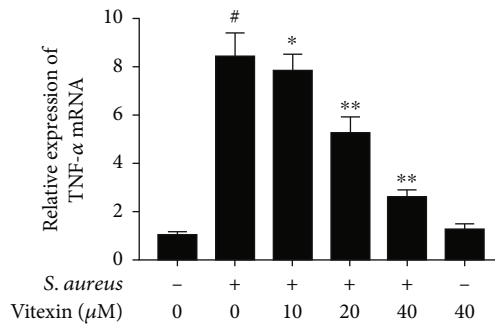
3.3. The Purified Substance Vitexin Had No Effect on the Viability of MAC-T Cells. Vitexin is the natural 8-C glucoside of the flavone apigenin (mung bean [45], chia leaf [46], *Prosopis cineraria* leaves [47], etc.), which is very likely to become a natural antioxidant. As illustrated in Figure 3(a),



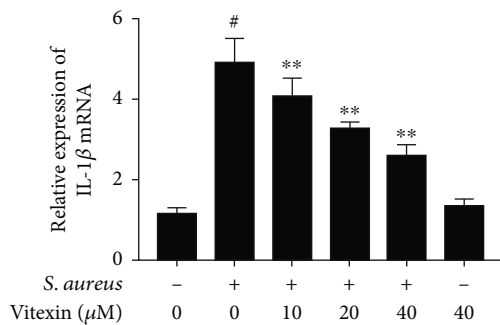
(a)



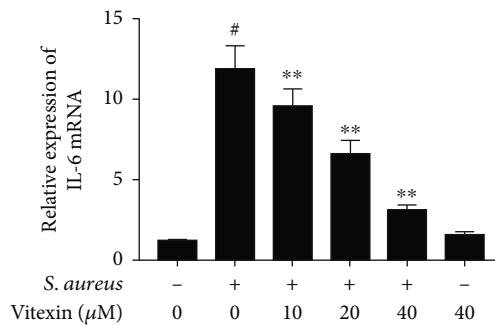
(b)



(c)



(d)



(e)

FIGURE 4: Continued.

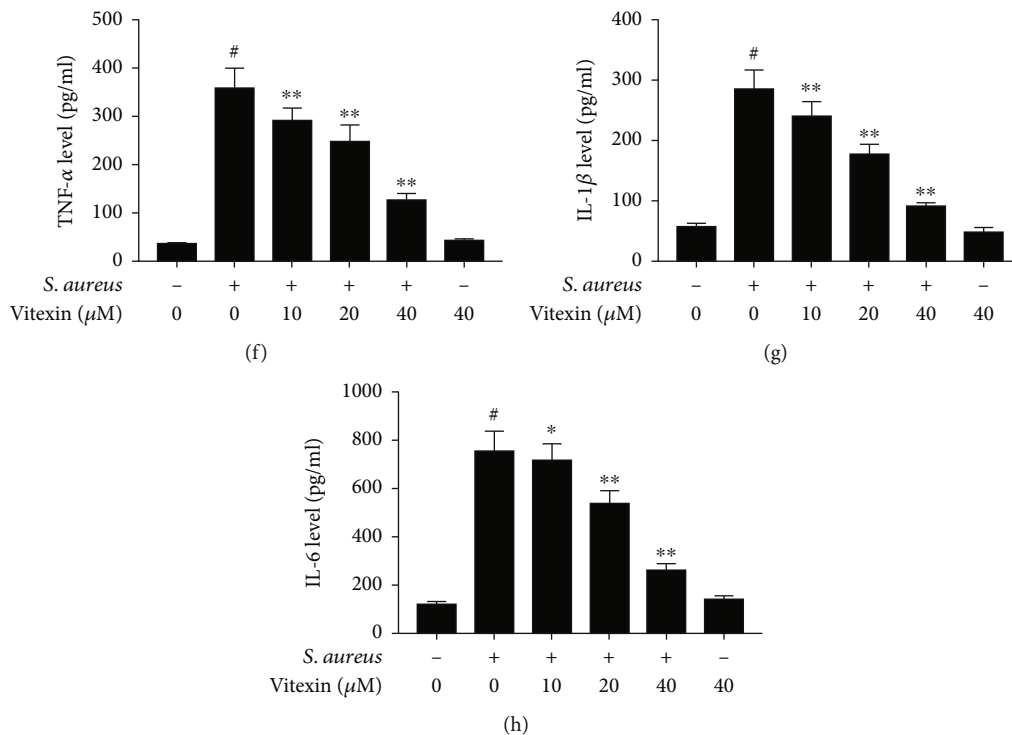
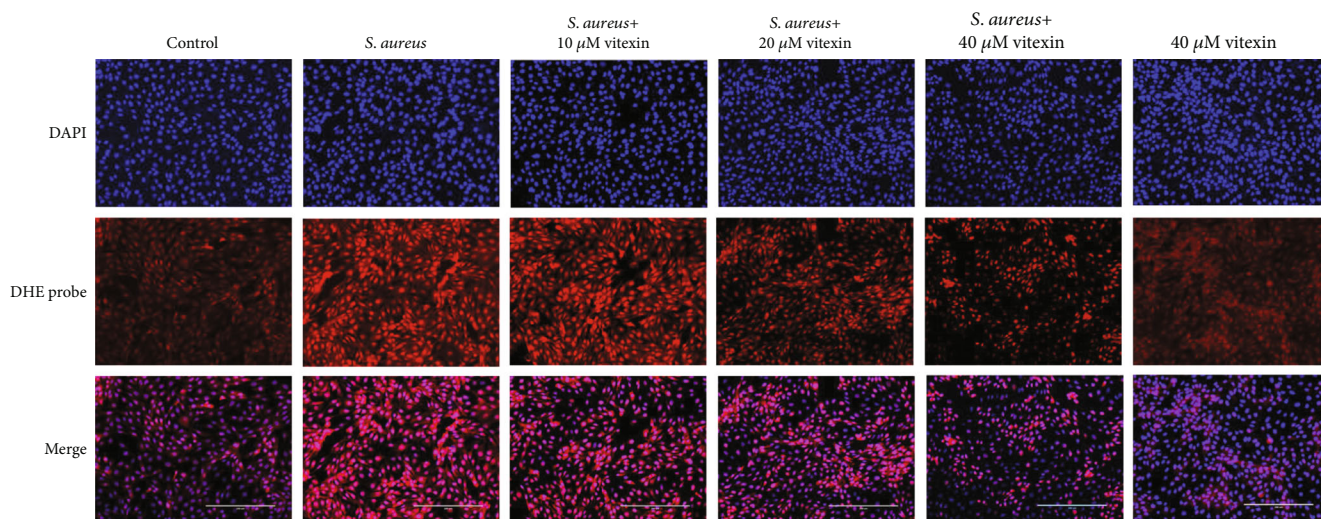


FIGURE 4: Vitexin ameliorated cell damage on *S. aureus* challenged-MAC-T cells. (a) MAC-T cells were stimulated with *S. aureus* at MOI of 100 for 6 h. And then, different concentrations of vitexin (10, 20, and 40 μM) were added to cocubate for 24 h. Flow cytometry was used to evaluate the effect of vitexin on the apoptosis of MAC-T cells stimulated by *S. aureus*. The horizontal axis represented Annexin V-FITC, and the vertical axis expressed PI. (b) Flow cytometry results were statistically analyzed for apoptosis rate by the GraphPad Prism 9.00 software. (c–e) The cells were dealt with *S. aureus* and/or vitexin; the relative expression of TNF- α , IL-1 β , and IL-6 mRNA was examined by RT-qPCR. GAPDH served as an internal reference gene. (f–h) The proinflammatory factors produced were tested by ELISA. Data were presented as means \pm SEM of three independent experiments. [#] $p < 0.01$ vs. the control group. ^{*} $p < 0.05$ vs. the *S. aureus* group; ^{**} $p < 0.01$ vs. the *S. aureus* group.

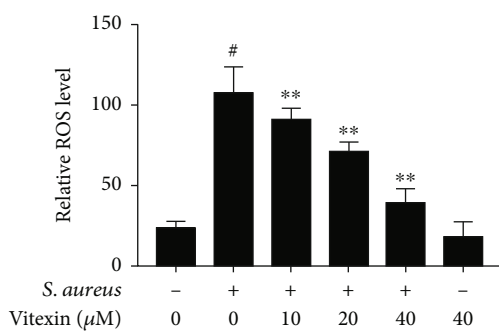
vitexin is a flavone glucoside, also known as apigenin-8-C- β -D-glucopyranoside. The purity of the extracted vitexin was detected by HPLC, and the extract was found to be a high-purity vitexin (Figure 3(b)). For the follow-up *in vivo* and *in vitro* experiments of vitexin, we tested and analyzed the effect of vitexin on cytotoxicity through CCK-8. CCK-8 results showed that vitexin was not toxic to MAC-T cells at least in the concentration range below 40 μM (Figure 3(c)).

3.4. Vitexin Ameliorated Cell Damage on *S. aureus* Challenged-MAC-T Cells. MAC-T cells infected with *S. aureus* experienced significant apoptosis (Figure 4(a)). But vitexin reduced the apoptosis rate of *S. aureus*-infected MAC-T cells in a dose-dependent manner (Figure 4(b)). In addition, the level of proinflammatory cytokine production was evaluated in *S. aureus*-induced MAC-T cells by qPCR and ELISA. The mRNA level of proinflammatory cytokines was greatly increased under the stimulation of *S. aureus*. On the other hand, vitexin inhibited the production of inflammatory factors in a dose-dependent manner (Figures 4(c)–4(e)). The released TNF- α , IL-1 β , and IL-6 concentrations in the cell supernatant were evaluated by ELISA, whose results were consistent with the trend of qPCR (Figures 4(f)–4(h)).

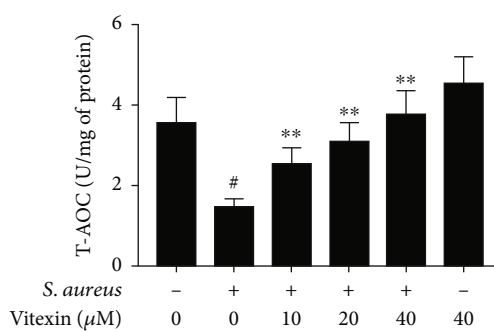
3.5. Vitexin Inhibited ROS Production on *S. aureus* Stimulated-MAC-T Cells. The level of intracellular ROS was evaluated by DHE probe, and the results revealed that *S. aureus* infection of MAC-T cells rapidly promoted the production of intracellular ROS. However, vitexin could effectively suppress the MAC-T cells stimulated by *S. aureus* to produce a large amount of ROS (Figures 5(a) and 5(b)). The body's antioxidant capacity is closely related to enzymes such as SOD, GSH-PX, and CAT, which eliminate free radicals and ROS so as not to trigger lipid peroxidation. We tested the T-AOC and the abovementioned enzyme activity. The T-AOC and enzyme activities of SOD, GSH-PX, and CAT in MAC-T cells stimulated by *S. aureus* were much lower than control, but vitexin obviously increased the T-AOC, SOD, GSH-PX, and CAT activities on *S. aureus* challenged-MAC-T cells (Figures 5(c)–5(f)). Conversely, vitexin prevented the production of MDA in a dose-dependent manner on MAC-T cells stimulated by *S. aureus* (Figure 5(g)). To further explore the mechanism of the antioxidant effect of vitexin, PPAR γ was predicted as an interacting protein by investigating the possible target genes of vitexin. Western blot results revealed that PPAR γ was inhibited after *S. aureus* infection, whereas vitexin greatly promoted



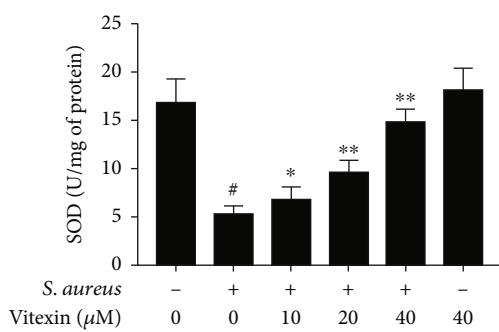
(a)



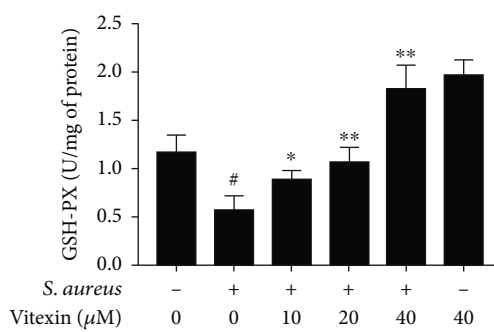
(b)



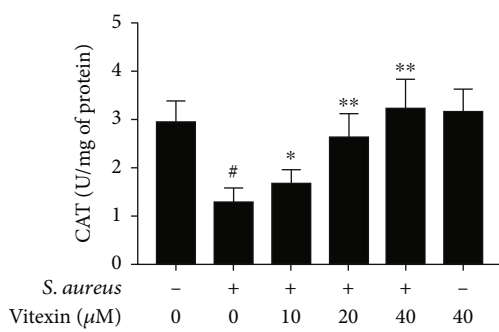
(c)



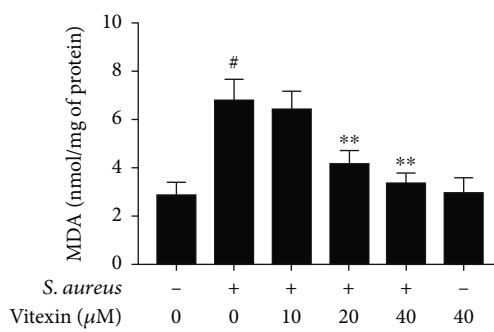
(d)



(e)



(f)



(g)

FIGURE 5: Continued.

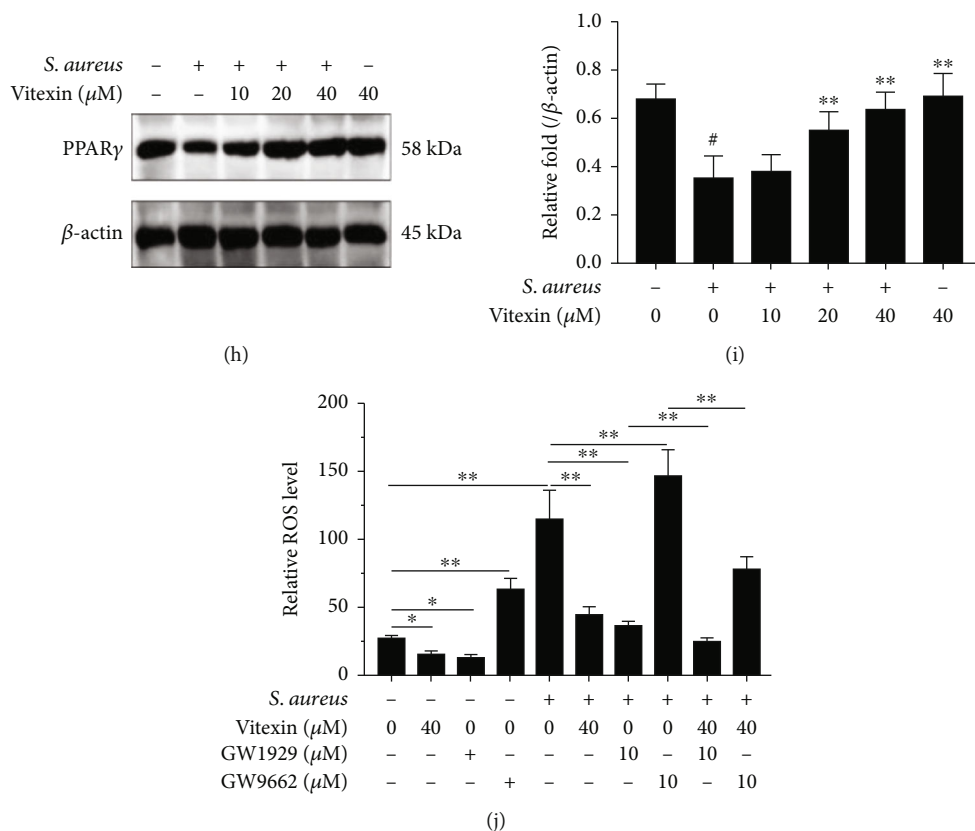


FIGURE 5: Vitexin inhibited ROS production on *S. aureus* stimulated-MAC-T cells. (a) The cells were stimulated with *S. aureus* for 6 h and then treated with different concentrations of vitexin (10, 20, and 40 μM) for 24 h. ROS red fluorescence was displayed with DHE probe. (b) ROS levels were quantified by the ImageJ software. Relative ROS levels were expressed as red fluorescence intensity/cell number. (c) The level of T-AOC. (d) The activity of SOD. (e) The activity of GSH-PX. (f) The activity of CAT. (g) The concentration of MDA. (h) Western blot detection of the expression level of PPAR γ . (i) PPAR γ gray values were measured by the ImageJ software. (j) MAC-T cells were pretreated with GW9662 (10 μM) or GW1929 (10 μM) for 30 min to downregulate or upregulate the expression of PPAR γ , respectively, then stimulated with *S. aureus* to mimic inflammatory stimulation, and finally treated with vitexin. ROS was detected with DHE probe. Data was expressed as means \pm SEM of three independent experiments. [#] $p < 0.01$ vs. the control group. ^{*} $p < 0.05$ vs. the *S. aureus* group; ^{**} $p < 0.01$ vs. the *S. aureus* group.

PPAR γ expression (Figures 5(h) and 5(i)). Agonists (GW1929) and antagonists (GW9662) of PPAR γ were hired to further study the effect of vitexin on PPAR γ . As shown in Figure 5(j), vitexin, like PPAR γ antagonists, reduced ROS levels in uninfected cells. ROS levels increased sharply under *S. aureus* stimulation, whereas agonists significantly reduced ROS levels in *S. aureus*-stimulated cells and were less effective than vitexin and agonist combination treatment. Meanwhile, PPAR γ antagonists accelerated the increase of ROS in *S. aureus*-infected cells, but when antagonists were used in combination with vitexin, GW9662 prevented the ROS inhibitory effect of vitexin under *S. aureus* challenge.

3.6. Vitexin Suppressed the Activation of MAPK and NF- κB Signaling Pathways by Blocking the ER Stress Caused by *S. aureus* on MAC-T Cells. To investigate the effect of vitexin on ER stress, ER stress-related proteins were examined by Western blot. The levels of BiP in *S. aureus*-infected cells were lower than normal cells, but vitexin greatly promoted their expression levels under the stimulation of *S. aureus*. Meanwhile, *S. aureus* infection drastically increased the

expression of PDI, Ero1- $\text{L}\alpha$, p-IRE1 α , PERK, p-eIF2 α , and CHOP, while vitexin repressed their expression (Figures 6(a) and 6(b)). In addition, Western blot was also hired to evaluate MAPK and NF- κB signaling pathways. The phosphorylation levels of JNK, ERK, p38, and p65 in *S. aureus*-induced MAC-T cells dramatically increased compared to the control. Reversely, vitexin significantly restricted the expression of p-JNK, p-ERK, p-p38, and p-p65 (Figures 6(c) and 6(d)).

3.7. Vitexin Improved *S. aureus*-Induced Mastitis in Mice. A mouse model of mastitis was established to assess the protective effect of vitexin. H&E staining was performed to evaluate the degree of damage to the mammary gland tissue of mice infected with *S. aureus*. As illustrated in Figure 7(a), the acinar cavity epithelial cells of mice mammary glands were attacked by *S. aureus* causing degeneration, necrosis, and even shedding to the acinar cavity. At the same time, the acinar cavity was also filled with serum and a large number of neutrophils and macrophages. Vitexin maintained the integrity of the acinar cavity epithelial cells and relieved the infiltration of inflammatory cells. Moreover, MPO was

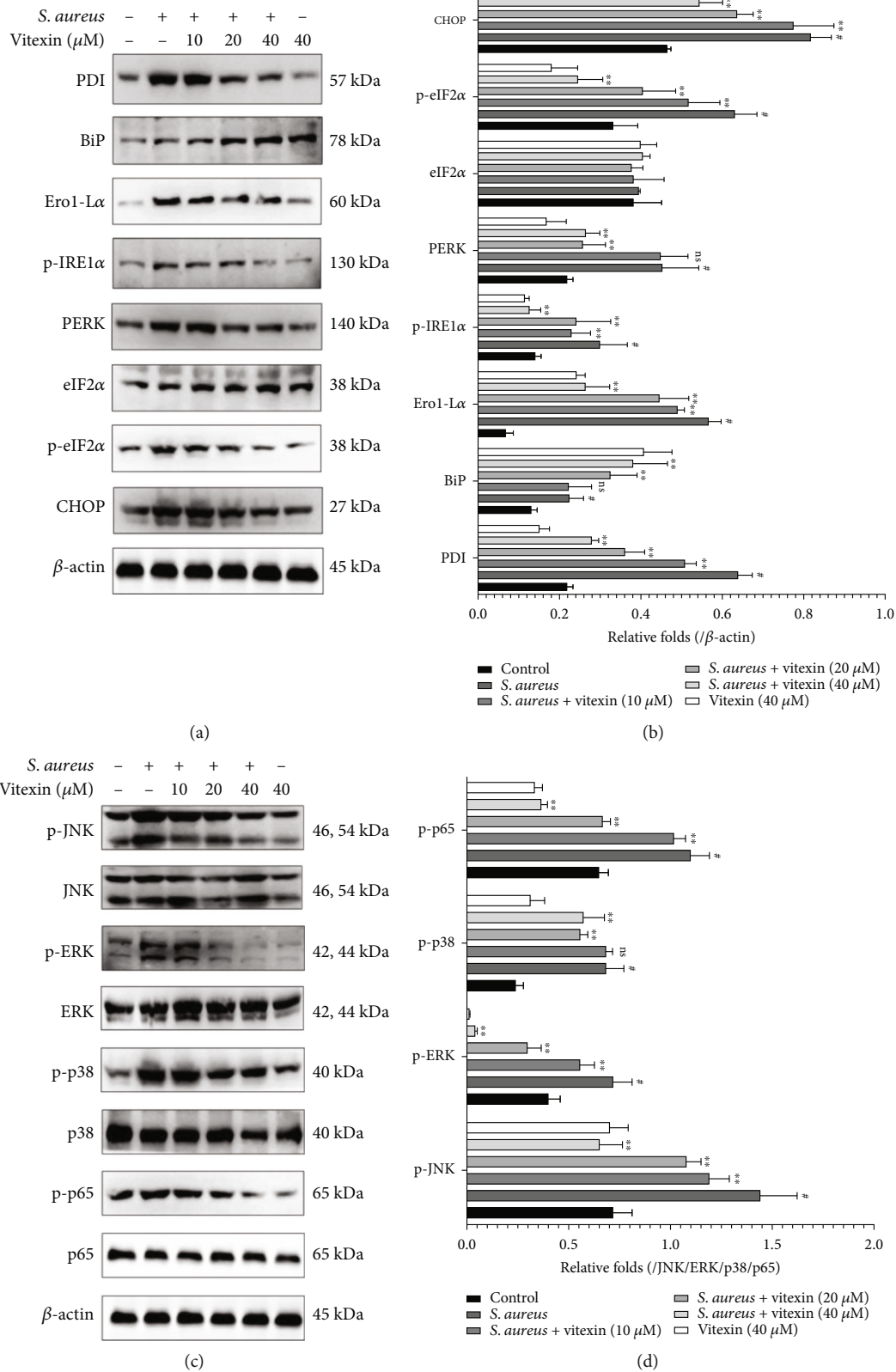


FIGURE 6: Vitexin suppressed the activation of MAPK and NF- κ B signaling pathways by blocking the ER stress caused by *S. aureus* on MAC-T cells. (a) The protein levels of PDI, BiP, Ero1- α , p-IRE1 α , PERK, p-eIF2 α , and CHOP were detected by Western blot on MAC-T cells. (c) The expression levels of JNK, ERK, p38, and p65 proteins in MAC-T cells were determined by Western blot. (b, d) Protein gray values were measured by the ImageJ software. Data was expressed as means \pm SEM of three independent experiments. * $p < 0.05$ vs. the *S. aureus* group; ** $p < 0.01$ vs. the *S. aureus* group.

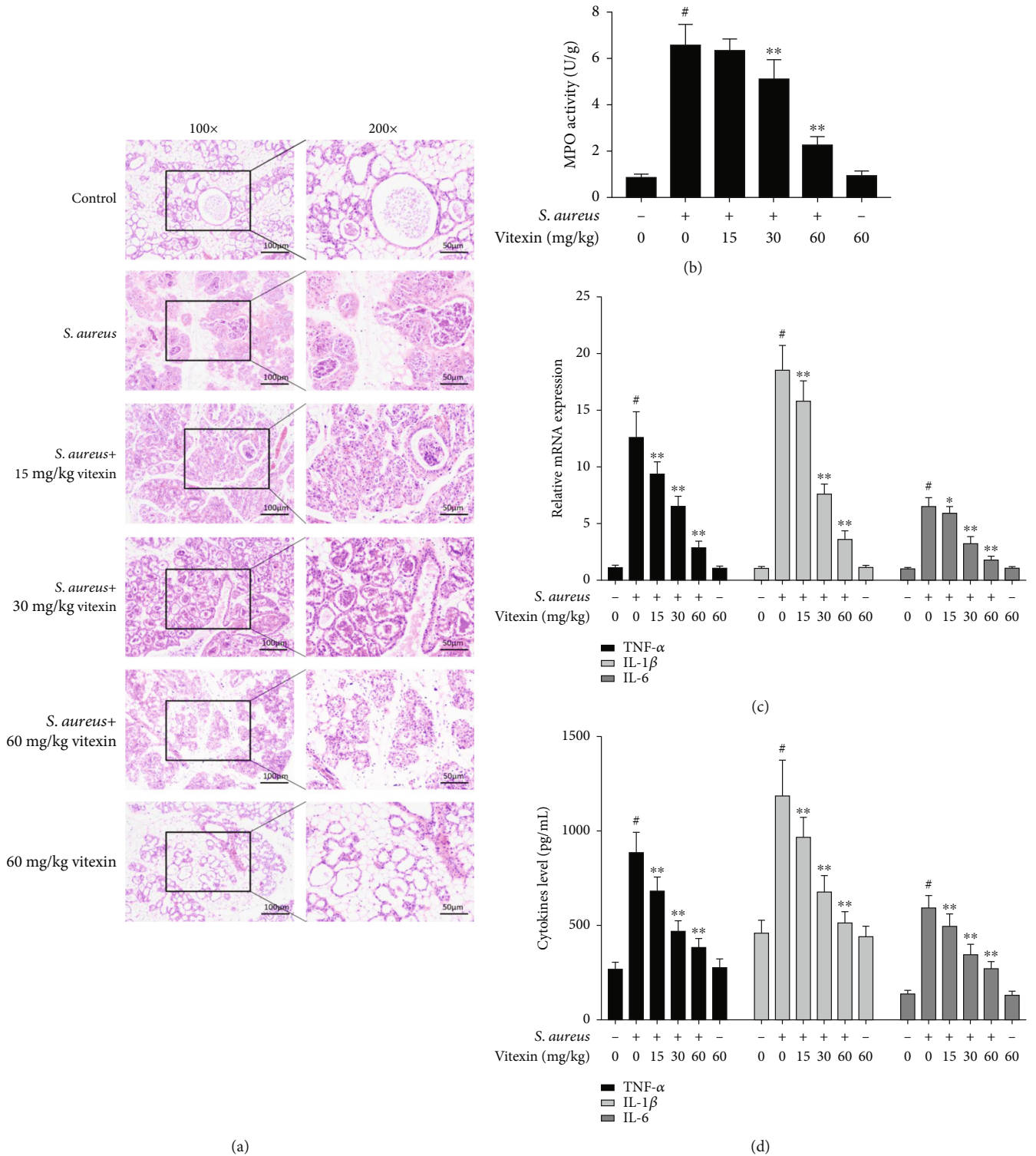


FIGURE 7: Vitexin improved *S. aureus*-induced mastitis in mice. All mouse mammary gland tissues were stimulated with *S. aureus* for 24 h, then intraperitoneally injected with different concentrations of vitexin (15, 30, and 60 mg/kg) three times. (a) Histopathological analysis of mammary gland tissues with H&E staining. Left images scale bar = 100 μ m, right large images scale bar = 50 μ m. (b) The activity of MPO. (c) The expression of TNF- α , IL-1 β , and IL-6 mRNA in vivo was measured by RT-qPCR. GAPDH was used as an endogenous control. (d) The proinflammation cytokines TNF- α , IL-1 β , and IL-6 in mammary gland tissues were detected by ELISA. Data was expressed as means \pm SEM of three independent experiments. [#] $p < 0.01$ vs. the control group. ^{*} $p < 0.05$ vs. the *S. aureus* group; ^{**} $p < 0.01$ vs. the *S. aureus* group.

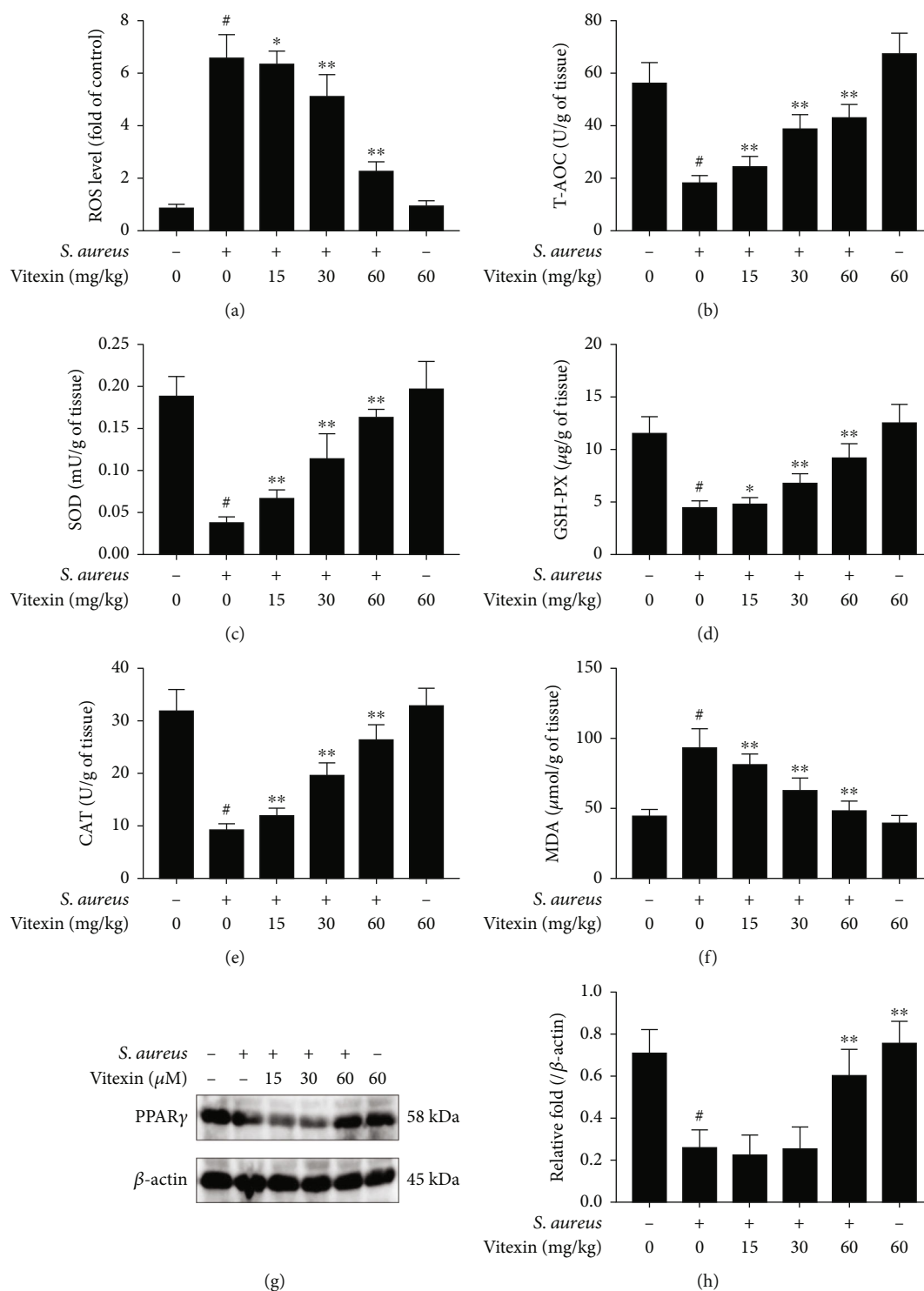


FIGURE 8: Vitexin reduced ROS production in mammary tissues of mice infected with *S. aureus*. (a) The level of tissue ROS. (b) The level of T-AOC. (c) The activity of SOD. (d) The activity of GSH-PX. (e) The activity of CAT. (f) The concentration of MDA. (g) PPAR γ protein was examined with Western blot. (h) PPAR γ gray values were calculated by the ImageJ software. Data was expressed as means \pm SEM of three independent experiments. #*p* < 0.01 vs. the control group. **p* < 0.05 vs. the *S. aureus* group; ***p* < 0.01 vs. the *S. aureus* group.

checked to evaluate the degree of inflammation in the mammary gland tissues, and the result indicated that vitexin remarkably suppressed MPO vitality in a dose-dependent manner (Figure 7(b)). In addition, qPCR and

ELISA were employed to examine proinflammatory cytokines (TNF- α , IL-1 β , and IL-6) which were depressed by vitexin both in mRNA and protein levels (Figures 7(c) and 7(d)).

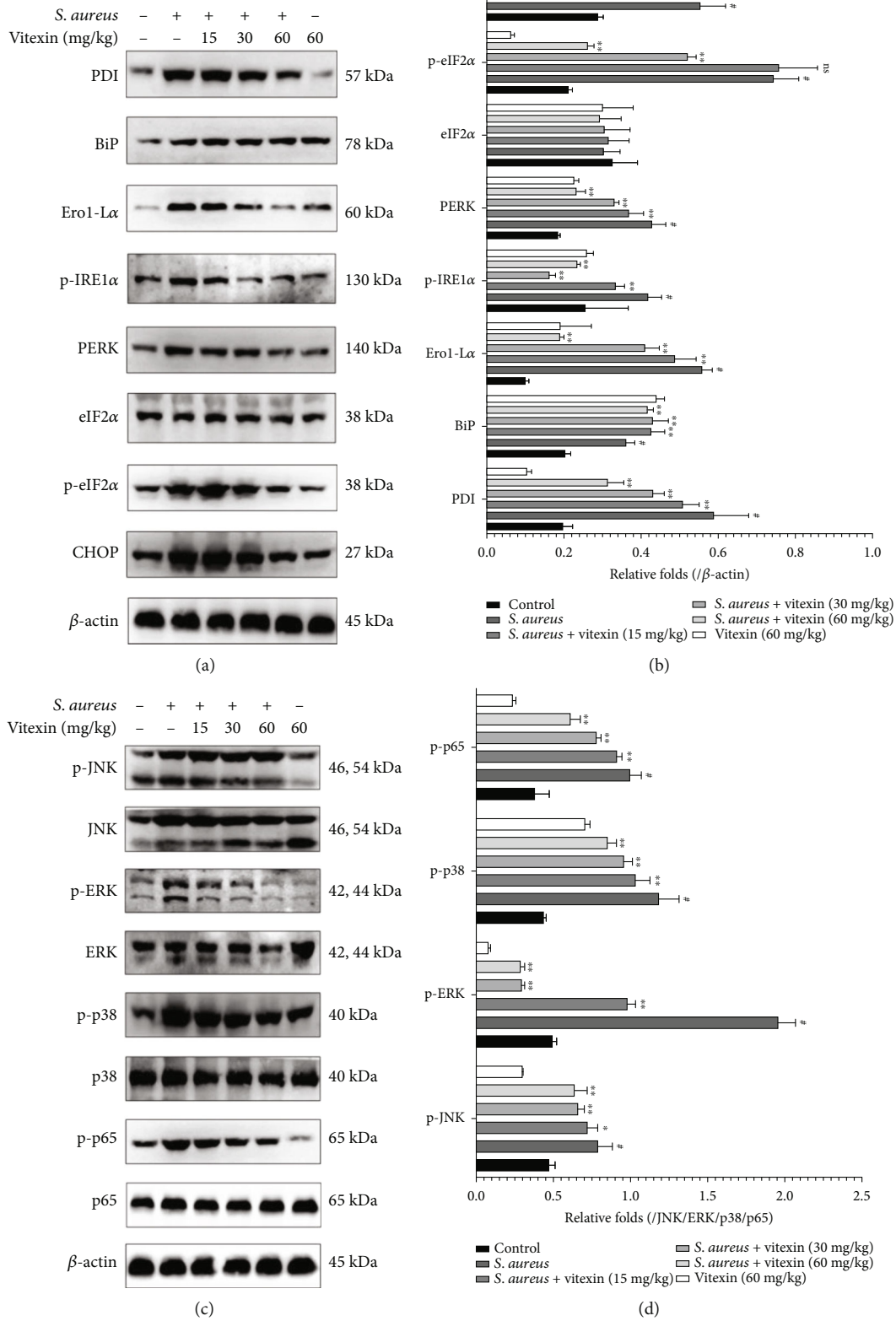


FIGURE 9: Vitexin relieved ER stress to inactivate MAPK and NF- κ B signaling pathways in *S. aureus*-induced mastitis on mice. (a) The protein levels of PDI, BiP, Ero1-L α , p-IRE1 α , PERK, p-eIF2 α , and CHOP in mammary gland tissues. (c) The expression levels of JNK, ERK, p38, and p65 proteins in mammary gland tissues. (b, d) Protein gray values were measured by the ImageJ software. Data was expressed as means \pm SEM of three independent experiments. # $p < 0.01$ vs. the control group. * $p < 0.05$ vs. the *S. aureus* group; ** $p < 0.01$ vs. the *S. aureus* group.

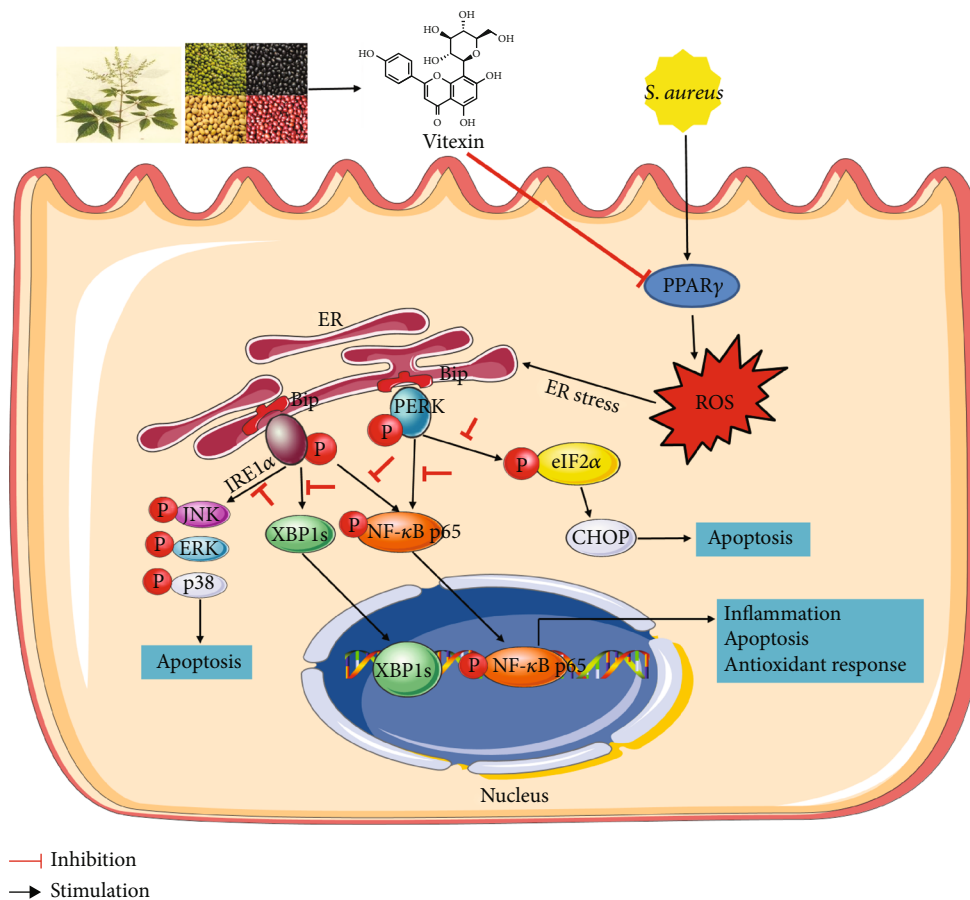


FIGURE 10: Schematic diagram of the therapeutic effect of vitexin on *Staphylococcus aureus*-induced mastitis. Vitexin inhibited the production of ROS by promoting PPAR γ activity, increased the activity of antioxidant enzymes, and reduced inflammatory cytokines and apoptosis by alleviating ER stress and inactivation MAPKs and NF- κ B signaling pathways.

3.8. Vitexin Reduced ROS Production in Mammary Tissues of Mice Infected with *S. aureus*. The tissue ROS and antioxidant capacity of mice with mastitis were determined. We found that *S. aureus* infected mouse mammary tissue strikingly increased the level of tissue ROS, whereas vitexin hindered the rise of ROS (Figure 8(a)). Furthermore, vitexin reversed *S. aureus* induced the fall of T-AOC (Figure 8(b)), SOD (Figure 8(c)), GSH-PX (Figure 8(d)), and CAT (Figure 8(e)). In contrast, MDA level was impeded by vitexin, compared with the *S. aureus* group (Figure 8(f)). PPAR γ protein levels were downregulated in *S. aureus*-infected cells, and vitexin reversed this decline (Figures 8(g) and 8(h)).

3.9. Vitexin Relieved ER Stress to Inactivate MAPK and NF- κ B Signaling Pathways in *S. aureus*-Induced Mastitis in Mice. To explore the molecular mechanism of vitexin's antioxidant and anti-inflammatory effects, Western blot was used to study the protein expression of ER stress and MAPK/NF- κ B pathway. As displayed in Figures 9(a) and 9(b), the expression of BiP in the mouse breast tissue stimulated by *S. aureus* was significantly reduced compared to the control group, while PDI, Ero1-L α , p-IRE1 α , PERK, and CHOP protein levels were restrained in the vitexin-treated mice with mastitis. Besides, p-JNK, p-ERK, p-p38, and p-

p65 proteins were decreased in the *S. aureus* + vitexin group compared with the *S. aureus* group (Figures 9(c) and 9(d)).

4. Discussion

Dairy cow mastitis drastically reduces milk production and milk quality, posing a serious threat to the economic benefits of the dairy industry [25, 48]. The decrease in milk production during mastitis in dairy cows is due to pathogens (such as *S. aureus* and *Escherichia coli*) that induce hypoxia, oxidative stress, and apoptosis, while suppressing the expression of milk genes (*Csn2*, *Lalba*, and *Csn1s1*) in the mammary gland [49, 50]. Through the analysis of the GEO dataset (GSE94056 and GSE139612), we also found that *S. aureus* infection caused a large number of DEGs in the bovine mammary gland tissues and cells, which are inseparable from the activation of oxidative stress induced-ER stress and inflammation-related signaling pathways. Therefore, looking for Chinese herbal medicines that have both antioxidant and anti-inflammatory properties is very likely to become drugs for the treatment of mastitis.

Vitexin, a natural flavonoid compound found in many plant species [35], has been widely reported to have antioxidant, anti-inflammatory, antiviral, neuroprotective, and

cardioprotective effects [27, 34]. However, few studies have explored the effect of vitexin on mastitis. In this study, in vivo and in vitro models of mastitis were successfully established. We found that vitexin reduced the production of ROS, protected the activity of antioxidant enzymes, and inhibited cell apoptosis and the production of proinflammatory cytokines in both MAC-T cell and mouse breast tissues. Previous studies have also confirmed that vitexin enhanced cell viability and/or decreased tissue damage by upregulating cell resistance to oxidative stress inducers [30, 31, 51]. Meanwhile, the anti-inflammatory activity of vitexin has attracted more and more attention, and there has been a lot of research involved. Vitexin downregulated the release of inflammatory cytokines (TNF- α , IL-1 β , and IL-6) and enzymes (iNOS) by regulating transcription factors and kinases (Nrf-2, NF- κ B, and MAPKs) [52, 53]. To explore the molecular mechanism of vitexin's antioxidation and anti-inflammation, we focused on the connection between ER stress and inflammation.

As a nuclear receptor transcription factor, PPAR γ is involved in the regulation of ROS by regulating redox and biosynthetic processes in mitochondria [54, 55]. Activation of PPAR γ inhibited oxidative stress and also negatively regulated the expression of AP-1, NF- κ B, and other inflammatory response genes [56]. In the present study, PPAR γ was found through the intersection of prediction target genes of vitexin and inflammatory disease-related genes. The expression level of PPAR γ was suppressed during *S. aureus* infection, while vitexin treatment enhanced its protein expression. Moreover, GW1929 significantly hindered the increase of ROS in *S. aureus*-infected cells. GW9662 reversed vitexin-induced ROS inhibition under *S. aureus*-stimulated conditions. From these results, we speculated that vitexin might alleviate oxidative stress by regulating PPAR γ . Oxidative stress is caused by the excessive production of ROS, which interferes with the ER protein folding mechanism to result in the accumulation of abnormal proteins in the ER, thereby causing ER stress [16, 52]. Our study found that vitexin significantly inhibited PDI, Ero1-L α , p-IRE1 α , PERK, and CHOP protein and promoted the expression of BiP in *S. aureus*-induced mastitis, suggesting that vitexin effectively prevented the production of ROS amplified by ER and programmed cell death triggered by CHOP.

ER stress is also involved in the regulation of immune signal pathways, such as MAPK and NF- κ B signaling pathways [57]. IRE1 α can stimulate the activation of apoptosis signal kinase-1 (ASK1) and then activate downstream kinases Jun-N-terminal kinase (JNK) and p38 mitogen-activated protein kinase (p38 MAPK) [21, 58]. In this study, p-JNK, p-ERK, and p-p38 were significantly increased under *S. aureus* challenge. Vitexin treatment downregulated MAPK signaling proteins in the infected group compared with the untreated group. Therefore, we conjectured that vitexin might reduce the production of inflammatory factors by inhibiting the activation of MAPKs. PERK can also indirectly induce NF- κ B through eIF2 α [59]. Vitexin inhibited p-p65 protein expression when *S. aureus* activated p65, indicating that vitexin alleviated inflammation and apoptosis partly by regulating the NF- κ B signaling pathway.

5. Conclusion

In summary, *S. aureus*-induced mastitis produced a large number of DEGs, which were mainly involved in immune signaling pathways, apoptosis, and ER stress. Vitexin could inhibit the production of ROS by promoting PPAR γ activity, increased the activity of antioxidant enzymes, and reduced inflammatory cytokines and apoptosis, possibly by alleviating ER stress and inactivation MAPKs and NF- κ B signaling pathway (Figure 10). Vitexin may become a potential drug for the treatment of mastitis in dairy cows.

Abbreviations

BiP:	Immunoglobulin heavy chain binding protein
CHOP:	C/EBP-homologous protein
DEGs:	Differentially expressed genes
ER:	Endoplasmic reticulum
Ero1-L α :	ER-residing protein endoplasmic oxidoreductin-1 like L α
GO:	Gene ontology
HPLC:	High pressure liquid chromatography
IRE1 α :	Inositol-requiring enzyme 1 α
JNK:	Jun N-terminal kinase
KEGG:	Kyoto Encyclopedia of Genes and Genomes
MAPK:	Mitogen-activated protein kinase
MPO:	Myeloperoxidase
NF- κ B:	Nuclear factor-kappa B
PPI:	Protein-protein interaction network
PPAR γ :	Peroxisome proliferator-activated receptor
PDI:	Protein disulfide isomerase
PERK:	Protein kinase R- (PKR-) like endoplasmic reticulum kinase
ROS:	Reactive oxygen species
<i>S. aureus</i> :	<i>Staphylococcus aureus</i>
UPR:	Unfolded protein response.

Data Availability

The data used to support the findings of this study are available from the corresponding author upon request.

Conflicts of Interest

The authors declare no conflict of interests.

Authors' Contributions

Y. C., G. D., and C. Q. conceived and designed the experiments. Y. C., J. Y., Z. H., B. Y., C. Y., and H. J. carried out the experiments. Y. C., J. Y., T. U., and S. G. processed the data. Y. C. wrote the paper. Y. C., T. U., X. Z., and M. G. revised the manuscript. The final manuscript was read and approved by all authors.

Acknowledgments

This work was funded by the National Natural Science Foundation of China (No. 32172925).

References

- [1] J. Kadariya, T. C. Smith, and D. Thapaliya, "Staphylococcus aureus and staphylococcal food-borne disease: an ongoing challenge in public health," *BioMed Research International*, vol. 2014, Article ID 827965, 9 pages, 2014.
- [2] G. Abril, T. G. Villa, J. Barros-Velázquez et al., "Staphylococcus aureus exotoxins and their detection in the dairy industry and mastitis," *Toxins*, vol. 12, no. 9, p. 537, 2020.
- [3] K. Artursson, R. Söderlund, L. Liu, S. Monecke, and J. Schelin, "Genotyping of Staphylococcus aureus in bovine mastitis and correlation to phenotypic characteristics," *Veterinary Microbiology*, vol. 193, pp. 156–161, 2016.
- [4] K. Tam and V. J. Torres, "Staphylococcus aureus secreted toxins and extracellular enzymes," *Microbiology spectrum*, vol. 7, no. 2, p. 10, 2019.
- [5] S. Denayer, L. Delbrassinne, Y. Nia, and N. Botteldoorn, "Food-borne outbreak investigation and molecular typing: high diversity of Staphylococcus aureus strains and importance of toxin detection," *Toxins*, vol. 9, no. 12, p. 407, 2017.
- [6] W. R. Schwan, "Staphylococcus aureus toxins: armaments for a significant pathogen," *Toxins*, vol. 11, no. 8, p. 457, 2019.
- [7] Y. Chen, Y. Wang, M. Yang, and M. Y. Guo, "Allicin inhibited Staphylococcus aureus-induced mastitis by reducing lipid raft stability via LxR α in mice," *Journal of Agricultural and Food Chemistry*, vol. 67, no. 39, pp. 10863–10870, 2019.
- [8] Z. B. Zhang, Y. F. Guo, C. Y. Li, C. W. Qiu, and M. Y. Guo, "Selenium influences mmu-miR-155 to inhibit inflammation in Staphylococcus aureus-induced mastitis in mice," *Food & Function*, vol. 10, no. 10, pp. 6543–6555, 2019.
- [9] W. N. Beavers and E. P. Skaar, "Neutrophil-generated oxidative stress and protein damage in Staphylococcus aureus," *Pathogens and disease*, vol. 74, no. 6, p. ftw060, 2016.
- [10] I. Sadowska-Bartosz, S. Galiniak, G. Bartosz, and M. Rachel, "Oxidative modification of proteins in pediatric cystic fibrosis with bacterial infections," *Oxidative Medicine and Cellular Longevity*, vol. 2014, Article ID 389629, 10 pages, 2014.
- [11] M. Muzila, K. Rumpunen, H. Wright et al., "Alteration of neutrophil reactive oxygen species production by extracts of devil's claw (Harpagophytum)," *Oxidative Medicine and Cellular Longevity*, vol. 2016, Article ID 3841803, 9 pages, 2016.
- [12] H. M. Zeeshan, G. H. Lee, H. R. Kim, and H. J. Chae, "Endoplasmic reticulum stress and associated ROS," *International Journal of Molecular Sciences*, vol. 17, no. 3, p. 327, 2016.
- [13] C. D. Ochoa, R. F. Wu, and L. S. Terada, "ROS signaling and ER stress in cardiovascular disease," *Molecular Aspects of Medicine*, vol. 63, pp. 18–29, 2018.
- [14] Y. Lin, M. Jiang, W. Chen, T. Zhao, and Y. Wei, "Cancer and ER stress: mutual crosstalk between autophagy, oxidative stress and inflammatory response," *Biomedicine & pharmacotherapy = Biomedecine & pharmacotherapie*, vol. 118, article 109249, 2019.
- [15] M. Mayer, U. Kies, R. Kammermeier, and J. Buchner, "BiP and PDI cooperate in the oxidative folding of antibodies in vitro," *The Journal of Biological Chemistry*, vol. 275, no. 38, pp. 29421–29425, 2000.
- [16] G. Di Conza and P. C. Ho, "ER stress responses: an emerging modulator for innate immunity," *Cell*, vol. 9, no. 3, p. 695, 2020.
- [17] J. A. Choi and C. H. Song, "Insights into the role of endoplasmic reticulum stress in infectious diseases," *Frontiers in Immunology*, vol. 10, p. 3147, 2019.
- [18] J. S. So, "Roles of endoplasmic reticulum stress in immune responses," *Molecules and Cells*, vol. 41, no. 8, pp. 705–716, 2018.
- [19] A. S. Martins, I. Alves, L. Helguero, M. R. Domingues, and B. M. Neves, "The unfolded protein response in homeostasis and modulation of mammalian immune cells," *International Reviews of Immunology*, vol. 35, no. 6, pp. 457–476, 2016.
- [20] S. E. Bettigole and L. H. Glimcher, "Endoplasmic reticulum stress in immunity," *Annual Review of Immunology*, vol. 33, no. 1, pp. 107–138, 2015.
- [21] H. Hu, M. Tian, C. Ding, and S. Yu, "The C/EBP homologous protein (CHOP) transcription factor functions in endoplasmic reticulum stress-induced apoptosis and microbial infection," *Frontiers in Immunology*, vol. 9, p. 3083, 2018.
- [22] M. I. Gómez, D. O. Sordelli, F. R. Buzzola, and V. E. García, "Induction of cell-mediated immunity to Staphylococcus aureus in the mouse mammary gland by local immunization with a live attenuated mutant," *Infection and Immunity*, vol. 70, no. 8, pp. 4254–4260, 2002.
- [23] M. Z. David and R. S. Daum, "Treatment of Staphylococcus aureus infections," *Current Topics in Microbiology and Immunology*, vol. 409, pp. 325–383, 2017.
- [24] A. M. Algammal, H. F. Hetta, A. Elkelish et al., "Methicillin-resistant Staphylococcus aureus (MRSA): one health perspective approach to the bacterium epidemiology," *Virulence Factors, Antibiotic-Resistance, and Zoonotic Impact, Infection and drug resistance*, vol. 13, pp. 3255–3265, 2020.
- [25] V. Krömker and S. Leimbach, "Mastitis treatment—reduction in antibiotic usage in dairy cows," *Zuchthygiene*, vol. 52, Suppl 3, pp. 21–29, 2017.
- [26] F. Babaei, A. Moafizad, Z. Darvishvand, M. Mirzababaei, H. Hosseinzadeh, and M. Nassiri-Asl, "Review of the effects of vitexin in oxidative stress-related diseases," *Food Science & Nutrition*, vol. 8, no. 6, pp. 2569–2580, 2020.
- [27] M. He, J. W. Min, W. L. Kong, X. H. He, J. X. Li, and B. W. Peng, "A review on the pharmacological effects of vitexin and isovitexin," *Fitoterapia*, vol. 115, pp. 74–85, 2016.
- [28] S. I. Rosa, F. Rios-Santos, S. O. Balogun, and D. T. Martins, "Vitexin reduces neutrophil migration to inflammatory focus by down-regulating pro-inflammatory mediators via inhibition of p38, ERK1/2 and JNK pathway," *Phytomedicine: international journal of phytotherapy and phytopharmacology*, vol. 23, no. 1, pp. 9–17, 2016.
- [29] S. Duan, X. Du, S. Chen et al., "Effect of vitexin on alleviating liver inflammation in a dextran sulfate sodium (DSS)-induced colitis model," *Biomedicine & pharmacotherapy = Biomedecine & pharmacotherapie*, vol. 121, article 109683, 2020.
- [30] S. Zhang, C. Guo, Z. Chen, P. Zhang, J. Li, and Y. Li, "Retracted: vitexin alleviates ox-LDL-mediated endothelial injury by inducing autophagy via AMPK signaling activation," *Molecular Immunology*, vol. 85, pp. 214–221, 2017.
- [31] Y. Lu, T. Yu, J. Liu, and L. Gu, "Vitexin attenuates lipopolysaccharide-induced acute lung injury by controlling the Nrf2 pathway," *PLoS One*, vol. 13, no. 4, article e0196405, 2018.
- [32] C. L. Venturini, A. Macho, K. Arunachalam et al., "Vitexin inhibits inflammation in murine ovalbumin-induced allergic asthma," *Biomedicine & pharmacotherapy = Biomedecine & pharmacotherapie*, vol. 97, pp. 143–151, 2018.
- [33] M. Krishnan and S. C. Kang, "Vitexin inhibits acrylamide-induced neuroinflammation and improves behavioral changes

- in zebrafish larvae,” *Neurotoxicology and Teratology*, vol. 74, article 106811, 2019.
- [34] S. Li, T. Liang, Y. Zhang et al., “Vitexin alleviates high-fat diet induced brain oxidative stress and inflammation via anti-oxidant, anti-inflammatory and gut microbiota modulating properties,” *Free Radical Biology & Medicine*, vol. 171, pp. 332–344, 2021.
- [35] Y. Peng, R. Gan, H. Li et al., “Absorption, metabolism, and bioactivity of vitexin: recent advances in understanding the efficacy of an important nutraceutical,” *Critical Reviews in Food Science and Nutrition*, vol. 61, no. 6, pp. 1049–1064, 2021.
- [36] Y. Chen, H. Jing, M. Chen et al., “Transcriptional profiling of exosomes derived from *Staphylococcus aureus*-infected bovine mammary epithelial cell line MAC-T by RNA-Seq analysis,” *Oxidative Medicine and Cellular Longevity*, vol. 2021, Article ID 8460355, 18 pages, 2021.
- [37] Y. Chen, S. Guo, K. Jiang, Y. Wang, M. Yang, and M. Guo, “Glycitin alleviates lipopolysaccharide-induced acute lung injury via inhibiting NF- κ B and MAPKs pathway activation in mice,” *International Immunopharmacology*, vol. 75, article 105749, 2019.
- [38] J. W. Min, J. J. Hu, M. He et al., “Vitexin reduces hypoxia-ischemia neonatal brain injury by the inhibition of HIF-1 α in a rat pup model,” *Neuropharmacology*, vol. 99, pp. 38–50, 2015.
- [39] J. Jiang, Y. Jia, X. Lu et al., “Vitexin suppresses RANKL-induced osteoclastogenesis and prevents lipopolysaccharide (LPS)-induced osteolysis,” *Journal of Cellular Physiology*, vol. 234, no. 10, pp. 17549–17560, 2019.
- [40] Y. Chen, Y. F. Zhao, J. Yang et al., “Selenium alleviates lipopolysaccharide-induced endometritis via regulating the recruitment of TLR4 into lipid rafts in mice,” *Food & Function*, vol. 11, no. 1, pp. 200–210, 2020.
- [41] J. Günther, W. Petzl, I. Bauer et al., “Differentiating *Staphylococcus aureus* from *Escherichia coli* mastitis: *S. aureus* triggers unbalanced immune-dampening and host cell invasion immediately after udder infection,” *Scientific Reports*, vol. 7, no. 1, p. 4811, 2017.
- [42] M. A. Islam, M. Takagi, K. Fukuyama et al., “Transcriptome Analysis of the Inflammatory Responses of Bovine Mammary Epithelial Cells: Exploring Immunomodulatory Target Genes for Bovine Mastitis,” *Pathogens*, vol. 9, p. 200, 2020.
- [43] T. Barrett, S. E. Wilhite, P. Ledoux et al., “NCBI GEO: archive for functional genomics data sets—update,” *Nucleic Acids Research*, vol. 41, no. Database issue, pp. D991–D995, 2013.
- [44] R. Edgar, M. Domrachev, and A. E. Lash, “Gene Expression Omnibus: NCBI gene expression and hybridization array data repository,” *Nucleic Acids Research*, vol. 30, no. 1, pp. 207–210, 2002.
- [45] M. Tao, R. Li, T. Xu et al., “Flavonoids from the mung bean coat promote longevity and fitness in *Caenorhabditis elegans*,” *Food & Function*, vol. 12, no. 17, pp. 8196–8207, 2021.
- [46] M. C. Zúñiga-López, G. Maturana, G. Campmajó, J. Saurina, and O. Núñez, “Determination of bioactive compounds in sequential extracts of chia leaf (*Salvia hispanica* L.) using UHPLC-HRMS (Q-Orbitrap) And a Global Evaluation of Antioxidant In Vitro Capacity,” *Antioxidants*, vol. 10, no. 7, p. 1151, 2021.
- [47] M. K. Sarkar, A. Kar, A. Jayaraman, S. Kar Mahapatra, and V. Vadivel, “Vadivel, vitexin isolated from *Prosopis cineraria* leaves induce apoptosis in K-562 leukemia cells via inhibition of the BCR-ABL-Ras-Raf pathway,” *The Journal of Pharmacy and Pharmacology*, vol. 74, p. 103, 2022.
- [48] P. L. Ruegg, “A 100-year review: mastitis detection, management, and prevention,” *Journal of Dairy Science*, vol. 100, no. 12, pp. 10381–10397, 2017.
- [49] A. J. Spitzer, Q. Tian, R. K. Choudhary, and F. Q. Zhao, “Bacterial endotoxin induces oxidative stress and reduces milk protein expression and hypoxia in the mouse mammary gland,” *Oxidative Medicine and Cellular Longevity*, vol. 2020, Article ID 3894309, 16 pages, 2020.
- [50] S. Schmitz, M. W. Pfaffl, H. H. Meyer, and R. M. Bruckmaier, “Short-term changes of mRNA expression of various inflammatory factors and milk proteins in mammary tissue during LPS-induced mastitis,” *Domestic Animal Endocrinology*, vol. 26, no. 2, pp. 111–126, 2004.
- [51] D. S. Malar, M. I. Prasanth, R. B. Shafreen, K. Balamurugan, and K. P. Devi, “*Grewia tiliaefolia* and its active compound vitexin regulate the expression of glutamate transporters and protect Neuro-2a cells from glutamate toxicity,” *Life Sciences*, vol. 203, pp. 233–241, 2018.
- [52] C. L. Xie, J. L. Li, E. X. Xue et al., “Vitexin alleviates ER-stress-activated apoptosis and the related inflammation in chondrocytes and inhibits the degeneration of cartilage in rats,” *Food & Function*, vol. 9, no. 11, pp. 5740–5749, 2018.
- [53] Y. H. Kim, T. W. Oh, E. Park et al., “Anti-inflammatory and anti-apoptotic effects of acer *Palmatum* Thumb. extract, KIOM-2015EW, in a hyperosmolar-stress-induced in vitro dry eye model,” *Nutrients*, vol. 10, no. 3, p. 282, 2018.
- [54] Z. Li, T. Liu, Y. Feng et al., “PPAR γ alleviates sepsis-induced liver injury by inhibiting hepatocyte pyroptosis via inhibition of the ROS/TXNIP/NLRP3 signaling pathway,” *Oxidative Medicine and Cellular Longevity*, vol. 2022, Article ID 1269747, 15 pages, 2022.
- [55] S. Nie, Z. Shi, M. Shi et al., “PPAR γ /SOD2 protects against mitochondrial ROS-dependent apoptosis via inhibiting ATG4D-mediated mitophagy to promote pancreatic cancer proliferation,” *Frontiers in cell and developmental biology*, vol. 9, article 745554, 2021.
- [56] S. Ni, D. Li, H. Wei, K. S. Miao, and C. Zhuang, “PPAR γ attenuates interleukin-1 β -induced cell apoptosis by inhibiting NOX2/ROS/p38MAPK activation in osteoarthritis chondrocytes,” *Oxidative Medicine and Cellular Longevity*, vol. 2021, Article ID 5551338, 15 pages, 2021.
- [57] F. Urano, X. Wang, A. Bertolotti et al., “Coupling of Stress in the ER to Activation of JNK Protein Kinases by Transmembrane Protein Kinase IRE1,” *Science*, vol. 287, no. 5453, pp. 664–666, 2000.
- [58] M. Corazzari, F. Rapino, F. Ciccocanti et al., “Oncogenic BRAF induces chronic ER stress condition resulting in increased basal autophagy and apoptotic resistance of cutaneous melanoma,” *Cell Death and Differentiation*, vol. 22, no. 6, pp. 946–958, 2015.
- [59] H. Y. Jiang, S. A. Wek, B. C. McGrath et al., “Phosphorylation of the alpha subunit of eukaryotic initiation factor 2 is required for activation of NF-kappaB in response to diverse cellular stresses,” *Molecular and Cellular Biology*, vol. 23, no. 16, pp. 5651–5663, 2003.

Review Article

Delving the Role of *Caralluma fimbriata*: An Edible Wild Plant to Mitigate the Biomarkers of Metabolic Syndrome

Rimsha Anwar,¹ Roshina Rabail,¹ Allah Rakha ,¹ Marcin Bryla,² Marek Roszko,² Rana Muhammad Aadil ,¹ and Marek Kieliszek ³

¹National Institute of Food Science and Technology, University of Agriculture, Faisalabad 38000, Pakistan

²Department of Food Safety and Chemical Analysis, Prof. Waclaw Dabrowski Institute of Agricultural and Food Biotechnology—State Research Institute, Rakowiecka 36, 02-532 Warsaw, Poland

³Department of Food Biotechnology and Microbiology, Institute of Food Sciences, Warsaw University of Life Sciences—SGGW, Nowoursynowska 159 C, 02-776 Warsaw, Poland

Correspondence should be addressed to Allah Rakha; arrehman_ft@uaf.edu.pk, Rana Muhammad Aadil; muhammad.aadil@uaf.edu.pk, and Marek Kieliszek; marek_kieliszek@sggw.pl

Received 3 May 2022; Revised 27 May 2022; Accepted 3 June 2022; Published 20 June 2022

Academic Editor: Yujie Chen

Copyright © 2022 Rimsha Anwar et al. This is an open access article distributed under the Creative Commons Attribution License, which permits unrestricted use, distribution, and reproduction in any medium, provided the original work is properly cited.

Metabolic syndrome (MS), commonly known as syndrome X or insulin resistance syndrome, is a collection of risk factors for cardiovascular diseases and type II diabetes. MS is believed to impact over a billion individuals worldwide. It is a medical condition defined by visceral obesity, insulin resistance, high blood pressure, and abnormal cholesterol levels, according to the World Health Organization. The current dietary trends are more focused on the use of functional foods and nutraceuticals that are well known for their preventive and curative role against such pathological disorders. *Caralluma fimbriata* is one such medicinal plant that is gaining popularity. It is a wild, edible, succulent roadside shrub with cactus-like leaves. Besides its main nutrient contents, various bioactive constituents have been identified and linked with positive health outcomes of appetite-suppressing, hypolipidemic, antioxidant, hepatoprotective, and anticancer potentials. Hence, such properties make *C. fimbriata* an invaluable plant against MS. The current review compiles recent available literature on *C. fimbriata*'s nutritional composition, safety parameters, and therapeutic potential for MS. Summarized data in this review reveals that *C. fimbriata* remains a neglected plant with limited food and therapeutic applications. Yet various studies explored here do prove its positive health-ameliorating outcomes.

1. Introduction

Food was mostly acquired from nature or forest resources in nomadic societies [1]. Plants have been the primary source of food, bioactive components, and a necessity for survival and environmental conservation [2]. Likewise, medicinal plants are a real gift from nature to mankind, aiding them in their pursuit of greater health. Such natural foods and their products have been recognized and used as the primary source of therapeutic medications since prehistoric times. They remain a source of effective bioactive compounds that can be utilized directly as medications. According to current estimates, the plant kingdom has about 250,000 species,

from which approximately 10% of medicinal plants have been investigated or discovered for the treatment of various diseases [3]. Hence, there is a dire need to explore more hidden components in the plant kingdom.

When compared to conventional medicine, many plants and herb-based therapies have a long history of usage in the prevention and management of various disorders [4]. According to the World Health Organization, the use of herbs, herbal materials, herbal preparations, finished herbal products containing active ingredients of plants, or combinations thereof as drugs are known as herbal, phyto, or botanical medicines [5]. Such medicinal herbs are widely distributed among plant sources and have wide therapeutic

applications [6]. The worth of such plants or herbs lies in their secondary metabolites, which are nonnutritive but can exert certain physiological actions in humans against different types of infectious diseases and metabolic disorders [7]. Various plant species throughout the world have been studied for their therapeutic properties, and bioactivity differs from plant to plant, as they pose diverse physiological impacts on the human body [8]. Medicinal plants play an important role in public health, particularly in underdeveloped countries owing to their better affordability and lower toxicity [9]. The extensive use of plants with therapeutic properties does not lead to intoxication, whereas overutilization of allopathic medicines has been associated with adverse effects. Drug residues may lead to the growth of drug-resistant microorganisms that are difficult to treat; hence, the globe is looking for safer alternatives [6].

Recent advances in nutraceuticals and functional foods research have proved that bioactive components in our diet have an important therapeutic role in the treatment of human maladies. Dietary scientists place a high value on isolating nutraceutical bioactive components from food sources [10]. Nutraceuticals, in contrast to traditional diets, are foods or part of food that combine nutritional and pharmacological effects. Hence, nutraceuticals contain any natural component with a nutritional value that has a positive effect on the human body, which are available in the form of powder/pill/dietary supplements or products containing concentrated food derivatives-nutrients. They are typically found in the most common functional foods. Some molecules, micronutrients, and macronutrients including alkaloids, polyphenols, terpenoids, some vitamins (A, B6, B12, C, D, and E), folate, and some trace elements like zinc, iron, selenium, and magnesium are present in these products that are believed to be responsible for the therapeutic effects [11]. *Caralluma* species are gaining more interest among nutraceutical companies owing to the presence of various phytochemicals with antioxidative potential [12]. *Caralluma* species have been extensively used for the treatment of various ailments like diabetes, rheumatism, leprosy, paralysis, malaria, and inflammation. A considerable number of active chemicals have been extracted from several *Caralluma* species. Therefore, scientists are working to produce nutraceuticals from natural products and their derivatives that can aid in enhancing human health while avoiding side effects [13].

Adherence to a nutritious plant-based diet and an active lifestyle, similar to that of our forefathers, may help in the prevention and management of this growing menace of MS. Among plant-based food sources, many indigenous, wild edible plants are still lacking the attention of food scientists, nutritionists, and processors. Thus, there is a need to target such underutilized plant resources to address these lifestyle-related disorders. Unfortunately, still no well-defined studies are conducted to encourage the utilization of historically known wild edible plants as a source of nutrition and therapeutic. Purposely, numerous studies on the nutritional content of wild edible plants are being carried out to raise public attention to their use [2]. One such overlooked plant with significant nutritional and nutraceutical potential is *C. fimbriata*. Henceforth, this review has been

designed to compile the latest available scientific literature on *C. fimbriata* to drive the attention of food and nutrition experts, food technologists, dietitians, and clinicians toward its nutritional and nutraceutical utilization at household, industrial, and clinical levels. The primary motivation was to select the underutilized medicinal plant, which is discussed in depth in this review, along with their mode of action and potential mechanism, and could potentially be utilized in the management and prevention of metabolic disorders. This review focuses on different varieties and their important bioactive compounds that have been presented to target MS to open up new avenues for various treatments/therapies [3]. Henceforth, this review has been designed to compile the latest available ten years of scientific studies on *C. fimbriata* to drive the attention of experts in food and nutrition departments towards its encouraged dietary utilization. For this purpose, scientific studies from 2012 onwards were collected using advanced search options on Google Scholar, ScienceDirect, and Scopus with the following keywords: “*Caralluma fimbriata*” OR “*Caralluma adscendens*” OR “Choong” AND “Metabolic Syndrome” OR “Diabetes” OR “Hyperlipidemia” OR “hypertension” OR “Obesity”.

2. *C. fimbriata*: An Edible Wild Medicinal Plant

The use of many indigenous medicinal plants is recommended by the WHO owing to their accessibility, affordability, and fewer adverse effects. Britain was the first to cultivate *C. fimbriata* formally in 1830 [14]. Unfortunately, authorities and agricultural entities continue to disregard or overlook the production/cultivation of such wild plants. Furthermore, as a result of overexploitation by the pharmaceutical industry, agriculture, mining, and fodder lopping, these plants are fast disappearing and may become extinct in the near future [15]. Therefore, to meet the global functional food and nutraceutical industry demands, new powerful strategies are required to end this threatening decline [16]. *C. adscendens* var. *fimbriata*, commonly known as *C. fimbriata* [17], is locally known as “Choong” or “Choonga” and “Kalli moolian” or “Karallamu” in Pakistan and India, respectively [18]. It is a resilient roadside shrub with cactus-like leaves and is well known in Ayurvedic medicine. The plant is about 20-30 cm tall, erect, branching herb with leafless four-angled green stem tapered to the tips. Its leaves are small that only appear on young branches and fall off quickly leaving spiky projections. Flowers bloom either singly or in groups at the ends of branches on short stalks. Its flowers are 2 cm in diameter, with small petals of purple color marked with golden and hairy borders [19]. Natural bioactive supplements are becoming increasingly popular for weight reduction, and *C. fimbriata* is currently regarded as one such functional plant that has exhibited potential outcomes [20].

C. fimbriata is an edible wild medicinal plant that grows in dry areas and is known as “famine food” by tribal Indians. Traditionally, it is eaten as a pickle or vegetable [21]. Through appropriate selection and climate adjustments, this wild plant can be easily adapted for its large-scale cultivation

[16]. History has reported its use during long hunting periods since hunting tribes in the form of chewable portions or chunks of the *C. fimbriata* to suppress hunger and quench thirst. No incidence of adverse effects has been reported after the use of *C. fimbriata* in the Indian subcontinent [22]. It contains pregnane glycosides that are known to suppress hunger and increase endurance. The plant has been studied for its antihyperglycemic and hypolipidemic properties, as well as hepatoprotective and antioxidant activities, yielding significant results [18, 23]. It is also used to treat pain, fever, and inflammation. The plant is commonly consumed by ethnic populations of Central India to manage obesity [24]. It also stimulates the central nervous system, and its therapeutic benefits are attributable to the pregnane group of glycosides found abundantly in them [25]. Flavone glycosides, pregnane glycosides, saponins, triterpenoids, and other flavonoids are important phytochemical constituents of *C. fimbriata* that have been studied against various pathological conditions and metabolic disorders. Pregnane glycosides are the secondary metabolites of *C. fimbriata* that are the steroidal compounds conjugated with sugar moiety [26]. They are related to altered lipid metabolism and inhibit the synthesis of fatty acids [18, 27]. They also act on the hypothalamus and cortisol, causing a feeling of fullness, thereby reducing hunger, and are most likely responsible for appetite suppression [28]. This occurs without any side effects compared to the known appetite suppressant drugs [29].

C. fimbriata extract (CFE) is commercially available in several countries including Australia and New Zealand [30]. CFE has been granted generally recognized as safe (GRAS) classification for use as a nutraceutical in the fight against the world's most significant public health problem (i.e., obesity) [31]. For example, GenaSlim is a brand of CFE that has been approved for weight loss programs. The use of CFE as a therapeutic intervention is well known in Ayurvedic medicine [32]. CFE can also be used as a natural antioxidant [33]. Other therapeutic applications of CFE reported in the literature include carminative, febrifugal, anthelmintic, antirheumatic, anti-inflammatory, antinociceptive, and antioxidant actions [25]. Therefore, CFE could serve as an appropriate chemically tested, safe, and effective appetite suppressant resulting in weight loss, blood glucose, and lipid reduction [34]. In addition, it has been used against malaria, hyperglycemia, ulcers, cancers, and other diseases. Future research for antiobesity and appetite-suppressant medications and nutraceuticals should focus on this significant phytochemical-pregnane glycoside [31]. It has been known to have hypolipidemic, antioxidant, hepatoprotective, antiobesogenic, and anticancer properties with few side effects [23].

In the Indian Health Ministry's comprehensive compilation of medicinal plants, it is listed as a vegetable [22]. Also, it is classified as famine food, hunger suppressor, and thirst quencher in Indian Materia Medica [35]. Its aerial parts are traditionally used as a culinary herb and cooked with meat during the winter [24]. For decades, tribal communities in India have consumed this as a traditional vegetable alternative. CFE is also largely available and easy to consume despite its bitter taste. Its safety and toxicity profile has been

thoroughly investigated [30]. While in the semiarid areas of Pakistan, its species have been used as emergency food for centuries [21]. *C. fimbriata*'s dietary or supplemental utilization is shown in Figure 1.

3. Nutritional and Phytochemical Constituents of *C. fimbriata*

C. fimbriata has about 45% moisture, 9% ash, 4.8% fat, 0.67% fiber, 0.66% protein, 40% carbohydrates, and 207 kcal/100 grams in terms of its nutritive value with a significant load of iron, manganese, zinc, and copper [36]. Another study indicated some variations but significant amounts of fats, ash, sugars, and caloric contents accounting for 8%, 6%, 30%, and 554 kcal/100 grams, respectively [20]. The examination of amino acid composition (mg/100 g dry weight) of aerial parts of *C. fimbriata* revealed aspartic acid 21.6, glutamic acid negligible, alanine 120.72, methionine 22.56, tyrosine 130.08, lysine 316.56, threonine negligible, proline 483.8, isoleucine 1578.24, phenylalanine 141.58, tryptophan 157.36, glycine 108.29, arginine 51.58, histidine 84.48, and valine 342.95. Likewise, moisture 82%, lipid 5.6%, carbohydrates 55.4%, protein 3.5%, total free amino acid 27.5%, crude fiber 15.3%, and ash 2.1% were also found [27]. Table 1 elaborates on the phytochemicals identified in *C. fimbriata* along with their bioactive potentials reported in various studies. Future investigations for bioactive peptides and genetic variations are still awaited in this regard [37, 38].

Extraction of CFE based on various extraction methods along with the detection and identification of bioactive nonnutritive compounds of *C. fimbriata* as explained in Table 2 revealed considerable amounts of steroids, coumarin, phytosterol, flavonoids, and alkaloids and medium levels of diterpenes and saponins while the relative absence of anthocyanins, phenols, tannins, phlobatannins, and cardinal glycosides. Similarly, steroids, coumarin, proteins, carbohydrates, diterpenes, phytosterol, flavonoids, saponins, and alkaloids were identified positively along with the high concentration of minerals and elemental compounds [22]. One more study looked into the existence of phytochemical ingredients, total phenolics, and flavonoid contents along with the antioxidant capacity of whole plant CFE utilizing various in vitro assays based on Soxhlet's extraction, 2,2-diphenyl-1-picrylhydrazyl (DPPH), nitric oxide (NO) scavenging, and ferric reducing antioxidant power test (FRAP) techniques. The total phenolic and flavonoid content of the plant ethanolic extract were found to be 80.08 ± 0.629 mg and 70.88 ± 1.170 mg, respectively. The ethanolic extract has higher antioxidant activity than the other extracts as measured by DPPH, NO, and FRAP [8]. Moreover, a study was conducted to check the phytochemical constituents of CFE using different solvents (aqueous, ethanolic, methanolic, and ethyl acetate). Methanolic extract revealed that the whole plant was rich in alkaloids, flavonoids, glycosides, phenolic compounds, saponins, and quinones. Mainly oleic acid (21.08%) and n-hexadecanoic acid (44.23%) were detected [61]. Another study indicated that *C. fimbriata* had total free phenolic 13.56 mg/100 g, while antinutritional compounds, namely, tannins (112 mg/100 g) and

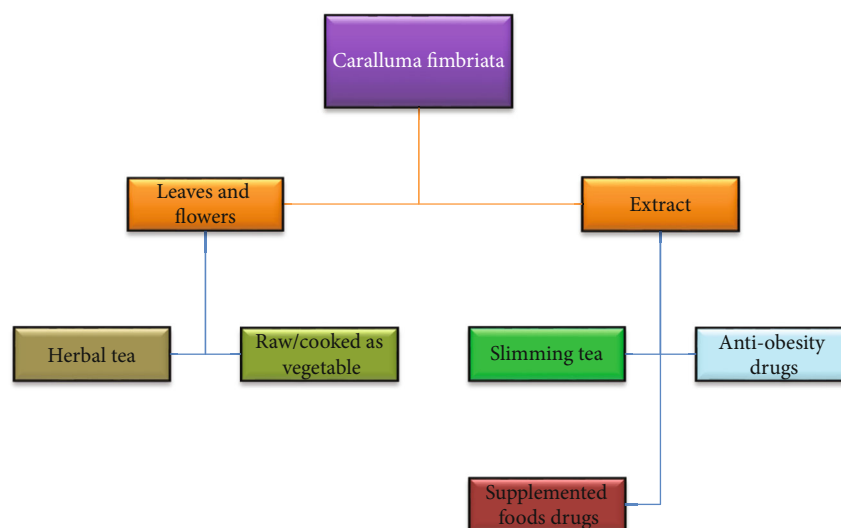


FIGURE 1: *C. fimbriata* utilization in various dietary and supplemental forms.

TABLE 1: Phytochemical constituents in *C. fimbriata*.

Phytochemical constituents	Bioactive potential	Reference
Total polyphenolic compounds	Antioxidant; cardioprotective; neuroprotective; and antihyperglycemic	[8, 22, 39, 40, 41, 42]
Flavonoids	Antioxidant; antiaging; anti-inflammatory; antifungal; immunomodulatory; cardioprotective; antiviral; antimicrobial; antibacterial; and antiparasitic	[8, 22, 34, 40, 43]
Saponins	Antitumor; antioxidative; anti-inflammatory; antidiabetic; and neuroprotective	[8, 22, 35, 40, 44]
Alkaloids	Antiadipogenic; antihyperglycemic; and antioxidant	[8, 22, 39, 42, 45]
Anthocyanins	Protective against cardiovascular diseases; cancers; neurodegenerative disorders; and aging-associated bone loss	[34, 46, 47]
Coumarins	Antioxidants; antitumor	[8, 22, 35, 48]
Tannins/gallic-tannins	Antiulcerative; anti-inflammatory; antioxidant; antidiabetic; anticancer; and cardioprotective	[8, 39, 40, 49, 50]
Steroids	—	[22, 34].
Diterpenes	Antiobesogenic; antihyperlipidemic; and anticarcinogenic	[51, 52, 22]
Phytosterol	Antihyperlipidemic; anticancer; antiapoptotic; cardioprotective; and anti-inflammatory	[8, 40, 53]
Quinones	—	[8]
Terpenoids	Anti-inflammatory; antitumor; and antiparasitic	[8]
Anthraquinones	Diuretic; antibacterial; antiulcer; anti-inflammatory; anticancer; and antinociceptive	[8, 54]
Pregnane glycosides	Antidiabetic; antiobesity; antinociceptive; antiulcer; anti-inflammatory; antiarthritis; and wound healing activities	[31, 55–58]
Pregnane steroids	—	[31]
Trigonelline	Anti-inflammatory; antioxidant; antipathogenic; and antiaging	[55, 59]
Glycosides	—	[60]

oxalates (125 mg/100 g), were also observed [2]. CFE included roughly 12% pregnane glycosides and 1.3% polyphenols according to phytochemical analyses. The current findings point to presumed *C. fimbriata* effects on ingestive behavior which are most likely mediated by cerebral and peripheral processes [55].

4. Therapeutic Potential and Bioactive Compounds of Genus *Caralluma*

There are almost 18,000 flowering plant species that account for nearly 11% of all plants in the world [6]. *Caralluma* is among such beneficial medicinal flowering plants that

TABLE 2: Extraction and biochemical activity of *C. fimbriata* extracts (CFE).

Extraction	Methodology	Result	References
Shade dried, powdered, and extracted in Soxhlet's apparatus using several solvents including pet ether (PE), chloroform (C), ethyl acetate (EA), ethanol (E), and aqueous (A)	Phytochemical screening: TPC, TFC, and antioxidant radical scavenging activity analysis	Ethanol extraction has shown a better antioxidant profile, whereas saponins were found in extracts of PE, C, and E Alkaloids and phenols in EA and E Anthraquinones in C, EA, and E Carbohydrates in C Flavonoids in E Steroids in C and EA Coumarins in EA, E, and A Quinones in C, EA, and E Tannins in C and EA	[8]
Dried (fluidized-bed drier at 45°C for 60 min) Homogenized (food processor) Mixed with hot water (at 65°C for 3 h in a temperature-controlled incubator shaker) Cooled (room temperature) Filtered (No.1 sinter glass funnel) Centrifuged extract	Phenolic and flavonoid content were analyzed	<i>C. fimbriata</i> acted as a natural antioxidant against acrylamide and oxidative deterioration due to higher phenolics and 1 flavonoid content	[33]
Slimaluma®, a dry ethanolic extract from the aerial portions of <i>C. fimbriata</i>	Phytochemical analysis using NMR spectroscopy	Amino acids: leucine, isoleucine, alanine, glutamine, and tryptophan Organic acids: lactate, acetate, and formate Carbohydrates: glucose, sucrose trigonelline, and pregnanes	[55]
Shade drying method	Nutritional and phytochemical analysis	Following phytochemicals detected steroid, coumarin, proteins, carbohydrates, diterpenes, phytosterol, flavonoids, and alkaloids	[22]
Shade drying method	Free phenolics and antinutritional content were analyzed	Total free phenolics and antinutritional content (tannin and oxalates) were detected positively	[2]
Shade dried, powdered, and extracted in Soxhlet's apparatus using several solvents including chloroform, ethyl acetate, methanol, and water	Phenolic and flavonoid content were analyzed	Methanol and water extraction has shown better antioxidant profiles and phenolic compounds	[21]
Shade drying method	The amino acid composition was checked	Following phytochemicals detected aspartic acid, alanine, methionine, tyrosine, lysine, isoleucine, glycine, and phenylalanine, negligible amounts detected for glutamic acid and threonine	[27]
Shade drying method using several extracts Aqueous, ethyl acetate, ethanolic, and methanolic extracts	GC-MS analyses were done	Alkaloids, flavonoids, glycosides, phenolic compounds, saponins, quinones, oleic acid, and n-hexadecanoic acid were positively detected in methanolic extract	[61]

belong to the family Apocynaceae and is found throughout Asia (Afghanistan, India, Iran, Pakistan, and Sri Lanka), Africa, Arabian Peninsula, Canary Islands, and Southeast Europe. The name "Caralluma" is derived from the Arabic word "qarh al-luhum" meaning "flesh wound" or "abscess" [24]. Caralluma has approximately 200 genera and 2500 species distributed all over the world, especially in tropical Asia and the Mediterranean regions [31, 62]. The chemical composition of different species of Caralluma depends on the growing conditions, morphological features, and genetic characterization. The presence of different phytochemical constituents makes them unique and diversified from one another [63]. Different species of Caralluma, i.e., *C. stalagmifera*, *C. adscendens* var. *attenuate*, *C. tuberculata*, *C. arab-*

ica, *C. attenuate* Wight, *C. burchardii*, *C. edulis*, *C. europaea*, *C. flava*, *C. indica*, *C. lasiantha*, *C. negevensis*, *C. sinaica*, and *C. umbellata* Haw, have been reported in the literature for their beneficial outcomes. These species have antimalarial, antiulcer, antioxidant, and antiproliferative properties and are extensively used in traditional medicines for the treatment of diabetes, rheumatism, paralysis, leprosy, and inflammation. Table 3 elaborates some of the major bioactive components of the Caralluma genus that are known for their role against MS including pregnane glycosides, flavonoid glycosides, flavones, magastigmane glycosides, pregnane steroids, steroidal glycosides, saturated and unsaturated hydrocarbons, aromatic and nonaromatic volatile chemicals, and β -sitosterol [31].

TABLE 3: Bioactive compounds isolated from various *Caralluma* species.

Bioactive component	Extraction	Therapeutic potential	Species variety	Reference
Pregnane glycosides (27 compounds)	Methanolic extraction	High cytotoxic activities	<i>C. gracilis</i> <i>C. dalzielii</i>	[64]
Novel Pregnane glycoside	Ether eluates of methanol and benzene fractions of ethanolic extract	—	<i>C. umbellata</i>	[64]
New pregnane glycosides (2-13)	Ethanolic and butanolic extraction	Appetite suppressant Antiobesity High cytotoxic activity	<i>C. fimbriata</i>	[64]
New pregnane glycosides (1-20)	Chloroform and methanol extracts	—	<i>C. negevensis</i> <i>C. russeliana</i> <i>C. sinaica</i>	[64]
Four tetrasaccharide pregnane glycosides (desflavasides A-D)	Sap	Antidiabetic and antiulcer	<i>C. flava</i>	[64]
Pregnane glycosides (nizwaside)	Sap	Anticancer Antidiabetic Antiulcer	<i>C. flava</i>	[64, 65]
Pregnane glycosides (carumbelloside-III and dihydro russelioside)	Ethanolic extraction	Antidiabetic Antiobesity Antinociceptive Antiulcer Anti-inflammatory Antiarthritis effects Wound healing activities	<i>C. pauciflora</i>	[58, 64]
Pregnane glycoside (russelioside B)	n-Butanol fraction of methanol extract	Antidiabetic Antihyperlipidemic	<i>C. quadrangular</i>	[64]
Five pregnane glycosides (caratuberside A-E); pregnant glycoside-russelioside	Chloroform fraction of MeOH extract	Antimalarial Antitrypanosomal Cytotoxic potential	<i>C. tuberculata</i>	[64]
Pregnane glycosides (desmiflavasides A and B)	Sap	Antiproliferative Antidiabetic Antiulcer	<i>C. flava</i>	[64, 65]
Pregnane glycosides (C15 oxypregnane glycosides (penicillosides A-C))	Chloroform fraction of ethanol extract	—	<i>C. penicillata</i>	[64]
Four acylated pregnane glycosides (russeliosides E-H)	Methanolic extraction; chloroform extracts; and n-butanol fraction of ethanol extract	—	<i>C. penicillata</i> <i>C. russeliana</i>	[64]
Five pregnane derivatives	HPLC-UV LC/MS-TOF	—	<i>C. fimbriata</i> <i>C. attenuata</i> <i>C. umbellata</i>	[66]
Polyoxy pregnane glycoside (retrospinoside 1)	n-butanol fraction of methanol extract; ether extracts	High cytotoxic activity	<i>C. retrospections</i>	[64]
Bisdesmosidic C21 pregnane steroidal glycosides (lasianthosides-A and B)	n-Butanol fraction of ethanolic extract; less polar solvent extraction	—	<i>C. lasiantha</i>	[64]
Pregnane steroidal glycoside (androstan glycoside)	Ethyl acetate extract	Moderate cytotoxic activity	<i>C. tuberculata</i>	[64]
Steroidal glycosides (stalagmoside I-IV)	Butanol fraction	Anti-inflammatory	<i>C. stalagmifera</i> <i>C. indica</i>	[64]
Steroidal glycosides (Caradalzieloside A-E)	CHCl ₃ /MeOH	—	<i>C. dalzielii</i>	[64]
Flavones glycoside (luteolin-4-O-neohesperidoside)	Methanolic extract; an n-butanol fraction of ethanol extract	—	<i>C. lasiantha</i> <i>C. russeliana</i>	[64]
	Methanolic extract	Anti-inflammatory	<i>C. negevensis</i>	[64]

TABLE 3: Continued.

Bioactive component	Extraction	Therapeutic potential	Species variety	Reference
Flavones glycoside (megastigmane glycosides)				
Flavone glycosides	Methanolic extract;	Antioxidant	<i>C. negevensis</i> <i>C. attenuate</i>	[64]
Steroids/triterpenoids; pentacyclic triterpenoid	n-Hexane; butanone, ethylene acetate, and n-butanol; ethanolic extraction; and chloroform extract	Antiapoptotic Neuroprotective Antioxidative Anticancer Anti-inflammatory Anti-inflammatory	<i>C. attenuate</i> <i>C.</i> <i>nilagiriana</i> <i>C. russeliana</i> <i>C. edulis</i>	[64, 67–69]
Stigmasterol	Less polar solvent extraction	Antiasthmatic Antioxidative Antiproliferative Neuroprotective	<i>C. lasiantha</i> <i>C.</i> <i>wissmannii</i>	[64, 70, 71]
Two sterols	Chloroform extract	—	<i>C. russeliana</i> <i>C. attenuate</i> <i>C.</i>	[64]
Flavonoids	Butanone, ethylene acetate, and n-butanol; ethanolic extraction; and chloroform extract	Antioxidant Antitumor Antimutagenic	<i>nilagiriana</i> <i>C. sinaica</i> <i>C. umbellate</i> <i>C.</i> <i>tuberculata</i> <i>C. edulis</i>	[64, 67, 72]
Rutin	Ethanolic extraction	Antidiabetic Antibacterial Anti-inflammatory Cardioprotective	<i>C.</i> <i>nilagiriana</i> <i>C. arabica</i>	[64, 73]
Alkaloids	Ethanolic extraction	Antiadipogenic	<i>C.</i> <i>nilagiriana</i> <i>C.</i> <i>tuberculata</i> <i>C. edulis</i>	[45, 64, 67, 72, 74]
Tannins	Ethanolic extraction	Anti-inflammatory Antioxidant Antidiabetic Anticancer Cardioprotective	<i>C.</i> <i>nilagiriana</i> <i>C. umbellate</i> <i>C. edulis</i>	[50, 64, 67]
Quercetin	—	Secondary metabolite Cardioprotective Neurological protection Antioxidant	<i>C. arabica</i>	[64, 74–76]
Polyphenols/phenolic compounds	Ethanolic extraction	Antioxidant	<i>C.</i> <i>nilagiriana</i> <i>C. edulis</i>	[64, 67]
Saponins	Butanone, ethylene acetate, and n-butanol	Immune system enhancers	<i>C. attenuate</i> <i>C. umbellate</i> <i>C.</i> <i>tuberculata</i> <i>C. edulis</i>	[64, 67, 72]

5. Metabolic Syndrome (MS)

Recent advancements in contemporary civilization have resulted in a convenient lifestyle accompanied by poor nutri-

tion, fast food intake, lack of physical activity, and excessive stress which are the major causes of many metabolic disorders. Among these, diabetes, hypertension, and hyperlipidemia are the most common ones that can lead to serious

TABLE 4: Different bioactive compounds of *C. fimbriata* against MS.

Target health problem	Bioactive compound	Mechanism of action	Reference
Diabetes mellitus	Pregnane glycoside	The hypoglycemic action is mainly due to the lowering of intestinal glucose absorption or stimulating pancreatic insulin production	[58]
	Quercetin	Stimulate the glucose uptake resulted in the translocation of glucose transporter 4 Reduced the production of sugars by downregulating the key gluconeogenesis enzymes	[82]
	Rutin	Improves insulin secretions Restore glycogen content Inhibit the formation of the advanced glycation end product	[83]
	Saponin	Induces insulin production Oxidative stress amelioration	[83]
Hyperlipidemia	Flavonoids	Exhibit inhibitory effect against pancreatic lipase Able to inhibit lipid peroxidation	[26]
	Quercetin	Decreased the production of reactive oxygen species and act as an anti-inflammatory Inhibit the production of lipoxygenase and cyclooxygenase which are induced by inflammation	[82]
Hypertension	Flavonoids	Able to modulate blood pressure by restoring the endothelial function or by affecting nitric oxide levels	[84]
Obesity	Pregnane glycoside	Aids in fat burning and hunger suppression Works by inhibiting the citrate lyase enzyme and stops the body to produce fat Inhibit malonyl-CoA and block fat synthesis and helps in burning of stored fat resulting in weight loss	[85]
	Quercetin	Decrease the action of an enzyme related to adipogenesis Downregulate the apoptosis while upregulating substrate acetyl-CoA carboxylase	[82]

ailments, i.e., cardiovascular diseases, atherosclerosis, cerebrovascular diseases, and cancers. All such pathological conditions have led to increased mortality attributable to noncommunicable diseases related. Metabolic syndrome (MS) is a collection of interrelated conditions that may lead to type 2 diabetes and cardiovascular diseases. Dyslipidemia (high levels of low-density lipoprotein (LDL), triglycerides (TG), or low levels of high-density lipoprotein (HDL)), high blood pressure, obesity, poor glucose metabolism, and/or insulin resistance are the key biomarkers of MS [77]. MS, also known as syndrome X or insulin resistance syndrome, is a group of risk factors for heart diseases affecting over a billion people worldwide [78]. MS is the leading cause of sickness and mortality in both developed and developing countries with significant economic consequences [79]. Obesity, diabetes mellitus, nonalcoholic fatty liver disease, stroke, and cardiovascular diseases have all reached epidemic proportions in recent decades and have become crucial for clinical and translational research [80]. Interestingly, each of these disorders has distinct physiological and clinical symptoms; they appear to share pathological traits such as intracellular stress and inflammation caused by metabolic disturbances resulting from excessive nutrition which is frequently aggravated by a modern sedentary lifestyle [81].

MS, whether inherited or acquired, has been regarded as a critically important health issue worldwide that needs quick and effective management. A significant proportion of these ailments is still difficult to manage effectively despite enormous advancements in contemporary medicines. Multi-

ple underlying causes including hereditary transmission, imbalanced diet, and unhealthy lifestyle are attributed to the growing burden of the said diseases [4]. Common biomarkers used for early detection and differential diagnosis of numerous metabolic disorders have been called into question owing to significant interindividual variability. For example, not all obese individuals have metabolic issues later in life, and 25–40% of them can lead healthy lives as well. Hence, early screening of high-risk individuals is critical for the prevention and management of MS [80]. The most prevalent features of the pathogenesis of MS are insulin resistance and visceral adiposity, even though it is diagnosed based on at least three metabolic abnormalities. Currently, scientists are concentrating their efforts on dietary components that have the potential to prevent a variety of chronic issues. As a result, consumers are shifting away from dietary supplements toward more nutritious eating habits [77].

6. Therapeutical Potential of *C. fimbriata* against MS

Various scientific studies have established the baselines for the potent therapeutical potential of *C. fimbriata* due to the wide range of phytochemicals therein with scientifically proven nutraceutical active potentials (as elaborated in Tables 1 and 2). Many of those nutraceutical components have been found protective against ailments of MS, i.e., diabetes mellitus, hypertension, hyperlipidemia, and obesity, for whom mechanisms of action have been listed in Table 4. Studies investigating the therapeutical potential

TABLE 5: Various studies of *C. fimbriata*'s therapeutic potential against MS.

Main component	Study subject	Material and method	Result	References
CFE	Overweight adults	Daily supplementation (16 weeks)	A significant effect on body weight maintenance was observed	[20]
CFE	Adults (97)	500 mg for 8 weeks	Significant reduction in stress and anxiety	[28]
CFE	A 14-year-old female (PWS)	CFE supplementation over 12 years	Significant effect against hyperphagia and obesity	[32]
Hydroalcoholic extract of <i>C. fimbriata</i>	Animal model (40 rats)	HFD-induced cardiac damage was analyzed	Cardiac protective outcomes were observed	[62]
<i>C. fimbriata</i>	Human colon cancer cells	MTT cell viability assay was performed on KB cell lines	Good antiproliferative activity against KB mouth cell line	[88]
Hydroalcoholic extract of <i>C. fimbriata</i>	Animal model (Wister rats)	Oxidative stress markers GSH, LO, PO, SDH, and AR were examined	Reduced oxidative and pancreatic damage caused by HFD	[89]
Hydroalcoholic extract of <i>C. fimbriata</i>	Animal model (HFD diabetic rats)	Carbohydrate metabolism was analyzed in rats with HFD	Significantly restore the levels of glycogen in the liver and muscles	[18]
Ethanol leaf extract of <i>C. fimbriata</i>	Human colon cancer cell	Antiproliferative effects were evaluated using MTT assays	Reduced cell proliferation by inducing cytotoxicity of COLO 320 cells	[88]
Commercially available CFE	Animal model (female rats)	Modulation of brain neuropeptides NPY and ORX	Significant reduction in weight gain	[55]
Ethanol leaf extract of <i>C. fimbriata</i>	Vitro approach	Alpha-amylase and alpha-glucosidase inhibitory assay with acarbose as control	Potent antihyperglycemic activity	[23]
Hydroalcoholic extract of <i>C. fimbriata</i>	Animal model (male Wister rats)	Renal functional and oxidative stress markers were checked	Effectively alleviated the HFD-induced renal damage	[35]
CFE and metformin	Wister rats	Lipid profile was analyzed	Significant reduction in lipid profile	[39]
CFE	Male Wister rats	Oxidative stress markers were checked	Significant protection against HF diet	[34]
CFE	Animal and human	Snord116 deletion	Significant alteration in appetite	[90]
CFE	PWS children and adolescents	Appetite behavior was recorded	Significant reduction in hyperphagia	[30]
CFE	Overweight and obese individuals	Anthropometry, appetite, and biochemical investigation done	No significant changes in the biochemical and clinical parameters	[91]
CFE	Animal model	Glucose, leptin, and triglycerides were measured	Significant reduction in insulin resistance and oxidative stress	[14]
CFE	Animal model	Metabolic parameters were assessed	Significant reduction in food intake and blood pressure	[92]
CFE	Animal model	Hepatotoxic, diabetic, and renal toxicities were analyzed	Significant reduction in diabetes	[87]
CFE	Animal model	Renal and liver function tests were measured	Significant reduction in body weight and lipid profile	[93]
CFE	Animal model	Serum lipid profile and blood glucose were measured	Significant alteration in lipid profile and body weight	[94]
CFE	Overweight and obese individuals	500 mg capsules twice for 12 weeks	CFE showed a reduction in BMI, weight gain, hip circumference, and systolic blood pressure	[95]

of *C. fimbriata* against MS have been enlisted in Table 5, and the important description of these studies has been discussed here under the relevant subheadings of this section.

6.1. Antidiabetic Potential of *C. fimbriata*. Diabetes mellitus is a metabolic disorder characterized by high blood glucose levels caused by insufficient or ineffective pancreatic insulin. According to WHO, diabetes affects 3% of the world's

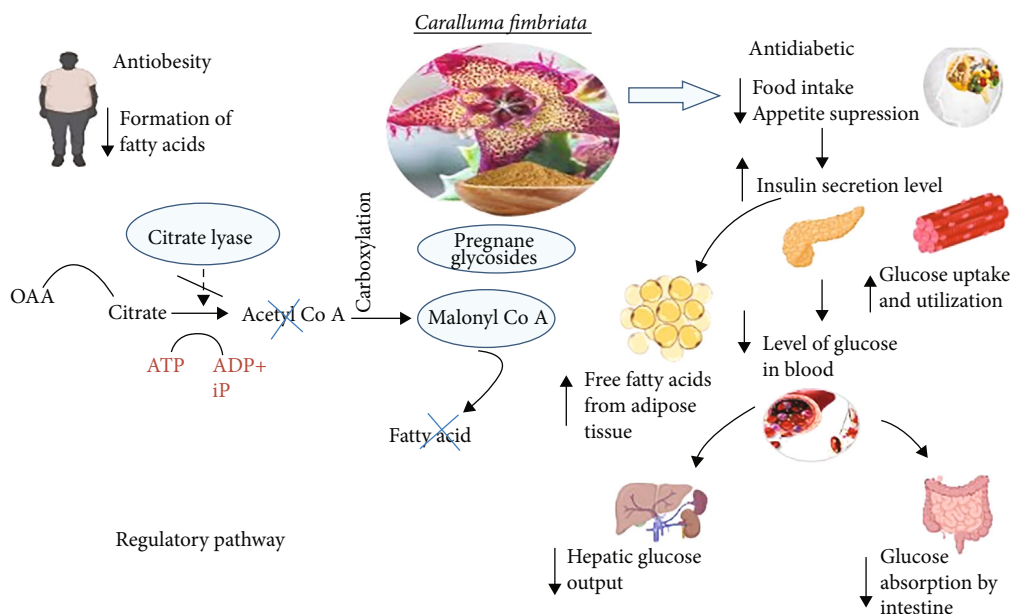


FIGURE 2: Regulatory pathways in the presence of *C. fimbriata* represent antiobesity and antidiabetic potential. *OAA: oxaloacetate; acetyl-CoA: acetyl coenzyme A; ATP: adenosine triphosphate; ADP: adenosine diphosphate; iP: inorganic phosphate*; ↓: decreasing/downregulation; ↑: increasing/upregulation.

population, and the prevalence is anticipated to double to 6.3% by 2025 [79]. According to statistics approximately 79.4 million people in India alone will be infected with the disease by 2030 [23]. As the prevalence of diseases rises, experts must look for more effective therapies with fewer side effects. Diabetes is treated with a wide variety of pharmacological medications. Although there are various types of oral hypoglycemic drugs and insulins available for the treatment of diabetes mellitus, people are increasingly seeking natural antidiabetic therapies with fewer adverse effects [86]. Currently, existing allopathic drugs have the potential to produce obesity and hyperandrogenemia while reducing blood glucose levels. Traditional medicinal herbs are used to treat diabetes mellitus all around the globe since they are less toxic and less costly and have fewer adverse effects than synthetic medicines. As a result, research on drugs derived from traditional medicinal plants has grown in importance [87].

Diet is one of the key elements that impact metabolic homeostasis including impaired glucose and lipid metabolism [18]. Insulin resistance and related disorders such as obesity and type 2 diabetes mellitus are linked to a high dietary fat intake. Controlling postprandial hyperglycemia and fat absorption through inhibition of enzymes responsible for glycoside and lipid hydrolysis should help to reduce MS complications [26]. The hypoglycemic action of the pregnane glycoside is mainly attributed to the lowering of intestinal glucose absorption or stimulation of pancreatic insulin production [58].

Figure 2 represents the regulatory mechanism involved in the antidiabetic and antiobesity potentials of *C. fimbriata*. A study was carried out to assess the CFE for its modulatory effects on carbohydrate metabolism and inhibition of α -amylase as measured by key enzyme activities and changes

in glycogen content (liver and muscle) in a high-fat diet (HFD-) fed diabetic rats. The results revealed that both CFE and metformin administration prevented changes in the activities of glucose metabolism enzymes and dramatically restored glycogen levels in the liver and muscle of HFD-fed rats. Furthermore, muscle myofiber degeneration and fat accumulation were less pronounced in these groups. Such findings suggest that CFE is beneficial in regulating carbohydrate metabolism associated with high-calorie diet consumption [18]. Another study investigated the antihyperglycemic properties of CFE. Purposely, α -amylase and α -glucosidase inhibitory assays were performed on different concentrations (1–1000 $\mu\text{g}/\text{mL}$) of the *C. fimbriata* leaf extract with controlled acarbose. The extract was used (100 $\mu\text{g}/\text{mL}$) in a glucose uptake experiment along with metformin and insulin as control treatments. CFE displayed a significant inhibitory effect on glucose metabolism enzymes. CFE showed highest glucose absorption (66.32 \pm 0.29%) at 100 $\mu\text{g}/\text{mL}$, 74.44 \pm 1.72% for metformin (10 g/mL), and 85.55 \pm 1.14% for insulin (10 μM). The results confirmed CFE to be safe because the IC_{50} of extract and metformin in the cell line examined was 1000 $\mu\text{g}/\text{mL}$ and 1000 μM , respectively [23].

Another investigation was aimed at checking the effects of CFE on insulin resistance and oxidative stress caused by the HFD in Wistar rats. The rats were given the HFD and CFE (200 mg/kg body weight/day) for 90 days. Hyperglycemia, hyperinsulinemia, hyperleptinemia, hypertriglyceridemia, and reduced insulin sensitivity were developed as a result of HFD. The rats fed on HFD had increased levels of lipid peroxidation, protein oxidation, lower growth-stimulating hormone (GSH) levels, and reduced enzymatic antioxidant activity in the liver, whereas CFE therapy corrected all these abnormalities. Moreover, the study revealed

that CFE helped to reduce insulin resistance and oxidative stress caused by HFD [14]. Another study was done to check the effect of CFE in diabetic rats. At different treatment periods, oral administration of CFE to diabetic rats at doses of 100 and 200 mg/kg body weight resulted in a significant reduction in blood glucose. Other parameters of the study included body weight, glycosylated hemoglobin (HbA1c), plasma insulin, total protein, liver, and renal biomarkers. The CFE-treated diabetic rats considerably recovered from hepatotoxicity, diabetes, and renal toxicity [87].

6.2. Antihypertensive Potential of *C. fimbriata*. Hypertension is defined as systolic blood pressure (≥ 140 mmHg) and diastolic blood pressure (≥ 90 mmHg). The use of antihypertensive medication is a major public health concern around the world. In 2000, 26.4% of people in the world had hypertension, which was expected to rise to 29.2% by 2025. In 2017, high blood pressure caused 10.4 million deaths along with 218 million disability-adjusted life-span worldwide [96]. Hypertension is among the major risk factors for heart diseases and strokes [97].

The development of atherosclerotic lesions due to the alterations in endothelial cell functioning contributes to the progression of cardiovascular disease. Increased generation of reactive oxygen species, oxidative stress, and reduced bioavailability of nitric oxide are all related to endothelial dysfunction, which can lead to arterial hardening and an increase in blood pressure. Flavonoids are the secondary metabolites and important constituents of *Caralluma* that act as antihypertensive agents by restoring endothelial function and by affecting the levels of nitric oxide [84]. The administration of CFE positively affected the metabolic markers in HFD-fed Wistar rats. After the intervention, organ weights, belly circumference, total cholesterol, triglycerides, and liver lipid content were all measured. The CFE appeared to have potential appetite-suppressing, antiobesity, and antihypertensive outcomes [92].

6.3. Antiobesity Potential of *C. fimbriata*. Obesity is one of the most serious public health problems of the 21st century. Obesity and overweight are both defined as an abnormal or excessive buildup of fat mass that has the potential to harm human health. According to the WHO, the global prevalence of obesity nearly quadrupled between 1975 and 2016 [98]. In 2016, the World Health Organization estimated that 39% of adults (1.9 billion) and 13% (650 million) were overweight or obese, respectively [99]. Obesity has been linked to a variety of ailments including heart disease, cancer, arthritis, hypertension, stroke, hyperlipidemia, and diabetes [100]. According to the National Health and Nutrition Examination Survey, the percentage of adults over the age of 20 who are obese in the United States grew from 13% to 30% between 1960 and 2000 [14]. Obesity treatment usually includes dietary modulations and physical activity adaptations in the form of lifestyle changes. When lifestyle modifications are ineffective, pharmacotherapy is generally prescribed as a second-line treatment [92]. *C. fimbriata* aids in fat burning and hunger suppression. It works by inhibiting the citrate lyase enzyme, causing our bodies to stop pro-

ducing fat and also inhibits the production of malonyl coenzyme A, which promotes the oxidation of stored fatty acids. Hence, it can be an effective intervention to block fat synthesis. Furthermore, it helps in the burning of stored fat resulting in weight loss [85].

A recent study was carried out to investigate how CFE affects satiety indicators and body composition in overweight adults. For this purpose, 83 men and women aged 20 to 50 years old took 1 g/day of CFE for 16 weeks. The placebo group's plasma leptin levels rose at week 16, whereas the CFE group remained the same. In addition, the CFE group's waist circumference decreased by 2.7 cm. The placebo group gained weight, but the CFE group dropped weight from the start (0.37 kg gain versus 0.33 kg loss). Evidently, the CFE has been shown to help people maintain their weight [20].

The CFE has also been used as a "natural slimming" dietary supplement because of its high concentration of pregnane glycosides. An efficacy trial on "Slimaluma" containing 100 mg/kg of CFE in female rats effectively modulated ingestive behavior and regulation of the brain neuropeptide Y (NPY) and orexin (ORX). Interference of CFE with the enzymes amylase and lipase has been examined in vitro as a possible adverse effect mechanism. The chemical composition of CFE was also figured out using NMR and spectrophotometric studies. According to the results of in vivo experiment, CFE did not affect blood parameters and liver/gut histomorphology. Increased water consumption and hypothalamic levels of NPY and ORX peptides were shown to minimize body weight gain [55]. A study was conducted to evaluate the efficacy of CFE in overweight and obese individuals. For this purpose, 89 patients were randomized into a treatment group and a placebo group. A capsule of 500 mg of CFE was given for 12 weeks daily. The results revealed that there were no significant changes in weight, body mass index, waist, and hip circumference [91]. Another study was conducted to investigate the effect of CFE on body weight, appetite, and lipid profile in obese rats. For this purpose, CFE was given 100 mg/kg for 50 days. The findings showed a significant reduction in body weight and lipid profile [93]. Likewise, the effect of CFE (500 mg twice daily) with restricted dietary intake and physical exercise was investigated in 33 overweight and obese subjects. The final results displayed a significant decline in BMI, body weight, hip circumference, total fat, and systolic blood pressure [95].

6.4. Antihyperlipidemic Potential of *C. fimbriata*. A study investigated the hypolipidemic potential of *C. fimbriata*. The results of the study revealed that HFD-induced heart damage in rats had increased the serum lipid profile such as total lipids, triglycerides, total cholesterol, and free fatty acids. All such abnormally raised values were considerably mitigated by CFE therapy due to an increase in lipid peroxidation and protein oxidation. The activity of antioxidant enzymes, i.e., creatine kinase, aldose reductase, and sorbitol dehydrogenase, was also significantly reduced. The study indicated that CFE was an adjuvant medication to prevent or manage heart damage caused by the HFD [62]. Similarly,

a study compared the protective effects of CFE and metformin against HFD-mediated oxidative stress, which contributes to pancreatic fibrosis in Wistar rats. Reduced glutathione, lipid oxidation, protein oxidation, and activity of antioxidant and polyol pathway enzymes, aldose reductase, and sorbitol dehydrogenase were measured in the pancreas after 90 days of intervention. Both CFE and metformin groups were able to avoid oxidative damage, while CFE had a better antioxidant status. The CFE therapy reduced acinar cell degeneration, necrosis, edema, and bleeding. Moreover, CFE proved an adjuvant therapy in the prevention or managing pancreatic damage caused by HFD [89]. Another study was conducted to check the effect of CFE (200 mg/kg body weight) and metformin (20 mg/kg body weight) on HFD-induced changes in lipid metabolism of Wistar rats. Hypercholesterolemia and hypertriglyceridemia with decreased HDL cholesterol, LDL cholesterol, and VLDL cholesterol were observed in HFD-fed group, while CFE/metformin proved valuable in ameliorating lipid metabolism biomarkers [35]. Similarly, a study was carried out to evaluate the impact of CFE (100 mg/kg/day) on lipid profile and body weight for the duration of 50 days. The results showed a significant reduction in lipid profile and body weight gain [94].

7. Nutraceutical Potentials of *C. fimbriata* against Other Diseases

7.1. Appetite-Suppressant Potential of *C. fimbriata*. Five mechanisms by which herbal medicines and their products can help people lose weight are as follows: (1) appetite suppression, thereby reducing energy intake, (2) stimulation of thermogenesis, (3) inhibition of pancreatic lipase activity, (4) reducing fat absorption, and (5) alteration in lipogenesis [99] (elaborated in Figure 1). *Caralluma* is a natural appetite suppressant that can be used as a weight loss supplement. Supplementation with *C. fimbriata* can lead to a clinically meaningful reduction in central adiposity, a key component of MS associated with other risk factors such as elevated blood pressure and cardiovascular disease. It contains pregnane glycosides, a class of naturally occurring compounds believed to inhibit the formation of fat [19]. A study revealed that a 14-year-old girl with Prader-Willi syndrome (PWS) was successfully treated for hyperphagia. At the age of two, the child began taking a supplemented CFE for appetite control. The CFE was given as a drink once a day, and the dose was gradually increased for appetite suppression. After extensive testing, blood count, vitamins, essential minerals, HbA1c, IGF-1, liver, and thyroid function tests were all within normal ranges. The study indicated that CFE may be effective in preventing hyperphagia and obesity in PWS through early intervention [32]. Another study explicated that supplementation of CFE reduced hyperphagia in children and adolescents with PWS. The CFE supplementation resulted in a substantial drop in hyperphagia at the highest dose of 1000 mg/day. The findings suggest that CFE may have a positive impact on PWS management [30].

7.2. Anticarcinogenic Potential of *C. fimbriata*. The Indian plant *C. fimbriata* has been shown to have cytotoxic activities against human colon cancer cell lines [88]. Human colon cancer is a malignant tumor of the digestive tract that is one of the major causes of death in both men and women worldwide. Colon cancer is currently the third most common cancer type in humans, the fourth most common cause of cancer-related death, and the second most common cancer type in terms of people living with cancer about 5 years after diagnosis. Every year, around 694,000 people worldwide die from colon cancer [88]. A study revealed against the KB mouth cell line CFE showed good antiproliferative action after assessing the drug's practical application and clinical efficacy; it may be utilized to treat oral cancer [92]. A study was done to see if CFE affected the COLO 320 cell line's cytotoxicity. For 24 hours, COLO 320 cells were treated with varying amounts of CFE (100–300 g/mL). In COLO 320 human colon cancer cells, CFE increased cytotoxicity. The most cytotoxic effect was seen at the highest dose of 300 μg with an IC_{50} of 233.87 μg . The results revealed that inducing cytotoxicity in COLO 320 cells with CFE reduced cell growth [88]. The 2,5-diphenyl-2H-tetrazolium bromide (MTT) cell viability experiment was done on KB cell lines that had been treated for 24 hours with increasing doses of ethanolic extract of *C. fimbriata*. The result was analyzed using cyclophosphamide as a positive control. In another study, viability of the cells at maximum concentration was found to be 28.47%, while the control showed 21.87% cell viability. CFE showed dose-dependent cytotoxicity with maximum toxicity of 71.52% at the maximum concentration. The inhibitory concentration (IC_{50}) value of CFE was found to be 28.39 $\mu\text{g}/\text{mL}$. Against the KB mouth cell line, CFE showed good antiproliferative action [88].

7.3. Antidepressant and Anti-Antioxidative Potential of *C. fimbriata*. In Western cultures, the global prevalence of diagnosed anxiety disorders is greater than 10%. There are also a significant number of people who suffer from anxiety but have not been diagnosed with a mental illness. Stress and subclinical (mild to moderate) anxiety are now widely accepted as lowering the quality of life [28]. Increased formation of free radicals causes oxidative stress which is linked to lower antioxidant levels in the myocardium and plays a crucial role in cardiovascular disease [62]. A study was done to check the effect of CFE in lowering anxiety and stress in healthy individuals. An 8-week double-blind randomized clinical experiment in which 97 people with mild to moderate anxiety were administered either 500 mg CFE ($n=49$) or 500 mg placebo ($n=48$) in a double-blind placebo-controlled trial. The GAD-7, perceived stress scale (PSS), positive and negative affect schedule (PANAS), and salivary cortisol were used to assess the timing of treatment impact at baseline, week 4, and week 8. CFE proved superior to placebo in lowering subclinical anxiety and stress over 8 weeks [28]. *C. fimbriata* revealed protection of testes of male Wistar rats from oxidative stress caused by the HFD. CFE was given orally to rats in groups C+CFE and HFD+CFE for 90 days (200 mg/kg body weight). HFD-fed rats had greater levels of lipid peroxidation, protein oxidation, polyol pathway enzymes,

reduced GSH levels, and decreased antioxidant activity in their testes, but CFE therapy corrected all of these abnormalities. CFE provided considerable protection against HFD-induced testicular oxidative damage [39]. A study used *C. fimbriata* as a natural antioxidant succulent cactus. The results revealed that fresh CFE had the maximum phenolic level of 96.4 ± 0.1 mg GAE/g, while the raw potato extract had a much lower phenolic content of 27.4 ± 0.3 mg GAE/g. The raw potato had 38.8 ± 0.2 mg QE/g of flavonoid content, while the fresh CFE had 54.4 ± 0.1 mg QE/g. After immersion treatment, CFE was found more effective in reducing acrylamide levels in French fries (42.5 g/kg) [33].

8. Safety and Tolerability/Toxicity Assessment

For human consumption, *C. fimbriata* is considered pharmacologically safe due to its natural occurrence and less toxicity. However, in some cases, it has been reported with no serious adverse effects by subjects of the study. The reported side effects were minor and limited to mild gastrointestinal symptoms such as constipation, flatulence, abdominal distention, and gastritis. All the above symptoms disappeared within a week, and the drug was shown to be nontoxic up to a dose of 2000 mg/kg. Hence, standardized extract of *C. fimbriata* was clinically tested and proven with no known side effects and was approved by TGA (Therapeutic Good Administration, Australia) [101]. Similarly, a study was done to check the toxicological assessment of CFE at different doses of 100, 300, and 1000 mg/kg body weight for six months in Sprague Dawley rats. No treatment-related toxicity or deaths were seen up to the maximum dose [102]. Another study was conducted to check the limitation of CFE, resulted in no reported adverse effects at the recommended dose of 1000 mg/kg [30]. Moreover, an efficacy study revealed that it was found to be nontoxic even up to the dose of 2000 mg/kg body weight [103].

9. Conclusion

The *Caralluma* genus comprises 260 species, and almost all of them have been considerably used for the treatment of various diseases. A large number of bioactive compounds like pregnane glycosides, megastigmane glycosides, alkaloids, quercetin, and flavone glycosides have been isolated from *Caralluma* species and used against obesity, diabetes, hypertension, ulcers, and cancer. One of these species, *C. fimbriata*, is an indigenous, wild, edible, succulent roadside shrub with cactus-like leaves. Exploration of the nutritional and nutraceutical potential of *C. fimbriata* has revealed significant bioactive constituents that have shown amelioration in cardiometabolic biomarkers, hyperglycemia, obesity, and appetite control. Hence, this neglected and underutilized vegetable should be more cultivated for its regular dietary utilization. The summarized data of this review has revealed that there is still very little work done on *C. fimbriata*. Therefore, more research on such a hidden miraculous plant and its reported active biomolecules should be done to authenticate its GRAS status. Further phytochemical and pharmacological research with more work done on innovative ideas to

incorporate CFE in diet or supplements should be done to address critical health concerns prevailing in developed as well as developing countries. As this plant still needs to get spotlighted in food and biomedical science, therefore, future investigations are welcomed to identify its therapeutic potential against different diseases either metabolic syndrome or not. Such studies can serve as a scientific baseline for designing a safer nutraceutical approach to these diseases.

Conflicts of Interest

The authors declare no conflict of interest.

References

- [1] A. J. Cortés, F. López-Hernández, and D. Osorio-Rodriguez, "Predicting thermal adaptation by looking into populations' genomic past," *Frontiers in Genetics*, vol. 11, pp. 1–14, 2020.
- [2] G. M. Kumar and N. Shiddamallayya, "Nutritional and anti-nutritional analysis of wild edible plants in Hassan District of Karnataka, India," *Indian Journal of Natural Products and Resources*, vol. 12, no. 2, pp. 281–290, 2021.
- [3] A. J. Siddiqui, S. Jahan, R. Singh et al., "Plants in anticancer drug discovery: from molecular mechanism to chemoprevention," *BioMed Research International*, vol. 2022, 18 pages, 2022.
- [4] H. Choudhury, M. Pandey, C. K. Hua et al., "An update on natural compounds in the remedy of diabetes mellitus: a systematic review," *Journal of Traditional and Complementary Medicine*, vol. 8, no. 3, pp. 361–376, 2018.
- [5] J. Zhang, K. Hu, L. Di et al., "Traditional herbal medicine and nanomedicine: converging disciplines to improve therapeutic efficacy and human health," *Advanced Drug Delivery Reviews*, vol. 178, p. 113964, 2021.
- [6] S. M. Samudra and H. P. Shinde, "Studies on ethnomedicinal plant diversity at Daund Tehsil, Pune, Maharashtra," *International Research Journal of Plant Science*, vol. 12, no. 1, pp. 1–13, 2021.
- [7] A. U. Tatiya, A. S. Kulkarna, S. J. Surana, and N. D. Bari, "Antioxidant and hypolipidemic effect of *Caralluma adscendens* Roxb. In Alloxanized Diabetic Rats," *International Journal of Pharmacology*, vol. 6, no. 4, pp. 400–406, 2010.
- [8] D. Yada, T. Sivakkumar, and M. Sudhakar, "Phytochemical evaluation and in-vitro antioxidant potential of whole plant of *Caralluma adscendens*," *Research Journal of Pharmacy and Technology*, vol. 14, no. 5, pp. 2774–2778, 2021.
- [9] M. Alam, S. Ali, S. Ahmed et al., "Therapeutic potential of ursolic acid in cancer and diabetic neuropathy diseases," *International Journal of Molecular Sciences*, vol. 22, no. 22, p. 12162, 2021.
- [10] S. A. Ashraf, M. Adnan, M. Patel et al., "Fish-based bioactives as potent nutraceuticals: exploring the therapeutic perspective of sustainable food from the sea," *Marine Drugs*, vol. 18, no. 5, pp. 1–20, 2020.
- [11] M. Ram, N. G. Cortes-perez, E. T. Quintana et al., "Functional foods, nutraceuticals and probiotics: a focus on human health," *Microorganisms*, vol. 10, no. 5, p. 1065, 2022.
- [12] M. Adnan, S. Jan, S. Mussarat et al., "A review on ethnobotany, phytochemistry and pharmacology of plant genus *Caralluma* R. Br.," *Journal of Pharmacy and Pharmacology*, vol. 66, no. 10, pp. 1351–1368, 2014.

- [13] S. A. Ashraf, A. E. O. Elkhalfifa, A. J. Siddiqui et al., "Cordycepin for health and wellbeing: a potent bioactive metabolite of an Entomopathogenic medicinal fungus Cordyceps with its nutraceutical and therapeutic potential," *Molecules*, vol. 25, no. 12, p. 2735, 2020.
- [14] G. Sudhakara, P. Mallaiah, N. Sreenivasulu, B. Sasi Bhusana Rao, R. Rajendran, and D. Saralakumari, "Beneficial effects of hydro-alcoholic extract of *Caralluma fimbriata* against high-fat diet-induced insulin resistance and oxidative stress in Wistar male rats," *Journal of Physiology and Biochemistry*, vol. 70, no. 2, pp. 311–320, 2014.
- [15] M. Ramachandra Naik, J. Rajappa Joga, N. Nagaraja, B. Nagashree, and N. Shankamma, "Micropropagation of *Caralluma adscendens* var. *fimbriata*-an indigenous medicinal plant of India," *Natural Products Chemistry & Research*, vol. 5, no. 278, p. 2, 2017.
- [16] A. J. Cortés and F. López-Hernández, "Harnessing crop wild diversity for climate change adaptation," *Genes*, vol. 12, no. 5, pp. 783–804, 2021.
- [17] R. Jayawardena, T. V. Francis, S. Abhayaratna, and P. Ranasinghe, "The use of *Caralluma fimbriata* as an appetite suppressant and weight loss supplement: a systematic review and meta-analysis of clinical trials," *BMC Complementary Medicine and Therapies*, vol. 21, no. 1, pp. 279–290, 2021.
- [18] S. Gujjala, M. Putakala, S. Nukala, M. Bangeppagari, R. Rajendran, and S. Desireddy, "Modulatory effects of *Caralluma fimbriata* extract against high-fat diet induced abnormalities in carbohydrate metabolism in Wistar rats," *Biomedicine and Pharmacotherapy*, vol. 92, pp. 1062–1072, 2017.
- [19] S. Asmi, T. Lakshmi, and R. Parameswari, "Caralluma fimbriata - pharmacological review," *Journal of Advanced Pharmacy Education and Research*, vol. 7, no. 3, pp. 175–177, 2017.
- [20] A. Rao, D. Briskey, C. dos Reis, and A. R. Mallard, "The effect of an orally-dosed *caralluma fimbriata* extract on appetite control and body composition in overweight adults," *Scientific Reports*, vol. 11, no. 1, pp. 1–10, 2021.
- [21] V. Maheshu, T. Priyadarsini, and M. Sasikumar, "Antioxidant capacity and amino acid analysis of *Caralluma adscendens* (Roxb.) Haw var. *fimbriata* (wall.) Grav. & Mayur. Aerial parts," *Journal of Food Science and Technology*, vol. 51, no. 10, pp. 2415–2424, 2014.
- [22] A. D. Padwal, S. N. Varpe, and M. B. Waman, "Phytochemical and nutritional analysis of *Caralluma fimbriata* L.," *International Journal of Researches in Biosciences and Agriculture Technology*, vol. 1, pp. 1–4, 2016.
- [23] A. Shenai and R. Anitha, "Antihyperglycemic activity of *Caralluma fimbriata*: an in vitro approach," *Pharmacognosy Magazine*, vol. 13, no. 51, pp. 499–504, 2017.
- [24] S. Malladi, V. N. Ratnakaram, and S. Babu, "Pharmacological review of *Caralluma r.Br.*: a potential herbal genus," *Asian Journal of Pharmaceutics*, vol. 12, no. 4, p. S1146, 2018.
- [25] M. Vajha and S. R. K. Chillara, "Evaluation of cellular antioxidant activity of selected species of *Caralluma* and *Boucerosia* on cell lines," *International Journal of Applied Sciences and Biotechnology*, vol. 2, no. 1, pp. 83–87, 2014.
- [26] M. A. Choucry, A. A. Shalabi, A. M. El Halawany et al., "New pregnane glycosides isolated from *Caralluma hexagona* lavranos as inhibitors of α -glucosidase, pancreatic lipase, and advanced glycation end products formation," *ACS Omega*, vol. 6, no. 29, pp. 18881–18889, 2021.
- [27] N. Qayyum, H. Rani, K. B. Mir, and A. Q. Khan, "Caralluma pharmacological attributes," *Journal of Food, Nutrition and Population Health*, vol. 2, no. 2, pp. 2–13, 2018.
- [28] G. Kell, A. Rao, and M. Katsikitis, "A randomised placebo controlled clinical trial on the efficacy of *Caralluma fimbriata* supplement for reducing anxiety and stress in healthy adults over eight weeks," *Journal of Affective Disorders*, vol. 246, pp. 619–626, 2019.
- [29] R. Ramaswamy and R. Kamala, "Pregnane glycoside compositions and *Caralluma* extract products and uses," *United States Patent*, vol. 2, no. 12, pp. 1–28, 2011.
- [30] J. L. Griggs, X. Q. Su, and M. L. Mathai, "Caralluma fimbriata supplementation improves the appetite behavior of children and adolescents with Prader-Willi syndrome," *North American Journal of Medical Sciences*, vol. 7, no. 11, pp. 509–516, 2015.
- [31] H. C. Dutt, S. Singh, B. Avula, I. A. Khan, and Y. S. Bedi, "Pharmacological review of *Caralluma r.Br.* with special reference to appetite suppression and anti-obesity," *Journal of Medicinal Food*, vol. 15, no. 2, pp. 108–119, 2012.
- [32] J. Griggs, "Single-case study of appetite control in Prader-Willi syndrome, over 12-years by the Indian extract *Caralluma fimbriata*," *Genes*, vol. 10, no. 6, pp. 447–454, 2019.
- [33] P. A. S. Babu, B. V. Aafrin, G. Archana et al., "Effects of polyphenols from *Caralluma fimbriata* on acrylamide formation and lipid oxidation—an integrated approach of nutritional quality and degradation of fried food," *International Journal of Food Properties*, vol. 20, no. 6, pp. 1378–1390, 2017.
- [34] S. Gujjala, M. Putakala, V. Gangarapu et al., "Protective effect of *Caralluma fimbriata* against high-fat diet induced testicular oxidative stress in rats," *Biomedicine and Pharmacotherapy*, vol. 83, pp. 167–176, 2016.
- [35] S. Gujjala, M. Putakala, S. Nukala, B. Manjunatha, R. Ramaswamy, and S. Desireddy, "Renoprotective effect of *Caralluma fimbriata* against high-fat diet-induced oxidative stress in Wistar rats," *Journal of Food and Drug Analysis*, vol. 24, no. 3, pp. 586–593, 2016.
- [36] R. M. Naik, V. Venugopalan, P. Kumaravelayutham, and Y. L. Krishnamurthy, "Nutritive value and mineral composition of edible *Caralluma* and *Boucerosia* species from the arid areas of Karnataka," *International Journal of Agriculture, Environment and Biotechnology*, vol. 5, no. 2, pp. 117–125, 2012.
- [37] A. J. Cortés, M. Restrepo-Montoya, and L. E. Bedoya-Canas, "Modern strategies to assess and breed Forest tree adaptation to changing climate," *Frontiers in Plant Science*, vol. 11, pp. 1606–1618, 2020.
- [38] R. Rabail, M. R. Khan, H. M. Mehwish et al., "An overview of chia seed (*Salvia hispanica* L.) bioactive peptides' derivation and utilization as an emerging nutraceutical food," *Frontiers in Bioscience - Landmark*, vol. 26, no. 9, pp. 643–654, 2021.
- [39] S. Gujjala, M. Putakala, R. Ramaswamy, and S. Desireddy, "Preventive effect of *Caralluma fimbriata* vs. metformin against high-fat diet-induced alterations in lipid metabolism in Wistar rats," *Biomedicine and Pharmacotherapy*, vol. 84, pp. 215–223, 2016.
- [40] N. Packialakshmi and S. Naziya, "Screening of antibacterial and phytochemical analysis of *Caralluma fimbriata*," *The Pharma Innovation Journal*, vol. 3, no. 6, pp. 65–69, 2014.
- [41] P. Cosme, A. B. Rodríguez, J. Espino, and M. Garrido, "Plant phenolics: bioavailability as a key determinant of their potential health-promoting applications," *Antioxidants*, vol. 9, no. 12, pp. 1–20, 2020.








- [42] Y. Y. Tang, X. M. He, J. Sun et al., "Polyphenols and alkaloids in byproducts of longan fruits (*Dimocarpus longan* Lour.) and their bioactivities," *Molecules*, vol. 24, no. 6, pp. 1186–1202, 2019.
- [43] M. M. Jucá, F. M. S. Cysne Filho, J. C. de Almeida et al., "Flavonoids: biological activities and therapeutic potential," *Natural Product Research*, vol. 34, no. 5, pp. 692–705, 2020.
- [44] L. T. Ngyuen, A. C. Farcas, S. A. Socaci et al., "An overview of saponins – a bioactive group," *Bulletin UASVM Food Science and Technology*, vol. 77, no. 1, pp. 25–36, 2020.
- [45] S. C. Baek, K. H. Nam, S. A. Yi et al., "Anti-adipogenic effect of β -carboline alkaloids from garlic (*Allium sativum*)," *Food*, vol. 8, no. 12, pp. 673–684, 2019.
- [46] V. Bendokas, K. Skemiene, S. Trumbeckaite et al., "Anthocyanins: from plant pigments to health benefits at mitochondrial level," *Critical Reviews in Food Science and Nutrition*, vol. 60, no. 19, pp. 3352–3365, 2020.
- [47] R. Hair, J. R. Sakaki, and O. K. Chun, "Anthocyanins, microbiome and health benefits in aging," *Molecules*, vol. 26, no. 3, pp. 537–554, 2021.
- [48] R. R. Khalil and Y. F. Mustafa, "Phytochemical, antioxidant and antitumor studies of coumarins extracted from granny smith apple seeds by different methods," *Systematic Reviews in Pharmacy*, vol. 11, no. 2, pp. 57–63, 2020.
- [49] N. Z. T. De Jesus, H. D. S. Falcao, I. F. Gomes et al., "Tannins, peptic ulcers and related mechanisms," *International Journal of Molecular Sciences*, vol. 13, no. 3, pp. 3203–3228, 2012.
- [50] I. E. Sallam, A. Abdelwareth, H. Attia et al., "Effect of gut microbiota biotransformation on dietary tannins and human health implications," *Microorganisms*, vol. 9, no. 5, pp. 965–998, 2021.
- [51] M. T. Islam, E. S. Ali, and M. S. Mubarak, "Anti-obesity effect of plant diterpenes and their derivatives: a review," *Phytotherapy Research*, vol. 34, no. 6, pp. 1216–1225, 2020.
- [52] C. Cavin, D. Holzhaeuser, G. Scharf, A. Constable, W. W. Huber, and B. Schilter, "Cafestol and kahweol, two coffee specific diterpenes with anticarcinogenic activity," *Food and Chemical Toxicology*, vol. 40, no. 8, pp. 1155–1163, 2002.
- [53] R. J. Ogbe, D. O. Ochalefu, S. G. Mafulul, and O. B. Olaniru, "A review on dietary phytosterols: their occurrence, metabolism and health benefits," *Asian Journal of Plant Science and Research*, vol. 5, no. 4, pp. 10–21, 2015.
- [54] M. Stompor Gorący, "The health benefits of emodin, a natural anthraquinone derived from rhubarb—a summary update," *International Journal of Molecular Sciences*, vol. 22, no. 17, pp. 9522–9538, 2021.
- [55] A. Vitalone, A. Di Sotto, C. L. Mammola et al., "Phytochemical analysis and effects on ingestive behaviour of a *Caralluma fimbriata* extract," *Food and Chemical Toxicology*, vol. 108, pp. 63–73, 2017.
- [56] A. A. Shalabi, A. M. El Halawany, M. A. Choucry et al., "New pregnane glycosides from *Caralluma hexagona* Lavranos and their in vitro α -glucosidase and pancreatic lipase inhibitory effects," *Phytochemistry Letters*, vol. 36, pp. 49–57, 2020.
- [57] A. M. SayedEl, E. AbdElSattar, and M. N. Khalil, "New calogenin pregnane glycoside derivative from *Huernia saudiarabica* and its lipase and α -glucosidase inhibitory activities," *Biomedicine and Pharmacotherapy*, vol. 127, p. 110143, 2020.
- [58] E. AbdEl-Sattar and D. E. Ali, "Russelioside B: a pregnane glycoside with pharmacological potential," *Revista Brasileira de Farmacognosia*, vol. 32, no. 2, pp. 188–200, 2022.
- [59] W. Y. Zeng, T. Lin, C. Han et al., "Trigonelline extends the lifespan of *C. elegans* and delays the progression of age-related diseases by activating AMPK, DAF-16, and HSF-1," *Oxidative Medicine and Cellular Longevity*, vol. 2021, 11 pages, 2021.
- [60] O. Kunert, V. G. Rao, G. S. Babu et al., "Pregnane glycosides from *Caralluma adscendens* var. *fimbriata*," *Chemistry and Biodiversity*, vol. 5, no. 2, pp. 239–250, 2008.
- [61] D. Priya, K. Rajaram, and K. P. Suresh, "Phytochemical studies and GC-MS analysis of *Caralluma fimbriata* wall," *International Journal of Pharmaceutical Research and Development*, vol. 3, no. 10, pp. 105–110, 2011.
- [62] S. Gujjala, M. Putakala, S. B. R. Bongu, R. Ramaswamy, and S. Desireddy, "Preventive effect of *Caralluma fimbriata* against high-fat diet induced injury to heart by modulation of tissue lipids, oxidative stress, and histological changes in Wistar rats," *Archives of Physiology and Biochemistry*, vol. 2, pp. 474–482, 2019.
- [63] Z. K. Shinwari, S. Sultan, and T. Mahmood, "Molecular and morphological characterization of selected *Mentha* species," *Pakistan Journal of Botany*, vol. 43, no. 3, pp. 1433–1436, 2011.
- [64] M. Sireesha, R. V. Nadh, K. S. Babu, and M. Sreenivasulu, "Phytochemical library of *Caralluma* genus," *International Journal of Research in Pharmaceutical Sciences*, vol. 9, no. 4, pp. 1201–1213, 2018.
- [65] M. A. Raees and Abstract, "A phytopharmacological review on an Arabian medicinal plant : *Caralluma flava* N.E. Br," *International Journal of Phytomedicine*, vol. 10, no. 3, pp. 148–152, 2018.
- [66] B. Avula, Y. J. Shukla, Y. H. Wang, and I. A. Khan, "Quantitative determination of pregnanes from aerial parts of *Caralluma* species using HPLC-UV and identification by LC-ESI-TOF," *Journal of AOAC International*, vol. 94, no. 5, pp. 1383–1390, 2011.
- [67] A. M. Minhas, A. U. Khan, and M. M. Ansari, "Anti-inflammatory effect of *Caralluma edulis* against acute and chronic inflammation," *Journal of Animal and Plant Sciences*, vol. 28, no. 1, pp. 264–269, 2018.
- [68] N. Yu, Y. Huang, J. Yu et al., "Ganoderma lucidum triterpenoids (GLTs) reduce neuronal apoptosis via inhibition of ROCK signal pathway in APP/PS1 transgenic Alzheimer's disease mice," *Oxidative Medicine and Cellular Longevity*, vol. 2020, 11 pages, 2020.
- [69] H. N. Nguyen, S. L. Ullevig, J. D. Short, L. Wang, Y. J. Ahn, and R. Asmis, "Ursolic acid and related analogues: triterpenoids with broad health benefits," *Antioxidants*, vol. 10, no. 8, pp. 1–24, 2021.
- [70] A. O. Antwi, D. D. Obiri, and N. Osafo, "Stigmasterol modulates allergic airway inflammation in guinea pig model of ovalbumin-induced asthma," *Mediators of Inflammation*, vol. 2017, 11 pages, 2017.
- [71] R. Pratiwi, C. Nantasenamat, W. Ruankham et al., "Mechanisms and neuroprotective activities of stigmasterol against oxidative stress-induced neuronal cell death via sirtuin family," *Frontiers in Nutrition*, vol. 8, pp. 1–12, 2021.
- [72] B. Ahmad, S. J. Abbas, F. Hussain, S. Bashir, and D. Ahmad, "Study on *Caralluma tuberculata* nutritional composition and its importance as medicinal plant," *Pakistan Journal of Botany*, vol. 46, no. 5, pp. 1677–1684, 2014.
- [73] R. Semwal, S. K. Joshi, R. B. Semwal, and D. K. Semwal, "Health benefits and limitations of rutin - a natural flavonoid

- with high nutraceutical value,” *Phytochemistry Letters*, vol. 46, pp. 119–128, 2021.
- [74] M. Khasawneh, H. M. Elwy, N. M. Fawzi, A. A. Hamza, A. R. Chevidenkandy, and A. H. Hassan, “Antioxidant activity and lipoxygenase inhibitory effect of *Caralluma arabica* and related polyphenolic constituents,” *American Journal of Plant Sciences*, vol. 5, no. 11, pp. 1623–1631, 2014.
- [75] I. U. H. Bhat and R. Bhat, “Quercetin: a bioactive compound imparting cardiovascular and neuroprotective benefits: scope for exploring fresh produce, their wastes, and by-products,” *Biology*, vol. 10, no. 7, pp. 1–34, 2021.
- [76] R. Khursheed, S. K. Singh, S. Wadhwa, M. Gulati, and A. Awasthi, “Enhancing the potential preclinical and clinical benefits of quercetin through novel drug delivery systems,” *Drug Discovery Today*, vol. 25, no. 1, pp. 209–222, 2020.
- [77] H. Rasheed, M. Shehzad, R. Rabail et al., “Delving into the nutraceutical benefits of purple carrot against metabolic syndrome and cancer: a review,” *Applied Sciences*, vol. 12, no. 6, p. 3170, 2022.
- [78] E. McCracken, M. Monaghan, and S. Sreenivasan, “Pathophysiology of the metabolic syndrome,” *Clinics in Dermatology*, vol. 36, no. 1, pp. 14–20, 2018.
- [79] E. Rodríguez-Correa, I. González-Pérez, P. I. Clavel-Pérez, Y. Contreras-Vargas, and K. Carvajal, “Biochemical and nutritional overview of diet-induced metabolic syndrome models in rats: what is the best choice,” *Nutrition and Diabetes*, vol. 10, no. 1, pp. 24–39, 2020.
- [80] X. Zheng, T. Chen, A. Zhao et al., “Hyochoolic acid species as novel biomarkers for metabolic disorders,” *Nature Communications*, vol. 12, no. 1, pp. 1–11, 2021.
- [81] I. L. Lemmer, N. Willemsen, N. Hilal, and A. Bartelt, “A guide to understanding endoplasmic reticulum stress in metabolic disorders,” *Molecular Metabolism*, vol. 47, p. 101169, 2021.
- [82] S. Chen, H. Jiang, X. Wu, and J. Fang, “Therapeutic effects of quercetin on inflammation, obesity, and type 2 diabetes,” *Mediators of Inflammation*, vol. 2016, 5 pages, 2016.
- [83] P. E. Aba and I. U. Asuzu, “Mechanisms of actions of some bioactive anti-diabetic principles from phytochemicals of medicinal plants: a review,” *Indian Journal of Natural Products and Resources*, vol. 9, no. 2, pp. 85–96, 2018.
- [84] J. L. Clark, P. Zahradka, and C. G. Taylor, “Efficacy of flavonoids in the management of high blood pressure,” *Nutrition Reviews*, vol. 73, no. 12, pp. 799–822, 2015.
- [85] B. Topiwala and R. Krishnamurthy, “*Hoodia gordonii* (African plant), *Caralluma fimbriata* and *Achyranthes aspera* (Indian plants): an appetite suppressant,” *BioTechnology: An Indian Journal*, vol. 7, no. 8, pp. 285–290, 2013.
- [86] B. B. Barton, A. Zagler, K. Engl, L. Rihs, and R. Musil, “Prevalence of obesity, metabolic syndrome, diabetes and risk of cardiovascular disease in a psychiatric inpatient sample: results of the metabolism in psychiatry (MiP) study,” *European Archives of Psychiatry and Clinical Neuroscience*, vol. 270, no. 5, pp. 597–609, 2020.
- [87] S. Latha, K. Rajaram, and P. Suresh Kumar, “Hepatoprotective and antidiabetic effect of methanol extract of *Caralluma fimbriata* in streptozocin induced diabetic albino rats,” *International Journal of Pharmacy and Pharmaceutical Sciences*, vol. 6, no. 1, pp. 665–668, 2014.
- [88] S. J. Suhasini, R. Anitha, G. Sosa, and T. Lakshmi, “The cytotoxic effect of *Caralluma fimbriata* on Kb cell lines,” *Research Journal of Pharmacy and Technology*, vol. 12, no. 10, pp. 4995–44998, 2019.
- [89] G. Sudhakara, P. Mallaiiah, R. Rajendran, and D. Saralakumari, “*Caralluma fimbriata* and metformin protection of rat pancreas from high fat diet induced oxidative stress,” *Biotechnic and Histochemistry*, vol. 93, no. 3, pp. 177–187, 2018.
- [90] J. L. Griggs, B. Sc Hons, P. Sinnayah, and A. M. L. Mathai, “Appetite stimulation and 5-HT_{2c} signalling in the Prader-Willi syndrome, Garvan Snord116 deletion mouse model, after eight-week administration of *Caralluma fimbriata* extract,” *Brain and Behavior*, vol. 8, no. 12, pp. 115–116, 2016.
- [91] V. Khajuria, A. Mahajan, A. Sharma et al., “To evaluate efficacy and safety of *Caralluma fimbriata* in overweight and obese patients: a randomized, single blinded, placebo control trial,” *Perspectives in Clinical Research*, vol. 6, no. 1, pp. 39–44, 2015.
- [92] K. J. Astell, M. L. Mathai, and X. Q. Su, “The effect of *Caralluma fimbriata* extract on metabolic parameters in high-fat fed Wistar rats,” *Journal of Nutrition & Intermediary Metabolism*, vol. 1, no. 2014, p. 43, 2014.
- [93] B. Ambadasu, S. V. Dange, and R. S. Wali, “Effect of *Caralluma fimbriata* extract on appetite, body weight & lipid profile in cafeteria diet-induced obesity in rats,” *International Journal of Pharmacy and Pharmaceutical Sciences*, vol. 5, no. 4, pp. 536–539, 2013.
- [94] B. Ambadasu, S. V. Dange, R. S. Wali, and P. S. Worlikar, “Effect of *Caralluma fimbriata* extract on appetite & lipid profile in rats fed with hypercalorie/cafeteria diet,” *International Journal of Pharma and Bio Sciences*, vol. 4, no. 2, pp. 788–793, 2013.
- [95] K. J. Astell, M. L. Mathai, A. J. McAinch, C. G. Stathis, and Q. S. Xiao, “A pilot study investigating the effect of *Caralluma fimbriata* extract on the risk factors of metabolic syndrome in overweight and obese subjects: a randomised controlled clinical trial,” *Complementary Therapies in Medicine*, vol. 21, no. 3, pp. 180–189, 2013.
- [96] L. Xiao, C. Le, G. Y. Wang et al., “Socioeconomic and lifestyle determinants of the prevalence of hypertension among elderly individuals in rural Southwest China: a structural equation modelling approach,” *BMC Cardiovascular Disorders*, vol. 21, no. 1, pp. 1–10, 2021.
- [97] J. Fang, C. Luncheon, A. Patel et al., “Self-reported prevalence of hypertension and antihypertensive medication use among Asian Americans: behavioral risk factor surveillance system 2013, 2015 and 2017,” *Journal of Immigrant and Minority Health*, vol. 23, no. 1, pp. 26–34, 2021.
- [98] M. Z. Aumeeruddy and M. F. Mahomoodally, “Traditional herbal medicines used in obesity management: a systematic review of ethnomedicinal surveys,” *Journal of Herbal Medicine*, vol. 28, p. 100435, 2021.
- [99] M. Payab, S. Hasani-Ranjbar, N. Shahbal et al., “Effect of the herbal medicines in obesity and metabolic syndrome: a systematic review and meta-analysis of clinical trials,” *Phytotherapy Research*, vol. 34, no. 3, pp. 526–545, 2020.
- [100] R. A. El-shiekh, D. A. Al-Mahdy, M. S. Hifnawy, and E. A. Abdel-Sattar, “In-vitro screening of selected traditional medicinal plants for their anti-obesity and anti-oxidant activities,” *South African Journal of Botany*, vol. 123, pp. 43–50, 2019.
- [101] B. Saboo and H. Zaveri, “Recent update in management of obesity and overweight patients: standardized extract of *Caralluma fimbriata* safe and effective therapy,” *International Journal of Computer Communication and Informatics*, vol. 2, pp. 5–9, 2011.

- [102] A. Y. Odendaal, N. S. Deshmukh, T. K. Marx, A. G. Schauss, J. R. Endres, and A. E. Clewell, "Safety assessment of a hydro-ethanolic extract of *Caralluma fimbriata*," *International Journal of Toxicology*, vol. 32, no. 5, pp. 385–394, 2013.
- [103] R. Rajendran, D. B. Ambikar, R. A. Khandare, V. D. Sannapuri, N. S. Vyawahare, and P. Clayton, "Nootropic activity of *Caralluma fimbriata* extract in mice," *Food and Nutrition Sciences*, vol. 5, no. 2, pp. 147–152, 2014.

Research Article

Resveratrol as a Promising Polyphenol in Age-Associated Cardiac Alterations

Denise Börzsei ¹, Judith Sebestyén,² Renáta Szabó ¹, Zelma Nadin Lesi,¹
Andrea Pálszabó,¹ Patrícia Pálszabó,¹ András Szász,³ Dániel Priksz ⁴, Béla Juhász ⁴,
Médea Veszélka ¹, Zsolt Turcsán,⁵ Zoltán Deim,¹ Csaba Varga ¹, and Anikó Pósa ¹

¹Department of Physiology, Anatomy and Neuroscience, Faculty of Science and Informatics, University of Szeged, 6726 Szeged, Hungary

²South-Pest Hospital Centre, National Institute for Infectology and Haematology, Department of Burns and Plastic Surgery, Budapest 1097, Hungary

³Institution of Physical Education and Sport Sciences, Faculty of Education, University of Szeged, 6725 Szeged, Hungary

⁴Department of Pharmacology and Pharmacotherapy, Faculty of Medicine, University of Debrecen, 4032 Debrecen, Hungary

⁵Gulyás János és Társa Ltd., 6645 Felgyő, Hungary

Correspondence should be addressed to Anikó Pósa; paniko@bio.u-szeged.hu

Received 25 March 2022; Accepted 10 June 2022; Published 18 June 2022

Academic Editor: Anderson J. Teodoro

Copyright © 2022 Denise Börzsei et al. This is an open access article distributed under the Creative Commons Attribution License, which permits unrestricted use, distribution, and reproduction in any medium, provided the original work is properly cited.

According to a widely accepted theory, oxidative stress is considered to be the number one trigger of aging-associated degenerative processes including cardiovascular diseases. In the context of aging-research, resveratrol receives special attention with its surprising number of health benefits. The aim of our study was to examine the anti-inflammatory and antioxidant effects of this dietary polyphenol in aging rat heart. 20-month-old female and male Wistar rats were divided into control (untreated) and resveratrol-treated groups. Resveratrol was administered at a dose of 0.05 mg/ml for 12 weeks dissolved in drinking water, while the control rats received *ad libitum* water. Cardiac level of reactive oxygen species (ROS), nuclear factor kappa B (NFκB), tumor necrosis factor alpha (TNF-α), and glutathione (GSH) parameters, as well as the activity of myeloperoxidase (MPO) and heme oxygenase (HO) enzymes were detected. Together with the biochemical measurements, hearts were isolated and used for an exposure of ischemic-reperfusion injury via Langendorff perfusion system. 12 week of resveratrol treatment suppressed the age-related inflammatory pathways including the expression of TNF-α, NFκB, and the activity of MPO while intensified the endogenous antioxidant defenses through the induction of GSH and HO system. Presumably, as a result of these processes, the necrotic area of the heart in response to an acute injury was also significantly reduced in the resveratrol-treated groups. Our findings confirmed that resveratrol has cardioprotective effects at several points by counteracting the aging-associated cellular malfunctions in the heart.

1. Introduction

Aging is a multifactorial biological process driven by a variety of cellular changes which ultimately affect protein homeostasis, chromosome structure, and genetic information. The hallmarks of aging are postulated to originate from oxidative damages and the resulting disrupted redox imbalance [1]. Oxidative stress can cause premature apoptosis or

senescence by impairing the cellular milieu, and this altered cellular fate serves as a major determinant of lifespan [2]. Furthermore, it is important to note that changes in cellular redox status and cell death signaling pathways are also causally related to the development of chronic inflammation [3]. Age-related oxidative stress and inflammation inevitably pose a threat to cardiovascular health; however, with the latest medical advancements, antioxidant active agents, and

lifestyle changes, it is now possible to slow down aging processes and avert the progression of age-related cardiovascular conditions [4–6].

Resveratrol (RESV) is a stilbenoid polyphenol originally extracted from the roots of *Veratrum grandiflorum* but has been detected in many other plants since then, such as grapes, berries, and peanuts. It exists in two isoforms, namely, *cis*-, *trans*-resveratrol, the latter of which is considered to be a more biologically active and stable form [7]. In 1992, Renaud and De Lorgeril were the first who set a parallel between wine-related polyphenols and reduced risk of adverse cardiovascular outcomes and named this phenomenon the “French paradox” [8]. RESV has gained an outstanding scientific interest ever since due to its wide-ranging biological effects. It has a remarkable ability to counteract a number of noncommunicable diseases and has been shown to be particularly effective in the treatment of cardiovascular diseases (CVD) thanks to its anti-inflammatory and antioxidant properties. [9–11]. Numerous experimental studies verified that RESV plays an important role in the prevention of CVDs by affecting cardiac Ca^{2+} homeostasis, hypertrophic signaling pathways, and myocyte apoptosis [12–14]. Additionally, it has also been demonstrated that RESV has an exceptional capability to extend the lifespan of multiple model organisms, bolstering hope that these findings can be translated into further medical studies in the future [15].

Based on the literature, we assumed that a long-term RESV intake may be an effective agent against age-derived myocardial damages in rat model. Therefore, the aim of our study was to explore the cardiac anti-inflammatory and antioxidant effects of RESV and whether these RESV-mediated protective effects are manifested in acute cardiac injury.

2. Materials and Method

2.1. Experimental Protocol. In this study, 20 month-old male and female Wistar rats ($n = 7 - 9$ rats per group) were used (Toxi-Coop, Hungary). Animals were kept under standard circumstances according to the regulations of the Directive 2010/63/EU. At the beginning of the study, within the sexes, rats were divided into the following two subgroups: control (CTRL) and RESV-consuming animals. Control rats received *ad libitum* water throughout the study, while RESV animals got 0.05 mg/ml *trans*-resveratrol (AK Scientific, USA) dissolved in their drinking water for 12 weeks [16]. This dose was chosen to provide the adequate mg/kg body-weight dose (7.5 mg/kg) based on the animals’ consumption [17]. Dissolved RESV was placed into the cages in a tinted glass in order to prevent photochemical isomerization. At the end of the study, rats were sacrificed, and their hearts were either perfused via Langendorff system in order to expose the size of infarction as a result of a left anterior descending coronary artery (LAD) occlusion or were clamped and stored at -80°C for further biochemical measurements. All procedures were approved by the National Scientific Ethical Committee on Animal Experimentation (XX./2317/2021.) and correspond to the ARRIVE guidelines.

2.2. Ischemia-Reperfusion Injury Modelling with Langendorff Perfusion System. After anesthesia, animals were subjected to cervical dislocation, and their hearts were removed by maximal aortic excision. Using an ice-cold Krebs-Henseleit buffer (1.24 mM KH_2PO_4 , 20.1 mM NaHCO_2 , 1.25 mM CaCl_2 , 4.7 mM KCl , 119 mM NaCl , 1.24 mM MgSO_4 , 11.2 mM glucose, and 1.24 mM MgSO_4), hearts were suspended through the aorta and placed on a Langendorff perfusion column. Retrograde perfusion of the hearts was performed under the following conditions: pressure 75 mm Hg, 5% CO_2 , 95% O_2 , and 37°C . Ischemic injury was modeled by LAD ligation for 30 min followed by reperfusion for 120 min. Hearts were then perfused with Evans blue solution (1%) and placed in a -20°C freezer until further analysis.

2.3. Determination of Infarct Size. To determine the area of infarct, frozen hearts were sliced into 2 mm-thick pieces perpendicular to the apico-basal axis and incubated at 37°C for 10 min in 1% 2,3,5-triphenyl tetrazolium chloride (TTC) solution. Slices were then immersed in 10% formalin solution and washed with phosphate buffer (pH 7.4). The heart slices were photographed between two glass slides, and the infarction area was evaluated using Image J program, its size was expressed as the percentage of the area at risk.

2.4. Determination of $\text{NF}\kappa\text{B}$, ROS, and $\text{TNF-}\alpha$ Concentration. Powdered heart tissues were homogenized with a given amount of phosphate-buffered saline (PBS; pH 7.4) with a handheld homogenizer. Samples were placed in the centrifuge for 20 minutes (at 2000 rpm, 4°C); then, supernatants were collected and kept on ice. Standards were diluted according to the manual of the Enzyme-linked Immunosorbent Assay (ELISA; GenAsia Biotech) kits. Sample solution wells included $40\ \mu\text{l}$ sample, $10\ \mu\text{l}$ antibody, and $50\ \mu\text{l}$ streptavidin-HRP. After covering the plate with a seal plate membrane, reagents together with samples were incubated at 37°C for 60 minutes. Color development was initiated by chromogen solutions A and B and stop solution. At the end of the assay, absorbance (OD) of each well was measured under 450 nm wavelength. The color shade of the samples is positively correlated with the concentration of the aforementioned enzymes. $\text{NF}\kappa\text{B}$ and $\text{TNF-}\alpha$ values were defined as pg/mg protein, while ROS concentration was expressed as $\mu\text{U}/\text{mg}$ protein.

2.5. Determination of MPO Activity. Heart tissues were homogenized twice for 10 seconds in a buffer containing PBS and 0.5% hexadecyltrimethylammonium bromide (HETAB). Samples were frozen and thawed four times, for better cell disruption; then, homogenates were centrifuged for 15 minutes, at 10 000 and 4°C . For the activity measurement, $12\ \mu\text{l}$ of standard or sample was added to a 96-well plate, followed by $280\ \mu\text{l}$ of o-dianisidine dihydrochloride. The reaction was started with $20\ \mu\text{l}$ of hydrogen peroxide, and after shaking the reaction mixture for 30 seconds, the activity of MPO was detected spectrophotometrically at 490 nm. The values were expressed as $\mu\text{U}/\text{mg}$ protein.

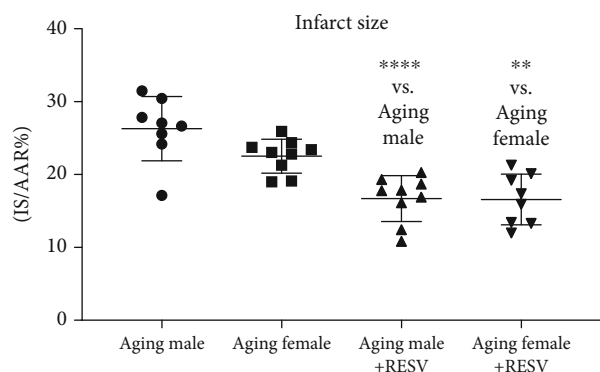


FIGURE 1: The effects of a 12-week-long resveratrol treatment on the magnitude of the infarct size in aged rats. Infarct size (IS) was calculated as the percentage of the area at risk (AAR). One-way ANOVA and Tukey posttest result is shown as mean \pm SD; $n = 8 - 9$ /group, ** $p < 0.01$, and **** $p < 0.0001$. Statistical significance between resveratrol-treated and nontreated control counterparts. RESV: Resveratrol; IS: Infarct size; AAR: Area at risk.

2.6. Determination of Total GSH+GSSG Content. Rat hearts were first homogenized on ice in a buffer [0.25 M sucrose, 20 mM Tris, and 1 mM dithiothreitol (DTT)], and the resulting homogenate (15 000g, 30 min, 4°C) was centrifuged. From the supernatant obtained after centrifugation, 1 ml was further homogenized with 200 μ l of homogenization buffer (0.25 M sucrose, 20 mM Tris, 1 mM DTT, and 0.1 M CaCl₂). After incubation on ice for 30 min, another centrifugation was performed (21 000g, 30 min, and 4°C). The resulting pure cytosolic fraction was used for enzyme assay. In a 96-well microplate, 40 μ l of sample or standard, 20 μ l of 5,5'-dithio-bis-2-nitrobenzoic acid, and 140 μ l of nicotinamide dinucleotide phosphate (NADPH) were added, and the resulting mixture was incubated for 5 min at 25°C. The reaction was started by adding 10 μ l of glutathione reductase. After shaking for 10 min, the formation of 2-nitro-5-thiobenzoic acid was measured at 405 nm, and the resulting GSH levels were expressed as nmol/mg protein.

2.7. Measurement of HO Activity. Cardiac tissues were homogenized in ice-cold buffer (10.0 mM N-2-hydroxyethylpiperazine-N'-2-ethanesulfonate, 0.10 mM ethylenediamine-tetraacetic acid disodium salt dihydrate, 1.0 mM DTT, 30.0 mM sucrose, 10 μ g/ml trypsin inhibitor, 2.0 μ g/ml aprotinin, 10.0 μ g/ml leupeptin, and pH 7.4), centrifuged at 15 000 \times g, for 20 min, at 4°C, and the remained supernatant was used for HO activity measurements. The reaction mixture consisted of 75 μ l of sample, 2.0 mM glucose-6-phosphate, 0.14 U/ml glucose-6-phosphate dehydrogenase, 15.0 μ M hemin, and 120.0 μ g/ml biliverdin reductase. For the determination of HO activity, two parallel measurements were performed, a so-called blind and NADPH line. For the NADPH measurement, 100 μ l of reduced β -nicotinamide adenine dinucleotide phosphate (β -NADPH) was added to the mixture to initiate the reaction and incubated at 37°C for 60 min, after which ice cooling was used to stop the reaction. For the blank measurements, a reaction mixture was prepared in which

β -NADPH was replaced with buffer. The NADPH and blank solutions were measured spectrophotometrically at 465 nm; the values obtained from the blank series were then subtracted from the NADPH values. HO activity was plotted as the amount of bilirubin formed in nmol/hour/mg protein.

2.8. Measurement of Protein Concentration (Bradford Method). In order to perform the protein measurements, the samples which were homogenized and centrifuged according to the previous measurements had to be diluted appropriately in parallel with the preparation of a new standard line. After the dilution, 200 μ l of Bradford reagent was added to both the standard bovine serum albumin (BSA) line and our samples. The protein concentration of the samples was measured at 595 nm by a spectrophotometer, results were expressed at μ g protein/ml.

2.9. Data Representation and Statistical Analysis. Experiments were designed to generate groups of equal size using randomization. Group sizes represent the number of independent samples/animals, not technical replicates. Raw data was analyzed by a blinded reader. Data presented as the mean value of the group \pm standard deviation (mean \pm SD). Normal distribution was estimated by Shapiro-Wilk normality test; after, statistical analysis was performed using one-way analysis of variance (ANOVA) followed by Tukey posttest (only if F in ANOVA achieved $p < 0.05$, and normality test was passed) or Kruskal-Wallis test followed by Dunn's posttest (when normality test was not passed). Statistical analysis was performed using the GraphPad Prism 8.4.2. (GraphPad Software Inc., La Jolla, CA, USA; RRID:SCR_002798). Probability values (p) less than 0.05 were considered significantly different; and the level of significance is marked with asterisks between the corresponding groups (*: $p < 0.05$; **: $p < 0.01$; ***: $p < 0.001$; ****: $p < 0.0001$).

3. Results

3.1. Measurement of Myocardial Infarct Size. As shown in Figure 1, aging CTRL animals have shown a higher rate of infarct size compared to the RESV-treated groups. As a result of the 12-week-long RESV consumption, a significant attenuation was detected in the necrotic extension of the heart in both sexes.

3.2. Cardiac TNF- α and NF κ B Concentration. Members of the inflammatory cascade, namely, TNF- α and NF κ B concentrations, were markedly elevated in aging CTRL groups compared to the RESV groups. 12 weeks of RESV administration was able to significantly mitigate these elevated pro-inflammatory values in both females and males. Data are presented in Figures 2(a) and 2(b).

3.3. Cardiac MPO Activity. Figure 3 presents that similar to the inflammatory TNF- α and NF κ B expression, CTRL aging female and male rats exhibited the highest MPO activities; whereas 12 weeks of RESV administration resulted in a decreased MPO activity in both sexes; furthermore, in females, this change was found to be significant.

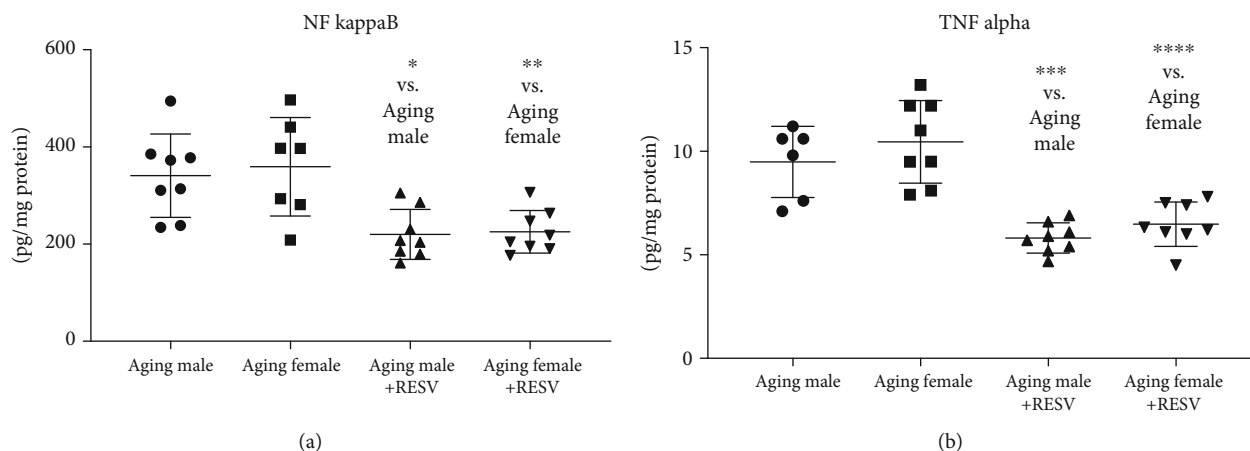


FIGURE 2: (a) The effects of a 12-week-long resveratrol treatment on cardiac NFκB concentration in aged rats (NFκB; expressed as pg/mg protein). One-way ANOVA and Tukey posttest result is shown as mean ± SD; $n = 7 - 8$ /group. (b) The effects of a 12-week-long resveratrol treatment on cardiac TNF- α expression in aged rats (TNF- α ; expressed as pg/mg protein). One-way ANOVA and Tukey posttest result is shown as mean ± SD; $n = 6 - 8$ /group. * $p < 0.05$, ** $p < 0.01$, *** $p < 0.001$, and **** $p < 0.0001$: Statistical significance between resveratrol-treated and nontreated control counterparts. RESV: Resveratrol; NFκB: Nuclear factor kappa B; TNF- α : Tumor necrosis factor alpha.

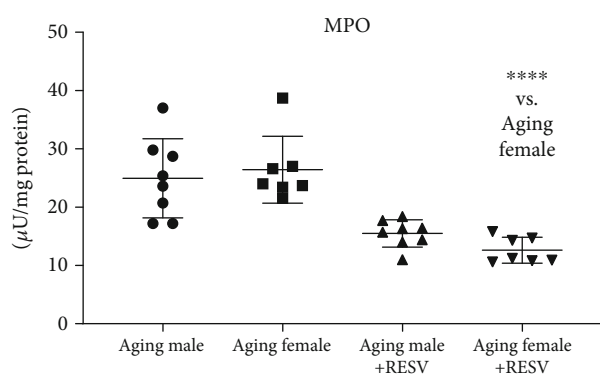


FIGURE 3: The effects of a 12-week-long resveratrol treatment on cardiac myeloperoxidase enzyme activity in aged rats (MPO; expressed as $\mu\text{U/mg protein}$). Non-Gaussian distribution and Kruskal-Wallis test with Dunn's post hoc test result is shown as mean ± SD; $n = 7 - 8$ /group. *** $p < 0.001$: Statistical significance between resveratrol-treated and nontreated control counterparts. RESV: Resveratrol; MPO: Myeloperoxidase.

3.4. Cardiac ROS Concentration. As shown in Figure 4, aging status resulted in a marked increase in the ROS expression of male and female rats. Nonetheless, for both sexes, RESV-treated rats possessed significantly lower ROS values in comparison with the CTRL animals.

3.5. Determination of Cardiac Total GSH+GSSG Content. As a result of the 12-week RESV treatment, a significant improvement was detected in the cardiac antioxidant status in both male and female aged rats. As for female rats, GSH+GSSG content alteration in response to the RESV administration was found to be significant. Data are presented in Figure 5.

3.6. Measurement of Cardiac HO Activity. As shown in Figure 6, RESV-consuming animals exhibited the highest

HO activity values, whereas a significant decrease was found in CTRL aging animals; thus, the reduced antioxidant values precipitated by aging were compensated by 12 weeks of RESV treatment.

4. Discussion

The quest to discover the secret of longevity has been ongoing for quite some time. It is apparent that life expectancy and cardiovascular aging are closely interrelated, both from a cause-and-effect perspective and from a prevalence point of view [2]. Based on the most widely accepted theories today, the primary cause of aging is the accretion of ROS and the resulting accumulative oxidative damage, since the efficacy of enzymatic and nonenzymatic antioxidant mechanisms dramatically declines with age [18]. The main source of ROS production is oxidative phosphorylation during mitochondrial metabolism. Since mitochondria build up 45% of cardiomyocytes, the ROS they generate are of paramount importance [19]. Cardiac vulnerability is strongly linked to this aggravated oxidative injury, as it is responsible for the premature apoptosis of the cardiomyocytes, by damaging intracellular macromolecules [20]. Our results clearly show that aging arise an elevated cardiac ROS production both in males and females; however, 12 weeks of RESV administration was able to moderate the oxidative processes by scavenging free radicals. RESV is considered to be an impressive antioxidant pharmacophore thanks to its 4-hydroxystilbene skeleton. The antioxidant activity of RESV is in part attributed to the existence of its free hydroxyl group. Besides, it potentiates endogenous antioxidant enzymes such as SOD, GSH, or HO by the interaction of Nrf2 which is considered to be the main target of RESV. RESV facilitates the translocation of Nrf2 to the nucleus and triggers the transcription of antioxidant defense enzymes [21]. It has been previously reported that RESV upregulates the gene expression of HO enzymes in a Nrf2-

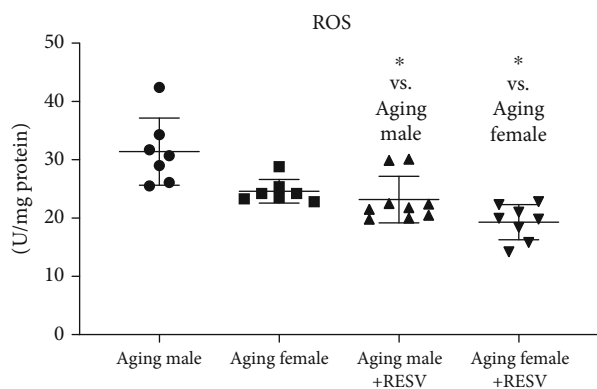


FIGURE 4: The effects of a 12-week-long resveratrol treatment on cardiac reactive oxygen species in aged rats (ROS; expressed as U/mg protein). Non-Gaussian distribution and Kruskal-Wallis test with Dunn's post hoc test result is shown as mean \pm SD; $n = 7 - 9$ /group and $*p < 0.05$: Statistical significance between resveratrol-treated and nontreated control counterparts. RESV: Resveratrol; ROS: Reactive oxygen species.

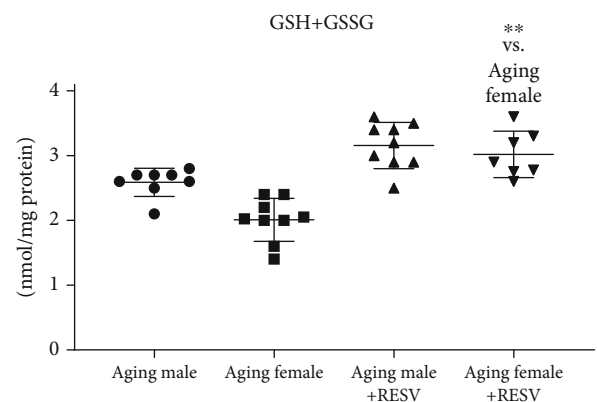


FIGURE 5: The effects of a 12-week-long resveratrol treatment on cardiac GSH+GSSG content in aged rats (GSH+GSSG; expressed as nmol/mg protein). Non-Gaussian distribution and Kruskal-Wallis test with Dunn's post hoc test result is shown as mean \pm SD; $n = 7 - 9$ /group and $**p < 0.01$: Statistical significance between resveratrol-treated and nontreated control counterparts. RESV: Resveratrol; GSH+GGSG: Total glutathione.

dependent manner, along this exact pathway [22]. During the breakdown of red blood cells, HO catalyzes the degradation of heme, resulting in the formation of biliverdin, ferrous iron, and carbon monoxide (CO). Biliverdin, with the help of biliverdin reductase, is converted to bilirubin which has been shown to protect against oxidative mechanisms by reducing oxygen radicals, NADPH oxidase, and adhesion molecules [23]. Moreover, a recent research regarding HO activity attributes its antioxidant role not only to the bilirubin/biliverdin redox cycle but also to CO [24]. CO, derived from HO activity, is responsible for regulating the GSH system as well [25]. GSH is a tripeptide of three amino acids that is synthesized as a primary line of antioxidant defense. Its free -SH group is capable of binding metal ions, and as a substrate for glutathione peroxidase (GPx), it is involved in the reduction of H_2O_2 and lipid peroxides [26]. Interest-

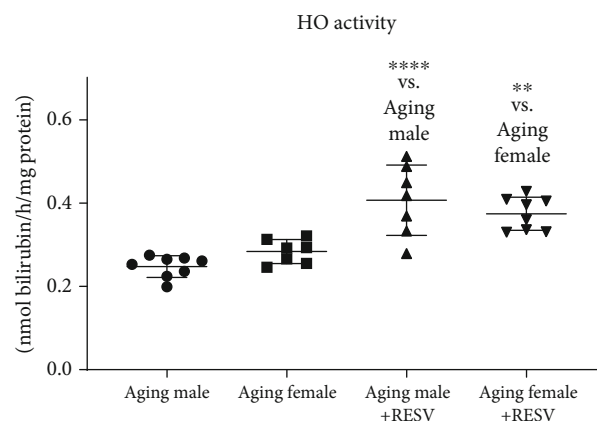


FIGURE 6: The effects of a 12-week-long resveratrol treatment on cardiac HO activity in aged rats (HO activity; expressed as nmol/bilirubin/h/mg protein). One-way ANOVA and Tukey posttest result is shown as mean \pm SD; $n = 7 - 8$ /group, $**p < 0.01$, and $****p < 0.0001$: Statistical significance between resveratrol-treated and nontreated control counterparts. RESV: Resveratrol; HO: Heme oxygenase.

ingly, the findings of Ungvari et al. supported that RESV also increases cellular GSH content via Nrf2 activation [27]. Previous work by our research group has shown that HO and GSH systems are inseparable, and their coordinated function is essential for the proper function of cardiac cells [28]. Several studies have shown that the efficiency of the HO and GSH system declines dramatically with age, resulting in a deterioration of the cell's tolerance to oxidative stress [28, 29]. Similarly, we observed that HO and GSH values were diminished in aged groups for both sexes. Nonetheless, a prolonged RESV treatment intensified the antioxidant mechanisms by boosting the synergic HO activity and GSH system. Supporting our results, mounting evidence indicates that RESV augments cellular antioxidant capacity through the reduction of reactive oxygen species (ROS) level, in parallel with the increase of glutathione (GSH), heme oxygenase (HO), and superoxide dismutase (SOD) activity [9]. It is also important to note that changes in the redox state of the cells are causally related to the systematic inflammatory processes. In the 2000s, Claudio Franceschi puts forward an interesting hypothesis, namely, that ageing organisms tend to develop a chronic inflammatory state characterized by persistently high level of proinflammatory cytokines (TNF- α , IL-1, and IL-6) in tissues and cells [30]. In this context, several lifespan-affecting biochemical pathways have been discovered over the last decades, the vast majority of which are mediated through the activation of NF κ B signaling. NF κ B is an important dimeric transcription factor and plays a fundamental role in biological processes associated with ageing, including inflammation, cell survival, and stress response. The inflammatory state resulting from ageing-associated dysregulated NF κ B signaling is characterized by increased MPO activity, elevated C reactive protein (CRP), and TNF- α concentrations [31, 32]. Ageing, in fact, is a progressive spread of inflammatory processes, and it is now clear that it is one of the main risk factors for CVDs

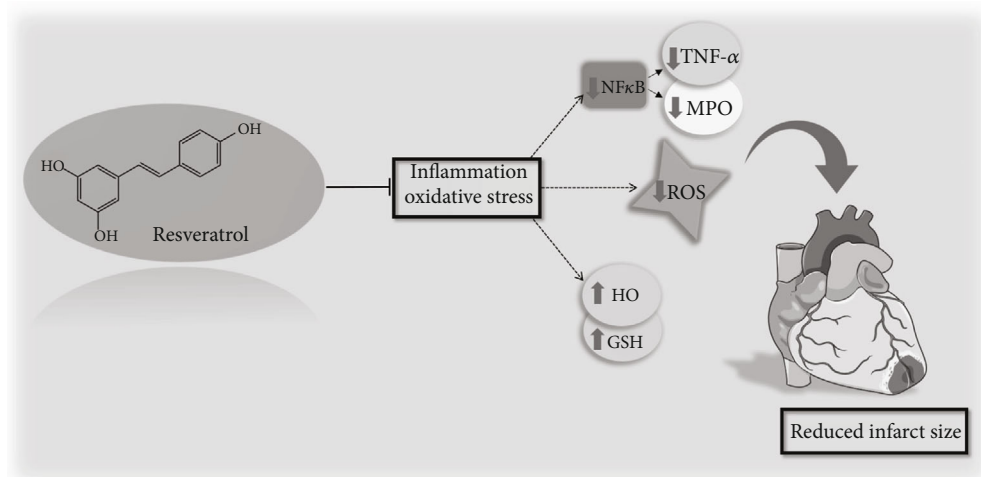


FIGURE 7: Summary of the study. Resveratrol sufficiently suppressed the age-related inflammatory pathways including the expression of TNF- α , NF κ B, and the activity of MPO while intensified the endogenous antioxidant defenses through the induction of GSH and HO system. Presumably, as a result of these processes, the necrotic extension of the heart was also significantly reduced. HO: Heme oxygenase; GSH+GGSG: Total glutathione; ROS: Reactive oxygen species; NF κ B: Nuclear factor kappa B; TNF- α : Tumor necrosis factor alpha; MPO: Myeloperoxidase enzyme.

[33]. Our findings have also underpinned that in the heart of aging females and males, a severe inflammatory state was manifested as a result of increased TNF- α concentration and MPO activity due to the upregulation of the NF κ B pathway. However, 12 weeks of RESV-treatment contributed to the moderation of cardiac inflammation by decreasing MPO activity, the expression of TNF- α and NF κ B. Confirming our results, both *in vivo* and *in vitro* studies substantiated the anti-inflammatory properties of RESV through the inhibition of inflammatory factors and pathways [34]. Previous studies verified that RESV suppresses NF κ B activation and gene expression along with the expression of proinflammatory cytokines [35]. According to Grujic Milanovic et al., RESV intake protected the cardiomyocytes through the inhibition of MPO activity, suggesting its promising anti-inflammatory and cardioprotective properties [36]. A remarkable finding from Yan et al. discussed that RESV improved cardiovascular function by decreasing circulating levels of proinflammatory cytokines such as of tumor necrosis factor- α (TNF- α) or interleukin-6 (IL-6) and by suppressing nuclear factor kappa B (NF- κ B) pathway [10]. Similarly, another study showed that RESV intake significantly reduced myocardial infarction areas together with myeloperoxidase (MPO) and TNF- α levels in the myocardium [11]. Along with the ability to decrease proinflammatory markers, RESV was observed to increase anti-inflammatory cytokines in the heart as well [37]. Maintaining a proper equilibrium between oxidant/antioxidant processes as well as between proinflammatory and anti-inflammatory agents provides the integrity of the body and the heart. In addition to the beneficial effects of RESV discussed in our study, it has proven to be cardioprotective in many other ways. RESV modulates the renin-angiotensin system and enhances the production of nitrogen monoxide (NO), thus proved to be effective in the pathomechanism of hypertension, atherosclerosis, or ischemic heart disease

[38, 39]. Growing evidence support that RESV exerts its cardioprotective effect by reducing oxidative stress and inflammation, improving Ca^{2+} homeostasis and decreasing cardiomyocyte apoptosis [40]. Interestingly, Fourny et al. found that RESV presents high potential to reduce ischemia-reperfusion injury in rat heart [41]. To support the cardioprotective effects of RESV, we analyzed the extent of cardiac damage induced by an acute cardiac injury. Our findings demonstrated that the necrotic area of the hearts was significantly attenuated as a result of 3-month long RESV treatment in both sexes. In accordance with our results, Xi et al. also verified the RESV-induced cardioprotection against ischemia-reperfusion injury [42]. Based on our results and other consistent data, we can conclude that RESV exerts its cardioprotective actions through its ability to balance inflammatory and oxidative mediators (Figure 7). RESV is proved to be a promising bioactive compound in several aspects of healthcare research and should be considered as a good therapeutic strategy in cardiovascular fields.

5. Conclusion

RESV is one of the most widely studied bioactive compounds, not only for its anti-inflammatory and antioxidant effects but also due its apparent lack of toxicity. It is clear that RESV was able to alleviate the age-related adverse changes in the heart of female and male rats, thereby making the myocardium more resistant to ischemic injury. Hence, our observations indicate that RESV can be considered as a potential bioactive compound in the regulation of redox homeostasis and inflammatory responses concurrent with cardioprotection. Research on RESV focusing its distinct mechanisms connected to the mitigation of ageing-related oxidative and inflammatory processes and their pathological

consequences could open up important preventive and therapeutic targets for CVD.

Data Availability

All data used to support the findings of this study are included within the article.

Conflicts of Interest

The authors declare no conflict of interest.

Authors' Contributions

Denise Börzsei and Judith Sebestyén contributed equally to this paper as first authors.

Acknowledgments

This research was supported by the 2019-1.1.1-PIACI-KFI-2019-00390 and by the ÚNKP-21-3-SZTE-426 (Börzsei Denise) new national excellence program of the ministry for innovation and technology from the source of the national research, development, and innovation fund. Additionally, Szegedi Tudományegyetem (University of Szeged) Open Access Fund was granted.

References

- [1] I. S. Pyo, S. Yun, Y. E. Yoon, J. W. Choi, and S. J. Lee, "Mechanisms of aging and the preventive effects of resveratrol on age-related diseases," *Molecules*, vol. 25, no. 20, p. 4649, 2020.
- [2] P. Pietri and C. Stefanadis, "Cardiovascular aging and longevity," *Journal of the American College of Cardiology*, vol. 77, no. 2, pp. 189–204, 2021.
- [3] T. Hussain, B. Tan, Y. Yin, F. Blachier, M. C. Tossou, and N. Rahu, "Oxidative stress and inflammation: what polyphenols can do for us?," *Oxidative Medicine and Cellular Longevity*, vol. 2016, Article ID 7432797, 9 pages, 2016.
- [4] D. E. Harrison, R. Strong, Z. D. Sharp et al., "Rapamycin fed late in life extends lifespan in genetically heterogeneous mice," *Nature*, vol. 460, no. 7253, pp. 392–395, 2009.
- [5] J. G. Wood, B. Rogina, S. Lavu et al., "Sirtuin activators mimic caloric restriction and delay ageing in metazoans," *Nature*, vol. 430, no. 7000, pp. 686–689, 2004.
- [6] E. Morselli, L. Galluzzi, O. Kepp et al., "Autophagy mediates pharmacological lifespan extension by spermidine and resveratrol," *Aging*, vol. 1, no. 12, pp. 961–970, 2009.
- [7] S. Galiniak, D. Aebisher, and D. Bartusik-Aebisher, "Health benefits of resveratrol administration," *Acta Biochimica Polonica*, vol. 66, no. 1, pp. 13–21, 2019.
- [8] S. Renaud and M. de Lorgeril, "Wine, alcohol, platelets, and the French paradox for coronary heart disease," *Lancet*, vol. 339, no. 8808, pp. 1523–1526, 1992.
- [9] X. N. Li, L. Y. Ma, H. Ji, Y. H. Qin, S. S. Jin, and L. X. Xu, "Resveratrol protects against oxidative stress by activating the Keap-1/Nrf2 antioxidant defense system in obese-asthmatic rats," *Experimental and Therapeutic Medicine*, vol. 16, no. 6, pp. 4339–4348, 2018.
- [10] F. Yan, X. Sun, and C. Xu, "Protective effects of resveratrol improve cardiovascular function in rats with diabetes," *Experimental and Therapeutic Medicine*, vol. 15, no. 2, pp. 1728–1734, 2018.
- [11] X. Cong, Y. Li, N. Lu et al., "Resveratrol attenuates the inflammatory reaction induced by ischemia/reperfusion in the rat heart," *Molecular Medicine Reports*, vol. 9, no. 6, pp. 2528–2532, 2014.
- [12] U. N. Das, "Anti-inflammatory nature of exercise," *Nutrition*, vol. 20, no. 3, pp. 323–326, 2004.
- [13] Q. Dong, Z. Wu, X. Li et al., "Resveratrol ameliorates cardiac dysfunction induced by pressure overload in rats via structural protection and modulation of Ca (2+) cycling proteins," *Journal of Translational Medicine*, vol. 12, no. 1, p. 323, 2014.
- [14] H. Kanamori, G. Takemura, K. Goto et al., "Resveratrol reverses remodeling in hearts with large, old myocardial infarctions through enhanced autophagy-activating AMP kinase pathway," *The American Journal of Pathology*, vol. 182, no. 3, pp. 701–713, 2013.
- [15] K. S. Bhullar and B. P. Hubbard, "Lifespan and healthspan extension by resveratrol," *Biochimica et Biophysica Acta*, vol. 1852, no. 6, pp. 1209–1218, 2015.
- [16] K. Robinson, C. Mock, and D. Liang, "Pre-formulation studies of resveratrol," *Drug Development and Industrial Pharmacy*, vol. 41, no. 9, pp. 1464–1469, 2015.
- [17] S. Han, N. B. Bal, G. Sadi, S. E. Usanmaz, M. O. Uludag, and E. Demirel-Yilmaz, "The effects of resveratrol and exercise on age and gender-dependent alterations of vascular functions and biomarkers," *Experimental Gerontology*, vol. 110, pp. 191–201, 2018.
- [18] C. Izzo, P. Vitillo, P. Di Pietro et al., "The role of oxidative stress in cardiovascular aging and cardiovascular diseases," *Lifestyles*, vol. 11, no. 1, p. 60, 2021.
- [19] J. Piquereau, F. Caffin, M. Novotova et al., "Mitochondrial dynamics in the adult cardiomyocytes: which roles for a highly specialized cell?," *Frontiers in Physiology*, vol. 4, p. 102, 2013.
- [20] G. Shi, Y. Wang, J. Yang et al., "Effect of cryptotanshinone on measures of rat cardiomyocyte oxidative stress and gene activation associated with apoptosis," *Cardiorenal Medicine*, vol. 11, no. 1, pp. 18–26, 2021.
- [21] N. Xia, A. Daiber, U. Forstermann, and H. Li, "Antioxidant effects of resveratrol in the cardiovascular system," *British Journal of Pharmacology*, vol. 174, no. 12, pp. 1633–1646, 2017.
- [22] Z. Ungvari, Z. Bagi, A. Feher et al., "Resveratrol confers endothelial protection via activation of the antioxidant transcription factor Nrf2," *American Journal of Physiology. Heart and Circulatory Physiology*, vol. 299, no. 1, pp. H18–H24, 2010.
- [23] D. Borzsei, R. Szabo, A. Hoffmann et al., "Distinct approaches of Raloxifene: its far-reaching beneficial effects implicating the HO-system," *Biomolecules*, vol. 10, no. 3, p. 375, 2020.
- [24] D. Stucki, J. Steinhausen, P. Westhoff et al., "Endogenous carbon monoxide signaling modulates mitochondrial function and intracellular glucose utilization: impact of the heme oxygenase substrate hemin," *Antioxidants*, vol. 9, no. 8, p. 652, 2020.
- [25] V. Consoli, V. Sorrenti, S. Grosso, and L. Vanella, "Heme Oxygenase-1 signaling and redox homeostasis in physiopathological conditions," *Biomolecules*, vol. 11, no. 4, p. 589, 2021.
- [26] M. H. Li, J. H. Jang, H. K. Na, Y. N. Cha, and Y. J. Surh, "Carbon monoxide produced by heme oxygenase-1 in response to nitrosative stress induces expression of glutamate-cysteine ligase in PC12 cells via activation of phosphatidylinositol 3-

- kinase and Nrf2 signaling," *The Journal of Biological Chemistry*, vol. 282, no. 39, pp. 28577–28586, 2007.
- [27] Z. Ungvari, N. Labinskyy, P. Mukhopadhyay et al., "Resveratrol attenuates mitochondrial oxidative stress in coronary arterial endothelial cells," *American Journal of Physiology. Heart and Circulatory Physiology*, vol. 297, no. 5, pp. H1876–H1881, 2009.
- [28] R. Szabó, A. Hoffmann, D. Börzsei et al., "Hormone replacement therapy and aging: a potential therapeutic approach for age-related oxidative stress and cardiac remodeling," *Oxidative Medicine and Cellular Longevity*, vol. 2021, Article ID 8364297, 9 pages, 2021.
- [29] M. Erden-Inal, E. Sunal, and G. Kanbak, "Age-related changes in the glutathione redox system," *Cell Biochemistry and Function*, vol. 20, no. 1, pp. 61–66, 2002.
- [30] C. Franceschi and J. Campisi, "Chronic inflammation (inflammaging) and its potential contribution to age-associated diseases," *The Journals of Gerontology. Series A, Biological Sciences and Medical Sciences*, vol. 69, Suppl 1, pp. S4–S9, 2014.
- [31] J. S. Tilstra, C. L. Clauson, L. J. Niedernhofer, and P. D. Robbins, "NF- κ B in aging and disease," *Aging and Disease*, vol. 2, no. 6, pp. 449–465, 2011.
- [32] G. J. Pan, B. S. Rayner, Y. Zhang, D. M. van Reyk, and C. L. Hawkins, "A pivotal role for NF- κ B in the macrophage inflammatory response to the myeloperoxidase oxidant hypothiocyanous acid," *Archives of Biochemistry and Biophysics*, vol. 642, pp. 23–30, 2018.
- [33] L. Ferrucci and E. Fabbri, "Inflammageing: chronic inflammation in ageing, cardiovascular disease, and frailty," *Nature Reviews. Cardiology*, vol. 15, no. 9, pp. 505–522, 2018.
- [34] R. Torregrosa-Munumer, E. Vara, J. A. Fernandez-Tresguerres, and R. Gredilla, "Resveratrol supplementation at old age reverts changes associated with aging in inflammatory, oxidative and apoptotic markers in rat heart," *European Journal of Nutrition*, vol. 60, no. 5, pp. 2683–2693, 2021.
- [35] T. Meng, D. Xiao, A. Muhammed, J. Deng, L. Chen, and J. He, "Anti-inflammatory action and mechanisms of resveratrol," *Molecules*, vol. 26, no. 1, p. 229, 2021.
- [36] J. Grujic-Milanovic, V. Jacevic, Z. Miloradovic et al., "Resveratrol protects cardiac tissue in experimental malignant hypertension due to antioxidant, anti-inflammatory, and anti-apoptotic properties," *International Journal of Molecular Sciences*, vol. 22, no. 9, p. 5006, 2021.
- [37] S. Liu, Y. Du, K. Shi, Y. Yang, and Z. Yang, "Resveratrol improves cardiac function by promoting M2-like polarization of macrophages in mice with myocardial infarction," *American Journal of Translational Research*, vol. 11, no. 8, pp. 5212–5226, 2019.
- [38] R. Gal, L. Deres, K. Toth, R. Halmosi, and T. Habon, "The effect of resveratrol on the cardiovascular system from molecular mechanisms to clinical results," *International Journal of Molecular Sciences*, vol. 22, no. 18, p. 10152, 2021.
- [39] P. Aguilar-Alonso, O. Vera-Lopez, E. Brambila-Colombres et al., "Evaluation of oxidative stress in cardiomyocytes during the aging process in rats treated with resveratrol," *Oxidative Medicine and Cellular Longevity*, vol. 2018, Article ID 1390483, 9 pages, 2018.
- [40] A. Riba, L. Deres, B. Sumegi, K. Toth, E. Szabados, and R. Halmosi, "Cardioprotective effect of resveratrol in a postinfarction heart failure model," *Oxidative Medicine and Cellular Longevity*, vol. 2017, Article ID 6819281, 10 pages, 2017.
- [41] N. Fourny, C. Lan, E. Seree, M. Bernard, and M. Desrois, "Protective effect of resveratrol against ischemia-reperfusion injury via enhanced high energy compounds and eNOS-SIRT1 expression in type 2 diabetic female rat heart," *Nutrients*, vol. 11, no. 1, p. 105, 2019.
- [42] J. Xi, H. Wang, R. A. Mueller, E. A. Norfleet, and Z. Xu, "Mechanism for resveratrol-induced cardioprotection against reperfusion injury involves glycogen synthase kinase 3 β and mitochondrial permeability transition pore," *European Journal of Pharmacology*, vol. 604, no. 1-3, pp. 111–116, 2009.

Research Article

Novel Compound Polysaccharides from Chinese Herbal Medicines: Purification, Characterization, and Antioxidant Activities

Xu Yang ¹, Haiyu Ji,² Yingying Feng,² Juan Yu,² and Anjun Liu ²

¹Tianjin Institute for Food Safety Inspection Technology, Tianjin 300308, China

²Key Laboratory of Food Nutrition and Safety, Ministry of Education, School of Food Science and Engineering, Tianjin University of Science and Technology, Tianjin 300457, China

Correspondence should be addressed to Xu Yang; yangxu1009@163.com and Anjun Liu; laj1456@163.com

Received 28 February 2022; Accepted 27 May 2022; Published 10 June 2022

Academic Editor: Felipe L. de Oliveira

Copyright © 2022 Xu Yang et al. This is an open access article distributed under the Creative Commons Attribution License, which permits unrestricted use, distribution, and reproduction in any medium, provided the original work is properly cited.

The present study investigated physicochemical properties and antioxidant activities *in vivo* and *in vitro* of purified compound polysaccharides (CPs-1) from Chinese herbal medicines, composed of lotus leaf, hawthorn, *Fagopyrum tataricum*, *Lycium barbarum*, *Semen cassiae*, and *Poria cocos* with the mass ratio of 2:4:2:1:1.5:1. The HPGPC profile and FT-IR spectra indicated that the average molecular weight of CPs-1 was 38.7 kDa and possessed the α - and β -D-pyranose, respectively. The methylation analysis and NMR spectrum demonstrated that CPs-1 had a $\rightarrow 6$ - β -D-Glcp-(1 \rightarrow 6)- β -D-Glcp(1 \rightarrow backbone. Furthermore, the antioxidant assays *in vitro* revealed that CPs-1 displayed high scavenging abilities for DPPH, hydroxyl, and reducing power, as well as ABTS and superoxide scavenging capacity. The antioxidant experiments *in vivo* revealed that CPs-1 could significantly enhance CAT, SOD, and GSH-Px activities and dramatically reduce MDA levels in liver and serum of high-fat mice. Therefore, CPs-1 could be potentially incorporated into pharmaceutical products or functional foods as a natural antioxidant.

1. Introduction

Free radicals are the generic terms of atoms, atomic groups, or molecules in a particular state containing unpaired electrons generated during biochemical reactions in the body [1]. Reactive oxygen species (ROS) are produced in the general physiological metabolism of human cells and tissues, significant in maintaining oxidative balance in antioxidant defense mechanisms [2]. However, excessive free radicals, especially ROS, lead to oxidative stress relevant to diabetes [3], Alzheimer [4] cardiovascular disease [5], nephrosis [6], cancer [7], arteriosclerosis [8], and many other aging-related disorders [9]. Antioxidants can protect the body against oxidative damage and delay chronic disease pathogenesis to a certain extent via restraining and scavenging ROS [10, 11]. Due to their antioxidant activity (one of the most important bioactivities of polysaccharides), polysaccharides from Chinese herbal medicines (CHMs) have been

broadly used as safe, stable, and effective natural antioxidants, because they possess less toxicity and side effects, compared with synthetic antioxidants [12, 13]. As a result, developing new multifarious CHM-derived polysaccharides has received considerable interest.

As CHMs, lotus leaf, hawthorn, *Semen cassiae*, *Fagopyrum tataricum*, *Poria cocos*, and *Lycium barbarum* are edible plants with medicinal benefits (called “medicine food homology” in China) [14]. Many studies have been published on the characterization and bioactivities of polysaccharides obtained from the above CHMs [15–18]. The compound polysaccharides (CPs) are complex with two or two more polysaccharides. It has been reported to show multiple pharmacological activities including antiviral, anti-inflammatory, antioxidant, and radioresistant and immunomodulating properties [19–22]. Furthermore, CPs prevent rats from obesity and related metabolic issues [23]. Moreover, CPs own higher radical scavenging activity than

that of the single polysaccharide [24]. The compound CHM ingredients can better enhance immunity than the single CHM ingredient [25]. The characterization and antioxidant activities of crude CPs from the above six CHMs have been investigated in our published article [26]. However, the purification, structure, and antioxidant activities of polysaccharides from the aforesaid crude CPs still remain unknown.

The current study designated to identify the characterization and antioxidant activities of purified CPs. Firstly, crude CPs were isolated with Sephadex G-75 column, and the preliminary structure was determined by methylation and nuclear magnetic resonance (NMR), high-performance gel permeation chromatography (HPGPC), chemical analysis, ion chromatography (IC), UV spectrum, and Fourier transform-infrared spectroscopy (FT-IR). Furthermore, *in vitro* and *in vivo* antioxidant activities of CPs were investigated based on their capacities to scavenge radical (DHHP, ABTS, hydroxyl, and superoxide anion) and reducing powers, as well as the murine serum and liver concentrations of catalase (CAT), glutathione peroxidase (GSH-Px), malondialdehyde (MDA), and superoxide dismutase (SOD).

2. Materials and Methods

2.1. Materials and Reagents. The fruits of *Poria cocos* (Schw.) Wolf, fruits of *Lycium barbarum* L., lotus leaves of *Nelumbo nucifera* Gaertn., seeds of *Cassia tora* Linn. (Semen cassiae), fruits of *Fagopyrum tataricum* (L.) Gaertn., and *Crataegus pinnatifida* (hawthorn) were obtained from Bozhou Shenghao Biotechnology Co., Ltd. (Anhui, China). Samples were gently processed for storage at 4°C. The dextran standards were purchased from Pharmacia Co. (New York, USA). Sephadex G-75 was gained from GE Healthcare Life Science (Piscataway, NJ, USA). The monosaccharide standards were purchased from Sigma-Aldrich Chemical Co. (St. Louis, USA). The assay kits of SOD, CAT, MDA, and GSH-Px were acquired from Nanjing Jiancheng Bioengineering Institute (Nanjing, China). Other chemicals or reagents were of analytical grade.

2.2. Extraction and Purification of CPs. The lotus leaf, hawthorn, *Fagopyrum tataricum*, *Lycium barbarum*, *Semen cassiae*, and *Poria cocos* were powdered using a grounding equipment (Model 800C, Yongkang Aizela Electric Appliance Co., Ltd., Zhejiang, China), respectively. Then, the fine powder was mixed at the mass ratio of 2:4:2:1:1.5:1 [27, 28]. According to our preliminary experiments [26], 10 g of the compound was extracted with deionized water (30 mL/g, 65°C, 45 min) three times using the ultrasonic-assistant extraction. After vacuum filtration, the aqueous extracts were mixed with 2% pectinase, at 50°C for 2 h, followed by a 5 min incubation at 95°C for enzyme inactivation. Then, a rotary evaporator was initially employed to remove excessive water from the mixture (SY-2000, Yarong Technology and Science Inc., Shanghai, China) at 55°C with the presence of vacuum, followed by mixing with ethyl alcohol (1:4 dilution ratio of concentrated mixture and ethyl alcohol). The diluted sample was stored overnight at 4°C. Then, the mixture was 15 min centrifuged at a speed of 4500 r/min. The pellets were three-time washed with dehydrated ethanol.

After redissolving of collected precipitate (termed crude CPs), dialysis and the lyophilization were subsequently conducted at -50°C under vacuum. Finally, the obtained solid was ground to powder.

CPs were dissolved in deionized water to reach 10 mg/mL, followed by separating into different fractions based on molecular weights (MWs) via ultrafiltration centrifugation with a 10 kDa MWCO (Sartorius, Göttingen, Germany) (at 4000 rpm for 20 min). Two fractions were obtained, i.e., CPs-1 (>10 kDa) and CPs-2 (1-10 kDa). The preexperiments revealed that CPs-1 presented stronger antioxidant activities than CPs-2. CPs-1 was purified using a permeation column (Sephadex G-75 gel, 4.5 × 60 cm) to acquire homogeneous polysaccharides. CPs-1 was eluted and collected using 5 mL deionized water at 1.0 mL/min flow rate. Total carbohydrate was determined by phenol-sulfuric acid. The protein in CPs-1 was examined by bovine serum albumin and Coomassie Brilliant Blue G-250.

2.3. Characterization of CPs-1

2.3.1. Analysis of Molecular Weight Distribution. The molecular weight distribution of CPs-1 was determined by HPGPC based on previously published method [29]. The calculation of the molecular weight of CPs-1 was based on the dextran standards.

2.3.2. Analysis of Monosaccharide Composition. The monosaccharide composition and molar ratios of CPs-1 were obtained using Dionex ICS-5000 chromatographic system (CA, USA). An aliquot of 5 mg CPs-1 sample was hydrolyzed in 1.0 mL trifluoroacetic acid (TFA, 2.0 mol/L) at 110°C for 4 h in a sealed tube. The recovery of TFA was achieved by adding methanol in a N₂ atmosphere. The 100 times dilution of the dried hydrolysate was obtained using 1.0 mL of deionized water. The elution was completed using NaAC (200 mM) and NaOH (10 mM) solutions at 0.5 mL/min flow rate at a column temperature of 30°C to generate 25 μL sample [30].

2.3.3. FT-IR and UV Spectrometric Analyses. Potassium bromide (KBr) was added into the CPs-1, and subsequently the mixture was pressed into a tablet. The resulting signal of FTIR spectra analysis at the detector (VECTOR-22 IR, Bruker, Karlsruhe, Germany) presents as a spectrum from 4000 cm⁻¹ to 400 cm⁻¹. A UV-2500PC spectrophotometer (Shimadzu, Kyoto, Japan) in 200-400 nm was utilized to document the UV spectra of CPs-1 [31].

2.3.4. Methylation Analysis. CPs-1 (5 mg) was methylated using a reported method [32], followed by hydrolyzation and acetylation in sequence. Then, the samples were evaluated by a gas chromatography-mass spectrometry (GC-MS) on a 4000 GC-MS system (Varian, CA, USA). The methodology from the previous literature [33] was employed to analyze the results of methylation.

2.3.5. NMR Spectroscopy Analysis. 0.5 mL of D₂O was mixed with 20 mg of lyophilized CPs-1. A Bruker DRX-400 NMR spectrometer (Rheinstetten, Germany) was used to document ¹H and ¹³C NMR spectra.

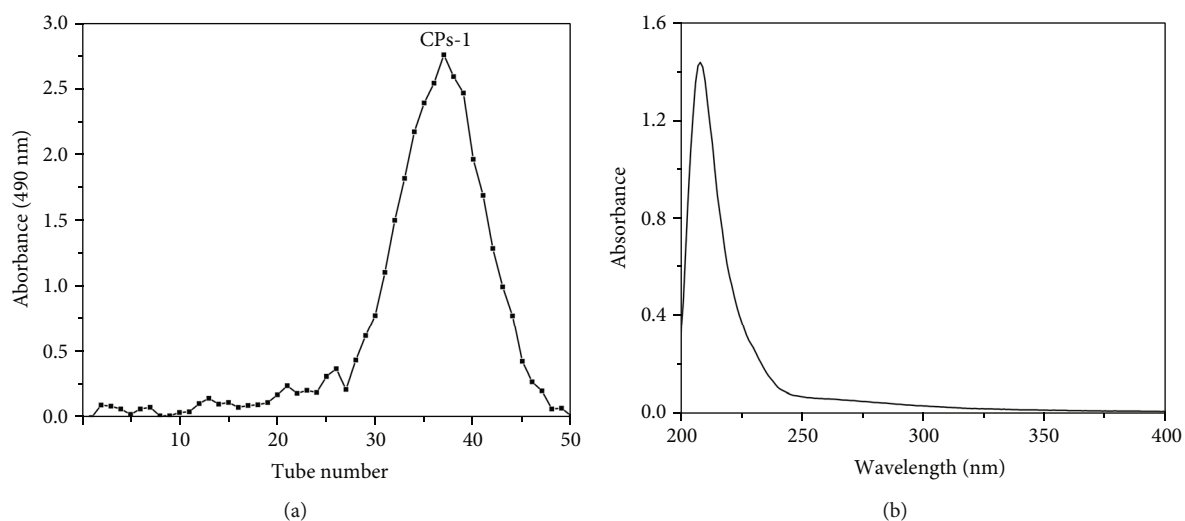


FIGURE 1: Elution profile of the fraction achieved from deionized water in a gel chromatography column (a) and UV spectrum of CPS-1 (b).

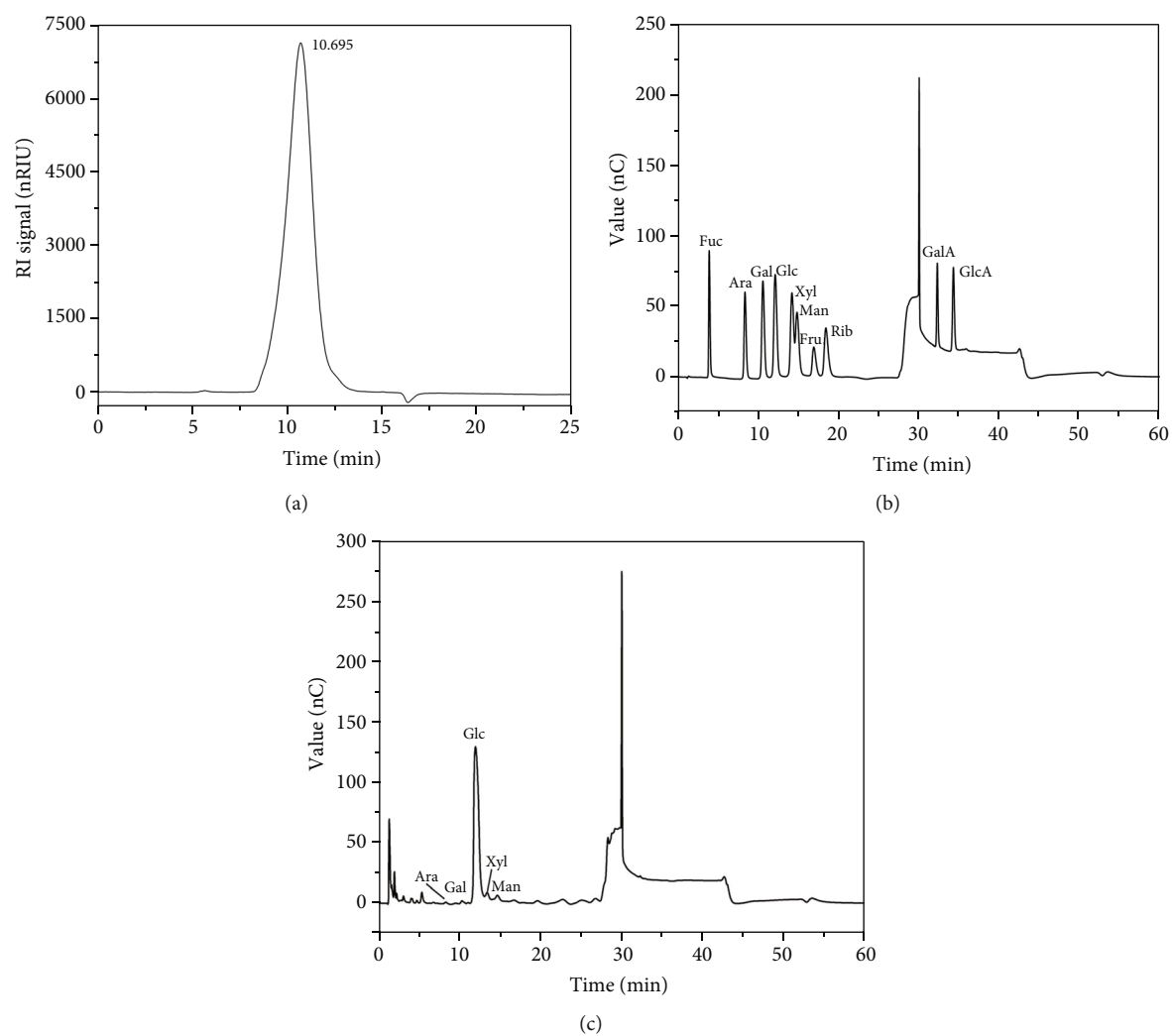


FIGURE 2: HPGPC of CPS-1 (a) and IC chromatogram of standard monosaccharides (b) and CPS-1 (c).

2.4. Antioxidant Activity of CPs-1 In Vitro. The radical scavenging abilities and reducing powers were estimated by following the published report [26]. 0.25, 0.5, 1.0, 2.0, and 4.0 mg/mL of different samples were conducted in this study. Vitamin C (VC) was served as the positive control.

2.5. Antioxidant Activity of CPs-1 In Vivo

2.5.1. Animal and Treatment. The mouse model generation and treatment of mice were based on previously published method with a slight modification [34]. Kunming mice (KM, male, 20 ± 2 g) were achieved from Si Pei Fu Biotech Co., Ltd. (Beijing, China), which the license number was SCXK (Jing) 2016-0002. Animal studies were conducted following China's Guidelines for the Care and Use of Laboratory Animals. The conduction conforms to the international uses of experimental animals. Mice were maintained in the standard experimental condition (relative humidity: 45-55%, adjustable temperature: 20-25°C), 12h/12h light/dark cycle. A normal control group consists of ten healthy KM randomly selected after one-week acclimatization and fed with the basal diet (0.9% normal saline, 0.2 mL/d). The remaining mice were fed with a high-fat diet, composed of 78.8% basic feed, 10% egg yolk powder, 10% lard, 1% cholesterol, and 0.2% sodium cholate, for 30 consecutive days.

After the high-fat mouse model was established, the high-fat mice were randomly grouped into five sections: model control (0.9% normal saline, 0.2 mL/d), positive control (simvastatin, 3.33 mg/kg, 0.2 mL/d), low dose (50 mg/kg, 0.2 mL/d), medium dose (100 mg/kg, 0.2 mL/d), and high dose (200 mg/kg, 0.2 mL/d) groups. Each group of ten mice received continuous gavage for 30 d. The normal control group, throughout the experiment, was fed a basal diet, while the others received ad libitum feeding of a high-fat diet.

When the last 12 h administration was completed, body weight and blood samples through eyeballs of the mice were collected. The serum was obtained by a centrifuge ($3000 \times g$) at 4°C for 10 min. The mice were sacrificed through cervical dislocation, and their livers were acquired and weighed. Serum and liver were preserved in the refrigerator at 4°C.

2.5.2. Antioxidant Activity of CPs-1 In Vivo. The indexes of antioxidant, including MDA, CAT, SOD, and GSH-Px, in serum and liver were determined with commercially available kits (Nanjing Jiancheng Bioengineering Institute).

2.6. Statistical Analysis. The experimental data were expressed as mean \pm standard deviation (SD). The one-way analysis of variance (ANOVA) was conducted using SPSS for Windows version 19.0 (SPSS Inc. Chicago, IL, USA). $P < 0.05$ was used as the cutoff indicating statistical significance.

3. Results and Discussion

3.1. Purification and Chemical Components of CPs-1. CPs were prepared in a $7.18 \pm 0.24\%$ yield from CHMs under optimal conditions based on the reported procedure [26]. Deproteinization and separation of CPs were performed using ultrafiltration centrifugation. As displayed in

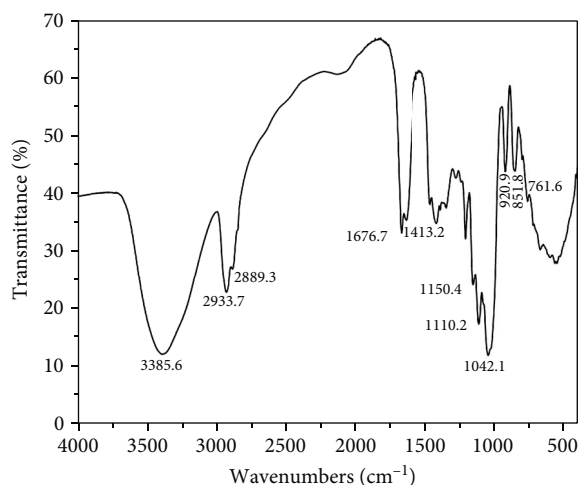


FIGURE 3: FT-IR spectrum of CPs-1.

Figure 1(a), the purified CPs-1 was obtained using the deionized water and Sephadex G-75 column.

The lyophilized CPs-1 was the white powder, with a total carbohydrate content of 97.87%, and no protein or uronic acid was detected, consistent with the results of UV analysis. The UV spectrum of CPs-1 is shown in Figure 1(b). The absence of absorption at 260 and 280 nm implied no protein and nuclear acid in CPs-1, respectively [35].

3.2. Molecular Weight Analysis and Composition of Monosaccharide in CPs-1. The homogeneity and average molecular weight of CPs-1 were characterized by HPGPC (Figure 2(a)). The HPGPC profile demonstrated a single symmetrical narrow peak at 10.695 min, suggesting the homogeneity and high purity of CPs-1. The HPGPC analysis revealed that the molecular weight of CPs-1 was 38.7 kDa in terms of the calibration curves of the standard dextrans.

IC was utilized to determine the composition of monosaccharide in CPs-1. Figures 2(b) and 2(c) demonstrated that CPs-1 included Gal, Ara, Xyl, Man, and Glc at a molar ratio of 0.5:0.5:2.7:2.7: 93.6, indicating that CPs-1 were heterogeneous and it is most likely that Glc was the backbone of CPs-1. The result was similar to other reports regarding the MW of polysaccharides extracted from *Poria cocos*. The composition of CPs-1 in the present work was consistent with that from *Semen cassiae* at an identical molar ratio of Gal and Glc [36].

3.3. FT-IR Analysis of CPs-1. The FT-IR spectra were used to analyze the functional groups and chemical bonds of CPs-1 [37]. As shown in Figure 3, the CPs-1 FT-IR spectrogram displayed the typical absorption peaks of polysaccharide, particularly in the regions of $800\text{-}1200\text{ cm}^{-1}$, $1400\text{-}1700\text{ cm}^{-1}$, $2800\text{-}3000\text{ cm}^{-1}$, and $3200\text{-}3500\text{ cm}^{-1}$ [26]. The broad and strong peak at approximately 3385 cm^{-1} was attributed to the O-H stretching vibration, associated with the existence of intramolecular and intermolecular hydrogen bonds. The small peaks at approximately 2933 and 2889 cm^{-1} were relevant to C-H stretching trembling from alkyl groups, including CH, CH₂, and CH₃ [26, 38]. The absorption peak at around 1676 cm^{-1}

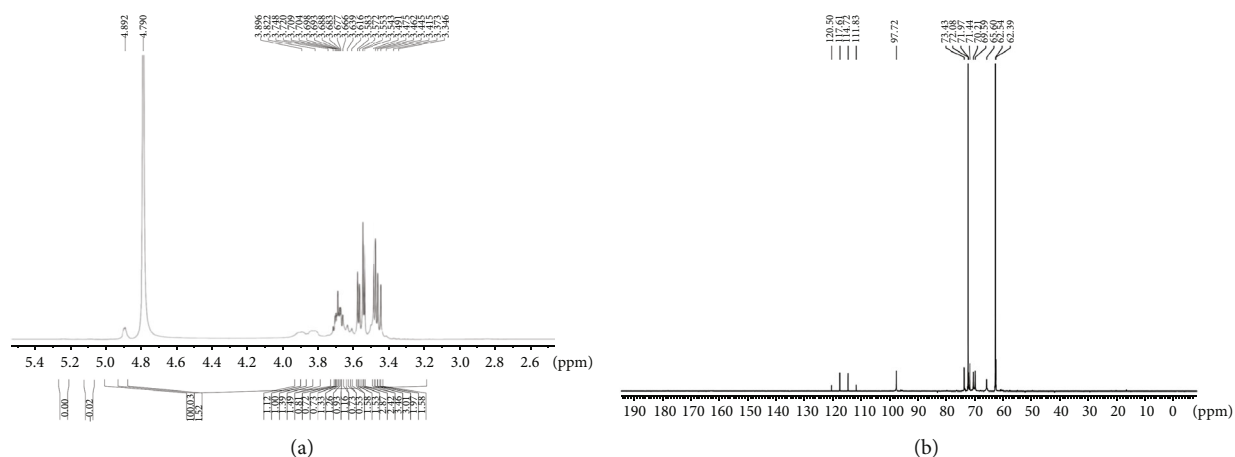


FIGURE 4: ^1H (a) and ^{13}C (b) NMR spectrum of CPs-1.

could be ascribed to the existence of bound water, while that at approximately 1413 cm^{-1} might be due to the C-H symmetrical deformation vibration [38]. The three absorption bands, i.e., 1150 , 1110 , and 1042 cm^{-1} , in the 1000 - 1200 cm^{-1} range demonstrated the presence of pyranose ring in the CPs-1 [39]. Moreover, the feature peaks at approximately 920 and 851 cm^{-1} were associated with β - and α -D-galactopyranose, respectively [40, 41]. The absorption peak at 761.6 cm^{-1} was correlated with α -D-xylopyranose [42]. The results were identical to those of monosaccharide composition. In summary, CPs-1 possessed the α - and β -D-pyranose, in agreement with other polysaccharides from hawthorn and lotus leaf in the previous study [43, 44].

3.4. Methylation Analysis of CPs-1. The methylation analysis was executed to evaluate molar ratios and the glycosidic linkage of sugar residues of CPs-1. The main methylated alditol acetates of CPs-1 are estimated to be 2,3,4,6-Me4-D-Glcp, 2,3,4-Me3-D-Glcp, and 2,4-Me2-D-Glcp with a molar ratio of 5.36:84.21:10.43. The corresponding peak times were 12.92, 16.67, and 19.44 min, respectively. Therefore, the results illustrated the presence of high concentration of the nonreducing terminal glucosyl, (1 \rightarrow 6)-linked-glucosyl and (1 \rightarrow 3, 6)-linked-glucosyl, and (1 \rightarrow 6)-linked-glucosyl in CPs-1. In addition, it was suggested that (1 \rightarrow 6)-linked-glucosyl was likely to form the backbone, while (1 \rightarrow 3, 6)-linked-glucosyl was identified as the branched residues. The relative molar ratio of (1 \rightarrow 6)-linked-glucosyl and (1 \rightarrow 3, 6)-linked-glucosyl was 8.07, revealing one branching point for every nine or ten residues of backbone. The nonreducing terminal of 1 \rightarrow linked glucosyl was detected in the branched residues [33].

3.5. NMR Analysis of CPs-1. As indicated in Figures 4(a) and 4(b), the ^1H and ^{13}C NMR spectra of CPs-1 are distributed in a narrow region within $\delta 3.0$ - 5.3 ppm (^1H NMR) and $\delta 60$ - 121 ppm (^{13}C NMR), correlated with polysaccharides [45]. Based on the composition of the monosaccharide, FT-IR, methylation analysis, and data from literature [33, 46-49], signals in ^1H and ^{13}C NMR spectra of CPs-1 were determined. Because of the overlapped peaks of the interference signal of

HDO ($\delta\text{H } 4.79\text{ ppm}$) and the absence of Ara and Gal in the CPs-1, two significantly weak anomeric proton signals occurred at $\delta\text{H } 5.0$ - 5.3 ppm , attributed to Ara and Gal. Additionally, other hydrogen on the anomeric carbon with the chemical shift ($\delta\text{H } 4.89\text{ ppm}$) was less than $\delta\text{H } 5.0\text{ ppm}$ caused by Glc. This suggested that CPs-1 had both α - and β -glycosidic bonds. The absences of proton signal peak at $\delta\text{H } 5.4\text{ ppm}$ and signal for sugar-ring carbons from $\delta\text{C } 82$ to 88 ppm (characteristic for furanosides) demonstrated that all sugar residues were pyranose in the CPs-1. The chemical shifts of anomeric carbons at $\delta\text{C } 120.50$, 117.61 , 114.72 , 111.83 , and 97.72 ppm corresponded to five monosaccharide residues, as well as α and β anomeric configurations in CPs-1, consistent with ^1H NMR analysis. The above results were identical with the monosaccharide composition and FT-IR analysis. At the anomeric region of the ^{13}C NMR spectrum, signals at 120.50 ppm were allocated to Ara and T-linked β -Glc. Signals at 117.61 and 114.72 ppm were generated from Gal and Glc, respectively, assigned to 1,6-linked β -Glc. Xyl was at 111.83 ppm , originated from 1,3,6-linked β -Glc. Signals at 97.92 ppm were caused by Man. The carbon resonances of CPs-1 from 62.39 to 73.43 ppm were attributed to carbons C2-C6 of various sugar moieties. In general, ^{13}C NMR spectrum signals from 67 to 70 ppm validated the existence of (1 \rightarrow 6) glycosidic linkages in CPs-1. The methylation analysis and ^1H and ^{13}C NMR spectra of CPs-1 indicated that the presence of (1 \rightarrow 6)- β -D-Glcp backbone and O-3 position of (1 \rightarrow 6)-linked β -D-Glcp was substituted by 1-linked β -D-Glcp branches, with one branching point for every 15 or 16 backbones on average.

3.6. Antioxidant Activities of CPs-1 In Vitro. DPPH has been extensively used to measure the oxidation resistance of various antioxidants, characterized by simple, rapid, and sensitive properties. The ABTS radical scavenging is also broadly applied to evaluate the total antioxidant capacity of polysaccharides. Removing hydroxyl radicals and superoxide anion will protect the body against oxidation-related damage. The strong reducing power indicates high antioxidant activities [26].

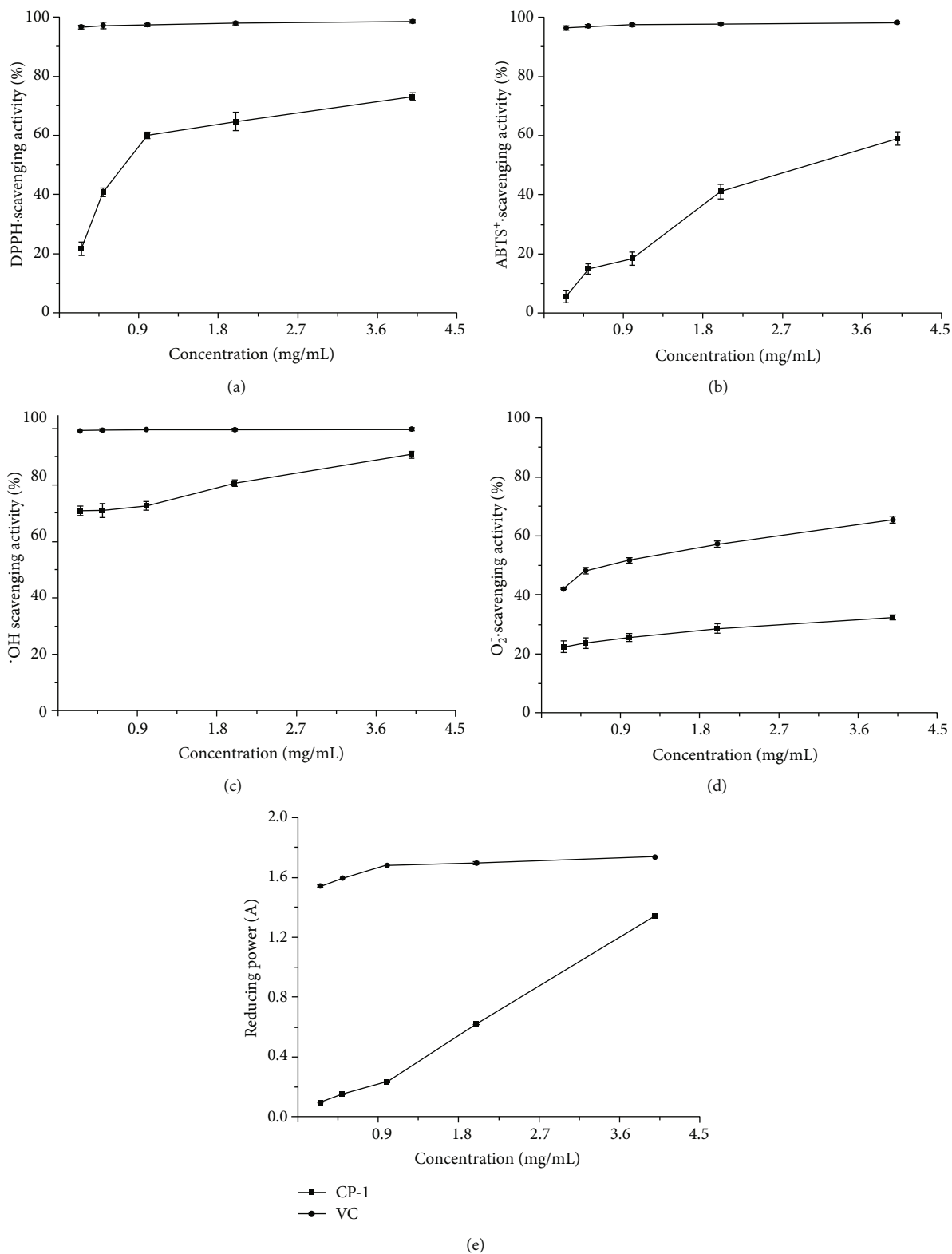


FIGURE 5: Antioxidant activities of CPs-1 for DPPH scavenging capacity compared to that of VC (a), for ABTS scavenging capacity compared to that of VC (b), for hydroxyl radical scavenging capacity compared to that of VC (c), for superoxide radical scavenging capacity compared to that of VC (d), and for reducing power compared to that of VC (e).

3.6.1. DPPH Radical Scavenging Activity. Figure 5(a) presents the scavenging ability of CPs-1 for DPPH compared to that of VC. It can be observed that the scavenging capacity

increases significantly with the polysaccharides from 0.25 to 4.0 mg/mL, inferior to that of VC at all concentrations. The scavenging activity of CPs-1 and VC at 4.0 mg/mL is 73.09

$\pm 1.35\%$ and $98.47 \pm 0.51\%$, respectively. The scavenging ability of CPs-1 at 2.0 mg/mL is higher than that of hawthorn polysaccharides (HTPs) and Lycium barbarum polysaccharides (LBPs) in previous research [43, 50]. Thus, CPs displayed noteworthy DPPH radical scavenging activity because an electron or a hydrogen atom could be easily provided.

3.6.2. ABTS Radical Scavenging Activity. CPs-1 displayed the scavenging capacity against ABTS, highly depending on the polysaccharide concentration of 0.25 to 4.0 mg/mL (Figure 5(b)). It was indicated that the ABTS scavenging ability is weaker than that of VC. At a concentration of polysaccharide (4.0 mg/mL), the scavenging activity is $58.93 \pm 2.17\%$, significantly lower than that of VC ($98.13 \pm 0.34\%$). The conclusion is in agreement with other published reports in the scavenging capacities for ABTS of HTPs and Fagopyrum tataricum polysaccharides (FTPs) [51, 52]. In short, CPs exhibited great scavenging ability for ABTS, enabling it potentially to be used as a novel antioxidant from natural resources.

3.6.3. Hydroxyl Radical Scavenging Activity. As demonstrated in Figure 5(c), the hydroxyl radical scavenging ability of CPs-1 is greatly correlated with the polysaccharides concentrations between 0.25 and 4.0 mg/mL. The scavenging capacity is $90.75 \pm 1.15\%$, lower than that of VC ($99.79 \pm 0.42\%$) at 4.0 mg/mL. The scavenging activity of CPs-1 for hydroxyl radical exceeds those in LBPs and Poria cocos polysaccharides (PCPs) reported in other publications [18, 53]. It is due to the fact that the hydroxyl radicals were scavenged by polysaccharides interacting with hydrogen with radicals and discontinued the radical chain reaction.

3.6.4. Superoxide Radical Scavenging Activity. As illustrated in Figure 5(d), the scavenging capacity of CPs-1 at 4.0 mg/mL for superoxide radical is $32.31 \pm 0.79\%$, compared with $65.54 \pm 1.17\%$ of VC. The superoxide radical scavenging abilities of CPs-1 are lower than those of the results from previous studies on HTPs, FTPs, LBPs, and Semen cassiae polysaccharides (SCPs) [16, 51, 53, 54]. To sum up, CPs-1 has relatively weak ability of scavenging the superoxide radical.

3.6.5. Reducing Power. The comparison of the absorbance between CPs-1 and VC is demonstrated in Figure 5(e). The absorbance of CPs-1 (4.0 mg/mL) and VC is 1.342 ± 0.002 and 1.738 ± 0.002 , respectively. The reducing power of CPs-1 is stronger than those of PCPs and LBPs in literature [18, 53].

The highly correlated relationship among the radical scavenging abilities (ABTS, hydroxyl, and superoxide anion), reducing powers, and CPs-1 concentration is described in Table 1, with correlation coefficients (R^2) of 0.9571, 0.9861, 0.9716, and 0.9923, respectively. In addition, a linear relationship ($R^2 = 0.9369$) was observed between the DPPH scavenging capacity and CPs-1 concentration.

3.7. Antioxidant Activities of CPs-1 In Vivo. SOD is specialized in scavenging superoxide anions and can improve the

TABLE 1: The correlation between antioxidant activity and concentration of CPs.

Antioxidant arrays	Optimal fitting functions	Determination coefficients (R^2)
DPPH	$Y_a = 18.28\text{Ln}(X_c) + 52.04$	0.9369
ABTS	$Y_a = 13.959X_c + 6.1463$	0.9571
Hydroxyl	$Y_a = 5.609X_c + 68.472$	0.9861
Superoxide-anion	$Y_a = 2.576X_c + 22.499$	0.9716
Reducing power	$Y_a = 0.3392X_c - 0.0375$	0.9923

X_c was the concentration of CPs, and Y_a was the antioxidant activity corresponding to X_c .

immunity and resistance of the body to ROS-induced diseases. As one of terminal oxidases, CAT is able to decompose hydrogen peroxide in cells, preventing tissue damage [55]. GSH-Px can reduce the free hydrogen peroxide to water and toxic lipid hydroperoxides preventing cells from ROS toxicity [56]. Therefore, CAT, GSH-Px, and SOD are the most crucial indexes to assess the antioxidant capacity. The MDA level reflects the oxidative damage severity and lipid peroxidation level *in vivo* [2].

3.7.1. Contents of CAT, GSH-Px, MDA, and SOD in Serum of Mice. Table 2 illustrates the effects of CPs-1 on serum concentrations of CAT, SOD, and GSH-Px, reflecting their remarkable increases in serum. Moreover, the MDA level in serum decreases gradually with the increase of the dosage of CPs-1. It was proved that the impacts of high-dosage CPs-1 on CAT, GSH-Px, and SOD concentrations in serum were substantially different from those of the model control ($P < 0.01$) and normal control ($P < 0.01$) groups, indicating significant differences in the influences of the medium-dose and the model control group on the concentrations of CAT, GSH-Px, and SOD in serum. In comparison with the model control group, the concentrations of MDA in serum with high- and medium-dosages of CPs-1 were substantially lower, where the significance level was 0.01 and 0.05, respectively. Compared with the normal control group, the contents of CAT, GSH-Px, and SOD in serum increased by 32.72%, 56.17%, and 87.24% in sequence with high-dosage CPs-1 ($P < 0.01$). These demonstrated that CPs-1 could dramatically reduce the concentration of MDA in serum since no significant difference was identified between these two groups ($P > 0.05$).

3.7.2. Concentrations of CAT, GSH-Px, MDA, and SOD in the Liver of Mice. The determinations of CAT, GSH-Px, MDA, and SOD in the liver of mice are displayed in Table 3. As shown in Table 3, the concentrations of CAT, GSH-Px, and SOD were substantially increased, while that of MDA was reduced gradually with increasing dosage of CPs-1, demonstrating the differential effects of high-dosage CPs-1 and the model control group ($P < 0.01$) on the concentrations of CAT, GSH-Px, MDA, and SOD in the liver. The concentrations of SOD in the liver with high- and

TABLE 2: Quantification of serum level CAT, GSH-Px, MDA, and SOD.

Groups	CAT contents (U/mL)	GSH-Px contents (U/mL)	MDA contents (nmol/mL)	SOD contents (U/mL)
Normal control	13.60 ± 1.01 ^a	664.23 ± 45.96 ^b	3.32 ± 0.35 ^a	100.12 ± 10.47 ^a
Model control	10.80 ± 0.70*	460.86 ± 43.37**	5.14 ± 0.78*	59.64 ± 19.68*
Low dose	12.36 ± 1.09	809.07 ± 107.74 ^{b*}	4.08 ± 0.91	79.53 ± 19.40 ^a
Medium dose	15.32 ± 1.28 ^b	924.65 ± 58.13 ^{b**}	3.53 ± 0.78 ^a	142.01 ± 10.88 ^{b*}
High dose	18.05 ± 1.30 ^{b**}	1037.31 ± 49.51 ^{b**}	3.02 ± 0.85 ^b	187.46 ± 25.19 ^{b**}

^aStatistical significance level: $P < 0.05$ (vs. the model control group). ^bStatistical significance level: $P < 0.01$ (vs. the model control group). *Statistical significance level: $P < 0.05$ (vs. normal control group). **Statistical significance level: $P < 0.01$ (vs. normal control group).

TABLE 3: Quantification of liver level CAT, GSH-Px, MDA, and SOD.

Groups	CAT contents (U/mgprot)	GSH-Px contents (U/mgprot)	MDA contents (nmol/mgprot)	SOD contents (U/mgprot)
Normal control	68.02 ± 5.07 ^b	832.90 ± 77.41 ^a	6.80 ± 0.58 ^b	287.92 ± 23.14 ^a
Model control	54.02 ± 3.48**	655.53 ± 36.96*	10.73 ± 1.03**	250.16 ± 8.76*
Low dose	61.79 ± 5.44	925.45 ± 62.27 ^b	7.70 ± 0.58 ^b	267.34 ± 8.24
Medium dose	74.34 ± 4.69 ^b	1213.37 ± 156.62 ^{b**}	6.85 ± 0.99 ^b	283.66 ± 14.19 ^a
High dose	79.85 ± 7.13 ^{b*}	1514.14 ± 94.76 ^{b**}	6.19 ± 0.76 ^b	316.06 ± 24.73 ^b

^aStatistical significance level: $P < 0.05$ (vs. the model control group). ^bStatistical significance level: $P < 0.01$ (vs. the model control group). *Statistical significance level: $P < 0.05$ (vs. normal control group). **Statistical significance level: $P < 0.01$ (vs. normal control group).

medium-dosage CPs-1 were evidently higher than those of the model control group, where the significance levels were 0.01 and 0.05, respectively. Compared with that of the normal control group, the concentrations of CAT, GSH-Px, and SOD in the liver of mice in the high-dosage group were increased by 17.39% ($P < 0.05$), 81.79% ($P < 0.01$), and 9.77%, respectively. Therefore, CPs-1 could prominently diminish MDA concentration in the liver of mice.

4. Conclusions

The CPs-1 were successfully purified from crude CPs by column chromatography, with an average molecular weight of 38.7 kDa. CPs-1 were heterogeneous polysaccharides, consisting of Gal, Ara, Xyl, Man, and Glc at a molar ratio of 0.5:0.5:2.7:2.7:93.6. In addition, the FT-IR spectra exhibited the presence of the α - and β -D-pyranose in CPs-1. The methylation analysis and NMR spectrum indicated that CPs-1 had a $\rightarrow 6$ - β -D-Glcp-(1 \rightarrow 6)- β -D-Glcp(1 \rightarrow backbone. The results of antioxidant activities *in vitro* suggested that CPs-1 showed high scavenging abilities for DPPH (73.09 ± 1.35%), hydroxyl (90.75 ± 1.15%), and reducing power (1.342 ± 0.002) at 4.0 mg/mL, as well as ABTS and superoxide scavenging capacity. Furthermore, CPs-1 could significantly enhance enzymatic activities (i.e., CAT, GSH-Px, and SOD) and distinctly reduce MDA serum- and liver-concentrations in high-fat mice. Hence, CPs-1 could function as a natural novel antioxidant for medicine and functional foods. Further research is currently performed to investigate the antioxidation mechanism of CPs-1.

Data Availability

Data is contained within the article.

Conflicts of Interest

The authors declare that there is no conflict of interest regarding the publication of this paper.

Authors' Contributions

Xu Yang, Haiyu Ji, and Anjun Liu conceived and designed the research. Haiyu Ji, Yingying Feng, and Juan Yu performed the experiments. Xu Yang, Haiyu Ji, and Yingying Feng analyzed the data. Xu Yang, Haiyu Ji, and Yingying Feng wrote the original draft. Juan Yu and Anjun Liu reviewed and edited the manuscript. Xu Yang, Haiyu Ji, and Yingying Feng contributed equally to this work.

Acknowledgments

This work was supported by the Tianjin Key R & D Program (21YFNSN00110), the Science and Technology Planning Project of State Administration for Market Regulation (2019MK005 and 2020MK010), and Tianjin Administration for Market Regulation (2019-W20) and State Criteria for Food Safety (spaq-2020-08 and spaq-2020-31).

References







- [1] C. Zeng and S. L. Feng, "The antioxidant capacity *in vitro* and *in vivo* of polysaccharides from *Bergenia emeiensis*,"

- International Journal of Molecular Sciences*, vol. 21, no. 20, p. 7456, 2020.
- [2] L. Chen, R. Long, G. L. Huang, and H. L. Huang, "Extraction and antioxidant activities *in vivo* of pumpkin polysaccharide," *Industrial Crops and Products*, vol. 146, p. 112199, 2020.
- [3] S. J. Yang, J. Q. Sun, D. X. Gu et al., "Antioxidant activities of sulfated codonopsis polysaccharides in acute oxidative stress," *Journal Food Biochemistry*, vol. 45, no. 12, 2021.
- [4] D. A. Butterfield and B. Halliwell, "Oxidative stress, dysfunctional glucose metabolism and Alzheimer disease," *Nature Reviews Neuroscience*, vol. 20, no. 3, pp. 148–160, 2019.
- [5] T. Donia and A. Khamis, "Management of oxidative stress and inflammation in cardiovascular diseases: mechanisms and challenges," *Environmental Science and Pollution Research*, vol. 28, no. 26, pp. 34121–34153, 2021.
- [6] Q. Yang, Y. H. Jiang, S. Fu et al., "Protective effects of *Ulva lactuca* polysaccharide extract on oxidative stress and kidney injury induced by D-galactose in mice," *Marine Drugs*, vol. 19, no. 10, p. 539, 2021.
- [7] A. M. Pisoschi, A. Pop, F. Iordache, L. Stanca, G. Predoi, and A. I. Serban, "Oxidative stress mitigation by antioxidants - An overview on their chemistry and influences on health status," *European Journal Medicinal Chemistry*, vol. 209, p. 112891, 2021.
- [8] H. J. Forman and H. Q. Zhang, "Targeting oxidative stress in disease: promise and limitations of antioxidant therapy," *Nature Reviews Drug Discovery*, vol. 20, no. 9, pp. 689–709, 2021.
- [9] J. Luo, K. Mills, S. L. Cessie, R. Noordam, and D. V. Heemst, "Ageing, age-related diseases and oxidative stress: What to do next?," *Ageing Research Reviews*, vol. 57, p. 100982, 2020.
- [10] G. J. Chen and J. Q. Kan, "Characterization of a novel polysaccharide isolated from *Rosa roxburghii* Tratt fruit and assessment of its antioxidant *in vitro* and *in vivo*," *International Journal of Biological Macromolecules*, vol. 107, no. Part A, pp. 166–174, 2018.
- [11] M. G. Yu, M. J. Chen, J. L. Gui et al., "Preparation of *Chlorella vulgaris* polysaccharides and their antioxidant activity *in vitro* and *in vivo*," *International Journal of Biological Macromolecules*, vol. 137, pp. 139–150, 2019.
- [12] H. L. Huang and G. L. Huang, "Extraction, separation, modification, structural characterization, and antioxidant activity of plant polysaccharides," *Chemical Biology & Drug Design*, vol. 96, no. 5, pp. 1209–1222, 2020.
- [13] M. Taghvaei and S. M. Jafari, "Application and stability of natural antioxidants in edible oils in order to substitute synthetic additives," *Journal Food Science and Technology-Mysore*, vol. 52, no. 3, pp. 1272–1282, 2015.
- [14] Y. Hou and J. G. Jiang, "Origin and concept of medicine food homology and its application in modern functional foods," *Food & Function*, vol. 4, no. 12, pp. 1727–1741, 2013.
- [15] C. L. Guo, S. H. Zhang, Y. Q. Wang, M. X. Li, and K. Ding, "Isolation and structure characterization of a polysaccharide from *Crataegus pinnatifida* and its bioactivity on gut microbiota," *International Journal of Biological Macromolecules*, vol. 154, pp. 82–91, 2020.
- [16] C. J. Liu, Q. Liu, J. D. Sun, B. Jiang, and J. F. Yan, "Extraction of water-soluble polysaccharide and the antioxidant activity from *Semen cassiae*," *Journal Food and Drug Analysis*, vol. 22, no. 4, pp. 492–499, 2014.
- [17] Y. R. Song, A. R. Han, T. G. Lim, E. J. Lee, and H. D. Hong, "Isolation, purification, and characterization of novel polysaccharides from lotus (*Nelumbo nucifera*) leaves and their immunostimulatory effects," *International Journal of Biological Macromolecules*, vol. 128, pp. 546–555, 2019.
- [18] N. Wang, Y. Zhang, X. Wang et al., "Antioxidant property of water-soluble polysaccharides from *Poria cocos* Wolf using different extraction methods," *International Journal of Biological Macromolecules*, vol. 83, pp. 103–110, 2016.
- [19] Y. Cai, W. Liu, Y. X. Lin et al., "Compound polysaccharides ameliorate experimental colitis by modulating gut microbiota composition and function," *Journal of Gastroenterology and Hepatology*, vol. 34, no. 9, pp. 1554–1562, 2019.
- [20] L. Y. Chen, Z. Z. Rong, L. Juan, and G. Z. Sheng, "Protective effects of total polysaccharides in compound Kuqinin canine parvovirus infection and its influence on the expression of *Bax* and *BCL-2* gene based on pathological, ultrastructural, and apoptotic changes," *Journal of Animal and Plant Science*, vol. 29, no. 4, pp. 919–929, 2019.
- [21] Q. Jin, L. Cheng, Y. L. Zhu et al., "Immune-related effects of compound astragalus polysaccharide and sulfated epimedium polysaccharide on newborn piglets," *Animal Biotechnology*, vol. 32, pp. 1–12, 2021.
- [22] X. L. Li, A. G. Zhou, and X. M. Li, "Inhibition of *Lycium barbarum* polysaccharides and *Ganoderma lucidum* polysaccharides against oxidative injury induced by γ -irradiation in rat liver mitochondria," *Carbohydrate Polymers*, vol. 69, pp. 172–178, 2007.
- [23] M. Y. Chen, B. Y. Lu, Y. Li et al., "Metabolomics insights into the modulatory effects of long-term compound polysaccharide intake in high-fat diet-induced obese rats," *Nutrition & Metabolism*, vol. 15, no. 1, pp. 8–22, 2018.
- [24] K. L. Yan, W. Zhang, H. B. Yu, H. X. Wang, and X. Y. Zhang, "New polysaccharide compounds derived from submerged culture of *Ganoderma lucidum* and *Lycium barbarum*," *Food Technology and Biotechnology*, vol. 48, no. 1, pp. 94–101, 2010.
- [25] G. Yin and Y. Dang, "Optimization of extraction technology of the *Lycium barbarum* polysaccharides by Box-Behnken statistical design," *Carbohydrate Polymers*, vol. 74, no. 3, pp. 603–610, 2008.
- [26] X. Yang, H. Y. Ji, Y. Y. Feng, J. Yu, and A. J. Liu, "A novel optimization of water-soluble compound polysaccharides from Chinese herbal medicines by quantitative theory and study on its characterization and antioxidant activities," *Chemistry & Biodiversity*, vol. 18, no. 1, p. e2000688, 2021.
- [27] S. Z. Li, *Compendium of Materia Medica*, Guangming Daily Press, Beijing, China, 2015.
- [28] J. Y. Liu and Q. Liu, *Study Essentials of 100 Classic Famous Prescriptions*, China Medical Science Press, Beijing, China, 2019.
- [29] Y. N. Zhao, H. Y. Sun, L. Ma, and A. J. Liu, "Polysaccharides from the peels of *Citrus aurantifolia* induce apoptosis in transplanted H22 cells in mice," *International Journal of Biological Macromolecules*, vol. 101, pp. 680–689, 2017.
- [30] X. Yang, H. Y. Ji, Y. Y. Feng, J. Yu, and A. J. Liu, "Structural characterization and antitumor activity of polysaccharides from *Kaempferia galanga* L.," *Oxidative Medicine and Cellular Longevity*, vol. 2018, Article ID 9579262, 10 pages, 2018.
- [31] X. Yang, X. Wang, X. Y. Chen, H. Y. Ji, Y. Zhang, and A. J. Liu, "Pinocembrin-lecithin complex: characterization, solubilization, and antioxidant activities," *Biomolecules*, vol. 8, no. 2, p. 41, 2018.

- [32] N. F. Wang, G. G. Jia, X. F. Wang et al., "Fractionation, structural characteristics and immunomodulatory activity of polysaccharide fractions from asparagus (*Asparagus officinalis* L.) skin," *Carbohydrate Polymers*, vol. 256, p. 117514, 2021.
- [33] J. H. Wang, J. L. Xu, J. C. Zhang, Y. Liu, H. J. Sun, and X. Q. Zha, "Physicochemical properties and antioxidant activities of polysaccharide from floral mushroom cultivated in Huangshan Mountain," *Carbohydrate Polymers*, vol. 131, pp. 240–247, 2015.
- [34] Y. Xu, X. Zhang, X. H. Yan et al., "Characterization, hypolipidemic and antioxidant activities of degraded polysaccharides from *Ganoderma lucidum*," *International Journal of Biological Macromolecules*, vol. 135, pp. 706–716, 2019.
- [35] L. P. Sun, X. J. Su, and Y. L. Zhuang, "Preparation, characterization and antiglycation activities of the novel polysaccharides from *Boletus snicus*," *International Journal of Biological Macromolecules*, vol. 92, pp. 607–614, 2016.
- [36] Z. Chen, W. Zhang, X. Y. Tang et al., "Extraction and characterization of polysaccharides from Semen cassiae by microwave-assisted aqueous two-phase extraction coupled with spectroscopy and HPLC," *Carbohydrate Polymers*, vol. 144, pp. 263–270, 2016.
- [37] M. Q. Zhu, R. M. Huang, P. Wen et al., "Structural characterization and immunological activity of pectin polysaccharide from kiwano (*Cucumis metuliferus*) peels," *Carbohydrate Polymers*, vol. 254, p. 117371, 2021.
- [38] Y. Q. Xu, X. J. Niu, N. Y. Liu et al., "Characterization, antioxidant and hypoglycemic activities of degraded polysaccharides from blackcurrant (*Ribes nigrum* L.) fruits," *Food Chemistry*, vol. 243, pp. 26–35, 2018.
- [39] L. Zhang, Y. Hu, X. Y. Duan et al., "Characterization and antioxidant activities of polysaccharides from thirteen boletus mushrooms," *International Journal of Biological Macromolecules*, vol. 113, pp. 1–7, 2018.
- [40] D. Liu, Q. W. Sun, J. Xu et al., "Purification, characterization, and bioactivities of a polysaccharide from mycelial fermentation of *Bjerkandera fumosa*," *Carbohydrate Polymers*, vol. 167, pp. 115–122, 2017.
- [41] Q. Wang, F. Liu, X. X. Chen, Z. J. Yang, and Y. Cao, "Effects of the polysaccharide SPS-3-1 purified from *Spirulina* on barrier integrity and proliferation of Caco-2 cells," *International Journal of Biological Macromolecules*, vol. 163, pp. 279–287, 2020.
- [42] Y. H. Liu, "Identification of polysaccharides from Chinese Yam (*Dioscoreae opposita* "Qi") by infrared spectroscopy," *Agricultural Science & Technology*, vol. 17, pp. 1941–1943, 2016.
- [43] I. Rjeibi and W. Jouida, "Characterization of polysaccharides extracted from pulps and seeds of *Crataegus azarolus* L. var. aronia: preliminary structure, antioxidant, antibacterial, α -amylase, and acetylcholinesterase inhibition properties," *Oxidative Medicine and Cellular Longevity*, vol. 2020, Article ID 1903056, 11 pages, 2020.
- [44] Y. R. Song, A. R. Han, S. G. Park, C. W. Cho, Y. K. Rhee, and H. D. Hong, "Effect of enzyme-assisted extraction on the physicochemical properties and bioactive potential of lotus leaf polysaccharides," *International Journal of Biological Macromolecules*, vol. 153, pp. 169–179, 2020.
- [45] R. N. Kasimu, C. L. Chen, X. Y. Xie, and X. Li, "Water-soluble polysaccharide from *Erythronium sibiricum* bulb: Structural characterisation and immunomodulating activity," *International Journal of Biological Macromolecules*, vol. 105, Part 1, pp. 452–462, 2017.
- [46] W. Liu, W. S. Lu, Y. Chai, Y. M. Liu, W. B. Yao, and X. D. Gao, "Preliminary structural characterization and hypoglycemic effects of an acidic polysaccharide SERP1 from the residue of *Sarcandra glabra*," *Carbohydrate Polymers*, vol. 176, pp. 140–151, 2017.
- [47] N. D. Sanandiya and A. K. Siddhanta, "Chemical studies on the polysaccharides of *Salicornia brachiata*," *Carbohydrate Polymers*, vol. 112, pp. 300–307, 2014.
- [48] M. B. Wu, F. F. Zhang, Z. P. Yu, J. P. Lin, and L. R. Yang, "Chemical characterization and *in vitro* antitumor activity of a single-component polysaccharide from *Taxus chinensis* var. *mairii*," *Carbohydrate Polymers*, vol. 133, pp. 294–301, 2015.
- [49] C. P. Zheng, Q. Dong, H. J. Chen, Q. F. Cong, and K. Ding, "Structural characterization of a polysaccharide from *Chrysanthemum morifolium* flowers and its antioxidant activity," *Carbohydrate Polymers*, vol. 130, pp. 113–121, 2015.
- [50] G. Gong, J. Fan, Y. Sun et al., "Isolation, structural characterization, and antioxidant activity of polysaccharide LBLP5-A from *Lycium barbarum* leaves," *Process Biochemistry*, vol. 51, no. 2, pp. 314–324, 2016.
- [51] P. P. Chu, Q. Q. Song, Y. T. Chen, L. Song, and Y. B. Qiao, "Evaluation on antioxidant activity of bitter buckwheat polysaccharide *in vitro*," *Tianjin Agricultural Sciences*, vol. 22, pp. 45–48, 2016.
- [52] P. P. Zheng, S. Li, L. R. Qi, Z. T. Yang, T. Zhang, and X. Y. Ao, "Extraction and antioxidant activity of hawthorn polysaccharides," *China Brewing*, vol. 34, pp. 107–113, 2015.
- [53] G. Gong, T. Dang, Y. Deng et al., "Physicochemical properties and biological activities of polysaccharides from *Lycium barbarum* prepared by fractional precipitation," *International Journal of Biological Macromolecules*, vol. 109, pp. 611–618, 2018.
- [54] X. Chen, H. B. Zhang, W. Q. Du et al., "Comparison of different extraction methods for polysaccharides from *Crataegus pinnatifida* Bunge," *International Journal of Biological Macromolecules*, vol. 150, pp. 1011–1019, 2020.
- [55] F. Chen, G. L. Huang, and H. L. Huang, "Preparation, analysis, antioxidant activities *in vivo* of phosphorylated polysaccharide from *Momordica charantia*," *Carbohydrate Polymers*, vol. 252, p. 117179, 2021.
- [56] W. Wang, X. W. Li, K. Chen, H. Y. Yang, B. Jialengbieke, and X. D. Hu, "Extraction optimization, characterization and the antioxidant activities *in vitro* and *in vivo* of polysaccharide from *Pleurotus ferulae*," *International Journal of Biological Macromolecules*, vol. 160, pp. 380–389, 2020.

Review Article

***Carica papaya* L. Leaves: Deciphering Its Antioxidant Bioactives, Biological Activities, Innovative Products, and Safety Aspects**

**Anshu Sharma,¹ Ruchi Sharma,² Munisha Sharma,³ Manoj Kumar ⁴,
Mrunal Deepak Barbhai ⁴, José M. Lorenzo,^{5,6} Somesh Sharma,² Mahesh Kumar Samota,⁷
Maria Atanassova,⁸ Gianluca Caruso ⁹, Mo. Naushad,² Radha,¹⁰ Deepak Chandran ¹¹,
Prasad Prakash,¹⁰ Muzaffar Hasan,¹² Nadeem Rais,¹³ Abhijit Dey ¹⁴,
Dipendra Kumar Mahato,¹⁵ Sangram Dhumal,¹⁶ Surinder Singh,¹⁷
Marisennayya Senapathy,¹⁸ Sureshkumar Rajalingam,¹⁹ Marthandan Visvanathan,²⁰
Lejaniya Abdul Kalam Saleena,²¹ and Mohamed Mekhemar ²²**

¹Department of FST, Dr. Yashwant Singh Parmar University of Horticulture and Forestry, Nauni, Solan 173230, India

²School of Bioengineering and Food Technology, Shoolini University, Solan 173229, Himachal Pradesh, India

³Sri Shankara Cancer Hospital and Research Centre, Bengaluru, Karnataka 560004, India

⁴Chemical and Biochemical Processing Division, ICAR—Central Institute for Research on Cotton Technology, Mumbai 400019, India

⁵Centro Tecnológico de la Carne de Galicia, Parque Tecnológico de Galicia, Avd. Galicia no. 4, San Cibrao das Viñas, 32900 Ourense, Spain

⁶Área de Tecnología de los Alimentos, Facultad de Ciencias de Ourense, Universidad de Vigo, 32004 Ourense, Spain

⁷Horticulture Crop Processing Division, ICAR-Central Institute of Post-Harvest Engineering and Technology, Abohar, Punjab, India

⁸Chemical Engineering, UCTM, Sofia 1734, Bulgaria

⁹Department of Agricultural Sciences, University of Naples Federico II, Portici, Naples, Italy

¹⁰School of Biological and Environmental Sciences, Shoolini University of Biotechnology and Management Sciences, Solan 173229, India

¹¹Department of Veterinary Sciences and Animal Husbandry, Amrita School of Agricultural Sciences, Amrita Vishwa Vidyapeetham University, Coimbatore 642109, India

¹²Agro Produce Processing Division, ICAR—Central Institute of Agricultural Engineering, Bhopal 462038, India

¹³Department of Pharmacy, Bhagwant University, Ajmer 305004, India

¹⁴Department of Life Sciences, Presidency University, 86/1 College Street, Kolkata 700073, India

¹⁵CASS Food Research Centre, School of Exercise and Nutrition Sciences, Deakin University, Burwood 3125, Australia

¹⁶Division of Horticulture, RSCM College of Agriculture, Kolhapur 416004, India

¹⁷Dr. S. S. Bhatnagar University Institute of Chemical Engineering and Technology, Panjab University, Chandigarh 160014, India

¹⁸Department of Rural Development and Agricultural Extension, College of Agriculture, Wolaita Sodo University, Wolaita Sodo, SNNPR, Ethiopia

¹⁹Department of Agronomy, Amrita School of Agricultural Sciences, Amrita Vishwa Vidyapeetham University, Coimbatore 642109, India

²⁰Department of Seed Science and Technology, Amrita School of Agricultural Sciences, Coimbatore, Tamil Nadu 642109, India

²¹Department of Food Science and Nutrition, Faculty of Applied Sciences, UCSI University, 56000 Cheras, Willayah Persekutuan, Kuala Lumpur, Malaysia

²²Clinic for Conservative Dentistry and Periodontology, School of Dental Medicine, Christian-Albrecht's University, 24105 Kiel, Germany

Correspondence should be addressed to Manoj Kumar; manojkumarpuniya114@gmail.com, Gianluca Caruso; gcaruso@unina.it, and Mohamed Mekhemar; mekhemar@konspar.uni-kiel.de

Received 5 April 2022; Revised 23 April 2022; Accepted 28 April 2022; Published 9 June 2022

Academic Editor: German Gil

Copyright © 2022 Anshu Sharma et al. This is an open access article distributed under the Creative Commons Attribution License, which permits unrestricted use, distribution, and reproduction in any medium, provided the original work is properly cited.

The prevalence of viral infections, cancer, and diabetes is increasing at an alarming rate around the world, and these diseases are now considered to be the most serious risks to human well-being in the modern period. There is a widespread practice in Asian countries of using papaya leaves (*C. papaya* L.) as herbal medicine, either alone or in combination with prescribed medications, to treat a variety of ailments. The importance of conducting the necessary descriptive studies in order to determine the safety of papaya leaf consumption is also emphasized in the context of their application in the healthcare sector. Electronic databases such as Google Scholar, Scopus, and PubMed were used to gather information on papaya leaves, their therapeutic potential, and clinical evidence-based studies. The literature was gathered from publications on papaya leaves, their therapeutic potential, and clinical evidence-based studies. The antidengue, anticancer, antidiabetic, neuroprotective, and anti-inflammatory effects of papaya leaves discussed in this article are supported by evidence from preclinical, *in vivo*, *in vitro*, and clinical trial studies, as well as from other sources. Leaves have been investigated for their mechanism of action as well as their potential to be used in the development of novel herbal products for the health business. According to the reports gathered, only a small number of research demonstrated that leaf extract at high concentrations was hazardous to certain organs. The collective literature reviewed in this review provides insights into the use of papaya leaves as a cure for epidemic diseases, highlighting the phytochemical composition and pharmacological attributes of papaya leaves, as well as the results of various preclinical and clinical studies that have been conducted so far on the subject. The review clearly demonstrates the successful medical evidence for the use of papaya leaf extracts in the healthcare system as a supplemental herbal medication in a variety of clinical settings.

1. Introduction

Chronic diseases are becoming an increasingly serious hazard to public health, necessitating the implementation of nutrition-based strategies to combat them. It can be difficult to obtain medical care for certain disorders, and the consumption of staple functional foods is vital in terms of preventing such ailments. Medical care accounts for 10 to 20% of the changeable contributors to human health, whereas social determinants, specifically healthy eating habits, account for 80 to 90% of the adjustable contributors. Healthy plant-based diets are more environmentally friendly and are connected with a lower risk of obesity, type 2 diabetes mellitus, viral infections, and some malignancies, among other health benefits. When it comes to addressing chronic human diseases, functional agriculture, specifically the cultivation of functional food crops like papaya leaves (*Carica papaya* L.), has emerged as a new frontier in nutritional research. The creation of functional food crops employing cutting-edge technology in combination with approaches from crop science, food science, and preventive medicine is therefore a significant topic of research [1].

C. papaya L. belongs to the family Caricaceae and is commonly known as papaya, pawpaw, and kates. It is a perennial horticultural shrub originated from Mesoamerican Centre, Central America, and southern Mexico [2–4] and is mainly cultivated in the tropical and subtropical regions of Brazil, Australia, Malaysia, China, India, Thailand, Myanmar, Philippines, and other adjoining [5]. Papaya is not only cultivated for the ripe sweet fruit, even other parts of the plant such as seeds, leaves, roots, flowers, barks, and latex have been traditionally used worldwide for the preparation of various medicinal formulations [6, 7]. However, leaves have been emerged as one of the most useful parts with plethora of health-promoting compounds and activities. In traditional medicines, the decoction of papaya fresh leaves is added into a tea to cure malaria, whereas dry and cured

leaves are used as cigar for smoking by persons suffering from respiratory disorders such as asthma. Fresh young leaves of papaya are consumed as a leafy vegetable after steaming in some countries. In India, boiled leaves of papaya are recommended by Ayurveda practitioners as relief from malarial and dengue fevers as papaya leaf extract is considered effective to elevate platelet count and red and white blood cells in patients after suffering from viral fever [8]. The extract has also been known to protect the patients against the sickling of red blood cells [9]. In many parts of Asia, papaya leaves are used for the treatment of beriberi [10]. Papaya leaves have been identified to have more than fifty bioactive components and therefore useful in the treatment of different human diseases [11, 12]. Scientific studies revealed the existence of considerable levels of glycosides, flavonoids, alkaloids, saponins, phenolic compounds, amino acids, lipids, carbohydrates, enzymes, vitamins, and minerals in papaya leaves [13, 14]. The crude form of ethyl acetate isolates of papaya leaves has very good antiplasmodial effect against *Plasmodium falciparum* and *P. falciparum*-resistant strains [15, 16]. Although the leaves of papaya are used in Ayurvedic medicines, the juice from green leaves has been gaining the attention of today's consumers as a functional food due to its potent antiviral and immunity-enhancing properties [17]. Tea prepared from the juice extracted from papaya leaves is also used as a synergistic therapeutic dietary supplement for patients suffering from the oxidative stress-related diseases because of its strong antioxidant potential [18]. Few of the studies reported that fresh papaya leaves possess antiseptic properties, while the dried leaves can be used as a tonic to purify the blood and to improve digestion. Leaf juice of papaya is now being known for its potent anticancer [19], antioxidative [4, 5], anti-inflammatory [7], antimicrobial [20], and antisickling properties [21] along with nephron protective [22], hepatoprotective [23], hypoglycaemic, and hypolipidemic effects [24] against toxins in the human system. In fact, polar isolates of papaya have exhibited

antihuman immunodeficiency virus (HIV), analgesic, and wound healing properties [25]. The imbalance in the activity of free radicals and the cellular antioxidant system is implicated to various lethal conditions such as cancer and cardiovascular diseases [26]. Recent research studies have been focusing on all-natural antioxidant-enriched plant parts, and in particular, papaya leaves are currently being consumed because a medical assessment of the leaf extract exhibited antiproliferative activity on cancerous cells along with its immune modulatory effects. There is a significant number of reviews regarding the functional properties of papaya fruits, but limited reviewing available relevant to the phytochemicals, biological activity, medical studies, and scope of using papaya's leaves in health industry. Therefore, this review is aimed at bridging this gap for better utilization of papaya leaves in the future due to their great medicinal potential. Electronic databases such as Google Scholar, Scopus, and PubMed were used to gather information on papaya leaves, their therapeutic potential, and clinical evidence-based studies. The literature was gathered from publications on papaya leaves, their therapeutic potential, and clinical evidence-based studies. The antidengue, anticancer, antidiabetic, neuroprotective, and anti-inflammatory effects of papaya leaves discussed in this article are supported by evidence from preclinical, *in vivo*, *in vitro*, and clinical trial studies, as well as from other sources. Leaves have been investigated for their mechanism of action as well as their potential to be used in the development of novel herbal products for the health business. The collective literature reviewed in this review provides insights into the use of papaya leaves as a cure for epidemic diseases, highlighting the phytochemical composition and pharmacological attributes of papaya leaves, as well as the results of various preclinical and clinical studies that have been conducted so far on the subject. The review clearly demonstrates the successful medical evidence for the use of papaya leaf extracts in the healthcare system as a supplemental herbal medication in a variety of clinical settings.

2. Phytochemical Composition of Papaya Leaves

Phytochemicals are chemical components, naturally found in different parts of plants, which make many species beneficial for therapeutic uses. Indeed, leaves of papaya are known to have various health-promoting phytochemicals, as it arose from chemical analysis performed in various studies which clearly illustrated the presence of significant amounts of alkaloids, saponins, glycosides, flavonoids, phenolic compounds, enzymes, amino acids, lipids, carbohydrates, vitamins, and minerals [13]. There were seven flavonoids found in papaya leaves, which were named as quercetin, kaempferol 3-rutinoside, quercetin3-(2G-rhamnosylrutinoside), quercetin 3-rutinoside, kaempferol 3-(2G-rhamnosylrutinoside), myricetin 3-rhamnoside. Caffeic acid, protocatechuic acid, quercetin, 5,7-dimethyl coumarin, p-coumaric acid, and chlorogenic acid are among the phenolic substances found in the leaves [19]. There is evidence to suggest that leaves contain a wide range of phytochemicals,

including carpaine, kaempferol 3-(2G-glucosylrutinoside), kaempferol 3-(2''-rhamnosylgalactoside), 7-rhamnoside, kaempferol 3-rhamnosyl-(1->2)-galactoside-7-rhamnoside, luteolin 7-galactosyl-(1->6)-galactoside, orientin 7-O-rhamnoside, 11-hydroperoxy-12,13-epoxy-9-octadecenoic acid, palmitamide, and 2-hexaprenyl-6-methoxyphenol [25]. Due to these potent bioactive components, extracts of the aforementioned leaves can be used to prepare nutraceuticals and herbal medicinal formulations. Chemical constituent and structure of some important compounds of *C. papaya* leaves are illustrated in Figure 1. There were reports that *C. papaya* leaves were used with other herbs to heal ailments. Traditional doctors in Nigeria use it to treat diabetes, while in Cameroon, they combine it with other herbs to treat malaria and other fungal infections and aboriginal Australians' record using decoctions of the leaf as an anticancer remedy [16, 19]. The functional bioactive components of leaves of papaya can elevate the overall antioxidant potential of blood. The leaves of papaya plant are well known to have papain, cystatin, chymopapain, tocopherol, phenolic acids, cyanogenic glucosides, glucosinolates, and vitamin C as main phytochemicals [27]. Mainly alkaloids, saponins, glycosides, phenolic compounds, and flavonoids are responsible for the anti-inflammatory and anticancerous properties of papaya leaves [28]. Vitamins, minerals, and amino acids of papaya leaves are quite helpful to improve the total haemoglobin, proteins, and immunity of human system [29]. Carpaine along with dehydrocarpaine I and dehydrocarpaine II are most important health-promoting and major bioactive components found in the leaves of papaya. Due to the presence of carpaine, these herbal leaves are utilized in Ayurveda formulations for treating various physical disorders and viral fevers such as dengue and chikungunya. The aforementioned alkaloid has the ability to calm high blood pressure and fast heart rate and is effective for the uterus marked relaxation, the bronchioles dilatation, and movement of the intestinal strips along with antiplasmodial properties [30]. Carpaine has also been reported to have potent anticancerous and antihelminthic properties [31]. Its concentration has been reported the highest in mature leaves of papaya, i.e., 9.30 mg/g, followed by fruit pulp, i.e., 4.90 mg/100 g, fruit peel, i.e., 1.99 mg/100 g, and seeds, i.e., 0.65 g/g [32]. Leaves constitute different components in varying proportions such as 8.3% of carbohydrates, 38.6% of vitamin C, 5.6% of pro- and 0.23% of phosphoric acid. A good amount of tannin ($0.85 \pm 10^{-3} \pm 1.76 \pm 10^{-4}$ M, 0.824%) in papaya leaf extract has been reported by a few researchers [33]. Papaya leaves has been found to have highest total phenolic compounds as 424.89 ± 0.22 mg GAE/100 g of the dry sample followed by the 339.91 ± 9.40 in unripe papaya, 272.66 ± 1.53 in ripe papaya, and 30.32 ± 6.90 mg GAE/100 g in seeds [34]. Due to the aforementioned bioactive compounds, a very good antioxidant potential of 90% has been recorded in its leaves already. Researchers also reported a good concentration of calcium and magnesium, i.e., 3480 mg/kg and 5928 mg/kg, respectively; other minerals like iron (558 mg/kg), zinc (33.4 mg/kg), manganese (22.88 mg/kg), chromium (7.50 mg/hg), and copper (2.16 mg/kg) were also found in fair amount [16]. Papaya

leaves have shown the highest ascorbic acid content with the concentration of 85.6 mg/100 g followed by 45.8 mg/100 g in ripe papaya, 37.8 mg/100 g in unripe papaya, and 14.4 mg/100 g in its seeds [34]. Biological enzymes, viz., papain and chymopapain, are in abundance in the leaves of papaya [35]. The concentration of papain in papaya leaf extract varies from 0.054 to 0.002 mg/mL [35] and due to which very powerful digestive action even higher than pepsin is seen, important phytochemical constituents of leaves along with their functional properties and structures.

3. Bioactivities of Papaya Leaf Extract

Papaya leaves have a very long history in terms of its medicinal uses and have been utilized in many Asian countries for treating various ailments. Because of the presence of the aforementioned important functional constituents, they are used to cure corns, warts, constipation, weakness, amenorrhea, menstruation problems, eczema, sinuses, cutaneous tubercle, glandular tumour, diabetes, ulcers, hypertension, dengue, etc. [8]. Traditionally, Australian aboriginal people consume papaya leaf extract for its anticancerous activity [36, 37]. In addition to their various cancer-fighting components, *C. papaya* leaves contain a significant amount of nutrients to improve the immunity. Beside vitamins E, A, and C, they have vitamin B-17 whose concentrated form is used to cure cancer patients in conventional chemotherapy treatment. Phytochemicals of papaya leaves have been reported to prevent bone marrow depletion and platelet destruction [2]. Juice of papaya leaf is quite helpful to elevate platelet count and red blood and white blood cells to normalize blood clotting and to repair the liver [18].

3.1. Antioxidant Effect. Many phytonutrients found in plants, such as fruits and vegetables, have come to the attention of food experts and the general public in recent years for their potential health benefits. Due to concerns about synthetic antioxidants' toxicity, these phytochemicals are commonly marketed as natural antioxidants as an alternative. Oxidative compounds present in many plants have antibacterial, antiviral, and cancer-fighting properties. They also have an array of other health benefits [19, 38]. Papaya peels are discarded after consuming the fruit. However, they contain antioxidants. Oxidative damage caused by free radicals has major implications in many chronic diseases [25]. By inhibiting the creation of free radicals, antioxidants can aid our health. New sources of natural antioxidants that are both safe and economically viable are now being investigated. Researchers made silver nanoparticles from *C. papaya* peel extract (CPPE) and examined their antioxidative properties to see if they worked. We found that the concentration-dependent activity of AgNPs was 56% for synthesised AgNPs and 38% for commercially available CPPE [39]. According to a recent study, the antioxidant activity of methanolic extract of papaya leaf was assessed by measuring its ability to neutralise free radicals (DPPH) [40]. DPPH free radical scavenging capacity was found to be best in hexane extract and lowest in aqueous extract in another investigation using papaya seed extracts and the results showed

[41]. Papaya leaf antioxidant activity has been studied by Nisa et al. using various cultivars, maturities, and solvents. During extraction, the solvents were water, methanol, and 70% ethanol. Results showed that water-extracted mature leaves had the highest antioxidant activity of any of the other types of leaves tested. PaMsrB1 (plant methionine sulfoxide reductase B1) from papaya leaf was studied with *Escherichia coli*, which has MBP (maltose-binding protein) at its N terminal protease activity, which assists in the digestion of MBP-tag and leads to the separation of the recombinant PaMsrB1. In the presence of dithiothreitol, the purified recombinant protein PaMsrB1 demonstrated reductase activity against methionine sulfoxide (MetSO). An affinity chromatography and LC/MS/MS study discovered several proteins that interact with PaMsrB1. Understanding the defensive mechanisms of PaMsrB1 against antioxidative stress is facilitated by these findings [41]. Antioxidant activity and total phenolic content (TPC) were measured by Ang et al. to determine the antioxidative capability of *C. papaya* peels. Ferric reducing/antioxidant power (FRAP) and the ABTS radical cation inhibition activity (ABTS-RCI) were used to evaluate antioxidant activities, and the Folin-Ciocalteu method was used to measure TPC. The TPC of the papaya peel was 15.18 g GAE/mL when extracted with 90% acetone (*v/v*) for 60 minutes. DPPH, FRAP, and ABTS assays found antioxidant activity of 37.34%, 19.70 $\mu\text{g TE/mL}$ extract, and 28.30%, respectively. The antioxidant potential of papaya peel may contribute to production of functional foods and nutraceutical in the near future utilising these papaya wastes [38]. Calvache et al. treated papaya peel residues with ethanol and drying them in a microwave oven to generate dietary fibre concentrates (DFCs), in order to demonstrate its antioxidant activity. Carotenoids, phenolics, ascorbic acid, proteocatechuic acid, manghaslin, quercetin 3-O-rutinoside, caffeoyl hexoside, ferulic acid, lutein, zeaxanthin, and beta-carotene were detected in the chromatographic analysis of the samples. Upon analysis of digestibility, it was found that about 65% of the polyphenols associated to peel DFCs were potentially bioaccessible in the small intestine and that the portion of indigestible fiber had antioxidant capacity [42]. *In vitro* antioxidant activity of papaya peel extracts, and their effects on endogenous glutathione, superoxide dismutase, catalase, cyclo-oxygenase-2 (COX-2), cyclo-oxygenase-3, and DNA fragmentation in HepG2 cells were investigated by Salla et al. Papaya peel extracts contained significant amounts of gallic acid (18.06 $\mu\text{g/g}$), caffeic acid (29.28 $\mu\text{g/g}$), p-coumaric acid (38.16 $\mu\text{g/g}$), ferulic acid (95.46 $\mu\text{g/g}$), and quercetin (3.17 $\mu\text{g/g}$). *In vitro* antioxidant capacity of papaya peels was determined by FRAP (31.86 $\mu\text{M Fe}^{+2}/\text{g}$), trolox equivalent antioxidant capacity (14.56 mM trolox equivalents/g), oxygen radical scavenging activity (30.88 mM TE/g), and 2,2-diphenyl-1-picrylhydrazyl radical scavenging ability (IC₅₀ = 8.33 mg/mL). SOD, CAT, GPx, GR activity, and GSH levels were decreased by 3.1, 1.46, 2.87, 1.34, and 1.32 times, respectively, when oxidative stress was induced. *Papaya* peel extracts, on the other hand, significantly increased SOD, CAT, GPx, GR, and GSH activities in cells compared to cells exposed to oxidative stress. It was found that papaya peel

TABLE 1: Antioxidant activities of *Carica papaya* L. leaf extract.

Type of extract	Method used	Responsible phytochemicals	References
Methanol	Peroxy-nitrite scavenging assay	Kaempferol 3-(2G-rhamnosylrutinoside)	[41]
Ethanol, methanol, and water	DPPH, FRAP	Flavonoids	[44]
Methanol	DPPH	Carpaine, kaempferol 3-(2G-glucosylrutinoside), kaempferol 3-(2''-rhamnosylgalactoside), 7-rhamnoside, kaempferol 3-rhamnosyl-(1->2)-galactoside-7-rhamnoside, luteolin 7-galactosyl-(1->6)-galactoside, orientin 7-O-rhamnoside, 11-hydroperoxy-12,13-epoxy-9-octadecenoic acid, palmitic amide, and 2-hexaprenyl-6-methoxyphenol	[25]
Methanol	DPPH	—	[45]
n-Hexane, dichloromethane, ethyl acetate, ethanol, methanol, n-butanol, and water	DPPH	Phenolics and flavonoids	[46]
Aqueous	DPPH, ABTS	Polyphenols	[5]
Methanol	Phosphomolybdenum method	Flavonoids	[47]
Aqueous	DPPH, ABTS ⁺ assay	Proteins and phenolic groups	[39]

extracts caused cell death by apoptosis cells by significantly reducing COX-2 activity, increasing caspase-3 activity, and triggering DNA fragmentation. Anticancer activities of papaya peel extracts may be attributed to the synergistic action of free radical scavenging, stimulation of antioxidant enzymes, and triggering apoptosis [43]. Similarly, antioxidant properties are directly and indirectly contributing towards imparting other bioactivities such as immunomodulatory activities, antiviral, antidiabetic, and others discussed in following subsections. Table 1 provides an overview of *C. papaya*'s antioxidant properties.

3.2. Antiviral (Antidengue) and Antithrombocytopenic Effect.

Dengue is an arboviral disease caused by dengue virus of the Flaviviridae family. Dengue fever occurs due to the infection transmitted by infected *Aedes aegypti* mosquito as a carrier of this virus [48]. The occurrence of this disease has increased by almost 30-fold in the previous three decades especially in developing countries. A number of infections caused by dengue virus ranges from 50 to 100 million per year [48], and every year, there is a new outbreak of dengue being reported. This viral infection leads to thrombocytopenia condition in infected patients [49]. The most common reason for thrombocytopenia is the poor production of platelets by the bone marrow, minimal survival of platelets, and sequestration of the platelets by the leptospirosis, malaria, dengue, and other viral infections. Major quantitative or qualitative dysfunction and reduction in the platelet count is the cause of mucocutaneous bleeding in the patients [50]. The platelet count drops below the normal level to an extent depending upon severity of viral infections. Moreover, viral fever is generally a self-limited illness which requires supportive care for complete recovery. Aspirin, antibiotics, nonsteroidal anti-inflammatory drugs, and corticosteroids must not be consumed by the patient as they are not so beneficial in viral infections. In fact, their consumption can cause gastritis or in severe cases internal bleeding too. One of the most disturbing aspects of the viral infections

is that there are no effective antiviral agents available to treat their complications. *In vivo* studies have indicated quite beneficial effects of papaya leaf extract to improve immunity against infections and to increase platelet counts in thrombocytopenic patients after suffering viral infections [51].

Various studies both with animal and human models have been conducted by researchers worldwide to confirm the anti-inflammatory effect [7] and platelet count improvement after administration of simple papaya leaf extract or ethanolic aqueous extract [8, 52–54]. The use of papaya extract is recommended to get early recovery in case of dengue with low platelet and red and white blood cell count [54]. As per few case studies conducted in recent years, its positive effect on total platelet count is clearly demonstrated. Researchers orally administered a 25 mL papaya leaf extract to the dengue patients daily in the morning as well as evening times for five days continuously [17]. There was significant improvement in platelet count and white blood cells and neutrophils (NEUT) just after the second day of oral consumption, and the count reached their healthy normal level at the end of course. Research was conducted, which is the study of multiple platelet transfusions to a baby suffering from congenital thrombocytopenia. The patient did not respond well to phototherapy, intravenous immunoglobulin, and two exchange transfusions with antifungal therapy and antibiotics. However, papaya leaf extract oral administration as much as 20 mg/kg/dose of patient body weight, three times a day, exhibited quite a positive effect on platelet count without any side effects in the baby even during the follow-up period [55]. Antiviral (antidengue) and antithrombocytopenic effect of papaya leaf extract is shown in Figure 2.

Like these aforementioned studies, there are various pre-clinical and clinical studies confirming the therapeutic effect of papaya leaves on thrombocyte animal models and are summarized in Table 2 for further enlightenment on its therapeutic potential against thrombocytopenia in dengue infection. The action mechanism of papaya leaf extract shows very good stabilizing properties to prevent platelet

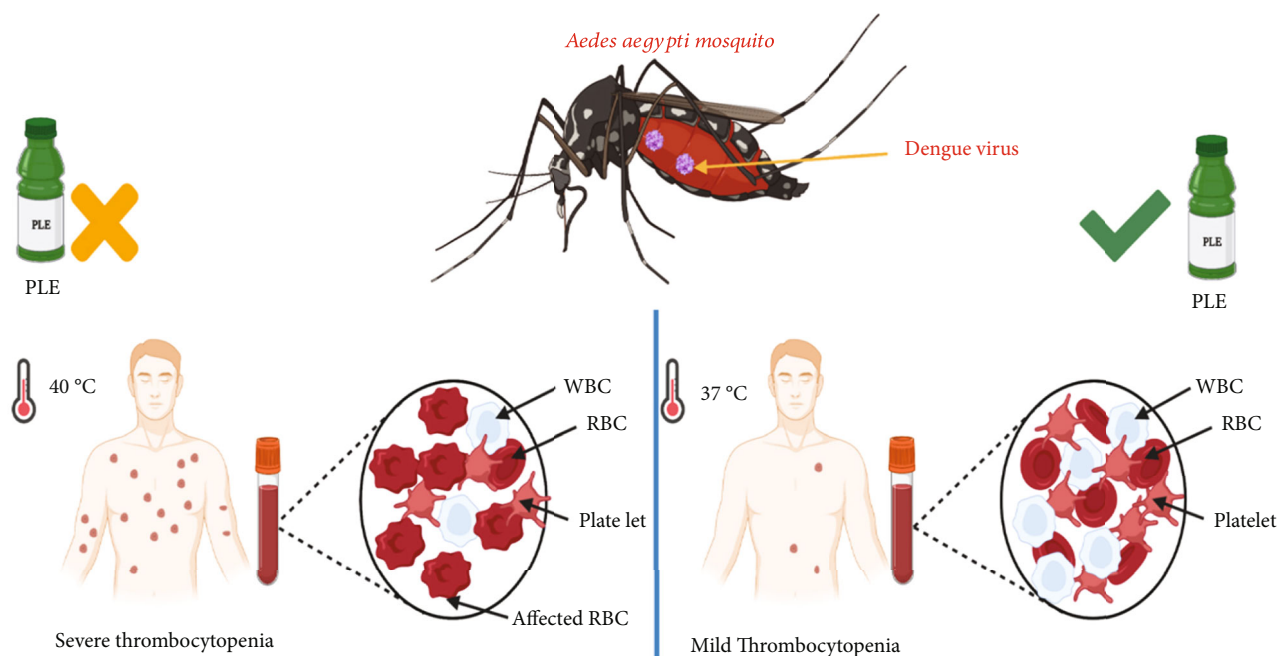


FIGURE 2: Antiviral (antidengue) and antithrombocytopenic effect of papaya leaves.

lysis and inhibits heat-induced and hypotonicity-induced haemolysis of erythrocytes even at the lower extract concentration. In the latter respect, the extracts are likely to possess membrane-stabilizing attributes and protect blood cells against stress-induced destruction. This property might be useful in patients with dengue where papaya leaf extracts could prevent platelet lysis, due to the presence of functional phytochemicals [56]. Some studies reported that papaya leaf extracts increase the arachidonate 12-lipoxygenase, 12S type activity, and platelet-activating factor receptor significantly in the body which consequently increases the platelet production in the patients administered with papaya leaf extract. The flavonoids present in this extract have also been found efficient in suppressing a protease found in viral assembly [57]. Further, Sharma et al. reported that papaya leaf extract was able to significantly increase the platelet count in thrombocytopenic rats. The authors also confirmed *in vitro* antiviral activity of papaya leaf extract using dengue-infected THP-1 cells (human leukemia monocytic cell line), and the possible mechanism noted was reduction in both envelop protein and NS1 protein expression. Further in thrombocytopenic rats treated with papaya leaf extract, decreased erythrocyte damage was observed along with increase in IFN- α expression and thrombopoietin levels indicating its potential to be used as therapeutic that can help in improving the platelet count and exhibit antiviral agent against dengue fever [58].

3.3. Anticancer Activity. Cancer is a huge group of diseases which can affect any organ of the human body with abnormal body cell growth. Cancer is also commonly known by the name of malignant tumour, and the cells affected by this disease have a tendency to spread from the originating organ to others very rapidly. Nowadays, cancer is one of the major

causes of death worldwide, with 9.6 million estimated deaths due to this lethal disease in a year [67]. Prostate, lung, colorectal, liver, and stomach cancers are commonly found in males, while breast, colorectal, thyroid, lung, and cervical cancers are the most reported in females [68]. The burden of this disease is continuously growing in the world, exerting tremendous emotional and financial strain on patients, their families and health systems, especially in low- and middle-income countries. Alternative therapy includes different plant extracts and their bioactive ingredients responsible for tremendous health improvement, including the prevention and treatment of cancer in many countries [69].

In one of the patents filed, it was declared that proliferation of cancer cells reduced while health improvement was noted when people having cancer (lung, stomach, colon, pancreatic, liver, neuroblastoma, ovarian, breast, solid, and blood cancer) were treated with brewed extract of papaya leaf or fractioned components [70]. Researchers also found ethanolic papaya leaf extracts with high levels of saponins more beneficial in suppressing cancer cell lines than aqueous extracts [71]. However, although there are significant sources denoting the anticancerous effects of papaya leaves, only a few studies have identified their exact effect on cancerous cells and mechanism of action [72].

Medicinal value of herbs is dependent on the chemical constituents present in them which are known for their positive pharmacological and physiological activities inside human system. Research studies on papaya has clearly denoted that the whole plant has great number of secondary metabolites [73] and are directly linked with the potent anticancerous activities inside human body [74, 75]. Recent studies were conducted to evaluate the effect of capsules of papaya on cancer-affected patients split in different age groups (pediatric: 3-8 years and adult: 18-72), including

TABLE 2: Medicinal potential of *Carica papaya* L. leaf extract against virus-induced thrombocytopenia.

Treatment	Results	References
Mature <i>C. papaya</i> leaf concentrate (0.72 mL/100 g bw of adult Wistar rats) administered for 3 days	(i) Increase in platelet count without toxicity in rats (ii) Increase in platelets by 76.50%, WBC by 30.51%, and RBCs by 9.08%	[57]
Fresh <i>C. papaya</i> leaf extract (0.2 mL (2 g)/mouse) for twenty-one days	(i) Increment in the platelet and the RBC count. (ii) The platelet count reached almost a fourfold higher at day 21 ($11.3 \times 10^5/\mu\text{L}$) and RBC count in the test group increased from $6 \times 10^6/\mu\text{L}$ to $9 \times 10^6/\mu\text{L}$ at the end of treatment.	[7]
<i>C. papaya</i> extract (150 mL) daily to dengue patient for five days	(i) Increase in no. of in thrombocytes ($28 \cdot 103/\text{mL}$ to $138 \cdot 103/\text{mL}$) and white blood cells BC ($3000/\text{mL} \cdot 7800/\text{mL}$) in a dengue adult patient (i) Increment in platelet count (ii) Third day onwards platelet count showed significantly positive results in the study group (82.96 ± 16.72) than control (66.45 ± 17.36). This trend of significant difference was the same on the fourth and fifth day of their studies.	[52]
Administration of 500 mg papaya leaf extract capsules on daily basis along with supportive medical treatment for five days to patients	(iii) Average platelet transfusion requirement in the study group was significantly less than the control group (0.685 units per patient vs. 1.19 units per patient)	[59]
Carpaine extracted from <i>C. papaya</i> leaf (2 mg/kg BW of thrombocytopenic Wistar rats) for twenty days	(i) Isolated carpaine from <i>C. papaya</i> leaf extract exhibited potent activity in sustaining normal platelet counts without acute toxicity.	[60]
Aqueous extract of <i>C. papaya</i> leaves (one spoonful of leaf paste) extract on dengue-infected children for two days	(i) Increase in number of a platelet count of dengue-infected children of age 10 and 14 (ii) After one-day administration, platelet count was 100,000 and within 2 days count reached up to 250,000	[61]
Aqueous extract of <i>C. papaya</i> leaves (25 mL) twice a day for two days	(i) Significant increase in the platelet an white blood cell count after 2 days of treatment	[62]
Standardized <i>C. papaya</i> leaf aqueous extract (50 and 150 mg/kg BW of Wistar rats) for two weeks	(ii) Oral administration showed a significant increase in thrombocytes ($1014.83 \text{ cells}/\text{mm}^3$), DTH response (0.16), and phagocytic index (63.15% increase)	[63]
<i>C. papaya</i> leaf extract capsules (290 mg) dose daily twice in thrombocytes postchemotherapy cancer patients for five days	(i) After 5 days, the mean increase in platelet counts from $101.93 \times 10^3/\mu\text{L}$ to $173.75 \times 10^3/\mu\text{L}$	[64]
Administration of papaya leaf extract (1.1 g) to total five hundred patients suffering from thrombocytopenia three times daily for five days	(i) A significant increase in counts of platelets were noticed in the study group.	[65]
Treatment of infected mice with 1000 mg/kg bw of FCPLJ (freeze-dried <i>C. papaya</i> L. leaf juice content) for four days	Increase in the number of total white blood cell and neutrophil counts by 1.44-fold.	[66]

males and females aged, with different body weights and ethnic backgrounds. They noticed a significant decrease in cancerous growth of the patients treated with papaya leaf extract of 0.16 g/kg body weight compared to control. Their findings suggested that papaya leaf extract has a great effect as anticancerous therapy for prevention and cure of prostate cancer due to presence of the phytochemicals (amino acids, flavonoids, alkaloids, and phenolics). However, the authors suggested that thorough research and understanding, the mechanism of action as anticancer agent is required before promoting use of papaya leaf extract as adjuvant treatment of cancer [37]. There are *in vitro* studies which clearly indicated a significant positive effect of this herbal extract on various tumour cell lines. However, still, further research needs to be conducted to provide concrete evidence and mechanism of

action of papaya leaf extract as anticancer agent. Table 3 summarizes the results of studies conducted by various researchers to find out the medicinal potential of papaya against different kind of cancer cells.

Papaya leaf extract (PLE) has ability to interact with a huge range of molecular targets and exerts disease preventive activities. The major molecular targets included in the anticancer prevention are inhibition of the activity of DNA topoisomerase I/II and change of signaling pathways. Previous studies suggested that anticancerous properties of papaya leaves might be due to two reasons, i.e., caspase-3/7 process activation and activation of p53-dependent mitochondrial pathway [36]. However, some researchers also revealed that PLE seizes the PCa cell in S phase of cell division, which leads to the cell death, thus responsible for anticancerous activity [79]. Molecular signaling pathways

TABLE 3: Medicinal potential of *Carica papaya* L. leaf extract against virus-induced thrombocytopenia.

Treatment	Effect on cancerous cells	References
Aqueous isolate of <i>C. papaya</i> leaves (1.25–27 mg/mL)	(i) Exhibited an effective anticancer property on cancer cell lines (stomach cancer cell line (AGS), pancreatic cancer cell line (Capan-1), colon cancer cell line (DLD-1), ovarian cancer cell line (Dov-13), lymphoma cell line (karpas), breast cancer cell line (MCF-7) (ii) Suppressed DNA synthesis by inhibiting the incorporation of 3H-thymidine	[70]
Aqueous extract of <i>C. papaya</i> leaves (0.625–20 mg/mL)	(i) Inhibition of proliferative responses of haematopoietic cell lines and solid tumour cell lines (ii) Increase in the expression of immune modulatory genes	[36]
Brewed leaf juice (20 mg/mL)	(i) Effective antiproliferative activity against cancerous cells of the prostate (ii) Suppression of SCC25 cells growth in a dose-dependent manner (iii) Survivability of 20% SCC25 cells, and 70% cancer-free human keratinocyte HaCaT cells remained viable with a dose of 20 mg/mL	[37]
Aqueous <i>C. papaya</i> leaf extract (659.63 µg/mL)	(i) Antiproliferative and apoptotic induced effect of papaya leaf inhibits the proliferation of human breast cancer cell (ii) Leaf extract exhibited apoptosis of MCF-7 cell line (22.54%)	[76]
Papaya leaf juice and its various extracts (0.25–0.1 mg/mL)	(i) Effective antiproliferative activity against cancerous cells of the prostate (ii) Potent growth inhibitory and cytotoxic activities on all prostate cells except the normal (RWPE-1 and WPMY-1) cells (iii) Medium polar fraction inhibited migration and adhesion of metastatic PC-3 cells	[77]
<i>C. papaya</i> leaf juice (0.01–1 mg/mL) in prostate epithelial cancer cells, benign tumor, and human prostate cancer cells	(i) Decrease the cancer cell proliferation (ii) Arrest the S phase cell cycle (iii) Induced apoptosis in prostate cancer cells	[7]
Silver nanoparticles (AgNPs) with papaya leaf extract (0.5, 1, 2.5, and 5 µg/mL) at 24 h and 48 h on human prostate carcinoma DU145 cells.	Reduction in cell proliferation and subsequent apoptosis of human prostate carcinoma DU145 cells.	[78]

and their cross-talk plays an important role in imparting the anticancerous activity such as repression of DNA topoisomerase I/II activities, lower gene expression of Bcl-2, CDK 4, cyclin D1, and B1, PCNA and higher expression of genes like Bax, Bak, cleaved caspase 3, and P53 [36, 37]. Anticancer activity of papaya leaf extracts and possible mechanism of action is shown in Figure 3.

Papaya leaf extract's immune modulatory potential is responsible for increasing the concentration of nitric oxide, CD80, TNF-alpha, and various other interleukins (IL-12p70, IL-12p40) and induction of apoptosis in cancer cells [37, 69]. However, papaya leaf extract at concentrations of 5 µg/mL on the release of cytokines exhibited percent inhibition of TNF- α (10.8%), IL-1 α (12.5%), IL-1 β (27.4%), IL-6 (42.9%), and IL-8 (8.4%) reported in some studies [80]. Possible mechanism of papaya leaf extract to act as an anticancerous agent is to lower down metastatic cancer by decreasing the extracellular matrix concentration which further acts as a chemo-attractants of PC-3 cells for adhesion as well as migration [76]. Thus, the extract shows the potential to reduce the procreation of cancer cells and conquer the process of DNA synthesis [70]. It might be inferred a prominent correlation between secretion of Th1 type cytokines

and increased cancer cell toxicity, which may result in the antitumour activity of papaya leaf extracts [36].

3.4. Immunomodulatory Effects. Other studies showed the immunomodulatory potential of papaya leaf extract and the cytokine ELISA profile of PBMC and revealed that papaya leaf extract downregulates IL-4 and IL-2 excretion in supernatants of cultures in a dose-reliant manner and presumed that leaf extract of papaya may bring apoptosis in PBMC, like similar effect on cancerous cells [36]. However, secretion of Th1 type cytokines like IL-12p70, IL-12p40, TNF- α , or IFN- γ applicable to anticancer immunity was interestingly upregulated even at low concentrations of leaf extract, with minor effect on IL-15, IL-6, IL-5, and IL-10 production [37]. Th1 (IFN- γ + CD4+) vs. Th2 (IL-4+ CD4+) T cells are important mediators of inflammatory reactions, and they may be influenced by regulatory T cells [81]. Flow cytometry was used by Abdullah et al. (2011) to investigate the effects of *C. papaya* on cells from healthy people. Significant downregulation of IFN- γ + CD4+ T cells, upregulation of IL-4+ CD4+ T cells, and upregulation of CD3+ CD4+ CD25+ CD127- T cells were observed after papaya consumption. Regulatory T cells were upregulated

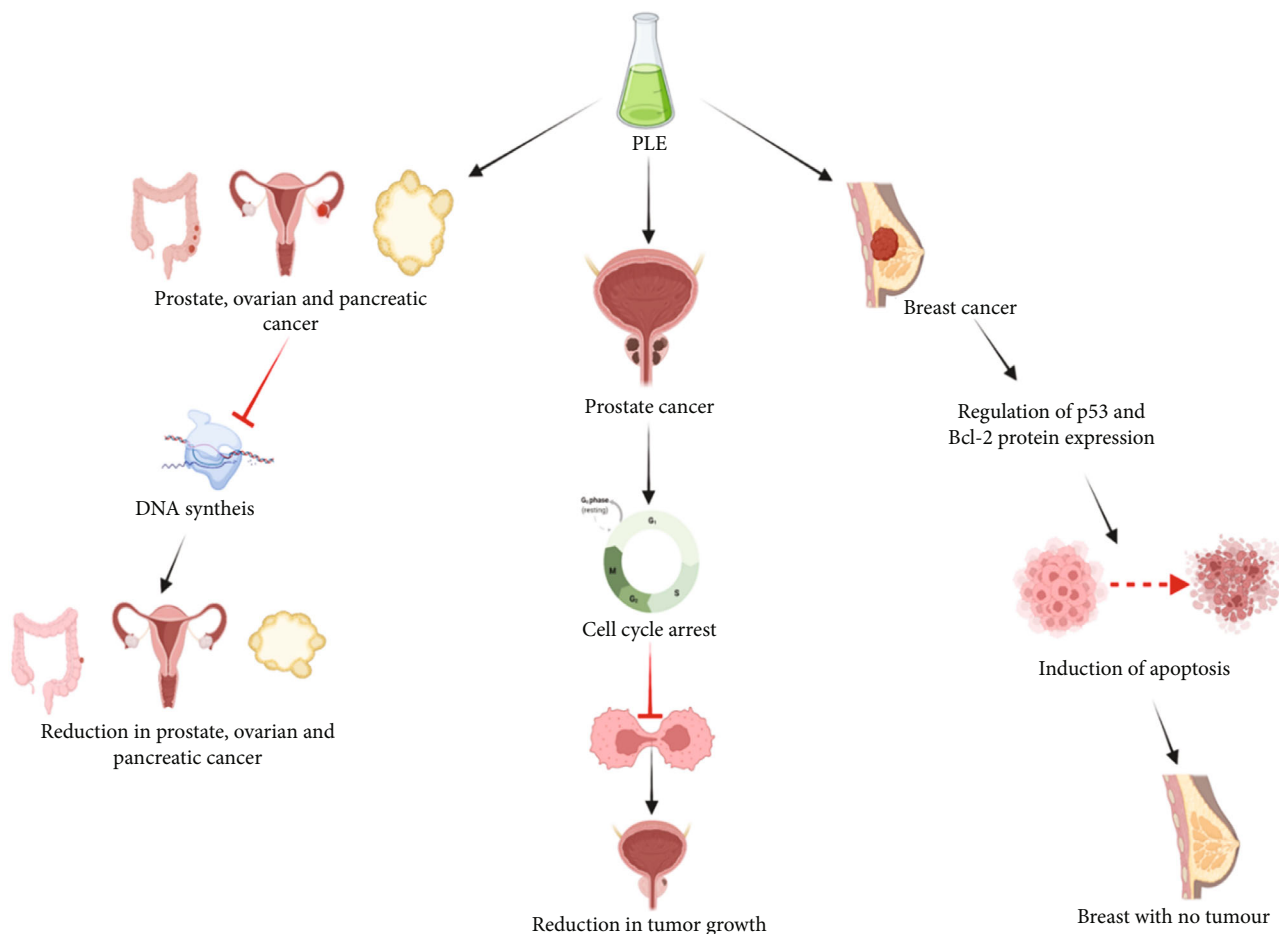


FIGURE 3: Anticancer activities of papaya leaf extract.

in male participants' *in vitro* cultures, and this was significantly associated with levels of IL-1 in culture supernatants [82]. There is a possibility that leaf extract of papaya may promote the control of Th2-mediated allergic ailment, or as an adjuvant of various vaccines by promoting an alteration from Th2 to Th1 type immune response [6]. The methanol (MeOH) extracts of *C. papaya* and on mice for 3 weeks were able to decrease the level of proinflammatory cytokine, and it was also found that use of standardized CPL aqueous extract (SCPLE) was significantly increasing the thrombocytes and phagocytic index in thrombocytopenic rats [80]. These findings help the researchers to screen out the anticancerous effects of papaya leaves on cancer cells *in vivo* studies. Studies conducted by various researchers with regard to immunomodulatory potential of papaya leaf extracts are summarized in Table 4.

3.5. Hypoglycemic and Antidiabetic Effects. Diabetes mellitus is a worldwide known disease caused by the failure of the pancreas to generate insulin or dysfunction of the human system to use insulin properly and has been emerging very rapidly worldwide. The increasing number of diabetes associated with the rough toxic effects of allopathic medicine has gained the attention of researchers to find out alternatives

with minor or no side effects [83]. This is a serious long-term condition which has been considered one of the major reasons of deaths in adult group globally, with four million estimated deaths in recent years [81, 84]. The term diabetes mellitus itself shows many diseases of abnormal carbohydrate metabolism which is associated to hyperglycaemia. It is connected to impairment in the insulin secretion along with varying degrees of resistance against insulin action. Diabetes also increases the risk of other diseases and disorders such as obesity, ageing, heredity, and genetic mutilation of beta-cell function/insulin receptor. Many plants are known for their effective antidiabetic, phytochemicals in conventional and today's medicine as well [84, 85]. Even various literature reports have shown the positive effects of different plant parts for treating this disease [86].

The decreasing trend in the blood glucose level of the treated animals with the consumption of plant part extracts has revealed in many studies that the extract of plant portions possesses potent antidiabetic effects and can be utilized for its cure. Among different plant parts, papaya leaves have been used in traditional Ayurveda medicines for diabetes [84].

Preclinical studies available in literature shows the antidiabetic effect of papaya leaves on diabetic rats, but no investigation has been undertaken as a clinical trial on human beings to

TABLE 4: Immunomodulatory potential of papaya leaf extract.

Treatment	Results	References
Oral administration of SCPLE (150 mg/kg) in thrombocytopenic rats	Significant ($p < 0.01$) increase in thrombocytes (1014.83×10^3 cells/mm ³), DTH response (0.16 ± 0.004), and phagocytic index	[63]
Administration of <i>C. papaya</i> and methanol (MeOH) extracts on mice for 3 weeks.	Proinflammatory cytokines (IL-10, IL-12, IL-1 β , IL-6, and TGF- β 1) were decreased.	[80]
Aqueous-extracted CP leaf fraction on the growth of various tumor cell lines	Production of IL-2 and IL-4 was reduced. IL12p40, IL-12p70, IFN-, and TNF- were enhanced without growth inhibition	[36]

TABLE 5: *In vivo* studies on the medicinal potential of *Carica papaya* L. leaf extract against diabetes.

Treatment	Results	References
The ethanolic aqueous extract of <i>C. papaya</i> (100 mg/kg) with water given to streptozotocin-induced diabetics for five days.	(i) Reduced glucose levels in the blood at the end of the fifth day of treatment. (ii) A great regeneration of the tissues of the liver. (iii) The tissues of kidney indicated a great recovery in the cuboidal tissue	[89]
The aqueous extract of <i>C. papaya</i> (0.75 g and 1.5 g/100 mL) for one month	(i) Delay in attaining the maximum plasma concentrations of amiodarone, extract and amiodarone increased the drug bioavailability (ii) Significant elevation in serum glucose levels (434.0 mg/dL) in comparison to the untreated rats (iii) Significant decrease in blood glucose levels up to 306.00 10.2 mg/dL	[90]
Aqueous extract of <i>C. papaya</i> leaf extract (400 mg/kg BW of diabetic albino rats) for twenty-one days	(i) Significant reduction in blood glucose level and serum lipid profile levels due to antihyperglycemic and hypolipidemic properties. (ii) Leaf extract showed 38.19 per cent reduction in the blood glucose level after completion of treatment	[91]
Ethanolic extract of <i>C. papaya</i> leaves (250-500 mg/kg BW of alloxan-induced diabetic rats) for twenty-one days	(i) Significant reduction in glucose level (123.50 mg/dL), total cholesterol, triglyceride (1.24 mg/dL), and serum urea (12.35 mg/dL). (ii) Significant increase in HDL cholesterol and total protein level (66.51 g/dL). (iii) Significant decrease in LDL cholesterol, creatinine, alanine aminotransferase and aspartate aminotransferase.	[92]
Ethanolic leaf extracts of <i>C. papaya</i> , i.e., 50, 150 and 300 mg/kg BW of diabetes-induced mice.	(i) Good effects on plasma insulin, cholesterol, triglyceride, and HDL cholesterol levels (ii) Hypoglycemic effect in diabetic rats after taking various doses of <i>C. papaya</i> extract	[87]
Aqueous extract of <i>C. papaya</i> leaf (120 mg/kg BW of albino rats) for eighteen days	(i) Significantly reduced glucose level from 275.00 to 85 mg/dL, total cholesterol from 117.70 to 98.50 mg/dL, total glycerides from 107.10 to 97.21 mg/dL, and LDL from 49.44 to 44.01 mg/dL	[93]
The administration at a dose of 1000 mg/kg body weight of papaya leaf ethanol extract in diabetic Wistar mice.	Reduce blood glucose levels in diabetic Wistar mice	[94]

examine the antidiabetic effect of this herbal leaf extracts till date. Researchers suggest that papaya leaves could be alternative medicine in the treatment of diabetes as it has no side effects. The presence of significant number of phytochemicals of this leaf extract has a great effect in reducing other secondary complications raised by diabetes [87]. First preclinical study on therapeutic effects of papaya on diabetic Wistar rats was conducted in 2007. Papaya ethanolic leaf extract (5.0 mg/kg BW of male Wistar rats) for twenty-four hours

was administered during the studies. A significant reduction in blood glucose of diabetic rats from 12.75 to 1.23 mmol/L within 24 hours of oral administration was observed by the researchers [88]. Studies conducted by various researchers are summarized in Table 5 and possible mechanism of papaya leaf extract as antidiabetic agent is shown in Figure 4.

Some studies suggested that the mechanism of action of aqueous papaya leaf extract consists in stimulating the beta cells with a higher pancreatic release of insulin, thus

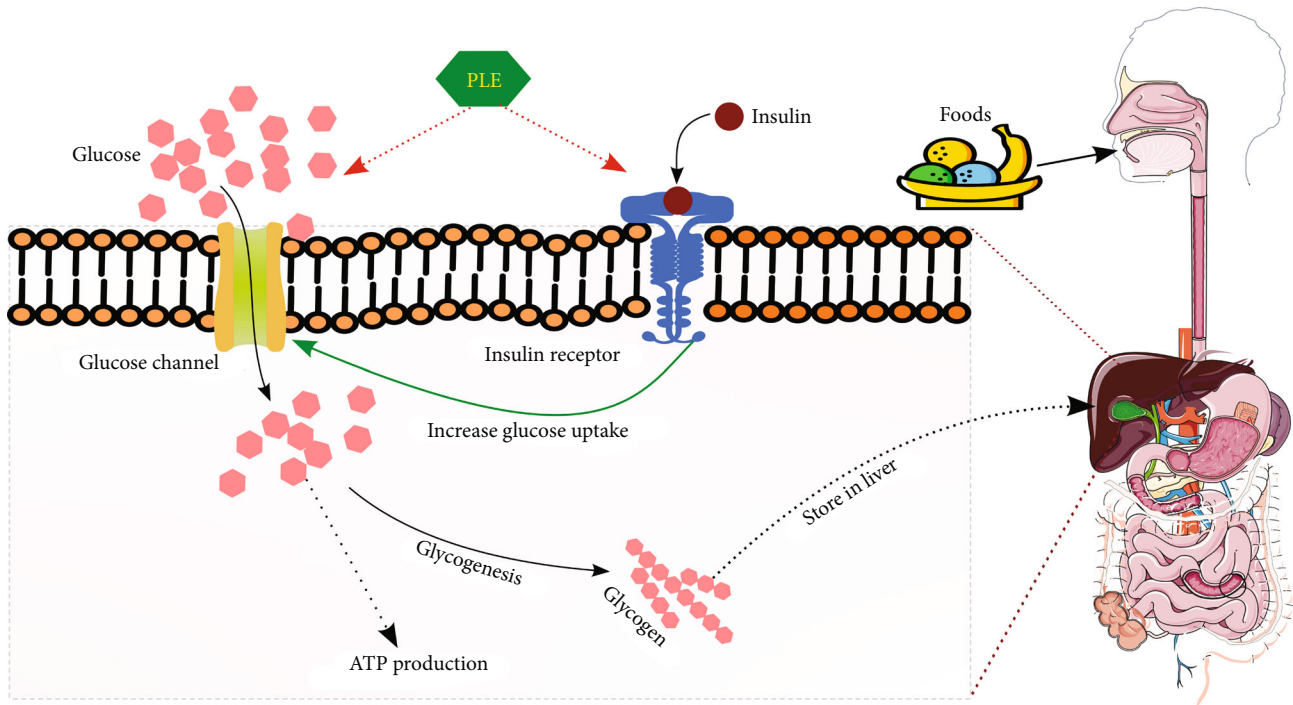


FIGURE 4: Antidiabetic activities of *Carica papaya* extract (CPE).

increasing peripheral glucose uptake or islets of Langerhans. Furthermore, reduced glycemic effect of papaya leaf extract is due to hampering of synthesis of fatty acids and cholesterologenesis decrease and due to an increasing amount of the latter parameters further increases the risk of overweight and diabetes. Different reports have shown that in diabetes, the islets appear to be preferentially affected by the destruction of insulin-secreting β -cells [95]. The mechanism triggered by papaya leaves consist in diminishing the lipid and carbohydrate hydrolyzing enzyme activity in the small intestines, which reduces disaccharides and triglycerides conversion into simpler easily absorbable monosaccharide and free fatty acids [96]. With the current available preclinical inputs, it is necessary to conduct more systematic, thorough cell line or animal model studies to prove the beneficial effect of papaya leaf extracts as hypoglycemic agent and before its implication as antidiabetic component.

3.6. Other Bifunctionalities of Papaya Leaves. No medical way has been proven to stop the death of brain cells in Alzheimer disease, though a few treatments only can help with both behavioural and cognitive symptoms. Aluminum leads to mitochondrial dysfunction with the generation of excessive free radicals and eventual damage in genetic material, peroxidation of lipids, and nitration of protein residues. Papaya leaf extract has shown a significant neuroprotective effect against aluminum-induced cognitive impairment and associated oxidative damage in an animal model [97]. Taking into account the presence of various alkaloids like carpaine, pseudocarpaine, dehydro-carpaine, and phenolic compounds, papaya leaves have been used as antispasmodic, analgesic, and antibacterial. Moreover, the boiled papaya

leaves along with some other plant parts such as stem bark and leaves of few medicinal plants were recommended for the treatment of arthritis and rheumatism like inflammation as well as for wound healing too [98]. Studies conducted by various researchers on neuroprotective, anti-inflammatory, and antibacterial effects is summarized in Table 6.

4. Papaya Leaf-Based Products

Though papaya leaves are a storehouse of many pharmaceutical properties, they have not been fully utilized up to date on a commercial scale for the production of different formulations. However, a few research studies have documented the development of leaf extract-based products of papaya for efficient utilization of its leaves.

4.1. Herbal Juice Beverages. For the preparation of aqueous extract of papaya leaves, the latter are needed to be collected excluding the sap and stalk for the extract preparation. Papaya leaf extract is prepared by chopping or crushing papaya leaves after proper washing, followed by water boiling in a saucepan allowing it to simmer till half-volume reduction and then by straining with a muslin cloth and filling in a glass container [103, 104]. Papaya leaf extract was made by putting papaya leaf powder in a Soxhlet extractor with ethanol and ethyl acetate (95%) for seventy-two hours, and after extraction, the leaf extract was filtered and concentrated through a rotary evaporator [105, 106]. Some researchers crushed the papaya leaves and completed the extraction in a round bottom glass flask at 80°C with water addition at three different times [105]. All the latter washings were blended and distilled under vacuum. The obtained syrup was dehydrated in a vacuum oven to obtain

TABLE 6: Medicinal potential of *Carica papaya* L. leaf extract as neuroprotective, anti-inflammatory, and antibacterial herbal medicine.

Treatment	Results	References
Ethanol extract of <i>C. papaya</i> leaves (25–200 mg/kg), carrageenan-induced paw oedema, cotton pellet granuloma, and formaldehyde-induced arthritis rats for ten days	(i) Reduction in inflammation and in carrageenan-induced paw edema, granuloma (cotton pellet induced) in arthritic mice (ii) Significant decrease in the amount of granuloma from 0.58 to 0.22 g	[99]
Aqueous <i>C. papaya</i> extract (0.625–2.5 mg/mL) in infected human beings	(i) Increment in protein content and also increased production of antibodies against ovalbumin (ii) Exhibited anti-inflammatory and antimicrobial activities at higher doses (iii) Leaf extract exhibited a decrease in gram-positive and gram-negative bacterial count and proliferation rate.	[100]
Alcoholic <i>C. papaya</i> leaf extract 200–400 mg/kg BW of male Wistar rats for forty-two days	(i) Neuroprotective effect of <i>C. papaya</i> leaves on an animal model (ii) Denoted a significant elevation in the level of acetylcholine, SOD, glutathione, and catalase and great reduction in total proteins	[101]
Methanol and aqueous extracts of <i>C. papaya</i> leaves (25 mg/mL–100 mg/mL).	Inhibits the growth of <i>Staphylococcus aureus</i> , <i>Escherichia coli</i> , and <i>Candida albicans</i>	[19, 102]

approximately papaya leaf extract. The juice was extracted by the cold juicing method, which has been reported to release bioactive components with more cytotoxic effects in comparison to other aqueous and ethanol isolates. In particular, leaves were washed with mineral water before slicing, and a grinder was used to extract papaya leaf juice. Approximately one kilogram of papaya leaves was blended in mineral water of 250 mL volume in the ratio of 1:0.25, and further, the juice was separated from papaya leaf waste through filtering to obtain a clear extract [72, 77].

The bitter taste of leaf extract makes its processed products undesirable for the consumers. A few studies reported the preparation of leaf extract and its blending with fruit pulps for achieving different processed products like jam and beverages, as an alternative for exploiting the leaf extract nutraceutical properties. Previous research revealed that the supplementation of a ready-to-serve beverage based on papaya leaf juice incorporated in guava for the treatment of dengue fever is very safe, as it also induced fast increment in the platelets count and improved immunity in its consumers.

Ready-to-serve beverages were prepared by blending papaya leaf and guava juice aiming to get early recovery of viral disease [10]. Several beverages produced by mixing papaya leaf juice in the banana pulp, pineapple, sweet orange, and pomegranate juice with the addition of papaya leaf extract were prepared to raise the nutritional composition of all the beverages [103]. Standardized formulation for preparation of mango-papaya leaf extract mixture-based nectar has been reported. Prior to beverage preparation, the aforementioned researchers extracted the juice by two hot pressing method, by heating the crushed papaya leaves for 10 minutes, and next passing them through the screw type juice extractor to extract the juice. Further, the leaf extract with 20% water was blended with mango pulp in the ratio of 70:30, so as to prepare the final good-flavoured nectar [98].

4.2. Herbal Green Tea. Papaya leaves are currently being used for the preparation of green tea in very few countries, thanks to their potent medicinal properties [10, 106]. Enzymes present in papaya leaf green tea have powerful anticancer activities against different types of tumors [36]. For drying, fresh leaves are washed and kept at ambient temperature for at least two hours, and then, they are cut into small pieces and weighed. For the complete removal of free moisture, fresh leaves are placed in mechanical cabinet dehydrator at a temperature of 60°C for few hours, followed by oven drying at 110°C just for a few minutes. After drying, leaves are crushed and packed in bags to store them in a cool and dry place [107].

4.3. Herbal Juice Powder and Capsules. Processing plant juices into powder form is a new method to increase the shelf life of the product at room temperature as well as for easy transportation of the reduced volume commodity. Spray drying is a technique applied in the processing industry to obtain fruit juice powder efficiently under controlled conditions. In order to keep these points in mind, researchers have performed spray drying of papaya leaf extract with a certain carrier material to preserve its internal constituents. Before spray drying, the papaya leaf juice is filtered twice to avoid blocking of the spray dryer atomizer. Maltodextrin at a concentration of 8.0–10% w/v as a carrier material is used to lower down the hygroscopicity of the prepared papaya leaf dried powder. After mixing with maltodextrin, the concentrated papaya leaf juice is conveyed into the spray drying machine with a feed flow rate of 350 mL/h and inside temperature of 130°C. Papaya leaf powder is stored under normal room temperature conditions [108].

Freeze-drying or lyophilization is another drying technique for the preparation of good quality juice powders. It is a preferred method for drying of food having compounds

that are heat sensitive and vulnerable to oxidation, taking into account that it operates at low temperatures under vacuum [109]. The ice sublimation during freeze-drying protects the main structure and the dried product shape, with minimal volume reduction, higher nutrient, and phytochemical retention due to low temperature. This technique has been successfully applied to diverse biological materials, and in this respect, researchers performed freeze-drying of the papaya leaves after proper cleaning with a veggie wash to scavenge unwanted soil and wax [110]. Further, they washed with reverse osmosis or mineral water prior to juice extraction in a juicer without water addition. After juice extraction, the residual husk was pressed with a clean cloth. The extracted juice was poured in a presterilized glass container and frozen at a temperature of -50°C prior to lyophilization in the dryer, so as to obtain the freeze-dried powdered form of papaya leaf juice with its maximum bioactive components. The obtained powder can be either stored in vials or encapsulated into capsule form for further applications [59]. Researchers dried papaya leaves before isolating them in a conical glass flask at 80°C three times with triple volume of mineral-free water. They collected all the obtained washings and distilled them under a vacuum of 20-30 TDS. The crude form of the obtained extract coming from the syrup dried in a vacuum oven can be used to form capsules [60].

4.4. Papaya Leaf-Based Silver Nanoparticles (AgNPs) as Health-Promoting Ingredient. Nanoparticles are an efficient mode for delivering drug nowadays, though the methods used for their synthesis are energy demanding and need harmful chemicals. Recently, researchers have been focusing on environmentally friendly methods of nanoparticles synthesis. The use of plant parts with valuable medicinal properties, appropriate microorganisms, and enzymes has been found effective as alternatives to antibiotics [111, 112]. Nanoparticle biosynthesis has been done by using strains of microbes, proteins, and other metabolites, plant extracts, and biodegradable products. Green synthesis of nanoparticles by utilizing *C. papaya* leaf extract has shown potent antimicrobial attributes. *C. papaya* silver nanoparticles biosynthesis is performed by adding a silver nitrate solution into *C. papaya* leaf extract, with the silver ions getting reduced due to chemical reaction between aqueous extract of leaf extract and silver nitrate solution. The *C. papaya* leaf silver nanomaterial, 5 to 200 nm sized, tends to penetrate into microbial cells and exhibit bacterial cell lysis. Due to antimicrobial effect of the *C. papaya* leaves, silver nanoparticles become more efficient with this extract, exhibit a great bactericidal efficiency, and could act as an alternative to antibiotic resistance [111]. More details on the synthesis of AgNPs from *C. papaya* leaves are discussed in Table 7.

5. Safety Assessment of Papaya Leaves

Various scientific studies revealed a great and selective growth inhibitory effect of different plant parts, whose beneficial components may work through different pathways to generate good biological responses. On the contrary,

undesired components or even high concentrations of beneficial components in the same parts can generate toxic or side effects, and to minimize the latter effects, the fractionation and standardization of their doses are needed. Papaya leaves have been utilized for the treatment of viral fevers, various cancers, etc., but despite their great uses, literature research reports regarding their detailed toxicity are not available yet up to date.

Studies on the acute toxic effect of papaya leaf extract at a concentration of 2.0 g/kg of the rat bodyweight have been conducted [28]. The latter authors found that the single oral dose of the papaya leaf extract did not turn out the reason of mortality without any significant transformations in the body weight and change in water and food consumption behavior; on the other hand, hemoglobin, red blood cells, and proteins were greatly raised. However, no deaths and no signs of toxicity were recorded during two weeks of investigation. Scientists performed a chemical analysis of *C. papaya* leaves and found that their extract had a significant amount of carpaine, manghaslin, organic acids, clitorin, nicotiflorin, rutin, and other minor chemical constituents [121]. These phytochemicals do not generate treatment-related change in body weight, food and water consumption habits, haematological parameters, and serum chemistry in treated rats after oral administration of the extract for one month. The dose of papaya leaf extracts up to 2000 mg/kg was considered relatively nontoxic during their studies. Similarly, studies to evaluate the subchronic toxicity effect of papaya leaf extract in rats with the administration of extract prepared from lyophilized leaves powder in clean water papaya leaf extract at concentrations of 0.00, 0.01, 0.14, and 2.00 g/kg weight of rats for almost three months were conducted [122]. Mortality, food, and water consumption behavior were recorded throughout the experimental duration. Their study revealed that leaf extract given for three months did not cause changes in the water and food intake behavior or the bodyweight of the treated rats and concluded that oral administration of papaya leaf extract for three months did not have any type of toxic effect in the rats [123].

In contradiction to the above-mentioned studies, some evaluated the effect of aqueous extract of papaya on rats and found that some concentrations were toxic in different ways [124]. The lethal concentration of the leaf extract with more than 5 g/kg body weight showed no signs of autonomic in acute studies. However, their results revealed that the aqueous extract of papaya had an adverse effect on liver and reproduction system in the rats. In the subacute study, rats were supplied with extract as much as 10-500 mg/kg of body weight for two weeks, and they found no effect on the formed elements of blood or haemoglobin, through an injury to the hepato-biliary system. In adult male rats, a significant reduction in sperm count, sperm viability, and testosterone was also observed, and in addition, female rats also showed fertility problems with increase of maternal mortality [125]. Therefore, it is essential to perform descriptive studies to identify and evaluate the leaf chemical constituents, their concentrations, and toxic side effects for further proper utilizations of papaya plant parts, in order to commercialize the relevant products for nutraceutical purposes.

TABLE 7: AgNPs synthesis using *C. Papaya* leaf with well-defined applications, characterization techniques, particle characteristics, and operating conditions.

Applications	Operating conditions	Characterization techniques used	Particle characteristics	Reference
(i) AgNPs exhibited inhibitory effect against both gram-positive and negative bacterial species	AgNO ₃ (1 mM); extract: AgNO ₃ (1 : 4), heated at 60°C for 5–10 min and incubated on sand bath for 30 min	UV-vis, FTIR, SEM-EDX, TEM, XRD	Size: 50–200 nm; shape: spherical	[112]
(i) Antibacterial activity against human pathogens such as <i>Bacillus subtilis</i> , <i>Enterococcus faecalis</i> , <i>Escherichia coli</i> , <i>Vibrio cholerae</i> , <i>Klebsiella pneumoniae</i> , and <i>Proteus mirabilis</i>	AgNO ₃ (2 mM); kept at 37°C in dark condition for 72 h	HR-TEM, UV-vis, FTIR, XRD	Size: 6–18 nm shape: face-centered cubic crystalline (fcc)	[113]
(ii) Cytotoxic effects against human breast carcinoma cell line (MCF 7)	AgNO ₃ (1 mM); aqueous leaf extract: AgNO ₃ (1 : 9); maintained at 27°C/24 h	FTIR, AFM, XRD	Size: 7–32 nm shape:	[114]
(i) NPs exhibited excellent antibacterial activity against <i>P. aeruginosa</i> and <i>E. coli</i> .	AgNO ₃ solution	UV-vis, FESEM, FTIR, EDX	Size: 13–69 nm shape: spherical	[115]
(ii) Exhibited binding activity against dengue type 2 virus NS1	AgNO ₃ (0.01 M); aqueous leaf extract: AgNO ₃ (1 : 4), heated on a sand bath at 70°C for 20 min	UV-vis, SEM	Size: 5 to 50 nm shape: spherical	[116]
(i) Showed antibacterial activity against <i>E. coli</i> and <i>B. Cereus</i>	1% silver nitrate (AgNO ₃); maintained at 40°C temperature for 24 h.	UV-Vis	Size: 250 nm shape: ND	[117]
(i) Showed inhibited inhibitory against both gram-positive and negative bacterial species	AgNO ₃ (1 mM); extract: AgNO ₃ (1 : 9); mixture was boiled at 45°C for 30 min	HE-TEM, XRD, FE-SEM, EDX	Size: 10 nm shape: spherical	[118]
(ii) Antimicrobial activity against <i>Pseudomonas aeruginosa</i> , <i>Escherichia coli</i> , <i>Bacillus subtilis</i> , and <i>Staphylococcus aureus</i>	AgNO ₃ (0.002 M); incubated for 24 h at 37°C	TEM, EDS, UV-vis	Size: 10–70 nm Shape: spherical	[119]
(i) Antioxidant	AgNO ₃ (1 mM)	UV-vis, FTIR, XRD, SEM, TEM	Size: 16 nm to 18 nm shape: spherical	[120]
(i) Blue CP and yellow 3RS dyes degradation	AgNO ₃ (1 mM); 200 µL extract: 10 mL AgNO ₃ ; solution was incubated in water bath at 50°C	TEM, STM, SEM, EDS, XRD, FTIR	Size: 10 to 20 nm shape: spherical	[7]
(ii) Antibacterial activity against gram negative (<i>E. coli</i>) and gram positive (<i>S. aureus</i>)	AgNO ₃ (1 mM); extract: AgNO ₃ (1 : 9); incubated for 24 h at 37°C	UV-vis, FTIR, SEM, EDX, DLS	Size: 80 nm shape: spherical	[111]
(i) Antibacterial activity against human pathogens (<i>Escherichia coli</i> and <i>Staphylococcus aureus</i>)	AgNO ₃ (1 mM); kept at 37°C for 3 hours	UV-vis, TEM, FTIR	Size: 13–17 nm shape: spherical	[121]
(i) Better efficacy against cancer cells and was also relatively less toxic to normal cells				
(i) Exhibited an excellent antibacterial activity against gram-positive and gram-negative pathogenic bacterial strains like (<i>Klebsiella pneumoniae</i> , <i>Staphylococcus aureus</i> , <i>Escherichia coli</i> , and <i>Yersinia enterocolitidis</i>)				

6. Conclusions

Research on papaya leaves has not yet received the attention it deserves throughout the world, despite the fact that the bioactive components found in the aforementioned plant parts should be harnessed for nutritional as well as therapeutic objectives. Indeed, papaya leaves have great potential to treat viral infections, to boost immunity along with antidiabetic, anticancer, anti-inflammatory, and many other disease preventive properties. More research studies are required to corroborate the main mechanisms of action shown by the phytochemicals present in papaya leaves as medicinal agents. In the latter respect, various studies found that papaya leaf extract resulted inhibitory effect on cancer cell growth and helped to reduce blood glucose levels. However, further descriptive clinical research is to be carried out to elucidate the functional properties of papaya plant parts on cancer cells and diabetic patients. The consumption of papaya leaves has been shown to have significant benefits in the recovery from viral illnesses like dengue fever. As new emerging viral infections have emerged as a major concern around the world, and as antiviral medications are currently unavailable to cure such diseases, the search for an alternative strategy for lethal corona virus-like diseases has become an urgent priority in recent years. Therefore, the evaluation of papaya leaf extract can be performed as preclinical trials or case-studies, in order to examine the actual effect of this extract and phytochemical responsible for preventing/curing other viral infections on human health.

It is necessary to do additional research in order to individually isolate phytochemicals, define their structure and medicinal properties, standardize the optimum doses, and investigate their toxicity. Because of their valuable phytochemical composition, papaya leaves have the potential to become a new functional food or nutraceutical for the future generations. However, only a few scientific studies have been conducted to date to formulate different papaya leaf-based products, and the commercial application of these products should be appropriately investigated. The leaves of this horticulture plant that is grown in underdeveloped nations have the potential to become a very attractive source of extremely nutritive and medicinal phytochemicals in the not-too distant future.

Conflicts of Interest

The authors declare no conflict of interest.

Authors' Contributions

A.S., R.S., M.K., M.A., R., M.M., and G.C. are responsible for conceptualization and supervision; A.S., M.S., M.K.S., S.S., D.K.M., S.D., M.N., P.P., M.H., S.S. (Surinder Singh), D.C., M.D.B., and J.M.L. for writing—original draft preparation; and M.S. (Marisennayya Senapathy), M.K., A.S., D.C., S.R., M. V., L.A.S., A.D., N.R., M.A., G.C., and M.M. for writing—review and editing. All authors have read and agreed to the published version of the manuscript.

Acknowledgments

The authors would like to thank the University of Kiel and Schleswig-Holstein for their support through the OA program.

References

- [1] Y. Zeng, M. K. Ali, J. Du et al., "Resistant starch in rice: its biosynthesis and mechanism of action against diabetes-related diseases," *Food Reviews International*, pp. 1–24, 2022.
- [2] C. Nandini, V. M. SubbaRao, V. R. Bovilla, A. K. Mohammad, N. S. Manjula, and K. Jayashree, "Platelet enhancement by *Carica papaya* L. leaf fractions in cyclophosphamide induced thrombocytopenic rats is due to elevated expression of CD110 receptor on megakaryocytes," *Journal of Ethnopharmacology*, vol. 275, article 114074, 2021.
- [3] G. Fuentes and J. M. Santamaría, "Papaya (*Carica papaya* L.): origin, domestication, and production," in *Genetics and Genomics of Papaya*, pp. 3–15, Springer, New York, NY, 2014.
- [4] J. Y. Yap, C. L. Hii, S. P. Ong, K. H. Lim, F. Abas, and K. Y. Pin, "Effects of drying on total polyphenols content and antioxidant properties of *Carica papaya* leaves," *Journal of the Science of Food and Agriculture*, vol. 100, no. 7, pp. 2932–2937, 2020.
- [5] F. Husin, H. Yaakob, S. N. A. Rashid, S. Shahar, and H. H. Soib, "Cytotoxicity study and antioxidant activity of crude extracts and SPE fractions from *Carica papaya* leaves," *Biocatalysis and Agricultural Biotechnology*, vol. 19, article 101130, 2019.
- [6] T. Vij and Y. Prashar, "A review on medicinal properties of *Carica papaya* Linn," *Asian Pacific Journal of Tropical Disease*, vol. 5, no. 1, pp. 1–6, 2015.
- [7] S. P. Singh, S. Kumar, S. V. Mathan et al., "Therapeutic application of *Carica papaya* leaf extract in the management of human diseases," *DARU Journal of Pharmaceutical Sciences*, vol. 28, no. 2, pp. 735–744, 2020.
- [8] S. L. C. A. Dharmarathna, S. Wickramasinghe, R. N. Waduge, R. P. V. J. Rajapakse, and S. A. M. Kularatne, "Does *Carica papaya* leaf-extract increase the platelet count? An experimental study in a murine model," *Asian Pacific Journal of Tropical Biomedicine*, vol. 3, no. 9, pp. 720–724, 2013.
- [9] N. O. A. Imaga, G. O. Gbenle, V. I. Okochi et al., "Antisickling property of *Carica papaya* leaf extract," *African Journal of Biochemistry Research*, vol. 3, pp. 102–106, 2006.
- [10] V. P. Krishna and T. Freeda, "Formulation, nutrient and microbial analysis of papaya leaves and guava incorporated RTS beverage," *International Journal of Current Microbiology and Applied Science*, vol. 3, no. 5, pp. 233–236, 2014.
- [11] C. Mantok, *Multiple usages of green papaya in healing at tao-garden*, Tao Garden Health spa & Resort, Thailand, 2015.
- [12] J. L. McLaughlin, "Paw paw and cancer: annonaceous acetogenins from discovery to commercial products," *Journal of Natural Products*, vol. 71, no. 7, pp. 1311–1321, 2008.
- [13] O. R. Alara, N. H. Abdurahman, and J. A. Alara, "*Carica papaya*: comprehensive overview of the nutritional values, phytochemicals and pharmacological activities," *Advances in Traditional Medicine*, vol. 22, pp. 17–47, 2022.

- [14] N. J. Ugo, A. R. Ade, and A. T. Joy, "Nutrient composition of *Carica papaya* leaves extracts," *Journal of Food Science and Nutrition Research*, vol. 2, no. 3, 2019.
- [15] P. Melariri, V. Campbell, P. Etusim, and P. Smith, "Antiplasmodial properties and bioassay-guided fractionation of ethyl acetate extracts from *Carica papaya* leaves," *Journal of Parasitology Research*, vol. 2011, Article ID 104954, 7 pages, 2011.
- [16] D. K. Sharma, B. Tiwari, R. K. Singh et al., "Estimation of minerals in *Carica papaya* leaf found in northern India by using ICP-OES technique," *International Journal of Scientific & Engineering Research*, vol. 4, no. 6, pp. 1012–1019, 2013.
- [17] N. Ahmad, H. Fazal, M. Ayaz, B. H. Abbasi, I. Mohammad, and L. Fazal, "Dengue fever treatment with *Carica papaya* leaves extract," *Pacific Journal of Tropical Biomedicine*, vol. 1, no. 33, p. 333, 2011.
- [18] E. Panzarini, M. Dwikat, S. Mariano, C. Vergallo, and L. Dini, "Administration dependent antioxidant effect of *Carica papaya* seeds water extract," *Evidence-based Complementary and Alternative Medicine*, vol. 2014, Article ID 281508, 13 pages, 2014.
- [19] A. Sharma, A. Bachheti, P. Sharma, R. K. Bachheti, and A. Husen, "Phytochemistry, pharmacological activities, nano-particle fabrication, commercial products and waste utilization of *Carica papaya* L.: a comprehensive review," *Current Research in Biotechnology*, vol. 2, pp. 145–160, 2020.
- [20] B. Callixte, N. J. Baptiste, and H. Arwati, "Phytochemical screening and antimicrobial activities of methanolic and aqueous leaf extracts of *Carica papaya* grown in Rwanda," *Molecular and Cellular Biomedical Sciences*, vol. 4, no. 1, pp. 39–44, 2020.
- [21] M. Adetayo, O. S. Adetayo, and A. Oyelese, "In-vitro antisickling and sickling-reversal activities of *Carica papaya* fruit at different stages of ripening," *Babcock University Medical Journal*, vol. 3, no. 2, pp. 10–18, 2020.
- [22] G. Gautam, B. Parveen, M. U. Khan et al., "A systematic review on nephron protective AYUSH drugs as constituents of NEERI-KFT (A traditional Indian polyherbal formulation) for the management of chronic kidney disease," *Saudi Journal of Biological Sciences*, vol. 28, no. 11, pp. 6441–6453, 2021.
- [23] S. A. Abdel-Halim, M. T. Ibrahim, M. M. Mohsen et al., "Phytochemical and biological investigation of *Carica papaya* Linn. leaves cultivated in Egypt (family Caricaceae)," *Journal of Pharmacognosy and Phytochemistry*, vol. 9, no. 5, pp. 47–54, 2020.
- [24] R. Agada, W. A. Usman, S. Shehu, and D. Thagariki, "In vitro and in vivo inhibitory effects of *Carica papaya* seed on α -amylase and α -glucosidase enzymes," *Heliyon*, vol. 6, no. 3, article e03618, 2020.
- [25] H. H. Soib, H. F. Ismail, F. Husin, M. H. Abu Bakar, H. Yaakob, and M. R. Sarmidi, "Bioassay-guided different extraction techniques of *Carica papaya* (Linn.) leaves on in vitro wound-healing activities," *Molecules*, vol. 25, no. 3, p. 517, 2020.
- [26] L. Tan, M. E. Norhaizan, W. P. P. Liew, and R. H. Sulaiman, "Antioxidant and oxidative stress: a mutual interplay in age-related diseases," *Frontiers in Pharmacology*, vol. 9, p. 1162, 2018.
- [27] P. Palanisamy and K. M. Basalingappa, "Phytochemical analysis and antioxidant properties of leaf extracts of *Carica papaya*," *Phytochemical Analysis*, vol. 13, no. 11, pp. 58–62, 2020.
- [28] R. Indran, V. Tufo, S. Pervaiz, and C. Brenner, "Recent advances in apoptosis, mitochondria and drug resistance in cancer cells," *Biochimica et Biophysica Acta- Bioenergetics*, vol. 1807, no. 6, pp. 735–745, 2011.
- [29] S. Z. Halim, N. R. Abdullah, A. Afzan, B. A. Rashid, I. Jantan, and Z. Ismail, "Acute toxicity study of leaf extract in Sprague Dawley rats," *Journal of Medicinal Plants Research*, vol. 5, no. 10, pp. 1867–1872, 2011.
- [30] T. Marie-Solange, A. A. Emma, and Z. G. Noël, "Ethnobotanical study of plants used to treat hypertension in traditional medicine by Abbey and Krobou populations of Agboville," *European Journal of Scientific Research*, vol. 35, pp. 85–98, 2009.
- [31] P. R. Dash and K. M. Mou, *Comprehensive Review on Five Medicinal Plants of Bangladesh. Chemical Constituents and Uses*, Anchor Academic Publishing, 2017.
- [32] P. L. Saran and V. Choudhary, "Drug bioavailability and traditional medicaments of commercially available papaya: a review," *African Journal of Agricultural Research*, vol. 8, no. 25, pp. 3216–3223, 2013.
- [33] O. Eleazu and K. C. Eleazu, "Physico-chemical properties and antioxidant potentials of 6 new varieties of ginger (*Zingiber officinale*)," *American Journal of Food Technology*, vol. 7, no. 4, pp. 214–221, 2012.
- [34] A. M. Maisarah, R. Asmah, and O. Fauziah, "Proximate analysis, antioxidant and anti-proliferative activities of different parts of *Carica papaya*," *Journal of Nutrition and Food Science*, vol. 5, no. 1, p. 267, 2014.
- [35] M. Parel and L. Gurditta, "Basketful benefits of papaya," *International Research Journal Pharmacognosy*, vol. 2, pp. 6–12, 2011.
- [36] N. Otsuki, N. H. Dang, E. N. Kumagai, A. Kondo, S. Iwata, and C. Morimoto, "Aqueous extract of *Carica papaya* leaves exhibits anti-tumor activity and immunomodulatory effects," *Journal of Ethnopharmacology*, vol. 127, no. 3, pp. 760–767, 2010.
- [37] T. T. Nguyen, P. N. Shaw, M. O. Parat, and A. K. Hewavitharana, "Anticancer activity of *Carica papaya*: a review," *Molecular Nutrition & Food Research*, vol. 57, no. 1, pp. 153–164, 2013.
- [38] Y. K. Ang, W. C. M. Sia, H. E. Khoo, and H. S. Yim, "Antioxidant potential of *Carica papaya* peel and seed," *Focusing on Modern Food Industry*, vol. 1, no. 1, pp. 11–16, 2012.
- [39] T. Kokila, P. S. Ramesh, and D. Geetha, "Biosynthesis of AgNPs using *Carica papaya* peel extract and evaluation of its antioxidant and antimicrobial activities," *Ecotoxicology and Environmental Safety*, vol. 134, Part 2, pp. 467–473, 2016.
- [40] P. G. Singh, S. B. Madhu, G. T. S. Shailasreesekhar, K. M. Basalingappa, and B. V. Sushma, "In vitro antioxidant, anti-inflammatory and anti-microbial activity of *Carica papaya* seeds," *Global Journal of Medical Research*, vol. 20, pp. 19–38, 2020.
- [41] W. Shen, J. Han, P. Yan et al., "Soluble expression of biologically active methionine sulfoxide reductase B1 (PaMsrb1) from *Carica papaya* in *Escherichia coli* and isolation of its protein targets," *Protein Expression and Purification*, vol. 146, pp. 17–22, 2018.
- [42] N. Calvache, M. Cueto, A. Farroni, P. M. de Escalada, and L. N. Gerschenson, "Antioxidant characterization of new dietary fiber concentrates from papaya pulp and peel (*Carica papaya* L.)," *Journal of Functional Foods*, vol. 27, pp. 319–328, 2016.

- [43] S. Salla, R. Sunkara, L. T. Walker, and M. Verghese, "Antioxidant and apoptotic activity of papaya peel extracts in HepG2 cells," *Food and Nutrition Sciences*, vol. 7, no. 6, pp. 485–494, 2016.
- [44] A. Nugroho, H. Heryani, J. S. Choi, and H. J. Park, "Identification and quantification of flavonoids in *Carica papaya* leaf and peroxynitrite-scavenging activity," *Asian Pacific Journal of Tropical Biomedicine*, vol. 7, no. 3, pp. 208–213, 2017.
- [45] V. Mohansrinivasan, S. V. Janani, P. Meghaswani et al., "Exploring the bioactive potential of *Carica papaya*," *The Natural Products Journal*, vol. 7, no. 4, 2017.
- [46] N. Asghar, S. A. R. Naqvi, Z. Hussain et al., "Compositional difference in antioxidant and antibacterial activity of all parts of the *Carica papaya* using different solvents," *Chemistry Central Journal*, vol. 10, no. 1, pp. 1–11, 2016.
- [47] A. M. Ibrahim and M. A. Ghareeb, "Preliminary phytochemical screening, total phenolic content, *in vitro* antioxidant and molluscicidal activities of the methanolic extract of five medicinal plants on *Biomphalaria alexandrina* snails," *Journal of Herbs Spices and Medicinal Plants*, vol. 26, no. 1, pp. 40–48, 2020.
- [48] P. Yogarajalakshmi, T. V. Poonguzhali, R. Ganesan, and S. Karthi, "Toxicological screening of marine red algae *Champia parvula* (C. Agardh) against the dengue mosquito vector *Aedes aegypti* (Linn.) and its non-toxicity against three beneficial aquatic predators," *Aquatic Toxicology*, vol. 222, article 105474, 2020.
- [49] A. Thomas, M. John, and B. Kanish, "Mucocutaneous manifestations of dengue fever," *Indian Journal of Dermatology*, vol. 55, no. 1, pp. 79–85, 2010.
- [50] A. M. Kirchmaier and D. Pillitteri, "Diagnosis and management of inherited platelet disorders," *Transfusion Medicine and Hemotherapy*, vol. 37, no. 5, pp. 237–246, 2010.
- [51] Y. Fenny, H. Endang, and K. Jusuf, "Effect of *Carica papaya* L. leaves extract capsules on platelet count and hematocrit in dengue patient," *International Journal of Medicinal Aromatic Plants*, vol. 2, pp. 573–578, 2012.
- [52] O. Siddique, A. Sundus, and M. F. Ibrahim, "Effects of papaya leaves on thrombocyte counts in dengue—a case report," *The Journal of the Pakistan Medical Association*, vol. 64, no. 3, pp. 364–366, 2014.
- [53] S. B. Vijeth, M. M. Kauser, V. Mangasuli, S. Sree, and S. A. Varghese, "Effect of *Carica papaya* leaf extract (CPLE) on thrombocytopenia among dengue patients of tertiary care hospital, Chitradurga, India," *International Journal of Advances in Medicine*, vol. 5, no. 4, p. 974, 2018.
- [54] A. Pandita, N. Mishra, N. G. Gupta, and R. Singh, "Use of papaya leaf extract in neonatal thrombocytopenia," *Clinical Case Reports*, vol. 7, no. 3, pp. 497–499, 2019.
- [55] P. Ranasinghe, W. K. M. Abeysekera, G. S. Premakumara, Y. S. Perera, P. Gurugama, and S. B. Gunatilake, "*In vitro* erythrocyte membrane stabilization properties of *Carica papaya* L. leaf extracts," *Pharmacognosy Research*, vol. 4, no. 4, pp. 196–202, 2012.
- [56] D. Charan, J. P. Saxena, J. P. Goyal, and S. Yasobant, "Efficacy and safety of *Carica papaya* leaf extract in the dengue: a systematic review and meta-analysis," *International Journal of Applied and Basic Medical Research*, vol. 6, no. 4, pp. 249–254, 2016.
- [57] A. Gammulle, W. D. Ratnasooriya, J. R. A. C. Jayakody, C. Fernando, C. Kanatiwela, and P. V. Udagama, "Thrombocytosis and anti-inflammatory properties and toxicological evaluation of *Carica papaya* mature leaf concentrate in a murine model," *International Journal of Medicinal Plants Research*, vol. 1, no. 2, pp. 21–30, 2012.
- [58] N. Sharma, K. P. Mishra, S. Chanda et al., "Evaluation of anti-dengue activity of *Carica papaya* aqueous leaf extract and its role in platelet augmentation," *Archives of Virology*, vol. 164, no. 4, pp. 1095–1110, 2019.
- [59] A. K. Gadhwal, B. S. Ankit, C. Chahar, P. Tantia, P. Sirohi, and R. P. Agrawal, "Effect of *Carica papaya* leaf extract capsule on platelet count in patients of dengue fever with thrombocytopenia," *Journal of Association of Physicians of India*, vol. 64, no. 4, pp. 22–26, 2016.
- [60] V. Zunjar, R. P. Dash, M. Jivrajani, B. Trivedi, and M. Nivsarkar, "Antithrombocytopenic activity of carpaïne and alkaloidal extract of *Carica papaya* Linn. leaves in busulfan induced thrombocytopenic Wistar rats," *Journal of Ethnopharmacology*, vol. 181, pp. 20–25, 2016.
- [61] C. P. Kala, "Leaf juice of *Carica papaya* L.: a remedy of dengue fever," *Medicinal Aromatic Plants*, vol. 1, p. 109, 2016.
- [62] R. Dhara, A. Rubeena, N. Shweta, P. Bhavisha, and B. Kinjal, "About dengue fever and *Carica papaya*, a leaf extract of papaya is used to treat dengue fever: -a review," *Indo American Journal of Pharmaceutical Research*, vol. 6, no. 8, pp. 6444–6449, 2016.
- [63] V. Anjum, P. Arora, S. H. Ansari, A. K. Najmi, and S. Ahmad, "Antithrombocytopenic and immunomodulatory potential of metabolically characterized aqueous extract of *Carica papaya* leaves," *Pharmaceutical Biology*, vol. 55, no. 1, pp. 2043–2056, 2017.
- [64] S. M. Hussain, M. H. Sohrab, A. K. Al-Mahmood, M. Shuayb, M. A. Al-Mansur, and C. M. Hasan, "Clinical use of *Carica papaya* leaf extract in chemotherapy-induced thrombocytopenia," *International Journal of Clinical and Experimental Medicine*, vol. 10, no. 2, pp. 3752–3756, 2017.
- [65] R. Venugopal, M. Suresh, and B. R. Halesha, "Role of *Carica papaya* leaf extract tablets/capsules on platelet counts in cases of dengue thrombocytopenia," *International Journal of Advances in Medicine*, vol. 5, no. 4, pp. 845–848, 2018.
- [66] M. R. Mohd Abd Razak, N. A. Norahmad, N. H. Md Jelas et al., "Immunomodulatory activities of *Carica papaya* L. leaf juice in a non-lethal, symptomatic dengue mouse model," *Pathogens*, vol. 10, no. 5, p. 501, 2021.
- [67] C. Mattiuzzi and G. Lippi, "Current cancer epidemiology," *Journal of Epidemiology and Global Health*, vol. 9, no. 4, pp. 217–222, 2019.
- [68] B. Farhood, B. Raei, R. Malekzadeh, M. Shirvani, M. Najafi, and T. Mortezaadeh, "A review of incidence and mortality of colorectal, lung, liver, thyroid, and bladder cancers in Iran and compared to other countries," *Contemporary Oncology*, vol. 23, no. 1, pp. 7–15, 2019.
- [69] M. Tigist, B. Getnet, K. Beza, M. Lulit, and M. Tinase, "Extraction and purification of papain enzymes from papaya leaf and the phytochemical components of the leaf," *Biotechnology International*, vol. 9, pp. 176–184, 2016.
- [70] C. Morimoto, N. H. Dang, and N. Y. S. Dang, "Therapeutic Co Ltd. cancer prevention and treating composition for pre-venting, ameliorating, or treating solid cancers, e.g. lung, or blood cancers, e.g. lymphoma, comprises components extracted from brewing papaya," 2008, Patent number-WO2006004226- A1; EP1778262-A1; JP2008505887 -W; US2008069907-A1.

- [71] Q. V. Vuong, S. Hirun, T. L. Chuen et al., "Antioxidant and anticancer capacity of saponin-enriched *Carica papaya* leaf extracts," *International Journal of Food Science & Technology*, vol. 50, no. 1, pp. 169–177, 2015.
- [72] T. T. Nguyen, M. O. Parat, P. N. Shaw, A. K. Hewavitharana, and M. P. Hodson, "Traditional aboriginal preparation alters the chemical profile of *Carica papaya* leaves and impacts on cytotoxicity towards human squamous cell carcinoma," *PLoS One*, vol. 11, no. 2, pp. 170–174, 2016.
- [73] P. B. Ayoola and A. Adeyeye, "Phytochemical and nutrient evaluation of *Carica papaya* (pawpaw) leaves," *International Journal of Current Research and Review*, vol. 5, no. 3, pp. 325–328, 2010.
- [74] A. M. Weli, S. Al-Salmi, H. Al Hoqani, and M. A. Hossain, "Biological and phytochemical studies of different leaves extracts of *Pteropyrum scoparium*," *Beni-Suef University Journal of Basic and Applied Sciences*, vol. 7, no. 4, pp. 481–486, 2018.
- [75] L. Amri and F. S. Hossain, "Comparison of total phenols, flavonoids and antioxidant potential of local and imported ripe bananas," *Egypt Journal of Basic and Applied Science*, vol. 5, no. 4, pp. 245–251, 2018.
- [76] Z. Nisa, M. Astuti, A. Murdiati, and S. M. Haryana, "Anti-proliferation and apoptosis induction of aqueous leaf extract of *Carica papaya* L. on human breast cancer cells MCF-7," *Pakistan Journal of Biological Sciences*, vol. 20, no. 1, pp. 36–41, 2016.
- [77] S. Pandey, C. Walpole, P. J. Cabot, P. N. Shaw, J. Batra, and A. K. Hewavitharana, "Selective anti-proliferative activities of *Carica papaya* leaf juice extracts against prostate cancer," *Biomedicine and Pharmacotherapy*, vol. 8, pp. 9515–9523, 2017.
- [78] S. P. Singh, A. Mishra, R. K. Shyanti, R. P. Singh, and A. Acharya, "Silver nanoparticles synthesized using *Carica papaya* leaf extract (AgNPs-PLE) causes cell cycle arrest and apoptosis in human prostate (DU145) cancer cells," *Biological Trace Element Research*, vol. 199, no. 4, pp. 1331–1361, 2021.
- [79] E. K. Salim and I. Jantan, "Inhibitory effect of selected medicinal plants on the release of pro-inflammatory cytokines in lipopolysaccharide-stimulated human peripheral blood mononuclear cells," *Journal of Natural Medicines*, vol. 68, no. 3, pp. 647–653, 2014.
- [80] A. H. Amin, F. A. Bughdadi, M. A. Abo-Zaid et al., "Immunomodulatory effect of papaya (*Carica papaya*) pulp and seed extracts as a potential natural treatment for bacterial stress," *Journal of Food Biochemistry*, vol. 43, no. 12, article e13050, 2019.
- [81] P. Saeedi, I. Petersohn, P. Salpea et al., "Global and regional diabetes prevalence estimates for 2019 and projections for 2030 and 2045: results from the International Diabetes Federation Diabetes Atlas, 9th edition," *Diabetes Research and Clinical Practice*, vol. 157, article 107843, 2019.
- [82] P. Abdullah, S. Chai, C. Y. Loh et al., "*Carica papaya* increases regulatory T cells and reduces IFN- γ +CD4⁺ T cells in healthy human subjects," *Molecular Nutrition & Food Research*, vol. 55, no. 5, pp. 803–806, 2011.
- [83] E. Ishihara, T. Miura, N. Shinya, and M. Usami, "Effect of the water extract of perilla leaves on glucose metabolism in diabetic rats," *Suzuka University of Medical Science Bulletin*, vol. 12, pp. 79–84, 2005.
- [84] K. Rao and S. Nammi, "Antidiabetic and renoprotective effects of the chloroform extract of *Terminalia chebula* Retz. seeds in streptozotocin-induced diabetic rats," *BMC Complementary and Alternative Medicine*, vol. 6, no. 1, 2006.
- [85] M. Prakash, M. Kumar, S. Kumari et al., "Therapeutic uses of wild plants by rural inhabitants of Maraog region in district Shimla, Himachal Pradesh, India," *Horticulturae*, vol. 7, no. 10, p. 343, 2021.
- [86] S. Moradi, S. Abbaszadeh, M. A. Shahsavari, and F. Beyranvand, "The most useful medicinal herbs to treat diabetes," *Biomedical Research and Therapy*, vol. 5, no. 8, pp. 2538–2551, 2018.
- [87] K. Sobia, M. A. Javaid, M. S. Ahmad et al., "Assessments of phytochemicals and hypoglycemic activity of leaves extracts of *Carica papaya* in diabetic mice," *International Journal of Pharmaceutical Sciences and Research*, vol. 7, no. 9, p. 3658, 2016.
- [88] T. O. Fakeye, T. Oladipupo, O. Showande, and Y. Ogunremi, "Effects of coadministration of extract of *Carica papaya* Linn (family Caricaceae) on activity of two oral hypoglycemic agents," *Tropical Journal of Pharmaceutical Research*, vol. 6, no. 1, pp. 671–678, 2007.
- [89] S. Sasidharan, V. Sumathi, N. R. Jegathambigai, and L. Y. Latha, "Antihyperglycaemic effects of ethanol extracts of *Carica papaya* and *Pandanus amaryfollius* leaf in streptozotocin-induced diabetic mice," *Natural Product Research*, vol. 25, no. 20, pp. 1982–1987, 2011.
- [90] E. Juarez-Rojop, J. C. Diaz-Zagoya, J. L. Ble-Castillo et al., "Hypoglycemic effect of *Carica papaya* leaves in streptozotocin-induced diabetic rats," *BMC Complementary and Alternative Medicine*, vol. 12, no. 1, 2012.
- [91] M. Yasmeen and B. Prabhu, "Anti-hyperglycemic and hypolipidemic activities of aqueous extract of *Carica papaya* Linn. leaves in alloxan-induced diabetic rats," *Journal of Ayurveda and Integrative Medicine*, vol. 3, no. 2, pp. 70–74, 2012.
- [92] A. F. Adenowo, M. F. Ilori, F. O. Balogun, and M. I. Kazeem, "Protective effect of ethanol leaf extract of *Carica papaya* Linn (Caricaceae) in alloxan-induced diabetic rats," *Tropical Journal of Pharmaceutical Research*, vol. 13, no. 11, pp. 1877–1882, 2014.
- [93] A. F. Ukpabi, M. N. Chukwu, J. N. Onyemaechi, V. Ibe, and E. F. Onus, "Antidiabetic and antihyperlipidemic effects of aqueous extract of *Carica papaya* leaf on the experimental model against single alloxan toxicity," *World Scientific Research*, vol. 6, no. 1, pp. 14–18, 2019.
- [94] T. I. Solikhah, B. Setiawan, and D. R. Ismukada, "Antidiabetic activity of papaya leaf extract (*Carica Papaya* L.) isolated with maceration method in alloxan-induced diabetic mice," *Systematic Reviews in Pharmacy*, vol. 11, no. 9, pp. 774–778, 2020.
- [95] T. T. P. Cushnie and A. J. Lamb, "Antimicrobial activity of flavonoids," *International Journal of Antimicrobial Agents*, vol. 26, no. 5, pp. 343–356, 2005.
- [96] I. E. Juárez-Rojop, C. Tovilla-Zárate, D. E. Aguilar-Domínguez et al., "Phytochemical screening and hypoglycemic activity of *Carica papaya* leaf in streptozotocin-induced diabetic rats," *Revista Brasileira de Farmacognosia*, vol. 24, pp. 341–347, 2014.
- [97] H. Bindhu and A. Vijayalakshmi, "Neuroprotective effect of *Carica papaya* leaf extract against aluminium toxicity: an experimental study on cognitive dysfunction and biochemical alterations in rats," *Indian Journal of Pharmaceutical Education and Research*, vol. 53, no. 3s, pp. s392–s398, 2019.

- [98] S. Gill, *Ethnomedical Uses of Plants in Nigeria*, Uniben Press, Benin, Nigeria, 1992.
- [99] V. Owoyele, O. M. Adebukola, A. A. Funmilayo, and A. O. Soladoye, "Anti-inflammatory activities of ethanolic extract of *Carica papaya* leaves," *Inflammo Pharmacology*, vol. 16, no. 4, pp. 168–173, 2008.
- [100] A. Gupta, S. S. Patil, and N. Pendharkar, "Antimicrobial and anti-inflammatory activity of aqueous extract of *Carica papaya*," *Journal of Herbmed Pharmacology*, vol. 6, no. 4, pp. 148–152, 2017.
- [101] S. Akhila and N. G. Vijayalakshmi, "Phytochemical studies on *Carica papaya* leaf juice," *International Journal of Pharmaceutical Science and Research*, vol. 6, pp. 880–883, 2015.
- [102] A. I. Airaodion, J. A. Ekenjoku, I. U. Akaninyene, and A. U. Megwas, "Antibacterial potential of ethanolic and aqueous extracts of *Carica papaya* leaves," *Asian Journal of Biochemistry, Genetics and Molecular Biology*, vol. 3, no. 2, pp. 33–38, 2020.
- [103] A. Sharma and A. Gupta, "Value addition in beverages with papaya leaves extract (*Carica papaya*)," *International Journal of Science and Research*, vol. 6, no. 7, pp. 2319–7064, 2015.
- [104] S. A. Junaid, A. O. Olabode, F. C. Onwuliri, A. E. Okworiu, and S. E. Agina, "The antimicrobial properties of *Ocimum gratissimum* extracts on some selected bacterial gastrointestinal isolates," *African Journal of Biotechnology*, vol. 5, pp. 2315–2321, 2006.
- [105] S. Hettige, "Salutary effects of *Carica papaya* leaf extract in dengue fever patients: a pilot study," *Srilankan Fam Physician*, vol. 29, pp. 17–19, 2008.
- [106] P. Kumar, C. Sharma, A. K. Verma, and A. Sharma, "Utilization of *Carica papaya* herbal leaf extract for preparation of a nutraceutical functional beverage," *Chemical Science Review and Letters*, vol. 9, no. 34, pp. 39–49, 2020.
- [107] E. Nwofia, P. Ojmelukwe, and C. Eji, "Chemical composition of leaves, fruit pulp and seeds in some *Carica papaya* (L) morphotypes," *International Journal of Medicinal and Aromatic Plants*, vol. 2, no. 1, pp. 200–206, 2012.
- [108] V. B. Babu Nagati, R. Koyyati, M. R. Donda, J. Alwala, K. R. Kundle, and P. R. M. Padigya, "Green synthesis and characterization of silver nanoparticles from *Cajanuscajan* leaf extract and its antibacterial activity," *International Journal of Nanomaterials and Biostructures*, vol. 2, no. 3, pp. 39–43, 2010.
- [109] R. Mabd Razak, N. M. Misnan, N. H. M. Jelas et al., "The effect of freeze-dried *Carica papaya* leaf juice treatment on NS1 and viremia levels in dengue fever mice model," *BMC Complementary and Alternative Medicine*, vol. 18, no. 1, 2018.
- [110] N. K. Palanisamy, N. Ferina, A. N. Amirulhusni et al., "Antibiofilm properties of chemically synthesized silver nanoparticles found against *Pseudomonas aeruginosa*," *Journal of Nanobiotechnology*, vol. 12, no. 1, pp. 2–7, 2014.
- [111] A. K. Dulta, P. C. Kumar, and P. Kumar Chauhan, "Eco-Friendly Synthesis of Silver Nanoparticles Using *Carica papaya* Leaf Extract and Its Antibiofilm Activity," in *International Conference on New Horizons in Green Chemistry & Technology*, Uttaranchal, Dehradun, India, 2018.
- [112] R. Banala, V. B. Nagati, and P. R. V. Karnati, "Green synthesis and characterization of *Carica papaya* leaf extract coated silver nanoparticles through X-ray diffraction, electron microscopy and evaluation of bactericidal properties," *Saudi Journal of Biological Sciences*, vol. 22, no. 5, pp. 637–644, 2015.
- [113] S. Chandrasekaran, P. Gnanasekar, R. Seetharaman, W. Keppanan, W. Arockiaswamy, and S. Sivaperumal, "Formulation of *Carica papaya* latex-functionalized silver nanoparticles for its improved antibacterial and anticancer applications," *Journal of Molecular Liquids*, vol. 219, pp. 232–238, 2016.
- [114] S. Renganathan, V. Aroulmoji, G. Shanmugam et al., "Silver nanoparticle synthesis from *Carica papaya* and virtual screening for anti-dengue activity using molecular docking," *Materials Research Express*, vol. 6, no. 3, article 035028, 2019.
- [115] A. Syafiuddin, T. Hadibarata, M. R. Salim, A. B. H. Kueh, and A. A. Sari, "A purely green synthesis of silver nanoparticles using *Carica papaya*, *Manihot esculenta*, and *Morinda citrifolia*: synthesis and antibacterial evaluations," *Bioprocess and Biosystems Engineering*, vol. 40, no. 9, pp. 1349–1361, 2017.
- [116] A. Yadav, S. Sar, and M. Upadhayay, "Biosynthesis and characterization of silver nanoparticle (CPLAgNps) from *Carica papaya* leaf, and their antibacterial activities," *Journal of Applied Chemistry*, vol. 10, no. 9, pp. 1–23, 2017.
- [117] C. Jackson, T. O. O. Uwah, A. A. Agboke, B. E. Udo, and E. M. Udofa, "Eco-friendly synthesis of silver nano particles using *Carica papaya* leaf extract," *Soft Nanoscience Letters*, vol. 8, no. 1, pp. 1–7, 2018.
- [118] P. Anbarasu, N. D. Karnan, and R. Usha, "*Carica papaya* mediated green synthesized silver nanoparticles," *International Journal of Current Pharmaceutical Research*, vol. 10, no. 3, pp. 15–20, 2018.
- [119] F. Jain, D. Ahmad, A. Gola et al., "Multi dye degradation and antibacterial potential of Papaya leaf derived silver nanoparticles," *Environmental Nanotechnology, Monitoring & Management*, vol. 14, article 100337, 2020.
- [120] A. Balavijayalakshmi and V. Ramalakshmi, "*Carica papaya* peel mediated synthesis of silver nanoparticles and its antibacterial activity against human pathogens," *Journal of Applied Research and Technology*, vol. 15, no. 5, pp. 413–422, 2017.
- [121] A. Afzan, N. R. Abdullah, S. Z. Halim et al., "Repeated dose 28-days oral toxicity study of *Carica papaya* L. leaf extract in Sprague Dawley rats," *Molecules*, vol. 17, no. 4, pp. 4326–4342, 2012.
- [122] Z. Ismail, H. Z. Halim, N. R. Abdullah, A. Afzan, B. A. Abdul Rashid, and I. Jantan, "Safety Evaluation of Oral Toxicity of *Carica papaya* Linn. Leaves: A Subchronic Toxicity Study in Sprague Dawley Rats," *Evidence-Based Complementary and Alternative Medicine*, vol. 2014, Article ID 741470, 10 pages, 2014.
- [123] C. H. Ansah, J. A. Appiah, K. Mensah, and P. Mante, "Aqueous leaf extract of *Carica papaya* (Caricaceae) Linn. causes liver injury and reduced fertility in rats," *International Journal of Pharmacy and Pharmaceutical Sciences*, vol. 8, pp. 261–265, 2016.
- [124] T. Omara, A. K. Kiprof, R. C. Ramkat et al., "Medicinal Plants Used in Traditional Management of Cancer in Uganda: A Review of Ethnobotanical Surveys, Phytochemistry, and Anticancer Studies," *Evidence-Based Complementary and Alternative Medicine*, vol. 2020, Article ID 3529081, 26 pages, 2020.
- [125] J. Nguyen, P. Kitzmiller, P. Khungar, N. Dabbade, K. T. Nguyen, and E. L. Flynn, "Phytochemical, hematologic and anti-tumor activity evaluations of *Carica papaya* leaf extract," *Journal of Translational Science*, vol. 3, no. 3, pp. 1–7, 2017.

Research Article

Epigallocatechin Gallate Relieved PM2.5-Induced Lung Fibrosis by Inhibiting Oxidative Damage and Epithelial-Mesenchymal Transition through AKT/mTOR Pathway

Zhou Zhongyin,¹ Wang Wei,² Xiong Juan ², and Fan Guohua ²

¹Department of Gastroenterology, Renmin Hospital of Wuhan University, Wuhan 430060, China

²Department of Thoracic Surgery, Renmin Hospital of Wuhan University, Wuhan 430060, China

Correspondence should be addressed to Fan Guohua; whurmyhxq@163.com

Zhou Zhongyin and Wang Wei contributed equally to this work.

Received 23 March 2022; Revised 7 May 2022; Accepted 20 May 2022; Published 6 June 2022

Academic Editor: German Gil

Copyright © 2022 Zhou Zhongyin et al. This is an open access article distributed under the Creative Commons Attribution License, which permits unrestricted use, distribution, and reproduction in any medium, provided the original work is properly cited.

Oxidative damage and epithelial-mesenchymal transition (EMT) are main pathological processes leading to the development of PM2.5-induced lung fibrosis. Epigallocatechin gallate (EG), a natural polyphenol extracted from green tea, possesses the ability to combat oxidative stress and inflammation. However, the potential roles of EG in PM2.5-induced lung fibrosis have not been reported yet. In the present study, we investigated whether EG could relieve PM2.5-induced lung injury and fibrosis *in vivo* and *in vitro*. To mimic PM2.5-induced lung fibrosis, C57/BL6 mice were intranasally instilled with PM2.5 suspension, and MLE-12 lung epithelial cells were stimulated with PM2.5 (100 $\mu\text{g}/\text{mL}$) *in vitro*. The results showed that intragastric administration of EG (20 mg/kg/d or 80 mg/kg/d for 8 weeks) significantly prevented lung injury, inflammation, and oxidative stress in PM2.5-induced mice, apart from inhibiting collagen deposition. Additionally, EG treatment also suppressed the activation of AKT/mTOR signaling pathway in lung tissues challenged with PM2.5. *In vitro* experiments further demonstrated that EG treatment could enhance cell viability in a concentration-dependent manner in PM2.5-treated MLE-12 lung epithelial cells. Also, the overexpression of constitutively active AKT could offset the inhibitory effects of EG on EMT and oxidative stress in PM2.5-treated MLE-12 lung epithelial cells. Finally, AKT overexpression also blocked the inhibitory effect of EG on the phosphorylation of mTOR in PM2.5-treated MLE-12 lung epithelial cells. In conclusion, EG could improve PM2.5-induced lung fibrosis by decreasing oxidative damage and EMT through AKT/mTOR pathway, which might be a potential candidate for the treatment of PM2.5-induced lung fibrosis.

1. Introduction

Air pollution has posed huge threat to human health, especially the cardiovascular system and respiratory system [1]. PM2.5 is defined as ambient air particulate matter with aerodynamic diameters less than 2.5 μm , which is one of the important pollutant compositions in air [2]. Increased PM2.5 is implicated with a variety of chronic diseases including bronchitis, chronic obstructive pulmonary disease (COPD) [3], asthma [4], coronary artery disease [5], and atherosclerosis [6]. PM2.5 can be easily inhaled into the air-

way and subsequently deposited in lung alveolar space due to its small size, the long-term deposition of which further gives rise to lung pathological injury and fibrosis by increasing oxidative stress and epithelial-mesenchymal transition (EMT) [7]. Thereby, candidates with antioxidative and anti-fibrotic effects possess the potential to attenuate PM2.5-induced lung injury and fibrosis.

At present, the pathogenesis of lung fibrosis has not been well clarified. Lung fibrosis originates from aberrant repair of the lung epithelial cells and repeated injury [8]. Some studies hold the view that the progressive pulmonary

dysfunction declining resulted from the lung epithelial injury as well as aberrant fibroblast proliferation participated in the development of inflammation and lung fibrosis [9, 10]. Additionally, EMT and excessive extracellular matrix (ECM) production also result in pulmonary structural remodeling [11, 12]. In recent years, a great many researchers have been immersed in the roles of lung epithelial cells and EMT in fibrosis. Lung epithelial cells could differentiate into a mesenchymal phenotype through EMT, which further secrete a series of fibrogenic cytokines to activate fibroblasts [13]. Protein kinase B (PKB, also known as AKT)/mechanistic target of rapamycin (mTOR) pathway serves as one of the most important pathways contributing to the activation of EMT, playing an essential role in the progression of lung fibrosis [14]. Hence, blocking AKT/mTOR pathway has been proposed to be a promising strategy to suppress EMT and combat lung fibrosis.

Epigallocatechin gallate (EG) is considered as the most abundant polyphenol with bioactivity in green tea isolated from *Camellia sinensis* [15]. As a bioactive dietary component, EG owns a great many pharmacological actions including antioxidation, anti-inflammation, antifibrosis, and inhibiting endoplasmic reticulum stress [16–18]. In acute lung injury induced by sepsis, acute pancreatitis, paraquat, and hip fracture, EG treatment could exert vital protective roles by different mechanisms [19–22]. In transverse aortic constriction-induced cardiac fibrosis, EG treatment significantly decreased collagen deposition and cardiomyocyte hypertrophy by blocking AKT/mTOR pathway [18]. These facts raised the possibility that EG may own the potential of pulmonary protection. Yet whether the EG could protect against chronic lung injury is still unknown.

In the current study, we aimed to explore whether EG can attenuate lung injury and fibrosis induced by PM2.5 in mice and to clarify the underlying mechanisms.

2. Materials and Methods

2.1. Regents and Chemicals. Epigallocatechin gallate with a purity of 99.87% was purchased from MedChemExpress Co., Ltd. (#: HY-13653, Shanghai, China). Primary antibodies against phosphorylated (P)-AKT, total (T)-AKT, P-mTOR, T-mTOR, and GAPDH were provided by Abcam (Cambridge, UK), while secondary antibody was obtained from LI-COR Biosciences (Lincoln, USA). Trypsin-EDTA (0.25%) phenol red and Dulbecco's modified Eagle's medium nutrient mixture F-12 (DMEM/F-12), fetal bovine serum (FBS), and trypsin-ethylenediaminetetraacetic acid (0.25%) phenol were provided by Invitrogen-Gibco (Grand Island, NY, USA).

2.2. The Extraction of PM2.5 Sampling. PM2.5 samples were obtained with a high flow PM2.5 sampler (Ecotech, Australia) in the Wuhan Environment Surveillance Centre. The extraction and analysis of PM2.5 sampling were carried out based on our previous study [23]. The PM2.5 particles were stored at -20°C and detached from filters by sonication, which were next desiccated by lyophilization. At last, these

PM2.5 solid particles were suspended in phosphate buffer saline (PBS) evenly by vortex concussion for intranasal instillation and cell experiments.

2.3. Mice and Models. C57/BL6J male mice weighing 24.3 ± 1.7 g (8–10 weeks) were provided by the Chinese Academy of Medical Sciences (Beijing). Mice were housed in a specific pathogen-free rooms with constant temperature ($22\text{--}25^{\circ}\text{C}$) and humidity (50–60%) under a 12 h light/dark cycle. Mice had ad libitum access to food and water. All animal experimental procedures were in accordance with the Guidelines for the Care and Use of Laboratory Animals published by the National Institutes of Health and were approved by the Committee on the Laboratory Animal Welfare & Ethics of Renmin Hospital of Wuhan University.

According to previous study, mice were intranasally instilled with PM2.5 particulates (100 mg/kg bodyweight) suspended in $50\ \mu\text{L}$ of sterile water or isovolumetric sterile saline once a week for four weeks to induce PM2.5-induced lung injury and fibrosis [24]. Meanwhile, EG (20 mg/kg/d or 80 mg/kg/d) or equal volume of sterile saline was administered orally to mice for continuous 8 weeks. 56 days after EG administration, mice were sacrificed by cervical dislocation after they were anaesthetized deeply by isoflurane inhalation. And the lungs were excised for molecular biological and histological detections. To keep the lungs in an extended status, 4% paraformaldehyde was instilled in the trachea.

2.4. Histopathological Analysis. The left lung tissues were embedded in paraffin, which were then sliced into $3\ \mu\text{m}$ -thick sections to expose the cross section of lung tissue. Subsequently, the sections were stained using hematoxylin for a few minutes and rinsed by tap water, followed by the differentiation with 1% hydrochloric acid alcohol for 3–5 seconds. After that, the sections were stained with eosin for 2–3 minutes. The lung injury was then observed and scored under a microscope. As described previously, a semiquantitative scoring system was applied to access lung injury based on the degree of neutrophil infiltration and pulmonary edema. Each index was scored by a pathologist according to the following criteria: 0, no injury; 1, injury up to 25% of the field; 2, injury up to 50% of the field; 3, injury up to 75% of the field; and 4, diffuse injury. A total lung injury score was calculated by summing up the two components (neutrophil infiltration and pulmonary edema) [25].

As for Masson staining, the lung sections were stained with iron hematoxylin for the nucleus after dewaxed in water. After that, the sections were stained with ponceau red, followed by phosphomolybdic acid aqueous solution. Next, the sections were stained with aniline blue and sealed with neutral resin. At last, the sections were observed and pictured under a light microscope.

2.5. Cell Culture and Treatment. The MLE-12 lung epithelial cells were provided by Kunming Cell Bank of Typical Cultures Preservation Committee, Chinese Academy of Sciences (Kunming, China). The cells were cultured in DMEM/F-12 supplemented with FBS (10%) at 37°C in an incubator with 5% CO_2 . To establish an *in vitro* model of PM2.5-induced

lung injury, the MLE-12 lung epithelial cells were stimulated with PM2.5 (100 $\mu\text{g}/\text{mL}$) with or without EG (20 μM) for 24 hours as described [23]. To activate AKT in MLE-12 lung epithelial cells constitutively, the adenoviral (Ad) vectors generated by Hanbio Biotechnology Co. (Shanghai, China) were used in the present study [26].

2.6. Western Blot and Quantitative Real-Time RT-PCR. The Western blot was carried out to access the levels of protein expression. The total proteins in lung tissues and lung epithelial cells were extracted using RIPA lysis buffer containing a protease inhibitor cocktail. A bicinchoninic acid (BCA) protein assay kit was used to detect and normalize the protein concentration. 10 μL of markers or quantitative protein samples (50 μg) was added into a 10% SDS-PAGE and separated before being transferred to the polyvinylidene fluoride (PVDF) membranes. Subsequently, 5% skim milk was used to block the nonspecific protein binding sites in the PVDF membranes. Then, the membranes were incubated with antibodies against GAPDH (1:1000), P-mTOR (1:500), T-mTOR (1:1000), P-AKT (1:5000), and T-AKT (1:1000) diluted in Tris-buffered saline+Tween (TBST) overnight at 4°C overnight, respectively. The next day, the PVDF membranes were incubated with the secondary antibodies after washed with TBST for 3 times. ECL detection kits were applied to access chemiluminescence using a LICOR Odyssey image system. The protein expression levels were normalized to GAPDH as an internal reference. The expression was quantified using the Image Lab software from Bio-Rad (Hercules, CA, USA).

Total RNA was extracted from murine lung tissues and cultured lung epithelial cells using the TRIzol reagent. Next, total RNA was reversely transcribed to complementary DNA by oligo primers using the Maxima First Strand cDNA Synthesis Kit. The transcriptional levels of target genes including TNF- α , IL-1 β , MCP-1, collagen I, collagen III, connective tissue growth factor (CTGF), E-Cadherin, α -SMA, Snail, thioredoxin-interacting protein (TXNIP), thioredoxin reductase 1 (TXNRD1), and thioredoxin 1 (TXN1) were detected with SYBR green. GAPDH was used as an internal reference gene to calculate the relative expression of target genes.

2.7. The Determination of Oxidative Stress. The fresh murine lung tissues (100 mg) were homogenized and then centrifuged for 10 min (X4230 g) to obtain the supernatant fractions. Then, the NADH oxidase (NOX) and superoxide dismutase (SOD) activities and malondialdehyde (MDA) level were detected using the commercially available kits according to the instructions [27].

2.8. CCK8 Assay. Cell Counting Kit-8 (CCK8) assay was performed to detect cell viability using a CCK8 assay kit. In detail, the lung epithelial cells were seeded into 96-well plates. Subsequently, 10 μL of CCK8 working solution was added into each well in a dark environment. Then, the plates were kept in an incubator (5% CO₂) at 37°C for 1 hour. Finally, the absorbance was measured at 450 nm to evaluate the cell viability of lung epithelial cells.

2.9. Data Analysis. All data in this study are presented as the mean \pm standard deviation (SD). One-way ANOVA followed by a post hoc Tukey's test was performed to analyze the differences among multiple groups, while an unpaired, two-sided Student *t* test was carried out to analyze the differences between 2 groups. *P* < 0.05 was defined as statistical significance.

3. Results

3.1. EG Treatment Decreased Pathological Injury and Inflammatory Response in Lung Tissues Treated with PM2.5. To begin with, lung pathological injury in each group was assessed by H&E staining. The results showed that EG (both 20 mg/kg/d and 80 mg/kg/d) could significantly alleviate interstitial thickening and inflammatory cell infiltration caused by PM2.5, which was reflected by decreased lung injury score (Figures 1(a) and 1(b)). The results from RT-PCR also indicated that EG treatment significantly decreased inflammatory response in PM2.5-induced lung tissues, which was evidenced by decreased mRNA levels of TNF- α , IL-1 β , and MCP-1 (Figures 1(c)–1(e)).

3.2. EG Treatment Inhibited Oxidative Stress in Lung Tissues Treated with PM2.5. Next, the levels of oxidative stress were evaluated using different methods. As shown in Figure 2(a), the level of lipid peroxidative product MDA in lung tissues from mice challenged PM2.5 was suppressed after EG (both 20 mg/kg/d and 80 mg/kg/d) treatment. Also, the activity of SOD and NOX was determined in each group. The results demonstrated that EG treatment could increase SOD activity and decrease NOX activity in PM2.5-induced lung tissues, indicating that EG exerted antioxidant effects (Figures 2(b) and 2(c)). Meanwhile, we observed the effects of EG on the mRNA levels of pro-oxidant gene TXNIP and antioxidant genes including TXN1 and TXNRD1. The results showed that EG treatment upregulated the mRNA levels of TXN1 and TXNRD1 and downregulated the mRNA level of TXNIP (Figures 2(d)–2(f)).

3.3. EG Alleviated Fibrosis and EMT in PM2.5-Induced Lung Tissues. Fibrosis is one of the most important features of PM2.5-induced lung injury [28]. Hence, we also observed the effects of EG on lung fibrosis of mice challenged with PM2.5. As shown in Figures 3(a) and 3(b), EG (both 20 mg/kg/d and 80 mg/kg/d) treatment significantly decreases the fibrotic area in lung tissues from mice treated with PM2.5. Furthermore, the mRNA levels of collagen I, collagen III, and CTGF in PM2.5-induced lung tissues were also inhibited by EG (Figures 3(c)–3(e)). Considering that EMT serves as one vital mechanism contributing to lung fibrosis, we also detected the markers of EMT in lung tissues. The results (Figures 3(f)–3(h)) showed that EG treatment significantly increased the level of E-Cadherin and decreased the levels of α -SMA and Snail, suggesting that EG shifted the phenotype from mesenchymal cells to epithelial cells.

3.4. AKT/mTOR Pathway Was Inhibited by EG in Lung Tissues Treated with PM2.5. Previous studies have illustrated that the abnormal activation of AKT/mTOR pathway was

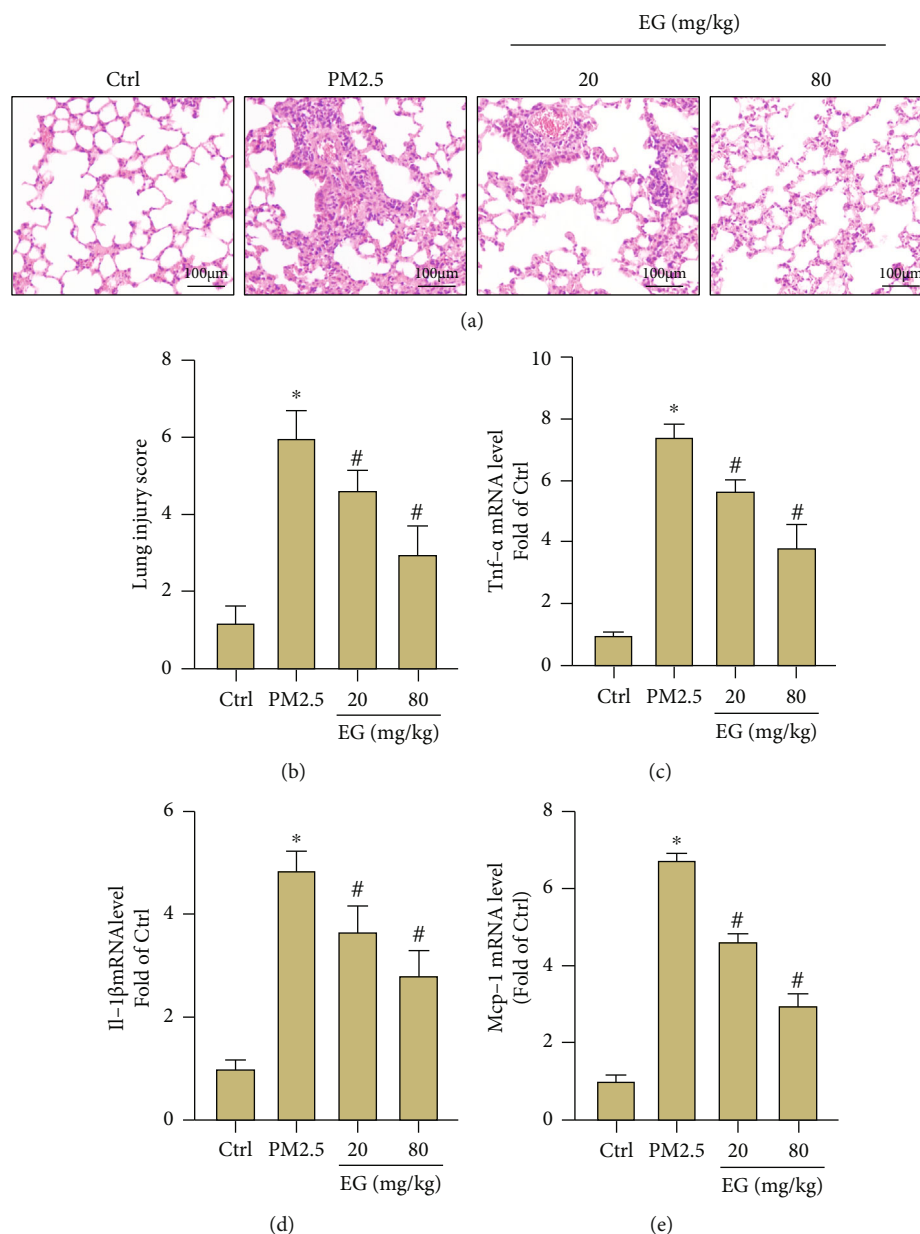


FIGURE 1: EG treatment decreased pathological injury and inflammatory response in lung tissues treated with PM2.5. (a–b) H&E staining of lung tissues in the indicated groups and lung injury scores ($n = 5$). Original magnification $\times 200$. (c–e) Comparison of mRNA levels of TNF- α , IL-1 β , and MCP-1 in lung tissues ($n = 5$). * $P < 0.05$ vs. Ctrl group, # $P < 0.05$ vs. PM2.5 group.

implicated with oxidative stress and EMT [29, 30]. Here, our data disclosed that PM2.5 stimulation significantly promoted the phosphorylation of AKT and mTOR in lung tissues (Figures 4(a)–4(c)). As expected, EG (both 20 mg/kg/d and 80 mg/kg/d) treatment obviously blocked the activation of AKT/mTOR pathway, hinting that the pulmonary protection from EG may be associated with the inhibition of AKT/mTOR pathway.

3.5. EG Relieved EMT and Oxidative Stress in PM2.5-Induced Lung Epithelial Cells in an AKT-Dependent Manner. Next, we investigated the roles of EG in PM2.5-induced lung epithelial cells. First, cell viability was detected in lung epithelial cells treated with different concentrations of EG. As shown

in Figure 5(a), the concentrations ranging from 0.1 to 50 μM display no effects on cell viability of lung epithelial cells. In PM2.5-induced lung epithelial cells, the concentrations ranging from 10 to 50 μM improved cell viability (Figure 5(b)). Based on these data, 20 μM was selected for the subsequent *in vitro* experiments. The results showed that EG (20 μM) could improve cell viability of PM2.5-induced lung epithelial cells, whereas constitutively active AKT overexpression by adenoviral infection blocked the effects of EG on cell viability (Figure 5(c)). Similarly, AKT activation also offset the inhibitory effects of EG on EMT in PM2.5-induced lung epithelial cells, evidenced by decreased mRNA level of E-Cadherin and increased mRNA level of α -SMA (Figures 5(d) and 5(e)). Additionally, the antioxidant effect

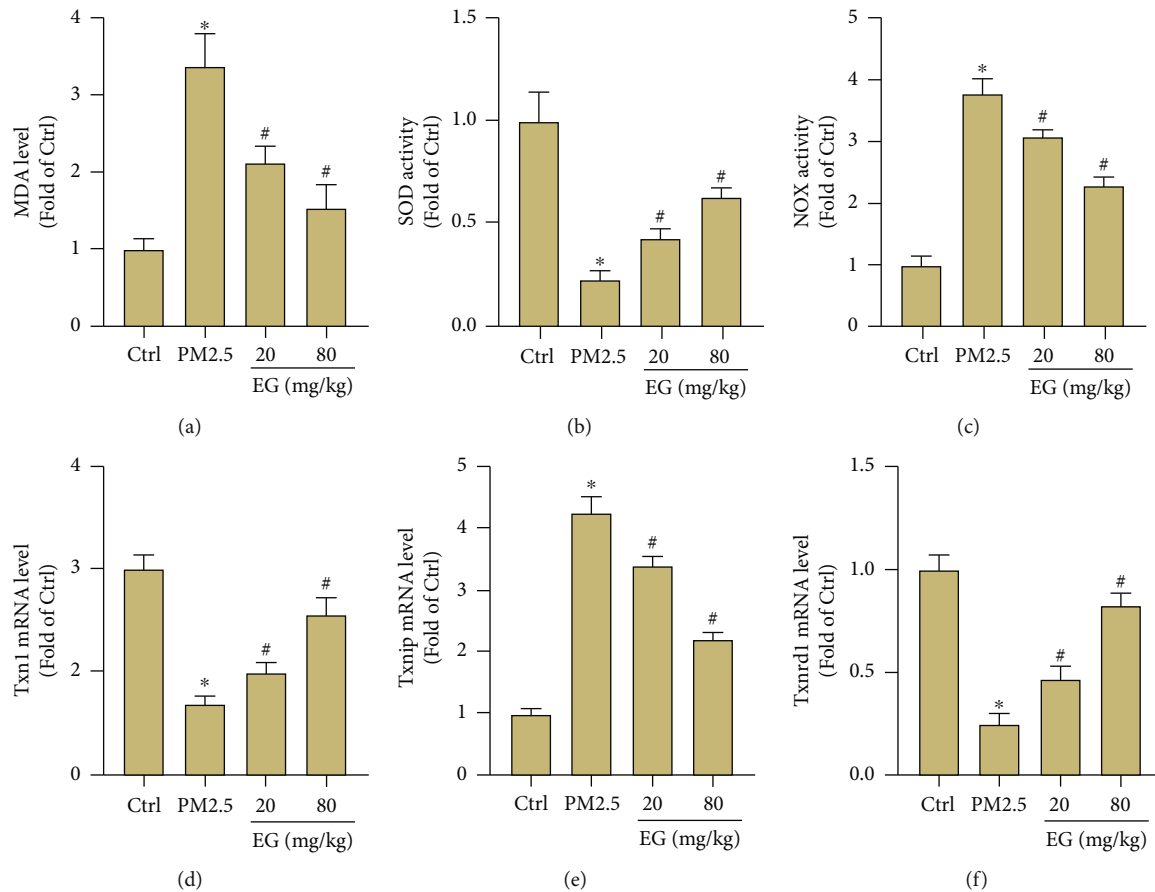


FIGURE 2: EG treatment inhibited oxidative stress in lung tissues treated with PM2.5. (a) MDA level in lung tissues ($n = 5$). (b–c) SOD activity and NOX activity in lung tissues ($n = 5$). (d–f) Comparison of mRNA levels of Txn1, Txnip, and Txnrd1 in lung tissues ($n = 5$). * $P < 0.05$ vs. Ctrl group, # $P < 0.05$ vs. PM2.5 group.

of EG on PM2.5-induced lung epithelial cells could also be counteracted after AKT activation (Figures 5(f) and 5(g)). Taken together, these results disclosed the fact that EG could inhibit EMT and oxidative stress in PM2.5-induced lung epithelial cells in an AKT-dependent manner.

3.6. AKT/mTOR Pathway Was Involved in Pulmonary Protection from EG in PM2.5-Induced Lung Epithelial Cells. Finally, we detected the protein levels of P-mTOR and T-mTOR in the indicated groups. As shown in Figures 6(a) and 6(b), EG could not inhibit mTOR at baseline, whereas it significantly decreased the protein level of P-mTOR in PM2.5-induced lung epithelial cells. As expected, AKT activation offset the inhibitory effects of EG on mTOR, which further solid the hypothesis that EG exerted its protective effects by blocking the activation of AKT/mTOR pathway in PM2.5-induced lung injury and fibrosis.

4. Discussion

Here, we disclosed that EG treatment prevents oxidative damage, inflammation, and lung fibrosis induced by PM2.5 for the first time. EG blocked the EMT of lung epithelial cells induced by PM2.5 *in vitro*. The pulmonary protection from

EG was associated with the inactivation of the AKT/mTOR pathway. Constitutive activation of AKT by adenovirus infection in lung epithelial cells could offset EG-elicited protection (Figure 7).

In many epidemiological studies, the relationship between respiratory diseases and ambient airborne fine particulate matter exposure has been well illustrated [31, 32]. To our knowledge, PM2.5 is comprised of a series of particles involving nitrate, black carbon, sulfate, polycyclic aromatic hydrocarbons, metals, and automobile exhaust particles, which could invade distal small airways and alveoli [33]. Excessive accumulation of PM2.5 in lung parenchyma could lead to irreversible lung fibrosis, apart from inducing inflammation and oxidative stress [34]. In the young and the elderly, long-term PM2.5 exposure gives rise to poorer lung function indices, evidenced by reduced forced vital capacity (FVC), and forced expiratory volume in 1 s (FEV1), as well as peak expiratory flow (PEF) [35]. At present, oxidative stress and EMT are regarded as two main factors contributing to lung fibrosis. Some animal experiments also showed that long-term PM2.5 exposure aggravates lung fibrosis by mediating oxidative stress and AKT activation [36]. PM2.5 displays a potent redox potential by elevating reactive oxygen species (ROS). In preexisting COPD rats stimulated with

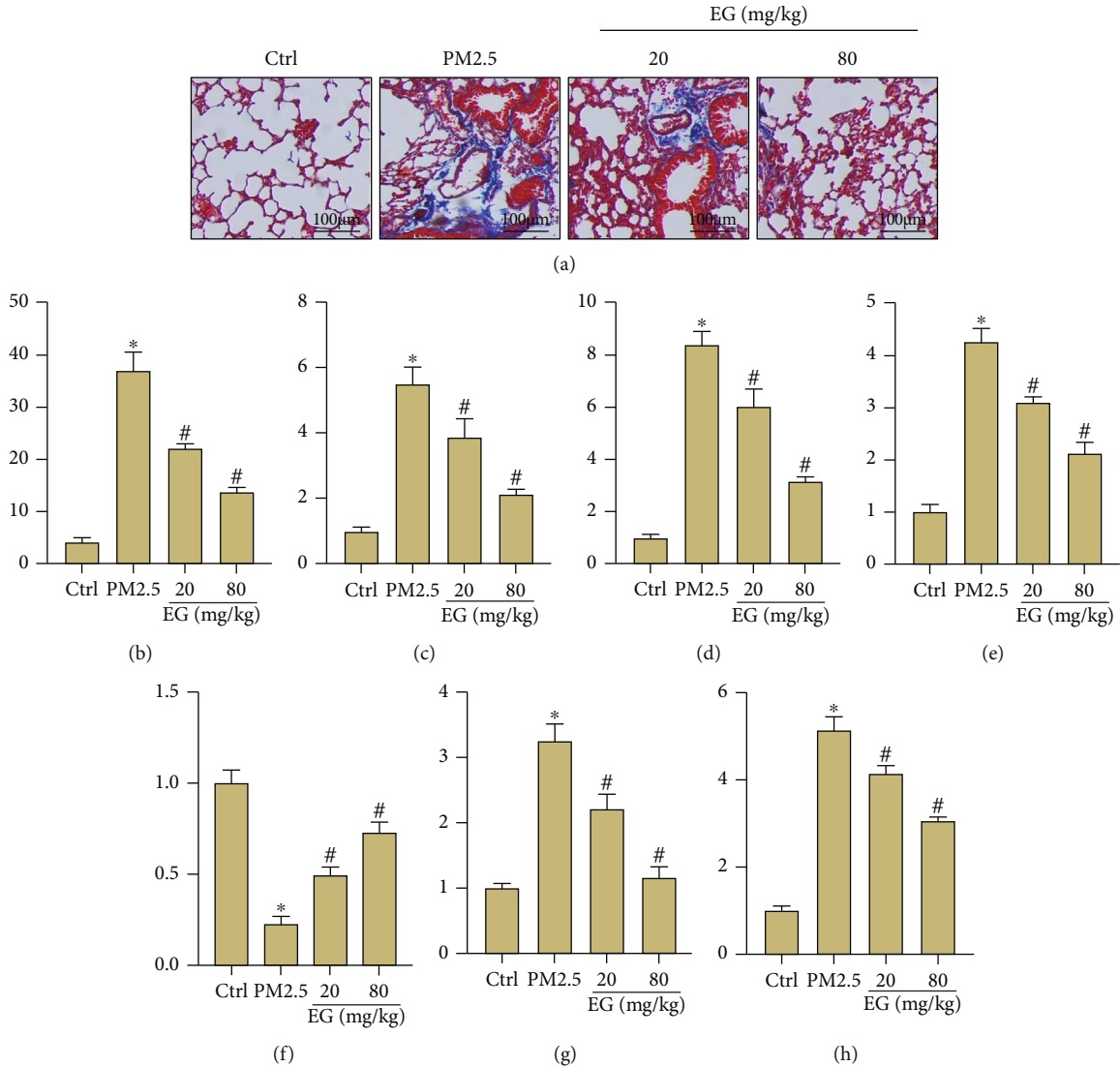


FIGURE 3: EG alleviated fibrosis and EMT in PM2.5-induced lung tissues. (a–b) Masson staining of lung tissues in the indicated groups and the quantification of fibrosis ($n = 5$). Original magnification $\times 200$. (c–e) Comparison of mRNA levels of fibrosis markers including collagen I, collagen III, and CTGF in lung tissues ($n = 5$). (f–h) Comparison of mRNA levels of EMT markers including E-Cadherin, α -SMA, and Snail in lung tissues ($n = 5$). * $P < 0.05$ vs. Ctrl group, # $P < 0.05$ vs. PM2.5 group.

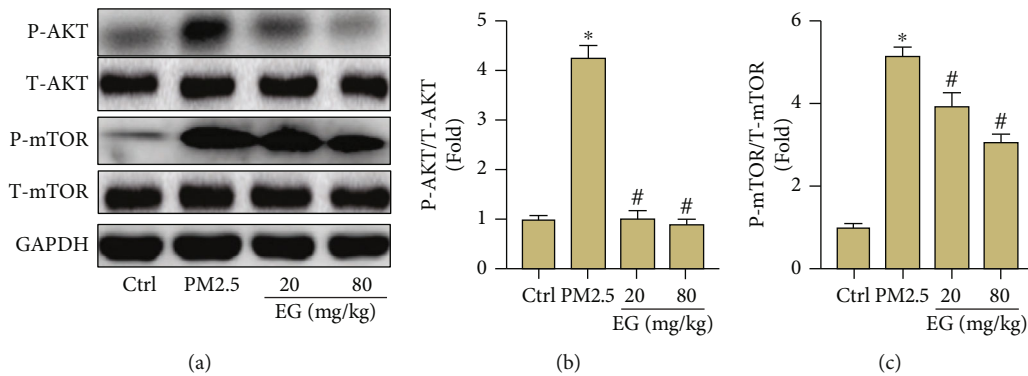


FIGURE 4: AKT/mTOR pathway was inhibited by EG in lung tissues treated with PM2.5. (a–c) Western blot analysis and statistical results for P-AKT, T-AKT, P-mTOR, and T-mTOR ($n = 5$). * $P < 0.05$ vs. Ctrl group, # $P < 0.05$ vs. PM2.5 group.

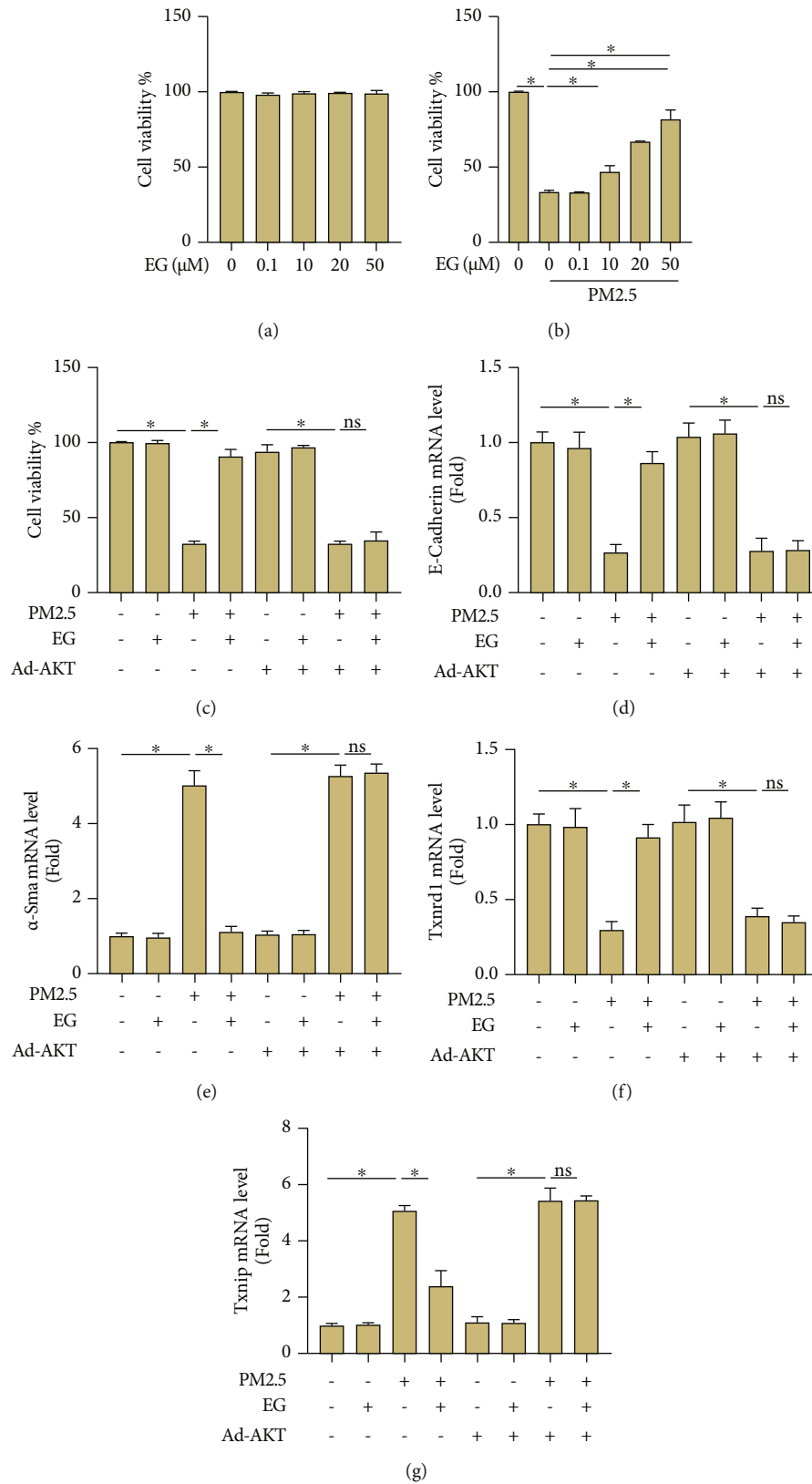


FIGURE 5: EG relieved EMT and oxidative stress in PM2.5-induced lung epithelial cells in an AKT-dependent manner. (a) Cell viability of lung epithelial cells treated with different concentrations of EG (n = 5). (b) Cell viability of PM2.5-induced lung epithelial cells treated with different concentrations of EG (n = 5). (c). Cell viability of PM2.5-induced lung epithelial cells treated with EG (20 μM) after AKT was overexpressed by adenovirus infection (n = 5). (d–e) Comparison of mRNA levels of EMT markers including E-Cadherin and α-SMA in the indicated groups (n = 5). *P < 0.05 vs. the indicated groups; ns: no significance.

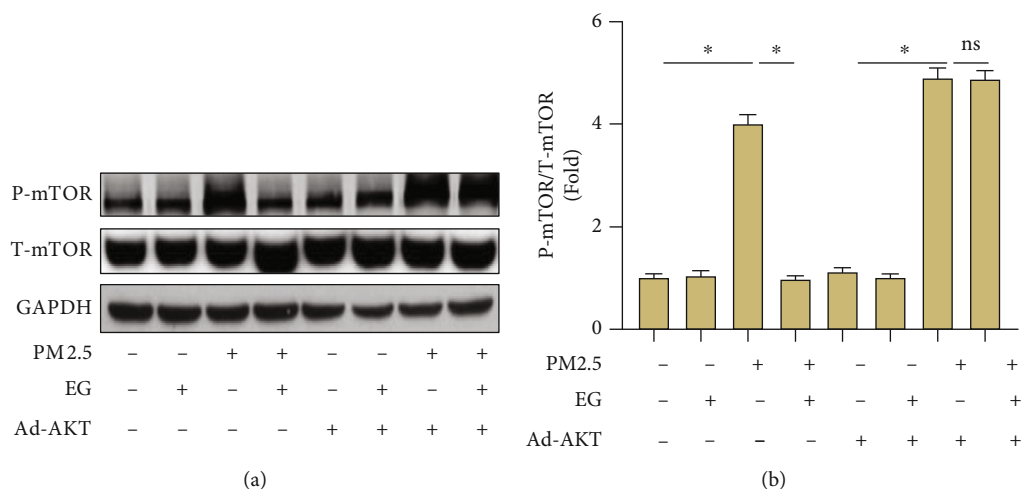


FIGURE 6: AKT/mTOR pathway was involved in pulmonary protection from EG in PM2.5-induced lung epithelial cells. (a–b) Western blot analysis and statistical results for P-mTOR and T-mTOR ($n = 5$). * $P < 0.05$ vs. the indicated groups; ns: no significance.

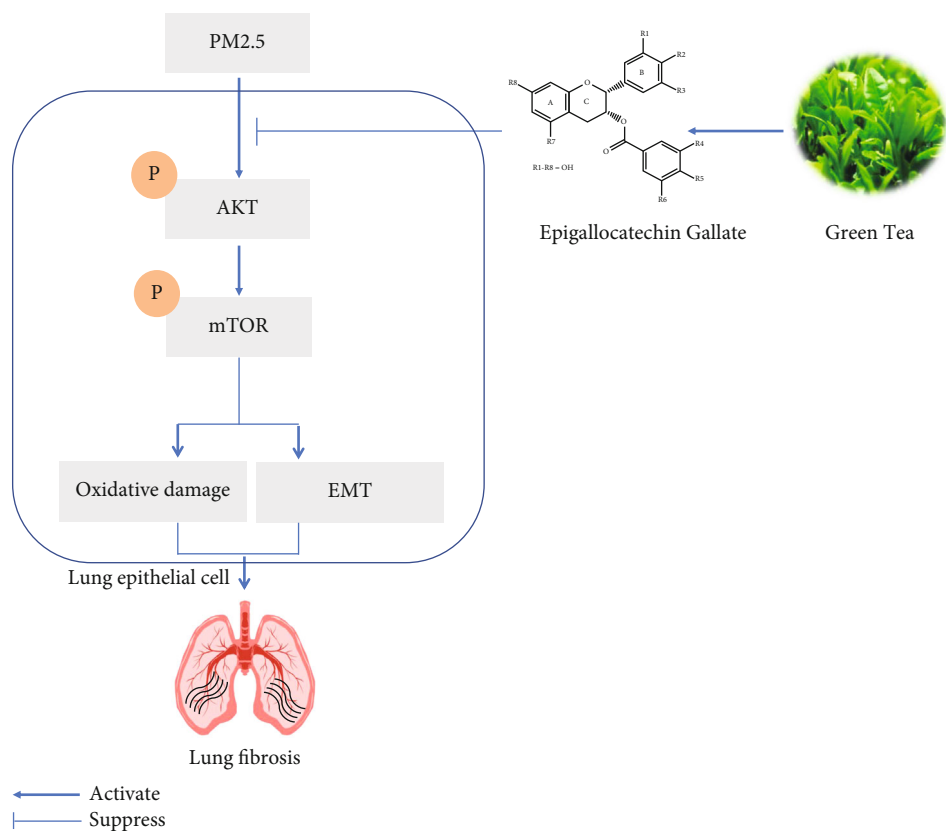


FIGURE 7: The possible mechanisms by which EG relieves PM2.5-induced lung fibrosis. PM2.5 could increase the phosphorylation of AKT, which subsequently phosphorylated mTOR in lung epithelial cell. The activated AKT/mTOR pathway further gave rise to oxidative damage and EMT, eventually causing lung fibrosis. The natural epigallocatechin gallate extracted from green tea could block the activation of AKT/mTOR, thus improving PM2.5-induced lung fibrosis by decreasing oxidative damage and EMT.

PM2.5, a significant reduction of some antioxidant factors including nuclear factor erythroid 2-related factor 2 (Nrf2), total superoxide dismutase, and heme oxygenase-1 was observed [37]. These studies hinted that oxidative stress serves as one critical mechanism contributing to PM2.5-induced lung fibrosis and injury. On the other one hand,

the interaction between epithelial cells and basal lamina could be altered by PM2.5, reflected by cytoskeletal and extracellular matrix with mesenchymal features [38]. In the present study, PM2.5 exposure promoted the development of EMT and oxidative damage *in vivo* and *in vitro*, which was significantly blocked by EG treatment.

Both AKT and mTOR (known as the mechanistic target of rapamycin) are serine-threonine protein kinases, participating in protein synthesis, metabolism pathways, autophagy, cell proliferation, and cell growth [39]. Activated AKT could phosphorylate mTOR, promoting the conversion of lung epithelial cells to fibroblasts, inducing lung fibrosis [40]. Additionally, the activation of AKT/mTOR pathway also gives rise to oxidative stress, which further aggravated the development of fibrosis [29, 41]. Here, our study unveiled that EG treatment not only decreased oxidative stress but also inhibited EMT during PM2.5-induced lung fibrosis by blocking the activation of AKT/mTOR pathway. In fact, Nrf2 also serves as a critical transcription factor in the development of fibrosis and antioxidant response. To be more specific, Nrf2 could dissociate from Keap1 and translocate to the nucleus. Subsequently, the transcriptional activity of Nrf2 is enhanced to activate the expression of some antioxidative genes [42, 43]. Previous study has unveiled that the activation of Nrf2 was also regulated by AKT, which was also involved in inflammatory and oxidative damage. Therefore, one of the limitations in the present study is that the status of Keap1/Nrf2 pathway was not investigated [44].

Natural therapeutic approaches have been recorded over 3,000 years. The secondary metabolites from natural products act as an endless frontier to develop compounds with medical and pharmaceutical purpose [45]. Green tea, a very popular beverage globally, is rich in flavonoids and phenolic acids, exhibiting important nutraceutical and medical properties [46]. EG is one of the most important polyphenolic compounds, owing seven hydroxyl radicals among three aromatic rings [47]. Previous studies reported that EG exerted antifibrotic effects by reducing collagen synthesis and blocking the major fibrosis-related pathways in keloids [48]. Also, in nonalcoholic fatty liver disease and cardiac remodeling, EG could decrease fibrogenic reaction and oxidative damage [18, 49]. Meanwhile, EG displays significant inhibitory effects on AKT/mTOR pathway in some diseases [50, 51]. In keeping with these studies, our results also disclosed that EG significantly decreased oxidative stress, apart from inhibiting the inflammatory factors including TNF- α , IL-1 β , and MCP-1 in mice exposed to PM2.5. And the protective effects of EG on mice exposed to PM2.5 were mediated by AKT/mTOR pathway.

In conclusion, we found that EG improved PM2.5-induced lung fibrosis by decreasing oxidative damage and EMT in an AKT-dependent manner. The present study provides proofs for the application of EG in the treatment of PM2.5-induced lung fibrosis.

Data Availability

All data supporting the findings in our study are available from the corresponding author upon reasonable request.

Conflicts of Interest

The authors declare no conflicts of interest.

Authors' Contributions

Zhou Zhongyin conceived and designed the experiments. Wang Wei, Xiong Juan, and Wang Wei carried out the experiments. Fan Guohua analyzed the data. Wang Wei completed the manuscript. All authors contributed to the article and approved the submitted version. Zhou Zhongyin and Wang Wei contributed equally to this work.

Acknowledgments

This work was supported by grants from Key Laboratory Opening Project of Hubei Province (no. 2021KFY052).

References

- [1] M. L. Aix, P. Petit, and D. J. Bicout, "Air pollution and health impacts during the COVID-19 lockdowns in Grenoble, France," *Environmental Pollution*, vol. 303, article 119134, 2022.
- [2] Q. Sun, X. Ren, Z. Sun, and J. Duan, "The critical role of epigenetic mechanism in PM2.5-induced cardiovascular diseases," *Genes and Environment*, vol. 43, no. 1, p. 47, 2021.
- [3] X. Guo, Y. Lin, Y. Lin et al., "PM2.5 induces pulmonary microvascular injury in COPD via METTL16-mediated m6A modification," *Environ Pollut*, vol. 303, article 119115, 2022.
- [4] L. Wang, Y. Cui, H. Liu, J. Wu, J. Li, and X. Liu, "PM2.5 aggravates airway inflammation in asthmatic mice: activating NF- κ B via MyD88 signaling pathway," *International Journal of Environmental Health Research*, pp. 1–12, 2022.
- [5] L. A. McGuinn, C. K. Ward-Caviness, L. M. Neas et al., "Association between satellite-based estimates of long-term PM_{2.5} exposure and coronary artery disease," *Environmental Research*, vol. 145, pp. 9–17, 2016.
- [6] Y. Gao, Q. Zhang, J. Sun et al., "Extracellular vesicles derived from PM2.5-exposed alveolar epithelial cells mediate endothelial adhesion and atherosclerosis in ApoE^{-/-} mice," *The FASEB Journal*, vol. 36, no. 2, article e22161, 2022.
- [7] M. M. Dysart, B. R. Galvis, A. G. Russell, and T. H. Barker, "Environmental particulate (PM2.5) augments stiffness-induced alveolar epithelial cell mechanoactivation of transforming growth factor beta," *PLoS One*, vol. 9, article e106821, no. 9, 2014.
- [8] X. Lv, C. Liu, S. Liu et al., "The cell cycle inhibitor P21 promotes the development of pulmonary fibrosis by suppressing lung alveolar regeneration," *Acta Pharmaceutica Sinica B*, vol. 12, no. 2, pp. 735–746, 2022.
- [9] V. C. Auyeung, M. S. Downey, M. Thamsen et al., "IRE1 α drives lung epithelial progenitor dysfunction to establish a niche for pulmonary fibrosis," *American Journal of Physiology Lung Cellular and Molecular Physiology*, vol. 322, no. 4, pp. L564–L580, 2022.
- [10] M. J. Roberts, L. T. May, A. C. Keen et al., "Inhibition of the proliferation of human lung fibroblasts by prostacyclin receptor agonists is linked to a sustained cAMP signal in the nucleus," *Frontiers in Pharmacology*, vol. 12, article 669227, 2021.
- [11] J. X. Duan, X. X. Guan, H. H. Yang et al., "Vasoactive intestinal peptide attenuates bleomycin-induced murine pulmonary fibrosis by inhibiting epithelial-mesenchymal transition:

- restoring autophagy in alveolar epithelial cells,” *International Immunopharmacology*, vol. 101, Part B, article 108211, 2021.
- [12] O. A. Grigorieva, M. A. Vigovskiy, U. D. Dyachkova et al., “Mechanisms of endothelial-to-mesenchymal transition induction by extracellular matrix components in pulmonary fibrosis,” *Bulletin of Experimental Biology and Medicine*, vol. 171, no. 4, pp. 523–531, 2021.
- [13] H. Ruan, S. Gao, S. Li et al., “Deglycosylated azithromycin attenuates bleomycin-induced pulmonary fibrosis via the TGF- β 1 signaling pathway,” *Molecules*, vol. 26, no. 9, p. 2820, 2021.
- [14] Y. Lu, Y. Zhang, Z. Pan et al., “Potential “therapeutic” effects of tocotrienol-rich fraction (TRF) and carotene “against” bleomycin-induced pulmonary fibrosis in rats via TGF- β /Smad, PI3K/Akt/mTOR and NF- κ B signaling pathways,” *Nutrients*, vol. 14, no. 5, p. 1094, 2022.
- [15] L. Lin, L. Zeng, A. Liu et al., “Role of epigallocatechin gallate in glucose, lipid, and protein metabolism and L-theanine in the metabolism-regulatory effects of epigallocatechin gallate,” *Nutrients*, vol. 13, no. 11, p. 4120, 2021.
- [16] A. E. Bulboacă, A. S. Porfire, V. Rus, C. A. Nicula, C. A. Bulboacă, and S. D. Bolboacă, “Protective effect of liposomal epigallocatechin-gallate in experimental gentamicin-induced hepatotoxicity,” *Antioxidants*, vol. 11, no. 2, p. 412, 2022.
- [17] B. Y. Li, H. Y. Li, D. D. Zhou et al., “Effects of different green tea extracts on chronic alcohol induced-fatty liver disease by ameliorating oxidative stress and inflammation in mice,” *Oxidative Medicine and Cellular Longevity*, vol. 2021, Article ID 5188205, 17 pages, 2021.
- [18] Y. Cui, Y. Wang, and G. Liu, “Epigallocatechin gallate (EGCG) attenuates myocardial hypertrophy and fibrosis induced by transverse aortic constriction via inhibiting the Akt/mTOR pathway,” *Pharmaceutical Biology*, vol. 59, no. 1, pp. 1305–1313, 2021.
- [19] M. Wang, H. Zhong, X. Zhang et al., “EGCG promotes PRKCA expression to alleviate LPS-induced acute lung injury and inflammatory response,” *Scientific Reports*, vol. 11, no. 1, article 11014, 2021.
- [20] Z. L. Luo, H. Y. Sun, X. B. Wu, L. Cheng, and J. D. Ren, “Epigallocatechin-3-gallate attenuates acute pancreatitis induced lung injury by targeting mitochondrial reactive oxygen species triggered NLRP3 inflammasome activation,” *Food & Function*, vol. 12, no. 12, pp. 5658–5667, 2021.
- [21] H. Shen, N. Wu, Z. Liu, H. Zhao, and M. Zhao, “Epigallocatechin-3-gallate alleviates paraquat-induced acute lung injury and inhibits upregulation of toll-like receptors,” *Life Sciences*, vol. 170, pp. 25–32, 2017.
- [22] X. D. Zhao, H. Liu, T. Li, Q. Gong, and W. L. Zhang, “Epigallocatechin Gallate attenuates hip fracture-induced acute lung injury by limiting mitochondrial DNA (mtDNA) release,” *Medical Science Monitor*, vol. 23, pp. 3367–3372, 2017.
- [23] F. Guohua, Z. Tiejuan, M. Xinpeng, and X. Juan, “Melatonin protects against PM2.5-induced lung injury by inhibiting ferroptosis of lung epithelial cells in a Nrf2-dependent manner,” *Ecotoxicology and Environmental Safety*, vol. 223, article 112588, 2021.
- [24] L. Yang, G. Liu, X. Li et al., “Small GTPase RAB6 deficiency promotes alveolar progenitor cell renewal and attenuates PM2.5-induced lung injury and fibrosis,” *Cell Death & Disease*, vol. 11, no. 10, p. 827, 2020.
- [25] L. Hou, J. Zhang, Y. Liu et al., “MitoQ alleviates LPS-mediated acute lung injury through regulating Nrf2/Drp1 pathway,” *Free Radical Biology & Medicine*, vol. 165, pp. 219–228, 2021.
- [26] Z. G. Ma, Y. P. Yuan, X. Zhang, S. C. Xu, S. S. Wang, and Q. Z. Tang, “Piperine attenuates pathological cardiac fibrosis via PPAR- γ /AKT pathways,” *eBioMedicine*, vol. 18, pp. 179–187, 2017.
- [27] Y. Zhang, S. Liu, X. Li, and J. Ye, “Protective effect of fasudil on hydrogen peroxide-induced oxidative stress injury of H9C2 cardiomyocytes,” *Disease Markers*, vol. 2021, Article ID 8177705, 9 pages, 2021.
- [28] M. Xu, X. Wang, L. Xu et al., “Chronic lung inflammation and pulmonary fibrosis after multiple intranasal instillation of PM2.5 in mice,” *Environmental Toxicology*, vol. 36, no. 7, pp. 1434–1446, 2021.
- [29] X. Zhang, Z. Liu, W. Yang et al., “Tetrahydrofolate alleviates the inhibitory effect of oxidative stress on neural stem cell proliferation through PTEN/Akt/mTOR pathway,” *Oxidative Medicine and Cellular Longevity*, vol. 2022, Article ID 9021474, 18 pages, 2022.
- [30] Y. Zhang, N. Yin, A. Sun et al., “Transient receptor potential channel 6 knockout ameliorates kidney fibrosis by inhibition of epithelial-mesenchymal transition,” *Frontiers in Cell and Development Biology*, vol. 8, article 602703, 2020.
- [31] J. Saers, L. Andersson, C. Janson, and J. Sundh, “Respiratory symptoms, lung function, and fraction of exhaled nitric oxide before and after assignment in a desert environment—a cohort study,” *Respiratory Medicine*, vol. 189, article 106643, 2021.
- [32] D. Tian, X. Chen, P. Hou et al., “Effects of exposure to fine particulate matter on the decline of lung function in rural areas in northwestern China,” *Environmental Science and Pollution Research International*, vol. 29, no. 10, pp. 14903–14913, 2022.
- [33] T. Zhao, W. Qi, P. Yang et al., “Mechanisms of cardiovascular toxicity induced by PM_{2.5}: a review,” *Environmental Science and Pollution Research* volume, vol. 28, no. 46, pp. 65033–65051, 2021.
- [34] R. Zheng, L. Tao, H. Jian et al., “NLRP3 inflammasome activation and lung fibrosis caused by airborne fine particulate matter,” *Ecotoxicology and Environmental Safety*, vol. 163, pp. 612–619, 2018.
- [35] S. Li, S. Cao, X. Duan et al., “Long-term exposure to PM2.5 and children’s lung function: a dose-based association analysis,” *Journal of Thoracic Disease*, vol. 12, no. 10, pp. 6379–6395, 2020.
- [36] L. Yang, Z. Lin, Y. Wang et al., “Nickel(II) ions exacerbate bleomycin-induced pulmonary inflammation and fibrosis by activating the ROS/Akt signaling pathway,” *Environmental Science and Pollution Research International*, vol. 25, no. 5, pp. 4406–4418, 2018.
- [37] J. Wang, Y. Li, P. Zhao et al., “Exposure to air pollution exacerbates inflammation in rats with preexisting COPD,” *Mediators of Inflammation*, vol. 2020, Article ID 4260204, 12 pages, 2020.
- [38] W. Liu, C. Gao, H. Dai et al., “Immunological pathogenesis of membranous nephropathy: focus on PLA2R1 and its role,” *Frontiers in Immunology*, vol. 10, p. 1809, 2019.
- [39] C. Shen, Y. He, Q. Chen et al., “Narrative review of emerging roles for AKT-mTOR signaling in cancer radioimmunotherapy,” *Ann Transl Med*, vol. 9, no. 20, p. 1596, 2021.

- [40] J. Wang, K. Hu, X. Cai et al., "Targeting PI3K/AKT signaling for treatment of idiopathic pulmonary fibrosis," *Acta Pharmaceutica Sinica B*, vol. 12, no. 1, pp. 18–32, 2022.
- [41] Z. He, S. Chen, T. Pan et al., "Ginsenoside Rg2 ameliorating CDAHFD-induced hepatic fibrosis by regulating AKT/mTOR-mediated autophagy," *Journal of Agricultural and Food Chemistry*, vol. 70, no. 6, pp. 1911–1922, 2022.
- [42] J. Li, Z. Yu, B. Han et al., "Activation of the GPX4/TLR4 signaling pathway participates in the alleviation of selenium yeast on deltamethrin-provoked cerebrum injury in quails," *Molecular Neurobiology*, vol. 59, no. 5, pp. 2946–2961, 2022.
- [43] X. Yang, Y. Fang, J. Hou et al., "The heart as a target for deltamethrin toxicity: inhibition of Nrf2/HO-1 pathway induces oxidative stress and results in inflammation and apoptosis," *Chemosphere*, vol. 300, article 134479, 2022.
- [44] U. Farooq, M. U. K. Sahibzada, T. Khan et al., "Folicitin isolated from hypericum oblongifolium exerts neuroprotection against lipopolysaccharide-induced neuronal synapse and memory dysfunction via p-AKT/Nrf-2/HO-1 signalling pathway," *Evidence-based Complementary and Alternative Medicine*, vol. 2022, Article ID 9419918, 10 pages, 2022.
- [45] M. Condello and S. Meschini, "Role of natural antioxidant products in colorectal cancer disease: a focus on a natural compound derived from prunus spinosa, trigonotis," *Cell*, vol. 10, no. 12, article 3326, 2021.
- [46] E. Mancini, C. Beglinger, J. Drewe, D. Zanchi, U. E. Lang, and S. Borgwardt, "Green tea effects on cognition, mood and human brain function: a systematic review," *Phytomedicine*, vol. 34, pp. 26–37, 2017.
- [47] M. Pervin, K. Unno, A. Takagaki, M. Isemura, and Y. Nakamura, "Function of green tea catechins in the brain: epigallocatechin gallate and its metabolites," *International Journal of Molecular Sciences*, vol. 20, no. 15, p. 3630, 2019.
- [48] G. Park, B. S. Yoon, J. H. Moon et al., "Green tea polyphenol epigallocatechin-3-gallate suppresses collagen production and proliferation in keloid fibroblasts via inhibition of the STAT3-signaling pathway," *The Journal of Investigative Dermatology*, vol. 128, no. 10, pp. 2429–2441, 2008.
- [49] G. Tang, Y. Xu, C. Zhang, N. Wang, H. Li, and Y. Feng, "Green tea and epigallocatechin gallate (EGCG) for the management of nonalcoholic fatty liver diseases (NAFLD): insights into the role of oxidative stress and antioxidant mechanism," *Antioxidants*, vol. 10, no. 7, article 1076, 2021.
- [50] Z. H. Liao, H. Q. Zhu, Y. Y. Chen et al., "The epigallocatechin gallate derivative Y₆ inhibits human hepatocellular carcinoma by inhibiting angiogenesis in MAPK/ERK1/2 and PI3K/AKT/HIF-1 α /VEGF dependent pathways," *Journal of Ethnopharmacology*, vol. 259, article 112852, 2020.
- [51] R. Wei, N. E. C. Penso, R. M. Hackman, Y. Wang, and G. G. Mackenzie, "Epigallocatechin-3-gallate (EGCG) suppresses pancreatic cancer cell growth, invasion, and migration partly through the inhibition of Akt pathway and epithelial-mesenchymal transition: enhanced efficacy when combined with gemcitabine," *Nutrients*, vol. 11, no. 8, p. 1856, 2019.

Review Article

Ginger for Healthy Ageing: A Systematic Review on Current Evidence of Its Antioxidant, Anti-Inflammatory, and Anticancer Properties

Mehtap Ozkur ¹, Necla Benlier ¹, Işıl Takan ^{2,3}, Christina Vasileiou ⁴,
Alexandros G. Georgakilas ⁴, Athanasia Pavlopoulou ^{2,3}, Zafer Cetin ^{5,6},
and Eyup Ilker Saygili ^{7,8}

¹Department of Medical Pharmacology, Faculty of Medicine, SANKO University, Gaziantep, Turkey

²Izmir Biomedicine and Genome Center, Balçova, Izmir 35340, Turkey

³Izmir International Biomedicine and Genome Institute, Dokuz Eylül University, Balçova, Izmir 35220, Turkey

⁴DNA Damage Laboratory, Physics Department, School of Applied Mathematical and Physical Sciences, National Technical University of Athens, 157 80 Athens, Greece

⁵Department of Medical Biology, School of Medicine, SANKO University, Gaziantep, Turkey

⁶Department of Biological and Biomedical Sciences, Graduate Education Institute, SANKO University, Gaziantep, Turkey

⁷Department of Medical Biochemistry, School of Medicine, SANKO University, Gaziantep, Turkey

⁸Department of Molecular Medicine, Graduate Education Institute, SANKO University, Gaziantep, Turkey

Correspondence should be addressed to Mehtap Ozkur; mozkur@sanko.edu.tr, Alexandros G. Georgakilas; alexg@mail.ntua.gr, and Eyup Ilker Saygili; isaygili@sanko.edu.tr

Received 23 February 2022; Accepted 11 April 2022; Published 9 May 2022

Academic Editor: German Gil

Copyright © 2022 Mehtap Ozkur et al. This is an open access article distributed under the Creative Commons Attribution License, which permits unrestricted use, distribution, and reproduction in any medium, provided the original work is properly cited.

The world's population is ageing at an accelerated pace. Ageing is a natural, physiological but highly complex and multifactorial process that all species in the Tree of Life experience over time. Physical and mental disabilities, and age-related diseases, would increase along with the increasing life expectancy. Ginger (*Zingiber officinale*) is a plant that belongs to the Zingiberaceae family, native to Southeast Asia. For hundreds of years, ginger has been consumed in various ways by the natives of Asian countries, both as culinary and medicinal herb for the treatment of many diseases. Mounting evidence suggests that ginger can promote healthy ageing, reduce morbidity, and prolong healthy lifespan. Ginger, a well-known natural product, has been demonstrated to possess antioxidant, anti-inflammatory, anticancer, and antimicrobial properties, as well as an outstanding antiviral activity due to a high concentration of antiviral compounds. In this review, the current evidence on the potential role of ginger and its active compounds in the prevention of ageing is discussed.

1. Introduction

According to the World Population Prospects 2019, it is estimated that one in six people will be over the age of 65 (16%) by 2050 and 1 in every 11 people (9%) in 2019, respectively [1]. Ageing is a natural, physiological but highly complex, multifactorial process that all organisms go through. The life expectancy is increasing at a steady pace, and as a result, the age-related diseases as well as the physical and mental dis-

abilities increase accordingly. While 80% of older people suffer from an age-related disease such as diabetes, hypertension, or heart disease, 50% have at least two age-related conditions. In fact, ageing has been considered as a “risk factor” for several diseases including cancer, diabetes, osteoarthritis, and cardiovascular and neurologic conditions [2, 3]. These diseases and disabilities pose a serious threat to the health of older people, thereby decreasing their quality of life and life expectancy. The biological consequences of

ageing remain largely unelucidated. However, studies in the last two decades have provided valuable information on the underlying cellular and molecular mechanisms of ageing and related diseases [4, 5].

Humans have used herbs for thousands of years to treat a variety of ailments. Clinical studies and epidemiological data suggest that some plant-based natural products may reduce and delay the molecular and cellular degradation over time as much as possible and also increase longevity in humans [4]. In this context, plant-based natural products can also be promising for the prevention and treatment of ageing and age-related diseases [6–8].

2. Ginger

Ginger (*Zingiber officinale*) is a member of the Zingiberaceae plant family, native to Southeast Asia. For centuries, ginger has been consumed in different ways by Asia's indigenous peoples, mainly in China and India, both as spice and sweetener in the local cuisine and as herbal medicine for treating many diseases. Specifically, in the traditional Chinese, Indian, and Ayurvedic medicine, ginger is believed to have therapeutic effects. It is used as a remedy for cough relief due to its expectorant action to loosen and expel phlegm. Ginger is also used for pain alleviation, treatment of nausea, vomiting, and poisoning and for facilitating digestion [9]. Currently, it is known that ginger has antioxidant, anti-inflammatory, and antitumor properties and its effectiveness in the prophylaxis and treatment of gastrointestinal, cardiovascular, respiratory, and neurological diseases has been demonstrated by several research studies [10]. Rhizome is the edible part of the plant. The nutraceutical value of ginger is attributed to the bioactive compounds contained in the rhizome, such as gingerols (GNs), shogaols (SGs), paradols, and zingiberene [9]. Volatile phenolic compounds, mainly 6-GN, as well as 4-, 8-, 10-, and 12-GNs, found in fresh ginger rhizome give ginger its pungent fragrance and unique aroma. These compounds are sensitive to pH and temperature changes, and gingerols are rapidly converted to their corresponding 6-, 8-, and 10-SGs during processes that require extreme heat such as drying and roasting. Extracts derived from rhizomes and processing methods may vary widely on chemical composition and associated properties, with dried ginger as a key player in antioxidant activity. Dry ginger powder is also known as *Sonth* in Hindi, *Sonti* in Telugu, *Soonth* in Gujarati, *Suntha* in Marathi, and *Shunti* in Kannada. The major phenolic compounds in ginger are mainly gingerols, the active constituent of fresh ginger. The other major polyphenols are abundant in active phytochemicals such as shogaols, paradols, zerumbone, zingerone, gingerols, and 1-dehydro-(10) gingerdione. Shogaols can be derived from ginger with heat treatment or long-term storage. Paradols can form shogaols after hydrogenation. Besides these, ginger raw fiber is also involved in polysaccharides, lipids, and organic acids. Ginger active compounds are critically implicated in different biological activities such as anti-inflammatory, antitumor, antimicrobial, and antioxidant activities (Figure 1) [10]. Therefore, dried ginger rhizome represents the major source of 6-SG which is the

most prominent dehydration product [11] (Figure 2). Recent studies have demonstrated that 6-SG has superior biological actions as compared to 6-GN [12, 13] with no associated side effects, and, as such, shuntha is considered more powerful medicinally than raw ginger [14, 15].

3. Ginger and Healthy Ageing

Active and healthy ageing is defined as the maintenance of one's ability to perform activities of daily living without being affected by cognitive and functional impairment and chronic illnesses [16]. Mounting evidence suggests that ginger can promote healthy ageing, reduce morbidity, and prolong healthy lifespan [16, 17]. For over three decades, studies have reported that the antioxidant, anti-inflammatory, antimicrobial, antitumor, and antihypercholesterolemic features of the bioactive compounds found in ginger account for its aforementioned health benefits [10, 17] (Figure 2).

It is believed that ginger can also protect, prevent, and even treat many diseases related to ageing by modulating molecular targets involved in their pathogenesis [6]. Furthermore, Natural Language Processing (NLP) was applied to uncover words most closely related to ginger. Briefly, PubMed literature search and article collection were conducted using the keyword "ginger". The natural language toolkit (NLTK: <https://www.nltk.org/>) and spaCy (<https://spacy.io/>), in a Python environment, were used for text processing. The word embedding algorithm Word2vec in the Gensim library in Python (<https://pypi.org/project/gensim/>) was used to train word vectors in the processed text. A list of all word-to-word distances was compiled. The similarity distances between each word pair were calculated using the *Word2Vec.most_similar* function in Gensim Word2vec model. Of the 4464 candidate articles, 4009 met the inclusion criteria, such as written in English, included an abstract, and contained adequate text. Only those words that appeared more than five times (i.e., minimum frequency threshold) were vectorized. The network depicted in Figure 3 provides information on the semantic terms associated with ginger, many of them related to the health effects of ginger.

Several of the health benefits of ginger and the underlying biological mechanisms are described below.

3.1. Ginger against Oxidative Stress. Free radicals are highly reactive atoms or molecules with one or more unpaired electrons in their outer shells. Reactive oxygen species (ROS) are formed when oxygen reacts with certain molecules in all aerobic cells. ROS can lead to the oxidative modification of major cellular macromolecules such as carbohydrates, lipids, proteins, and DNA [18]. The free radical ageing theory, later termed as "oxidative stress theory of ageing," is based on the hypothesis that age-related functional losses actually result from the accumulation of this oxidative damage.

Oxidative stress is associated with the reduced production of antioxidant enzymes and the activation of inflammatory pathways. Therefore, both oxidative stress and chronic inflammation lead to many molecular and cellular changes including genomic instability, epigenetic alterations,

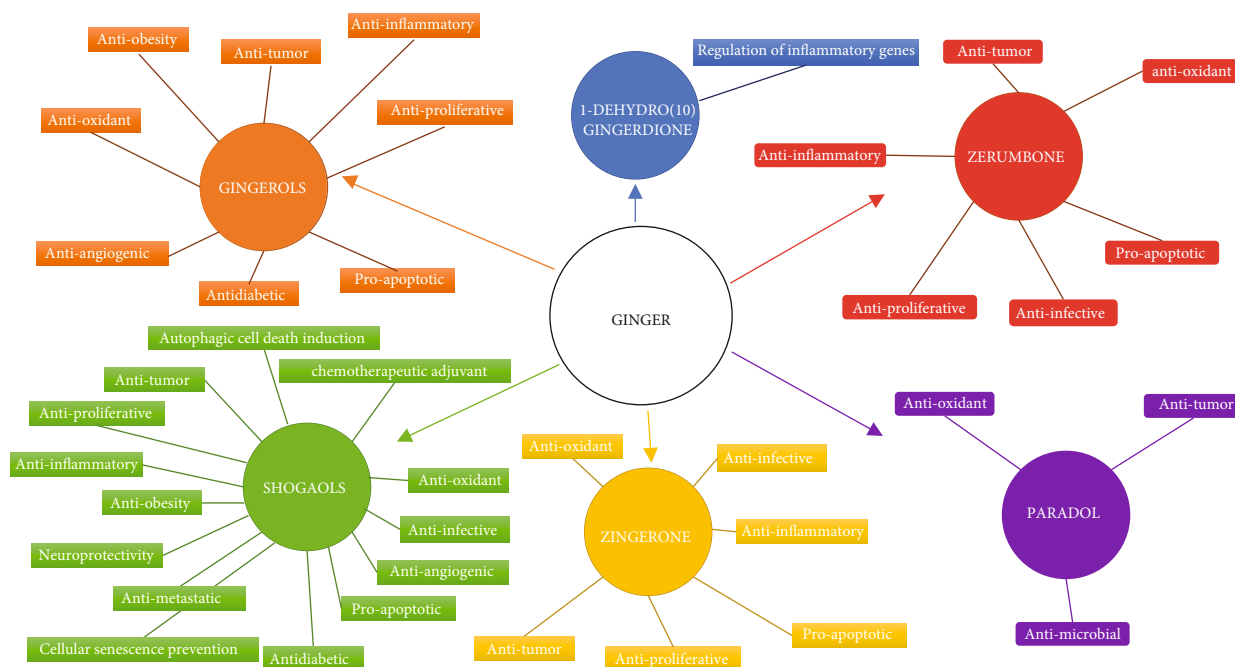


FIGURE 1: Illustration of the wide range of the health effects of ginger. A great range of those natural products' beneficial effects for the human organism have been verified and investigated at a molecular and mechanistic basis. Emphasis is given in this review on the antioxidant, anti-inflammatory, and anticarcinogenic properties of ginger.

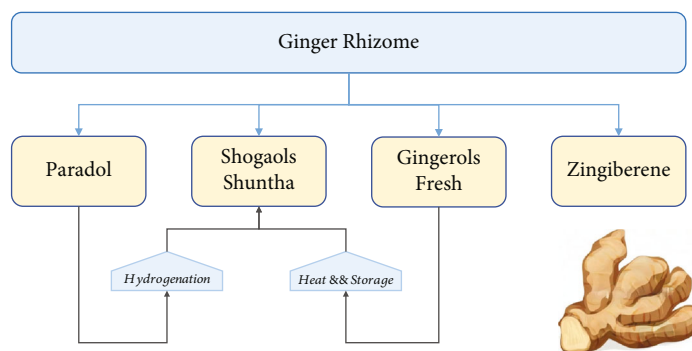


FIGURE 2: Ginger rhizome active compounds.

mitochondrial dysfunction, cellular senescence, and stem cell loss. These physiological/pathological changes play a key role in the development of age-related metabolic and degenerative disorders as well as cell ageing [18].

Several phytochemical extracts from ginger have been demonstrated to possess a number of antioxidant properties, like scavenging superoxide, hydroxyl, and nitric oxide radicals *in vitro* in a dose-dependent manner [19]. In one study, pretreatment with ginger extract inhibited the IL-1 β -induced elevation of ROS and lipid peroxidation and significantly the increased gene expression of the corresponding antioxidant enzymes in C28/I2 human chondrocytes [20]. In rats, ginger showed a marked renoprotective effect on biochemical, histological, and immunohistochemical markers in nephrotoxicity induced by gentamicin and cadmium; this effect was attributed to the antioxidant and free radical scavenging activities of polyphenolic compounds such as 6-GN

and 6-SG [21, 22]. Exogenous 6-SG and 6-, 8-, and 10-GN exhibited considerable antioxidant activities, with IC₅₀ values ranging from 8.05 to 26.3 μ M against DPPH (1,1-diphenyl-2-picrylhydrazyl) radical, 0.85-4.05 μ M against superoxide radicals, and 0.72-4.62 μ M against hydroxyl radicals. In that study, 6-SG was reported as the most potent antioxidant and anti-inflammatory compound, with 6-GN exhibiting the least antioxidant activity [23].

In addition to antioxidant activity, the bioactive components of ginger can also exert a modulating effect on antioxidant enzymes or enzymatic systems. In a study investigating the effect of ginger extract on oxidative hepatic toxicity induced by lead acetate (PbAc) in rats, the extract reduced the levels of malondialdehyde (MDA), a marker of oxidative stress in the liver, and caused a significant increase both in the concentration (by 112-228%) and mRNA expression (1.4- to 8-fold) of antioxidant enzymes and molecules

methods including sun drying (at 28–44°C for 3 days), oven drying (at 60°C for 4 days), and freeze drying (at -30°C for 3 days) on the antioxidant and anti-inflammatory activities of ginger rhizome, all drying processes, primarily sun drying, were reported to enhance the aforementioned properties of the plant significantly as compared to fresh ginger [33].

In a study examining the effects of storage time and temperature on the activities of ginger phytochemical compounds such as phenolics, flavonoids, 6-GN, and 6-SG, storage temperature was observed to affect free radical scavenging activity to a greater extent than storage time. It has been suggested that when stored at 5°C, the qualities of fresh rhizome can be preserved for up to 4 months in terms of both antioxidant and antibacterial activities [34].

There is a growing interest globally in organic farming because organic foods are considered healthier. In a study by Min and colleagues, it was found that organic ginger rhizomes and leaves have a significantly greater phytochemical and antioxidant capacity than their nonorganic counterparts. Moreover, applications of mycorrhiza combined with tissue culture for organic farming resulted in a marked increase in the total phenolic and flavonoid contents, as well as 6-GN and 8-gingerol concentrations, in ginger rhizomes [35].

3.2. Anti-Inflammatory and Immunomodulatory Activities.

Inflammation can be defined as the body's protective response that develops following invasion by microorganisms, antigen exposure, and damage to cells and tissues. It involves complex interactions among many cell types, mediators, receptors, and signaling pathways. In particular, chronic inflammation has a central role in the pathogenesis of many diseases such as atherosclerosis, cancer, diabetes, and rheumatoid arthritis as well as ageing. Studies have long shown that ginger and its various active compounds have anti-inflammatory activity. It was initially suggested that the anti-inflammatory activity of ginger is mainly associated with its inhibitory action on prostaglandin and leukotriene synthesis [15]. Both fresh ginger (mainly composed of gingerols) and dried ginger extracts (major source of shogaols) were demonstrated to inhibit lipopolysaccharide- (LPS-) induced prostaglandin E2 (PGE2) production [36, 37]. This activity of 6-, 8-, and 10- gingerols was attributed to their inhibitory action on COX-2 mRNA expression and the corresponding COX-2 enzyme, with 10-gingerol exhibiting the strongest inhibitory effect depending on the length of the side chains. However, 6-, 9-, and 10-shogaols were found to have lesser inhibitory effect on COX-2 mRNA expression [38].

In a carrageenan-induced rat paw edema model in which the anti-inflammatory activity of ginger extract was evaluated at different doses, the extract was shown to reduce the levels of the inflammatory mediators PGE2, TNF- α , IL-6, monocyte chemoattractant protein-1 (MCP-1), and myeloperoxidase (MPO) by 32% to 60% in a dose-dependent manner (25–200 mg/kg). The anti-inflammatory activity of ginger extract was found to be significantly greater than that of diclofenac at the same concentration, and 6-SG was more potent than other shogaols. At a dose of 200 mg/kg, ginger

extract prevented histopathological effects induced by carrageenan and increased total antioxidant capacity. The authors suggested that the anti-inflammatory activity of ginger extract mainly involves inhibition of cell migration and activation of inflammatory cells [39].

Several studies showed that 6-GN (i) inhibited inducible nitric oxide synthase (iNOS) and TNF- α expression in mouse macrophages stimulated by LPS, (ii) reduced IL-6, IL-8, and ROS levels in hepatic HuH7 cells stimulated by IL-1 β , (iii) decreased IL-8, IL-6, IL-1 β protein, and mRNA levels in intestinal epithelial cell inflammation induced by *Vibrio cholerae*, (iv) reduced secretion and expression of TNF- α , IL-1 β , IL-6, PGE2, COX-2, and iNOS in murine RAW 264.7 monocyte/macrophage-like cells exposed to LPS, and (v) downregulated expression of iNOS and COX-2 protein in murine skin cells exposed to 12-O-tetradecanoylphorbol 13-acetate (TPA) by either modulating or inhibiting a NF- κ B- (nuclear factor kappa-light-chain-enhancer of activated B cells-) mediated signaling pathway or via its interaction with various endogenous mediators such as PI3K/Akt/I kappaB kinases (IKK) and MAPK [40–44]. In addition, the inhibitory effect of 6-GN on COX-2 enzyme has been reported to contribute to its anti-inflammatory activity [41].

Systemic administration of 6-GN caused hypothermia by slowing the metabolic rate in rats and led to inhibition of acetic acid-induced writhing response and formalin-induced licking time in mice. These data suggest that 6-GN may potentially have antipyretic and analgesic properties as well as anti-inflammatory activity [45, 46].

It was reported that 6-SG inhibited the release of TNF- α , IL-1 β , and NO in LPS-activated RAW264.7 macrophages, suggesting that it may have a therapeutic potential in chronic inflammatory events primarily involving macrophages [47]. It was also shown to inhibit activation of a NF- κ B-mediated pathway and subsequent release of TNF- α , IL-1 β , IL-6, and PGE2 in BV2 microglia cells exposed to LPS. Upregulation of peroxisome proliferator-activated receptor gamma (PPAR- γ) by 6-SG was found to play a role in its anti-inflammatory action [48].

Toll-like receptors (TLRs) play a crucial role in innate immunity. TLRs are expressed by the elements of the innate body defense system such as macrophages and dendritic cells and trigger the immune system following breaching of physical barriers, such as skin or intestinal mucosa, by microorganisms. During this process, myeloid differentiation factor 88 (MyD88) and Toll-interleukin-1 (IL-1) receptor domain-containing adapter inducing interferon beta (TRIF) act as signal transducers. In one study by Park et al., 6-SG was shown to inhibit activation of NF- κ B and IRF3, as well as their target genes, COX2 and IFN- β , by suppressing the TRIF pathway of TLR3 and TLR4 [49]. These data provide important clues for elucidating the anti-inflammatory mechanism(s) of action of 6-SG in bacterial and viral infections. Moreover, the antipyretic and analgesic effects of 6-GN, as compared to 6-SG, were found to be more potent, when both were administered intravenously at doses ranging from 1.75 to 3.5 mg/kg and orally at doses from 70 to 140 mg/kg [50].

According to two recently published meta-analyses, where the effects of ginger supplementation on inflammatory markers in humans were examined, significantly lower levels of serum CRP, TNF- α , IL-6, and PGE2 were reported within a period of 2-3 months versus controls [51, 52].

In male endurance runners, intake of 500 mg capsules of ginger powder during a 6-week vigorous training period significantly lowered the postexercise levels of the proinflammatory cytokines IL-1 β , IL-6, and TNF- α , known as “indicators of athletes’ acute immune function,” and also reduced the fatigue-like symptoms induced by these cytokines [53].

3.3. DNA Damage and Ginger’s Anticancer Activity. Data in literature are mainly focused on the actions of a ginger extract, the polyphenolic alkenone, 6-GN [2, 54]. Anticancer, anti-inflammatory, antitumor, and proapoptotic activities have been identified as potential effects of 6-GN. Relevant effects have been found in a variety of cancers [55–62]. The underlying biological pathways include, but are not limited to, DNA damage-associated cell cycle regulation, apoptosis, and chromatin regulation. These effects, in combination with the absence of toxicity in healthy cells, can have promising future use in clinical setup underlining its differential effect on cancer and normal cells.

Results from human cervical cancer cells *in vitro* and *in vivo* have shown that 6-GN treatment may significantly increase DNA damage [63]. Results from the sensitive and reliable biomarker of gamma-H2AX have shown that the main pathway depends on the generation of intracellular ROS, which led to p53 reactivation followed by the p53-mediated G2/M cell cycle arrest. Amplification of apoptotic effects of cisplatin also occurred, presumably due to ROS-mediated induction of DNA damage and increased apoptotic effects. Similar results are also present in both acute and chronic myeloid leukemia cell lines, as examined via p-H2AX and comet assay in Rastogi et al.’s study [54]. Increased levels of the phosphorylated histone do confirm significant underlying DNA damage. Cell viability assays were also performed in this study where ROS-mediated DNA damage resulted in G2/M cell cycle arrest. This was further validated with flow cytometry-based TUNEL assay. Significant cell cycle arrest at G2/M checkpoint has also been observed in human colon cancer cell lines; the increased population of cells in G2 phase in combination with p53 phosphorylation indicates increased DNA damage effects [64]. Apart from 6-GN, another phenolic agent extract from ginger, zingerone, has shown comparable effects in colon cancer cells. Comet assay results indicate a significant increase in DNA damage following zingerone treatment in these cell lines, leading to decreased cell proliferation and proapoptotic effects. Herein, there is a possible speculation on the involvement of the ROS-mediated apoptosis pathway.

A different experimental setup has been employed in murine sarcoma cell lines by Lima et al. [57], where decreased cell viability was observed in high concentration of 6-GN compared to another antineoplastic agent. In this study, a cytogenetic approach of micronuclei formation

was employed, where at high concentrations nucleoplasmic bridges and nuclear buds were observed with concomitant increase in apoptosis. Interestingly, pretreatment with 6-GN may also enhance IR-induced cell apoptosis in gastric cancer cell lines [55]. This piece of evidence, in combination with cell proliferation inhibition and increased cell radio sensitization, can be taken into consideration in the combined therapeutic effects of chemoradiotherapy. Radiosensitization in cancer cell lines has also been reported in colorectal cancer cell lines, where Zerumbone pretreatment is associated with radiation-induced cell cycle arrest and apoptosis [65]. Concurrently, the dose and route of administration-dependent (comparing to earlier studies) radioprotective effects in mice have been reported for another hydroalcoholic extract of ginger rhizome, zinger. Radiation toxicity syndromes and associated lethality presented ameliorated effects in whole body gamma irradiation [66]. 10-Gingerol (10-GN) reports, albeit limited, are aiming towards similar direction as 6-GN. Decreased cell proliferation and accumulation of cells in S phase (cell cycle arrest) were reported in TNBC [67] and human colon cancer cells [68].

On the other hand, the results on the influence of simple dietary change, where mice were pretreated with samples of a lyophilized extract of rhizome ginger (i.e., hydroalcoholic extraction containing ~2.54% gingerols), are not in agreement with previous reports on the inhibition of bladder cancer induced by N-butyl-N-(4-hydroxybutyl) nitrosamine mouse bladder tumors [67].

Studies on ginger spice as supplement (i.e., powder ethanol-dried) have demonstrated the protective effects and decrease in DNA damage induced by hydrogen peroxide in 3T3-L1 fibroblasts. Ginger, as compared to other dietary supplements, showed significant DNA protective activity in various concentrations and also the overall maximum antioxidant activity [69].

The incidence rate of the majority of cancers is increasing with age (<https://www.cancer.gov/about-cancer/causes-prevention/risk/age>). Despite extensive research efforts on elucidating the molecular basis of cancer and developing strategies for its accurate diagnosis and effective treatment, cancer remains a major health problem with a rapidly increasing incidence. This has attracted interest for functional foods that are believed to have cancer preventive and tumor growth retarding potential. Over the last 25 years, many studies have demonstrated chemopreventive potential for the active compounds of ginger such as 6-GN and 6-SG in animal models, cell lines, and human cancers. The anti-neoplastic activities of these compounds have been associated with their antioxidant, anti-inflammatory, antiangiogenic, antiproliferative, and proapoptotic features.

Similarly, an active ingredient of ginger, 6-SG, has been found to inhibit breast cancer cell invasion, by reducing matrix metalloproteinase-9 expression via blockade of NF- κ B activation. In addition, 6-SG was demonstrated to induce apoptosis in hepatocellular carcinoma, NB4, MOLT4, and Raji leukemia cells and prostate cancer cells by modulating endoplasmic reticulum stress and a caspase-3-mediated pathway, p53, BAX and BCL2, and STAT3 pathways,

respectively [70–72]. Recently, Bawadood et al. suggested that 6-SG suppressed autophagy in breast cancer cells and also induced apoptosis by targeting the NOTCH signaling pathway [73].

However, a recent study demonstrated that ginger extract suppresses progression of cell cycle in the human pancreatic PANC-1 cancer cell line and induces autotic cell death. Unlike apoptosis and necroptosis, autosis results in a variety of morphological changes in cancer cells including nuclear shrinking, focal membrane rupture, electron-dense mitochondria, and vacuolation. In the same study, both the ginger extract and 6-SG were reported to increase the LC3-II/LC3-I ratio and decrease SQSTM1/p62 expression and, at the same time, activate AMPK and inhibit mTOR, all of which are indicators of autophagy. The authors concluded that ginger exerts its anticancer activity by inducing the formation of ROS in cancer cells [74]. Similarly, 6-SG was shown to induce autophagic cell death by promoting LC3 expression in breast cancer cells and by inhibiting the AKT/mTOR pathway in non-small-cell lung cancer A549 cells [75, 76].

Although the findings of these studies seem to contradict those of previous studies, data suggest that autophagy is a strategic survival mechanism, that is, cancer cells may have turned to autophagy to escape apoptotic death [75].

It was considered that PTHrP, which is normally secreted by some cancer cells, may promote metastasis to the bone by interacting with osteoblasts and osteoclasts [77]. The chemical agent 2-amino-1-methyl-6-phenylimidazo [4,5-b] pyridine (PhIP) is found in processed and red meat and is regarded as a potential carcinogen for renal cell carcinoma (RCC). Human 786-O renal cell carcinoma cells upon induction by PhIP showed increased secretion of both parathyroid hormone-related protein (PTHrP) and IL-8. Subsequently, cultures of human osteoblasts with PhIP-stimulated condition medium of 786-O increased the expression of the macrophage colony-stimulating factor (M-CSF) and receptor activator of NF- κ B ligand (RANKL) and decreased the expression of osteoprotegerin (OPG). It was reported that 6-SG decreased PTHrP and IL-8 expression in RCC cells and decreased RANK expression in osteoblasts. Overall, these findings demonstrate that PhIP is an important risk factor for bone metastasis in RCC and may enhance osteoclastic bone resorption, suggesting that 6-SG could exhibit antimetastatic activity by blocking PhIP-induced bone resorption in an *in vitro* RCC model [77].

Meanwhile, it was observed that 6-GN, the other bioactive compound of ginger, downregulates the NF- κ B, AKT, and *Bcl2* genes in HeLa cells and increases the expression of TNF α , BAX, and *cytochrome c* as well as *caspase-3* and *PARP*. These data suggest that 6-GN induces death of cancer cells possibly through caspase-3-mediated apoptosis and autophagy [78]. In another study, treatment with 6-GN inhibited cell growth and colony formation in a time- and dose-dependent manner in renal cell carcinoma, by exerting its effect on the AKT-GSK 3 β -cyclin D1 signaling pathway, and caused cell cycle arrest at the G1 phase [79].

Benzo(a)pyrene intake is known to play a pivotal role in the development of colorectal cancer in humans. In a

murine colorectal cancer model induced by benzo(a)pyrene, 6-GN was shown to inhibit tumorigenesis via its anti-inflammatory, antiproliferative, antiangiogenic, and apoptotic actions [80]. Moreover, 6-GN was reported to exhibit anti-inflammatory activity by decreasing TNF- α , IL-1 β , INOS, and COX-2 expression and also inhibit cell proliferation by increasing the expression of *WNT3a*, *DVL-2*, and β -*catenin* and, conversely, decreasing *cyclin D1* and *Ki 67* expression. In the same study, 6-GN displayed antiangiogenic activity by reducing the expression of *VEGF*, *angiopoietin-1*, *FGF*, and *GDF-15* and also apoptotic activity by increasing *APC* and *p53* expression [80]. A semisynthetic derivative of 6-GN (i.e., SSi6) was reported to both inhibit migration and invasion of cancer cells and exhibit cytotoxic effect on human epithelial-like breast cancer cells [81].

3.3.1. Ginger Supplements. In a population of humans at high risk for colorectal cancer, supplementation with ginger extract at a dose of 2 g/day for 28 days reduced the expression of the telomerase reverse transcriptase (hTERT) and MIB-1 (epitope of Ki-67), two markers of cell proliferation, and elevated the expression of the *BAX* gene (an indicator of apoptosis) as demonstrated by biopsy samples of colon mucosa [82]. In another study, supplementation with ginger extract was found to decrease *COX-1* expression in individuals at increased risk for developing colorectal cancer. It is known that the COX-1 enzyme has an integral role in the synthesis of PGE2, which is primarily involved in the development of colorectal cancer. This finding suggests that ginger supplementation may lower the risk for developing colorectal cancer through its COX-1 inhibitory effect [83].

3.3.2. Ginger in Antineoplastic Combination Therapies. Combination therapy with two or more drugs or agents can elicit a synergistic and/or additive effect in the treatment of cancer and reduce drug resistance and drug toxicity. The combination of γ -tocotrienol and 6-GN was shown to induce cytotoxicity and apoptosis synergistically in HT-29 and SW837 human colorectal cancer cells [84]. In another study conducted by the same research team, the combination of ginger extract and Gelam honey was reported to exhibit chemopreventive activity in HT29 colon cancer cells by modulating the Ras/ERK and PI3K/AKT pathways in a synergistic manner [85]. Additionally, treatment with a combination of 6-GN and epigallocatechin gallate (EGCG), the latter with reported antineoplastic properties, was shown to synergistically induce apoptosis and inhibit growth of cancer cells [86].

In a murine breast cancer model, Ashmawy et al. demonstrated that combined use of ginger extract with doxorubicin (DOX) increases the survival rate of mice as compared to the group receiving DOX alone, reduces tumor mass, and increases apoptosis [87]. Recently, 6-SG was shown to increase the antineoplastic efficacy of the anticancer drugs 5-fluorouracil, oxaliplatin, and irinotecan in SW480 and SW620 colon cancer cell lines by increasing their ability to induce apoptosis and autophagy [88]. The aforementioned data suggest that addition of ginger extract

or 6-SG in conventional chemotherapeutic regimens may improve treatment outcomes [87, 88].

3.3.3. Ginger in Nausea and Vomiting Induced by Antineoplastic Drugs. Nausea and vomiting are the most frequent and bothersome side effects experienced by cancer patients receiving chemotherapy. Despite the availability of effective drug and antineoplastic combination therapies in recent years, the treatment success rate is not adequate [89]. Several animal and human studies reported that ginger extract can be effective in the management of chemotherapy-induced nausea and vomiting (CINV) [90]. CINV is classified as both acute and delayed side effect according to the time of onset. In two recent meta-analyses, ginger (in the form of oral extracts or capsules) was found to be more effective in preventing acute nausea and vomiting in patients receiving chemotherapy treatment [91]. It was concluded that its antiemetic effect was more pronounced especially when ginger supplementation was received at a maximum dose of 1 g for more than 3 days, starting from the first day of chemotherapy [92]. The mechanism of action of ginger and its active components in CINV remain unclear. Studies have reported that ginger shows an antagonistic action by binding to a distinct site on 5HT-3 receptors, other than the sites that antiemetic drugs (e.g., ondansetron) bind to and, therefore, may elicit a synergistic inhibitory effect when administered with 5HT-3 receptor antagonists [90]. Additionally, many preclinical studies demonstrated that the inhibitor activity of ginger in CINV is mediated by its antagonistic effects on neurokinin-1 and dopamine receptors, together with its antioxidant and anti-inflammatory actions [90].

3.4. Neuroprotective Activity. The prevalence of neurodegenerative diseases such as Alzheimer's disease, Parkinson's disease, and dementia increases with ageing. Recent studies have suggested that ginger may have neuroprotective effects on these chronic, noncurable disorders mediated by mechanisms other than those underlying its known antioxidant, anti-inflammatory, and antiapoptotic properties [6].

3.4.1. Alzheimer's Disease. Alzheimer's disease (AD) is the most common neurodegenerative disorder in the elderly. AD is a progressive disorder and one of the major causes of dementia in this age group. It is characterized by β -amyloid protein deposition leading to plaque formation, aggregates of hyperphosphorylated *tau* protein that form tangles of neurons, oxidative stress, and reduction in acetylcholinesterase (AChE) levels in certain areas of the brain [4].

In a rat model of AD induced by oral aluminum chloride and injection of intracerebroventricular β -amyloid protein, ginger extract was shown to increase SOD and CAT expression in the brain and decrease secretion and expression of NF- κ B, IL-1 β , and MDA levels, leading in this way to improvement of the behavioral dysfunction [93]. In a murine model of AD induced by injection of β -amyloid plaques, fermented ginger (to increase bioavailability) was reported to significantly reduce synaptic disorder and neuron cell loss as compared to nonfermented ginger [94]. In

a separate study, ginger extract was found to inhibit AChE activity as well as lipid peroxidation induced by administration of prooxidant substances in the rat brain [95].

Cholinergic neuron loss in the hippocampus is associated with memory loss and attention problems in AD. In an HT22 hippocampal neuron cell culture known to express cholinergic markers, 6-SG reduced the production of hydrogen peroxide (H_2O_2) ROS and increased cholinergic activity. The brain-derived neurotrophic factor has been suggested to contribute to the neuroprotective effect of 6-SG [96]. In a mouse model of AD induced by β -amyloid protein, 6-SG was shown to exert neuroprotective effects via its antagonistic action against the cysteinyl leukotriene 1 receptor, which is known to have a central role in the pathogenesis of AD [94]. In mouse hippocampal HT22 cells, 6-SG activated sortilin-related receptor 1 (SORL1), which is reported to decrease amyloid precursor protein in the brain [97].

Additionally, by investigating the effects of 6-GN on cytotoxicity and apoptotic cell death induced by β -amyloid in rat pheochromocytoma cells (PC12 cells) and human neuroblastoma SH-SY5Y cells, 6-GN was observed to decrease ROS levels and increase the antioxidant enzyme activity in these cells [98, 99]. In middle-aged women, ginger extract supplementation was found to improve cognitive function when received at a dose of 400-800 mg daily [100].

3.4.2. Parkinson's Disease. Parkinson's disease (PD) is a neurodegenerative disorder characterized by a progressive loss of dopamine-producing neurons in certain regions of the brain with ageing [6].

In a murine model of PD induced by 1-methyl-4-phenyl-4-propionoxypiperidine (MPTP), ginger extract was shown to protect neurons against apoptosis, increase dopamine levels in the globus pallidus and striatum, and reduce TNF- α , NO, and ROS levels, resulting in this way in improved PD symptoms of motor coordination disorder and bradykinesia [101]. In another study, 6-SG was reported to exert neuroprotective effects *in vivo* (C57/BL cells) and *in vitro* (rat mesencephalic cell cultures) PD models [102].

Recent studies have demonstrated that the treatment of intestinal dysfunction is important in neurodegenerative disorders such as PD. In C57BL/6J mice (i.e., resistant to audiogenic seizures) with intestinal damage induced by MPTP, ginger and 6-SG suppressed the elevation of NOS, TNF- α , and IL-1 β , exhibited protective effects on enteric dopaminergic neurons, and maintained intestinal integrity [103].

3.5. Cardioprotective Activity. Ageing is one of the leading risk factors for developing cardiovascular diseases. It is known that dyslipidemia and hypertension are important predisposing factors for many cardiovascular conditions including coronary heart disease and stroke. Recent studies have shown that ginger and some of its active constituents may be useful in lowering blood lipid levels and blood pressure and preventing platelet aggregation.

It was reported that intravenous administration of fresh ginger extract lowers blood pressure in anesthetized rats, and this activity was attributed to its inhibitory effect on voltage-dependent calcium channels [104]. In a rat model

of hypertension induced by the NOS inhibitor L-NAME, pretreatment with ginger rhizomes was shown to lower blood pressure, inhibit the angiotensin-1-converting enzyme (ACE) and arginase activities, and increase vasodilator nitric oxide (NO) levels [105]. Another study showed that 6-GN inhibits the activation of angiotensin II type 1 receptors [106]. As it is known, ACE converts angiotensin I to angiotensin II, which is a potent vasoconstrictor peptide primarily involved in the pathogenesis of hypertension and exerts its effect via angiotensin II type 1 receptors. In a study where several *in vitro* cell cultures were used, 6-GN was reported to normalize the expression of major biomarkers related to hypertension through the peroxisome proliferator-activated receptor delta (PPAR δ) [107]. Recently, in a rat hypertension model induced by L-NAME, *Zingiber officinale* was reported to increase both the antihypertensive effectiveness and plasma concentration of losartan, an antihypertensive drug and an angiotensin II type 1 receptor antagonist [108]. These data suggest that ginger may also act on hepatic microsomal enzymes that are involved in the metabolism of some antihypertensive drugs.

In a meta-analysis of clinical trials, it was concluded that ginger supplementation at a dose of >3 g daily for two months is effective in lowering blood pressure in middle-aged individuals [109].

Elevation of blood lipids is considered the leading cause of atherosclerosis. In rats fed a high-fat diet, the combination of aerobic exercise and ginger extract resulted in a significant reduction in serum triglyceride (TG), low-density lipoprotein (LDL), and total cholesterol levels and a marked increase in the levels of high-density lipoprotein (HDL); these observations suggest that ginger may confer protection against atherosclerosis [110]. Of note, in recent years, it has been reported that oxidation of apoA-I, a component of HDL, may result in the production of dysfunctional HDL in hyperlipidemic states. In one study, ginger extract was found to stimulate functional HDL production by restoring apoA-I function via inhibition of oxidative stress in hamsters fed a high-fat diet. In the same study, it was also found that ginger increased fecal excretion of cholesterol [111].

Transforming-growth factor beta (TGF- β) increases the binding potential of LDL, by inducing proteoglycan synthesis in vascular smooth muscle cells. Because of this activity, which has a crucial role in the development of atherosclerosis, TGF- β exhibits also proatherogenic properties. In one study, it was suggested that 6-GN may have a protective role against the development of atherosclerosis by inhibiting proteoglycan synthesis [112].

Many recent studies have demonstrated blood-lowering effects of ginger supplementation in humans. A significant reduction in serum/cholesterol levels was reported in hyperlipidemic patients who were given ginger supplement at a dose of 3 g/day for 45 days in one study and for 4 weeks in another study [113, 114].

Platelet aggregation is a well-established risk factor for coronary heart disease and stroke. Recently, potent *in vitro* antiplatelet activity of ginger was demonstrated in platelet aggregation stimulated by adenosine 5-diphosphate (ADP),

bovine thrombin, and arachidonic acid as compared to aspirin (positive control) [115].

3.6. Endocrine Diseases. Age is the major risk factor for the development of type 2 diabetes mellitus (DM). The pathogenesis of DM involves insulin resistance and pancreatic beta cell dysfunction.

In type 2 diabetic Lepr^{db/db} mice, 6-GN was shown to increase glucose-stimulated insulin secretion, which was mediated by glucagon-like peptide-1 (GLP-1). In the same study, 6-GN was reported to increase the presence of glucose transporter type 4 (GLUT-4) molecules in skeletal muscle cells and facilitate glycogen storage, resulting in this way to improvement of hyperglycemia [116].

In diabetes, long-standing hyperglycemia is known to induce protein glycation, which is associated with covalent binding of glucose to plasma proteins. In turn, protein glycation results in the formation of advanced glycation end products (AGEs), which accelerate the development of diabetic complications such as nephropathy, retinopathy, neuropathy, and cardiomyopathy. In an *in vitro* study, 6-GN and 6-SG were shown to inhibit protein glycation by trapping methylglyoxal, a highly reactive AGE precursor in diabetes [117].

Vascular calcification plays an important role in the morbidity and mortality in diabetic patients, due to associated cardiovascular complications. Recently, 6-SG has been shown to antagonize hyperglycemia-induced vascular calcification by inhibiting the Akt/ROS signaling pathway and NLRP3/caspase 1/IL-1 β inflammasome in human arterial smooth muscle cells [118]. In addition, treatment with ginger extract and 6-SG was reported to alleviate pain associated with diabetic neuropathy via its effects at the spinal cord [119].

In a recent meta-analysis, regular ginger supplementation (3 grams daily in some studies) [6] was reported to reduce fasting blood glucose concentration, insulin resistance, and HbA1c level in type 2 DM patients [120].

Collectively, these data suggest that ginger and its active components may have beneficial effects on the short- and long-term control of blood glucose, insulin resistance, and protective effects against the development of vascular complications in diabetes.

Obesity is an important risk factor for diabetes, hypertension, and many cardiovascular diseases, as well as an important metabolic disease that accelerates the ageing process.

PPAR δ is the main regulator of energy metabolism in skeletal muscle and adipose tissue. Activation of PPAR δ has been shown to induce fatty acid oxidation and reduce obesity in mice [121]. In one study, ginger extract reduced diet-induced obesity in mice and increased exercise endurance capacity by increasing skeletal muscle fat catabolism; it was suggested that this effect may be mediated by the modulatory actions of 6-SG and 6-GN on the PPAR δ signaling pathway [122].

Recent studies suggest that gut microbiota may represent an important target in the treatment of obesity. In a recent study, ginger supplementation has been reported to reduce

body weight, fatty liver, and insulin resistance by restoring gut microbiota in rats fed a high-fat diet [123].

Steamed ginger ethanolic extract (SGE) is rich in 6-SG. A marked reduction in average body weight, body mass index, and body fat content was observed in healthy obese individuals taking 100 mg SGE supplementation daily for 12 weeks [107, 124]. These findings suggest that supplementation with a ginger extract rich in 6-SG along with lifestyle changes, such as diet control and/or physical activity, may have a significant potential in lowering body mass index [124].

3.7. Anti-Infective Actions. Reduced immune function and comorbidities related to ageing increase the risk for developing infections in older people. Recent studies have shown that ginger and its bioactive constituents have antibacterial, antifungal, and antiviral activities. In particular, ginger and/or its active components were reported to be active against drug-resistant bacteria such as *Escherichia coli*, *Salmonella typhi*, *Staphylococcus aureus*, *Pseudomonas aeruginosa*, *Mycobacterium tuberculosis*, and *Enterococcus faecalis* and fungi such as *Candida albicans* [14, 125, 126].

The cytokine interferon- γ (IFN- γ), which is produced by natural killer cells and activated by T lymphocytes, has a critical role in protecting our body against viral and bacterial infections. 6-SG was found to enhance IFN- γ transcription and expression in a dose-dependent manner in human T lymphocyte cells [127].

3.8. Ginger and COVID-19. Ginger has been demonstrated to have an outstanding antiviral activity due to a high concentration of antiviral compounds [14, 128]. Coronavirus disease 2019 (COVID-19) is an infectious respiratory tract disease caused by the severe acute respiratory syndrome coronavirus 2 (SARS-CoV-2). Since its discovery in 2019, the virus has spread worldwide, causing the COVID-19 pandemic. The disease can be fatal especially in elderly infected patients with comorbidities [129]. Although there is no definitive treatment or a fully effective vaccine for COVID-19, extensive research is ongoing. The viral nonstructural protein 15 (Nsp15) is increasingly being considered as an important therapeutic target for the viral replication of SARS-CoV-2. In a recent *in vitro* study using hydroxychloroquine (one of the few drugs recommended for the management of COVID-19) as a positive control, it was suggested that gingerol can inhibit viral replication by binding to the Nsp15 viral protein of SARS-CoV-2 [130]. Additionally, in a very recent publication, it was stated that ginger extract may be used as an adjunctive treatment for COVID-19 due to its demonstrated beneficial effects in acute respiratory distress syndrome (ARDS), pulmonary fibrosis, pneumonia, and sepsis, which also occur in COVID-19 patients [131]. In 2020, Ahkam et al. designed an *in silico* study to investigate the potential utilization of the antiviral properties of ginger in counteracting SARS-CoV-2 infection based on the interaction of ligand ginger compounds with the viral spike (S) protein and main protease (MPro) [132]. Thus, a promising therapeutic strategy would be to develop structure-dependent antiviral drugs based on phytochemical compounds that inhibit essential SARS-CoV-2 proteins.

3.9. Sarcopenia. Sarcopenia is an age-related condition characterized by reduced skeletal muscle mass, muscle atrophy, and functional loss. It represents a significant health problem in the elderly, since it is associated with slowing of movements, imbalance, pain, and serious injuries due to falls. There is currently no medical treatment available for sarcopenia. However, various management approaches have been proposed (reviewed in Rondanelli et al. (2016)) to delay sarcopenia progression including an adequate and balanced diet and regular exercise [133].

Myoblasts are the primary progenitor cells that differentiate in the embryonic phase and play an integral role in the development of muscle tissue. One study reported overproduction of ROS, an increase in oxidative stress markers, and a reduction in myogenic differentiation and proliferation capacity in senescent myoblasts [133]. In a more recent *in vitro* study, a standardized ginger extract containing 6-GN and 6-SG was shown to prevent cellular senescence and promote myoblast differentiation in myoblast cells [134]. Moreover, many studies demonstrated that ginger supplementation at a dose of 2–4 g daily may alleviate muscle pain related to vigorous exercise and reduce the loss of muscle strength [133]. These data suggest that ginger and its active nutraceuticals may have a beneficial role in sarcopenia by reversing the ageing of myoblasts, possibly through their antioxidant and anti-inflammatory activities, and may be effective for maintaining the overall skeletal muscle health.

3.10. Osteoarthritis. Osteoarthritis is the most common joint disease in the world, characterized by degeneration of cartilage, pain, inflammation, impaired mobility, and dysfunction, especially in older populations. Although osteoarthritis is not regarded as an inflammatory arthritis, its pathogenesis involves various degrees of inflammation in the cartilage and surrounding tissues. Old age constitutes a risk factor for osteoarthritis. Osteoarthritis is among the leading causes of disability and chronic pain especially in individuals over the age of 65 years [135]. Ginger extract was shown to inhibit the production of the inflammatory mediators PGE2 and NO in osteoarthritic chondrocyte cell cultures in one study and, also, to inhibit oxidative stress and apoptosis in IL-1 β -induced C28I2 human chondrocytes [20, 136]. A very recent meta-analysis concluded that oral ginger supplementation is more effective in pain relief and improvement of joint function in patients with knee osteoarthritis as compared to placebo, possibly through its anti-inflammatory and antioxidant activities [137].

3.11. Skin Ageing. In addition to protecting the body from a large variety of external aggressors, the skin also has important cosmetic functions. Skin changes are among the most visible signs of ageing. Wrinkles, loss of elasticity, and laxity occur in the skin with ageing. Notably, long-term exposure to solar ultraviolet (UV) radiation is the major determinant for extrinsic skin ageing [138]. Fibroblast-derived elastase enzyme is known to contribute to the formation of wrinkles by causing loss of elasticity in the skin exposed to UV-B [139]. Ginger extract, previously shown to inhibit fibroblast-derived elastase, was reported to prevent UV-B-

induced loss of skin elasticity when administered topically to mouse and rat skin [139]. In another study, a reduction in the signs of skin ageing was observed in individuals using a ginger oil body cream for four weeks, probably attributed to the antioxidant activity of the plant [140].

4. Side Effects of Ginger

Ginger acts directly on the gastrointestinal tract by increasing muscle tone and peristalsis via its anticholinergic and antiserotonin action. Ginger can ameliorate the central nervous system side effects associated with antiemetic drugs. Similar to onion and garlic, ginger extracts can inhibit blood coagulation *in vitro* [141–143]. Ginger has few adverse effects, and only mild side effects have been reported including heartburn and diarrhea. In large doses, ginger may increase antiprostaglandin activity and gastric exfoliation *in vitro* [142, 143].

5. Conclusion and Future Directions

Ageing is a complex process that is determined by multiple and interdependent genetic, cellular, and environmental factors. Ginger, one of the most commonly used natural products both for gastronomic and medicinal purposes, has documented antioxidant, anti-inflammatory, anti-infection, and chemopreventive properties. In this review, the effectiveness of ginger in the prophylaxis and treatment of several and diverse ageing-associated diseases, like gastrointestinal, cardiovascular, respiratory, and neurological diseases, as well as the underlying biological mechanisms, is discussed thoroughly. However, the number of studies on the effective dosage, pharmacodynamics, and pharmacokinetics of ginger, which can be used to delay ageing and prevent degenerative diseases, is rather limited. Therefore, additional studies on ginger as a powerful natural product need to be conducted so as to enhance our understanding of the role and mechanism(s) of ginger in the prevention of disease.

Data Availability

The data used to support the findings of this study are all included and available within the article.

Conflicts of Interest

The authors declare no conflicts of interest.

Authors' Contributions

M.O. and E.I.S. were responsible for conceptualization; I.T. and A.P. were responsible for software; all authors were responsible for writing—original draft preparation; all authors were responsible for writing—review and editing; M.O., A.G.G., and E.I.S. were responsible for supervision; M.O., A.G.G., and E.I.S. were responsible for project administration. All authors have read and agreed to the current version of the manuscript.

References

- [1] U. Desa, *World population prospects 2019: highlights*, vol. 11, United Nations Department for Economic and Social Affairs, New York (US), 2019.
- [2] J. Shlisky, D. E. Bloom, A. R. Beaudreault et al., “Nutritional considerations for healthy aging and reduction in age-related chronic disease,” *Advances in Nutrition*, vol. 8, no. 1, pp. 17.2–1726, 2017.
- [3] T. Niccoli and L. Partridge, “Ageing as a risk factor for disease,” *Current Biology*, vol. 22, no. 17, pp. R741–R752, 2012.
- [4] Y. Liu, W. Weng, R. Gao, and Y. Liu, “New insights for cellular and molecular mechanisms of aging and aging-related diseases: herbal medicine as potential therapeutic approach,” *Oxidative Medicine and Cellular Longevity*, vol. 2019, Article ID 4598167, 25 pages, 2019.
- [5] K.-H. Wagner, D. Cameron-Smith, B. Wessner, and B. Franzke, “Biomarkers of aging: from function to molecular biology,” *Nutrients*, vol. 8, no. 6, p. 338, 2016.
- [6] N. F. N. Mohd Sahardi and S. Makpol, “Ginger (*Zingiber officinale* Roscoe) in the prevention of ageing and degenerative diseases: review of current evidence,” *Evidence-based Complementary and Alternative Medicine*, vol. 2019, Article ID 5054395, 13 pages, 2019.
- [7] I. Domínguez-López, M. Yago-Aragón, A. Salas-Huetos, A. Tresserra-Rimbau, and S. Hurtado-Barroso, “Effects of dietary phytoestrogens on hormones throughout a human lifespan: a review,” *Nutrients*, vol. 12, no. 8, p. 2456, 2020.
- [8] Y. Yang, C. Ren, Y. Zhang, and X. Wu, “Ginseng: an non-negligible natural remedy for healthy aging,” *Aging and Disease*, vol. 8, no. 6, pp. 708–720, 2017.
- [9] Y. Liu, J. Liu, and Y. Zhang, “Research progress on chemical constituents of *Zingiber officinale* Roscoe,” *BioMed research international*, vol. 2019, Article ID 5370823, 21 pages, 2019.
- [10] R. B. Semwal, D. K. Semwal, S. Combrinck, and A. M. Viljoen, “Gingerols and shogaols: important nutraceutical principles from ginger,” *Phytochemistry*, vol. 117, pp. 554–568, 2015.
- [11] S. Ok and W.-S. Jeong, “Optimization of extraction conditions for the 6-shogaol-rich extract from ginger (*Zingiber officinale* Roscoe),” *Preventive Nutrition and Food Science*, vol. 17, no. 2, pp. 166–171, 2012.
- [12] S. Bhattarai, V. H. Tran, and C. C. Duke, “Stability of [6]-gingerol and [6]-shogaol in simulated gastric and intestinal fluids,” *Journal of Pharmaceutical and Biomedical Analysis*, vol. 45, no. 4, pp. 648–653, 2007.
- [13] M. H. Pan, M. C. Hsieh, J. M. Kuo et al., “6-Shogaol induces apoptosis in human colorectal carcinoma cells via ROS production, caspase activation, and GADD 153 expression,” *Molecular Nutrition & Food Research*, vol. 52, no. 5, pp. 527–537, 2008.
- [14] Q.-Q. Mao, X.-Y. Xu, S.-Y. Cao et al., “Bioactive compounds and bioactivities of ginger (*Zingiber officinale* Roscoe),” *Food*, vol. 8, no. 6, p. 185, 2019.
- [15] A. H. Rahmani, “Active ingredients of ginger as potential candidates in the prevention and treatment of diseases via modulation of biological activities,” *International journal of physiology, pathophysiology and pharmacology*, vol. 6, no. 2, pp. 125–136, 2014.
- [16] W. H. Organization, *World report on ageing and health*, World Health Organization, 2015.

- [17] M. S. Butt and M. T. Sultan, "Ginger and its health claims: molecular aspects," *Critical Reviews in Food Science and Nutrition*, vol. 51, no. 5, pp. 383–393, 2011.
- [18] I. Liguori, G. Russo, F. Curcio et al., "Oxidative stress, aging, and diseases," *Clinical Interventions in Aging*, vol. 13, pp. 757–772, 2018.
- [19] G. Jagetia, M. Baliga, and P. Venkatesh, "Ginger (*Zingiber officinale* Rosc.), a dietary supplement, protects mice against radiation-induced lethality: mechanism of action," *Cancer Biotherapy & Radiopharmaceuticals*, vol. 19, no. 4, pp. 422–435, 2004.
- [20] A. Hosseinzadeh, K. B. Juybari, M. J. Fatemi et al., "Protective effect of ginger (*Zingiber officinale* roscoe) extract against oxidative stress and mitochondrial apoptosis induced by interleukin-1 β in cultured chondrocytes," *Cells, Tissues, Organs*, vol. 204, no. 5-6, pp. 241–250, 2017.
- [21] A. M. Hegazy, M. M. Mosaed, S. H. Elshafey, and N. A. Bayomy, "6-Gingerol ameliorates gentamicin induced renal cortex oxidative stress and apoptosis in adult male albino rats," *Tissue and Cell*, vol. 48, no. 3, pp. 208–216, 2016.
- [22] S. A. Gabr, A. H. Alghadir, and G. A. Ghoniem, "Biological activities of ginger against cadmium-induced renal toxicity," *Saudi Journal of Biological Sciences*, vol. 26, no. 2, pp. 382–389, 2019.
- [23] S. Dugasani, M. R. Pichika, V. D. Nadarajah, M. K. Balijepalli, S. Tandra, and J. N. Korlakunta, "Comparative antioxidant and anti-inflammatory effects of [6]-gingerol, [8]-gingerol, [10]-gingerol and [6]-shogaol," *Journal of Ethnopharmacology*, vol. 127, no. 2, pp. 515–520, 2010.
- [24] O. I. Mohamed, A. F. El-Nahas, Y. S. El-Sayed, and K. M. Ashry, "Ginger extract modulates Pb-induced hepatic oxidative stress and expression of antioxidant gene transcripts in rat liver," *Pharmaceutical Biology*, vol. 54, no. 7, pp. 1164–1172, 2016.
- [25] K. Al Syaad, F. Elsaid, M. Abdraboh, and A. Al-Doaiss, "Effect of graviola (*annona muricata* L.) and ginger (*zingiber officinale* roscoe) on diabetes mellitus induced in male wistar albino rats," *Folia biologica*, vol. 65, no. 5-6, pp. 275–284, 2019.
- [26] E. B. Lee, J. H. Kim, C. W. An et al., "Longevity and stress resistant property of 6-Gingerol from *Zingiber officinale* Roscoe in *Caenorhabditis elegans*," *Biomolecules & Therapeutics*, vol. 26, no. 6, pp. 568–575, 2018.
- [27] J. A. Michiels, C. Kevers, J. Pincemail, J. O. Defraigne, and J. Dommès, "Extraction conditions can greatly influence antioxidant capacity assays in plant food matrices," *Food Chemistry*, vol. 130, no. 4, pp. 986–993, 2012.
- [28] K. P. P. Gunathilake and H. V. Rupasinghe, "Inhibition of human low-density lipoprotein oxidation in vitro by ginger extracts," *Journal of Medicinal Food*, vol. 17, no. 4, pp. 424–431, 2014.
- [29] S. Adel and J. Prakash, "Chemical composition and antioxidant properties of ginger root (*Zingiber officinale*)," *Journal of Medicinal Plants Research*, vol. 4, pp. 2674–2679, 2010.
- [30] Y. Sueishi, H. Masamoto, and Y. Kotake, "Heat treatments of ginger root modify but not diminish its antioxidant activity as measured with multiple free radical scavenging (MULTIS) method," *Journal of Clinical Biochemistry and Nutrition*, vol. 64, no. 2, pp. 143–147, 2019.
- [31] E. W. C. Chan, Y. Y. Lim, S. K. Wong et al., "Effects of different drying methods on the antioxidant properties of leaves and tea of ginger species," *Food Chemistry*, vol. 113, no. 1, pp. 166–172, 2009.
- [32] L. Khodaie and O. Sadeghpour, "Ginger from ancient times to the new outlook," *Jundishapur journal of natural pharmaceutical products*, vol. 10, no. 1, article e18402, 2015.
- [33] I. Mustafa, N. L. Chin, S. Fakurazi, and A. Palanisamy, "Comparison of phytochemicals, antioxidant and anti-inflammatory properties of sun-, oven- and freeze-dried ginger extracts," *Food*, vol. 8, no. 10, p. 456, 2019.
- [34] A. Ghasemzadeh, H. Z. Jaafar, and A. Rahmat, "Changes in antioxidant and antibacterial activities as well as phytochemical constituents associated with ginger storage and polyphenol oxidase activity," *BMC Complementary and Alternative Medicine*, vol. 16, no. 1, pp. 1–11, 2016.
- [35] B. R. Min, L. E. Marsh, K. Brathwaite, and A. O. Daramola, "Effects of tissue culture and mycorrhiza applications in organic farming on concentrations of phytochemicals and antioxidant capacities in ginger (*Zingiber officinale* roscoe) rhizomes and leaves," *Journal of Food Science*, vol. 82, no. 4, pp. 873–881, 2017.
- [36] S. D. Jolad, R. C. Lantz, A. M. Solyom, G. J. Chen, R. B. Bates, and B. N. Timmermann, "Fresh organically grown ginger (*Zingiber officinale*): composition and effects on LPS-induced PGE₂ production," *Phytochemistry*, vol. 65, no. 13, pp. 1937–1954, 2004.
- [37] S. D. Jolad, R. C. Lantz, G. J. Chen, R. B. Bates, and B. N. Timmermann, "Commercially processed dry ginger (*Zingiber officinale*): composition and effects on LPS-stimulated PGE₂ production," *Phytochemistry*, vol. 66, no. 13, pp. 1614–1635, 2005.
- [38] R. Lantz, G. Chen, M. Sarihan, A. Solyom, S. Jolad, and B. Timmermann, "The effect of extracts from ginger rhizome on inflammatory mediator production," *Phytomedicine*, vol. 14, no. 2-3, pp. 123–128, 2007.
- [39] S. M. Ezzat, M. I. Ezzat, M. M. Okba, E. T. Menze, and A. B. Abdel-Naim, "The hidden mechanism beyond ginger (*Zingiber officinale* Rosc.) potent *in vivo* and *in vitro* anti-inflammatory activity," *Journal of Ethnopharmacology*, vol. 214, pp. 113–123, 2018.
- [40] T.-Y. Lee, K.-C. Lee, S.-Y. Chen, and H.-H. Chang, "6-Gingerol inhibits ROS and iNOS through the suppression of PKC- α and NF- κ B pathways in lipopolysaccharide-stimulated mouse macrophages," *Biochemical and Biophysical Research Communications*, vol. 382, no. 1, pp. 134–139, 2009.
- [41] X.-H. Li, K. C. McGrath, V. H. Tran et al., "Attenuation of proinflammatory responses by S-[6]-gingerol via inhibition of ROS/NF-kappa B/COX2 activation in HuH7 cells," *Evidence-based Complementary and Alternative Medicine*, vol. 2013, Article ID 146142, 8 pages, 2013.
- [42] P. Saha, A. Katarkar, B. Das, A. Bhattacharyya, and K. Chaudhuri, "6-gingerol inhibits vibrio cholerae-induced proinflammatory cytokines in intestinal epithelial cells via modulation of NF- κ B," *Pharmaceutical Biology*, vol. 54, no. 9, pp. 1606–1615, 2016.
- [43] N. Liang, Y. Sang, W. Liu, W. Yu, and X. Wang, "Anti-inflammatory effects of gingerol on lipopolysaccharide-stimulated RAW 264.7 cells by inhibiting NF- κ B signaling pathway," *Inflammation*, vol. 41, no. 3, pp. 835–845, 2018.
- [44] M. H. Pan, M. C. Hsieh, P. C. Hsu et al., "6-Shogaol suppressed lipopolysaccharide-induced up-expression of iNOS

- and COX-2 in murine macrophages,” *Molecular Nutrition & Food Research*, vol. 52, no. 12, pp. 1467–1477, 2008.
- [45] S. Ueki, M. Miyoshi, O. Shido, J. Hasegawa, and T. Watanabe, “Systemic administration of [6]-gingerol, a pungent constituent of ginger, induces hypothermia in rats via an inhibitory effect on metabolic rate,” *European Journal of Pharmacology*, vol. 584, no. 1, pp. 87–92, 2008.
- [46] H.-Y. Young, Y.-L. Luo, H.-Y. Cheng, W.-C. Hsieh, J.-C. Liao, and W.-H. Peng, “Analgesic and anti-inflammatory activities of [6]-gingerol,” *Journal of Ethnopharmacology*, vol. 96, no. 1-2, pp. 207–210, 2005.
- [47] A. Levy and O. Simon, “Six-shogaol inhibits production of tumour necrosis factor alpha, interleukin-1 beta and nitric oxide from lipopolysaccharide-stimulated RAW 264.7 macrophages,” *West Indian Medical Journal*, vol. 58, no. 4, pp. 295–300, 2009.
- [48] Q. Han, Q. Yuan, X. Meng, J. Huo, Y. Bao, and G. Xie, “6-Shogaol attenuates LPS-induced inflammation in BV2 microglia cells by activating PPAR- γ ,” *Oncotarget*, vol. 8, no. 26, pp. 42001–42006, 2017.
- [49] S.-J. Park, M.-Y. Lee, B.-S. Son, and H.-S. Youn, “TBK1-targeted suppression of TRIF-dependent signaling pathway of toll-like receptors by 6-shogaol, an active component of ginger,” *Bioscience, Biotechnology, and Biochemistry*, vol. 73, no. 7, pp. 1474–1478, 2009.
- [50] M. Suekawa, A. Ishige, K. Yuasa, K. Sudo, M. Aburada, and E. Hosoya, “Pharmacological studies on ginger. I. Pharmacological actions of pungent constituents, (6)-gingerol and (6)-shogaol,” *Journal of Pharmacobio-Dynamics*, vol. 7, no. 11, pp. 836–848, 1984.
- [51] M. Jalali, M. Mahmoodi, S. P. Moosavian et al., “The effects of ginger supplementation on markers of inflammatory and oxidative stress: a systematic review and meta-analysis of clinical trials,” *Phytotherapy Research*, vol. 34, no. 8, pp. 1723–1733, 2020.
- [52] M. Morvaridzadeh, S. Fazelian, S. Agah et al., “Effect of ginger (*Zingiber officinale*) on inflammatory markers: a systematic review and meta-analysis of randomized controlled trials,” *Cytokine*, vol. 135, article 155224, 2020.
- [53] F. Zehsaz, N. Farhangi, and L. Mirheidari, “Clinical immunology the effect of *Zingiber officinale* R. rhizomes (ginger) on plasma pro-inflammatory cytokine levels in well-trained male endurance runners,” *Central-European journal of immunology*, vol. 2, pp. 174–180, 2014.
- [54] N. Rastogi, R. K. Gara, R. Trivedi et al., “(6)-Gingerol-induced myeloid leukemia cell death is initiated by reactive oxygen species and activation of miR-27b expression,” *Free Radical Biology and Medicine*, vol. 68, pp. 288–301, 2014.
- [55] Y. Luo, X. Chen, L. Luo et al., “[6]-Gingerol enhances the radiosensitivity of gastric cancer via G2/M phase arrest and apoptosis induction,” *Oncology Reports*, vol. 39, no. 5, pp. 2252–2260, 2018.
- [56] P. Su, V. P. Veerarahavan, S. Krishna Mohan, and W. Lu, “A ginger derivative, zingerone—a phenolic compound—induces ROS-mediated apoptosis in colon cancer cells (HCT-116),” *Journal of biochemical and molecular toxicology*, vol. 33, no. 12, article e22403, 2019.
- [57] R. M. de Lima, A. C. Dos Reis, J. V. de Oliveira Santos et al., “Antitumoral effects of [6]-gingerol [(S)-5-hydroxy-1-(4-hydroxy-3-methoxyphenyl)-3-decanone] in sarcoma 180 cells through cytogenetic mechanisms,” *Biomedicine & Pharmacotherapy*, vol. 126, article 110004, 2020.
- [58] A. A. Oyagbemi, A. B. Saba, and O. I. Azeez, “Molecular targets of [6]-gingerol: its potential roles in cancer chemoprevention,” *BioFactors*, vol. 36, no. 3, pp. 169–178, 2010.
- [59] D. Chen, K. R. Landis-Piowar, M. S. Chen, and Q. P. Dou, “Inhibition of proteasome activity by the dietary flavonoid apigenin is associated with growth inhibition in cultured breast cancer cells and xenografts,” *Breast Cancer Research*, vol. 9, no. 6, pp. 1–8, 2007.
- [60] D. Chen, K. G. Daniel, M. S. Chen, D. J. Kuhn, K. R. Landis-Piowar, and Q. P. Dou, “Dietary flavonoids as proteasome inhibitors and apoptosis inducers in human leukemia cells,” *Biochemical Pharmacology*, vol. 69, no. 10, pp. 1421–1432, 2005.
- [61] K. B. Pandey and S. I. Rizvi, “Plant polyphenols as dietary antioxidants in human health and disease,” *Oxidative Medicine and Cellular Longevity*, vol. 2, no. 5, pp. 270–278, 2009.
- [62] F. Di Domenico, C. Foppoli, R. Coccia, and M. Perluigi, “Antioxidants in cervical cancer: chemopreventive and chemotherapeutic effects of polyphenols,” *Biochimica et Biophysica Acta (BBA)-Molecular Basis of Disease*, vol. 1822, pp. 737–747, 2012.
- [63] N. Rastogi, S. Duggal, S. K. Singh et al., “Proteasome inhibition mediates p53 reactivation and anti-cancer activity of 6-gingerol in cervical cancer cells,” *Oncotarget*, vol. 6, no. 41, pp. 43310–43325, 2015.
- [64] J. K. Kundu, H.-K. Na, and Y.-J. Surh, “Ginger-derived phenolic substances with cancer preventive and therapeutic potential,” *Food Factors for Health Promotion*, vol. 61, pp. 182–192, 2009.
- [65] G. C. Jagetia, M. S. Baliga, P. Venkatesh, and J. N. Ulloor, “Influence of ginger rhizome (*Zingiber officinale* Rosc) on survival, glutathione and lipid peroxidation in mice after whole-body exposure to gamma radiation,” *Radiation Research*, vol. 160, pp. 584–592, 2003.
- [66] C.-B. Lin, C.-C. Lin, and G. J. Tsay, “6-Gingerol inhibits growth of colon cancer cell LoVo via induction of G2/M arrest,” *Evidence-based Complementary and Alternative Medicine*, vol. 2012, Article ID 326096, 7 pages, 2012.
- [67] R. Jayakumar and M. Kanthimathi, “Dietary spices protect against hydrogen peroxide-induced DNA damage and inhibit nicotine-induced cancer cell migration,” *Food Chemistry*, vol. 134, no. 3, pp. 1580–1584, 2012.
- [68] M. M. Bernard, J. R. McConnery, and D. W. Hoskin, “[10]-Gingerol, a major phenolic constituent of ginger root, induces cell cycle arrest and apoptosis in triple-negative breast cancer cells,” *Experimental and Molecular Pathology*, vol. 102, no. 2, pp. 370–376, 2017.
- [69] A. Deorukhkar, N. Ahuja, A. L. Mercado et al., “Zerubone increases oxidative stress in a thiol-dependent ROS-independent manner to increase DNA damage and sensitize colorectal cancer cells to radiation,” *Cancer Medicine*, vol. 4, no. 2, pp. 278–292, 2015.
- [70] R. Hu, P. Zhou, Y.-B. Peng et al., “6-Shogaol induces apoptosis in human hepatocellular carcinoma cells and exhibits anti-tumor activity in vivo through endoplasmic reticulum stress,” *PLoS One*, vol. 7, no. 6, article e39664, 2012.
- [71] C. Chatupheeraphat, C. Nantasenammat, K. Deesrisak, S. Roytrakul, U. Anurathapan, and D. Tanyong, “Bioinformatics and experimental studies of anti-leukemic activity from 6-gingerol demonstrate its role in p53 mediated apoptosis pathway,” *EXCLI Journal*, vol. 19, pp. 582–595, 2020.

- [72] A. Saha, J. Blando, E. Silver, L. Beltran, J. Sessler, and J. DiGiovanni, "6-Shogaol from dried ginger inhibits growth of prostate cancer cells both in vitro and in vivo through inhibition of STAT3 and NF- κ B signaling," *Cancer Prevention Research*, vol. 7, no. 6, pp. 627–638, 2014.
- [73] A. S. Bawadood, F. A. Al-Abbasi, F. Anwar, A. M. El-Halawany, and A. M. Al-Abd, "6-Shogaol suppresses the growth of breast cancer cells by inducing apoptosis and suppressing autophagy via targeting notch signaling pathway," *Biomedicine & Pharmacotherapy*, vol. 128, article 110302, 2020.
- [74] M. Akimoto, M. Iizuka, R. Kanematsu, M. Yoshida, and K. Takenaga, "Anticancer effect of ginger extract against pancreatic cancer cells mainly through reactive oxygen species-mediated autotic cell death," *PLoS One*, vol. 10, no. 5, article e0126605, 2015.
- [75] A. Ray, S. Vasudevan, and S. Sengupta, "6-Shogaol inhibits breast cancer cells and stem cell-like spheroids by modulation of Notch signaling pathway and induction of autophagic cell death," *PLoS One*, vol. 10, no. 9, article e0137614, 2015.
- [76] J.-Y. Hung, Y.-L. Hsu, C.-T. Li et al., "6-Shogaol, an active constituent of dietary ginger, induces autophagy by inhibiting the AKT/mTOR pathway in human non-small cell lung cancer A549 cells," *Journal of Agricultural and Food Chemistry*, vol. 57, no. 20, pp. 9809–9816, 2009.
- [77] I.-J. Yeh, S.-C. Chen, M.-C. Yen, Y.-H. Wu, C.-H. Hung, and P.-L. Kuo, "6-Shogaol suppresses 2-amino-1-methyl-6-phenylimidazo [4, 5-b] pyridine (PhIP)-induced human 786-O renal cell carcinoma osteoclastogenic activity and metastatic potential," *Nutrients*, vol. 11, no. 10, p. 2306, 2019.
- [78] D. Chakraborty, K. Bishayee, S. Ghosh, R. Biswas, S. K. Mandal, and A. R. Khuda-Bukhsh, "[6]-Gingerol induces caspase 3 dependent apoptosis and autophagy in cancer cells: drug-DNA interaction and expression of certain signal genes in HeLa cells," *European Journal of Pharmacology*, vol. 694, no. 1-3, pp. 20–29, 2012.
- [79] S. Xu, H. Zhang, T. Liu et al., "6-Gingerol induces cell-cycle G1-phase arrest through AKT–GSK 3 β –cyclin D1 pathway in renal-cell carcinoma," *Cancer Chemotherapy and Pharmacology*, vol. 85, no. 2, pp. 379–390, 2020.
- [80] E. O. Farombi, B. O. Ajayi, and I. A. Adedara, "6-Gingerol delays tumorigenesis in benzo[a]pyrene and dextran sulphate sodium-induced colorectal cancer in mice," *Food and Chemical Toxicology*, vol. 142, article 111483, 2020.
- [81] L. Luna-Dulcey, J. A. da Silva, and M. R. Cominetti, "SSi6 promotes cell death by apoptosis through cell cycle arrest and inhibits migration and invasion of MDA-MB-231 human breast cancer cells," *Anti-Cancer Drugs*, vol. 31, no. 1, pp. 35–43, 2020.
- [82] J. Citronberg, R. Bostick, T. Ahearn et al., "Effects of ginger supplementation on cell-cycle biomarkers in the normal-appearing colonic mucosa of patients at increased risk for colorectal cancer: results from a pilot, randomized, and controlled trial," *Cancer Prevention Research*, vol. 6, no. 4, pp. 271–281, 2013.
- [83] X. M. Zhao, W. Tian, R. Jiang, and J. Wan, "Long noncoding RNAs-related diseases, cancers, and drugs," *Scientific World Journal*, vol. 2013, article 350358, 7 pages, 2013.
- [84] M. Yusof, S. Makpol, R. Jamal, R. Harun, N. Mokhtar, and W. Ngah, " γ -Tocotrienol and 6-gingerol in combination synergistically induce cytotoxicity and apoptosis in HT-29 and SW837 human colorectal cancer cells," *Molecules*, vol. 20, no. 6, pp. 10280–10297, 2015.
- [85] A. A. Tahir, N. F. A. Sani, N. A. Murad, S. Makpol, W. Z. W. Ngah, and Y. A. M. Yusof, "Combined ginger extract & Gelam honey modulate Ras/ERK and PI3K/AKT pathway genes in colon cancer HT29 cells," *Nutrition Journal*, vol. 14, no. 1, pp. 1–10, 2015.
- [86] A. A. Rahman, S. Makpol, R. Jamal, R. Harun, N. Mokhtar, and W. Z. W. Ngah, "Tocotrienol-rich fraction, [6]-gingerol and epigallocatechin gallate inhibit proliferation and induce apoptosis of glioma cancer cells," *Molecules*, vol. 19, no. 9, pp. 14528–14541, 2014.
- [87] N. E. El-Ashmawy, N. F. Khedr, H. A. El-Bahrawy, and H. E. Abo Mansour, "Ginger extract adjuvant to doxorubicin in mammary carcinoma: study of some molecular mechanisms," *European Journal of Nutrition*, vol. 57, no. 3, pp. 981–989, 2018.
- [88] M. Woźniak, S. Makuch, K. Winograd, J. Wiśniewski, P. Ziółkowski, and S. Agrawal, "6-Shogaol enhances the anti-cancer effect of 5-fluorouracil, oxaliplatin, and irinotecan via increase of apoptosis and autophagy in colon cancer cells in hypoxic/aglycemic conditions," *BMC Complementary Medicine and Therapies*, vol. 20, no. 1, pp. 1–10, 2020.
- [89] P. Fernández-Ortega, M. Caloto, E. Chirveches et al., "Chemotherapy-induced nausea and vomiting in clinical practice: impact on patients' quality of life," *Supportive Care in Cancer*, vol. 20, no. 12, pp. 3141–3148, 2012.
- [90] W. Marx, K. Ried, A. L. McCarthy et al., "Ginger—mechanism of action in chemotherapy-induced nausea and vomiting: a review," *Critical Reviews in Food Science and Nutrition*, vol. 57, no. 1, pp. 141–146, 2017.
- [91] W. P. Chang and Y. X. Peng, "Does the oral administration of ginger reduce chemotherapy-induced nausea and vomiting?: a meta-analysis of 10 randomized controlled trials," *Cancer Nursing*, vol. 42, no. 6, pp. E14–E23, 2019.
- [92] M. Crichton, S. Marshall, W. Marx, A. L. McCarthy, and E. Isenring, "Efficacy of Ginger (*Zingiber officinale*) in Ameliorating Chemotherapy-Induced Nausea and Vomiting and Chemotherapy-Related Outcomes: A Systematic Review Update and Meta-Analysis," *Journal of the Academy of Nutrition and Dietetics*, vol. 119, no. 12, pp. 2055–2068, 2019.
- [93] G. F. Zeng, Z. Y. Zhang, L. Lu, D. Q. Xiao, S. H. Zong, and J. M. He, "Protective effects of ginger root extract on Alzheimer disease-induced behavioral dysfunction in rats," *Rejuvenation Research*, vol. 16, no. 2, pp. 124–133, 2013.
- [94] J.-Y. Na, K. Song, J.-W. Lee, S. Kim, and J. Kwon, "6-Shogaol has anti-amyloidogenic activity and ameliorates Alzheimer's disease via CysLT1R-mediated inhibition of cathepsin B," *Biochemical and Biophysical Research Communications*, vol. 477, no. 1, pp. 96–102, 2016.
- [95] G. Oboh, A. O. Ademiluyi, and A. J. Akinyemi, "Inhibition of acetylcholinesterase activities and some pro-oxidant induced lipid peroxidation in rat brain by two varieties of ginger (*Zingiber officinale*)," *Experimental and Toxicologic Pathology*, vol. 64, no. 4, pp. 315–319, 2012.
- [96] S. Shim and J. Kwon, "Effects of [6]-shogaol on cholinergic signaling in HT22 cells following neuronal damage induced by hydrogen peroxide," *Food and Chemical Toxicology*, vol. 50, no. 5, pp. 1454–1459, 2012.
- [97] J.-Y. Na, K. Song, J.-W. Lee, S. Kim, and J. Kwon, "Sortilin-related receptor 1 interacts with amyloid precursor protein and is activated by 6-shogaol, leading to inhibition of the amyloidogenic pathway," *Biochemical and Biophysical Research Communications*, vol. 484, no. 4, pp. 890–895, 2017.

- [98] G.-f. Zeng, S.-h. Zong, Z.-y. Zhang et al., "The role of 6-gingerol on inhibiting amyloid β protein-induced apoptosis in PC12 cells," *Rejuvenation Research*, vol. 18, no. 5, pp. 413–421, 2015.
- [99] C. Lee, G. H. Park, C.-Y. Kim, and J.-H. Jang, "[6]-Gingerol attenuates β -amyloid-induced oxidative cell death via fortifying cellular antioxidant defense system," *Food and Chemical Toxicology*, vol. 49, no. 6, pp. 1261–1269, 2011.
- [100] N. Saenghong, J. Wattanathorn, S. Muchimapura et al., "*Zingiber officinale* improves cognitive function of the middle-aged healthy women," *Evidence-based Complementary and Alternative Medicine*, vol. 2012, Article ID 383062, 9 pages, 2012.
- [101] A. Bassiouny, A. Zaky, and E. M. Reda, "conferenceseries.com," *Journal of Neurology*, vol. 4, 2016.
- [102] G. Park, H. G. Kim, M. S. Ju et al., "6-Shogaol, an active compound of ginger, protects dopaminergic neurons in Parkinson's disease models via anti-neuroinflammation," *Acta Pharmacologica Sinica*, vol. 34, no. 9, pp. 1131–1139, 2013.
- [103] E. Huh, J. G. Choi, D. Noh et al., "Ginger and 6-shogaol protect intestinal tight junction and enteric dopaminergic neurons against 1-methyl-4-phenyl 1, 2, 3, 6-tetrahydropyridine in mice," *Nutritional Neuroscience*, vol. 23, no. 6, pp. 455–464, 2020.
- [104] M. N. Ghayur and A. H. Gilani, "Ginger lowers blood pressure through blockade of voltage-dependent calcium channels," *Journal of Cardiovascular Pharmacology*, vol. 45, no. 1, pp. 74–80, 2005.
- [105] A. J. Akinyemi, G. R. Thome, V. M. Morsch et al., "Effect of dietary supplementation of ginger and turmeric rhizomes on angiotensin-1 converting enzyme (ACE) and arginase activities in L-NAME induced hypertensive rats," *Journal of functional foods*, vol. 17, pp. 792–801, 2015.
- [106] Q. Liu, J. Liu, H. Guo et al., "[6]-Gingerol: a novel AT₁ antagonist for the treatment of cardiovascular disease," *Planta Medica*, vol. 79, no. 5, pp. 322–326, 2013.
- [107] Y.-J. Lee, Y.-N. Jang, Y.-M. Han, H.-M. Kim, and H. S. Seo, "6-Gingerol normalizes the expression of biomarkers related to hypertension via PPAR δ in HUVECs, HEK293, and differentiated 3T3-L1 cells," *PPAR Research*, vol. 2018, Article ID 6485064, 14 pages, 2018.
- [108] A. Ahad, M. Raish, Y. A. Bin Jordan, M. A. Alam, A. M. Al-Mohizea, and F. I. Al-Jenoobi, "Effect of *Hibiscus sabdariffa* and *Zingiber officinale* on the antihypertensive activity and pharmacokinetic of losartan in hypertensive rats," *Xenobiotica*, vol. 50, no. 7, pp. 847–857, 2020.
- [109] H. Hasani, A. Arab, A. Hadi, M. Pourmasoumi, A. Ghavami, and M. Miraghajani, "Does ginger supplementation lower blood pressure? A systematic review and meta-analysis of clinical trials," *Phytotherapy Research*, vol. 33, no. 6, pp. 1639–1647, 2019.
- [110] M. Khosravani, M. A. Azarbayjani, M. Abolmaesoomi et al., "Ginger extract and aerobic training reduces lipid profile in high-fat fed diet rats," *European Review for Medical and Pharmacological Sciences*, vol. 20, no. 8, pp. 1617–1622, 2016.
- [111] T. Barbalata, M. Deleanu, M. G. Carnuta et al., "Hyperlipidemia determines dysfunctional HDL production and impedes cholesterol efflux in the small intestine: alleviation by ginger extract," *Molecular Nutrition & Food Research*, vol. 63, no. 19, article 1900029, 2019.
- [112] D. Kamato, H. Babaahmadi Rezaei, R. Getachew et al., "(S)-[6]-Gingerol inhibits TGF- β -stimulated biglycan synthesis but not glycosaminoglycan hyperelongation in human vascular smooth muscle cells," *Journal of Pharmacy and Pharmacology*, vol. 65, no. 7, pp. 1026–1036, 2013.
- [113] R. Alizadeh-Navaei, F. Roozbeh, M. Saravi, M. Pouramir, F. Jalali, and A. A. Moghadamnia, "Investigation of the effect of ginger on the lipid levels. A double blind controlled clinical trial," *Saudi Medical Journal*, vol. 29, no. 9, pp. 1280–1284, 2008.
- [114] Y. Zhao and Z.-Y. Chen, "Roles of spicy foods and their bioactive compounds in management of hypercholesterolemia," *Journal of Agricultural and Food Chemistry*, vol. 66, no. 33, pp. 8662–8671, 2018.
- [115] C. Chen, Q. Zhang, F.-Q. Wang et al., "In vitro anti-platelet aggregation effects of fourteen fruits and vegetables," *Pakistan Journal of Pharmaceutical Sciences*, vol. 32, no. 1, pp. 185–195, 2019.
- [116] M. B. Samad, M. Mohsin, N. A. Bin et al., "[6]-Gingerol, from *Zingiber officinale*, potentiates GLP-1 mediated glucose-stimulated insulin secretion pathway in pancreatic β -cells and increases RAB8/RAB10-regulated membrane presentation of GLUT4 transporters in skeletal muscle to improve hyperglycemia in Leprdb/db type 2 diabetic mice," *BMC Complementary and Alternative Medicine*, vol. 17, no. 1, pp. 1–13, 2017.
- [117] Y. Zhu, Y. Zhao, P. Wang, M. Ahmedna, and S. Sang, "Bioactive ginger constituents alleviate protein glycation by trapping methylglyoxal," *Chemical Research in Toxicology*, vol. 28, no. 9, pp. 1842–1849, 2015.
- [118] T.-C. Chen, C.-K. Yen, Y.-C. Lu et al., "The antagonism of 6-shogaol in high-glucose-activated NLRP3 inflammasome and consequent calcification of human artery smooth muscle cells," *Cell & Bioscience*, vol. 10, no. 1, pp. 1–10, 2020.
- [119] F. A. Fajrin, A. E. Nugroho, A. Nurrochmad, and R. Susilowati, "Ginger extract and its compound, 6-shogaol, attenuates painful diabetic neuropathy in mice via reducing TRPV1 and NMDAR2B expressions in the spinal cord," *Journal of Ethnopharmacology*, vol. 249, article 112396, 2020.
- [120] J. Zhu, H. Chen, Z. Song, X. Wang, and Z. Sun, "Effects of ginger (*Zingiber officinale* Roscoe) on type 2 diabetes mellitus and components of the metabolic syndrome: a systematic review and meta-analysis of randomized controlled trials," *Evidence-based complementary and alternative medicine*, vol. 2018, Article ID 5692962, 11 pages, 2018.
- [121] T. Tanaka, J. Yamamoto, S. Iwasaki et al., "Activation of peroxisome proliferator-activated receptor δ induces fatty acid β -oxidation in skeletal muscle and attenuates metabolic syndrome," *Proceedings of the National Academy of Sciences*, vol. 100, no. 26, pp. 15924–15929, 2003.
- [122] K. Misawa, K. Hashizume, M. Yamamoto, Y. Minegishi, T. Hase, and A. Shimotoyodome, "Ginger extract prevents high-fat diet-induced obesity in mice via activation of the peroxisome proliferator-activated receptor δ pathway," *The Journal of Nutritional Biochemistry*, vol. 26, no. 10, pp. 1058–1067, 2015.
- [123] J. Wang, P. Wang, D. Li, X. Hu, and F. Chen, "Beneficial effects of ginger on prevention of obesity through modulation of gut microbiota in mice," *European Journal of Nutrition*, vol. 59, no. 2, pp. 699–718, 2020.
- [124] S.-H. Park, S.-J. Jung, E.-K. Choi et al., "The effects of steamed ginger ethanolic extract on weight and body fat loss: a

- randomized, double-blind, placebo-controlled clinical trial,” *Food Science and Biotechnology*, vol. 29, no. 2, pp. 265–273, 2019.
- [125] A. Bhaskar, A. Kumari, M. Singh et al., “[6]-Gingerol exhibits potent anti-mycobacterial and immunomodulatory activity against tuberculosis,” *International Immunopharmacology*, vol. 87, article 106809, 2020.
- [126] B. O. Oyedemi, E. Kotsia, P. D. Stapleton, and S. Gibbons, “Capsaicin and gingerol analogues inhibit the growth of efflux-multidrug resistant bacteria and R-plasmids conjugal transfer,” *Journal of Ethnopharmacology*, vol. 245, article 111871, 2019.
- [127] Y. Ouyang, X. Zhong, H. Liao, P. Zhu, K. Luo, and H. Zhu, “A new method for screening natural products to stimulate IFN- γ production in Jurkat human T lymphocytes,” *Slas Discovery: Advancing The Science Of Drug Discovery*, vol. 26, no. 1, pp. 130–139, 2021.
- [128] I. Ahmed, A. Aslam, G. Mustafa, S. Masood, M. A. Ali, and M. Nawaz, “Anti-avian influenza virus H9N2 activity of aqueous extracts of *Zingiber officinalis* (ginger) and *Allium sativum* (garlic) in chick embryos,” *Pakistan Journal of Pharmaceutical Sciences*, vol. 30, pp. 1341–1344, 2017.
- [129] S. Yavuz and S. Ünal, “Antiviral treatment of COVID-19,” *Turkish journal of medical sciences*, vol. 50, no. SI-1, pp. 611–619, 2020.
- [130] S. Kumar, P. Kashyap, S. Chowdhury, S. Kumar, A. Panwar, and A. Kumar, “Identification of phytochemicals as potential therapeutic agents that binds to Nsp15 protein target of coronavirus (SARS-CoV-2) that are capable of inhibiting virus replication,” *Phytomedicine*, vol. 85, article 153317, 2021.
- [131] S. M. Thota, V. Balan, and V. Sivaramkrishnan, “Natural products as home-based prophylactic and symptom management agents in the setting of COVID-19,” *Phytotherapy Research*, vol. 34, no. 12, pp. 3148–3167, 2020.
- [132] A. H. Ahkam, F. E. Hermanto, A. Alamsyah, I. H. Aliyyah, and F. Fatchiyah, “Virtual prediction of antiviral potential of ginger (*Zingiber officinale*) bioactive compounds against spike and MPro of SARS-CoV2 protein,” *Berkala Penelitian Hayati Journal Of Biological Researches*, vol. 25, no. 2, pp. 52–57, 2020.
- [133] M. Rondanelli, A. Miccono, G. Peroni et al., “A systematic review on the effects of botanicals on skeletal muscle health in order to prevent sarcopenia,” *Evidence-based Complementary and Alternative Medicine*, vol. 2016, Article ID 5970367, 23 pages, 2016.
- [134] N. F. N. Mohd Sahardi, F. Jaafar, M. F. Mad Nordin, and S. Makpol, “*Zingiber officinale* Roscoe prevents cellular senescence of myoblasts in culture and promotes muscle regeneration,” *Evidence-based Complementary and Alternative Medicine*, vol. 2020, Article ID 1787342, 13 pages, 2020.
- [135] P. K. Sacitharan, “Ageing and osteoarthritis,” *Biochemistry and cell biology of ageing: part II clinical science*, vol. 91, pp. 123–159, 2019.
- [136] C.-L. Shen, K.-J. Hong, and S. W. Kim, “Comparative effects of ginger root (*Zingiber officinale* Rosc.) on the production of inflammatory mediators in normal and osteoarthrotic sow chondrocytes,” *Journal of Medicinal Food*, vol. 8, no. 2, pp. 149–153, 2005.
- [137] F. Araya-Quintanilla, H. Gutierrez-Espinoza, M. J. Munoz-Yanez, U. Sanchez-Montoya, and J. Lopez-Jeldes, “Effectiveness of ginger on pain and function in knee osteoarthritis: a PRISMA systematic review and meta-analysis,” *Pain Physician*, vol. 23, no. 2, pp. E151–E161, 2020.
- [138] S. Zhang and E. Duan, “Fighting against skin aging: the way from bench to bedside,” *Cell Transplantation*, vol. 27, no. 5, pp. 729–738, 2018.
- [139] K. Tsukahara, H. Nakagawa, S. Moriwaki, Y. Takema, T. Fujimura, and G. Imokawa, “Inhibition of ultraviolet-B-induced wrinkle formation by an elastase-inhibiting herbal extract: implication for the mechanism underlying elastase-associated wrinkles,” *International Journal of Dermatology*, vol. 45, no. 4, pp. 460–468, 2006.
- [140] P. Leelapornpisid, R. R. Wickett, S. Chansakaow, and N. Wongwattananukul, “Potential of native Thai aromatic plant extracts in antiwrinkle body creams,” *Journal of Cosmetic Science*, vol. 66, no. 4, pp. 219–231, 2015.
- [141] K. Srivastava, “Isolation and effects of some ginger components on platelet aggregation and eicosanoid biosynthesis,” *Prostaglandins, Leukotrienes and Medicine*, vol. 25, no. 2-3, pp. 187–198, 1986.
- [142] K. Srivastava, “Effects of aqueous extracts of onion, garlic and ginger on platelet aggregation and metabolism of arachidonic acid in the blood vascular system: in vitro study,” *Prostaglandins, Leukotrienes and Medicine*, vol. 13, no. 2, pp. 227–235, 1984.
- [143] A. Lumb, “Mechanism of antiemetic effect of ginger,” *Anaesthesia*, vol. 48, no. 12, pp. 1118–1118, 1993.